AD NUMBER

AD456000

NEW LIMITATION CHANGE

TO

Approved for public release, distribution unlimited

FROM

Distribution authorized to U.S. Gov't. agencies and their contractors; Administrative/Operational Use; JAN 1965. Other requests shall be referred to Air Force Materials Laboratory, Attn: Research and Technology Division, Wright-Patterson AFB, OH.

AUTHORITY

DOT ltr, 6 Jul 1987

UNCLASSIFIED

AD 456000L

DEFENSE DOCUMENTATION CENTER

FOR

SCIENTIFIC AND TECHNICAL INFORMATION

CAMERON STATION ALEXANDRIA. VIRGINIA

AFML-TR-64-399
Volume I

FATIGUE BEHAVIOR OF SHEET MATERIALS

FOR THE SUPERSONIC TRANSPORT

Volume I - Summary and Analysis of Fatigue and Static Test Data

A. J. McCulloch
M. A. Melcon
L. Young

Lockheed-California Company

Technical Report AFML-TR-64-399, Volume I

January 1965

SUPERSONIC TRANSPORT RESEARCH PROGRAM
SPONSORED BY THE
FEDERAL AVIATION AGENCY

Jointly directed by: RTD, FAA, and NASA

Air Force Materials Laboratory
Research and Technology Division
Air Force Systems Command
Wright-Patterson Air Force Base, Ohio

NOTICES

When Government drawings, specifications, or other data are used for any
purpose other than in connection with a definitely related Government procure-
ment operation, the United States Government thereby incurs no responsibility
nor any obligation whatsoever; and the fact that the Government may have form-
ulated, furnished, or in any way supplied the said drawings, specifications, or
other data, is not to be regarded by implication or otherwise as in any manner
licensing the holder or any other person or corporation, or conveying any
rights or permission to manufacture, use, or sell any patented invention that
may in any way be related thereto.

The distribution of this report is limited because the information con-
tained herein is a part of a national undertaking sponsored by the Federal
Aviation Agency with administrative and technical support provided by the
Department of Defense, Research and Technology Division, Air Force Systems
Command with contributing basic research and technical support provided by the
National Aeronautics and Space Administration.

Copies have been placed in the DDC Collection. U.S. Government agencies
may obtain copies from DDC. Other qualified DDC users may request through:

Office of the Dep/Adm for SST Development
Federal Aviation Agency
800 Independence Ave. S. W.
Washington 25, D. C.

This report must not be cited, abstracted, reprinted, or given further
distribution without written approval of the above-named controlling office.

Copies of this report should not be returned to the Research and Technol-
ogy Division unless return is required by security considerations, contractual
obligations, or notice on a specific document.

ABSTRACT

To obtain comparative fatigue test data on three sheet materials selected for possible use on supersonic transports, a multi-phase program of tests was carried out using specimens of duplex-annealed 8-1-1 titanium, PH14-8 Mo (SRH 1050) stainless steel and Inco 718 alloy in the 20 percent cold rolled and aged condition. Unnotched, center-notched, fusion-welded and spotwelded specimens were used.

Constant load amplitude (S-N) fatigue tests were conducted at room temperature, 400 and 650°F on specimens having no prior exposure and on specimens with prior exposure to a constant load at 400 or 650°F for 100, 1000 or 5000 hours. An evaluation was also made of the effect of applying contaminants during S-N testing at 550 and 650°F to specimens having no prior exposure and to specimens exposed to load and contaminant at 550°F for 1000 hours.

In addition to the constant load amplitude fatigue tests, variable amplitude loadings and cyclic temperatures selected to conservatively represent service conditions in the wing root region of a supersonic transport were applied in flight-by-flight sequences. For one group of such tests, a representative time of approximately one hour at temperature during each "flight" was chosen. For a second group, the time at temperature was minimized A limited additional investigation of the effects of contaminants was carried out in these flight-by-flight tests.

Tests were also conducted to evaluate the effects of the cycle of heating and pressurization loading that occurs in fuselage skins once during each flight. These tests were performed on specimens having no prior exposure and on specimens exposed to load at 650°F for 5000 hours.

TABLE OF CONTENTS

LIST OF TABLES

ix

e	Percent elongation in a 2.00 inch gage length
f_{axp}	Gross area stress during exposure
f_{gross}	Gross area stress = load/gross area at the section of minimum width
f_{net}	Net area stress = load/net area at the section of minimum width
f_{max}	Highest value of gross area stress
f_{mean}	Mean gross area stress
f_{min}	Lowest value of gross area stress
f_{vary}	Maximum gross area stress minus mean gross area stress
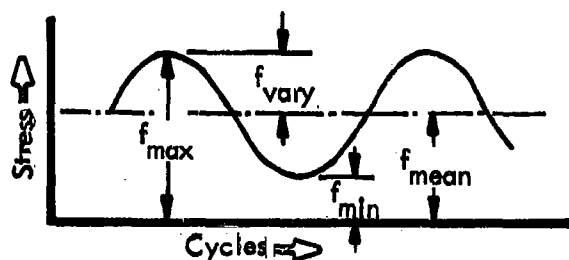
$f_{1g_{Ref}}$	Gross area stress for steady state (one g) flight at design gross weight of airplane
Δf	Change in gross area stress
F_{tu}	Static gross area tensile ultimate strength
F_{ty}	Static gross area tensile stress at which the departure from linearity of the stress-strain curves equal 0.002 inches per inch in a two inch gage length
$°F$	Degrees Fahrenheit
ksi	Kips (1000 pounds) per square inch
L	Length in inches
ΔL	Change in length in inches
$\Delta L/L$	Strain in inches per inch
R	Ratio of minimum to maximum stress
RT	Room Temperature
ρ	Density in pounds per cubic inch

SECTION 1

INTRODUCTION

To attain the levels of safety, reliability, and economical performance essential in a successful commercial supersonic transport (SST), the design of the airframe structure must reflect realistic evaluations of the fatigue characteristics of the candidate structural materials. These evaluations are distinguished from those made for subsonic transports by the addition of temperature-time effects to the list of variables to be considered.

In the design of subsonic transports for long service lives, the selection of materials and the evaluation of processes have been guided by comparisons of data obtained at normal temperatures using constant load amplitude test conditions. For the evaluation of the potential service life of a material as used in airframes, however, service experience and a growing fund of test data demonstrate the need for more complex tests. This need stems from the basic nonlinearity in the growth of fatigue damage which markedly reduces the reliability of calculating the effects of complex time histories of loadings. Direct integrations of the effects of complex service conditions must be obtained in tests. The results of such tests provide the best guides to the selection of fatigue design parameters which can be obtained prior to actual service.

In the design of supersonic transports, the difficulties and uncertainties in the handling of the fatigue problem are compounded by the introduction of the effects of elevated temperatures. Thermal gradients produce complex additions to the operating stress histories. Prolonged exposure to elevated temperatures may degrade the materials used and increase their susceptibility to the effects of contaminants. Test evaluations of these temperature effects must be obtained to guide the selection of SST materials and processes to ensure adequate service life.

To obtain such data, fatigue tests were performed using unnotched, notched, and welded specimens made from one steel, one titanium, and one nickel base alloy. S-N data were obtained on specimens having no prior exposure and on specimens exposed before testing to stress at elevated temperature for periods up to 5,000 hours. The additional effects of applying contaminants during the S-N tests were evaluated on unexposed specimens and on specimens exposed to contaminants while under stress at elevated temperature for a period of 1,000 hours.

In addition to these relatively simple constant load amplitude tests, loading spectra and thermal cycles selected to conservatively represent the service conditions on the wing surface of a supersonic transport were applied in flight-by-flight sequences. In one set of these variable load amplitude tests, the time spent at temperature during each "flight" was the average time

1

at temperature expected during service. Since this average time at temperature during each "flight" is approximately one hour, these tests will cover a long period of time. In a second set of tests, the same loading and thermal stress magnitudes and sequences were employed with the time at temperature minimized during each "flight". Base line flight-by-flight test data were also obtained from tests run at room temperature and at constant elevated temperature using the same loading magnitudes and sequences. Comparisons of the results from these sets of tests provide indications of the effects of short-and long-term intermittent exposure to elevated temperature, the effect of thermal cycling and the effect of loading at elevated temperature.

To provide an indication of the effect of the quite different loading sequences in fuselage structure, tests were carried out during which repeated cycles of combined loading and heating were applied to simulate the pressurization and aerodynamic heating cycle which occurs at least once each flight.

Finally, static tensile tests were performed to obtain data on the effects of prior exposure to load and temperature on static tensile properties.

The scope of the test program is indicated by the detailed listing in Tables 1-4 of the test conditions and the number of specimens tested.

TABLE 1   SUMMARY OF STATIC TENSILE TESTS

	PROGRAM		
	PHASE I		PHASE III—EVALUATION OF CONTAMINANT & CORROSIVE EFFECTS
	SPECIMEN CONDITION		
	NO PRIOR EXPOSURE	PRIOR EXPOSURE TO STRESS[1] AT ELEVATED TEMPERATURES	PRIOR EXPOSURE TO STRESS[1] AND CONTAMINANT AT ELEVATED TEMPERATURES
Materials	8-1-1 Titanium PH14-8Mo Stainless Steel and INCO 718	⟵————⟶	8-1-1 Titanium, PH14-8Mo Stainless Steel, & INCO 718
Specimen Configurations	Standard Tensile and Fusion-Welded	Standard Tensile and Fusion-Welded	Standard Tensile
Exposure Temperatures	———	400°F and 650°F	550°F
Exposure Times	———	100 hr, 1000 hr, and 5000 hr	1000 hr
Test Temperatures	RT, 400°F, and 650°F	RT, 400°F, and 650°F	650°F
Contaminants	———	———	Synthetic Sea Water (ASTM), MIL-O-7277 Mineral Oil, and Versilube F-50
Avg. No. of Specimens Each	3	3	3
Total Number of Specimens	83[2]	324	27

(1) Gross area stress for stainless steel and INCO 718 = 40,000 psi and for titanium = 25,000 psi.

(2) Includes 38 preliminary material evaluation tests.

3

TABLE 2 SUMMARY OF CONSTANT LOAD AMPLITUDE FATIGUE TESTS TO DEFINE S-N CURVES

PROGRAM

	PHASE I - CONSTANT LOAD AMPLITUDE TESTS				PHASE III-EVAL. OF CONTAMINANTS AND CORROSIVE EFFECTS	
	NO PRIOR EXPOSURE	SPECIMEN CONDITION			NO PRIOR EXPOSURE	PRIOR EXPOSURE TO STRESS & CONTAMINANT AT ELEVATED TEMPERATURE[1]
		PRIOR EXPOSURE TO ELEVATED TEMPERATURE	PRIOR EXPOSURE TO STRESS AT ELEVATED TEMPERATURE[1]			
Materials	8-1-1 Titanium, PH14-8Mo Stainless Steel, & INCO 718					8-1-1 Titanium, PH14-8Mo Stainless Steel & INCO 718
Specimen	Unnotched, Center Notched, & Fusion Welded	Fusion Welded [2]	Unnotched, Center Notched Prior to Exposure & Fusion Welded	Center Notched After Exposure	Unnotched, Center Notched, & Fusion Welded	Unnotched, Center Notched, & Fusion Welded
Exposure Temperatures	—	—	400°F & 650°F	400°F & 650°F	—	550°F
Exposure Times	—	—	100 hr, 1000 hr & 5000 hr	5000 hr	—	1000 hr
Test Temperature	RT, 400°F & 650°F	RT	RT, 400°F & 650°F	RT, 400°F & 650°F	650°F [3]	650°F
Contaminants					[4]	[4]
Constant Stress Ratios (R)	0.1 and -0.5	0.1 [5]	0.1 and -0.5	0.1 [5]	0.1 [5]	0.1 [5]
Number of S-N Plots	54	3	324	18	27	27
Avg. No. of Spec. per S-N Plot	12	3	12	3	3	3
Total Number of Specimens	653 [6]	9	3680	54	89	79

(1) Gross area stress for stainless steel and INCO 718 = 40,000 psi and for titanium = 25,000 psi.
(2) Unpolished welds.
(3) 6 8-1-1 titanium specimens were tested at 550°F
(4) Synthetic sea water (ASTM), MIL-O-7277 mineral oil, and Versilube F-50.
(5) One stress level only.
(6) In addition, 25 spotwelded specimens were tested.

TABLE 3 SUMMARY OF REALISTIC WING LOAD SPECTRA FATIGUE TESTS

	PHASE II - REAL TIME TESTS	PHASE II - ACCELERATED TESTS			PHASE III-EVALUATION OF CONTAMINANT AND CORROSIVE EFFECTS
		SPECIMEN TEST CONDITION(1)			
	TESTED WITH THERMAL CYCLE	TESTED AT ROOM TEMPERATURE	TESTED AT CONSTANT ELEVATED TEMPERATURE	TESTED WITH THERMAL CYCLE	SPECIMENS TESTED WITH CONTAMINANT AND THERMAL CYCLE
Materials	8-1-1 Titanium, PH14-8Mo Stainless Steel & INCO 718				8-1-1 Titanium, PH14-8Mo Stainless Steel & INCO 718
Specimen Configurations	Center-Notched and Spotwelded Doubler			Center-Notched and Spotwelded Doubler	Center-Notched
Contaminants	—	—	—	—	MIL-O-7277 Mineral Oil & Synthetic Sea Water (ASTM)(2)
Test Temperature	RT to 500°F(3)	RT	550°F	RT to 550°F(3)	550°F
Time at Elevated Temperature	60 min/flight	None	All	1 sec/flight	All
Avg. No. of Specimens Each	6	8(4)	4	4	2(2)
Total Number of Specimens	36	78(4)	28	31	8

(1) No prior soak.
(2) MIL-O-7277 mineral oil was applied on two specimens of each material and the synthetic sea water was applied only to two titanium specimens.
(3) To conserve test time in coupon testing, room temperature (RT) was defined as > 90°F.
(4) Includes specimens for exploratory tests.

5

TABLE 4 FUSELAGE LOADING FATIGUE TESTS

	PROGRAM	
	PHASE II - FUSELAGE LOADING EVALUATION	
	SPECIMEN CONDITION	
	NO PRIOR EXPOSURE	PRIOR EXPOSURE TO STRESS(1) AT ELEVATED TEMPERATURE
Materials	8-1-1 Titanium, PH 14-8Mo Stainless Steel and INCO 718	8-1-1 Titanium, PH14-8Mo Stainless Steel and INCO 718
Specimen Configuration	Center-Notched and Fusion-Welded	Center-Notched and Fusion-Welded
Exposure Temperatures	——	650°F
Exposure Time	——	5000 hrs.
Test Temperature	RT to 550°F(2)	RT to 550°F(2)
Number of Specimens Each	4(3)	2
Total Number of Specimens	24(3)	12

(1) Gross area stress for stainless steel and INCO 718 = 40,000 psi & for titanium = 25,000 psi
(2) To conserve test time in coupon testing, room temperature (RT) was defined as ≈ 120°F.
(3) Includes specimens for exploratory tests.

SECTION 2

SUMMARY

An extensive, comparative evaluation of the fatigue properties of 8-1-1 duplex-annealed titanium, PH14-8Mo (SRH 1050) and Inco 718 cold rolled 20 percent and aged was carried out using unnotched, center-notched and welded sheet specimens. A total of approximately 5300 tests are reported.

Data were obtained in conventional constant load amplitude tests and also in tests in which variable amplitude loadings were applied in flight-by-flight sequences. These tests showed marked superiority of the 8-1-1 titanium material for supersonic transport airframe applications.

The largest body of data was obtained in the constant load amplitude tests. The intent in these tests was the evaluation of the materials on the basis of the indicated effects of prior exposure to load at elevated temperature. S-N curves were defined for constant values of stress ratio, R, (minimum/maximum) of 0.1 and -0.5 at room temperature, 400°F and 650°F for specimens without prior exposure and also for specimens with prior exposures under constant load at temperatures of 400°F or 650°F for periods of 100, 1000 or 5000 hours. The number of combinations of material, specimen geometry, test temperature, exposure temperature and exposure time was therefore very large. This fact together with m..ked non-uniformity in trends displayed by the data posed difficult evaluation problems.

For evaluation, the S-N curves for constant values of R were first grouped by material, specimen geometry and test temperature and are presented in Appendix VI of this volume of the report for possible comparison with similarly defined data for other materials. This form of presentation does not, however, lend itself to the most direct use in airframe material selections. To provide more directly applicable data for design situations in which constant values of mean stress are important parameters, the S-N curves for constant values of R were used to construct S-N diagrams from which S-N curves for representative values of mean stress were derived. These curves were then grouped by material, specimen geometry and test temperature. These groupings of curves are presented in Appendix VII. An examination of the highly variable trends shown by these groupings led to a further summarization of the data. This summarization, which is presented and discussed in Section 5 of the report. shows for each material-specimen geometry combination the percentage changes in varying stress for preselected values of test life as functions of exposure temperature, exposure time and test temperature. The plots of data in this form show highly non-uniform trends which may indicate changes in the stability of the materials. However, a rating of the materials on the basis of their indicated stability would be premature. For each material, the data are based on a relatively small number of specimens taken from sheets

7

of a single thickness produced from a single heat and tested in a type of test which ordinarily produces large scatter in test data.

The most informative comparison of the materials provided by the S-N data is believed to be one based on envelopes of the constant mean stress curves for all exposure and test conditions expressed in terms of varying stress divided by material density. Such envelopes are presented in Figures 1 through 9. An examination of these figures leads to the conclusion that, for the range of specimen exposure and test conditions covered in these tests, the 8-1-1 duplex-annealed titanium specimens showed marked superiority for supersonic transport airframe applications over the other materials tested. The ratings of the material-specimen geometry combinations based on the figures are presented in Table 5, Page 27.

To supplement the fatigue test evaluations of the materials, static tensile tests of plain and fusion-welded specimens were made for the same set of exposure conditions and test temperatures. The envelopes of the data are presented in Figures 10 through 13. These envelopes indicate that stressed exposure had the largest effect on the static strength properties of PH14-8Mo specimens and the least effect on those of Inco 718. In general, the effects of exposure on static strength properties do not correlate with the effects on fatigue test data.

Based on the lower boundaries of the envelopes, the ultimate strength to density ratios for both plain and fusion-welded specimens and the elongations of the plain specimens rate the materials for all test temperatures in the order, 8-1-1 titanium, PH14-8Mo and Inco 718. On the basis of the yield strength to density ratio for plain specimens tested at room temperature the rating is the same. However, for tests at 650°F these ratings would be reversed; and for tests at 400°F the rating is PH14-8Mo, 8-1-1 titanium and Inco 718.

Additional comparative evaluations of the materials were provided by tests in which direct integrations of the effects of flight-by-flight sequences of loading are made by the test specimens. Exploratory tests were carried out at room temperature and at a constant temperature of 550°F before testing with thermal cycles was undertaken. The thermal cycles were applied in minimum times with a maximum temperature of 550°F. In these tests the magnitudes and sequences of loading were conservatively tailored to those anticipated at a beam cap in the wing root region of a supersonic transport. The results obtained for center-notched specimens and specimens with single spotwelds are presented graphically in Figures 14 and 15. The data for center-notched specimens lead to the simpler, more clearly defined, rating of 8-1-1 titanium, Inco 718 and PH14-8Mo in that order. For specimens with single spotwelds, the data show that, in 8-1-1 titanium, shorter test lives were obtained than those for center-notched specimens. The data for the single spotweld specimens in both of the other materials show much longer test lives than those for the notched specimens. In a few preliminary tests of fusion welded specimens, the data for all materials in this type of test indicate very long potential service lives.

The tests with flight-by-flight sequences of loadings and thermal cycles supply in relatively short test times the most directly applicable rating of

materials for an important class of applications in airframes. However, such tests cannot reflect the possible effects of long-term intermittent exposure to elevated temperature acting in conjunction with flight-by-flight sequences of loading. To provide data on this aspect of the fatigue evaluation of the test materials, tests have been started in which the specimens are exposed to 500°F for approximately one hour during the cruise phase of each test "flight." In these tests the loading magnitudes and sequences are the same as those used in the tests described above in which the thermal cycle was applied in the minimum practical time. These "real time" tests will provide a more informative evaluation of material stability than can be provided by S-N type testing after exposure to constant load and temperature.

Continuation of these long-term tests beyond the period of the current program has been proposed.

To provide data on the effects of quite different loading sequences occurring in airframes, specimens were subjected to simultaneous application of loading and heating cycles to simulate the effect in fuselage skins of the cycle of pressurization loading and aerodynamic heating which occurs each flight. Specimens without prior exposure and specimens with prior exposure to moderate load for 5000 hours at 650°F were tested. Comparisons of the data with S-N data obtained at constant temperature indicate that such S-N data can be used to conservatively predict the test lives in the more complex tests. The rating of the materials for these tests is therefore the same as the rating presented on the basis of S-N data.

The tests which have been described provide ratings of the materials when they are tested without contaminants. To explore the effects of contaminants, intermittent application of synthetic sea water, MIL-O-7277 mineral oil or Versilube F-50 was made at room temperature during constant load amplitude testing of specimens without prior exposure and also of specimens given intermittent applications of the contaminants during 1000 hour exposure at 550°F. The test results indicated that these exposures had no significant consistent effect when compared with the constant load amplitude test lives for specimens not exposed to contaminants. However, in a limited series of tests in which contaminants were intermittently applied during the application of flight-by-flight loading sequences at a constant temperature of 550°F, more clearly defined effects were obtained. In these tests, the mineral oil was applied to center-notched specimens of each material and salt water was applied to center-notched 8-1-1 titanium specimens. The application of the mineral oil reduced the test lives of the center-notched specimens of Inco 718 and PH14-8Mo by 32 and 17 percent, respectively. The application of the synthetic sea water and the mineral oil had no effect on the test lives for center-notched specimens of 8-1-1 titanium. The test lives are shown in Figure 14.

In static tensile tests at 650°F of plain specimens after the 1000 hour exposure to contaminants at 550°F, small effects were produced by the contaminants. The data for specimens tested with and without contaminant exposure are presented in Figure 16.

9

Metallographic examination at 200X of selected test specimens used in the program indicated that none of the test or exposure conditions including those with contaminants had produced evidence of surface corrosion, intergranular attack or subsurface cracking.

In addition, relatively crude measurements of creep elongations on unnotched rectangular specimens after exposure under moderate load for 5000 hours at 400°F or 650°F were made. The measurements showed essentially zero creep for the 8-1-1 titanium and Inco 718 specimens and very small values for the PH14-8Mo specimens.

Comparisons of the S-N data obtained in this program with data reported by Boeing-North American under contract AF33(657)-11461 showed that shorter test lives were obtained for the transverse, unnotched specimens used in this program than those for the longitudinal specimens tested by Boeing-North American. The agreement between the two sets of S-N data for fusion welded specimens is considered to be good. A comparison between similar sets of static test data for plain and fusion-welded specimens was also in good agreement.
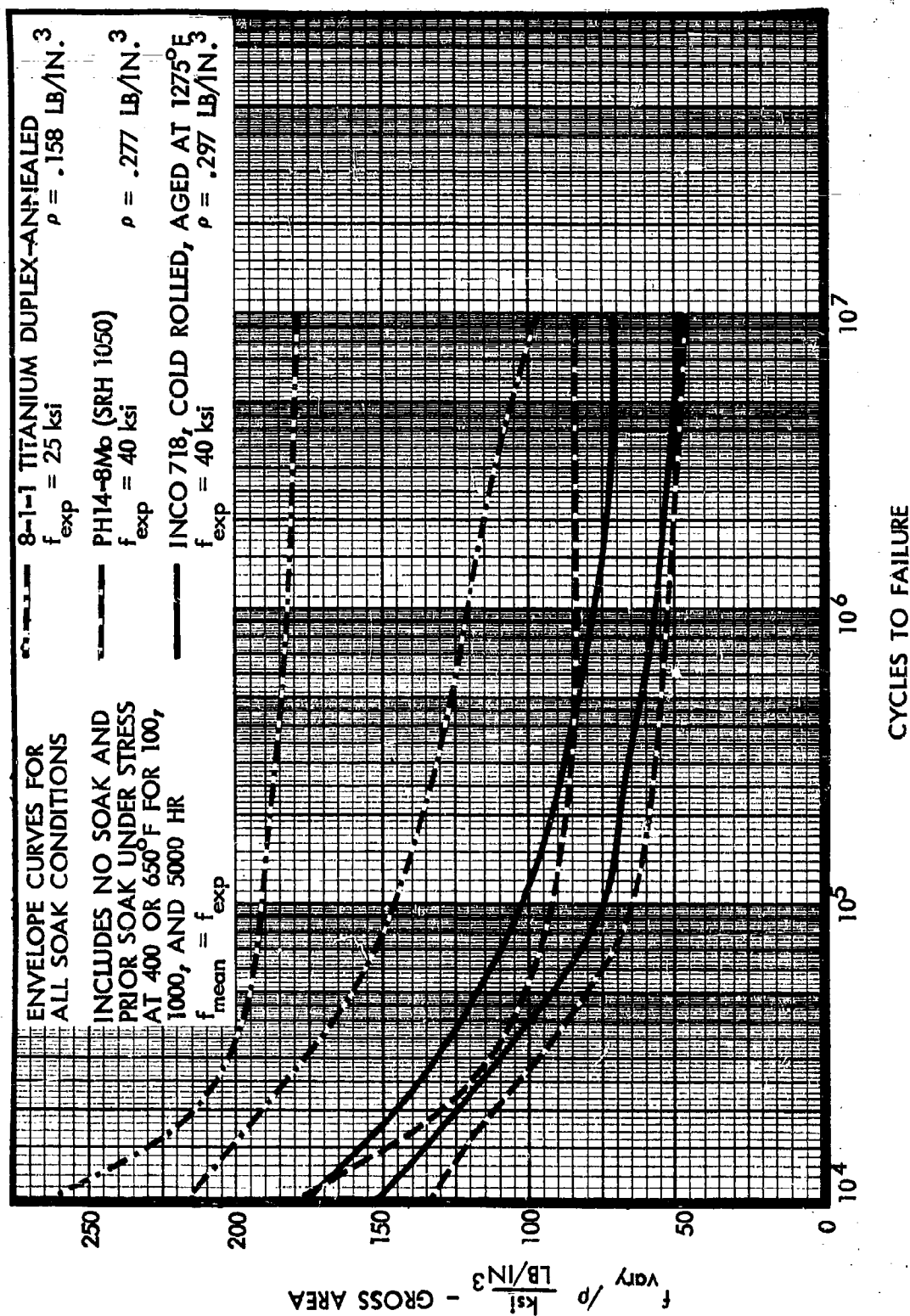
Figure 1. Comparison of S–N Curves at Room Temperature, Center–Notched Specimens, $f_{mean} = f_{exp}$

11
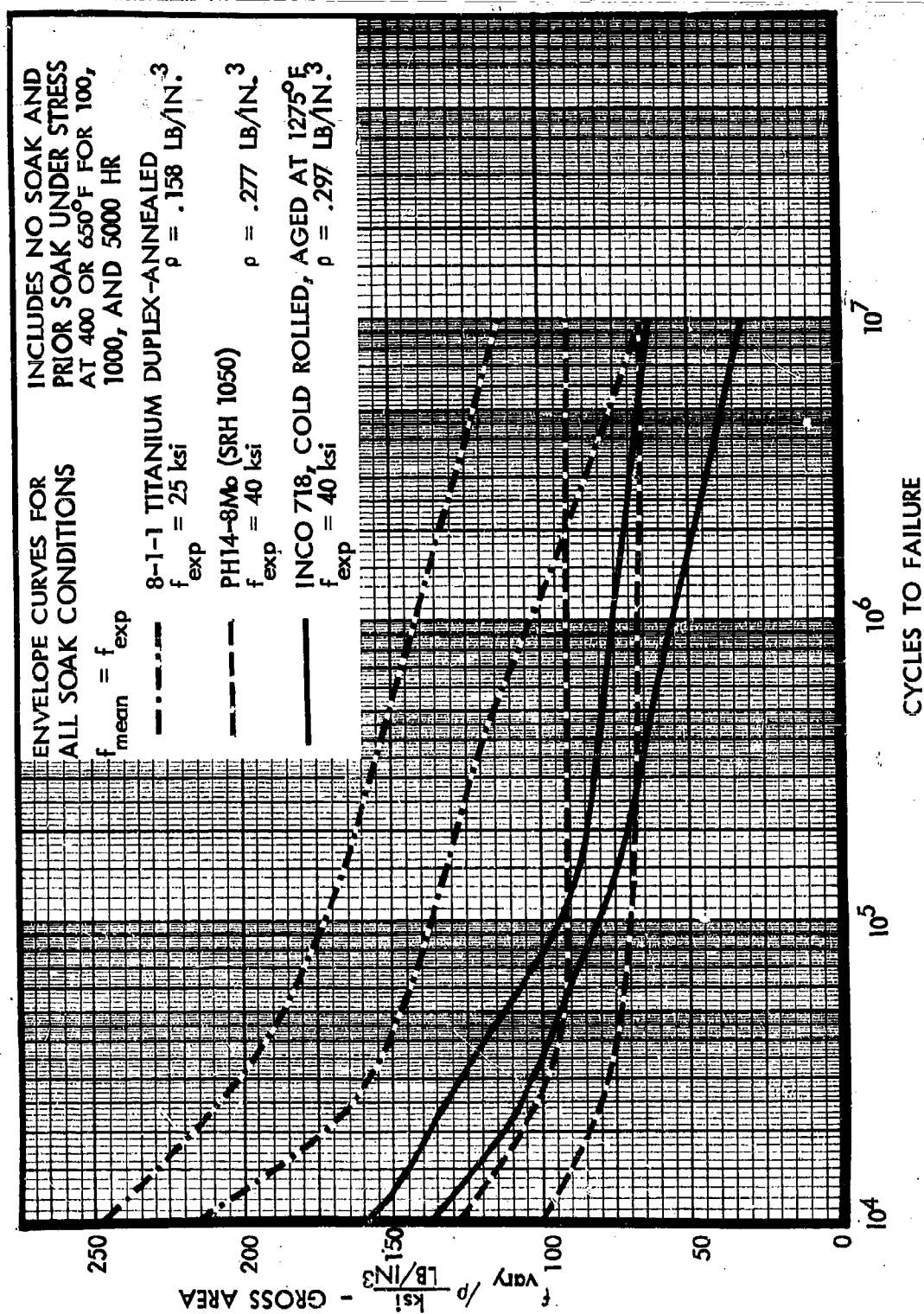
Figure 2. Comparison of S-N Curves at 400°F, Center-Notched Specimens, $f_{mean} = f_{exp}$

12
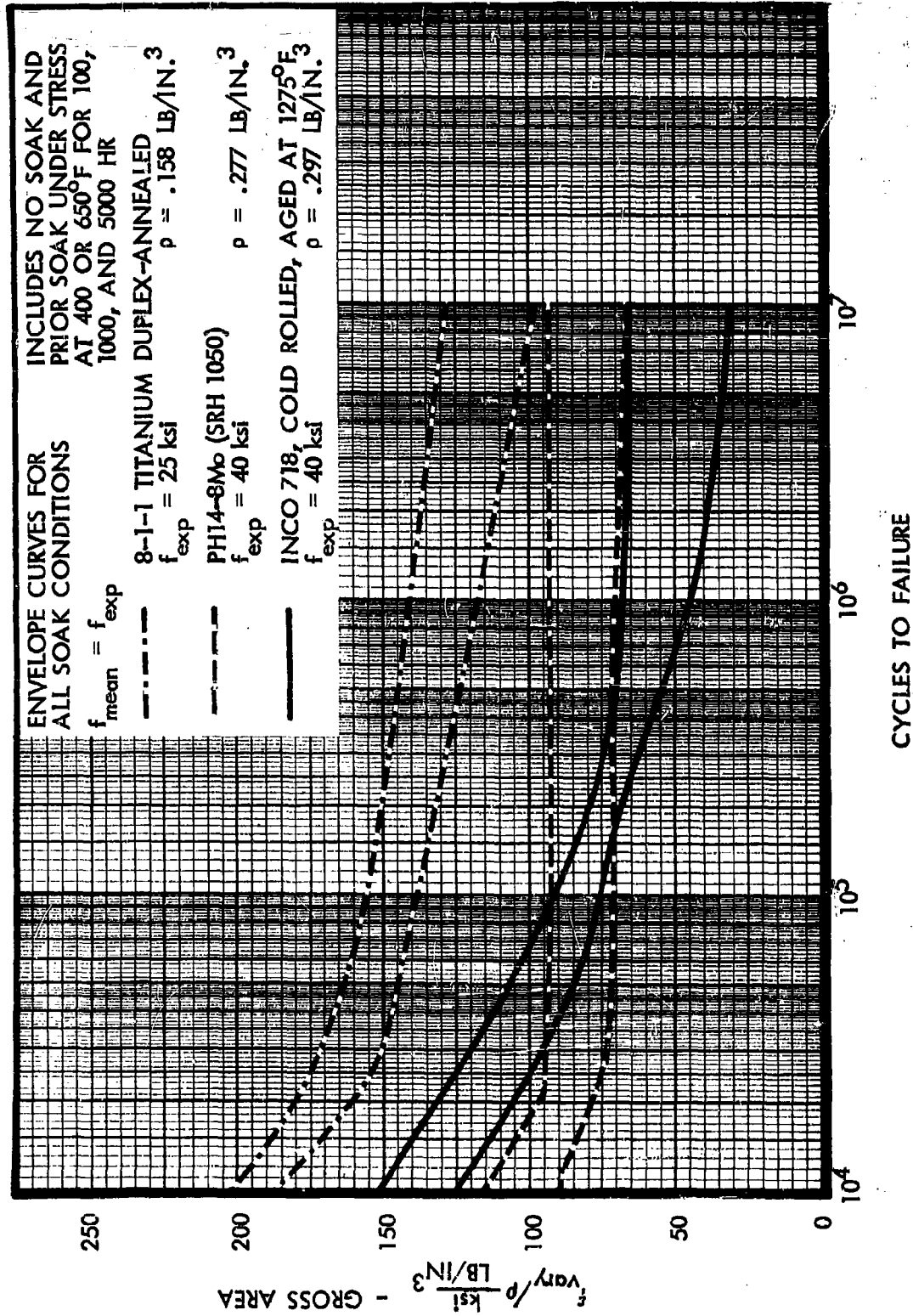
Figure 3. Comparison of S-N Curves at $650°F$, Center-Notched Specimens, $f_{mean} = f_{exp}$

ENVELOPE CURVES FOR
ALL SOAK CONDITIONS

INCLUDES NO SOAK AND
PRIOR SOAK UNDER STRESS
AT 400 OR $650°F$ FOR 100,
1000, AND 5000 HR

$f_{mean} = f_{exp}$

8-1-1 TITANIUM DUPLEX-ANNEALED
$f_{exp} = 25$ ksi $\rho = .158$ LB/IN.^{3}

PH14-8Mo (SRH 1050)
$f_{exp} = 40$ ksi $\rho = .277$ LB/IN.^{3}

INCO 718, COLD ROLLED, AGED AT $1275°F$
$f_{exp} = 40$ ksi $\rho = .297$ LB/IN.^{3}

CYCLES TO FAILURE

$\frac{f_{vary}/\rho}{\frac{ksi}{LB/IN^3}}$ - GROSS AREA

13

ENVELOPE CURVES FOR ALL SOAK CONDITIONS

$f_{mean} = f_{exp}$

INCLUDES NO SOAK AND PRIOR SOAK UNDER STRESS AT 400 OR 650°F FOR 100, 1000, AND 5000 HR

- — ·· — · 8-1-1 TITANIUM DUPLEX-ANNEALED
  $f_{exp} = 25$ ksi $\rho = .158$ LB/IN.^{3}

- — — PH14-8Mo (SRH 1050)
  $f_{exp} = 40$ ksi $\rho = .277$ LB/IN.^{3}

- ——— INCO 718, COLD ROLLED, AGED AT 1275°F,
  $f_{exp} = 40$ ksi $\rho = .297$ LB/IN.^{3}

CYCLES TO FAILURE

$f_{vary} / \rho \quad \dfrac{ksi}{LB/IN^3}$

Figure 4. Comparison of S-N Curves at Room Temperature, Unnotched Specimens, $f_{mean} = f_{exp}$

14
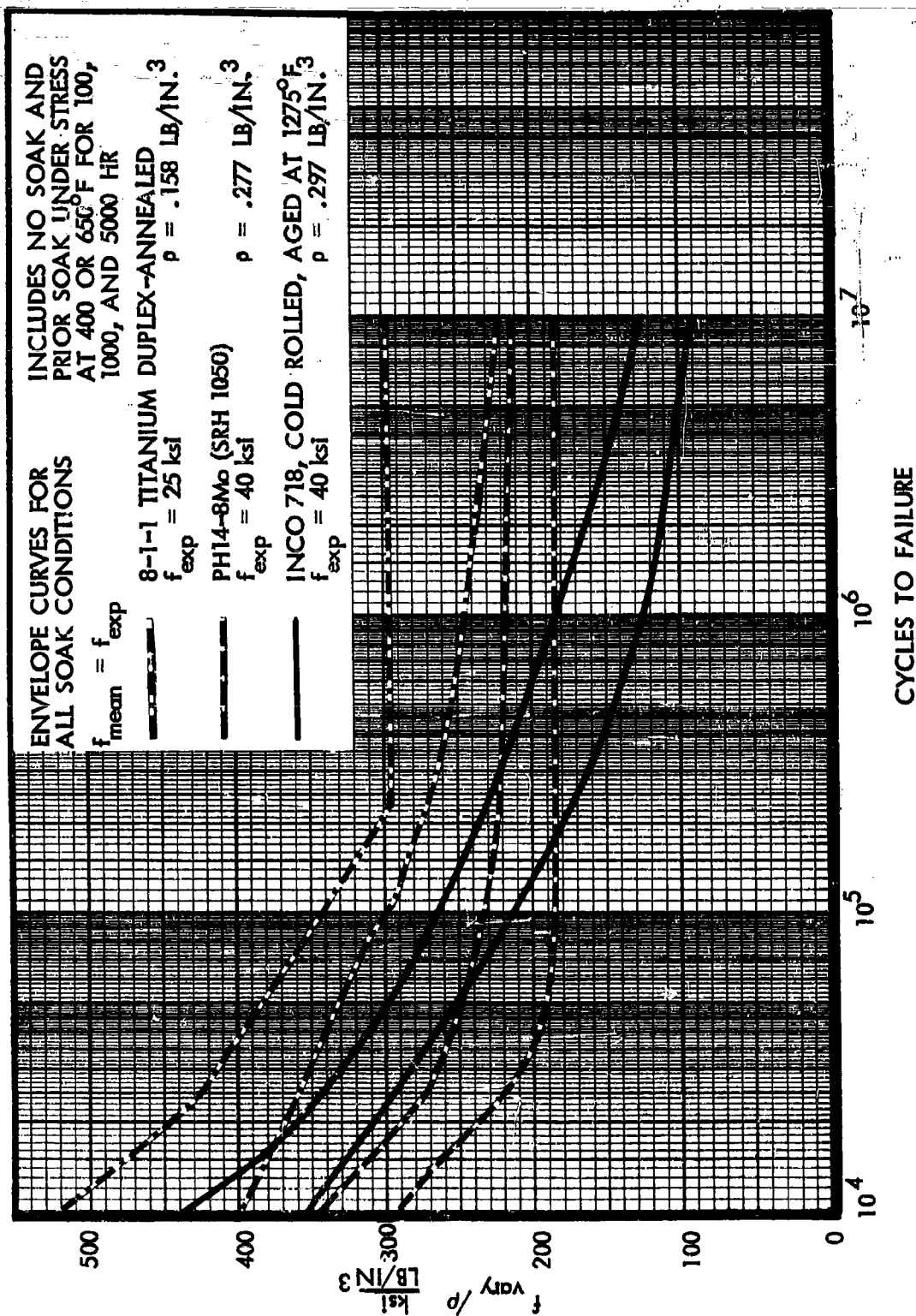
Figure 5. Comparison of S-N Curves at 400°F, Unnotched Specimens, $f_{mean} = f_{exp}$

ENVELOPE CURVES FOR
ALL SOAK CONDITIONS

INCLUDES NO SOAK AND
PRIOR SOAK UNDER STRESS
AT 400 OR 650°F FOR 100,
1000, AND 5000 HR

$f_{mean} = f_{exp}$

8-1-1 TITANIUM DUPLEX-ANNEALED
$f_{exp} = 25$ ksi $\rho = .158$ LB/IN.^{3}

PH14-8Mo (SRH 1050)
$f_{exp} = 40$ ksi $\rho = .277$ LB/IN.^{3}

INCO 718, COLD ROLLED, AGED AT 1275°F
$f_{exp} = 40$ ksi $\rho = .297$ LB/IN.^{3}

CYCLES TO FAILURE

$\frac{f_{vary}}{\rho}$ $\frac{ksi}{LB/IN3}$

15
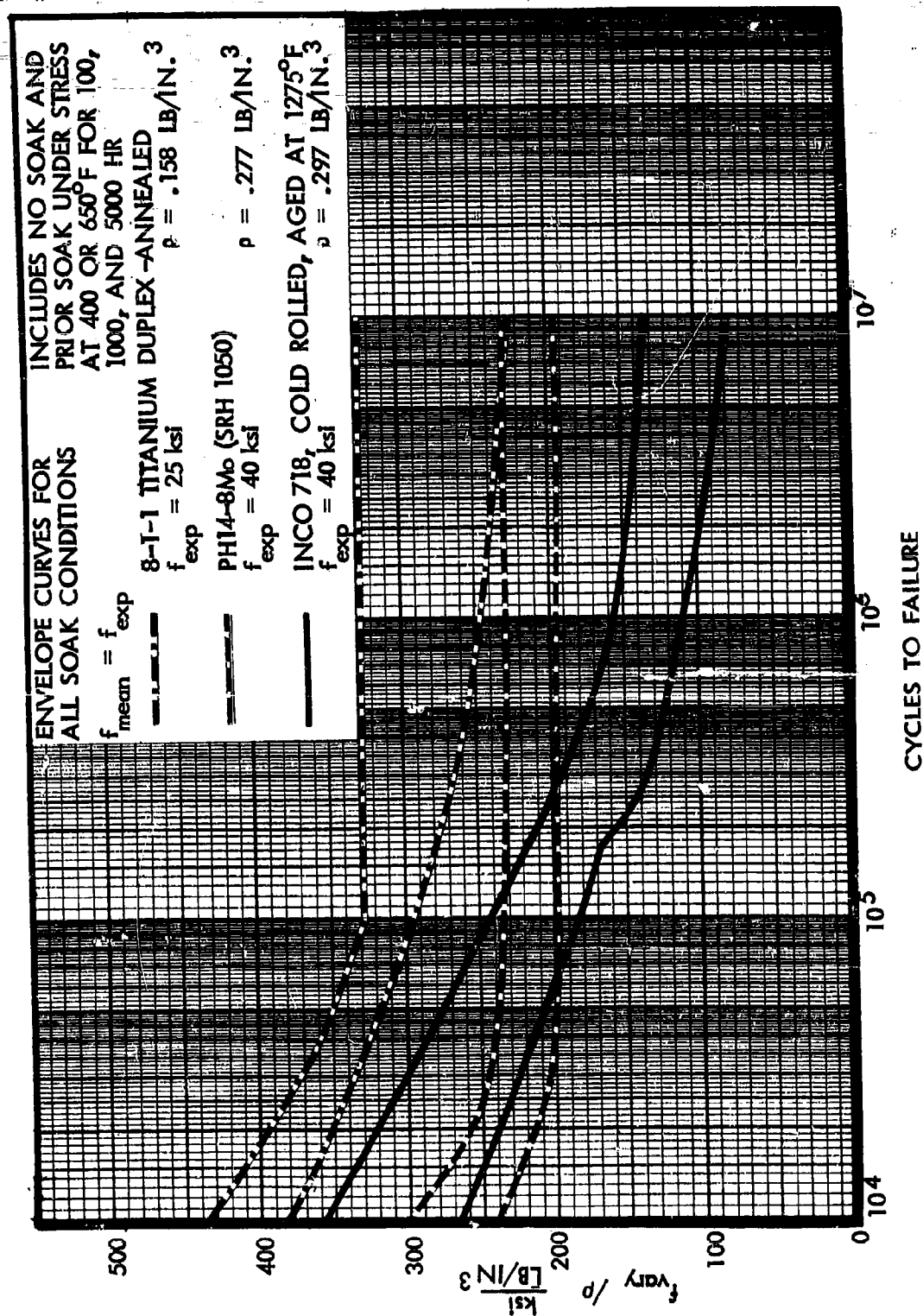
Figure 6. Comparison of S-N Curves at 650°F, Unnotched Specimens, $f_{mean} = f_{exp}$

16
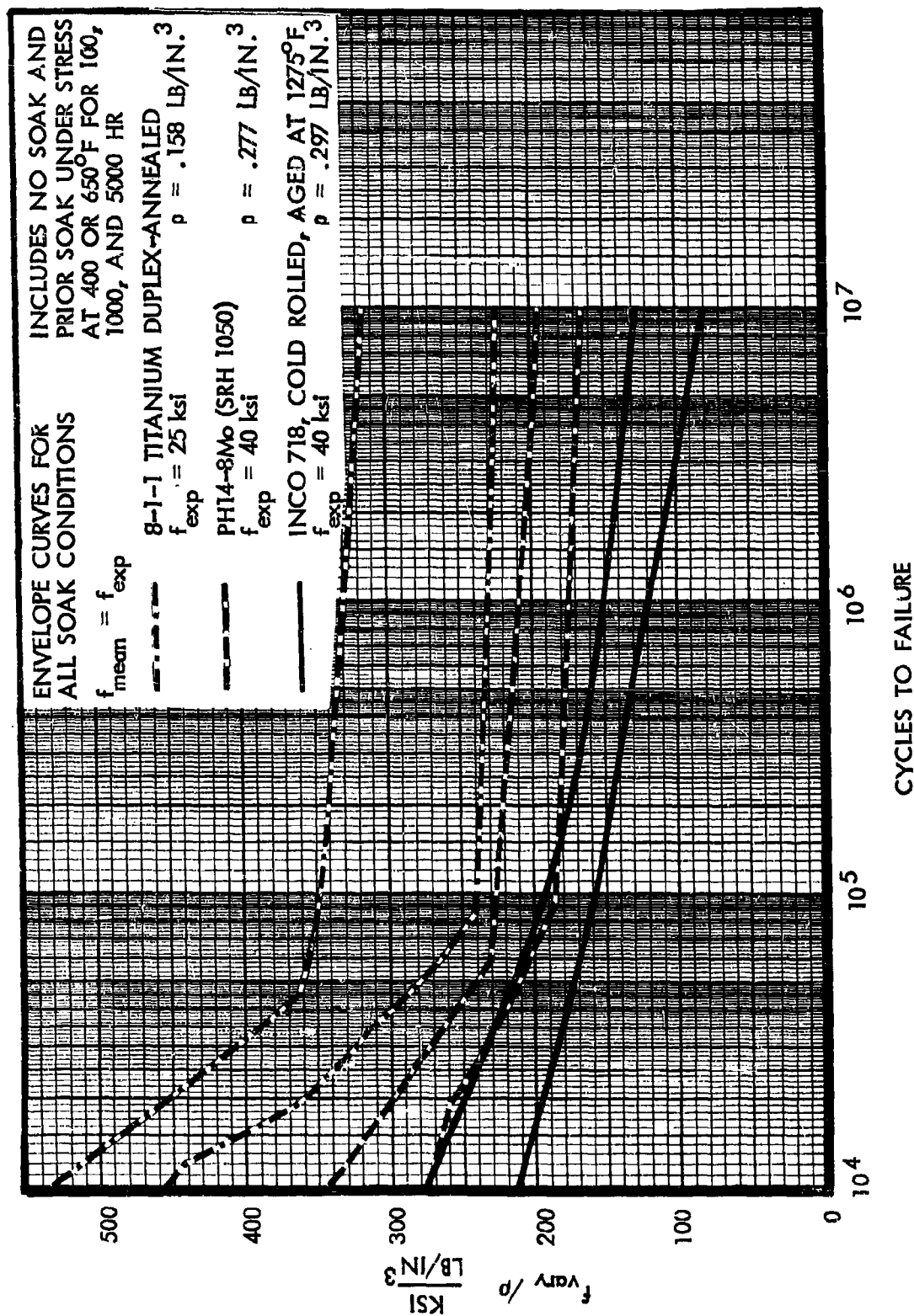
Figure 7. Comparison of S-N Curves at Room Temperature, Fusion-Welded Specimens, $f_{mean} = f_{exp}$

17
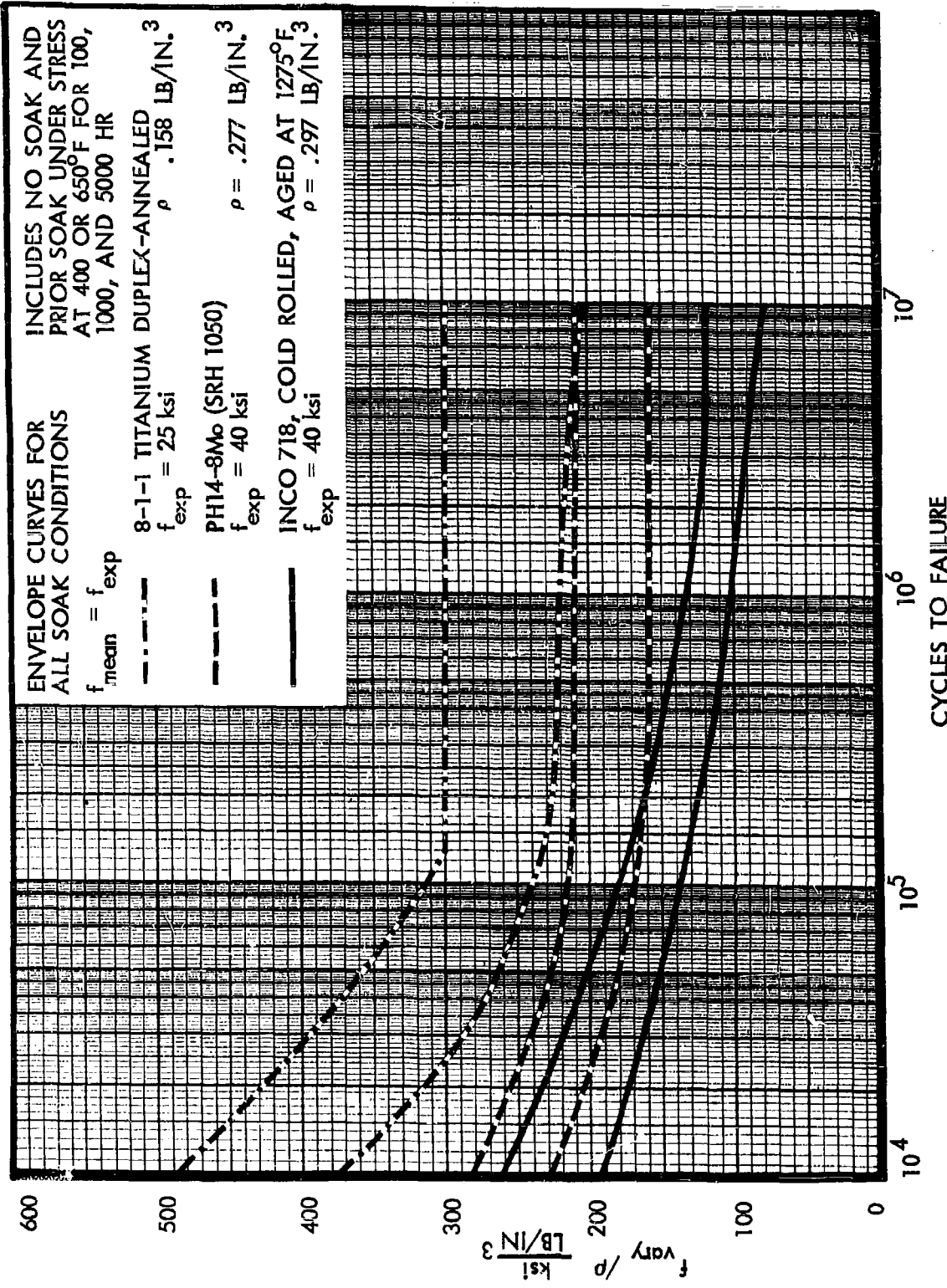
Figure 8. Comparison of S-N Curves at 400°F, Fusion-Welded Specimens, $f_{mean} = f_{exp}$
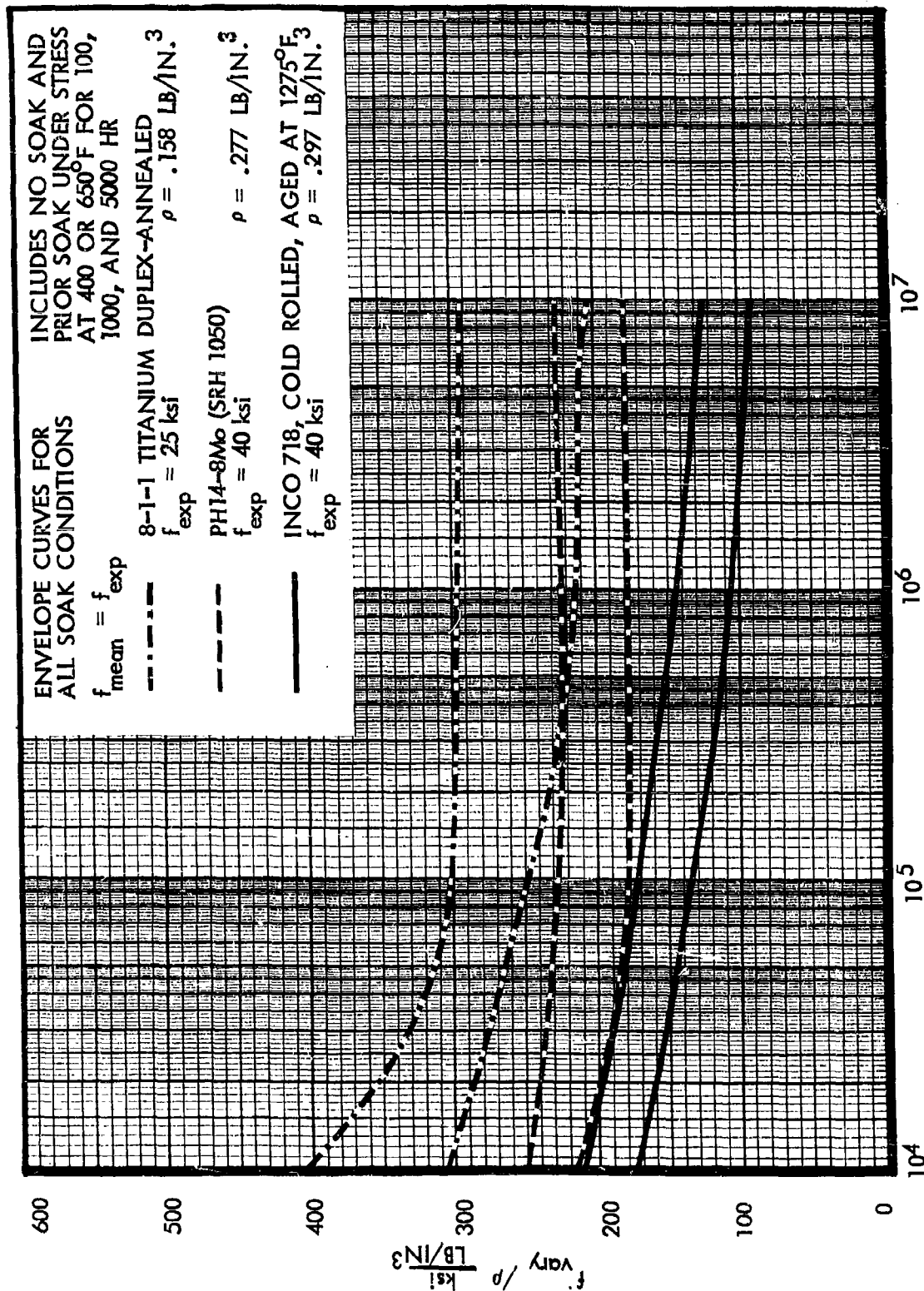
Figure 9. Comparison of S–N Curves at 650°F, Fusion-Welded Specimens, $f_{mean} = f_{exp}$
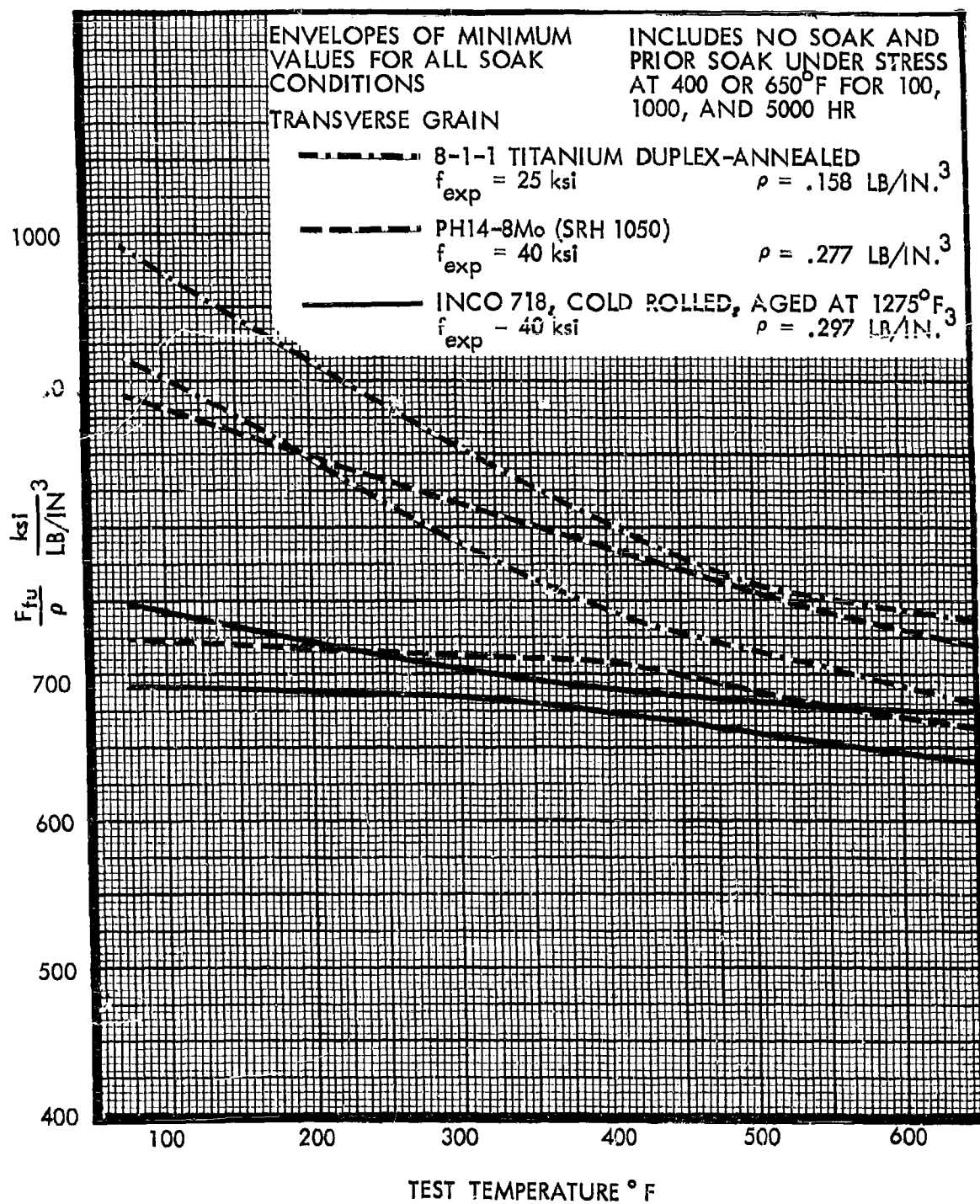
Figure 10. Ultimate Tensile Strength to Density Ratio versus Test Temperature, Plain Specimens

ENVELOPES OF MINIMUM VALUES FOR ALL SOAK CONDITIONS

INCLUDES NO SOAK AND PRIOR SOAK UNDER STRESS AT 400 OR 650°F FOR 100, 1000, AND 5000 HR

TRANSVERSE GRAIN

— · — · — · 8-1-1 TITANIUM DUPLEX-ANNEALED
f_{exp} = 25 ksi ρ = .158 LB/IN.^{3}

— — — — PH14-8Mo (SRH 1050)
f_{exp} = 40 ksi ρ = .277 LB/IN.^{3}

———— INCO 718, COLD ROLLED, AGED AT 1275°F
f_{exp} = 40 ksi ρ = .297 LB/IN.^{3}
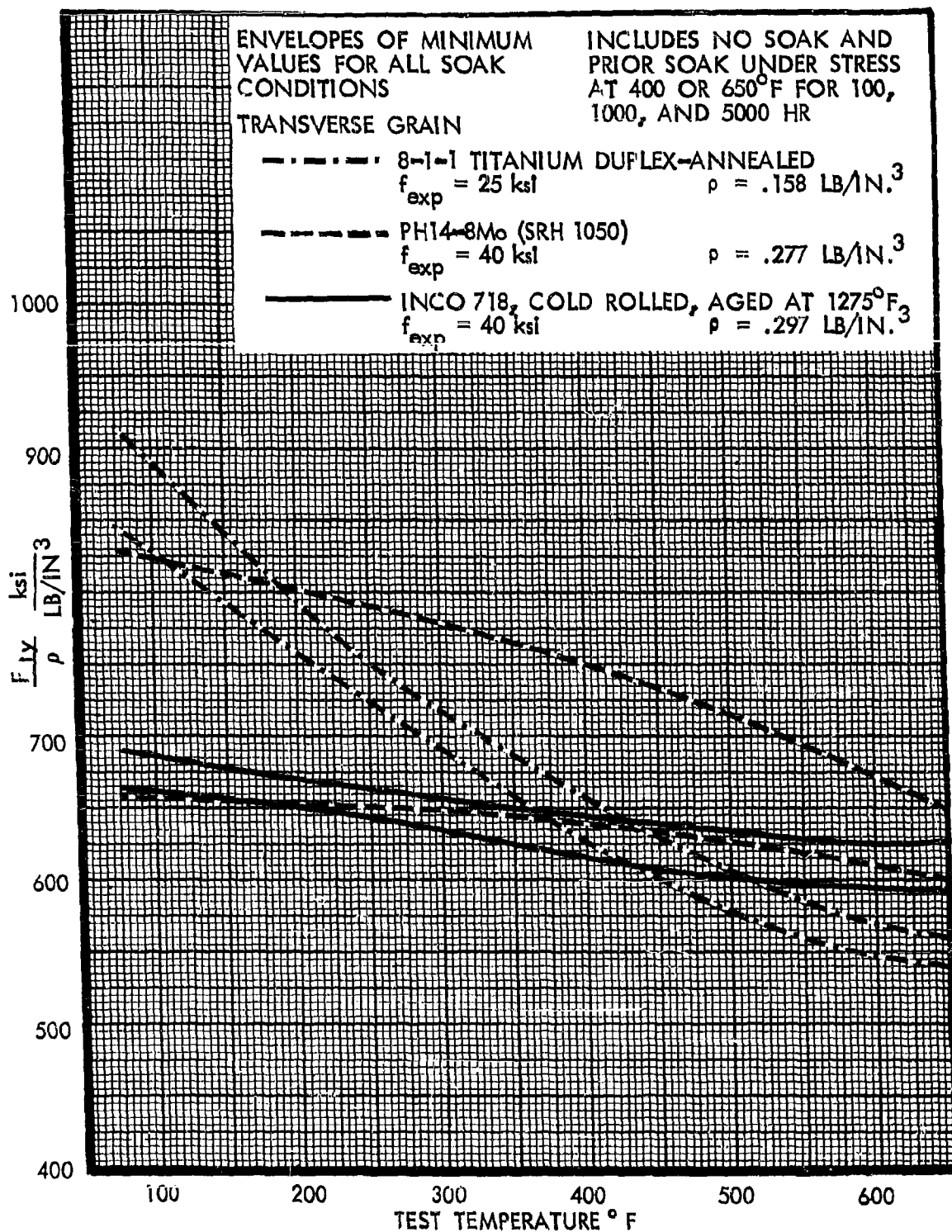
Figure 11. Yield Strength to Density Ratio versus Test Temperature, Plain Specimens

21
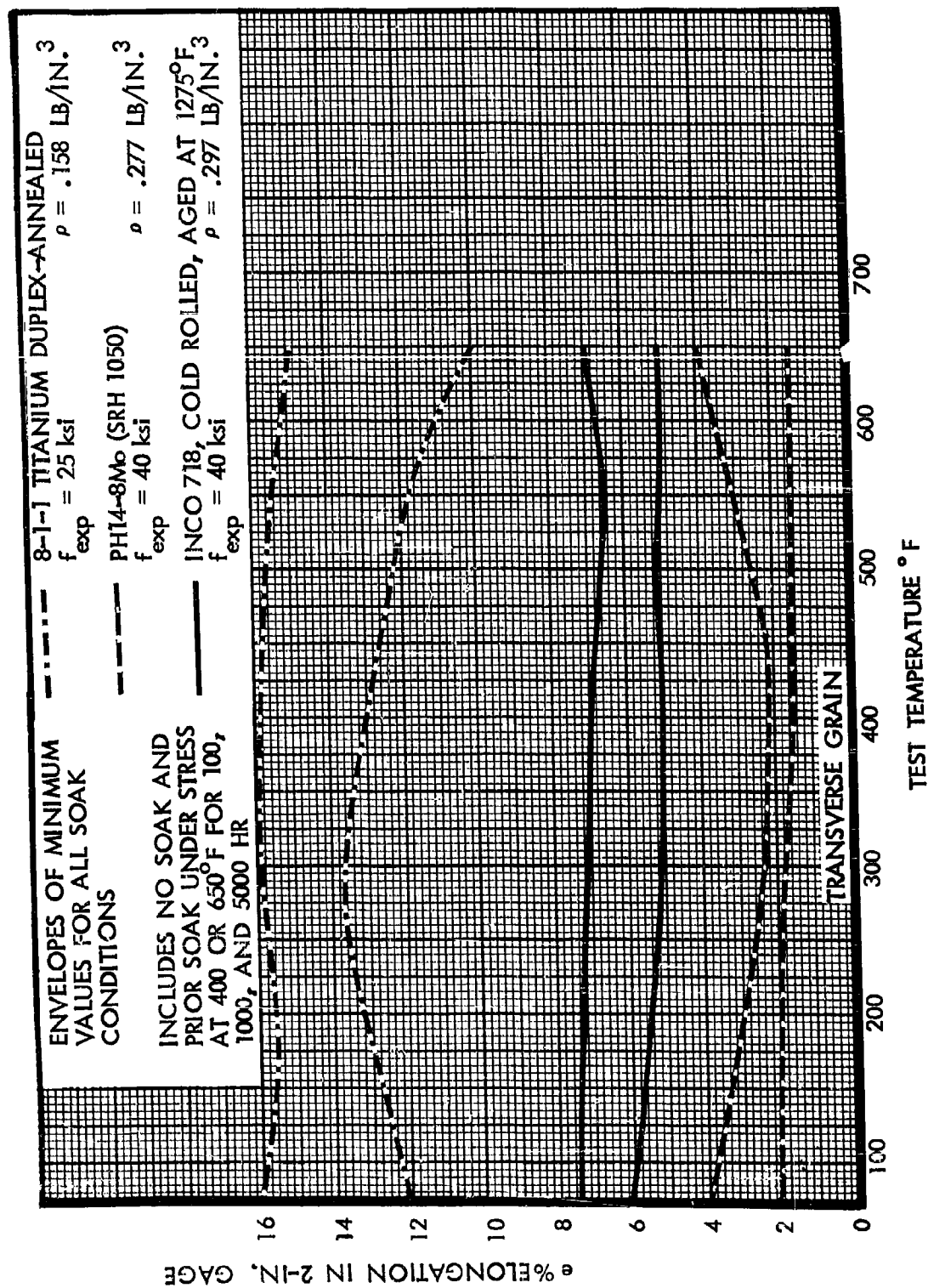
Figure 12.   Elongation versus Test Temperature, Plain Specimens

22
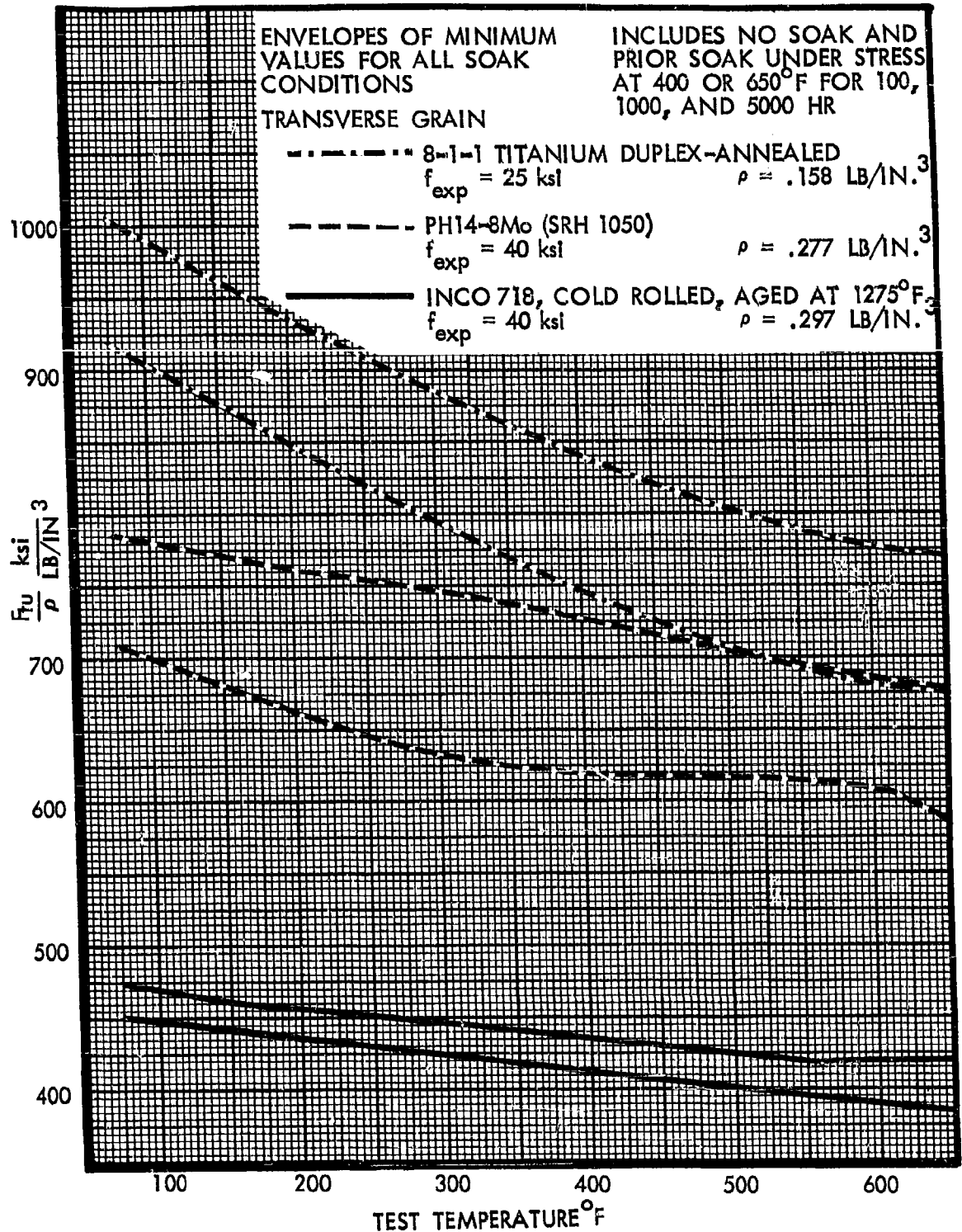
Figure 13. Ultimate Tensile Strength to Density Ratio versus Test Temperature, Fusion-Welded Specimens

23

NUMBER OF FLIGHTS

NO. OF SPECIMENS	8	4	4	4	4	4	4	2	2	2	2	4	3	4
MATERIAL *	8-1-1 Ti	PH14-8Mo	INCO 718	8-1-1 Ti	PH14-8Mo	INCO 718	8-1-1 Ti	8-1-1 Ti	PH14-8Mo	INCO 718	8-1-1 Ti	PH14-8Mo	8-1-1 Ti	INCO 718
CONTAMINANT APPLIED DURING TEST	NONE			NONE			SALT WATER	MIL-O-7277 OIL				NONE		
TEST TEMPERATURE	ROOM TEMP			550°F								90 TO 550° F		
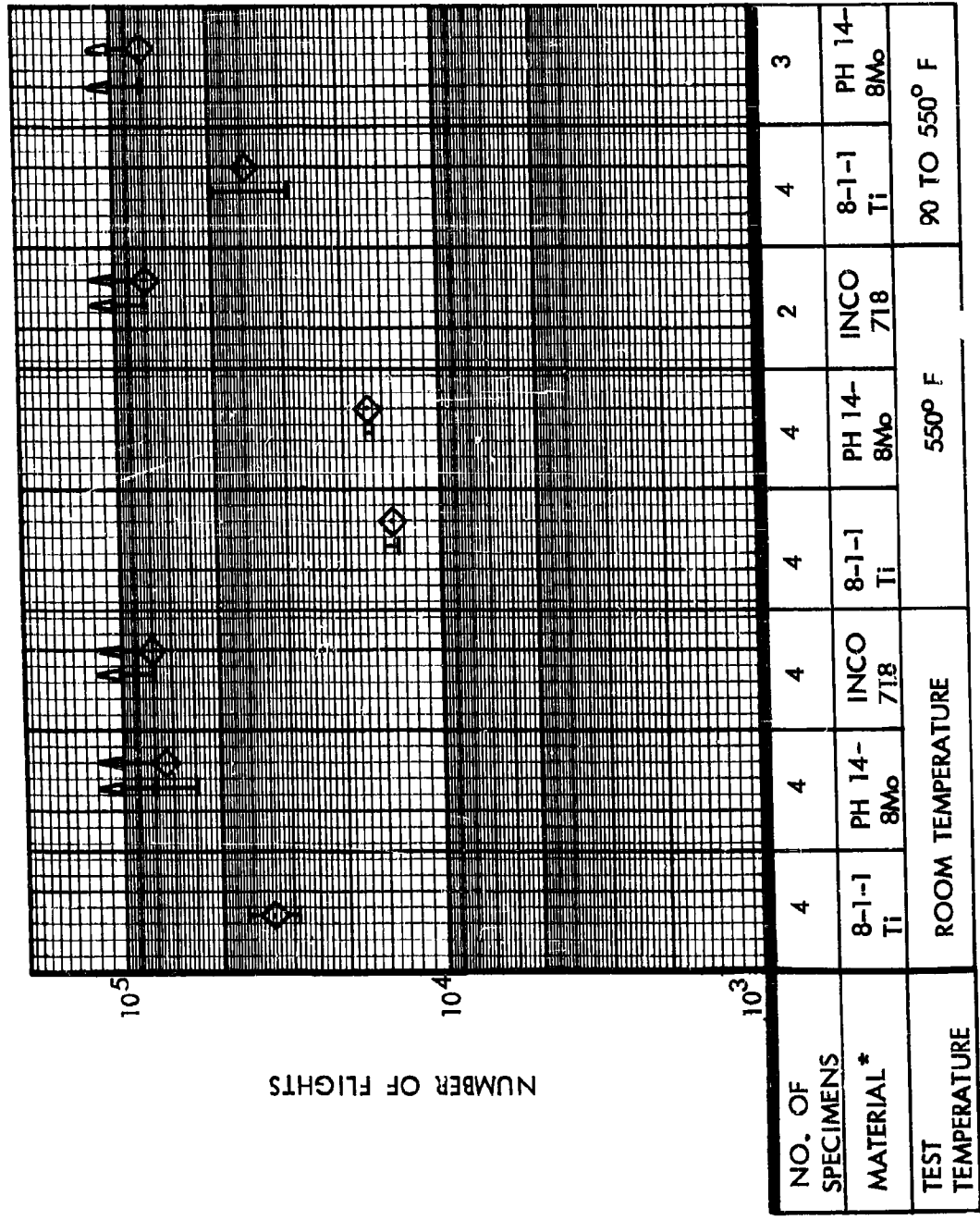
* NO PRIOR SOAK

I SCATTERBAND
◇ AVERAGE TEST LIFE

Figure 14. Comparison of Accelerated Flight-by-Flight Test Results for Spectra C, Center-Notched Specimens

24

Figure 15. Comparison of Accelerated Flight-by-Flight Test Results for Spectra C, Spotwelded Specimens

Figure 16. Effects of Prior Soak with Contaminants on Static Tensile Properties
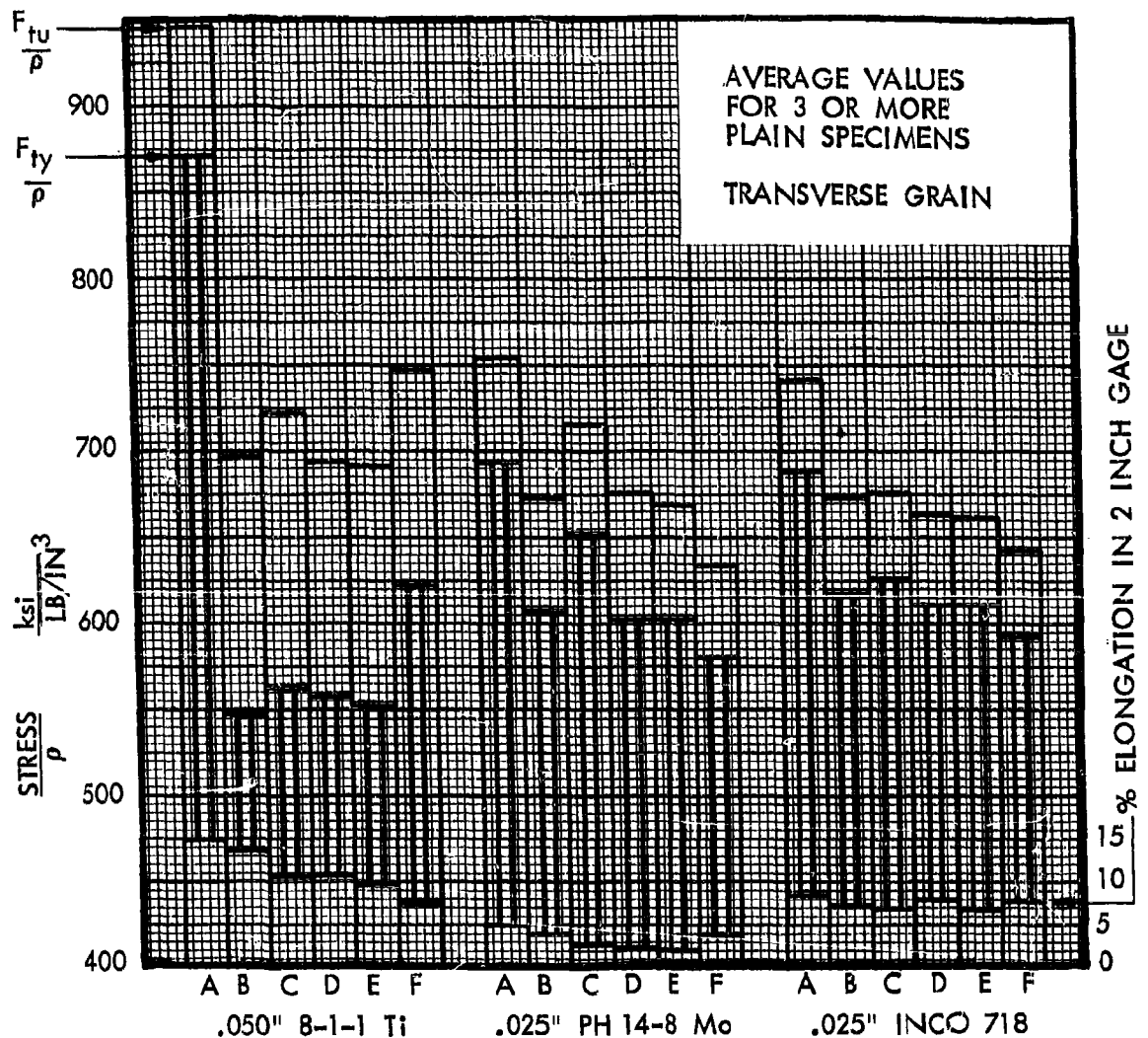
A. Test at R.T., No Prior Soak — No Contaminant

B. Test at 650°F, No Prior Soak — No Contaminant

C. Test at 650°F, Prior Soak at f_{exp} and 650°F for 1000 hr — No Contaminant

D. Test at 650°F, Prior Soak with f_{exp} and Salt Water at 550°F for 1000 hr

E. Test at 650°F, Prior Soak with f_{exp} and MIL-O-7277 Oil at 550°F for 1000 hr

F. Test at 650°F, Prior Soak with f_{exp} and Versilube F-50 at 550°F for 1000 hr

f_{exp} = 25,000 psi for Titanium and 40,000 psi for Steel and Nickel

TABLE 5   RATING OF MATERIALS BASED ON S-N DATA

	RATING	TYPE OF SPECIMEN		
		CENTER NOTCHED	UNNOTCHED	FUSION-WELDED & PLANISHED
HIGH STRESS[1] LOW CYCLE RANGE	1 2 3	8-1-1 TITANIUM INCO 718 PH 14-8Mo	8-1-1 TITANIUM INCO 718 PH 14-8Mo	8-1-1 TITANIUM PH 14-8Mo INCO 718
LOW STRESS[2] HIGH CYCLE RANGE	1 2 3	8-1-1 TITANIUM PH 14-8Mo INCO 718	8-1-1 TITANIUM PH 14-8Mo INCO 718	8-1-1 TITANIUM PH 14-8Mo INCO 718

(1) $N \lesssim 2 \times 10^5$ CYCLES
(2) $N \gtrsim 2 \times 10^5$ CYCLES

SECTION 3

MATERIALS

The sheet materials selected for evaluation and the quantities received are shown below.

MATERIAL	CONDITION AS RECEIVED	SHEET SIZE	NO. OF SHEETS	HEAT NUMBER
8-1-1 Titanium	Dup.-Annealed	.050 x 36 x 96	10	D 4539
PH14-8Mo Steel	Sol.-Annealed	.025 x 44 x 96	8	33347
INCO 718	20% Cold Rolled	.025 x 24 x 72	20	6905-FV

The available data on the processing of the materials before delivery are presented in Table 6.

To provide a preliminary evaluation of these materials, static tensile tests were made shortly after the sheets of materials were received. In these tests, one longitudinal and one transverse plain tensile test specimen was cut from each sheet, heat treated if required, and tested at room temperature. The material properties obtained during these tests are reported in Volume II. Adequate material quality was demonstrated in these tests as shown below by the average values of the static strength properties.

MATERIAL	NO. OF SPECIMENS	LONGITUDINAL GRAIN			TRANSVERSE GRAIN			ρ
		F_{tu} (ksi)	F_{ty} (ksi)	e*	F_{tu} (ksi)	F_{ty} (ksi)	e*	LB/IN^3
8-1-1 Titanium	10	147.2	135.6	14.4	149.4	135.7	14.9	.158
PH14-8Mo Steel	8	203.6	184.8	6.2	209.0	191.2	5.0	.277
INCO 718	20	222.0	209.8	9.2	219.9	204.3	8.3	.297

* Elongation in 2 inches

TABLE 6   PROCESSING TECHNIQUES REPORTED BY MANUFACTURER

STEP	MATERIAL/MANUFACTURER		
	8-1-1 TITANIUM TITANIUM METALS CORPORATION OF AMERICA	PH14-8Mo ARMCO STEEL CORPORATION	INCO 718 HUNTINGTON ALLOYS PRODUCT DIVISION OF INTERNATIONAL NICKEL
1.	Ingot hot forged until 19 inches square.	Melted in electric arc air furnace	Vacuum melted ingot.
2.	Ingot reheated.	Casted into 20 to 21 inch thick ingot.	Ingot hot rolled into semi-finished rectangular bloom.
3.	Ingot hot forged until 15 inches square	Ingot hot rolled to 4 to 5 inches thick bar.	Bloom hot rolled into bar.
4.	Ingot ground and forged to 7 x 11 in.	Bar rolled to .18 in. thick sheet.	Bar cut into sections.
5.	Ingot ground and forged to 2-7/8 in. x 12 in. bar.	Sheet annealed and pickled.	Sections are hot cross rolled.
6.	Bar given ultra-sonic test.	Sheet cold rolled to .100 in. thickness.	Sections cold rolled to oversize sheet.
7.	Bar ground and cut to length.	Sheet annealed and pickled.	Sheet annealed.
8.	Bar pickled and rolled to .050 in. sheet	Sheet cold rolled to .050 in. thickness.	Sheet pickled.
9.	Sheet annealed and descaled.	Sheet annealed and pickled.	Sheet cold rolled 20% to .025 gage.
10.	Sheet annealed and blasted by grit.	Sheet cold rolled to .025 in. thickness.	Sheet leveled.
11.	Sheet pickled and scrubbed for uniform color.	Sheet annealed and pickled.	

30

SECTION 4

TEST SPECIMEN GEOMETRY

Five specimen designs were originally specified. The geometries of these specimens are defined in Figure 17 . All specimens were taken in the transverse grain direction with the exception of one longitudinal grained specimen taken from each sheet and tested as a part of the material inspection procedure. Specimens A and B in the figure were used for static tensile tests. Specimen B includes an aircraft quality butt fusion weld produced by the mechanical tungsten inert gas arc welding method. These specimens make provision for the use of stress-strain curve generating equipment. Specimen C was used extensively in the test program to obtain fatigue test data for unnotched material. Specimen D was employed in the fatigue test evaluation of fusion welded specimens. These four specimens required the matching of contoured edges to produce a test section having substantially smaller cross-sectional area than the ends of the specimens to ensure failure in the test area. Specimen E is a center-notched specimen with a quarter-inch diameter hole. A simple rectangular shape was used for this specimen since experience has shown that the severity of the notch effect provided by the hole ensures fatigue cracking at the hole. The use of a rectangular shape minimizes the cost of specimen preparation and provides the smallest ratio of hole diameter to specimen width. This ratio produces the largest effective stress concentration factor for a given hole diameter and a moderate specimen width. The half-inch holes in the ends of the specimens shown in Figure 17 were used in the mounting of specimens in preconditioning apparatus.

During the course of the program, specimens with doublers attached by multiple- and single-spotwelds were added in the evaluation of the effects of flight-by-flight loading histories. The geometries used are shown in Figure 18. Since preconditioning was not required, holes were omitted at the ends of these specimens.

The details of the preparation of specimens are presented in Appendix I, the development of fixtures to support the specimens under compressive loading is described in Appendix II and the development of a method of attaching thermocouples to specimens subjected to thermal cycling is described in Appendix III.
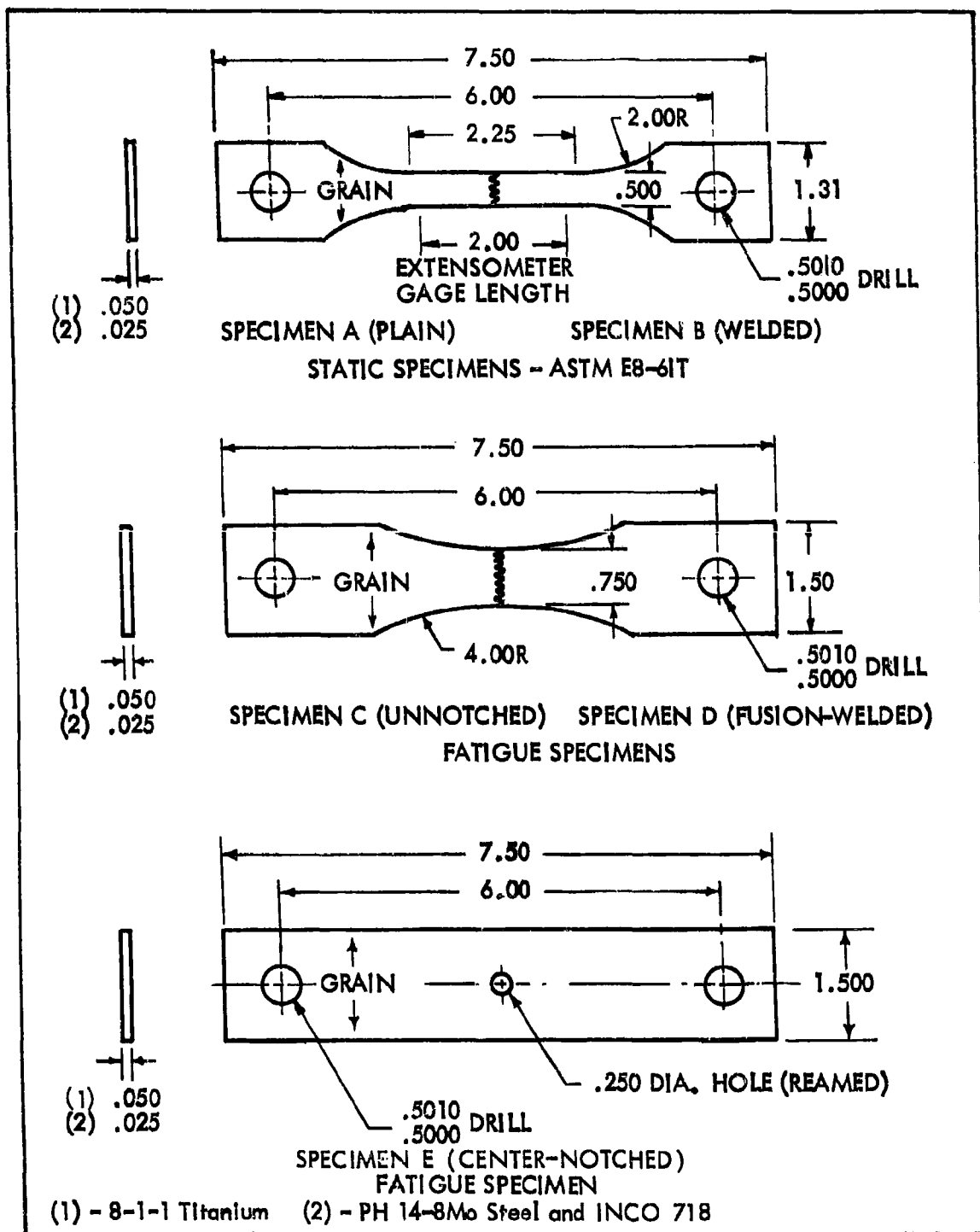
Figure 17. Unnotched, Fusion-Welded and Notched Test Specimens
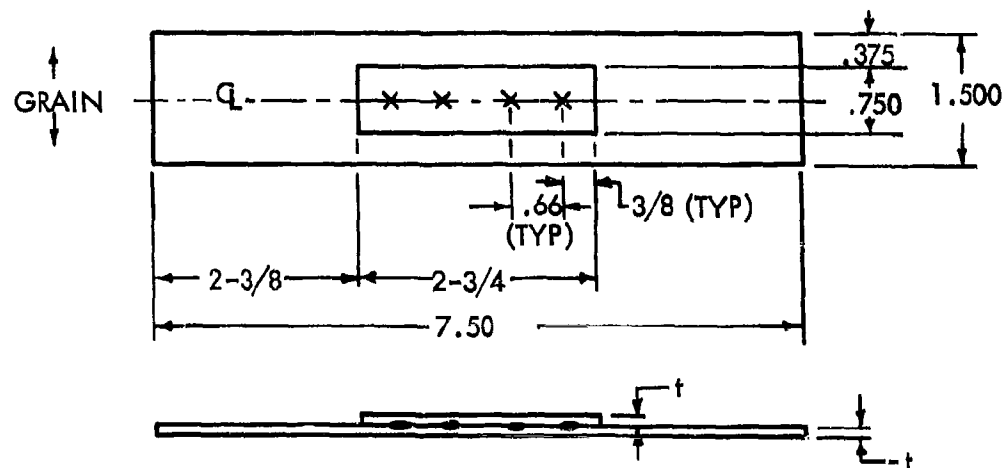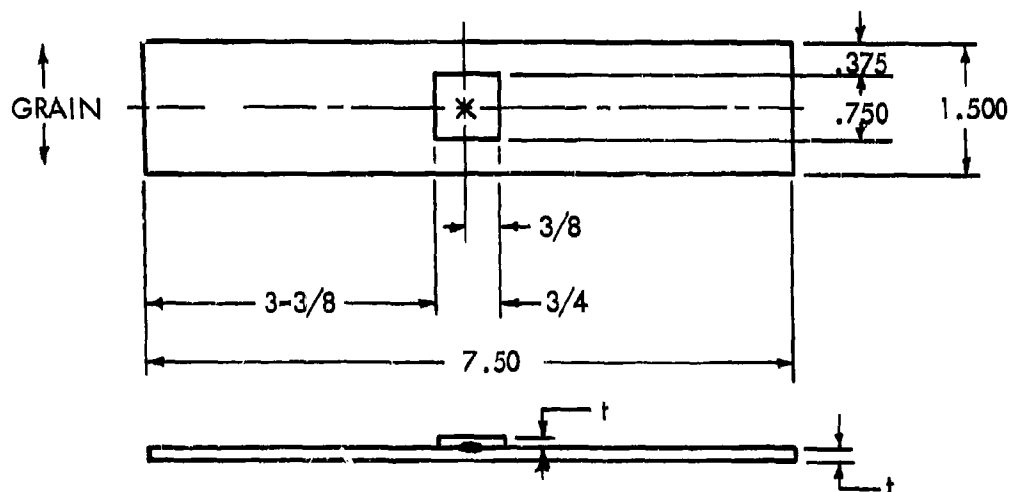
Figure 18. Test Specimens with Spotwelded Doubler

SECTION 5

EVALUATION OF MATERIALS

PHASE I - CONSTANT LOAD AMPLITUDE AND STATIC TENSILE TESTS

A. CONSTANT LOAD AMPLITUDE (S-N) TESTS

Constant load amplitude (S-N) tests of specimens which had not been preconditioned were carried out at room temperature, 400°F and 650°F at constant stress ratios, R (minimum/maximum stress) of 0.1 and - 0.5. To evaluate the effect of prior exposure to load and temperature, additional groups of specimens were preconditioned by steady stressing under axial load at temperature. The nominal gross area tensile stresses during this preconditioning were 40,000 psi for the PH14-8Mo and Inco 718 specimens and 25,000 psi for the 8-1-1 titanium specimens.

Groups of specimens were preconditioned for periods of 100, 1000 or 5000 hours at temperatures of 400 or 650°F in the ovens described in Appendix IV. The specimens were then tested at the R values defined above at room temperature, 400 or 650°F. The test equipment used for these tests is also described in Appendix IV.

The test data are reported in Volume II where they are used to define S-N curves for constant values of R. To define these curves, the test data were first plotted in terms of log stress versus log cycles and straight lines were fitted to the mean values in the high stress-low cycle range of data and also in the low stress-high cycle range. Semi-log representations of these lines were then faired to produce the conventional S-N curves.

A statistical analysis of the test data was not made because the relatively small number of data points for each of the large number of combinations of test variables did not permit the definition of statistically significant results with a reasonable degree of confidence. A discussion of this aspect of the definition of S-N curves is presented in Appendix V.

The S-N curves for constant values of R provide the most direct representations of the test data. Because of this, they were grouped by material and specimen geometry to show graphically the effects of differing exposure temperatures and times. This grouping which is presented in Appendix VI reduces the number of data plots from 189 to 54. However, uniform trends are not shown for any one set of curves. Under these conditions, detailed evaluations of test condition effects and comparisons of materials and specimen geometries pose very real difficulties. To provide for a reduction in the number of graphs to be examined and to provide more directly informative comparisons for use by airframe design personnel, curves were drawn for constant values of mean stress.

To provide a basis for drawing S-N curves for constant mean stresses, S-N diagrams were derived from the constant R curves. These diagrams are presented in Volume II. From these diagrams, S-N curves for a mean tensile stress of 25,000 psi were developed for the 8-1-1 titanium specimens and curves for a mean tensile stress of 40,000 psi were developed for the PH14-8Mo and Inco 718 specimens. These mean stresses are approximately proportional to the material strengths and are considered to represent first approximations to design steady flight stresses in SST wing root material at maximum aircraft weight.

The 27 groupings of such curves required to show the effects of test variables on each material and specimen geometry are presented in Appendix VII. Again, as in the case of the constant R curves, marked and non-uniform variations in the response of the nine combinations of material and specimen geometry to the twenty one different combinations of test temperature and exposure conditions lead to undue difficulty in detailed evaluation of the data when it is presented in this form. For this reason, another form of presentation was selected for data evaluation.

For compactness in presentation, the data for each material-specimen geometry combination are presented on one graph. Each graph shows the percent changes in cyclic stress for a preselected test life as a function of test temperature, prior exposure temperature and exposure time. Since the S-N curves for each material-specimen geometry combination are not parallel, an evaluation at a single number of cycles to failure could be misleading. For this reason, data are shown for test lives of both 10^4 and 10^7 cycles. The set of such graphs is presented in Figures 19 through 27.

In the use of these graphs it must be remembered that the data represent the results obtained with a very small number of specimens for each test condition and that the specimens for each material represent one sheet thickness produced from one heat. Extrapolation of the data to longer exposure times is not warranted.

With these reservations, an examination of the graphs leads to the following comments.

The data for the center-notched 8-1-1 titanium specimens presented in Figure 19 show some increases in varying stress after exposure for 1000 hours but for all exposure and test conditions, the stresses at both N = 10^4 and N = 10^7 cycles after exposure for 5000 hours are lower than those for the 1000 hour exposure. The largest changes are shown for N = 10^7 cycles.

In view of the limited data and the general difficulty in the definition of stresses for 10^7 cycle life, the significance of the trends must not be over-emphasized. For the 5000 hour exposure, the range of stress changes at N = 10^7 for all test conditions is ± 22 percent. This range corresponds to stress changes of ± 3000 psi for specimens exposed at 400° and 650°F and tested at 400°F.

The data for the unnotched 8-1-1 titanium specimens presented in Figure 20 show moderate changes at N = 10^4 cycles with the largest change of -22 percent being produced by the 5000 hour exposure at 650° in tests at room temperature. At N = 10^7 cycles, the trends at 1000 hours exposure generally change to show

lower values for 5000 hours exposure. The exception is shown by specimens exposed at 400°F and tested at room temperature. However, after 5000 hours exposure, the percentage changes from values for unexposed specimens fall in the range of 0 to -25 percent.

For the fusion-welded and planished specimens of 8-1-1 titanium, the data in Figure 21 for $N = 10^4$ cycles show moderate changes with exposure which decrease to negligibly small changes for 5000 hours exposure. At $N = 10^7$ cycles, the data for 5000 hours exposure show a trend toward the values for unexposed specimens. For the 5000-hour exposure, the percentage changes range from +13 to -11 percent.

The data for center-notched PH14-8Mo specimens presented in Figure 22 shows slight changes in values for $N = 10^4$ cycles up to 1000 hours exposure, followed by small reductions in values for 5000 hours exposure when tested at elevated temperatures. At $N = 10^7$ cycles the general trend is for peak values to occur for 1000 hours exposure, with reductions up to 35 percent after 5000 hour exposure.

As shown in Figure 23, the unnotched PH14-8Mo specimens showed very small percentage changes at both $N = 10^4$ and $N = 10^7$ cycles for all exposures, with the exception of a 23 percent decrease in tests at room temperature of specimens exposed for 1000 hours at 400°F.

The fusion-welded and planished specimens of PH14-8Mo showed relatively consistent trends with slight increases of the order of 10 percent for tests at 650°F after exposure at 650°F and decreases of the order of 20 percent for tests at 400°F after exposure at 400°F. The data are presented in Figure 24.

The data for center-notched Inco 718 specimens presented in Figure 25 show small changes at $N = 10^4$ cycles but relatively large changes at $N = 10^7$ cycles. For tests after exposure for 5000 hours at 650°F, increases up to 22 percent are shown. However, for tests after exposure for 5000 hours at 400°F, decreases of as much as 42 percent are presented.

For unnotched specimens of Inco 718, Figure 26 indicates decreases in relative fatigue strength with increasing exposure time with the exception of values at $N = 10^4$ cycles for tests at 400°F and a value at $N = 10^7$ cycles for tests at 650°F after 5000 hours exposure at 650°F. At $N = 10^7$ cycles after exposure for 5000 hours, the percentage changes range from an increase of 15 percent to a decrease of 31 percent.

Finally, the data for fusion-welded and planished specimens of Inco 718 presented in Figure 27 show moderate changes at $N = 10^4$ cycles and also at $N = 10^7$ cycles for tests other than those at room temperature. For the room temperature tests, increases occur at $N = 10^7$ cycles in fatigue strengths relative to those for unexposed specimens. The increases range from 35 to 57 percent after exposure for 5000 hours at temperatures of 400°F and 650°F, respectively.

These summarizations of the basic S-N data obtained during the program emphasize the variability of the data for all materials.

37

A more generally informative summarization of the constant-mean stress data is provided by Figures 28, 29 and 30. These figures present lower boundaries of the S-N curves for all exposure conditions and test temperatures expressed in terms of varying stress divided by material density. When the data are presented in this form, it is clear that, for all specimen geometries, the 8-1-1 duplex-annealed titanium sheet demonstrated marked superiority for airframe applications. The ratings of the materials are shown in Table 7, Page 52.

The figures also show that the fusion-welded specimens had much greater resistance to repeated loading than the notched specimens with this resistance approaching that of the unnotched specimens at the longer test durations. In addition, the figures show that unnotched PH14-8Mo specimens had greater resistance at elevated temperature than at room temperature for durations greater than 10^5 cycles. For this range of durations, the fusion-welded PH14-8Mo specimens had slightly greater resistance at 650°F than they had in room temperature tests.

In the group of specimens which have been discussed in the preceding paragraphs, the center-notched specimens were notched by drilling a hole before the specimens were exposed to steady load at temperature. To explore the effect of drilling such a hole after specimen exposure for 5000 hours at 400°F or at 650°F, a group of specimens was exposed and then drilled before test. This notching after exposure tended to reduce the fatigue strength of the 8-1-1 titanium sheet at all test temperatures. It had no effect on PH14-8Mo specimens. For Inco 718 specimens, tests at room temperature showed no effect of delayed notching but in tests at 400 and 650°F moderate reductions in test life were obtained. The comparative data are shown in Figures 31-48 and the test data for specimens notched after exposure are listed in Table 8, Page 71.

In the preparation of the large number of fusion-welded specimens required for the basic program, light planishing of the welds was employed. To provide an indication of the effect of this operation a group of specimens with unplanished welds was prepared and tested. These tests indicated that the planishing operation had little effect on the fatigue resistance of the specimens. The comparative data are shown in Figures 49, 50, and 51, and the test data for unplanished specimens are listed in Table 9, Page 75.

An item of interest in testing of fusion-welded specimens is the location of failure. The fusion-welded 8-1-1 titanium specimens were tested with no subsequent heat treatment of the weld. In these specimens, fatigue cracks generally initiated at the interface between weld metal and heat affected zone and propagated across the weld. The PH14-8Mo specimens were heat treated after welding. In these specimens failures usually occurred in the base metal or the heat affected zone. These results are considered to be typical for fusion welded specimens heat treated after welding. The fusion-welded Inco 718 specimens were not heat treated after welding. These specimens usually failed in the weld metal since the strength of the weld metal is appreciably less than that of the cold rolled and aged base metal. The failure locations for fusion welded specimens are listed in Table 10, Page 76.

When these failure locations were compared with those reported for the fatigue tests conducted in the Boeing-North American Joint Venture under

Air Force Contract AF33(650)-11461, the failure locations for the fusion-welded 8-1-1 titanium and Inco 718 specimens were found to be the same. However, the failure locations for the .025 inch fusion-welded PH14-8Mo specimens were slightly different. During the tests now being reported, the steel specimens failed in the heat affected zone and base metal while during those conducted by Boeing-North American most of the failures occurred in the weld or heat affected zone.

Figures 52 through 57 provide comparisons of test data presented in this report with test data reported by Boeing-North American under Air Force Contract AF33(650)-11461. Figures 52 through 54 show that somewhat shorter test lives were obtained in the current work for specimens taken in the transverse direction than those reported for the longitudinal specimens tested by Boeing-North American. For the data on fusion-welded specimens shown on Figures 55 through 57 good agreement is shown between the two sets of data.

During the long term exposure of specimens at temperature under load, creep was not measured. However, to provide some indication of the magnitude of creep, measurements of the apparent change in the lengths of unnotched specimens were made at the end of the 5000-hour exposure period. Change in lengths between the specimen mounting holes are reported in Table 11, Page 83. Although these values do not have the weight of precise creep strain measurements, they indicate that the creep during the 5000 hours was small. The negative values of creep reported for titanium and Inco 718 specimens may be due to small lattice changes.

To assist in the evaluation of the exposure and fatigue test conditions, a metallographic examination was made of several of the notched and welded specimens. The specimens selected for this examination represented the most adverse combination of material, specimen configuration, pretest conditions and test loadings considered in this section of the report. These metallographic examinations, which are presented and discussed in Appendix VIII, indicate no subsurface cracking or metallurgical defects.
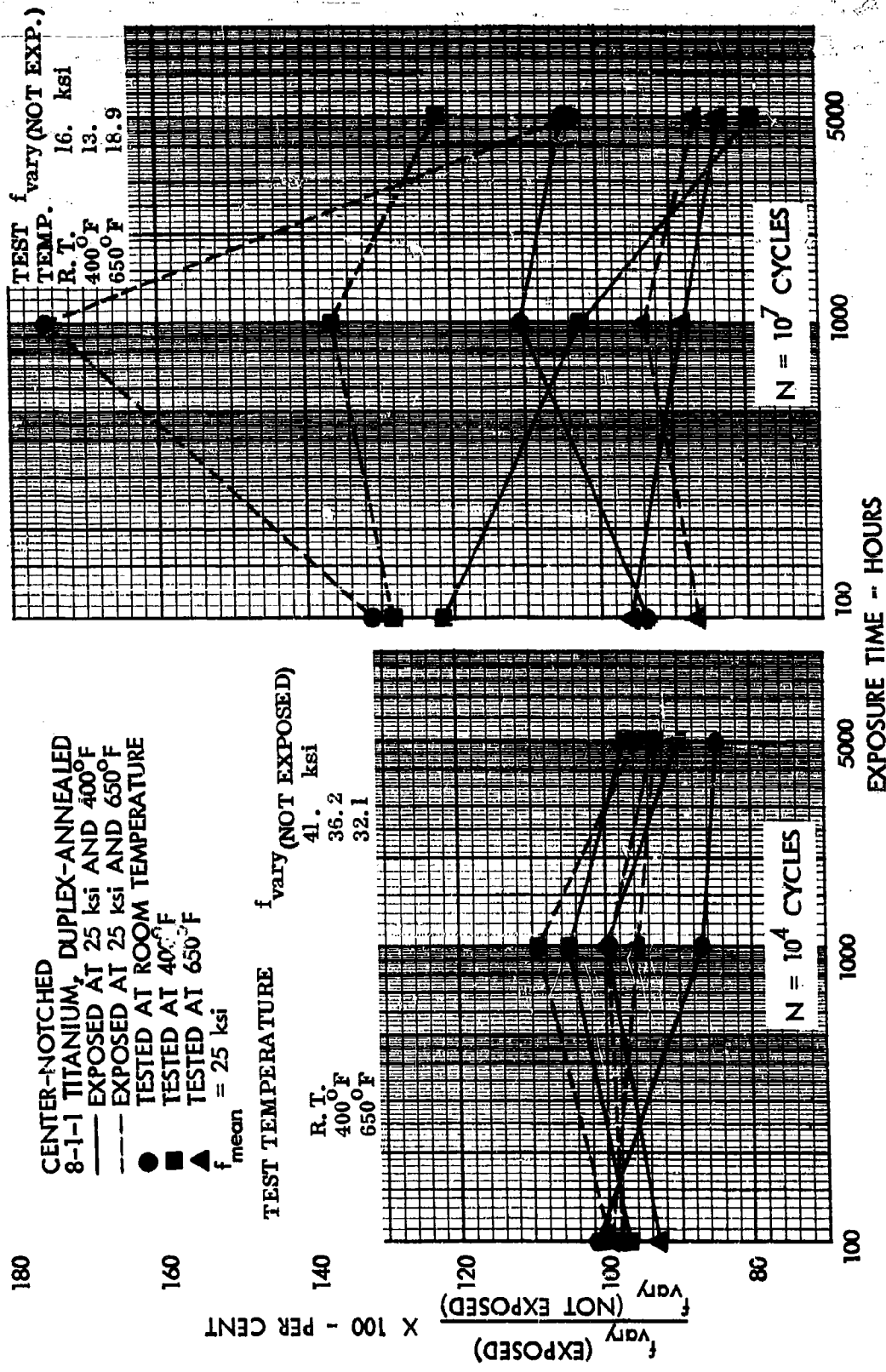
Figure 19. Change in Fatigue Strengths vs Exposure Time, 8-1-1 Titanium, Center-Notched

40
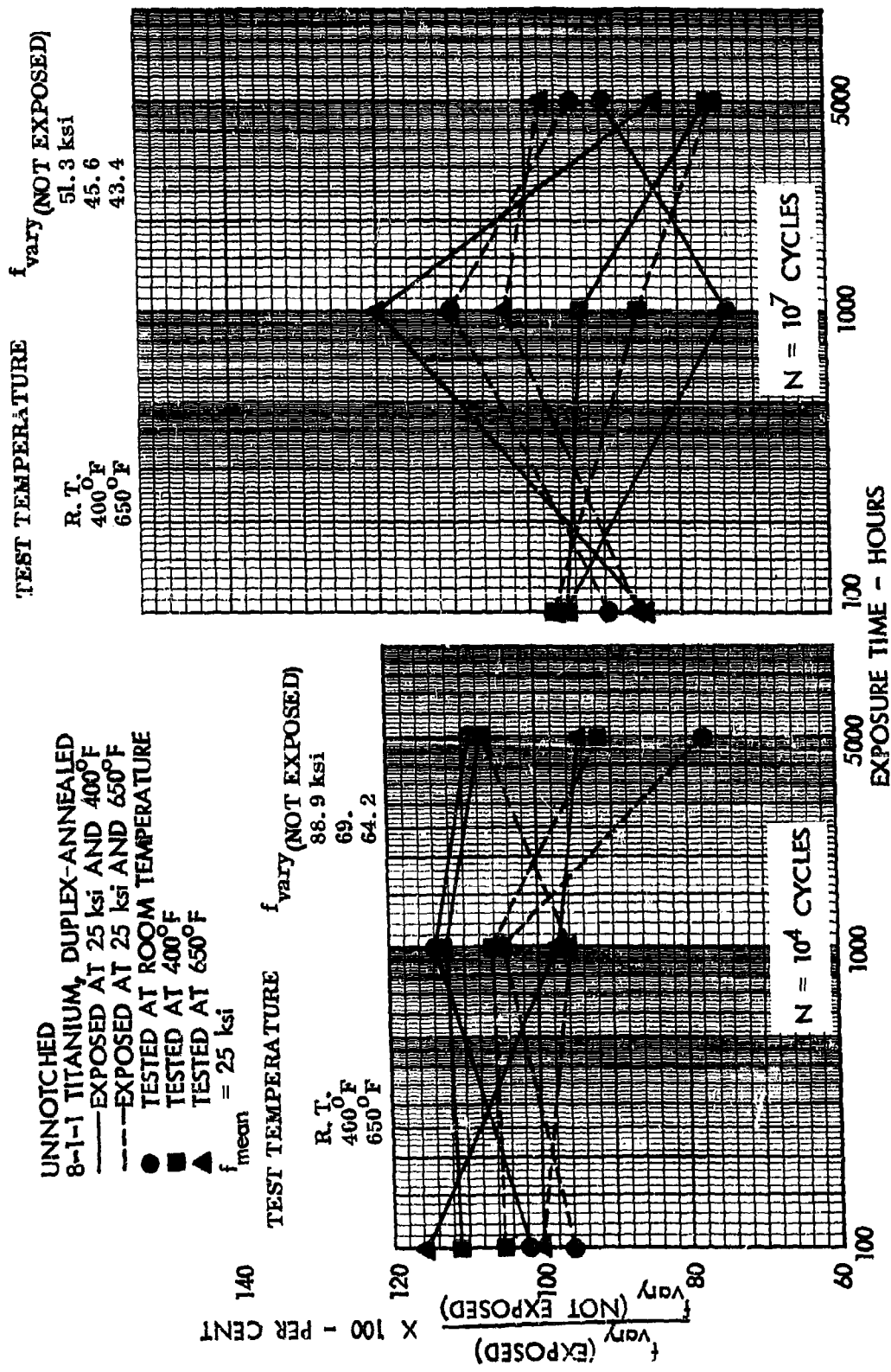
Figure 20. Change in Fatigue Strengths vs Exposure Time, 8-1-1 Titanium, Unnotched
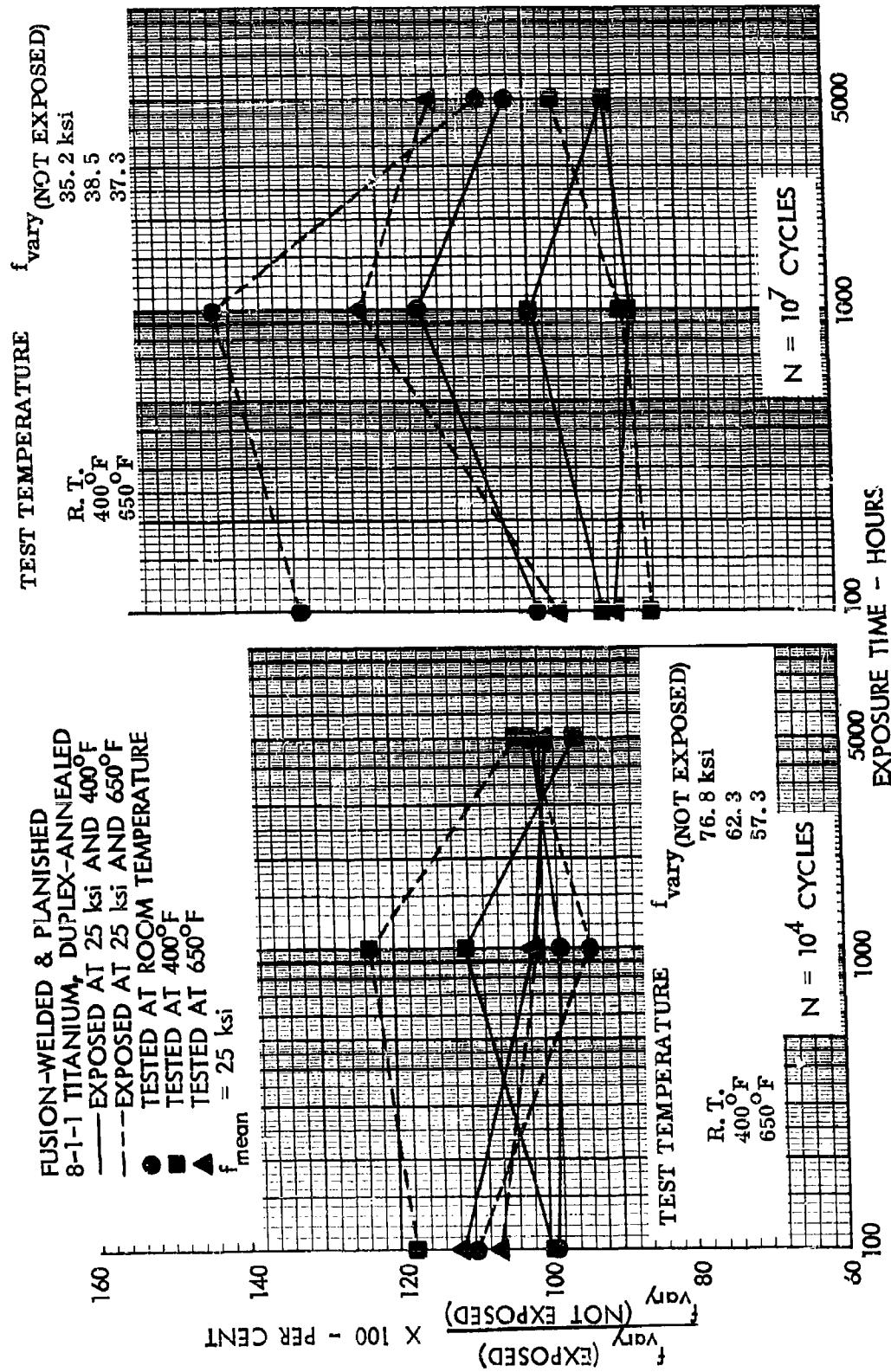
Figure 21. Change in Fatigue Strengths vs Exposure Time, 8-1-1 Titanium, Fusion-Welded & Planished
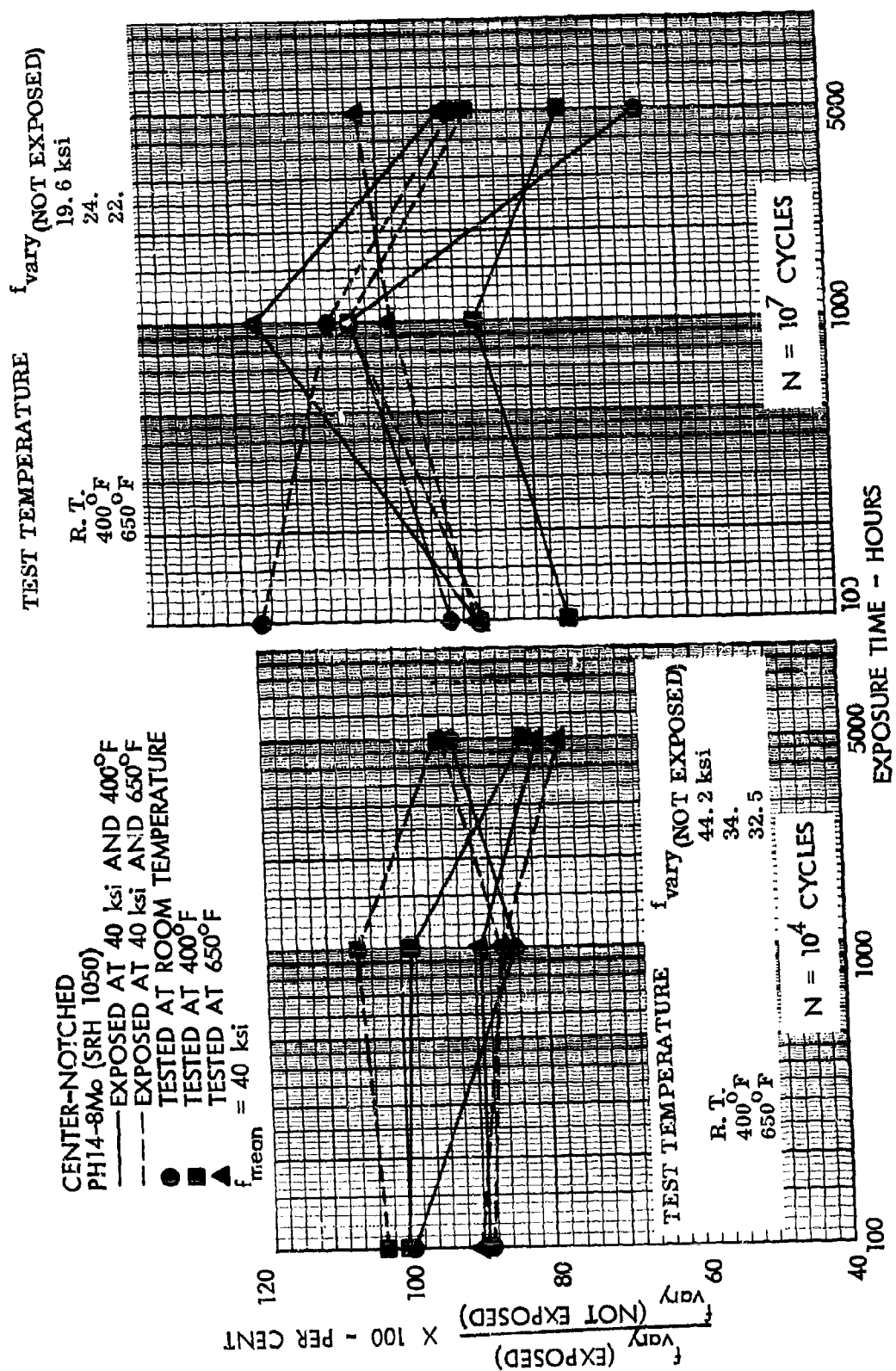
Figure 22. Change in Fatigue Strengths vs Exposure Time, PH 14-8Mo, Center-Notched

43
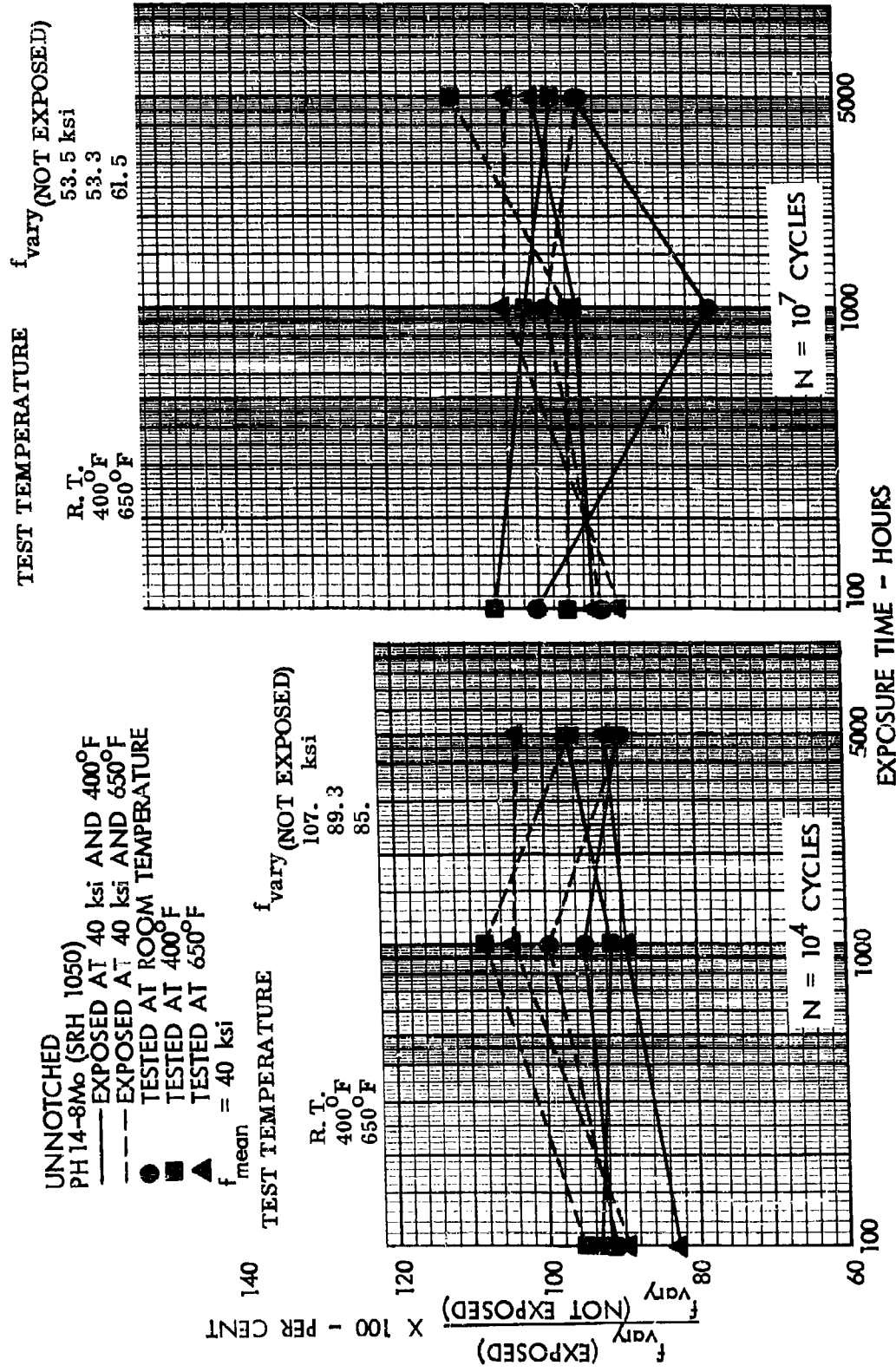
Figure 23. Change in Fatigue Strengths vs Exposure Time, PH 14-8Mo, Unnotched
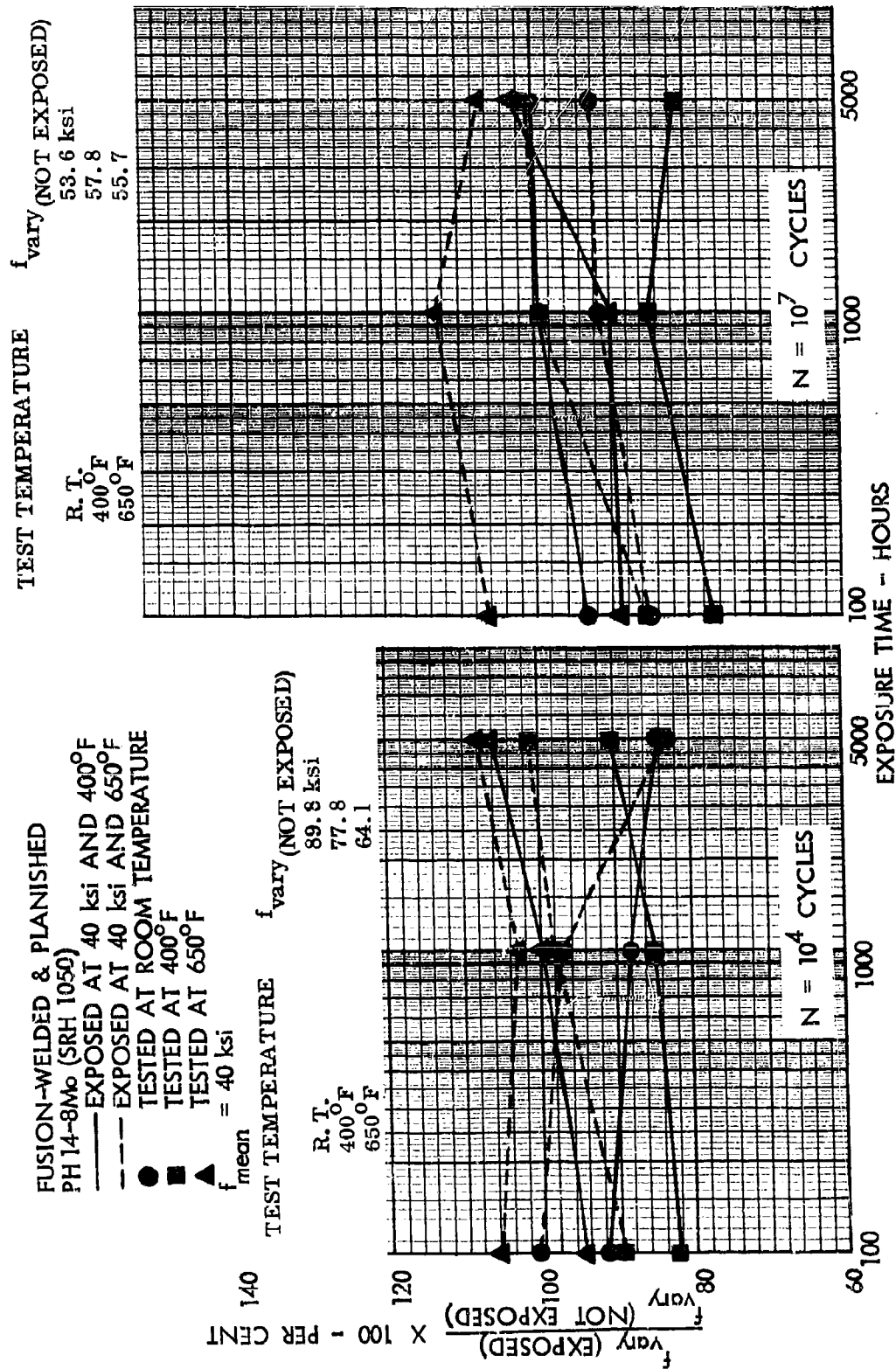
Figure 24. Change in Fatigue Strengths vs Exposure Time, PH 14-8Mo, Fusion-Welded & Planished

45

CENTER-NOTCHED
INCO 718, COLD ROLLED, AGED AT 1275°F
——— EXPOSED AT 40 ksi AND 400°F
– – – EXPOSED AT 40 ksi AND 650°F
● TESTED AT ROOM TEMPERATURE
■ TESTED AT 400°F
▲ TESTED AT 650°F
f_{mean} = 40 ksi

TEST TEMPERATURE $f_{vary(NOT\ EXPOSED)}$
R.T.   18.1 ksi
400°F   14.
650°F   16.

N = 10^7 CYCLES

TEST TEMPERATURE $f_{vary(NOT\ EXPOSED)}$
R.T.   49.6 ksi
400°F   46.
650°F   41.7

N = 10^4 CYCLES

EXPOSURE TIME – HOURS

$\dfrac{f_{vary}\ (EXPOSED)}{f_{vary}\ (NOT\ EXPOSED)}$ X 100 – PER CENT

Figure 25.   Change in Fatigue Strengths vs Exposure Time, INCO 718, Center-Notched

46
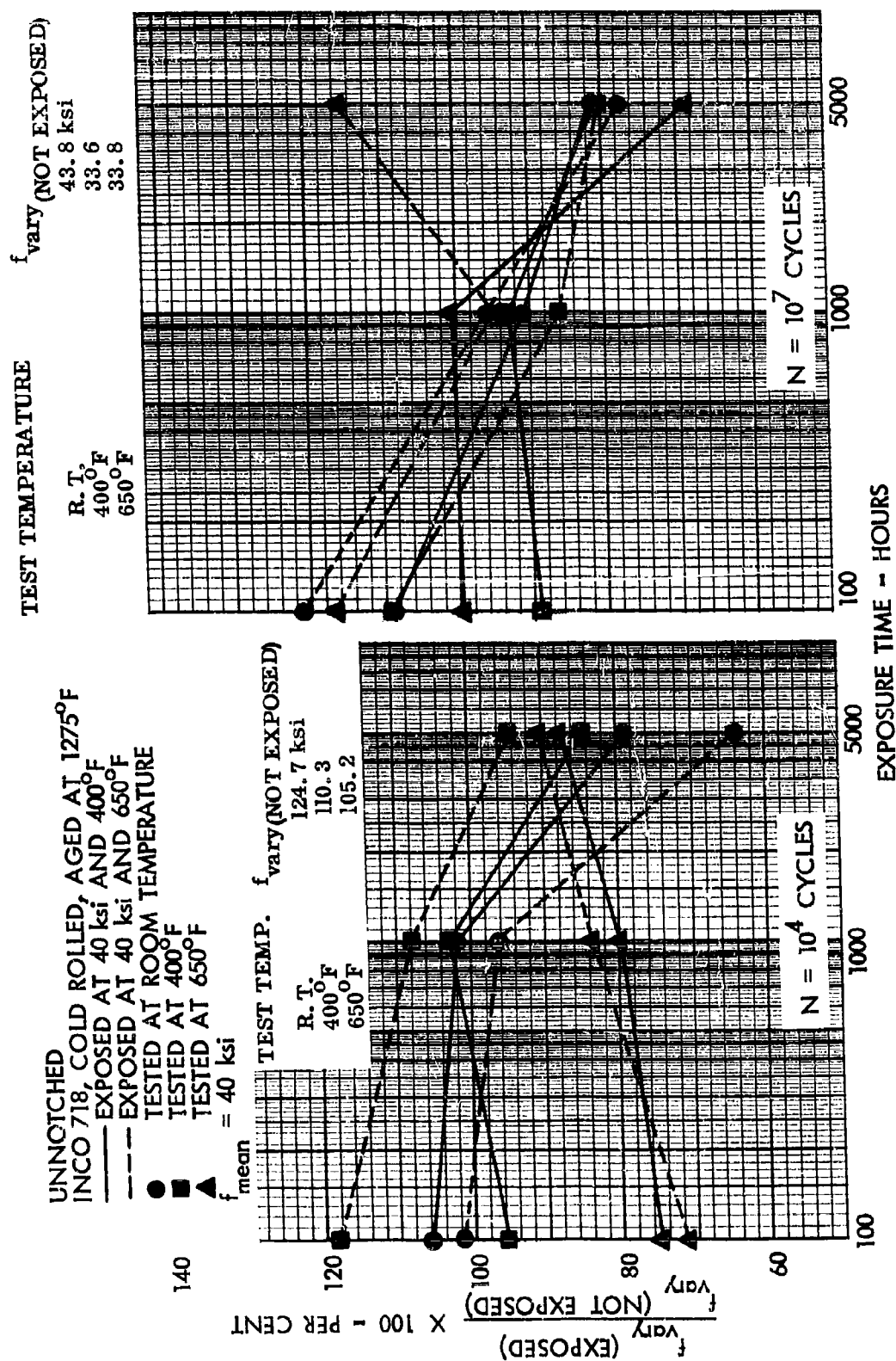
Figure 26. Change in Fatigue Strengths vs Exposure Time, INCO 718, Unnotched

47
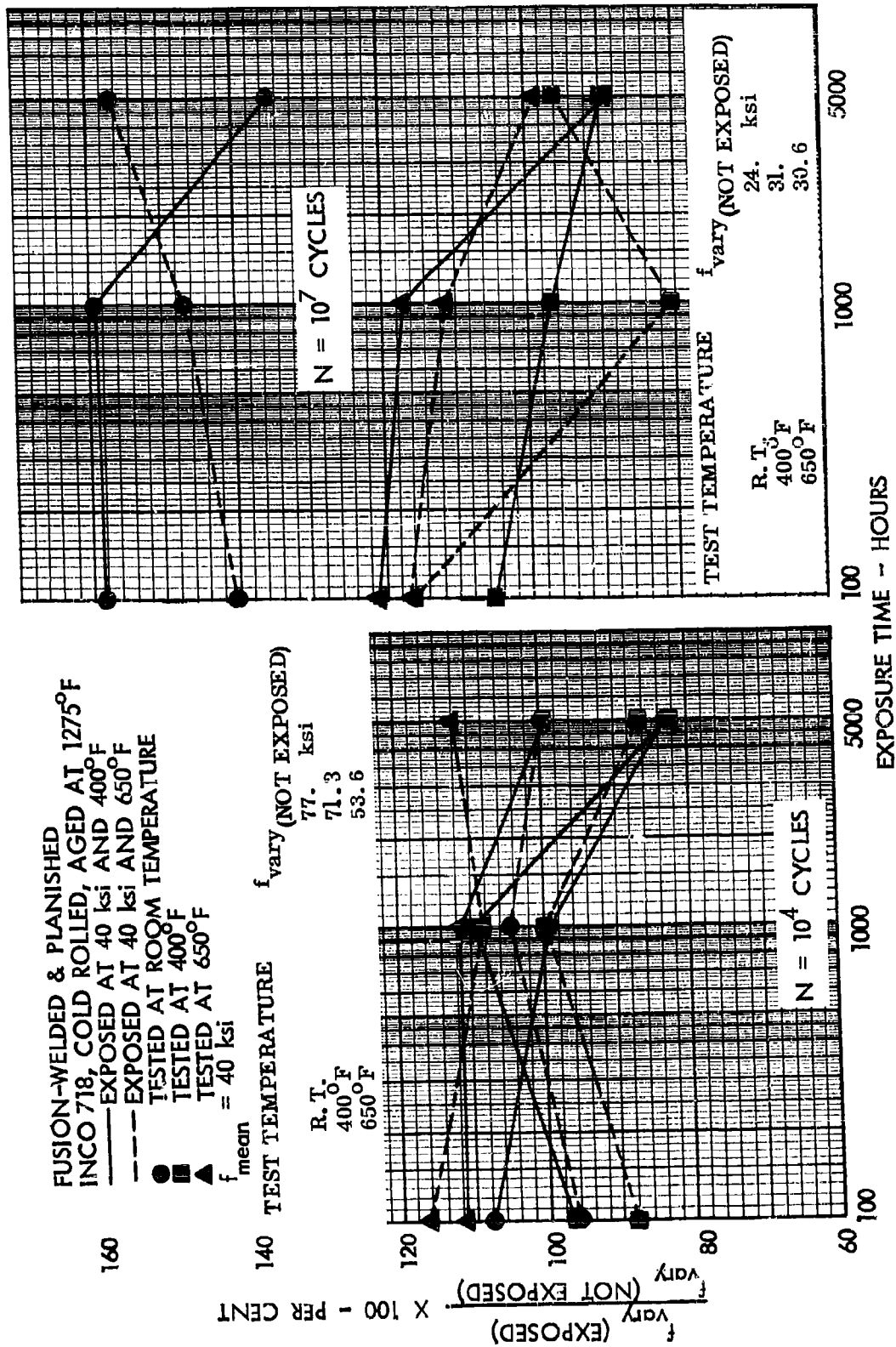
Figure 27. Change in Fatigue Strengths vs Exposure Time, INCO 718, Fusion-Welded & Planished

48
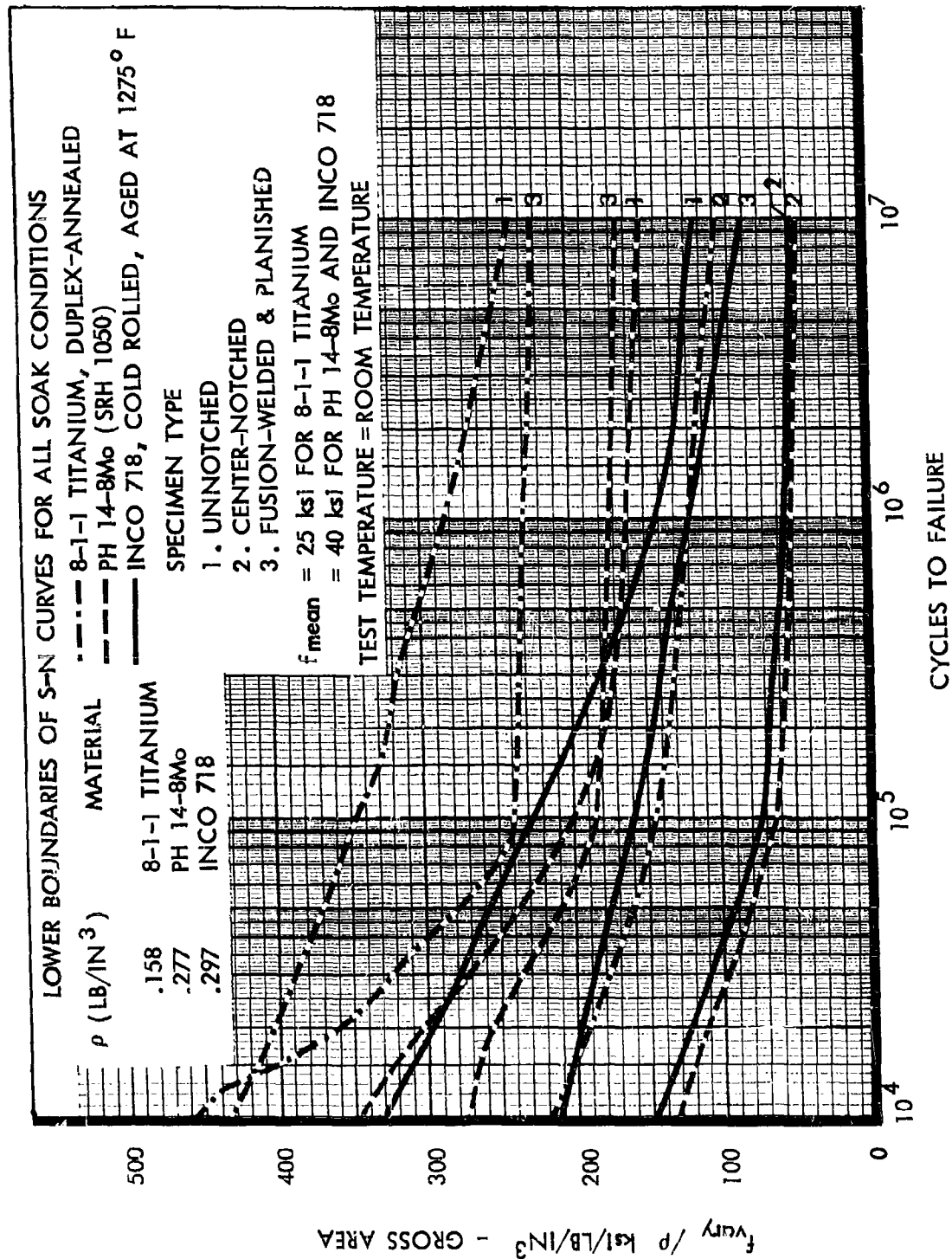
Figure 28.   Comparison of S-N Curves at Room Temperature, f_{mean} = Constant
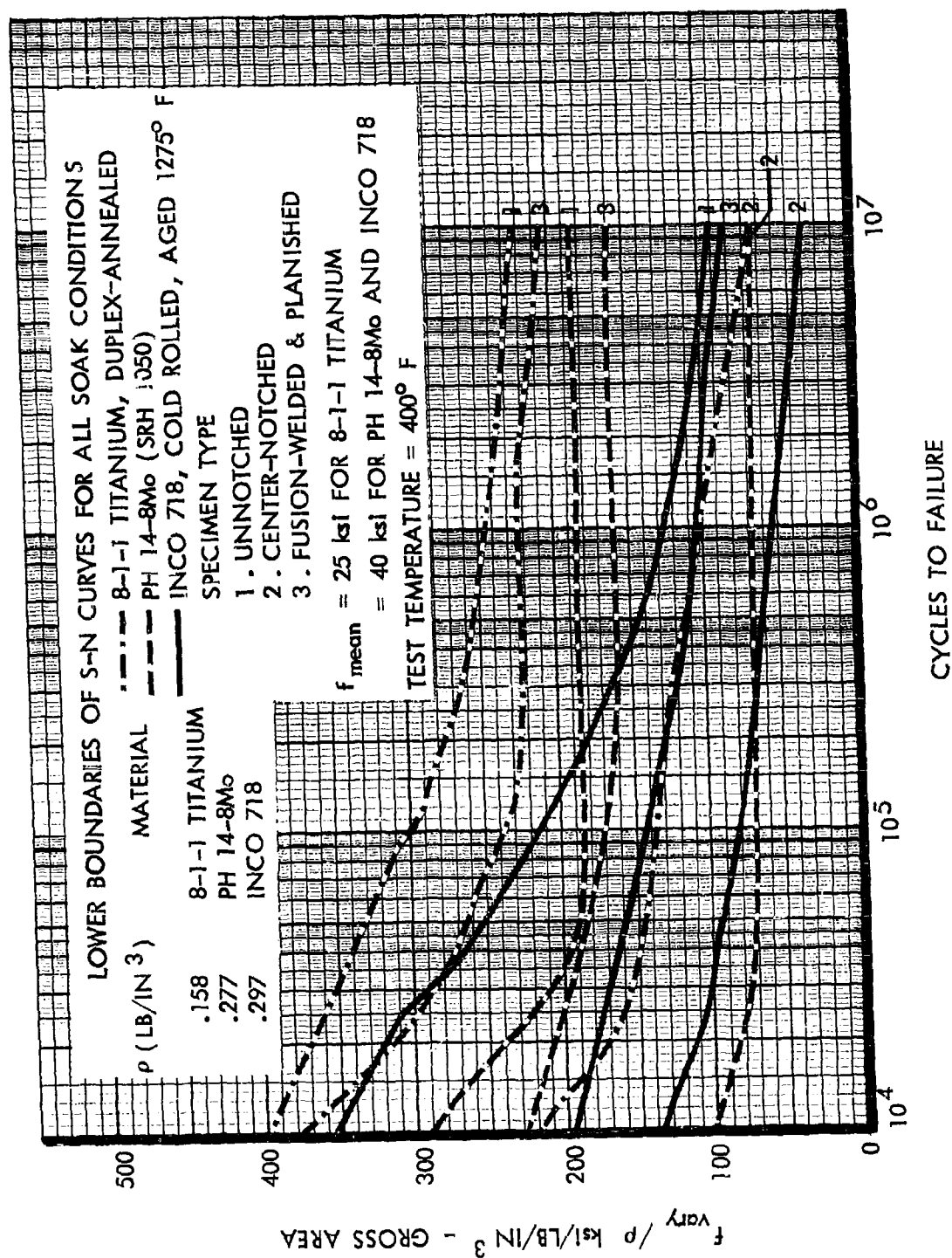
Figure 29. Comparison of S-N Curves at 400°F, f_{mean} = Constant
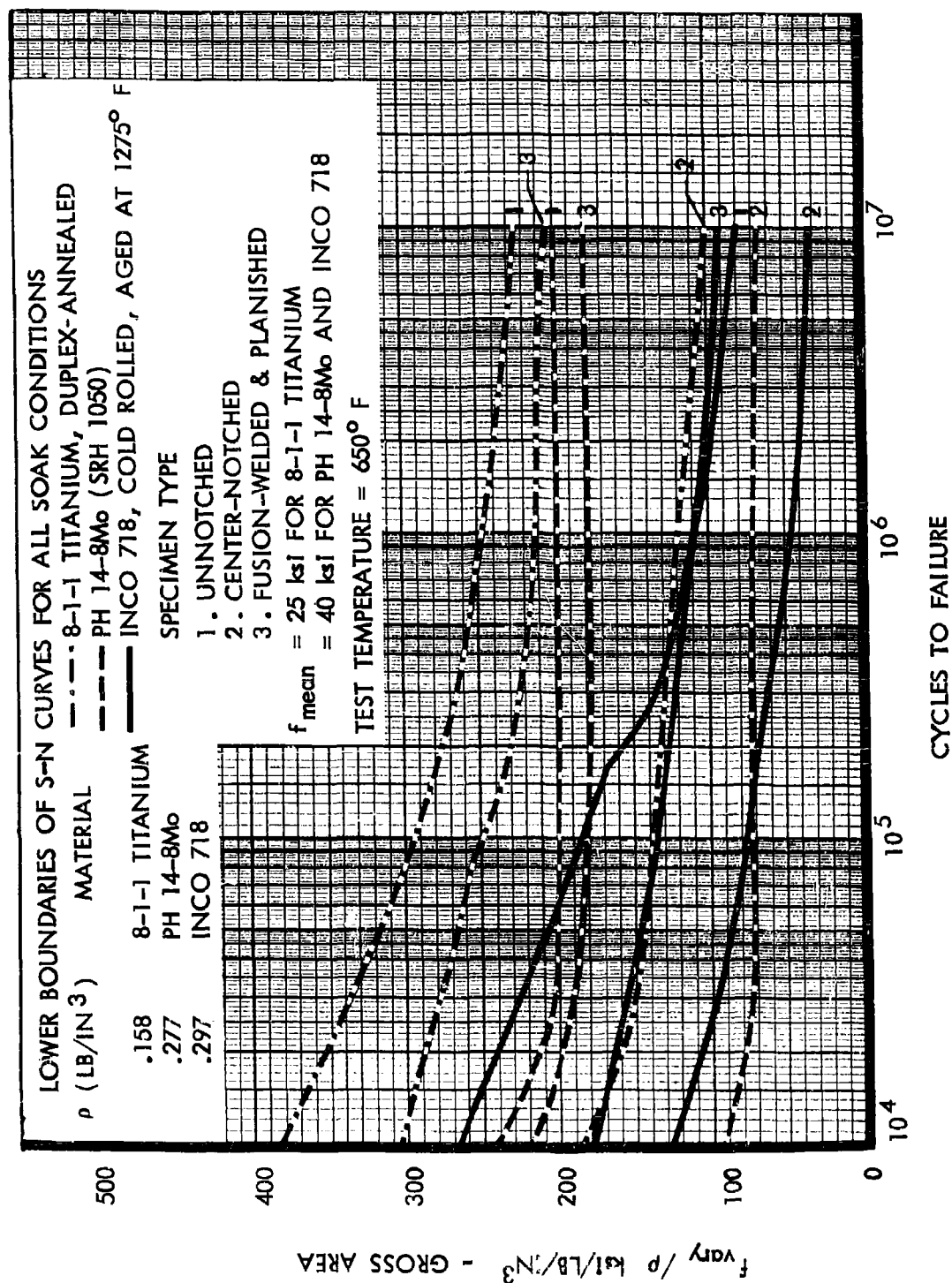
Figure 30. Comparison of S-N Curves at 650°F, f_{mean} = Constant

TABLE 7 RATING OF MATERIALS BASED ON S-N DATA

RATING	TYPE OF SPECIMEN		
	Center-Notched	Unnotched	Fusion-Welded & Planished
(1) High Stress Low Cycle Range			
1	8-1-1 Ti	8-1-1 Ti	8-1-1 Ti
2	INCO 718	INCO 718	PH14-8Mo
3	PH14-8Mo	PH14-8Mo	INCO 718
(2) Low Stress High Cycle Range			
1	8-1-1 Ti	8-1-1 Ti	8-1-1 Ti
2	PH14-8Mo	PH14-8Mo	PH14-8Mo
3	INCO 718	INCO 718	INCO 718

(1) $N \leq \approx 2 \times 10^5$ Cycles

(2) $N > \approx 2 \times 10^5$ Cycles
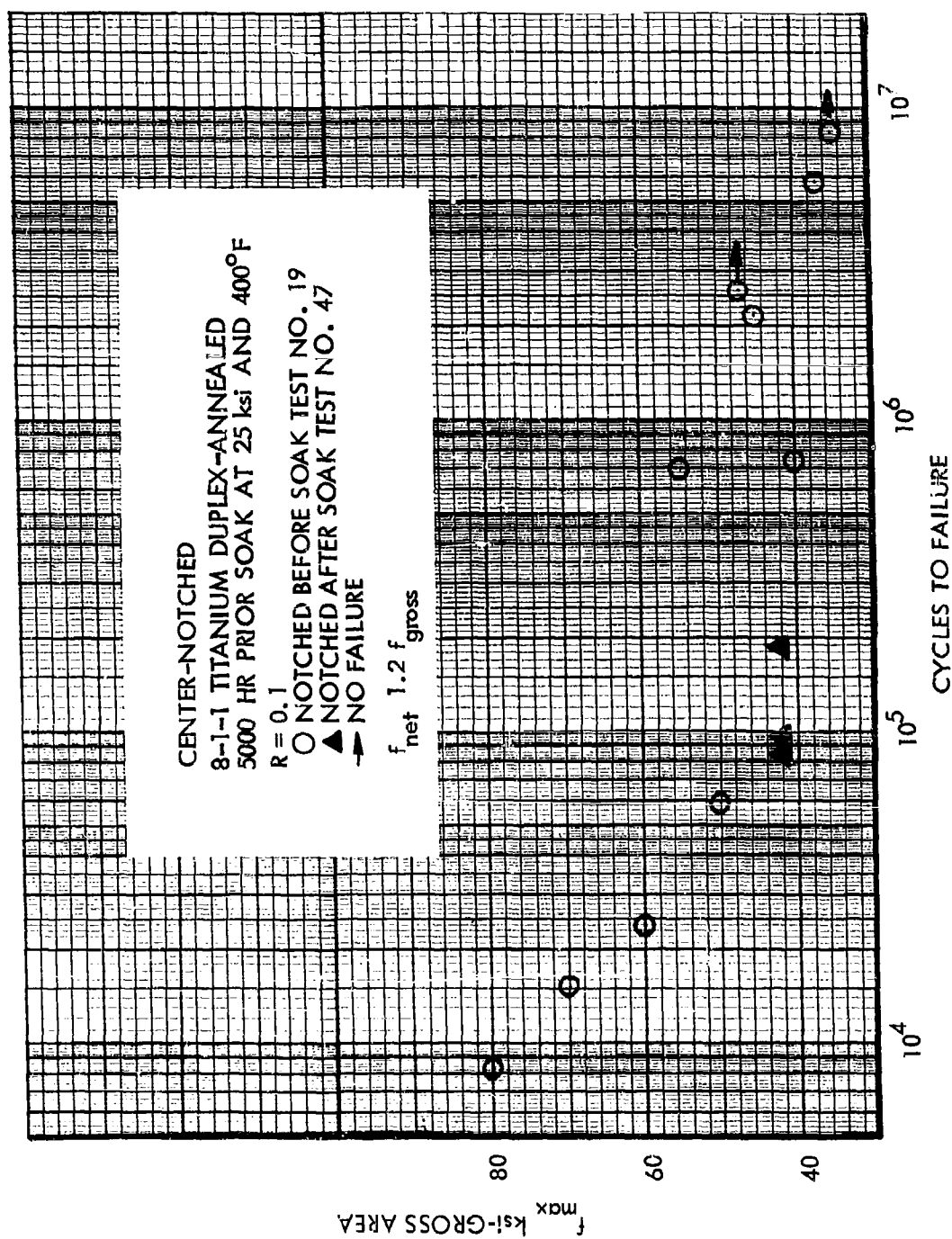
Figure 31. Comparison of S-N Data at Room Temperature, 8-1-1 Titanium, Notched Before and After Soak

53

Figure 32. Comparison of S-N Data at Room Temperature, 8-1-1 Titanium, Notched Before and After Soak

CENTER-NOTCHED
8-1-1 TITANIUM DUPLEX-ANNEALED
5000 HR PRIOR SOAK AT 25 ksi AND 650°F
R = 0.1
○ NOTCHED BEFORE SOAK TEST NO. 37
▲ NOTCHED AFTER SOAK TEST NO. 50
↶ FAILED AT CLAMP

$f_{net} = 1.2 f_{gross}$

CYCLES TO FAILURE

f_{max} ksi-GROSS AREA

54
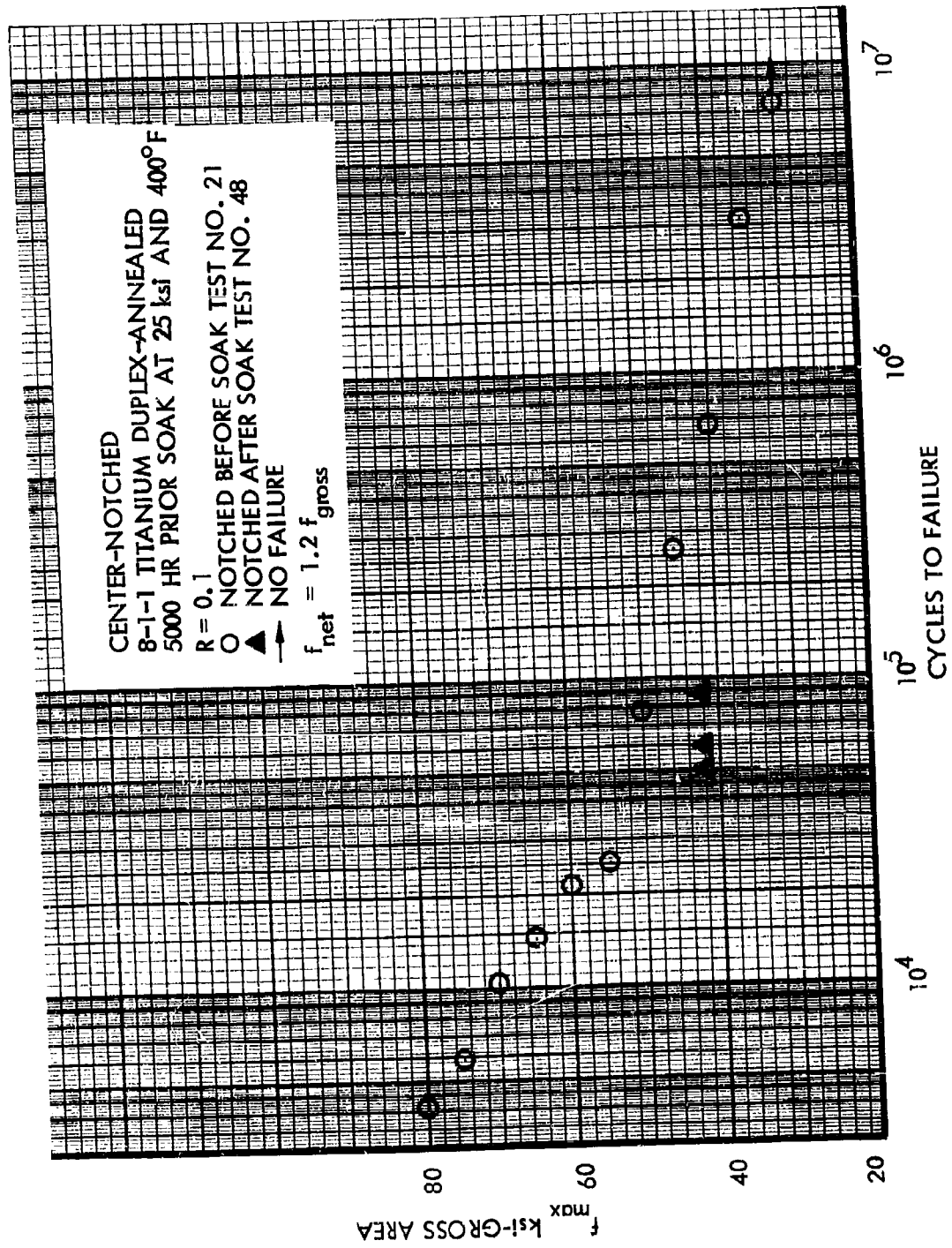
Figure 33. Comparison of S-N Data at 400°F, 8-1-1 Titanium, Notched Before and After Soak

55
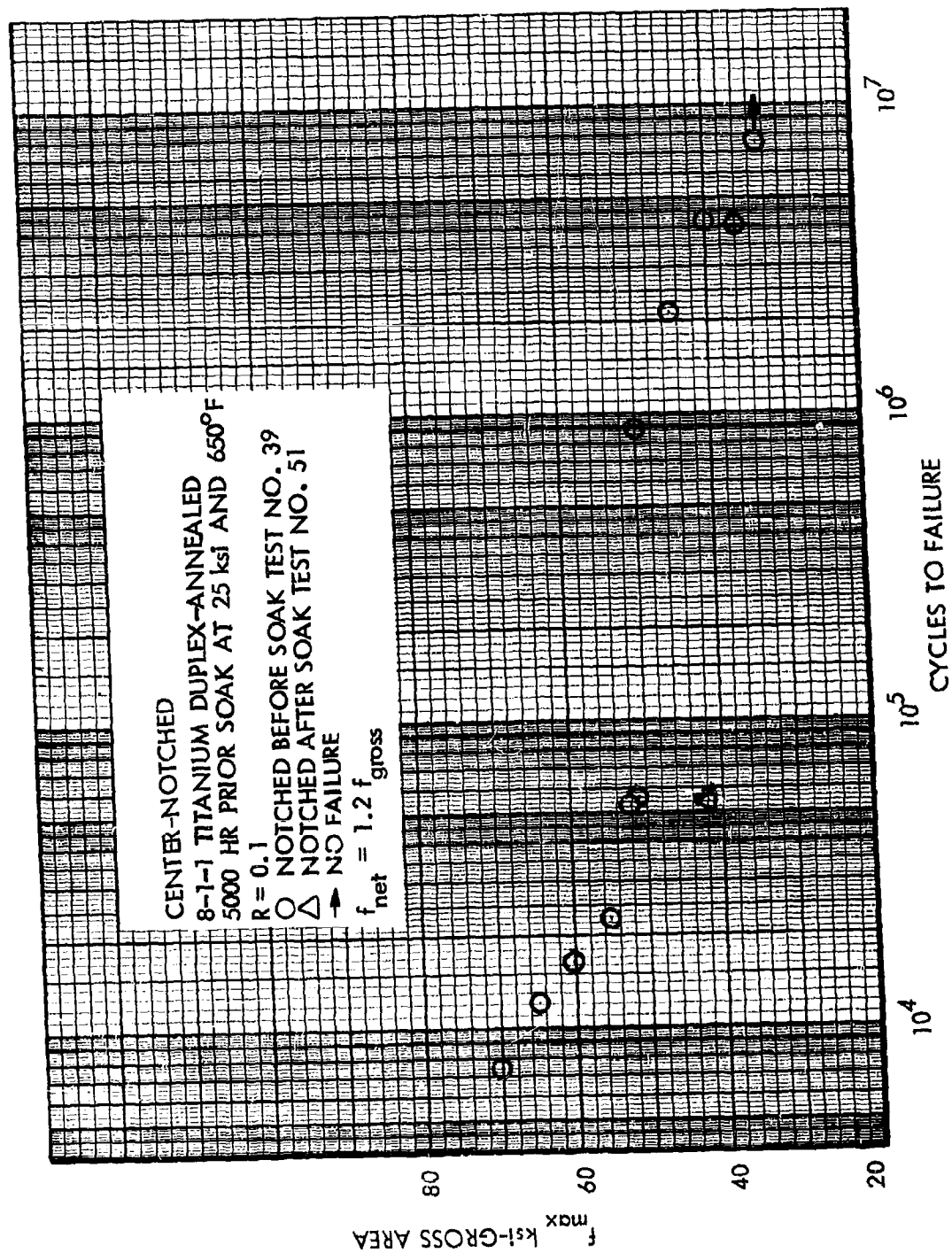
Figure 34. Comparison of S-N Data at 400°F, 8-1-1 Titanium, Notched Before and After Soak

The chart contains the following labels:

CENTER-NOTCHED
8-1-1 TITANIUM DUPLEX-ANNEALED
5000 HR PRIOR SOAK AT 25 ksi AND 650°F
R = 0.1
○ NOTCHED BEFORE SOAK TEST NO. 39
△ NOTCHED AFTER SOAK TEST NO. 51
↑ NO FAILURE
$f_{net} = 1.2\ f_{gross}$

X-axis: CYCLES TO FAILURE (10^4, 10^5, 10^6, 10^7)

Y-axis: f_{max} ksi-GROSS AREA (20, 40, 60, 80)

Figure 35. Comparison of S-N Data at 650°F, 8-1-1 Titanium, Notched Before and After Soak
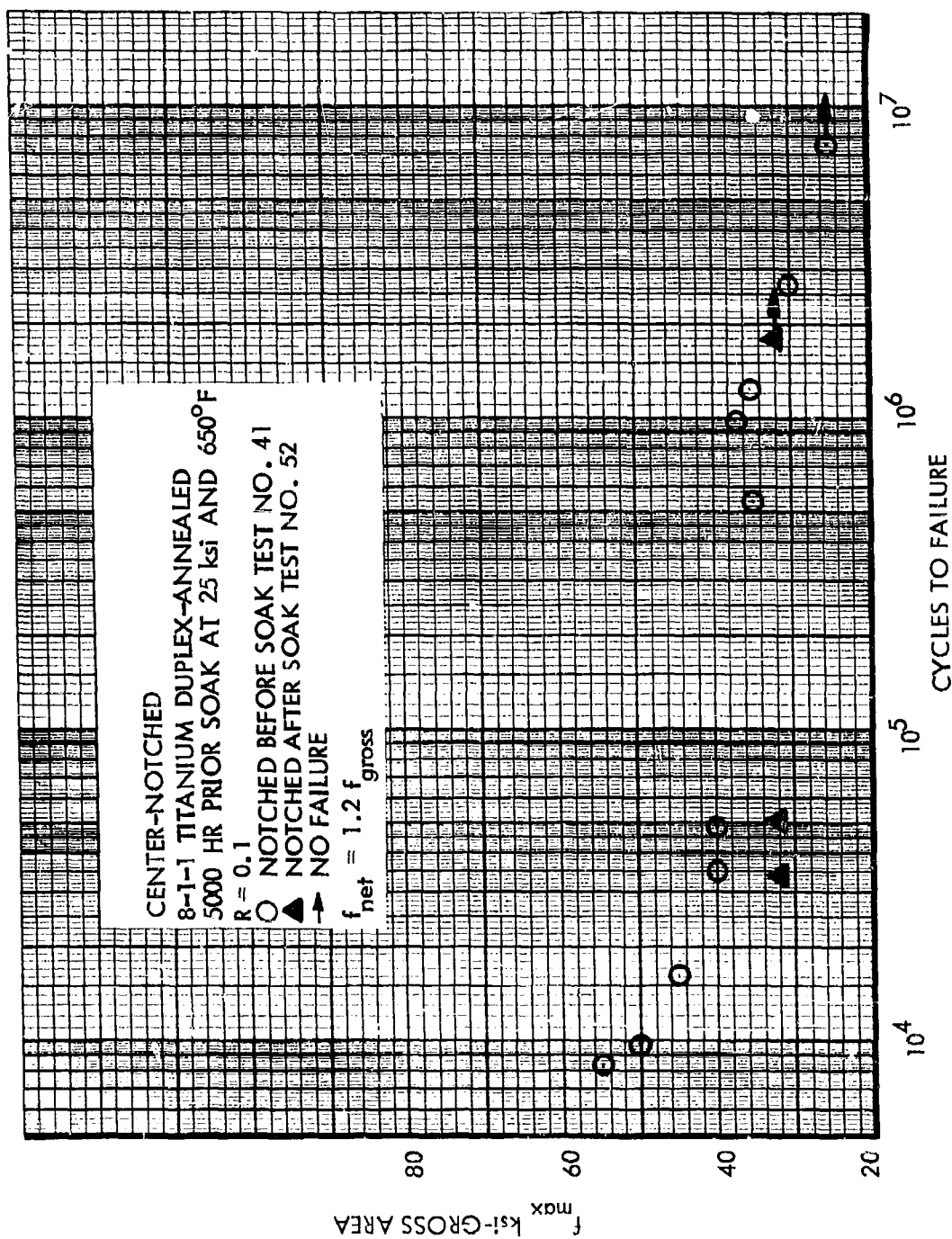
Figure 36. Comparison of S-N Data at $650°F$, 8-1-1 Titanium, Notched Before and After Soak
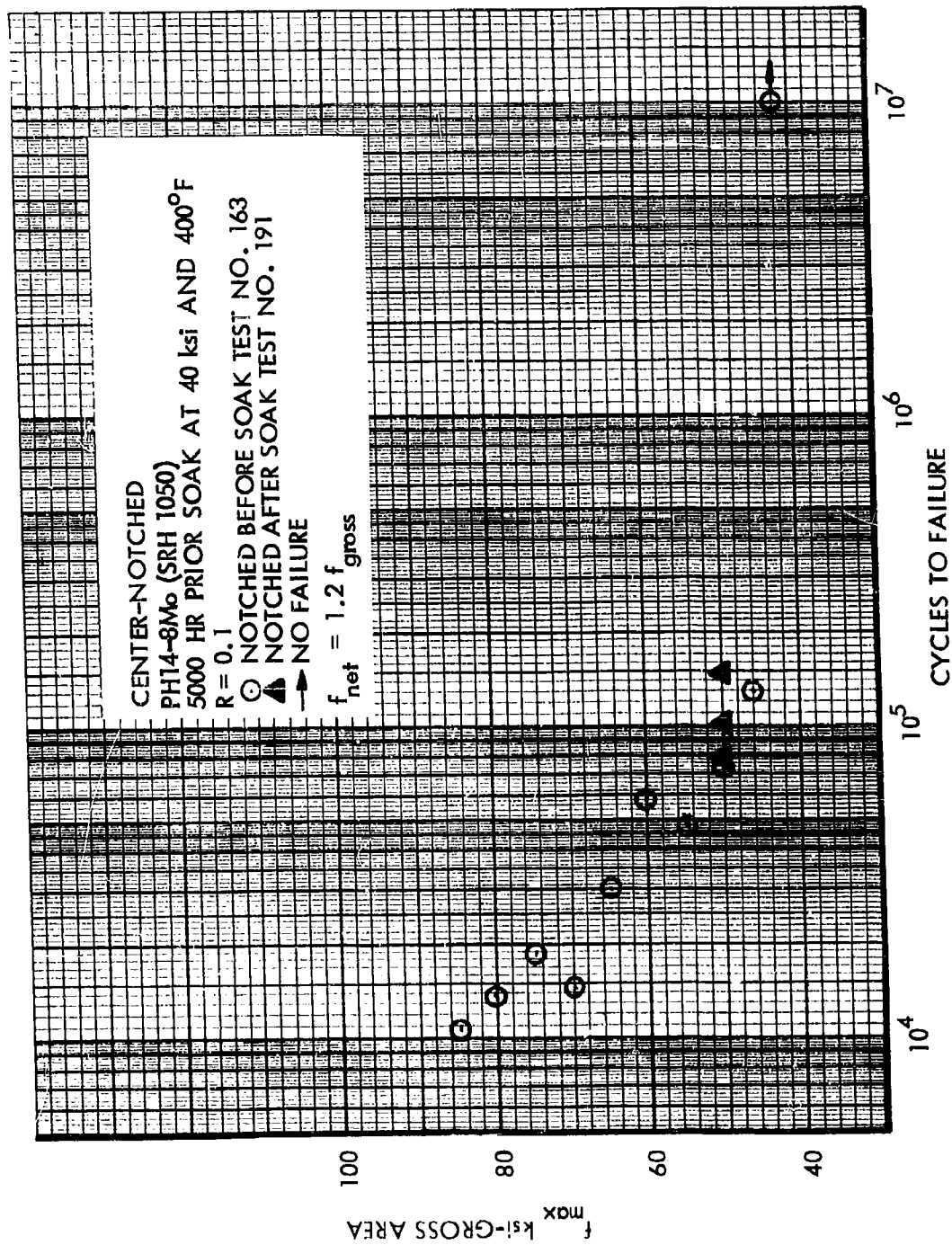
Figure 37. Comparison of S–N Data at Room Temperature, PH14–8Mo, Notched Before and After Soak

CENTER–NOTCHED
PH14–8Mo (SRH 1050)
5000 HR PRIOR SOAK AT 40 ksi AND 400°F
R = 0.1
⊙ NOTCHED BEFORE SOAK TEST NO. 163
▲ NOTCHED AFTER SOAK TEST NO. 191
→ NO FAILURE
$f_{net} = 1.2 f_{gross}$

CYCLES TO FAILURE

f_{max} ksi–GROSS AREA

Figure 38. Comparison of S-N Data at Room Temperature, PH14-8Mo, Notched Before and After Soak
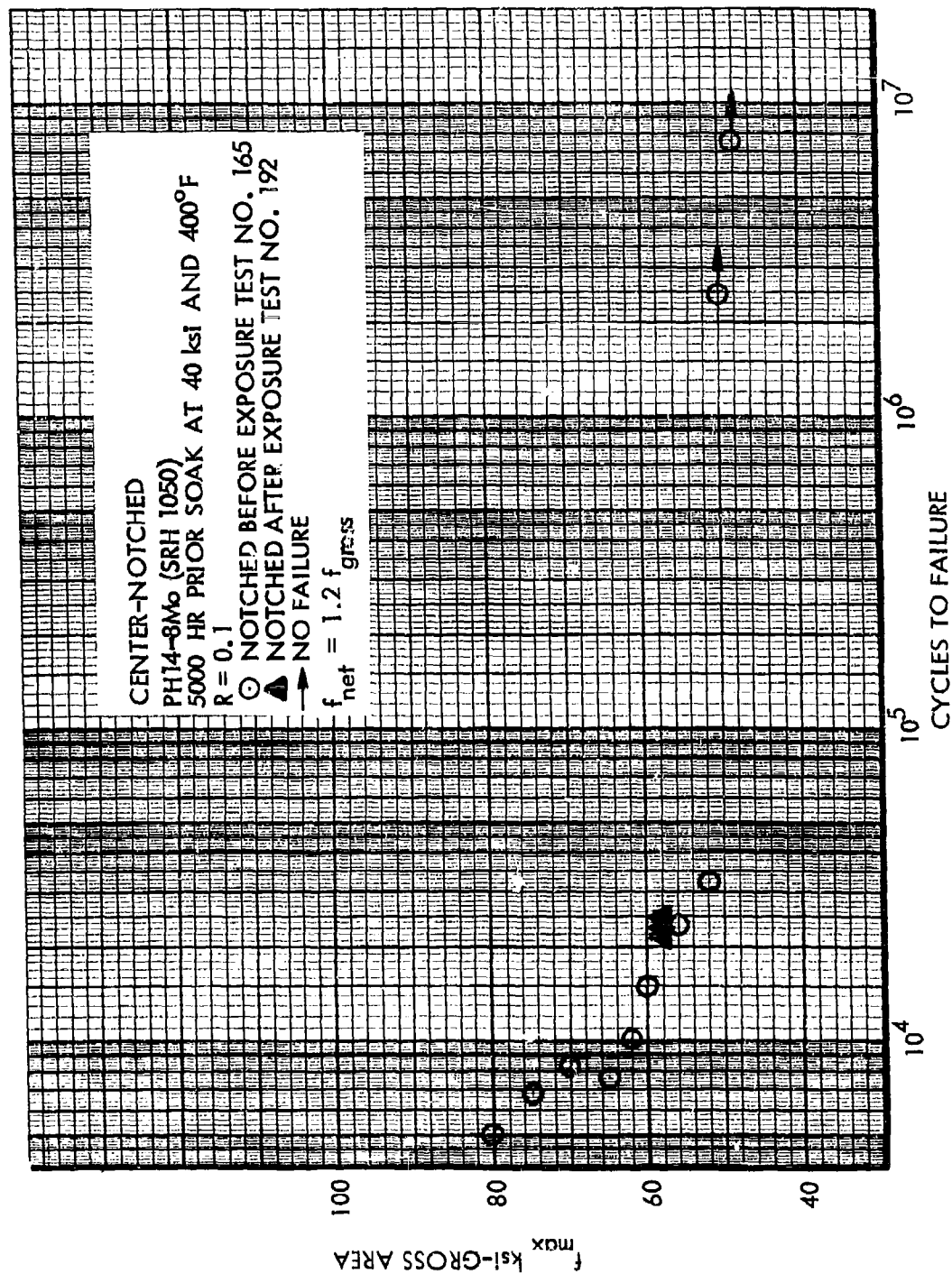
Figure 39. Comparison of S-N Data at 400°F, PH14-8Mo, Notched Before and After Soak

CENTER-NOTCHED
PH14-8Mo (SRH 1050)
5000 HR PRIOR SOAK AT 40 ksi AND 400°F
R = 0.1
⊙ NOTCHED BEFORE EXPOSURE TEST NO. 165
▲ NOTCHED AFTER EXPOSURE TEST NO. 192
↑ NO FAILURE
$f_{net} = 1.2 f_{gross}$
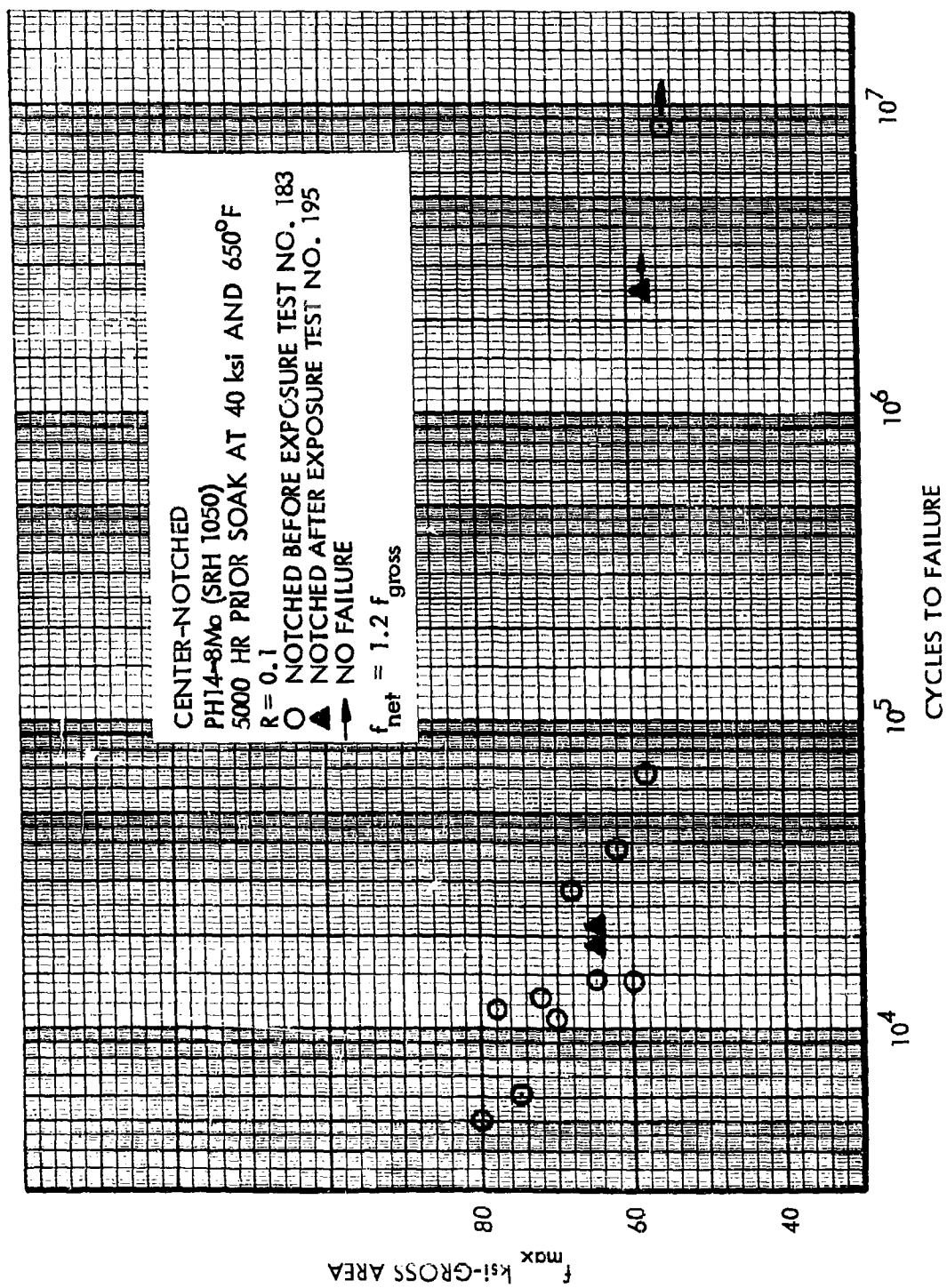
Figure 40. Comparison of S-N Data at 400°F, PH14-8Mo, Notched Before and After Soak

62
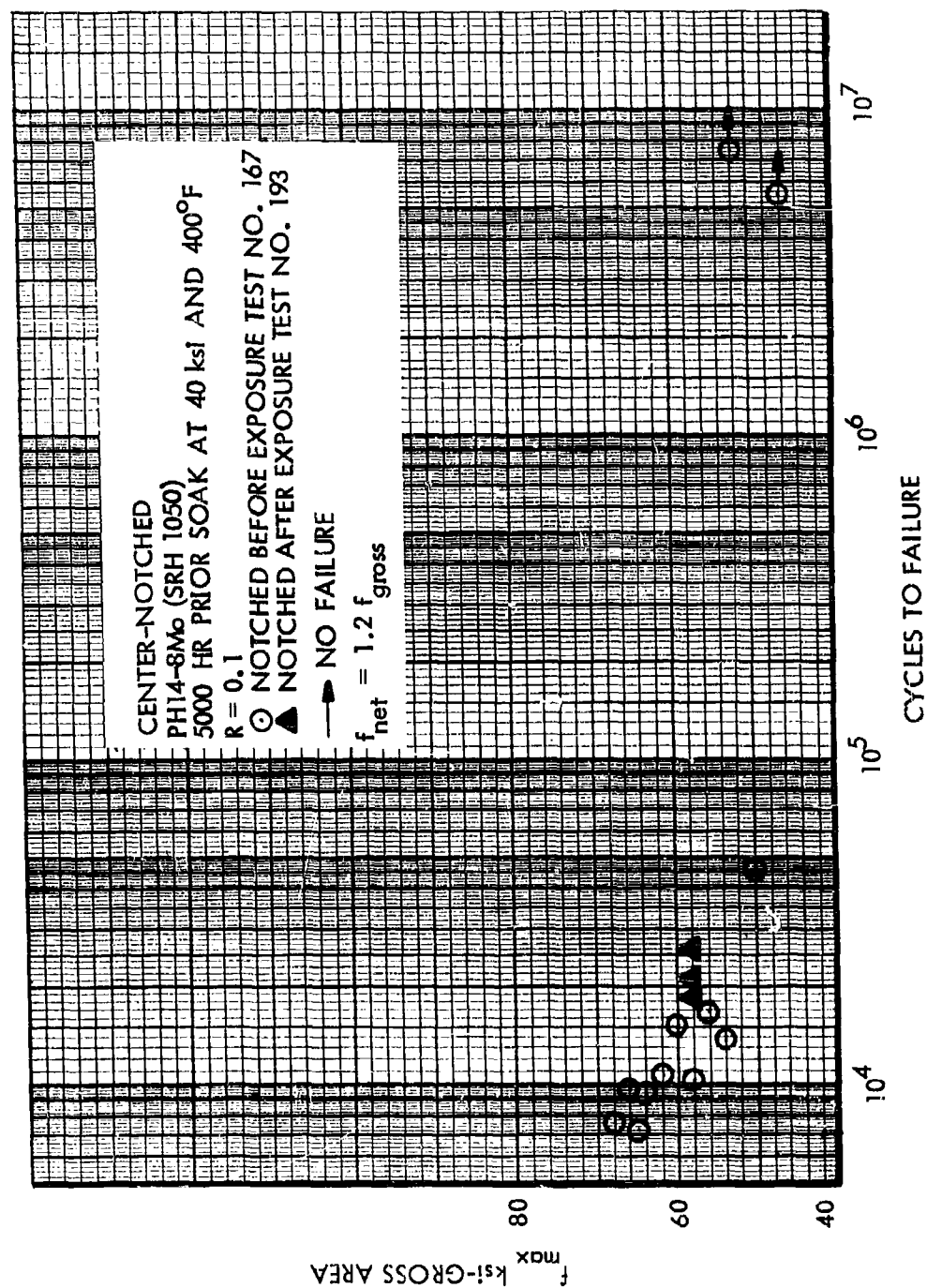
Figure 41. Comparison of S–N Data at 650°F, PH 14–8Mo, Notched Before and After Soak
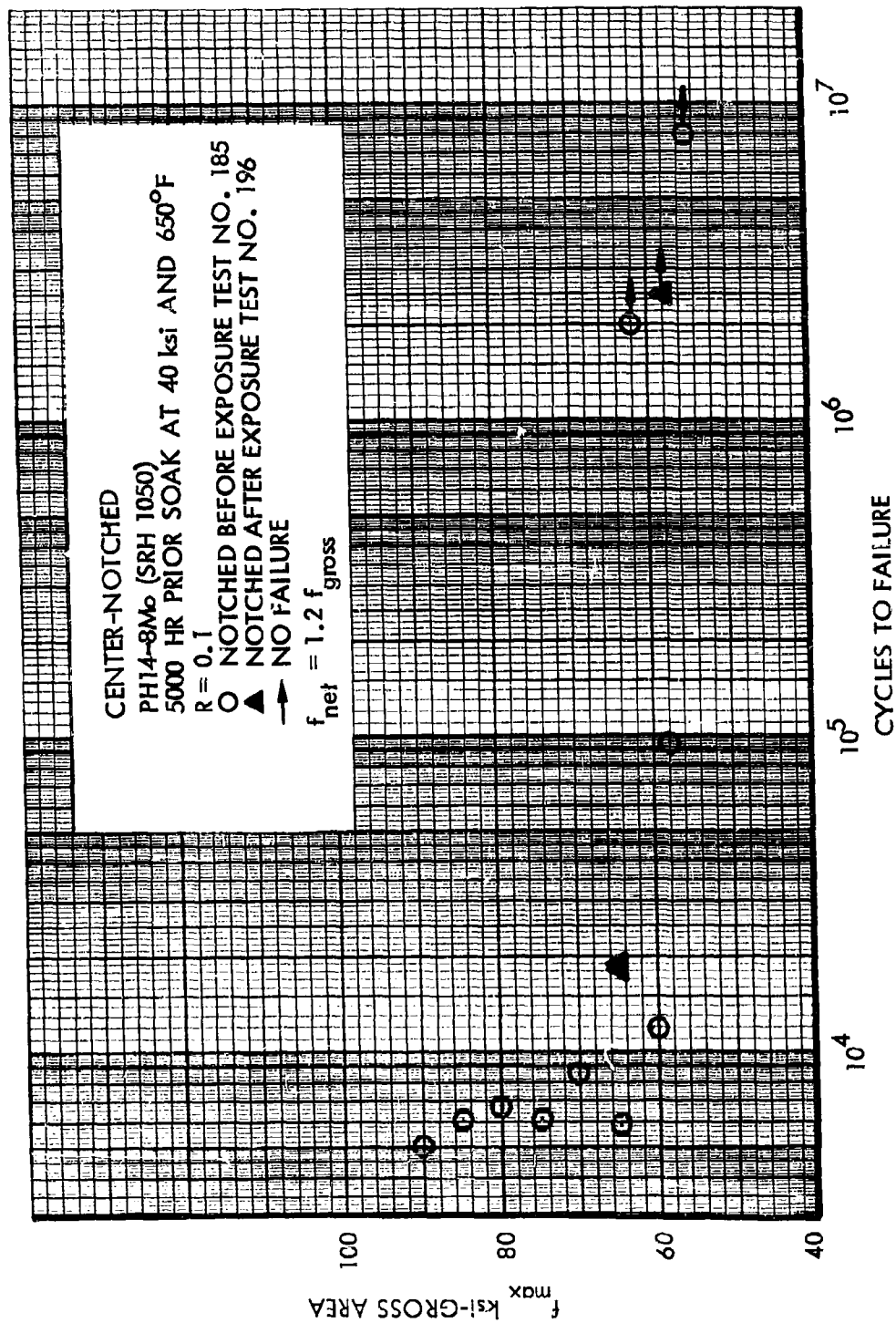
Figure 42. Comparison of S–N Data at 650°F, PH 14–8Mo, Notched Before and After Soak
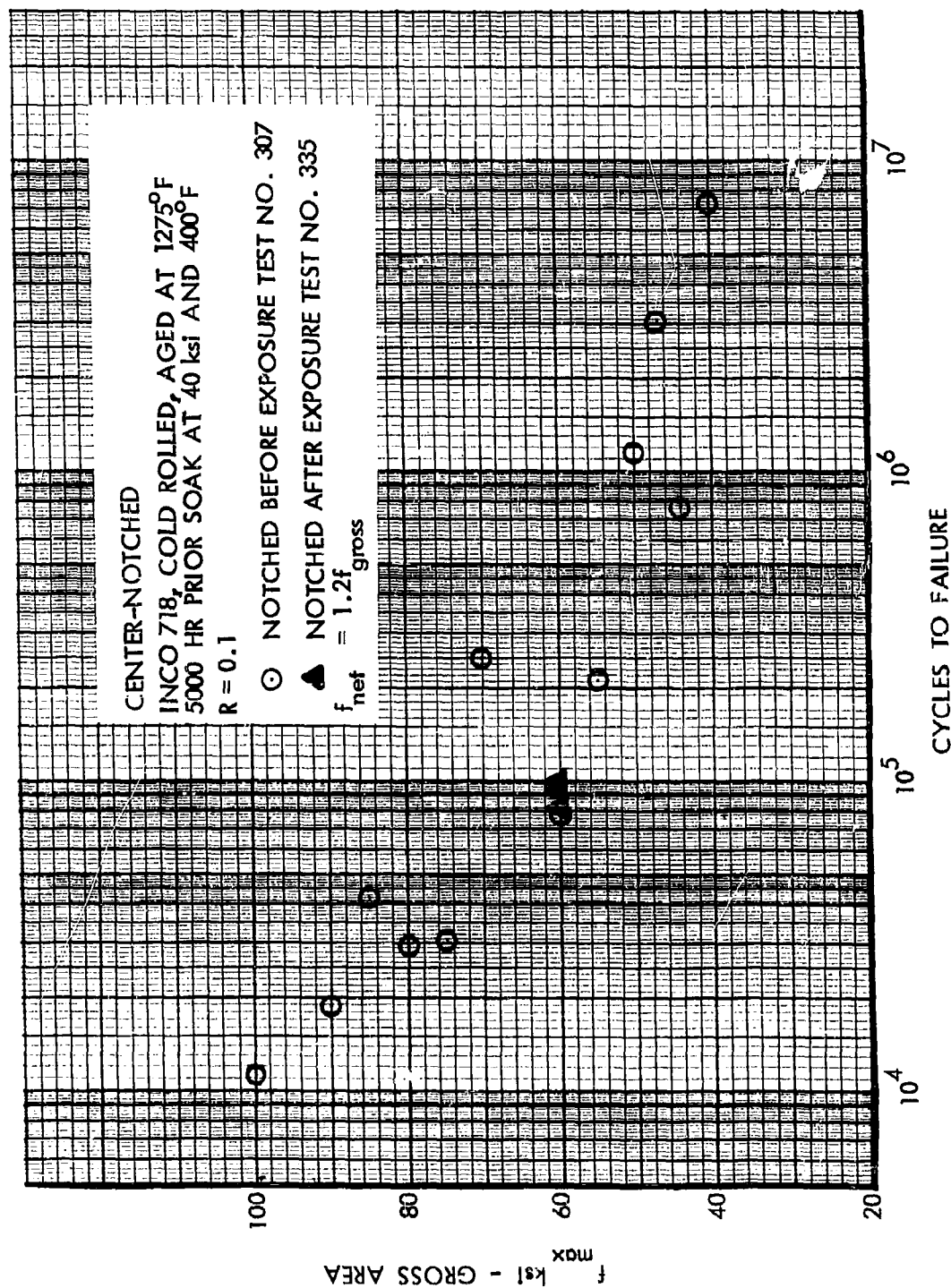
Figure 43.   Comparison of S–N Data at Room Temperature, INCO 718, Notched Before and After Soak

65
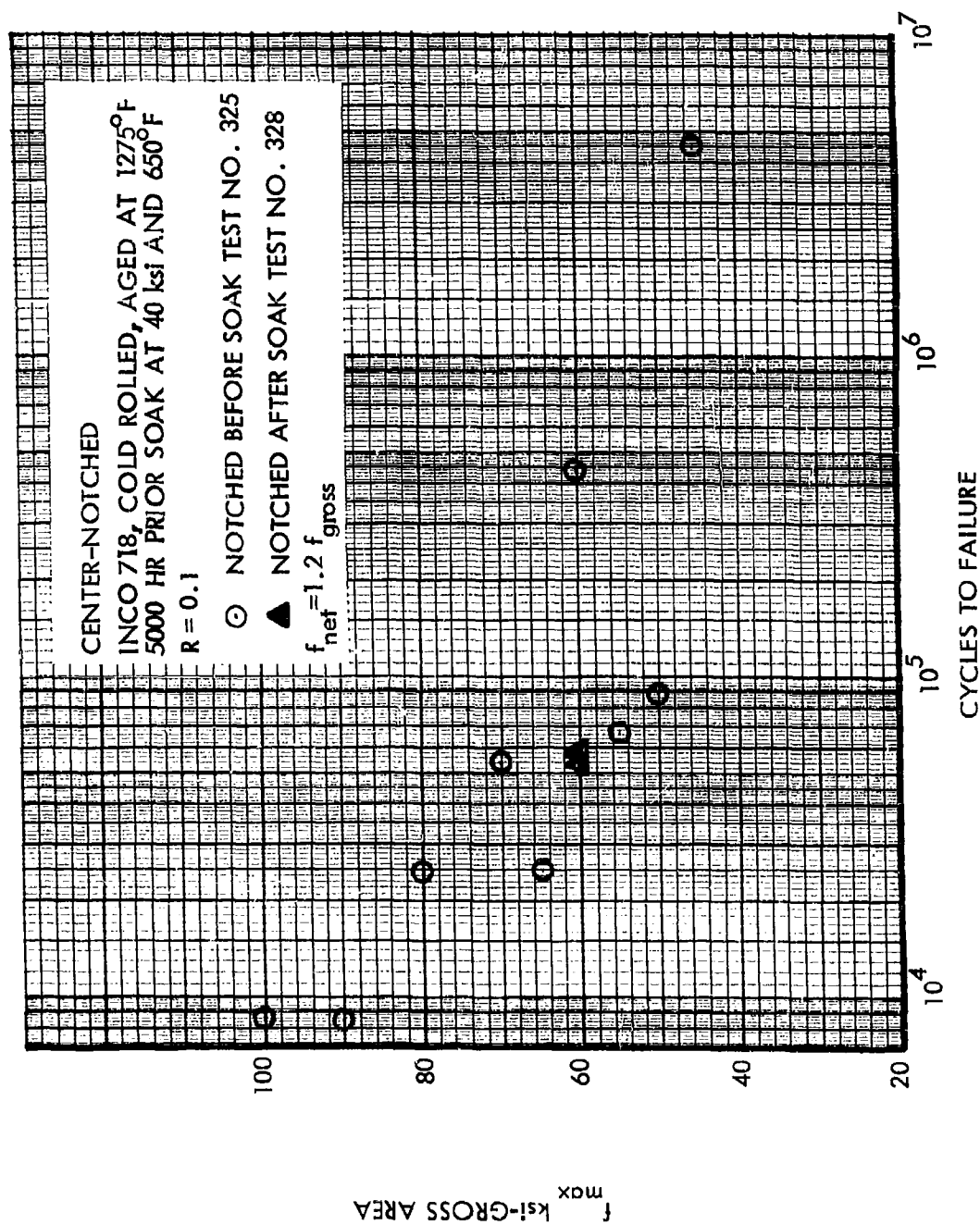
Figure 44. Comparison of S–N Data at Room Temperature, INCO 718, Notched Before and After Soak
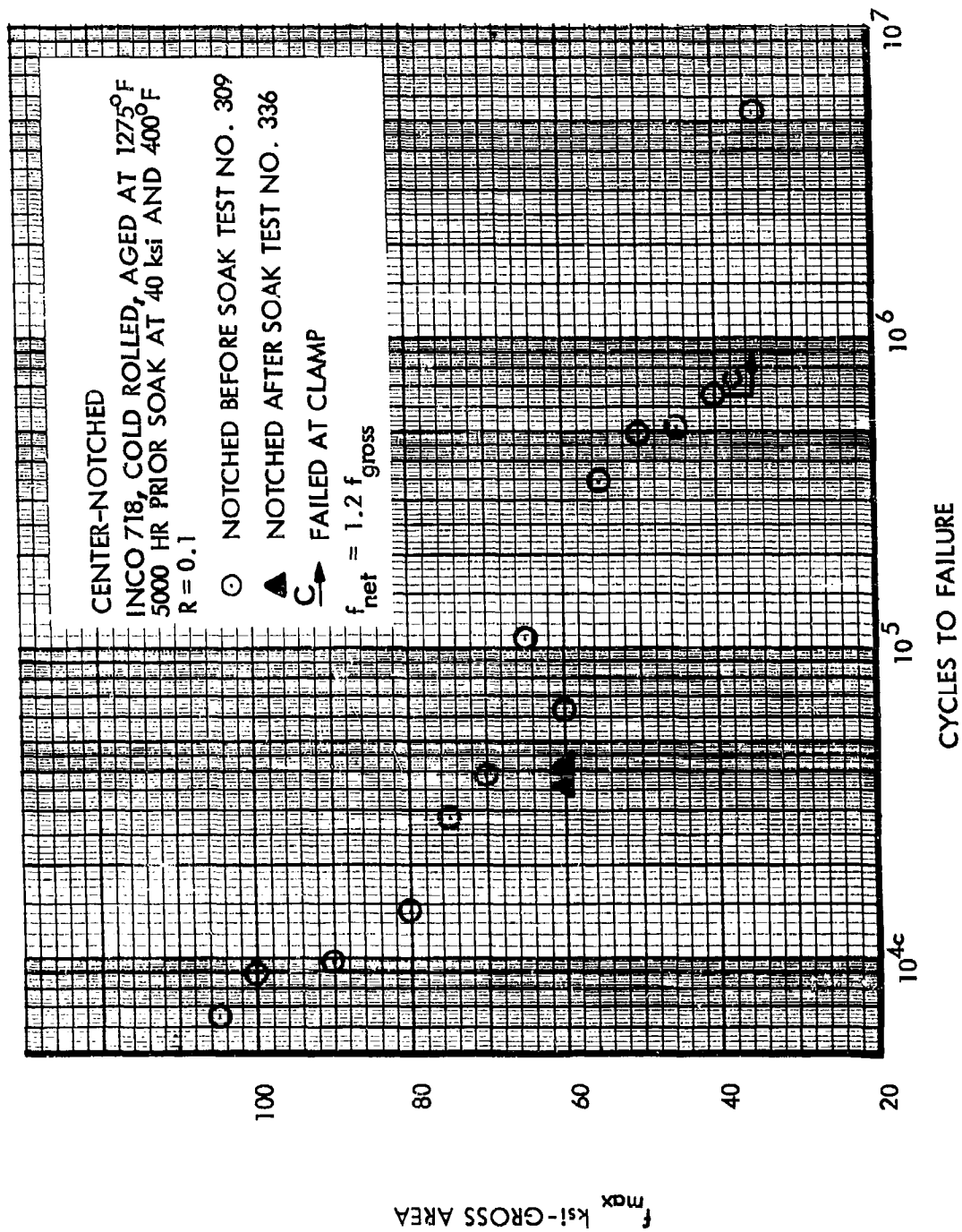
Figure 45. Comparison of S-N Data at 400°F, INCO 718, Notched Before and After Soak.
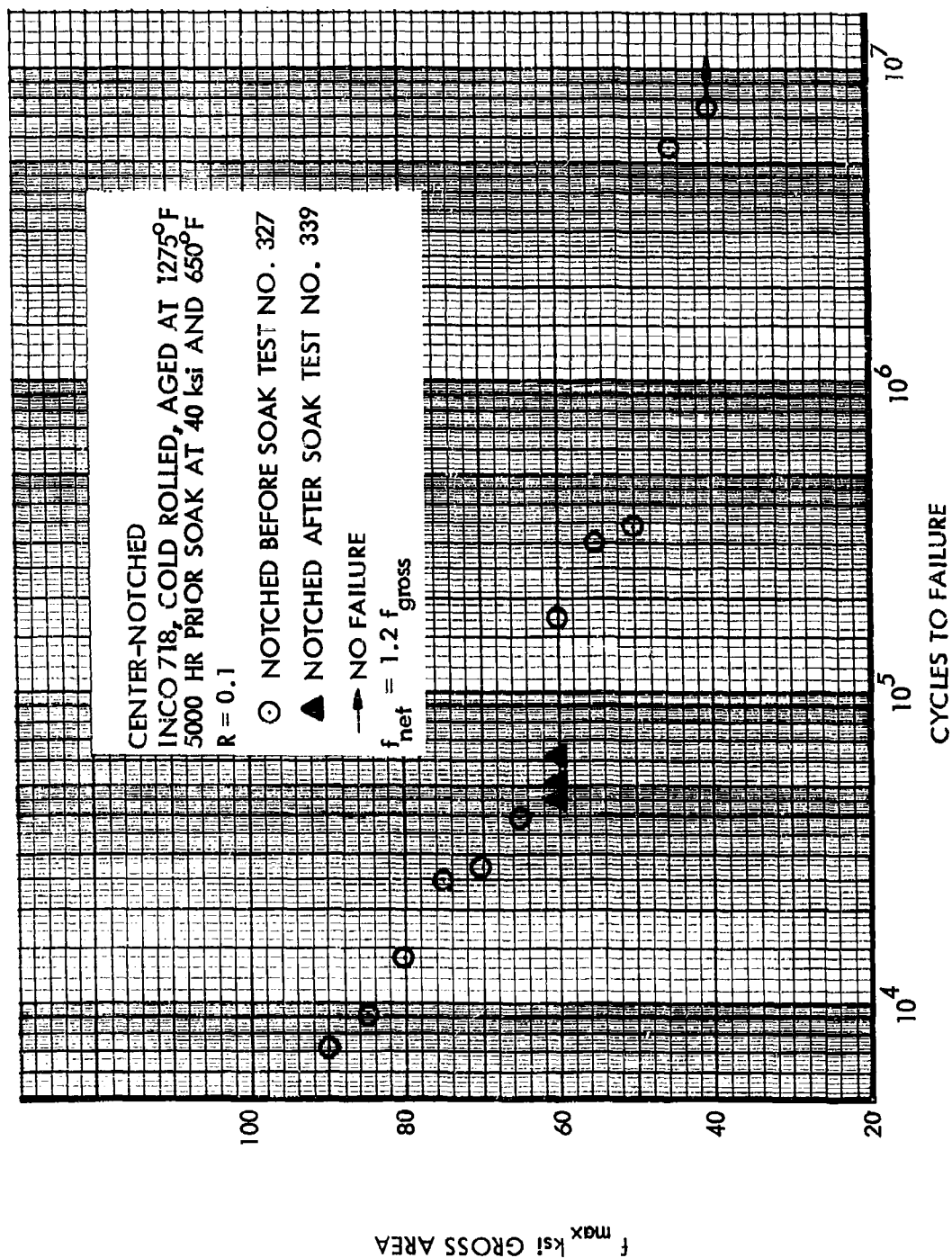
Figure 46. Comparison of S-N Data at 400°F, INCO 718, Notched Before and After Soak

CENTER-NOTCHED
INCO 718, COLD ROLLED, AGED AT $1275°F$
5000 HR PRIOR SOAK AT 40 ksi AND $400°F$
R = 0.1
⊙ CENTER NOTCHED BEFORE SOAK TEST NO. 311
▲ CENTER NOTCHED AFTER SOAK TEST NO. 337
→ NO FAILURE
$f_{net} = 1.2\ f_{gross}$

f_{max} ksi-GROSS AREA

100   80   60   40   20   0

10^4 10^5 10^6 10^7

CYCLES TO FAILURE
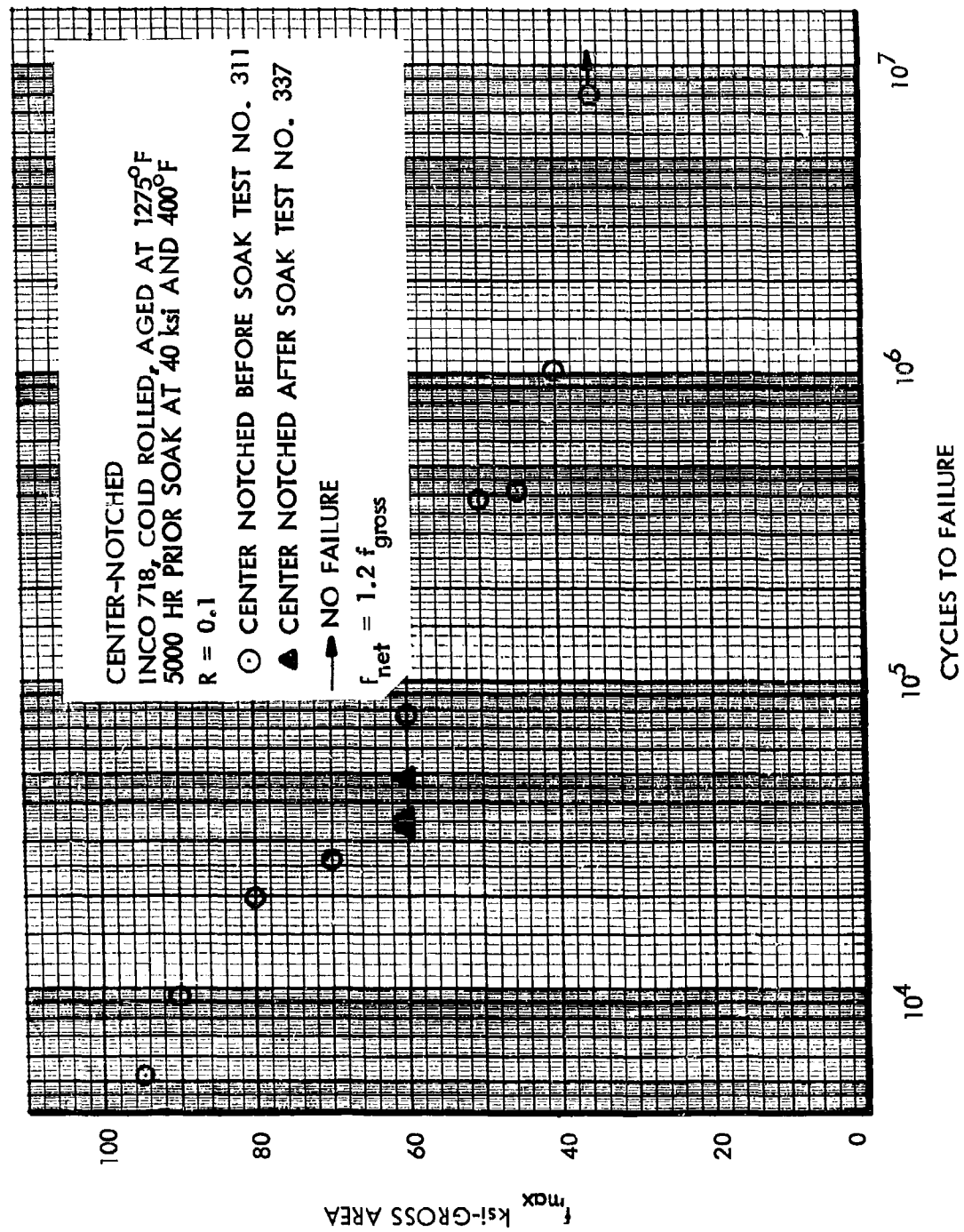
Figure 47. Comparison of S-N Data at $650°F$, INCO 718, Notched Before and After Soak

69

Figure 48. Comparison of S-N Data at 650°F, INCO 718, Notched Before and After Soak

70

TABLE 8 CONSTANT AMPLITUDE FATIGUE TEST DATA FOR SPECIMENS CENTER-NOTCHED AFTER EXPOSURE FOR 5000 HOURS

R = 0.1

MATERIAL	PRIOR SOAK 5000 HRS	TESTED AT ROOM TEMP.				TESTED AT 400°F				TESTED AT 650°F			
		TEST NO.	SPEC. NO.	f_{max} (ksi)	CYCLES TO FAILURE	TEST NO.	SPEC. NO.	f_{max} (ksi)	CYCLES TO FAILURE	TEST NO.	SPEC. NO.	f_{max} (ksi)	CYCLES TO FAILURE
8-1-1 Titanium Duplex Annealed	25 ksi 400°F	47	1 2 3	42 42 42	97,560 85,140 189,900	48	4 5 6	42 42 42	50,220 60,120 88,740	49	7 8 9	42 42 42	35,100 34,560 26,820
	25 ksi 650°F	50	13 14 15	42 42 42	64,260 40,140 69,480	51	16 17 18	42 42 42	54,180 55,080 55,800	52	19 20 21	42 42 42	33,840 50,760 1,800,000*
PH14-8Mo (SRH 1050)	40 ksi 400°F	191	1 2 3	50 50 50	101,160 78,660 148,500	192	4 5 6	58 58 58	21,420 23,220 25,020	193	7 8 9	58 58 58	18,540 21,240 26,100
	40 ksi 650°F	194	13 14 15	50 50 50	114,300 97,020 61,560	195	16 17 18	58 65 65	2,500,000* 18,900 21,780	196	19 20 21	58 65 65	2,500,000* 18,900 18,180
INCO 718 Cold Rolled, Aged at 1275°F	40 ksi 400°F	335	1 2 3	60 60 60	94,140 82,080 100,260	336	4 5 6	60 60 60	36,000 40,500 42,300	337	7 8 9	60 60 60	35,820 33,480 48,060
	40 ksi 650°F	338	13 14 15	60 60 60	58,860 56,880 53,100	339	16 17 18	60 60 60	50,760 62,100 44,820	340	19 20 21	60 60 60	31,140 39,060 57,260

*No failure

71

Figure 49. Comparison of S-N Data at Room Temperature, 8-1-1 Titanium, Planished and Unplanished Fusion Welds

72
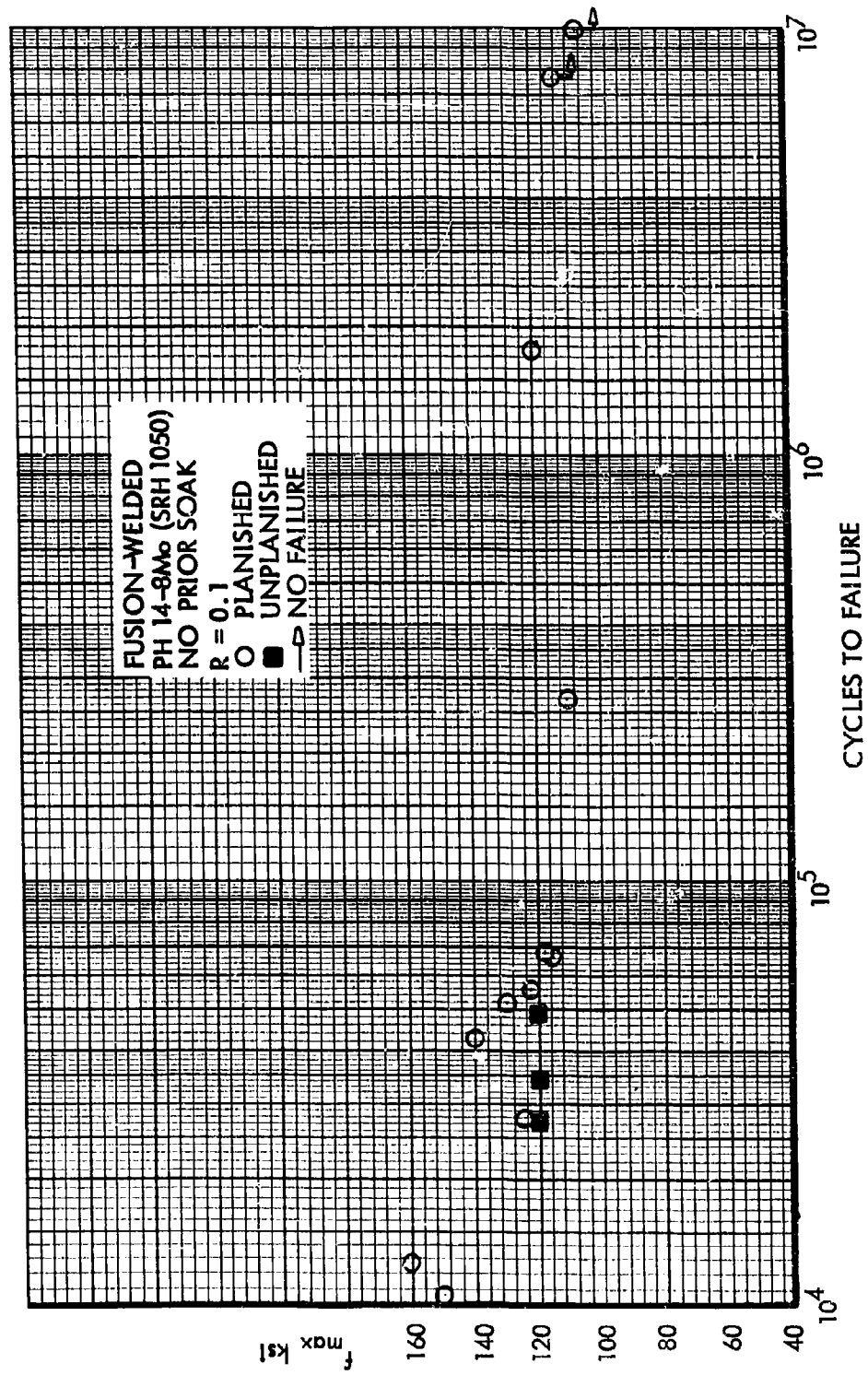
Figure 50. Comparison of S-N Data at Room Temperature, PH 14-8Mo, Planished and Unplanished Fusion Welds
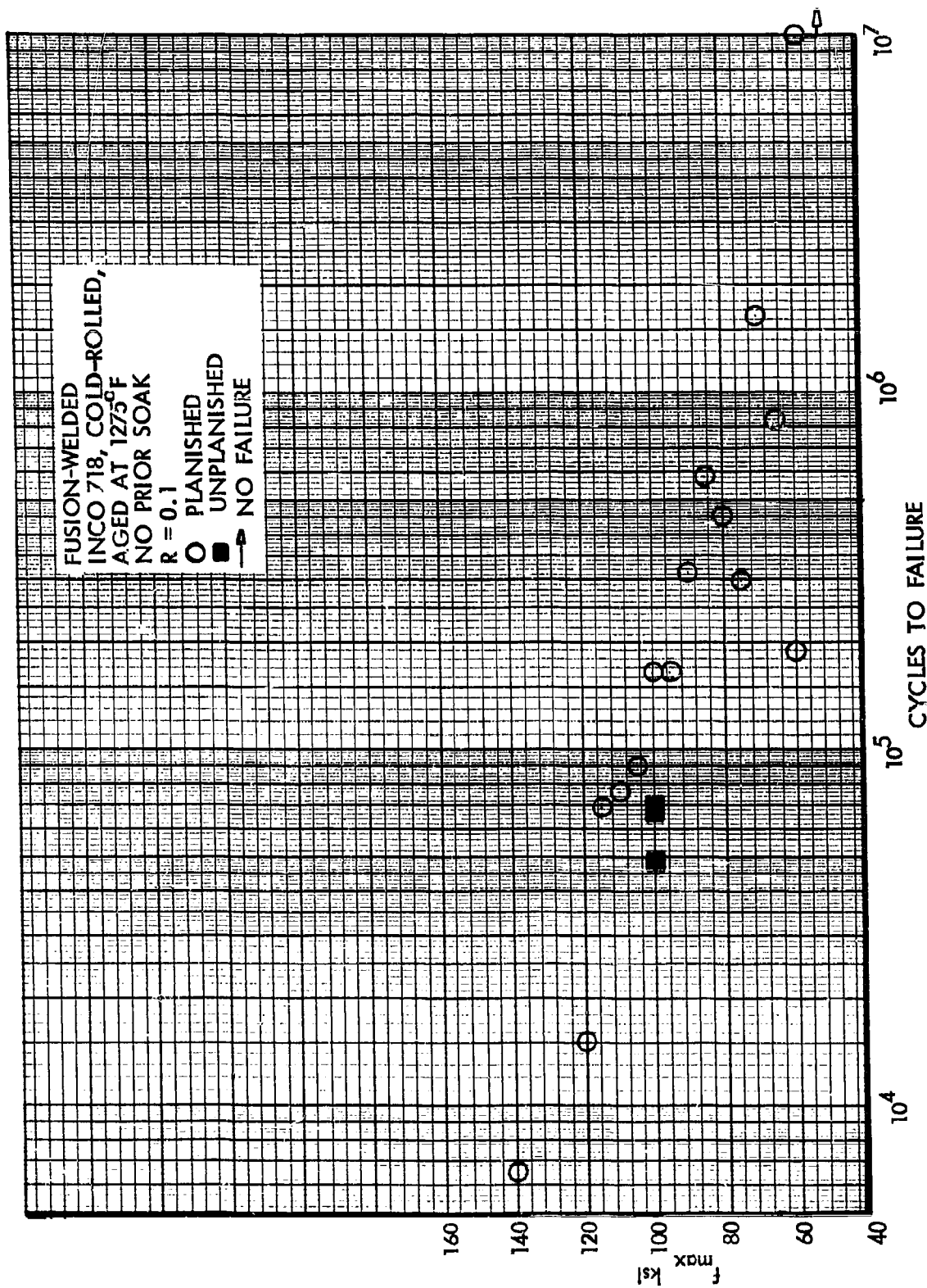
Figure 51. Comparison of S–N Data at Room Temperature, INCO 718, Planished and Unplanished Fusion Welds

TABLE 9   CONSTANT LOAD AMPLITUDE FATIGUE TESTS AT ROOM TEMPERATURE

UNPIANISHED FUSION-WELDED SPECIMENS

TRANSVERSE GRAIN
NO PRIOR SOAK
R = 0.1

Specimen Material	Test No.	f_{max} (ksi)	Cycles to Failure
8-1-1 Titanium Duplex-Annealed	99a	100 100 100	140,400 147,240 66,960
PH14-8Mo (SRH 1050) Stainless Steel	243a	120 120 120	34,380 27,540 48,780
INCO 718 Cold Rolled, Aged at 1275°F	387a	100 100 100	48,600 70,740 67,500

TABLE 10 LOCATION OF FAILURES IN FUSION-WELDED FATIGUE TEST SPECIMENS

Material	Total Number of Specimens Examined	Percent of Failures		
		Thru Weld	At Edge of Weld	Away From Weld
8-1-1 Ti Duplex Annealed	278	94.6 *	2.2	3.2
PH14-8Mo (SRH 1050) Stainless Steel	133	4.5	51.9	43.6
INCO 718 Cold Rolled, Aged at 1275°F	228	87.7	7.9	4.4

NOTE: No correlation was found between location of failure and scatter in S-N data.

* Through weld and heat affected zone.
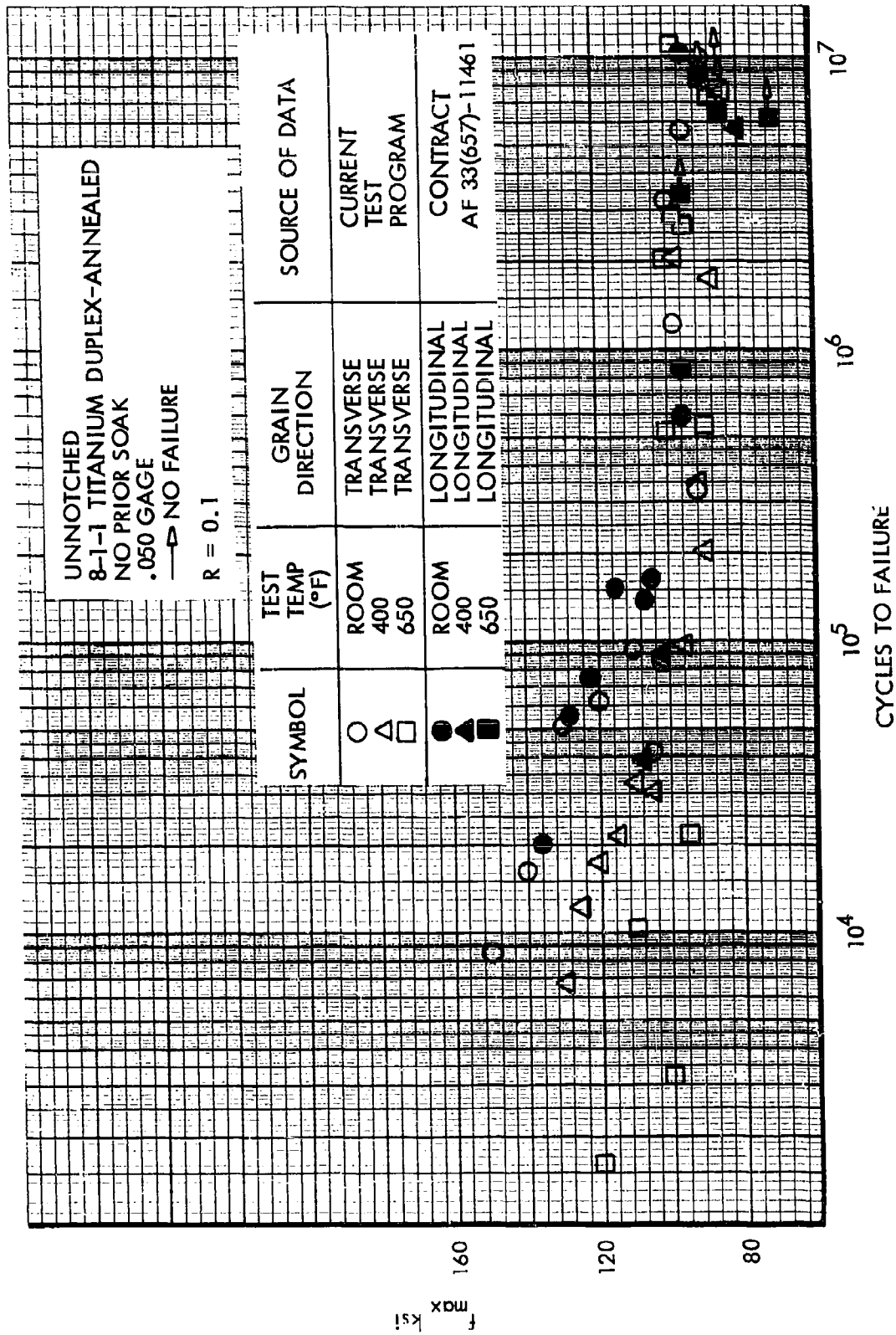
Figure 52. Comparison of S–N Data with Similar Data Obtained under AF 33(657)-11461, Unnotched 9-1-1 Titanium
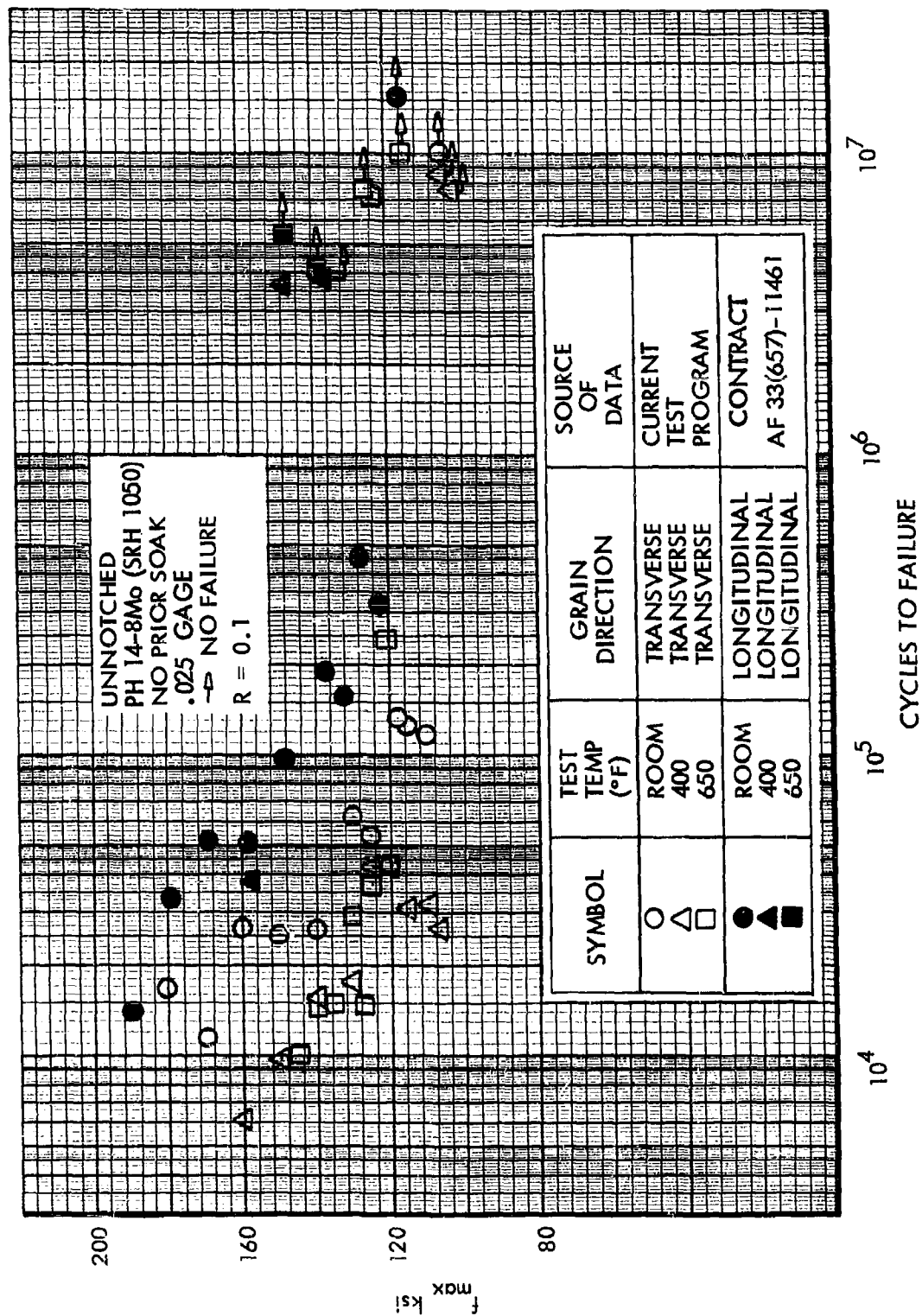
Figure 53. Comparison of S-N Data with Similar Data Obtained under AF 33(657)-11461, Unnotched PH 14-8Mo
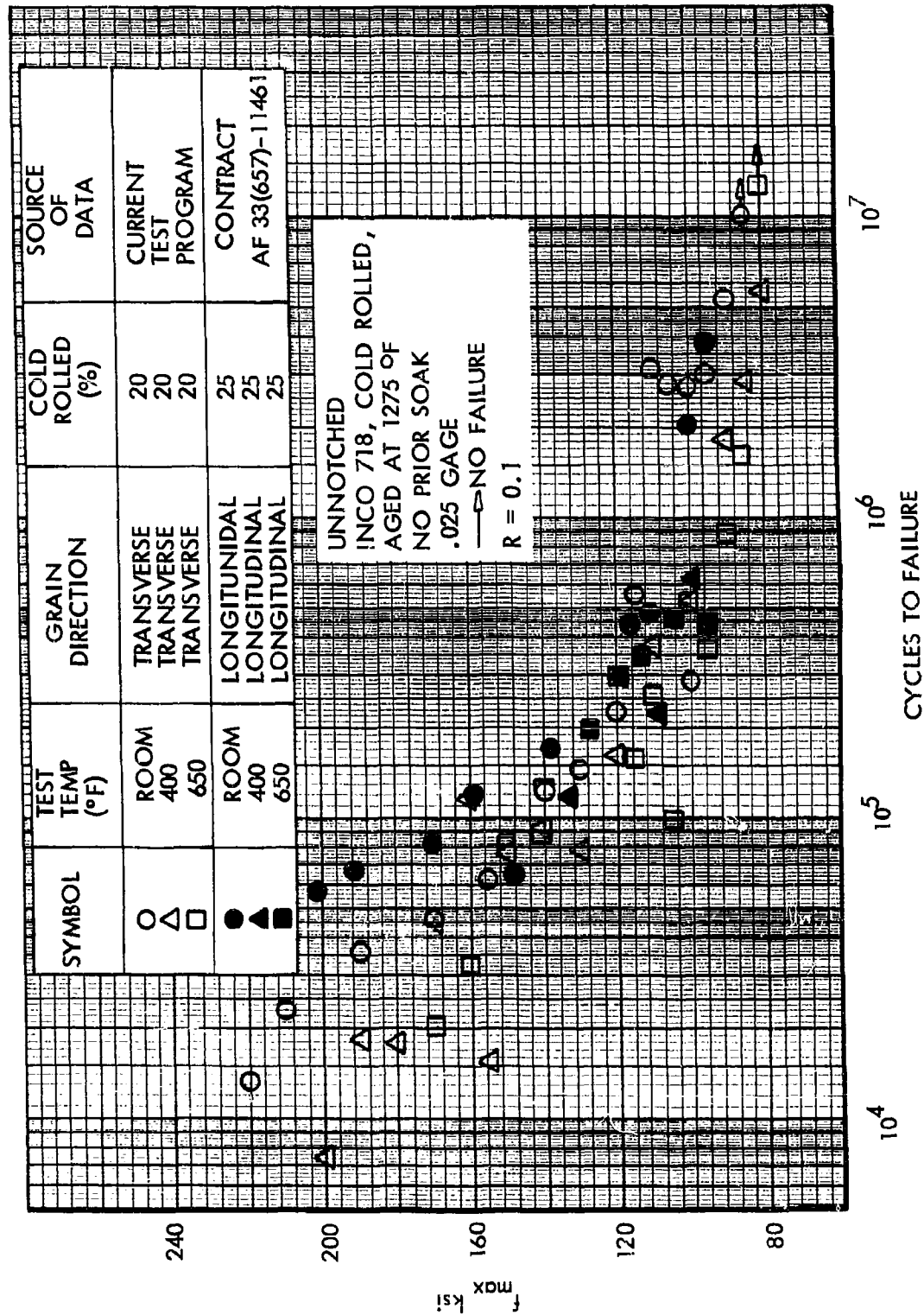
Figure 54. Comparison of S-N Data with Similar Data Obtained under AF 33(657)-11461, Unnotched INCO 718

The figure contains the following legend table:

SYMBOL		TEST TEMP (°F)	GRAIN DIRECTION	COLD ROLLED (%)	SOURCE OF DATA
○		ROOM	TRANSVERSE	20	CURRENT TEST PROGRAM
△		400	TRANSVERSE	20	
□		650	TRANSVERSE	20	
●		ROOM	LONGITUNIDAL	25	CONTRACT AF 33(657)-11461
▲		400	LONGITUDINAL	25	
■		650	LONGITUDINAL	25	

UNNOTCHED
INCO 718, COLD ROLLED, AGED AT 1275 °F
NO PRIOR SOAK
.025 GAGE
→ NO FAILURE

R = 0.1

CYCLES TO FAILURE

f_{max} ksi

79

Figure 55. Comparison of S-N Data with Similar Data Obtained under AF 33(657)-11461, Fusion-Welded 8-1-1 Titanium
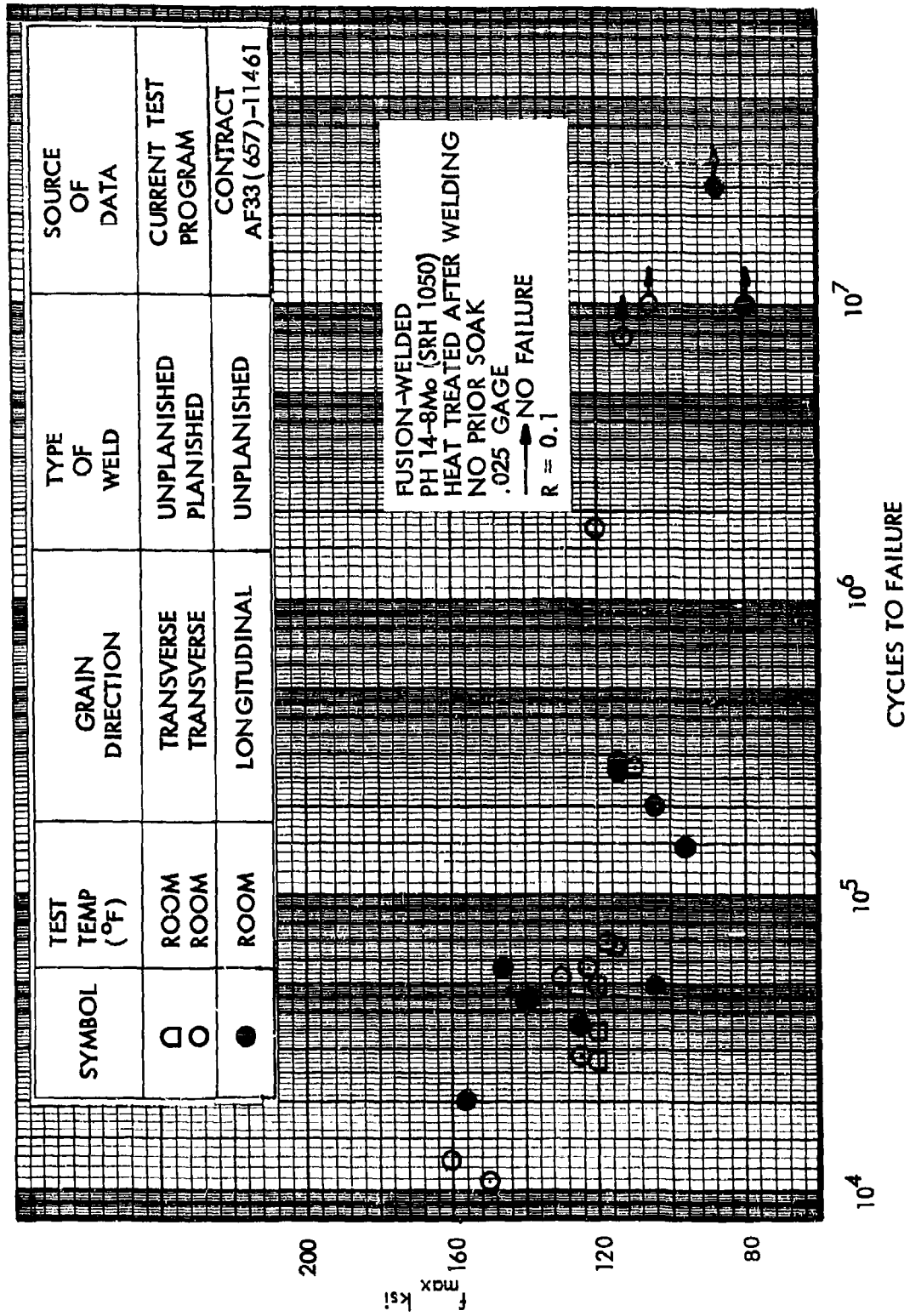
Figure 56. Comparison of S-N Data with Similar Data Obtained under AF 33(657)-11461, Fusion-Welded PH 14-8Mo

81
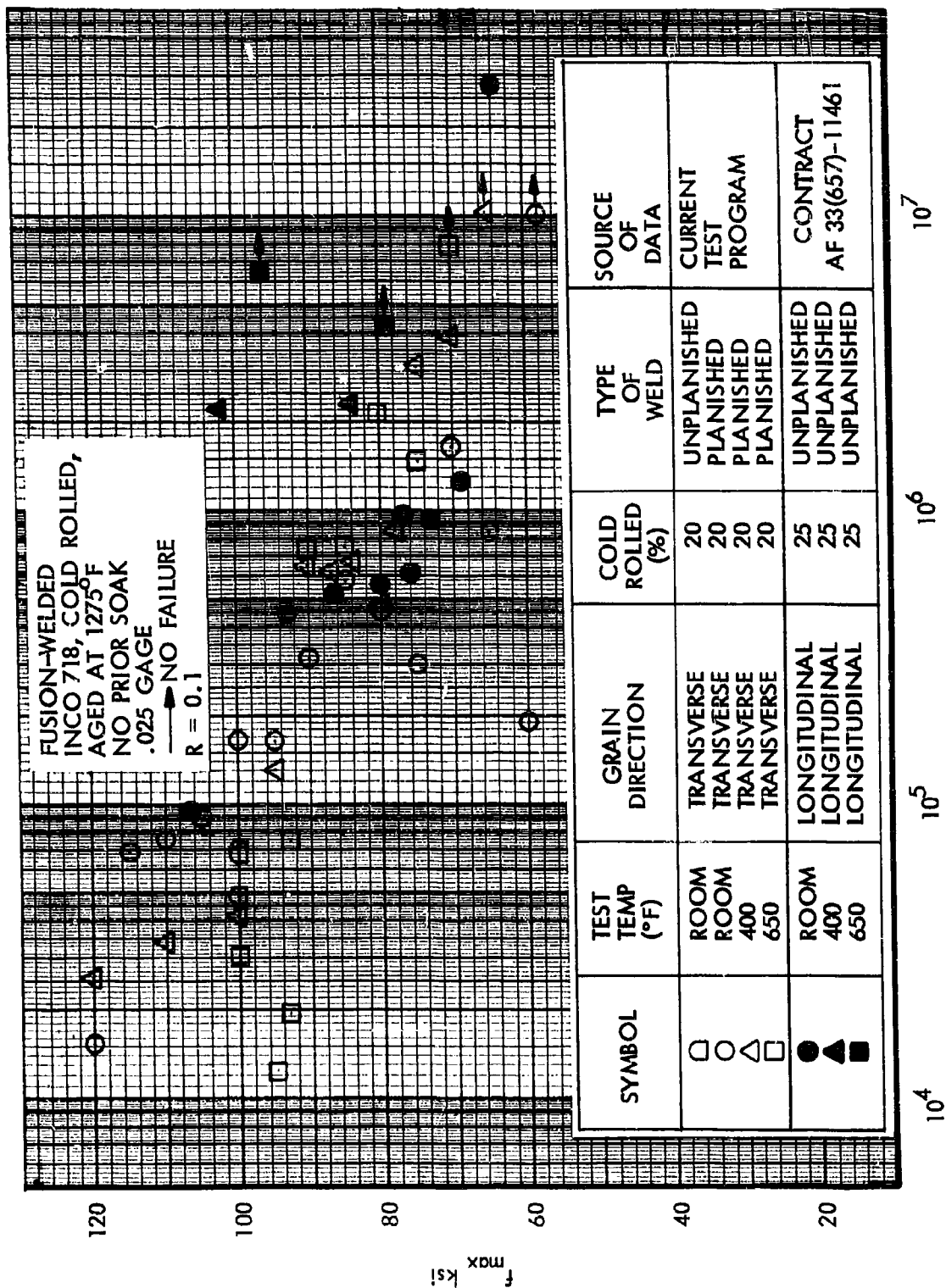
Figure 57. Comparison of S–N Data with Similar Data Obtained under AF 33(657)–11461, Fusion–Welded INCO 718

TABLE 11   CHANGE IN LENGTH AFTER 5000 HOURS OF EXPOSURE

PLAIN RECTANGULAR SPECIMENS TO BE CENTER-NOTCHED AFTER EXPOSURE
SIX INCH SPECIMEN LENGTH (L) BASED ON DISTANCE BETWEEN CENTERLINES
OF THE HOLES DRILLED AT ENDS OF SPECIMEN

SPEC. NO.	8-1-1 TITANIUM			PH14-8Mo			INCO 718		
	PRIOR SOAK	Δ L (in)	Δ L/L (in/in)	PRIOR SOAK	Δ L (in)	Δ L/L (in/in)	PRIOR SOAK	Δ L (in)	Δ L/L (in/in)
1		-.0055	-.00092		.0202	.00337		-.0078	-.00130
2		-.0055	-.00092		.0193	.00321		-.0090	-.00150
3		-.0056	-.00093		.0172	.00287		-.0080	-.00133
4	25 ksi	-.0058	-.00097	40 ksi	.0203	.00338	40 ksi	-.0057	-.00095
5	and	-.0053	-.00088	and	.0200	.00333	and	-.0054	-.00090
6	400°F	-.0056	-.00093	400°F	.0218	.00363	400°F	-.0062	-.00103
7	for	-.0038	-.00063	for	.0232	.00387	for	-.0063	-.00105
8	5000	-.0042	-.00070	5000	.0160	.00267	5000	-.0070	-.00117
9	hrs.	-.0018	-.00030	hrs.	.0213	.00355	hrs.	-.0073	-.00122
10		-.0042	-.00070		.0210	.00350		-.0063	-.00105
11		-.0048	-.00080		.0225	.00375		-.0054	-.00090
12		-.0018	-.00030		.0210	.00350		-.0067	-.00112
Average		-.0045	-.00075		.0203	.00339		-.0067	-.00111
13		0	0		.0195	.00325		-.0063	-.00105
14		0	0		.0100	.00167		-.0055	-.00092
15	25 ksi	0	0	40 ksi	.0196	.00327	40 ksi	-.0075	-.00125
16	and	0	0	and	.0195	.00325	and	-.0044	-.00073
17	650°F	0	0	650°F	.0195	.00175	650°F	-.0050	-.00083
18	for	0	0	for	.0170	.00283	for	-.0089	-.00148
19	5000	0	0	5000	.0102	.00170	5000	-.0093	-.00155
20	hrs.	0	0	hrs.	.0122	.00203	hrs.	-.0095	-.00158
21		0	0		.0102	.00170		-.0090	-.00150
22		0	0		.0193	.00322		-.0078	-.00130
23		0	0		.0125	.00208		-.0063	-.00105
24		0	0		.0145	.00243		-.0078	-.00130
Average		0	0		.0146	.00243		-.0073	-.00121

83

B. STATIC TENSILE TESTS

Static tensile tests were conducted at room temperature, 400 and 650°F to provide data on the effect of test temperature on the static strength properties of specimens with no prior exposure and to supplement the information on the effects of prior exposure which is provided by S-N data.

The Baldwin-Lima-Hamilton static test machine and the auxiliary test equipment used for these tests is described in Appendix IV. The test data are presented in Volume II and graphical presentations of lower boundaries of the data are presented in this section in Figures 58 through 69.

For specimens with no prior exposure, the reductions from room temperature values in the ultimate and yield strengths of plain 8-1-1 titanium specimens tested at 650°F were approximately 25 and 37 percent. For plain PH14-8Mo and Inco 718 specimens the corresponding reductions were approximately 6 and 9 percent. For fusion-welded specimens, the reductions in ultimate strength at 650°F were 26 percent for the 8-1-1 titanium, 19 percent for PH14-8Mo and 12 percent for Inco 718.

With the exception of moderate changes in the static yield and ultimate strength of PH14-8Mo steel, the effect on strength of prior exposures to constant load at temperature was small. Significant effects on specimen elongation were obtained for all materials. However, these effects can seldom be correlated with the effects of prior exposure on S-N data. For example, in the constant load amplitude tests, the unnotched specimens of PH14-8Mo were affected most by exposure conditions at 400°F while in the static tests the most pronounced effect on plain specimens was produced by exposure at 650°F.

A detailed examination of the data presented graphically on Figures 58 to 69 leads to the following comments.

For the plain 8-1-1 duplex-annealed titanium specimens, slight increases occurred in the ultimate tensile and yield strength after stressed exposure to temperature. The largest increase in F_{tu} at any of the test temperatures for these specimens was approximately 8 percent at 400°F after stressed exposure for 5000 hours at 650°F. The maximum increase in F_{ty} was 7 percent in tests conducted at room temperature after stressed exposure for 1000 hours at 650°F. The elongation of these specimens was decreased by several of the exposure conditions. The largest decrease in ductility was approximately 26 percent in tests at 650°F after 1000 hours of stressed exposure at 650°F. However, there was a 14 percent increase in ductility in tests at room temperature after the exposure described above and a 12 and 11 percent increase in tests at 650°F when the exposure time at 650°F was increased to 5000 hours. In tests at room temperature the only decrease in ductility occurred after prior exposure at 400°F for 1000 hours.

For PH14-8Mo plain specimens, the ultimate tensile and yield strengths showed significant increases after 1000 and 5000 hours of stressed exposure at

650°F. The largest increases of 23 and 26 percent in F_{tu} and F_{ty}, respectively, occurred in tests at room temperature after the 5000 hour exposure period. Such gains in strength after extended exposure at 650°F are typical of precipitation hardened steels. Also typical is a general tendency for a reduction in ductility. A 50 percent reduction was obtained in tests at room temperature after 1000 hours of stressed exposure at 650°F and 25 and 50 percent reductions occurred in tests at 400 and 650°F respectively, after 1000 hours exposure at 400°F. However, a 33 percent increase in ductility was obtained in tests at 650°F after 5000 hours of exposure at 650°F.

For Inco 718 plain specimens, none of the exposure conditions had any significant effect on the ultimate and yield strength of the material. The maximum changes in F_{tu} were approximately a 4 percent increase in tests at room temperature after 1000 hours of stressed exposure at 400°F and a 5 percent decrease in tests at 650°F after 5000 hours of exposure at 400°F. The largest change in F_{ty} was a 4 percent increase in tests at room temperature after 5000 hours of stressed exposure at 650°F. The significant changes in elongation were a 14 percent decrease in tests at room temperature after 5000 hours of stressed exposure at 400°F and a 23 percent decrease in tests at 400°F after stressed exposure for 5000 hours at 400°F or 1000 hours at 650°F. All other changes in elongation after stressed exposure were less than 8 percent.

The effects of stressed exposure to temperature on fusion-welded specimens were also evaluated in static tests conducted at room temperature, 400 and 650°F. During these tests, extensometers were not used to measure the elongation and yield strength because abrupt specimen failures could lead to instrument damage.

The general effect of exposure on fusion-welded 8-1-1 titanium specimens was an increase in tensile strength. The largest increase occurred after 1000 hours of stressed exposure at 650°F and ranged from 10 percent at a test temperature of 400°F to 6 percent in tests conducted at room temperature. The only stressed exposure condition to reduce the ultimate tensile strength of 8-1-1 titanium was 5000 hours at 400°F with the resulting reductions ranging from 4 percent at a test temperature of 650°F to 2 percent at the 400°F test temperature.

For PH14-8Mo fusion-welded specimens, the ultimate tensile strength was increased by 12 percent at a test temperature of 650°F after being exposed to stress at 650°F for 1000 hours. A 12 percent increase in ultimate tensile strength occurred at a test temperature of 400°F after 5000 hours of stressed exposure at 650°F. The ultimate strength of fusion-welded PH14-8Mo specimens is also reduced after stressed exposure. The peak reduction of 5 percent occurs at a test temperature of 400°F after 5000 hours of stressed exposure at 400°F.

The tensile strength of the fusion-welded Inco 718 specimens was generally reduced a small amount by stressed exposure at temperature. The largest reduction of 6 percent occurred at a test temperature of 650°F after 1000 hours of stressed exposure at the same temperature.

During the static tests conducted on the fusion-welded specimens, it was

noted that failures occurred at different locations for each material. The fusion-welded 8-1-1 titanium specimens always failed in the base metal away from the weld. These specimens had static strengths comparable to the plain specimens, as shown in Figures 58 and 67.

While all failures were in or immediately adjacent to the weld in the fusion-welded PH14-8Mo specimens, the static tensile strength was only slightly reduced below that for the parent metal. This is to be expected since these specimens were heat treated after welding.

Most of the fusion-welded Inco 718 specimens failed in the weld zone since the weld metal strength was appreciably less than that of the cold rolled and aged parent metal.

The failure locations for the fusion-welded 8-1-1 titanium and Inco 718 specimens were the same as those obtained in the Boeing-North American Joint Venture under Air Force Contract AF33(657)-11461. However, all of the .025 inch thick PH14-8Mo specimens which were heat treated after welding failed in or near the weld zone in this test program while the majority of the corresponding Boeing-North American test specimens failed in the base metal during static tests.

A comparison of the tensile properties of plain and fusion-welded specimens reported by Boeing-North American with those obtained in the current program is provided by the data listed in Table 12. The data from the two programs are considered to show good agreement.

In order to compare the materials on the basis of static tensile properties, the lower boundaries of values for all exposure conditions are presented in Figures 70 and 71. These figures show that, using the ultimate strength to density ratio for both the plain and fusion-welded specimens, the 8-1-1 titanium would be rated first, PH14-8Mo steel second and Inco 718 third at all test temperatures. The same rating would also apply to comparisons of the elongations along a two inch gage length for these materials. This rating does not apply when using the yield strength to density ratio for plain specimens. In tests conducted at room temperature, the 8-1-1 titanium would be rated first, Inco 718 second and PH14-8Mo third. In tests conducted at 650°F, these ratings would be reversed. For the 400°F test temperature, PH14-8Mo is rated first, 8-1-1 titanium second and Inco 718 third.

The comparison of ultimate tensile strengths of plain and fusion welded specimens presented in Figure 71 emphasizes the large decrease in strength of Inco 718 specimens when they contain fusion welds which are not heat treated after welding.
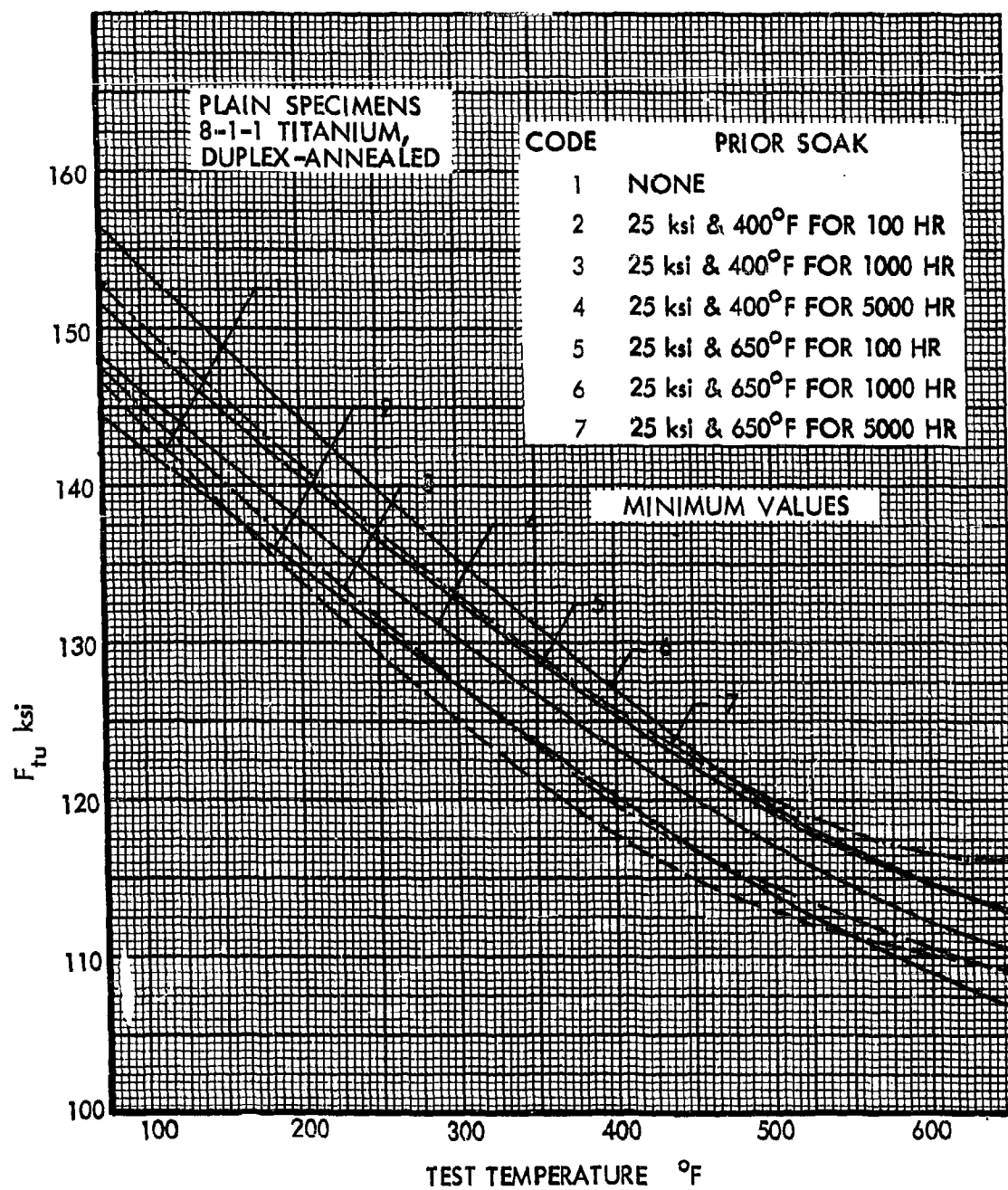
Figure 58. Effects of Prior Soak on Ultimate Tensile Strength,
Plain Specimens, 8-1-1 Titanium
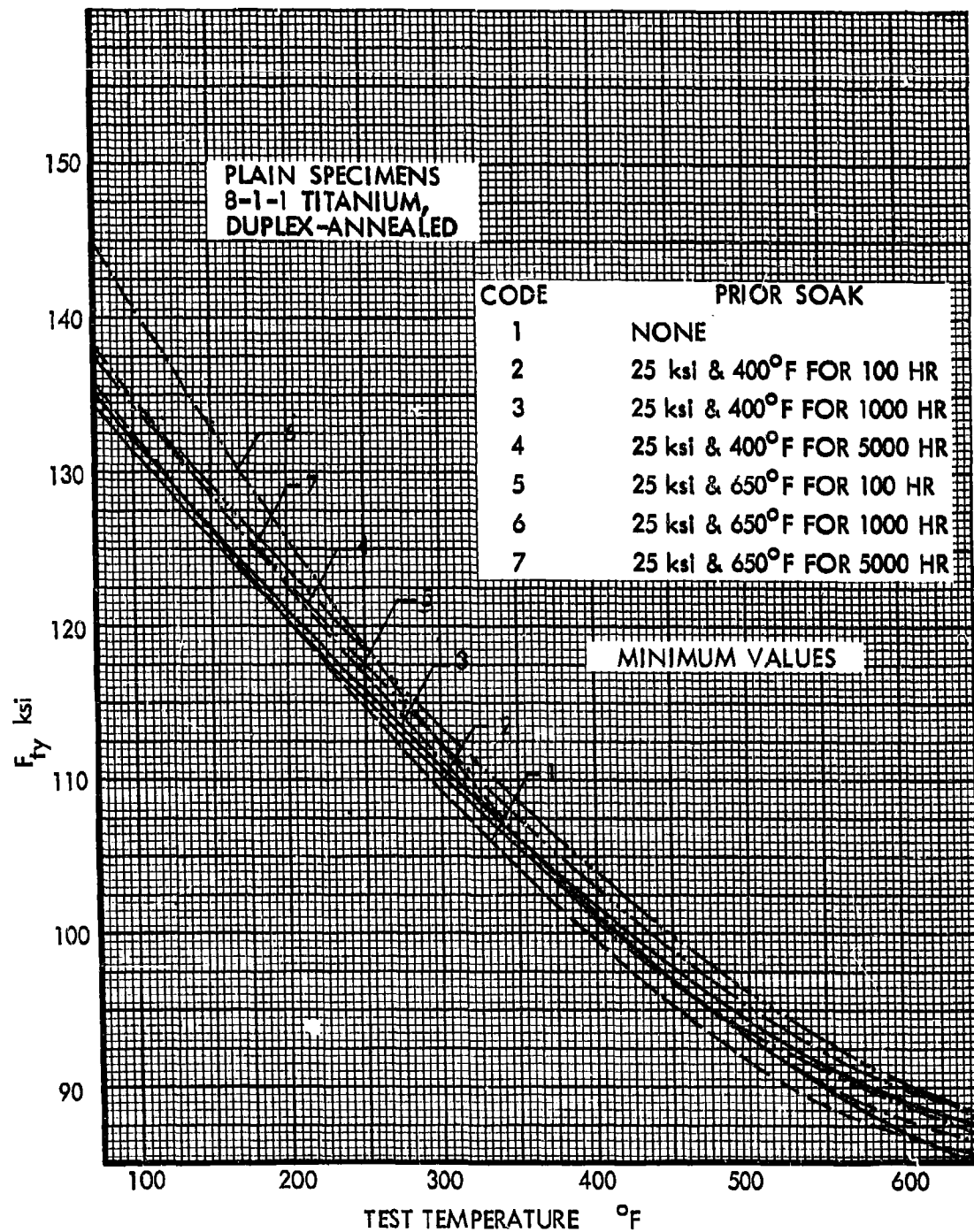
Figure 59. Effects of Prior Soak on Yield Strength, Plain Specimens, 8-1-1 Titanium
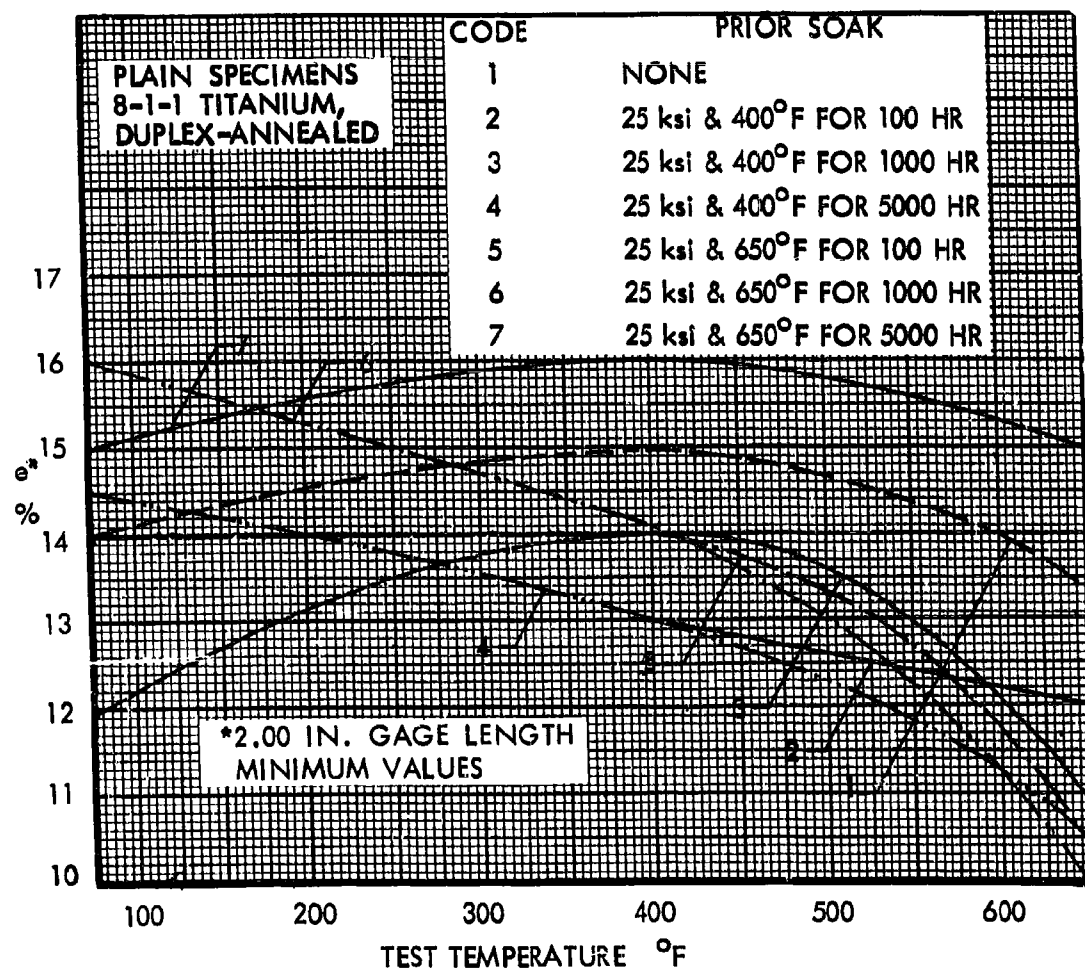
Figure 60. Effects of Prior Soak on Elongation, Plain Specimens, 8-1-1 Titanium

89
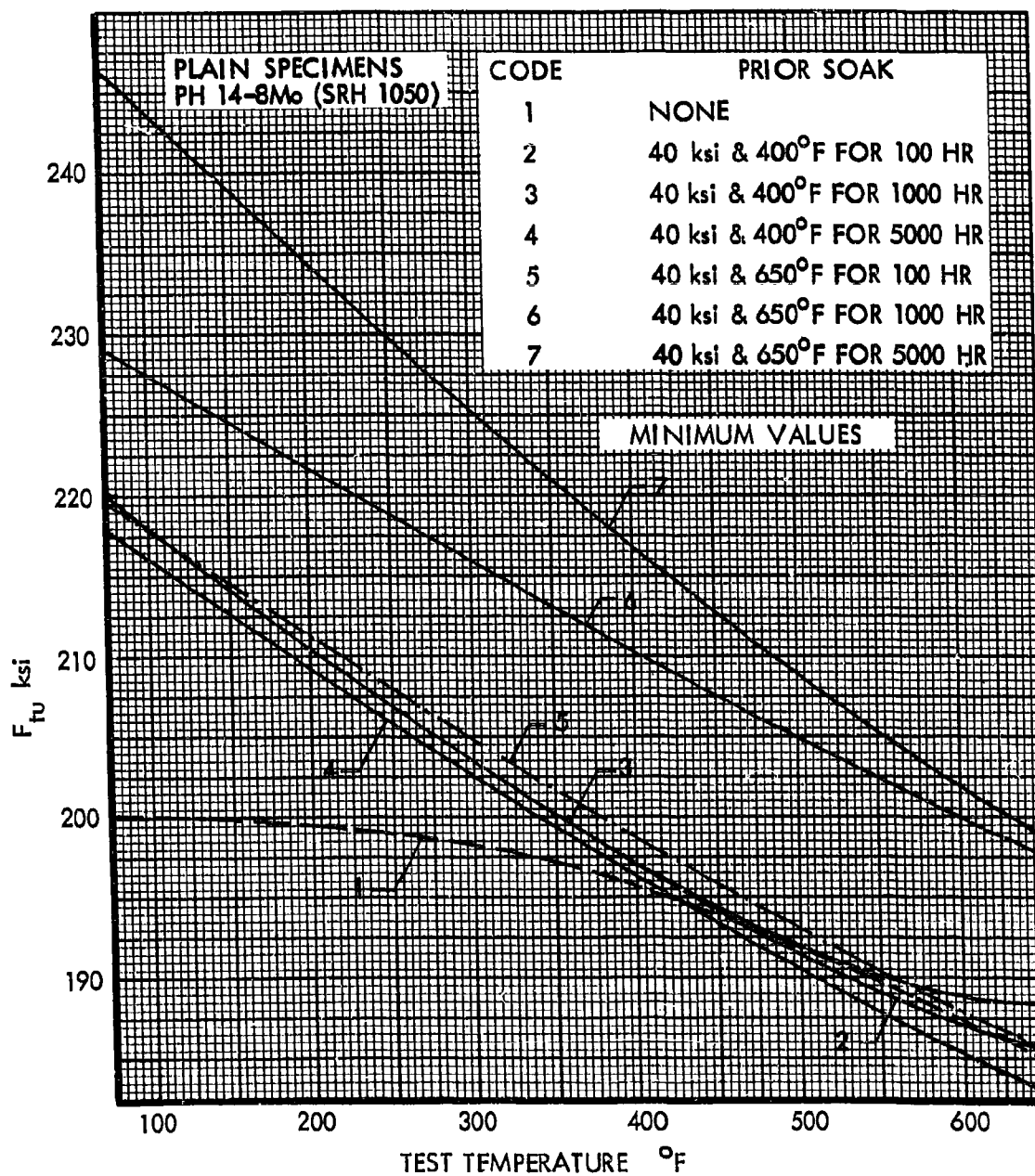
Figure 61. Effects of Prior Soak on Ultimate Tensile Strength,
Plain Specimens, PH 14-8Mo
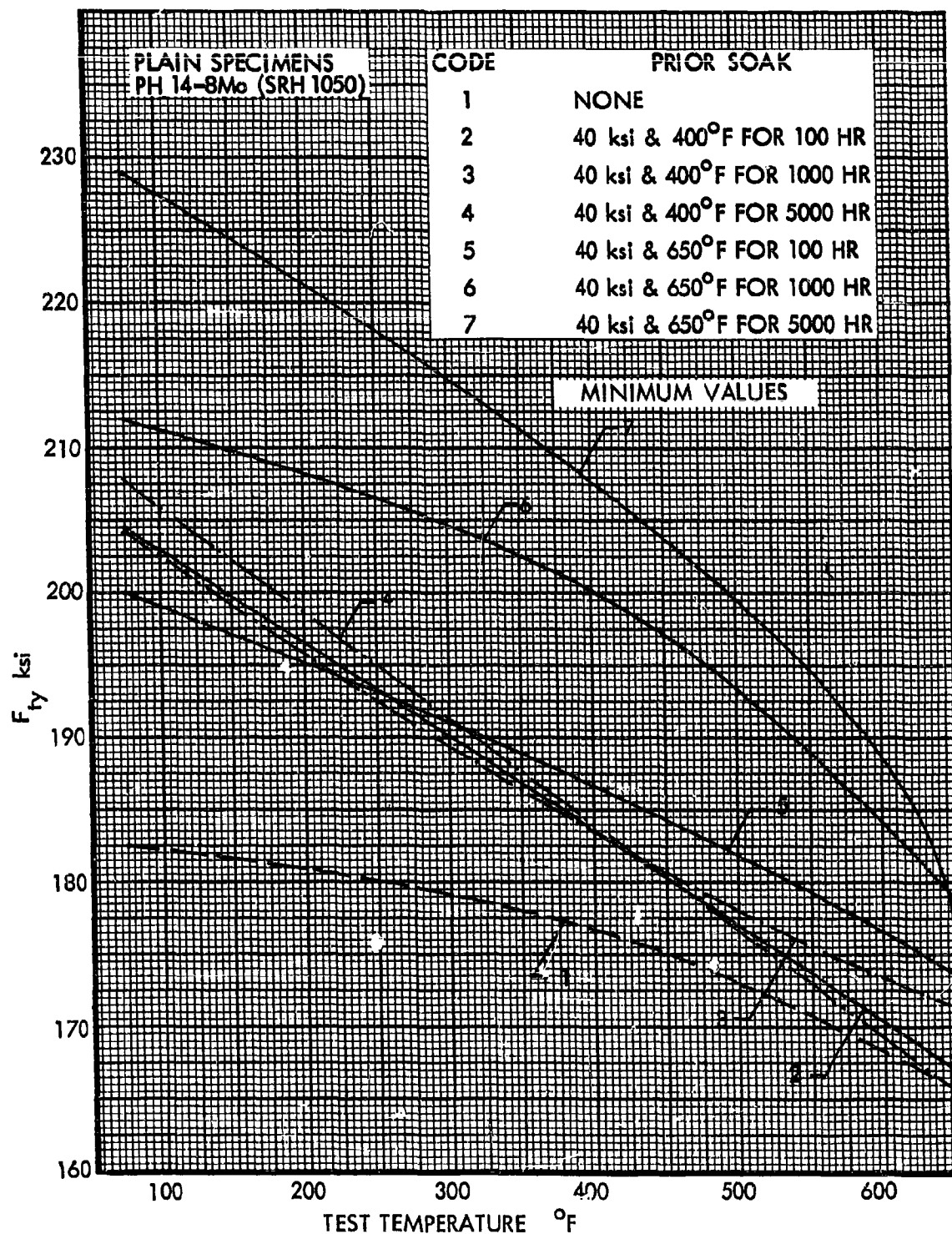
Figure 62. Effects of Prior Soak on Yield Strength, Plain Specimens, PH 14-8Mo

Code table:

CODE	PRIOR SOAK
1	NONE
2	40 ksi & 400°F FOR 100 HR
3	40 ksi & 400°F FOR 1000 HR
4	40 ksi & 400°F FOR 5000 HR
5	40 ksi & 650°F FOR 100 HR
6	40 ksi & 650°F FOR 1000 HR
7	40 ksi & 650°F FOR 5000 HR
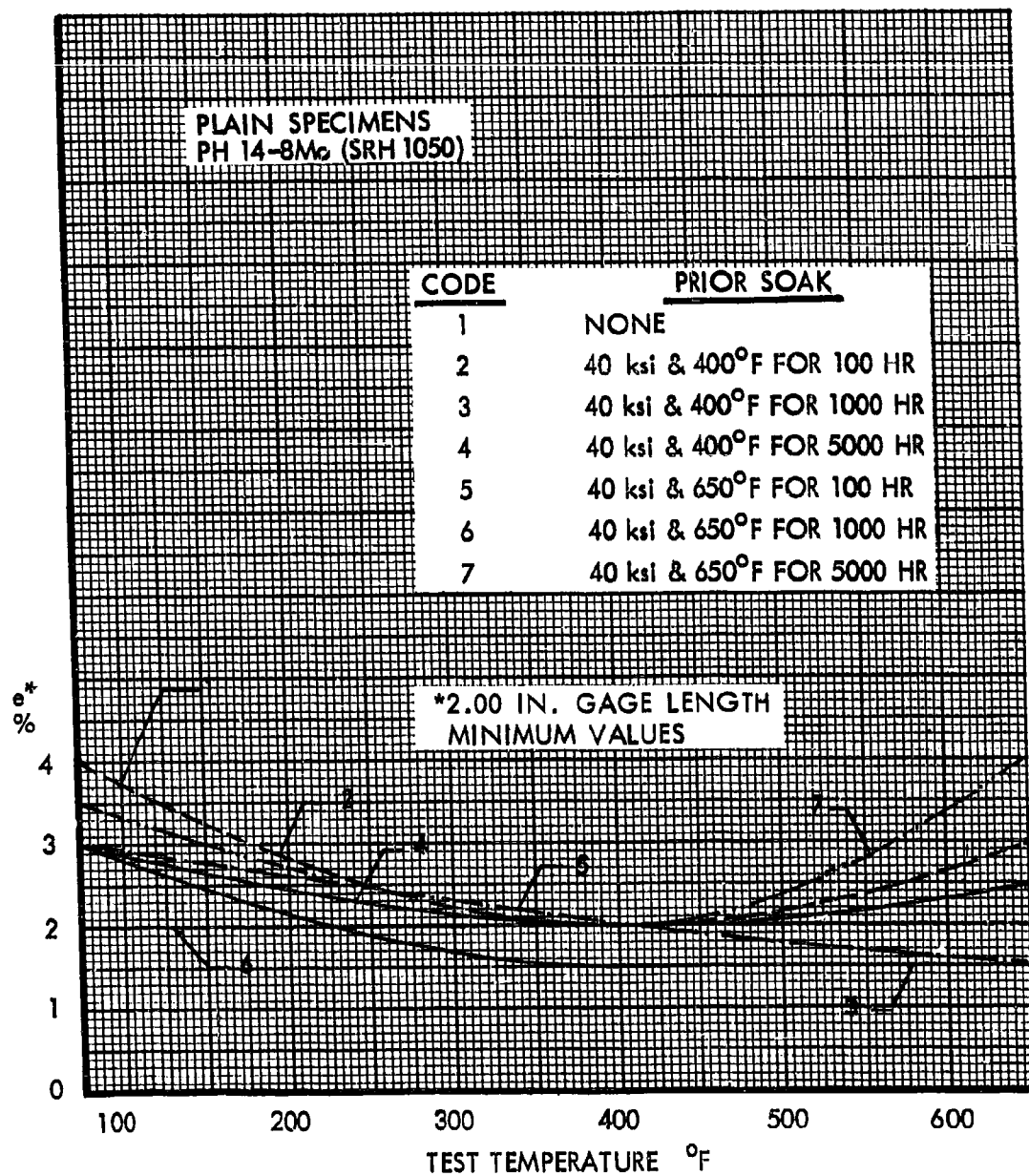
Figure 63.   Effects of Prior Soak on Elongation, Plain Specimens, PH14-8Mo
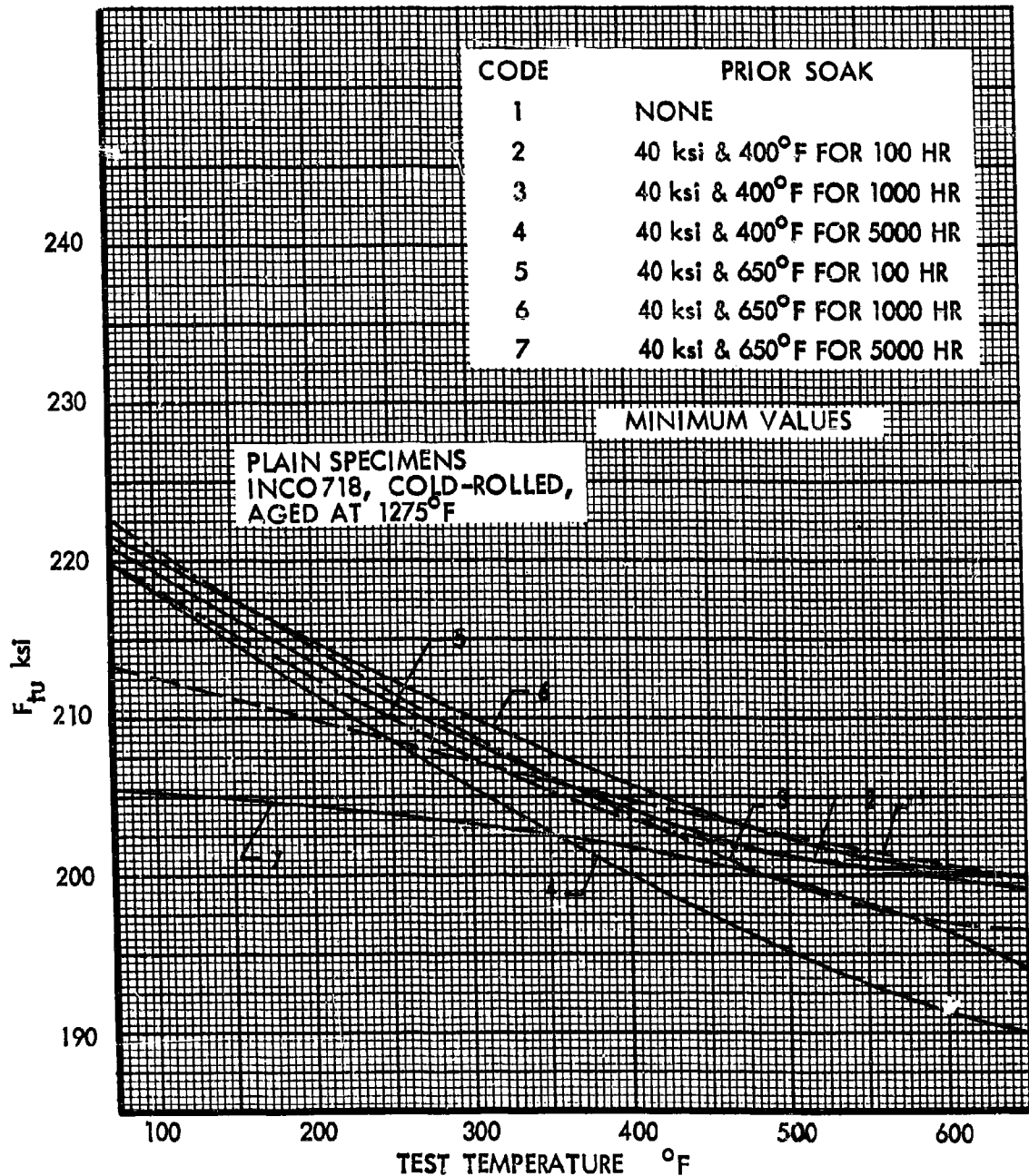
Figure 64.   Effects of Prior Soak on Ultimate Tensile Strength,
Plain Specimens, INCO 718
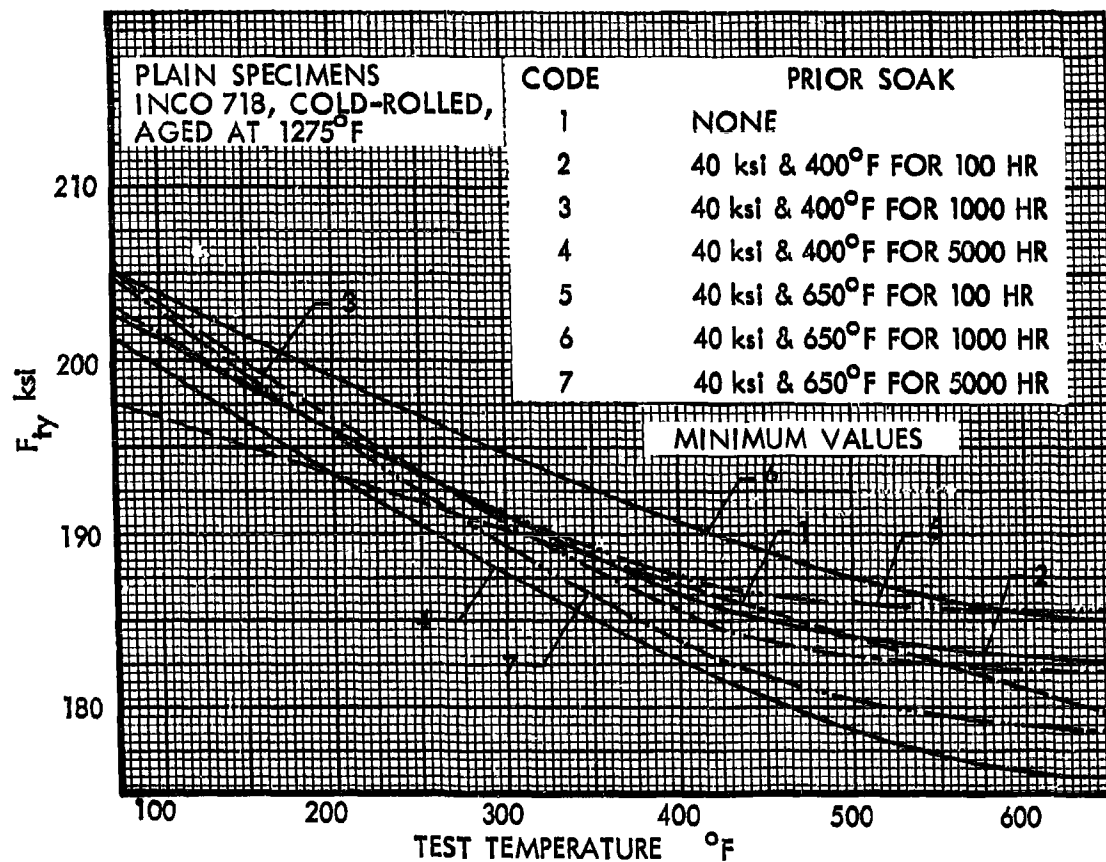
Figure 65. Effects of Prior Soak on Yield Strength, Plain Specimens, INCO 718
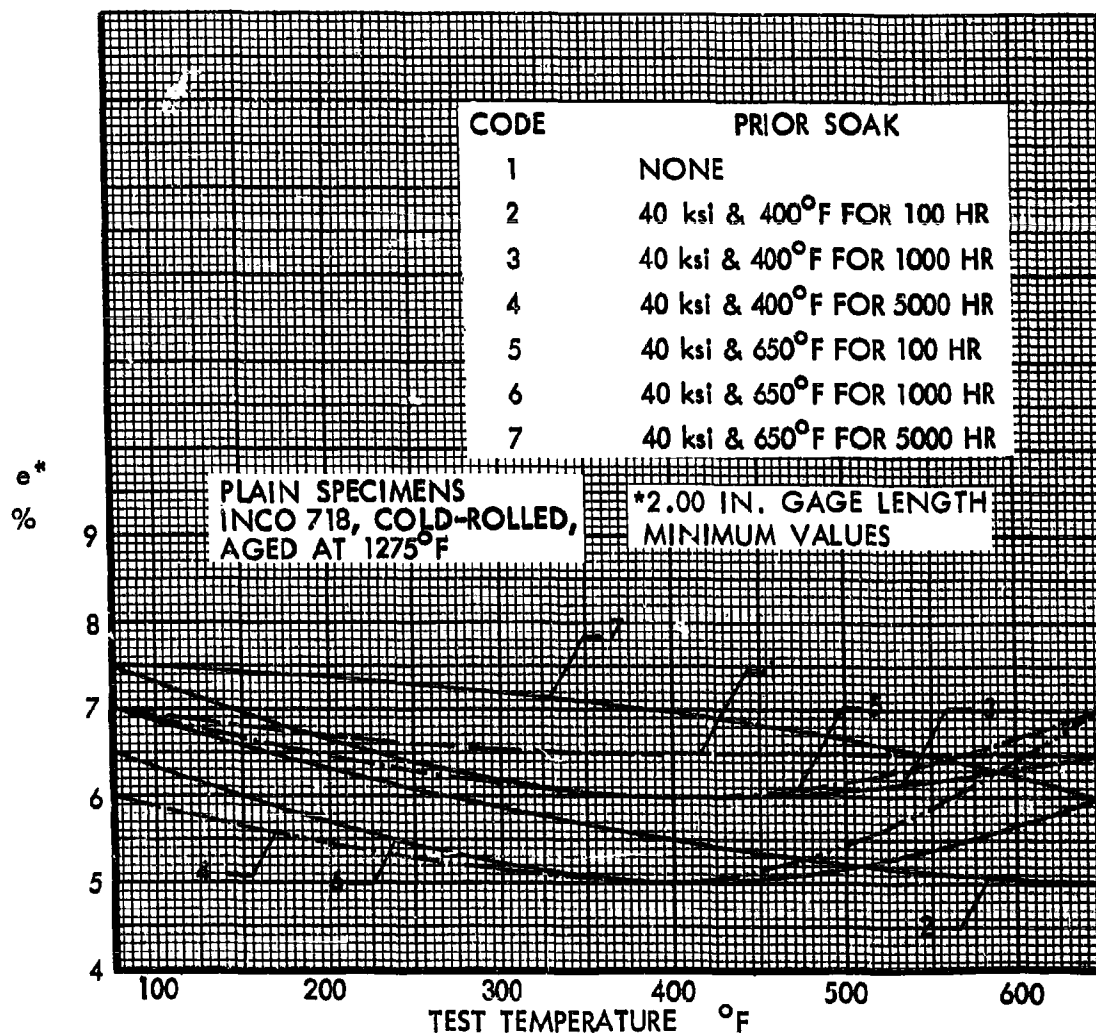
Figure 66. Effects of Prior Soak on Elongation, Plain Specimens, INCO 718

CODE	PRIOR SOAK
1	NONE
2	25 ksi & 400°F FOR 100 HR
3	25 ksi & 400°F FOR 1000 HR
4	25 ksi & 400°F FOR 5000 HR
5	25 ksi & 650°F FOR 100 HR
6	25 ksi & 650°F FOR 1000 HR
7	25 ksi & 650°F FOR 5000 HR

MINIMUM VALUES

FUSION-WELDED
& PLANISHED
8-1-1 TITANIUM,
DUPLEX-ANNEALED

TEST TEMPERATURE °F

F_{tu} ksi
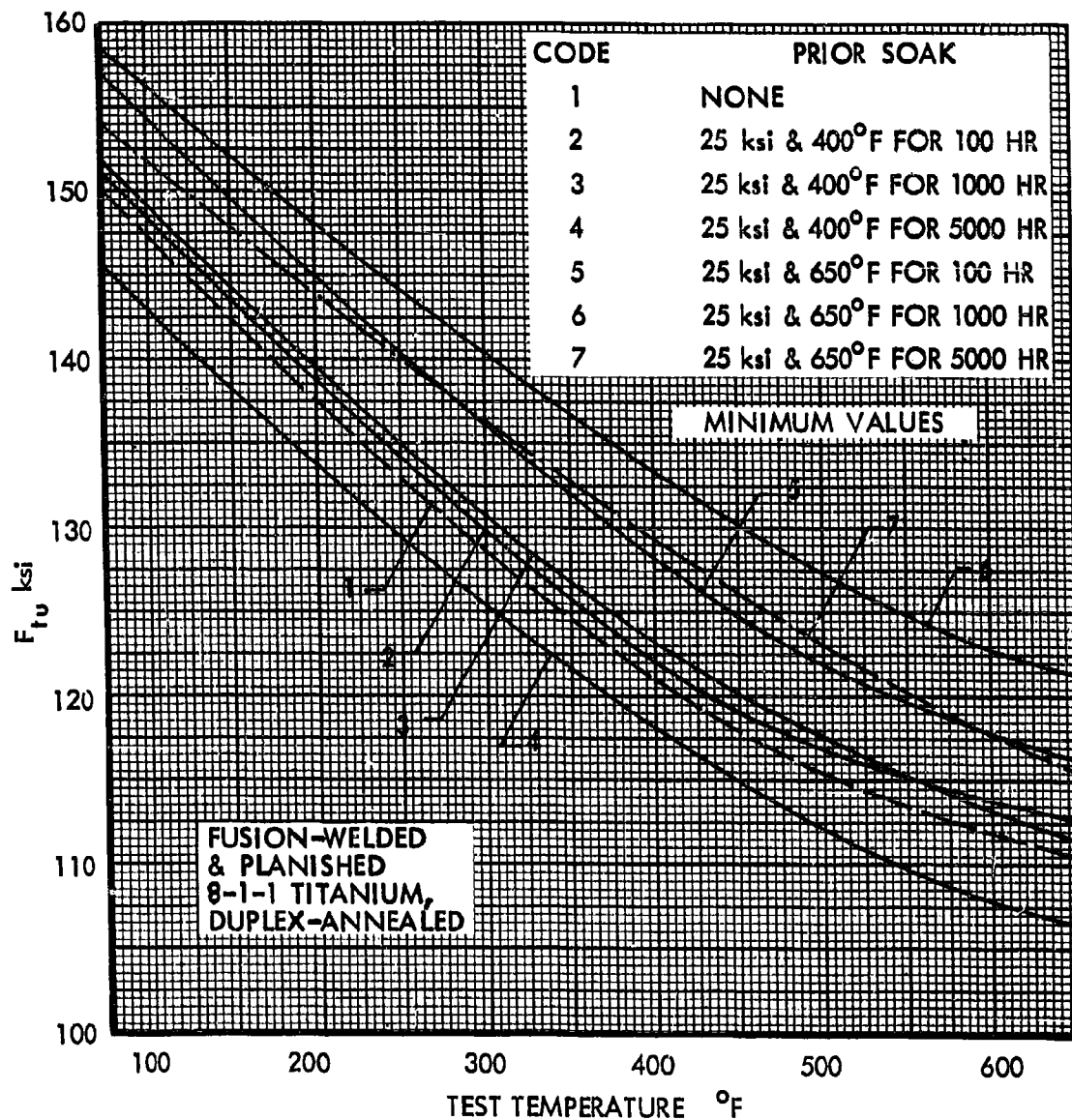
Figure 67.   Effects of Prior Soak on Ultimate Tensile Strength,
Fusion-Welded 8-1-1 Titanium

96
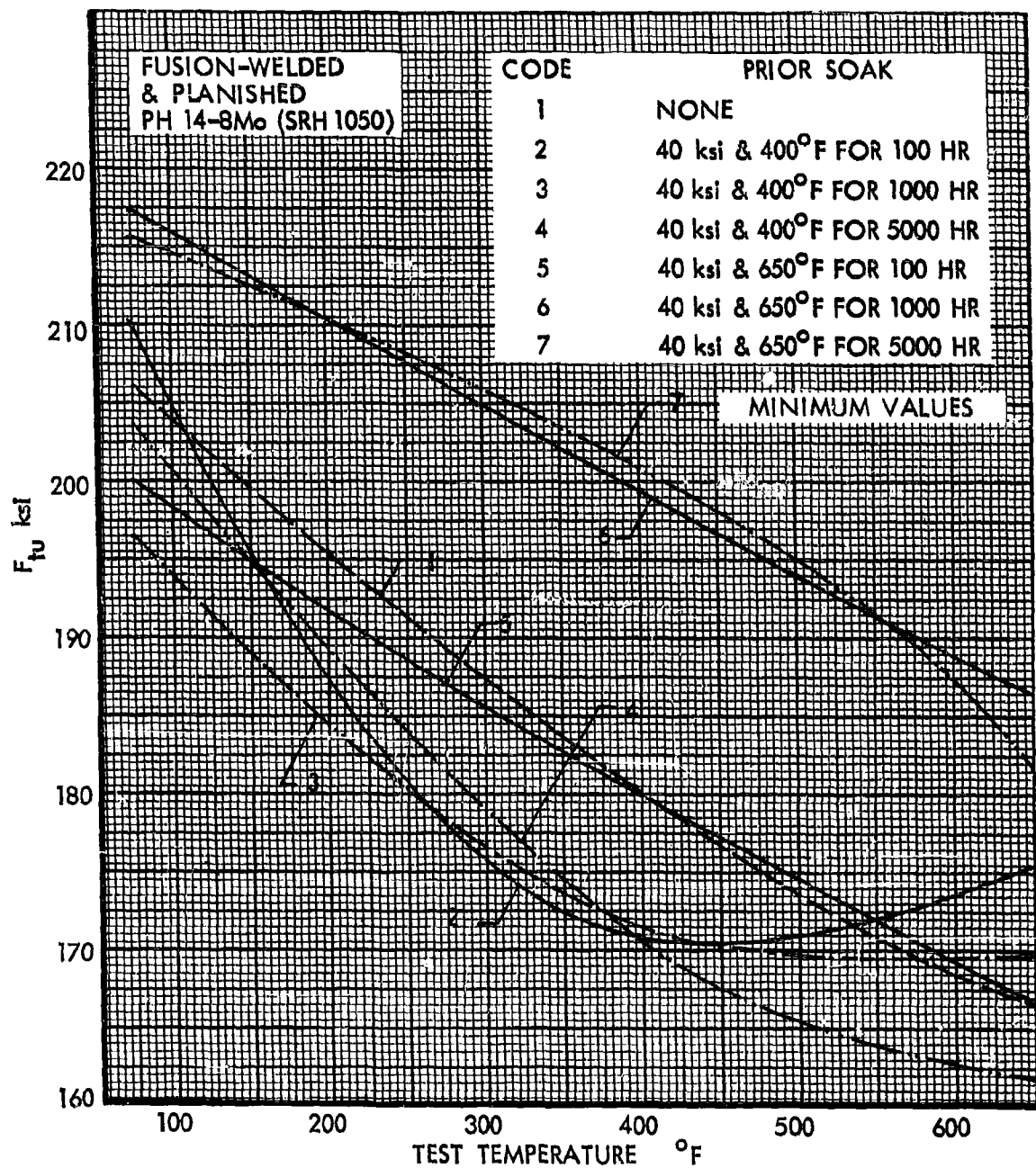
Figure 68. Effects of Prior Soak on Ultimate Tensile Strength,
Fusion-Welded PH14-8Mo

CODE	PRIOR SOAK
1	NONE
2	40 ksi & 400°F FOR 100 HR
3	40 ksi & 400°F FOR 1000 HR
4	40 ksi & 400°F FOR 5000 HR
5	40 ksi & 650°F FOR 100 HR
6	40 ksi & 650°F FOR 1000 HR
7	40 ksi & 650°F FOR 5000 HR

FUSION-WELDED & PLANISHED INCO718, COLD-ROLLED, AGED AT 1275°F

MINIMUM VALUES

F_{tu} ksi

TEST TEMPERATURE °F
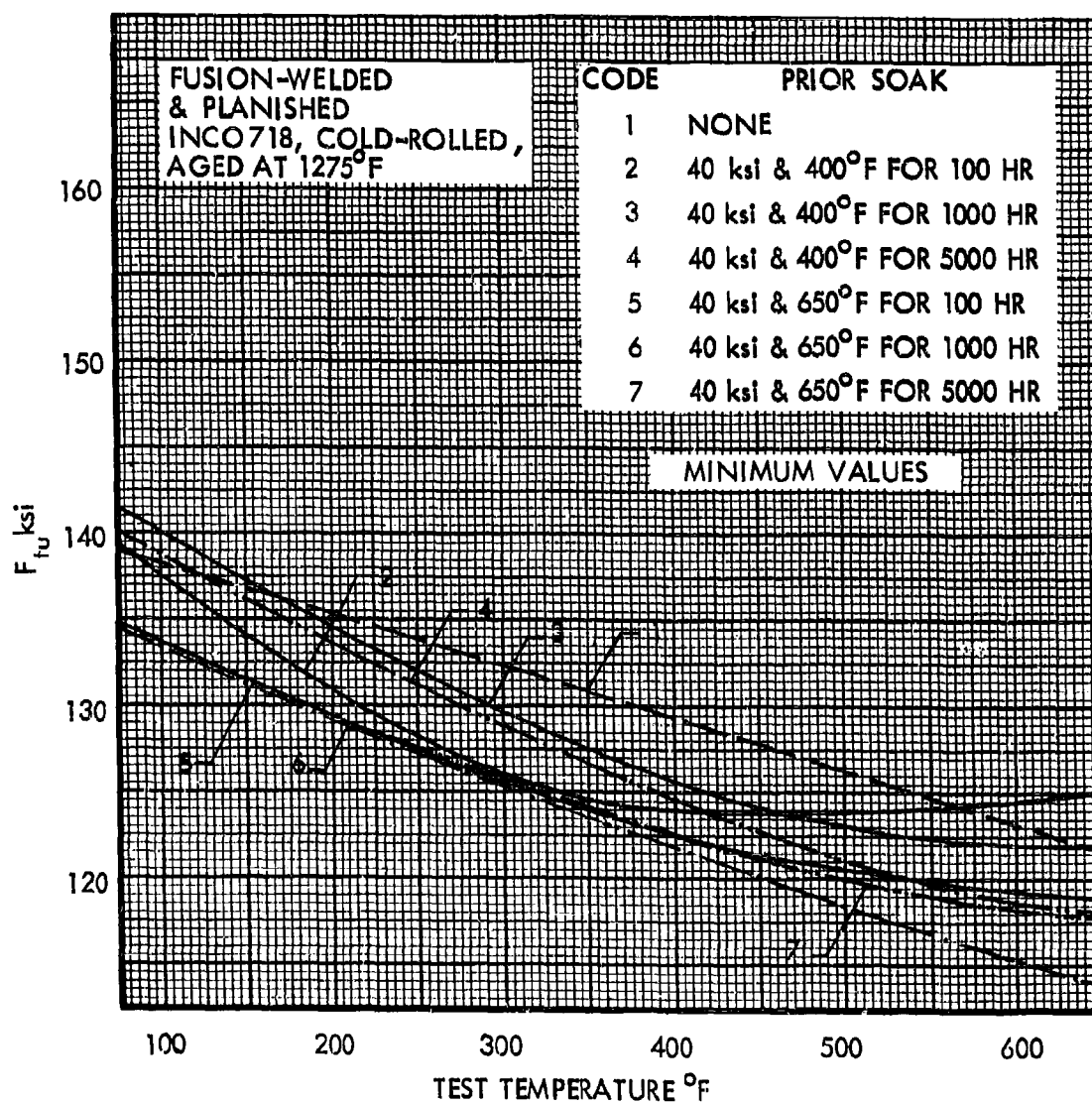
Figure 69. Effects of Prior Soak on Ultimate Tensile Strength, Fusion-Welded INCO 718

TABLE 12   COMPARISON OF AVERAGE STATIC TEST PROPERTIES WITH THOSE OBTAINED UNDER CONTRACT AF33(657)-11461
8-1-1 TITANIUM DUPLEX ANNEALED; PH14-8Mo (SRH 1050); INCO 718,
COLD ROLLED AND AGED AT 1275°F; .050 GAGE FOR TITANIUM AND .025 GAGE FOR STEEL AND NICKEL ALLOY
NO PRIOR SOAK

Test Program *	Material	TESTED AT ROOM TEMP.				TESTED AT 400°F				TESTED AT 650°F			
		No.of Speci-mens	Ftu (ksi)	Fty (ksi)	e** (%)	No.of Speci-mens	Ftu (ksi)	Fty (ksi)	e** (%)	No.of Speci-mens	Ftu (ksi)	Fty (ksi)	e** (%)
							PLAIN SPECIMENS						
A	8-1-1 Titanium	10	149.4	137.5	14.9	3	119.5	100.8	15.3	3	110.2	86.8	13.8
B		6	143.3	130.0	14.0	3	119.7	99.0	13.0	3	106.0	84.5	11.5
A	PH14-8Mo	8	209.0	191.2	5.0	3	197.4	179.9	2.0	3	186.3	167.8	3.5
B		3	210.7	202.2	3.5	3	195.8	182.3	2.5	3	183.8	166.8	2.5
A	INCO 718	20	219.9	204.3	8.3	3	206.1	188.8	6.8	3	199.9	183.6	7.2
B		3	212.3	196.5	10.0	3	197.7	183.0	7.0	3	188.7	176.8	7.0
							FUSION-WELDED AND PLANISHED SPECIMENS						
C	8-1-1 Titanium	3	150.6	-	-	3	123.5	-	-	3	112.4	-	-
D		3	141.8	125.8	10.0	-	-	-	-	3	104.1	81.0	8.5
C	PH14-8Mo ***	3	207.8	-	-	3	189.5	-	-	3	173.1	-	-
D		3	207.7	197.8	3.5	-	-	-	-	3	177.7	162.2	2.5
C	INCO 718	3	141.1	-	-	3	130.5	-	-	3	124.1	-	-
D		3	132.2	89.3	2.0	-	-	-	-	3	113.3	72.9	2.0

Notes: *   A - Current program
              B - Boeing-North American joint venture under contract AF33(657)-11461
              C - Current program with welds roll planished
              D - Boeing-North American joint venture with welds ground flush

         **   2.0 inch gage length

        ***   All of the steel specimens were heat treated after welding

99
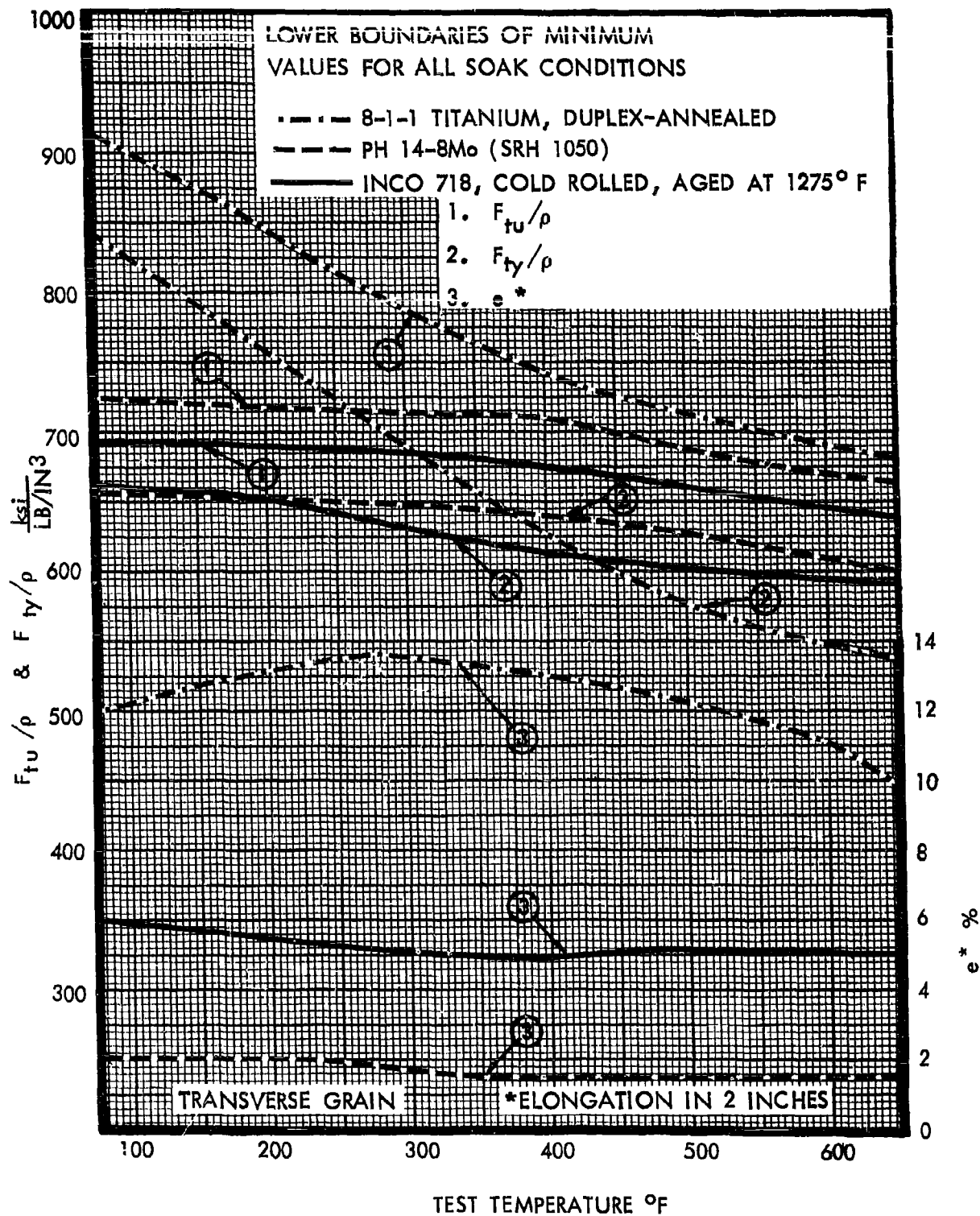
Figure 70. Comparison of Static Tensile Properties, Plain Specimens

100
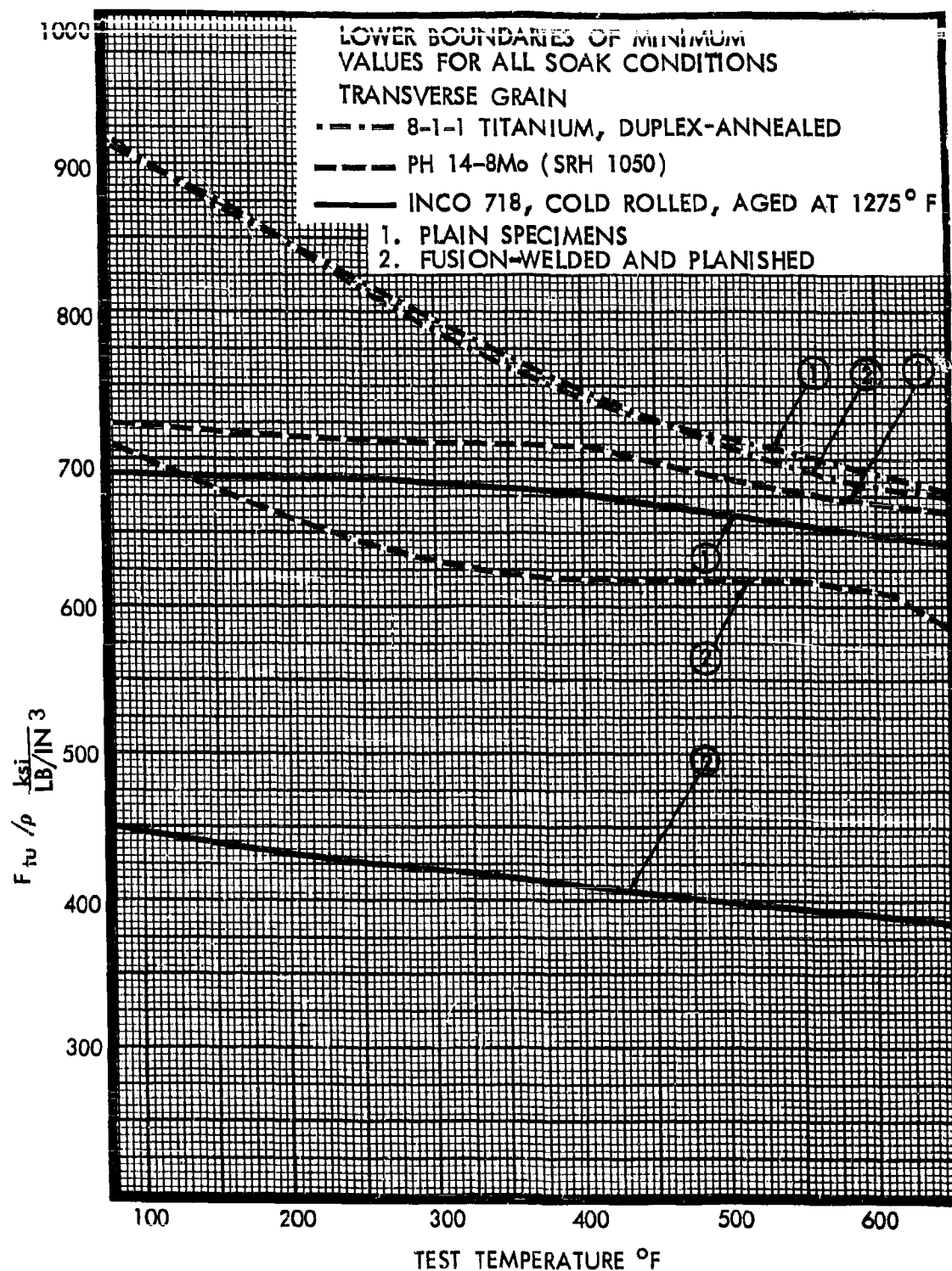
Figure 71. Comparison of Ultimate Tensile Strength, Plain and Fusion-Welded Specimens.

PHASE II - FLIGHT-BY-FLIGHT LOADING SEQUENCE TESTS

The constant load amplitude tests carried out in Phase I of the program provide one basis for the comparison of sheet materials proposed for possible use in SST structure. In general, however, such tests cannot adequately indicate the effects of the sequences of loadings and thermal cycles anticipated in service. To provide data on these effects, tests must be conducted in which reasonable, conservative, simulations of the service conditions are generated. Such tests have been carried out using test conditions which simulate service conditions in the lower surface of the wing root structure and also using test conditions which simulate the very different service conditions anticipated along the sides of fuselages.

A. WING ROOT LOADING CONDITIONS

To simulate the service conditions in the wing root region, two types of tests were undertaken. In one type, the average time at temperature anticipated for each service flight is developed during each test "flight". This type of test should provide the best test evaluation of long term intermittent exposures to elevated temperature occurring in conjunction with anticipated sequences of loading. However, such tests are inevitably of long duration and are probably not practical for design development testing. To explore the possibilities of accelerated tests, sets of specimens must also be tested using the same loading sequences and thermal cycles but with a minimum practical time at elevated temperature. Comparisons of the number of flights obtained in the two sets of tests will provide guides to the interpretation of SST design development tests. The latter tests must be conducted in relatively short times for the test information to be useful in the design process.

For the tests to be practical, the test durations expressed in number of flights must be short enough to be demonstrated in reasonable calendar times but the severity of the test conditions must not be unrealistic. To explore the selection of appropriate loading severities, preliminary work with SST structures suggested the use, in tests at room temperature, of the spectra shown in Tables 13,14,15 and 16 and in Figure 72 employing the test sequences shown in Figure 73. The test load magnitudes are defined in terms of a reference 1g stress. For the 8-1-1 titanium specimens the value of the 1g stress was selected as 25,000 psi and for the PH14-8Mo steel and Inco 718 specimens the value selected was 40,000 psi. These values were also used as steady state or mean stresses in the evaluation of the constant load amplitude tests carried out under Phase I of the Program. The values are believed to reflect conservative selections of allowable design stresses which are consistent with the ultimate static strengths of the materials.

For conservatism in the selection of the sequence and magnitude of test loadings, attention was focused on a point in wing structure which is below the surface such as a beam cap. At such a location, a significant tensile stress will be developed during heating. The sequence shown in Figure 73 reflects this choice of structural location.

TABLE 13   CLIMB SPECTRUM

$\dfrac{f_{vary}}{f_{1g_{Ref}}}$	UNIT SPECTRUM[1]	ADDITIONAL NUMBER OF DISCRETE CYCLES OF $\dfrac{f_{vary}}{f_{1g_{Ref}}}$ APPLIED EVERY[2]								TOTAL NUMBER OF DISCRETE CYCLES IN 8×10^4 FLTS.
		100 FLIGHTS	500 FLIGHTS	1,000 FLIGHTS	5,000 FLIGHTS	10,000 FLIGHTS	20,000 FLIGHTS	40,000 FLIGHTS	80,000 FLIGHTS	
.15	7									560,000
.25	2									160,000
.35		62								49,600
.45		22								17,600
.55		7								5,600
.65			13							2,080
.75			6							960
.85			2							320
.95			1							160
1.05				1						80
1.15					2					32
1.25					1					16
1.35						1				8
1.45							2			8
1.55							1			4
1.65								1	1	3
1.75									1	1
1.85									1	1
1.95									1	1
2.05									1	1

(1) Automatically controlled on a flight-by-flight basis.
(2) Manually controlled in real-time tests and automatically controlled in accelerated tests.

103

TABLE 14 CRUISE SPECTRUM

$\dfrac{f_{vary}}{f_{lg_{Ref}}}$	UNIT SPECTRUM[1]	ADDITIONAL NUMBER OF DISCRETE CYCLES OF $\dfrac{f_{vary}}{f_{lg_{Ref}}}$ APPLIED EVERY[2]								TOTAL NUMBER OF DISCRETE CYCLES IN 8×10^4 FLTS.
		100 FLIGHTS	500 FLIGHTS	1,000 FLIGHTS	5,000 FLIGHTS	10,000 FLIGHTS	20,000 FLIGHTS	40,000 FLIGHTS	80,000 FLIGHTS	
.15	3	80								304,000
.25		48								38,400
.35		7								5,600
.45		1								800
.55				1	3					128
.65					1	1				24
.75							1	1		6
.85									1	1
.95									1	1

(1) Automatically controlled on a flight-by-flight basis.

(2) Manually controlled in real-time tests and automatically controlled in accelerated tests.

104

TABLE 15   DESCENT SPECTRUM

$\dfrac{f_{vary}}{f_{lg_{Ref}}}$	UNIT SPECTRUM[1]	ADDITIONAL NUMBER OF DISCRETE CYCLES OF $\dfrac{f_{vary}}{f_{lg_{Ref}}}$ APPLIED EVERY[2]								TOTAL NUMBER OF DISCRETE CYCLES IN 8×10^{4} FLTS.
		100 FLIGHTS	500 FLIGHTS	1,000 FLIGHTS	5,000 FLIGHTS	10,000 FLIGHTS	20,000 FLIGHTS	40,000 FLIGHTS	80,000 FLIGHTS	
.15	7	75								620,000
.25	1	30								104,000
.35		25								20,000
.45		5	2							4,320
.55		1	1							960
.65				3	1					256
.75				1						80
.85						3				24
.95							2	1		10
1.05								2		4
1.15								1		2
1.25									1	1
1.35									1	1

(1) Automatically controlled on a flight-by-flight basis.
(2) Manually controlled in real-time tests and automatically controlled in accelerated tests.

TABLE 16   TAXI SPECTRUM FOR SPECTRA A

$\dfrac{\Delta f}{f_{lg_{Ref}}}$ (3)	UNIT SPECTRUM (1)	ADDITIONAL NUMBER OF DISCRETE LOADINGS OF $\dfrac{\Delta f}{f_{lg_{Ref}}}$ APPLIED EVERY (2)								TOTAL NUMBER OF LOADINGS IN 8×10^4 FLTS.
		100 FLIGHTS	500 FLIGHTS	1,000 FLIGHTS	5,000 FLIGHTS	10,000 FLIGHTS	20,000 FLIGHTS	40,000 FLIGHTS	80,000 FLIGHTS	
1.58	1									80,000
1.62		75								60,000
1.66		41								32,800
1.70		25								20,000
1.74		14								11,200
1.78		8								6,400
1.82		5								4,000
1.86		3								2,400
1.90			8							1,280
1.94			4							640
1.98			2							320
2.02			1							160
2.06				1	1					96
2.10					3					48
2.14						4				32
2.18						2				16
2.22							2	1		10
2.26								3		6
2.30								1		2
2.34								1		2
2.38									1	1
2.42									1	1

(1) Automatically controlled on a flight-by-flight basis.

(2) Manually controlled in real time tests and automatically controlled in accelerated tests.

(3) The discrete loadings are applied as negative half cycles below the descent spectrum mean.

106

CUMULATIVE FREQUENCY OF OCCURRENCE (CYCLES)
IN 80,000 FLIGHTS

Figure 72. Loading Spectra A for Preliminary Flight-by-Flight Tests at Room Temperature
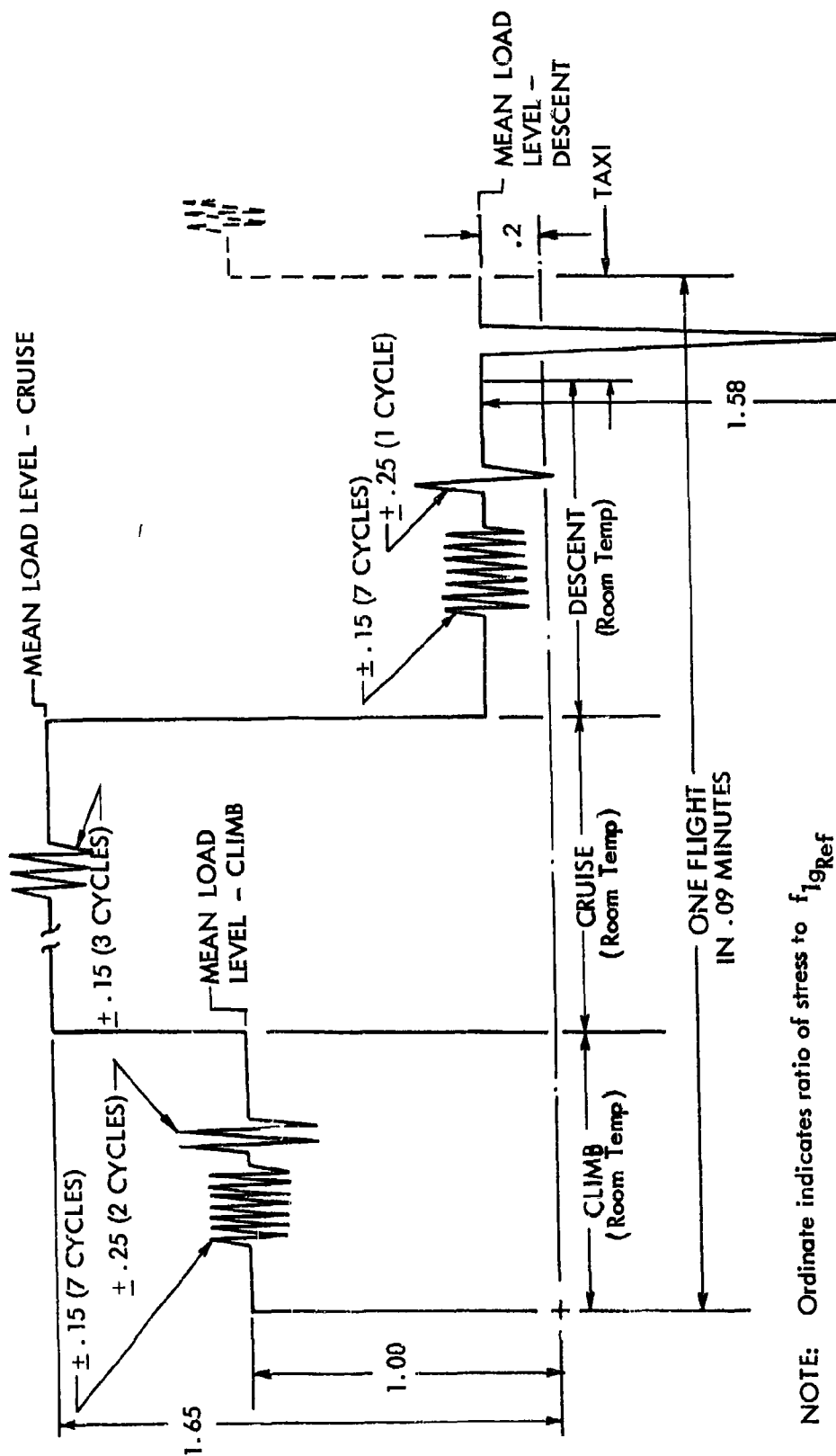
107

Figure 73.   Unit Flight-By-Flight Loading Sequences and Magnitudes - Spectra A

NOTE: Ordinate indicates ratio of stress to $f_{1g_{Ref}}$

where $f_{1g_{Ref}}$ = 25,000 psi for 8-1-1 Titanium and
                40,000 psi for PH-14-8Mo Steel and Inco 718
         Growth in Magnitude of Cyclic Loads with Time is Given in Tables 13 - 16

108

The effect of thermally induced load was represented during the cruise portion of each "flight" by a tensile increment of 0.8 times the reference 1g load. This load, when superimposed on the decrement of 0.15 times the reference value which is due to reduced fuel weight, leads to the net increment of 0.65 units shown on the figure. While the thermal increment will decrease during actual cruising flight as the structural temperatures approach equilibrium, a constant value was applied in the tests. During descent, a reversal of the thermally induced load will occur and a maximum value of compression increment will be generated. For the initial tests, a thermal decrement of 0.4 units superimposed on a decrement of 0.4 units due to weight loss, when subtracted from the reference 1g load, leads to the net value of 0.2 shown in Figure 73 for the steady state value about which the oscillatory descent loadings were applied.

During the descent phase of each service flight, the majority of the applied loadings will probably occur at relatively low altitudes when the structure will have cooled appreciably. For simplicity in the conduct of the tests, these descent loadings are defined to be applied at minimum test temperature.

The ground loadings were represented by a single excursion to the largest compressive stress anticipated during each flight. This expedient was adopted to retain the effect of intermittent compressive loadings but to avoid the substantial extension of test time required to apply a spectrum of ground loadings.

The growth of cyclic load magnitudes with test time which is defined by the spectra was represented by the application of the larger loadings during particular test flights. The order of application of these loadings is defined in the tables.

The spectra, which are identified as Spectra A, were defined as flight-by-flight sequence traces on magnetic tapes. The tapes were used with the test apparatus described in Appendix IV in tests at room temperature of center notched and fusion-welded specimens. These tests produced the test lives listed in Table 17 and shown graphically in Figure 74.

In these preliminary tests, the test loadings produced relatively short test lives (4400 to 9700 flights) for specimens notched by an unloaded hole and very long test lives for specimens containing a fusion weld. The results for the notched specimens led to a re-evaluation of the bases for the spectra and the conclusion that they were unrealistically severe. The results for the fusion-welded specimens, coupled with additional evidence of a low effective stress concentration provided by the S-N test values reported under Phase I, led to the conclusion that additional spectrum loading testing of these specimens was not warranted.

The re-evaluation of the basis for the spectra indicated that the need for a reasonably conservative but not unrealistic representation of wing root loadings dictated a marked reduction in the maximum stress ranges produced in the first set of tests.

To obtain an indication of the effect of such a reduction, the magnetic tapes defining the loading histories identified as Spectra A were used in tests of an additional set of notched specimens. In these tests, however,

TABLE 17 - ACCELERATED FLIGHT-BY-FLIGHT TEST RESULTS

FOR SPECTRA A AT ROOM TEMPERATURE

SPECIMEN MATERIAL	SPECIMEN TYPE	REFERENCE 1g STRESS (ksi)	SPECIMEN TEMP. ($^{\circ}$F)	NUMBER OF FLIGHTS TO DEVELOPMENT OF VISUAL CRACKING
8-1-1 Titanium Duplex Annealed	Center-Notched	25	Room	8,500 8,500 8,500 8,500 plus } a
				8,500 8,900 9,450 9,700
	Fusion-Welded			76,000 plus 76,000 plus } b
	Multi-Spotwelded Doubler			3,000 3,000 3,000 3,000 } c
	Single-Spotwelded Doubler	25		11,000 12,750
PH 14-8Mo (SRH1050) Stainless Steel	Center-Notched	40		2,278 2,304 2,500 2,500
	Fusion-Welded			31,000 76,000 plus 110,000 plus 110,000 plus } b
INCO 718 Cold Rolled, Aged at 1275°D	Center-Notched			4,400 5,050 5,100 5,380
	Fusion-Welded	40	Room	14,000 plus 14,000 plus 24,000 plus 24,000 plus } d 64,750 68,188

a. Malfunction of load programmer resulted in inadvertent failure of two specimens outside of notched area - a visual inspection revealed three cracked specimens.

b. No failure - testing discontinued.

c. During 3000th flight, one specimen failed catastrophically through an end spotweld. An inspection revealed cracks at end spotweld in remaining three (3) specimens.

d. Overload inadvertently applied - testing discontinued.
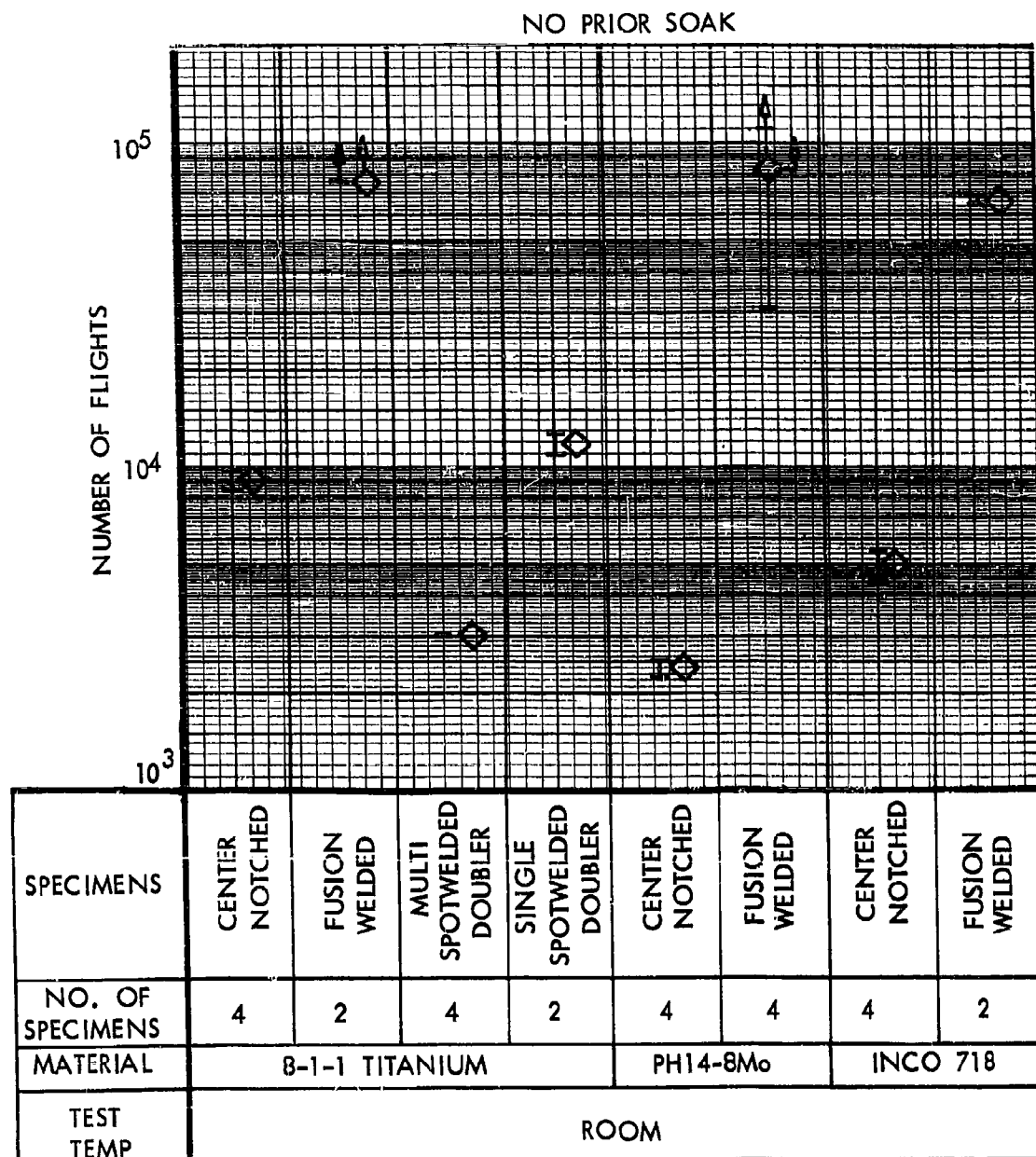
110

Figure 74. Preliminary Accelerated Flight-by-Flight Test Results
for Spectra A at Room Temperature

the magnitudes of all loadings were reduced to 80% of those applied in the first set of tests. The test lives obtained at room temperature with this arbitrary reduction of all load magnitudes ranged from 27,000 to greater than 76,000 flights for 8-1-1 titanium, from 6,800 to 7,600 flights for PH14-8Mo and from 11,400 to 14,900 for Inco 718. The results are reported in Table 18 and shown in Figure 75 where the loadings are identified as Spectra B. These results demonstrate the sensitivity of test life to loading severity and show the generally expected trend to larger test scatter with reductions in test severity. They also provide one guide to the description of a new set of loadings of reduced severity which would not produce excessively long test lives. An additional requirement imposed by the need for realism was the retention of the original definitions of reference stress levels and oscillatory flight loadings with the selection of a more representative tensile thermal stress increment and a more representative simulation of ground loadings.

The new set of loadings had a value of tensile thermal stress increment of 0.6 times the reference 1g stress rather than 0.8 and a ground loading spectrum of reduced severity. The ground loading spectrum is listed in Table 19 and the new set of spectra, identified as Spectra C, are shown in Figure 76. Figure 77 shows a schematic of the loading sequences and magnitudes. This figure may be compared with the corresponding representation in Figure 73 of the test sequences and magnitudes used in the first set of tests.

New loading tapes containing flight-by-flight loading histories defined for Spectra C were prepared and used in tests at room temperature of notched specimens. These tests led to lives ranging from 26,500 to 105,000 flights for 8-1-1 titanium from 8,100 to 10,400 flights for PH14-8Mo and 11,600 to 12,000 flights for Inco 718. The results of the tests are listed in Table 20 and shown in Figure 78. The test lives were considered to be satisfactory for the purpose of the test program and so the loading histories defined for Spectra C were established as the standard for the program.

To replace the fusion-welded specimens in the series of spectrum loading tests specimens with mechanically fastened joints were considered. However, the retention of a form of welded attachment was believed to be desirable. Therefore, exploratory tests of spotwelded specimens were undertaken.

The geometry of the multi-spot specimens used in the initial tests is shown in Section IV, and the details of the spotwelding procedure are presented in Appendix I. Several 8-1-1 titanium specimens of this type were prepared and tested using repeated constant amplitude loadings and flight-by-flight loadings.

The S-N type test results are listed in Table 21 and are presented graphically in Figure 79 where they may be compared with data for notched specimens. The flight-by-flight test lives are shown in Figures 74, 75 and 78. The relatively short test lives obtained in both types of test led to the selection of a second specimen type having a single spotweld. This type of specimen simulates the situation in structure in which a transverse stiffening member is attached to skin by a single row of spotwelds.

Several specimens of this geometry were prepared and tested at room temperature. The S-N type test data obtained are listed in Table 21 and shown in Figures 79 - 81 and the type of failure is shown in Figure 82. The flight-by-flight test lives are shown in Figures 74 and 78. These latter results indicated that use of this type of specimen would provide informative data and that the test lives would be more nearly compatible with those of notched titanium specimens than the lives obtained for fusion-welded specimens. A reasonable compatibility of test lives was considered desirable for different types of specimens. This will be particularly important in the real-time tests of material stability.

Upon completion of the accelerated tests at room temperature, additional sets of specimens were tested at a constant temperature of $550^{\circ}F$ using the Spectra C loading tapes.

The intent of these tests was to establish probable lower boundaries of the test lives to be obtained in later tests in which a temperature cycle is required during each flight. The results of these tests are listed in Table 22 and shown in Figure 83. A comparison of these results with those obtained in tests at room temperature shows that application of all loading sequences at a constant temperature of $550^{\circ}F$ produced a significant reduction in the number of flights to failure.

With the sets of base line tests at room temperature and constant elevated temperature complete, tests were undertaken in which the flight-by-flight sequence of loadings is accompanied by the flight-by-flight sequence of temperature changes.

Much greater importance is attached to these tests than to the exploratory tests carried out at room temperature and at constant elevated temperature. When thermal cycles accompany the flight-by-flight loading sequences, the most realistic conditions are represented in tests of minimum duration. In addition, the test lives obtained in these tests will be compared with the results of tests of much longer duration in which real-time at temperature will be developed. These latter tests will be described in later paragraphs. The comparison of test lives in these two types of test will provide a basis for assessing the significance of SST design development tests which must be carried out in minimum calendar times.

For these reasons, the evaluation of the flight-by-flight test data is focused on the results of the tests with thermal cycles.

The average test duration of approximately 55,000 flights for notched 8-1-1 titanium specimens listed in Table 23 and shown in Figure 84 establish a standard for the test conditions. By comparison, the average test durations of approximately 4,500 and 10,000 flights shown for the notched PH14-8 Mo and Inco 718 specimens are considered to demonstrate the marked superiority of the 8-1-1 titanium material in SST airframe applications. The data for the specimens with a single spotweld indicate that, for the loading conditions and specimen support conditions employed in these tests, the endurance of the titanium specimens

was appreciably less than that of the notched specimens. For PH14-8Mo specimens, the endurance of the spotwelded specimens is much greater than that of the notched specimens. For Inco 718 specimens the same conclusion is believed to apply. Since durations greater than 80,000 flights were obtained in tests of Inco 718 spotwelded specimens at room temperature and at a constant temperature of 550°F, no testing with thermal cycles was undertaken.

The evaluations of materials and specimen geometries based on tests incorporating flight-by-flight sequences of loadings and of minimum time temperature cycles are the most directly applicable, relatively rapid, evaluations for many design situations. However, the total time at temperature in such tests is quite short. The tests cannot provide assurance that the interactions of loading and temperature effects occurring over a long period of service do not appreciably affect the fatigue resistance of the materials. The data reported under Phase I on the effects of exposure to steady load and constant temperature for 5,000 hours are reassuring but they cannot be accepted as adequate.

To provide data on the long term effects produced by loading sequences and intermittent exposure to elevated temperature, a test has been started. In this test groups of six notched and spotwelded specimens of each of the materials being evaluated are being exposed to flight-by-flight loading sequences with approximately one hour at maximum temperature during each test flight. The time at temperature was selected to represent the average time in cruising flight anticipated in service operations. The loadings are those defined by Spectra C. The test apparatus developed for these tests is described in Appendix IV.

A comparison of the number of flights endured by the test specimens in this test with the number endured in the tests with minimum time at temperature will be made. This comparison will provide the most informative indication of the effect on the materials of long exposure to elevated temperature under simulated service conditions.

For the data in the two types of tests to be directly comparable, a maximum test temperature of 550°F was initially employed in the tests with real time at temperature. However, detailed information on the temperature distributions anticipated on the SST indicate the applicability in this long term test of a 500°F temperature. The test temperature was changed to this value. The total time at the higher temperature was approximately 600 hours. The effect of this change in test temperature on the test life comparisons is believed to be very small. In the very short total times at temperature in the tests carried out on an accelerated basis, the relative effect on test life of maximum temperatures of 500 or 550°F is probably small.

Continuation of the tests with real time at temperature beyond the period covered by this report has been proposed. As of December 31, 1964, 1697 flights have been applied with no specimen failures.

To provide an indication of the utility of conventional fatigue test life calculations, such calculations have been carried out for center-notched specimens and are reported in Appendix IX. They indicate the need for use of a very severe representation of the ground-air-ground transition cycle.

TABLE 18   ACCELERATED FLIGHT-BY-FLIGHT TEST RESULTS FOR SPECTRA B* AT ROOM TEMPERATURE

SPECIMEN MATERIAL	SPECIMEN TYPE	REFERENCE 1g STRESS (ksi)	SPECIMEN TEMP. (°F)	NUMBER OF FLIGHTS TO DEVELOPMENT OF VISUAL CRACKING	COMMENTS
8-1-1 Titanium Duplex Annealed	Center-Notched	20	Room	27,000 34,377 43,106 76,000 plus	No failure – testing discontinued
	Multi-Spotwelded Doubler	20		3,000 3,000	
PH14-8Mo (SRH 1050) Stainless Steel	Center-Notched	32		6,800 7,200 7,400 7,600	
INCO 718 Cold Rolled, Aged at 1275°F	Center-Notched	32	Room	11,400 11,780 13,080 14,880	

*All load magnitudes in Spectra B were 80% of the corresponding loadings defined by Spectra A.
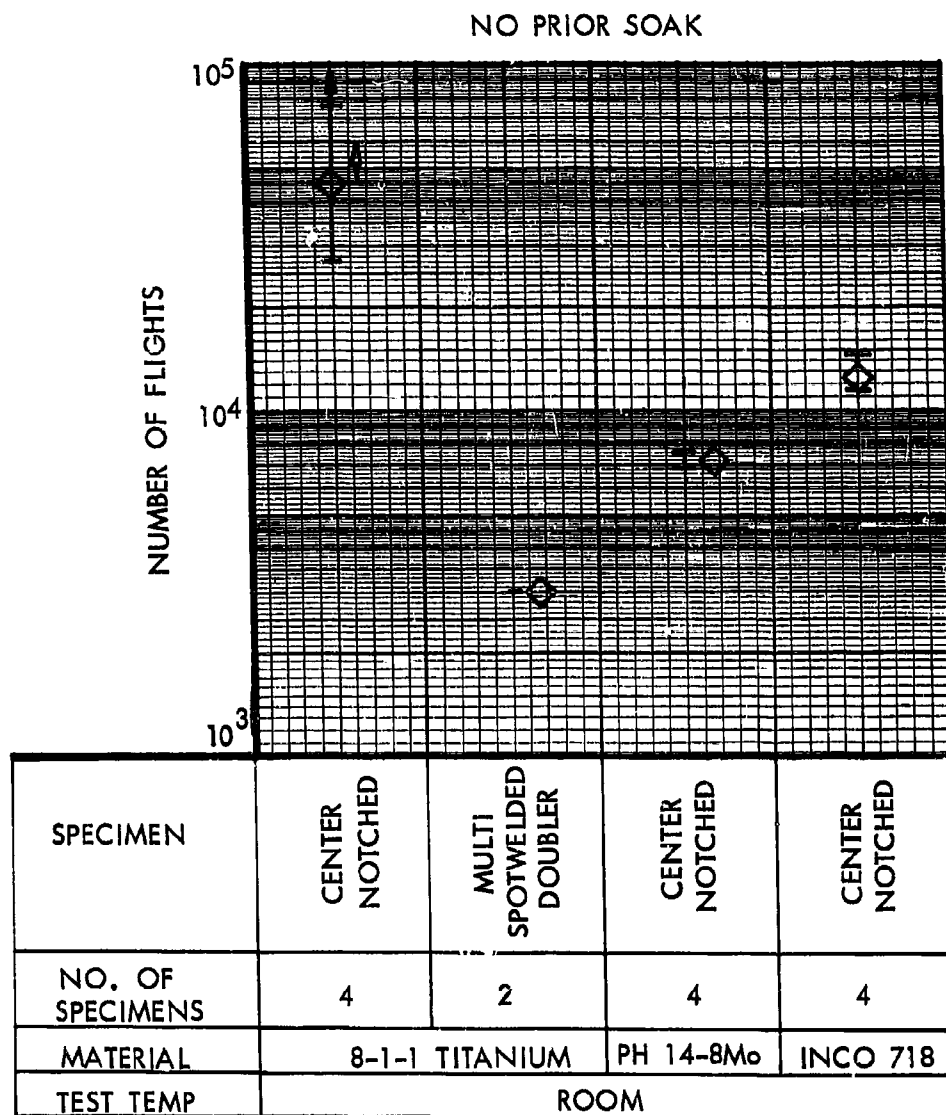
NO PRIOR SOAK

SPECIMEN	CENTER NOTCHED	MULTI SPOTWELDED DOUBLER	CENTER NOTCHED	CENTER NOTCHED
NO. OF SPECIMENS	4	2	4	4
MATERIAL	8-1-1 TITANIUM		PH 14-8Mo	INCO 718
TEST TEMP	ROOM			

I SCATTERBAND FOR TEST RESULTS

◇ AVERAGE OF TEST RESULTS

⚘ INDICATES INCLUSION OF TESTS
WITH NO FAILURE

Figure 75. Preliminary Accelerated Flight-by-Flight Test Results
for Spectra B at Room Temperature

TABLE 79   TAXI SPECTRUM FOR SPECTRA C

$\frac{\Delta f}{f_{1g_{Ref}}}$ (3)	UNIT SPECTRUM (1)	ADDITIONAL NUMBER OF DISCRETE LOADINGS OF $\frac{\Delta f}{f_{1g_{Ref}}}$ APPLIED EVERY(2)								TOTAL NUMBER OF DISCRETE LOADINGS IN 8×10^4 FLTS.
		100 FLIGHTS	500 FLIGHTS	1,000 FLIGHTS	5,000 FLIGHTS	10,000 FLIGHTS	20,000 FLIGHTS	40,000 FLIGHTS	80,000 FLIGHTS	
.95	1									80,000
1.05		22	1	1						17,840
1.15		2	2							1,920
1.25			1	1	1	1				264
1.35					2					32
1.45							1			4

(1) Automatically controlled on a flight-by-flight basis.

(2) Manually controlled in real time tests and automatically controlled in accelerated tests.

(3) The discrete loadings are applied as negative half cycles below the descent spectrum mean.

117

Figure 76. Loading Spectra C for Real Time and Accelerated Time Tests
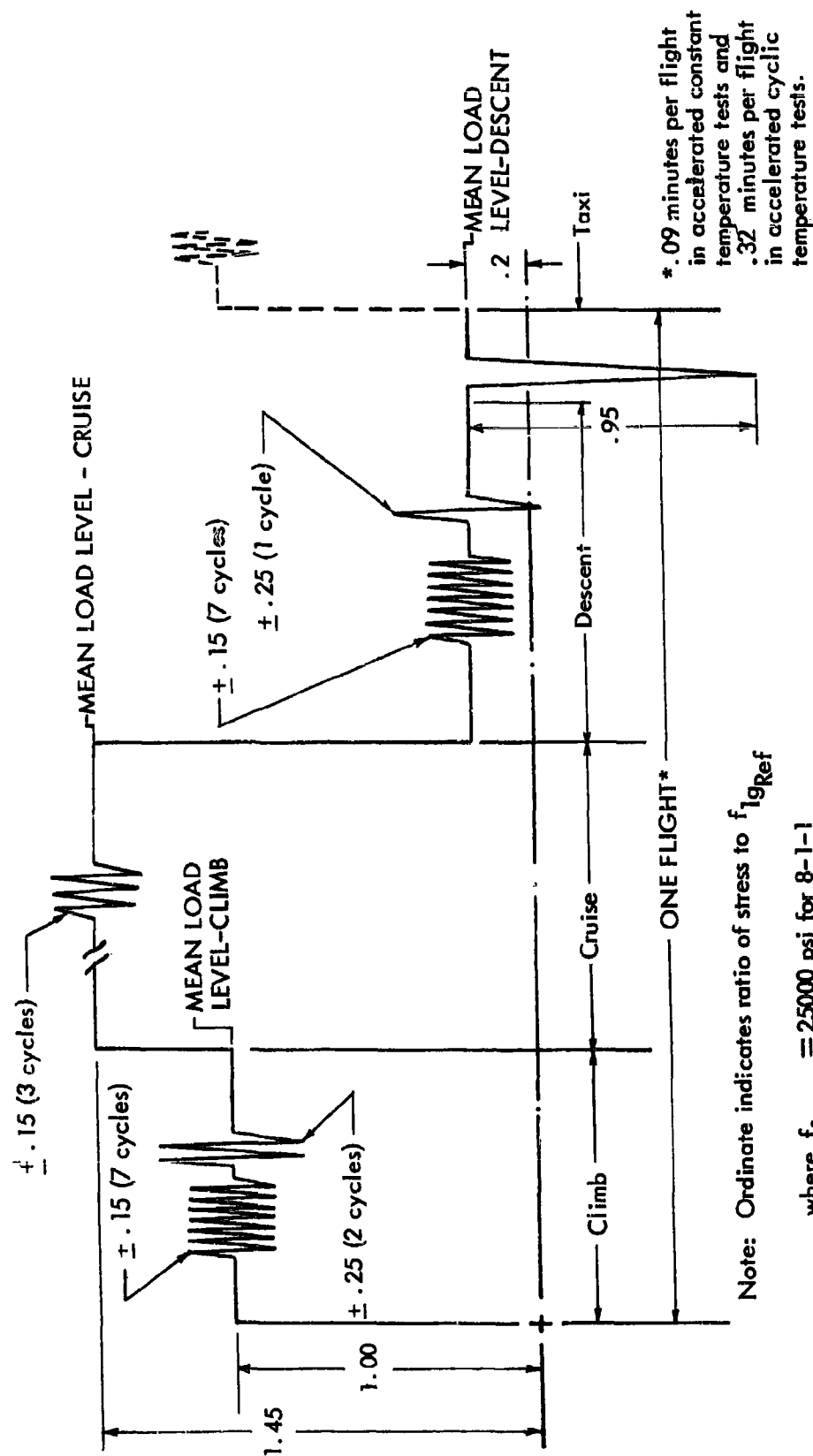
118

Figure 77. Unit Flight-by-Flight Loading Sequences and Magnitudes – Spectra C

Note: Ordinate indicates ratio of stress to $f_{1g_{Ref}}$

where $f_{1g_{Ref}}$ = 25000 psi for 8-1-1 Titanium and

40000 psi for PH 14-8Mo Steel and Inco 718

Growth in Magnitudes of Cycle Loads with Time is Given in Tables 13-15 and 19

*.09 minutes per flight in accelerated constant temperature tests and .32 minutes per flight in accelerated cyclic temperature tests.

119

TABLE 20 - ACCELERATED FLIGHT-BY-FLIGHT TEST RESULTS FOR SPECTRA C AT ROOM TEMPERATURE

SPECIMEN MATERIAL	SPECIMEN TYPE	REFERENCE 1g STRESS (ksi)	SPECIMEN TEMP. (°F)	NUMBER OF FLIGHTS TO DEVELOPMENT OF VISUAL CRACKING	COMMENTS
8-1-1 Titanium Duplex Annealed	Center-Notched	25	Room	26,500 29,500 54,340 56,000 57,000 83,000 105,000 75,900	
	Multi Spotwelded Doubler			6,000 9,400	
	Single Spot-welded Doubler			29,000 30,000 38,000 41,400	
PH14-8Mo (SRH 1050) Stainless Steel	Center-Notched	40		8,100 8,500 8,500 10,380	
	Single Spot-welded Doubler			59,000 77,000 80,000 80,000	No failure, testing discontinued
INCO 718 Cold Rolled, Aged at 1275°F	Center-Notched		Room	12,750 13,750 14,500 16,100	
	Single Spot-welded Doubler			80,000 80,000 80,000 80,000	No failure, testing discontinued

NO PRIOR SOAK

SPECIMEN	CENTER NOTCHED	SINGLE SPOTWELDED DOUBLER	MULTI SPOTWELDED DOUBLER	CENTER NOTCHED	SINGLE SPOTWELDED DOUBLER	CENTER NOTCHED	SINGLE SPOTWELDED DOUBLER
NO. OF SPECIMENS	8	2	4	4	4	4	4
MATERIAL	8-1-1 TITANIUM			PH 14-8Mo		INCO 718	
TEST TEMP.	ROOM						

$\mathcal{I}$ SCATTER BAND FOR TEST RESULTS

$\diamondsuit$ AVERAGE TEST RESULTS

ϕ INDICATES INCLUSION OF TESTS WITH
    NO FAILURE

Figure 78. Accelerated Flight-by-Flight Test Results for Spectra C at Room Temperature

TABLE 21　　CONSTANT LOAD AMPLITUDE FATIGUE TESTS AT ROOM TEMPERATURE
SPECIMENS CONTAINING SPOTWELDED DOUBLERS

TRANSVERSE GRAIN
NO PRIOR SOAK
$R = 0.1$

Specimen Material	Specimen Type	f_{max} (ksi)	Cycles to Failure
8-1-1 Titanium Duplex-Annealed	Multi Spotwelded Doubler	60 40 30	5,940 17,460 36,720
	Single Spotwelded Doubler	70 60 50 40 30 30 25	12,420 21,600 34,560 72,720 169,740 226,260 10,000,000*
PH14-8Mo (SRH 1050) Stainless Steel	Single Spotwelded Doubler	110 90 80 70 60 60 50	23,100 70,740 93,060 146,520 181,260 186,000 3,000,000*
INCO 718 Cold Rolled, Aged at 1275°F	Single Spotwelded Doubler	110 100 90 80 75 70 65 55	23,580 28,800 77,580 170,460 139,500 92,700 124,380 256,500

*No failure

Figure 79. Comparison of S-N Data at Room Temperature Notched and Spotwelded 8-1-1 Titanium

123
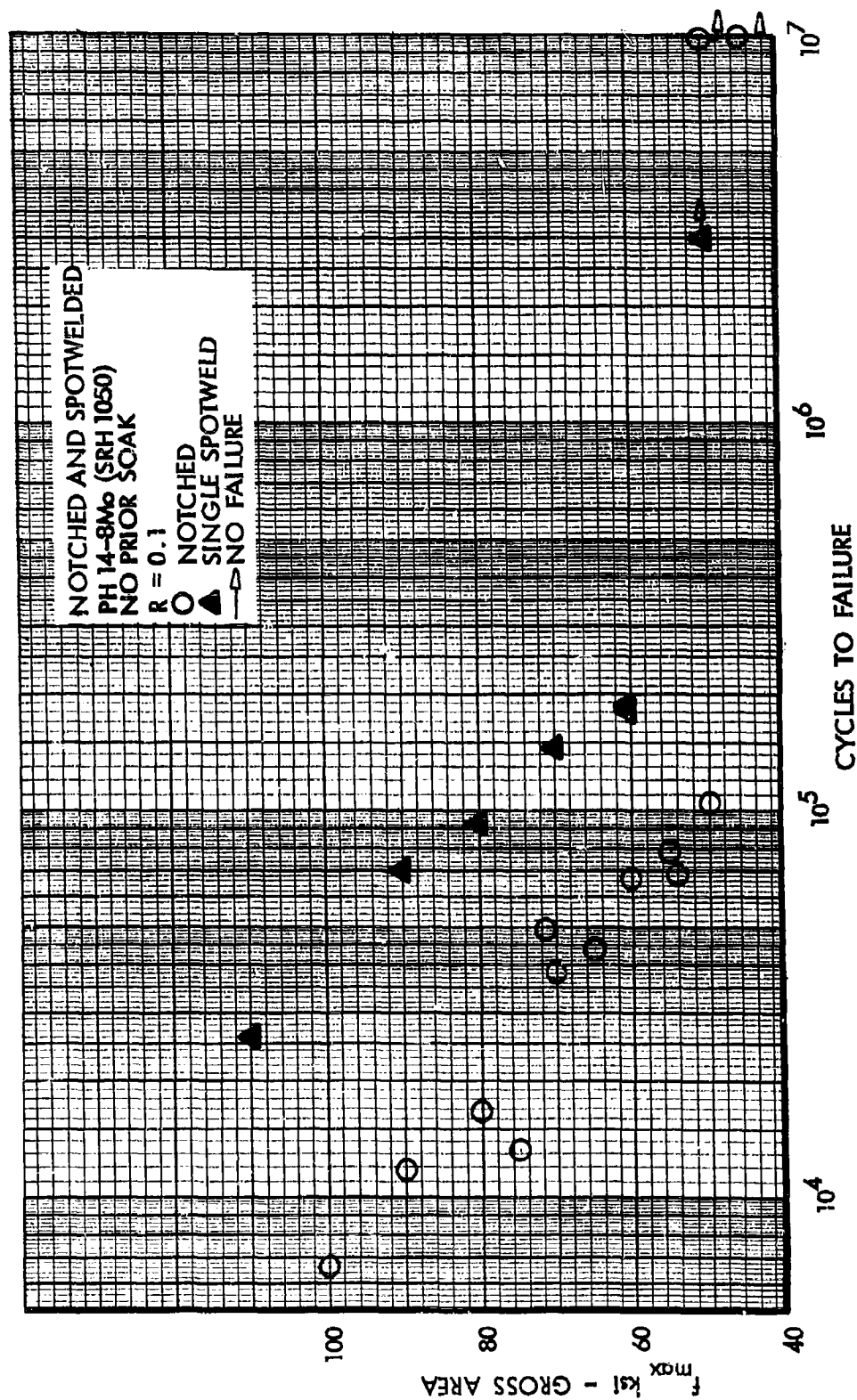
Figure 80. Comparison of S-N Data at Room Temperature
Notched and Spotwelded PH 14-8Mo
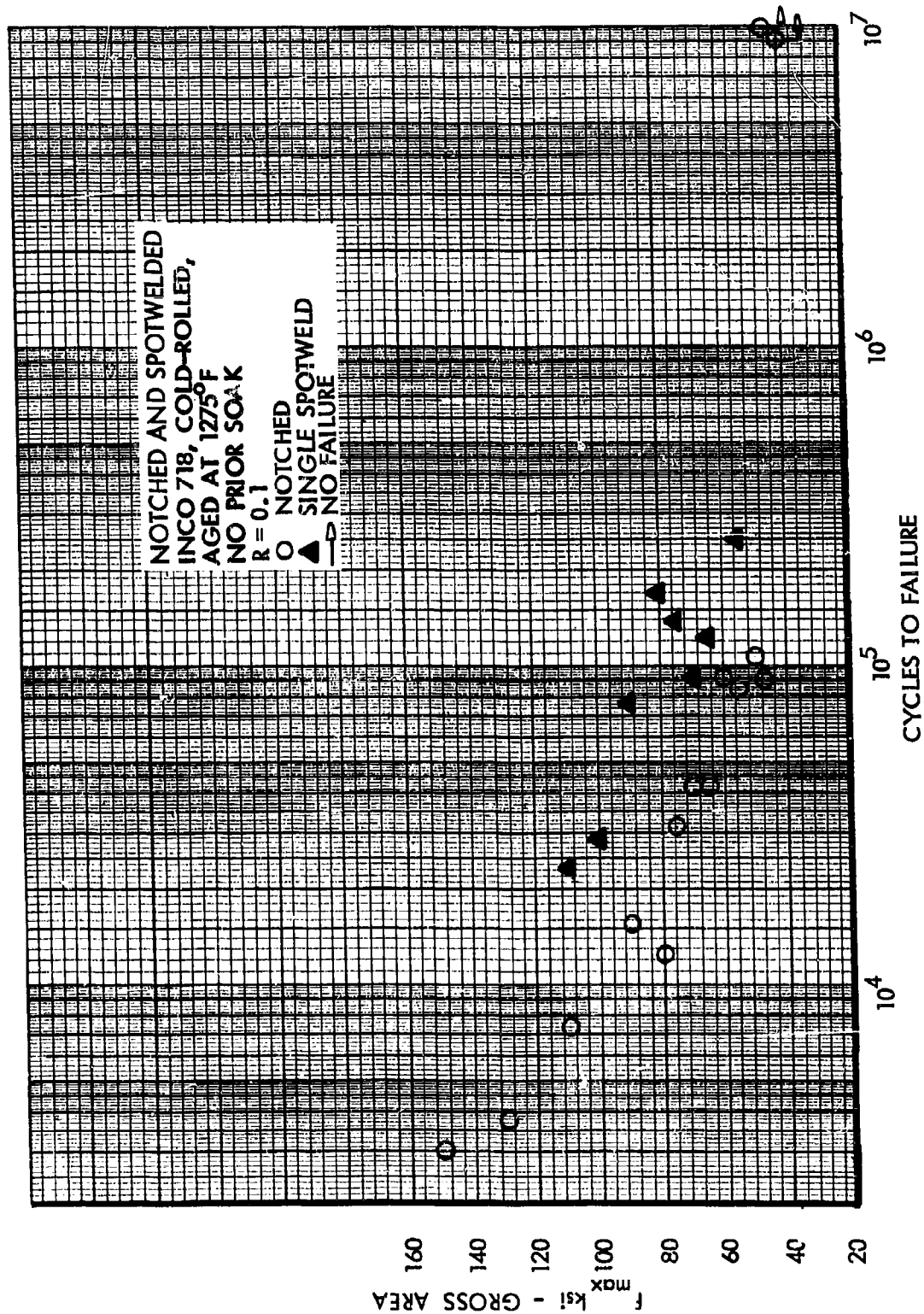
Figure 81.   Comparison of S-N Data at Room Temperature
Notched and Spotwelded INCO 718

125
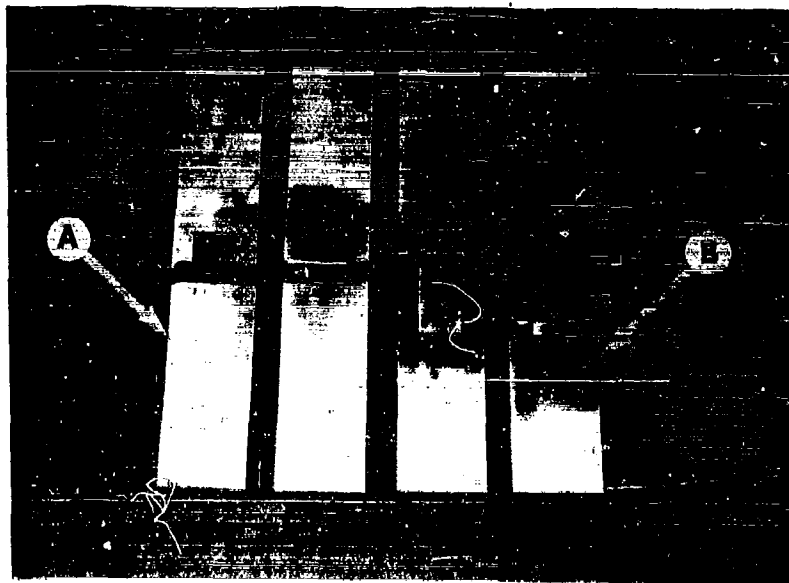
A. Single-Spotwelded Doubler
B. Multi-Spotwelded Doubler

Figure 82. Typical Fractures of Spotwelded 8-1-1 Titanium Fatigue Specimens

TABLE 22   ACCELERATED FLIGHT-BY-FLIGHT TEST RESULTS FOR SPECTRA C AT 550°F

SPECIMEN MATERIAL	SPECIMEN TYPE	REFERENCE Lg STRESS (ksi)	SPECIMEN TEMP. (°F)	TIME AT 550°F (hours)	NUMBER OF FLIGHTS TO DEVELOPMENT OF VISUAL CRACKING	COMMENTS
8-1-1 Titanium Duplex Annealed	Center Notched	25	550	23.85 / 23.85 / 27.60 / 27.90	15,900 / 15,900 / 18,400 / 18,600	
	Single Spotwelded Doubler	25		22.50 / 21.00 / 21.00 / 20.40	15,000 / 14,000 / 14,000 / 13,600	
PH14-8Mo (SRH 1050) Stainless Steel	Center Notched	40		4.88 / 4.50 / 4.88 / 4.50	3,250 / 3,000 / 3,250 / 3,000	
	Single Spotwelded Doubler			25.50 / 24.00 / 25.50 / 25.50	17,000 / 16,000 / 17,000 / 17,000	
INCO 718 Cold Rolled, Aged at 1275°F	Center Notched			17.47 / 17.47 / 18.00 / 18.00	11,650 / 11,650 / 12,000 / 12,000	
	Single Spotwelded Doubler	40	550	52.50 / 79.50 / 79.95 / 120.00 / 120.00 / 120.00 / 120.00	35,000 / 53,000 } / 53,300 / 80,000 plus / 80,000 plus } / 80,000 plus / 80,000 plus }	Loads were 14% too high. / Specimen overheated / No failure, testing discontinued

NO PRIOR SOAK.

SPECIMEN	CENTER NOTCHED	SINGLE SPOTWELDED DOUBLER	CENTER NOTCHED	SINGLE SPOTWELDED DOUBLER	CENTER NOTCHED	SINGLE SPOTWELDED DOUBLER
NO. OF SPECIMENS	4	4	4	4	4	5
MATERIAL	8-1-1 TITANIUM		PH 14-8Mo		INCO 718	
TEST TEMP.	550°F					

I   SCATTER BAND FOR TEST RESULTS
◇   AVERAGE OF TEST RESULTS
↑   INDICATES INCLUSION OF
    TESTS WITH NO FAILURE

Figure 83. Accelerated Flight-by-Flight Test Results for Spectra C
at Constant Elevated Temperature

128

TABLE 23   ACCELERATED FLIGHT-BY-FLIGHT TEST RESULTS FOR SPECTRA C WITH CYCLIC TEMPERATURE

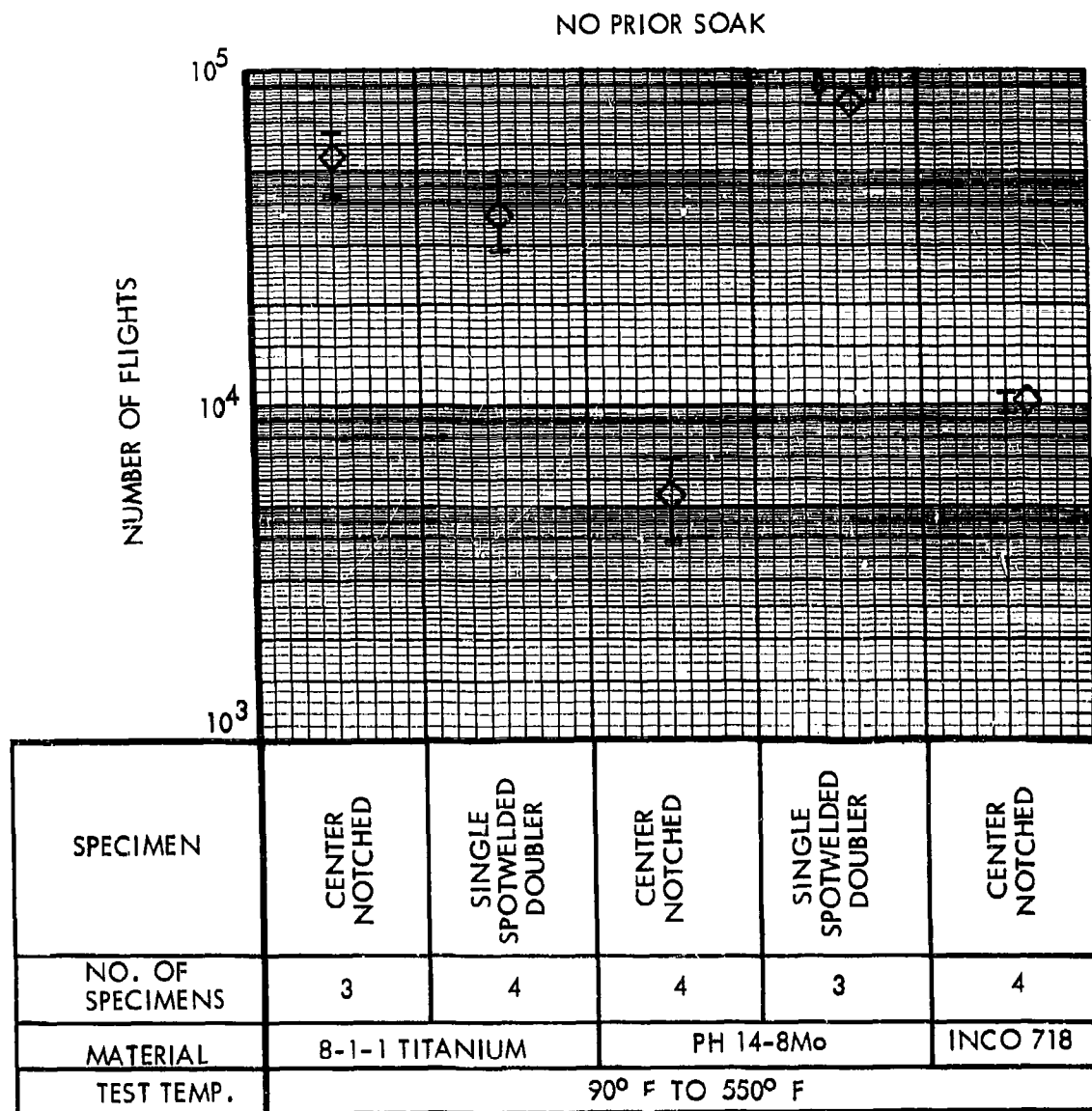| SPECIMEN MATERIAL	SPECIMEN TYPE	REFERENCE 1g STRESS (ksi)	SPECIMEN TEMP. (°F)	TIME AT 550°F (hours)	NUMBER OF FLIGHTS TO DEVELOPMENT OF VISUAL CRACKING	COMMENTS
8-1-1 Titanium Duplex Annealed	Center Notched	25	90 to 550	3.61	13,000	Specimens overheated
				4.22	15,200	
				4.86	17,500	
				4.86	17,500	Specimens overloaded
				11.64	41,900	
				11.64	41,900	
				16.42	59,100	
				18.00	64,800	
	Single Spotwelded Doubler	25		8.03	28,900	
				8.17	29,400	
				10.39	37,400	
				13.68	49,250	
PH14-8Mo (SRH 1050) Stainless Steel	Center Notched	40		.94	3,400	Loads were 14% too high
				1.11	4,000	
				1.92	6,900	
				1.92	6,900	
				.94	3,400	Loads were 14% too high
				.97	3,500	
				1.08	3,900	
				1.08	3,900	
	Single Spotwelded Doubler			14.25	51,300	Failed at edge of clamp
				22.22	80,000 plus	No failure, testing discontinued
				22.22	80,000 plus	
				22.22	80,000 plus	
INCO 718 Cold Rolled, Aged at 1275°F	Center Notched	40	90 to 550	2.92	10,500	3000 flights with loads 14% too high
				2.78	10,000	14% too high
				3.25	11,700	Overloaded by unknown high compressive load
				3.06	11,000	
				2.69	9,700	
				2.64	9,500	
				3.03	10,900	

NO PRIOR SOAK

SPECIMEN	CENTER NOTCHED	SINGLE SPOTWELDED DOUBLER	CENTER NOTCHED	SINGLE SPOTWELDED DOUBLER	CENTER NOTCHED
NO. OF SPECIMENS	3	4	4	3	4
MATERIAL	8-1-1 TITANIUM		PH 14-8Mo		INCO 718
TEST TEMP.	90° F TO 550° F				

I   SCATTER BAND FOR TEST RESULTS

◇ AVERAGE OF TEST RESULTS

♀ INDICATES INCLUSION OF
    TESTS WITH NO FAILURE

Figure 84.   Accelerated Flight-by-Flight Test Results for Spectra C
with Cyclic Temperature

130

B. FUSELAGE LOADING CONDITIONS

In the tests described in the preceding section, the load magnitudes and sequences are appropriate to lifting surfaces. In other portions of an airframe, quite different conditions occur which require different test evaluations. One of the more important of these is the region of fuselage skin which is loaded principally by fuselage pressurization. A reasonable approximation to the significant service loadings is obtained by the use of simultaneously applied cycles of loading and heating. The test loading and heating cycle represents the cycle of hoop tension load and aerodynamic heating produced once per flight in service.

To provide an evaluation of the effect on this loading-heating cycle, notched and fusion-welded specimens were tested in specially constructed apparatus which is described in Appendix IV. Each load cycle ranged from approximately zero to a constant tensile maximum and each temperature cycle ranged from 120°F to 550°F.

Two cycles of heating and cooling were produced during each minute of test time so the total time at maximum temperature in these tests was relatively small. To obtain an indication of the effects of extended exposure to stress at elevated temperature on the test results, an additional set of specimens was tested after previous exposure under constant load for 5,000 hours at 650°F. The exposure conditions for these specimens were the same as those employed for the sets of exposed specimens tested under Phase I.

The S-N data obtained under the Phase I testing indicated the need for relatively high test stresses. However, in this type of test in which simple repetitions of constant test conditions are applied, the test lives obtained for large load magnitudes provide assurance of much longer test lives at lower, more realistic, magnitudes.

The results obtained in these tests are listed in Table 24 and shown graphically on Figures 85 through 90. These figures also present conventional S-N Curves for specimens with and without prior exposure. The S-N curves were taken from Volume II.

The test lives for all specimens indicate that very long test durations would be obtained at the lower maximum design stresses considered to be suitable for the skins of pressurized fuselages. In addition, the data indicate that prior exposure of specimens for 5000 hours at 650°F had very little effect on the test lives.

Within the scope of the data, it appears that the test lives for the conditions in this type of test could be predicted reasonably well and conservatively from conventional S-N data obtained at constant temperature. The ratings of the materials on the basis of stress to density ratio are then the same as those presented for the S-N testing in Phase I. In other words, duplex-annealed 8-1-1 titanium sheet is rated first for all specimen configurations. PH14-8Mo is rated second for the fusion-welded specimens. For the center-notched specimens, Inco is rated second in the high stress low cycle range while PH14-8Mo is rated second in the low stress high cycle range.

131

TABLE 24 FUSELAGE LOADING TESTS WITH TEMPERATURE CYCLES FROM 120 TO 550°F

SPECIMEN MATERIAL	SPECIMEN TYPE (1)	PRIOR SOAK	MAX STRESS (ksi) R ≈ 0	CYCLES TO FAILURE
8-1-1 Titanium Duplex Annealed	Center Notched	None	70 70	7,750 (2) 7,841 (2)
		None	60 60	36,527 43,098
		25 ksi at 650°F for 5000 hr	65 65	6,662 8,262
	Fusion Welded and Planished	None	88 88	19,605 (2) 20,000 (2)
		None	80 80	36,988 37,927 (3)
		25 ksi at 650°F for 5000 hr	95 95	16,824 27,374
FH14-8Mo (SRH 1050) Stainless Steel	Center Notched	None	65 65	16,587 (2) 22,598 (2)
		None	60 60	26,010 80,000 (4)
		40 ksi at 650°F for 5000 hr	65 65	9,699 12,362
	Fusion Welded and Planished	None	130 130	8,490 (2) 20,480 (2)
		None	110 110	80,000 (4) 80,000 (4)
		40 ksi at 650°F for 5000 hr	130 130	13,337 23,837
INCO 718 Cold-Rolled Aged at 1275°F	Center Notched	None	80 80	25,491 (2) 27,000 (2)
		None	76 76	52,962 55,335
		40 ksi at 650°F for 5000 hr	76 76	51,391 53,718
	Fusion Welded and Planished	None	120 120	1,150 (2) 1,150 (2)
		None	108 108	24,493 33,185
		40 ksi at 650°F for 5000 hr	108 108	13,077 41,150

(1) Transverse grain, all specimens.
(2) Exploratory test results.
(3) Failed at the thermocouple attachment.
(4) No failure, testing stopped.

Figure 85. Comparison of Fuselage Loading Test Lives with S-N Curves, Unexposed 8-1-1 Titanium

CYCLES TO FAILURE

Figure 86. Comparison of Fuselage Loading Test Lives with S-N Curves,
Unexposed PH 14-8Mo

CYCLES TO FAILURE

Figure 87. Comparison of Fuselage Loading Test Lives with S-N Curves,
Unexposed INCO 718

135
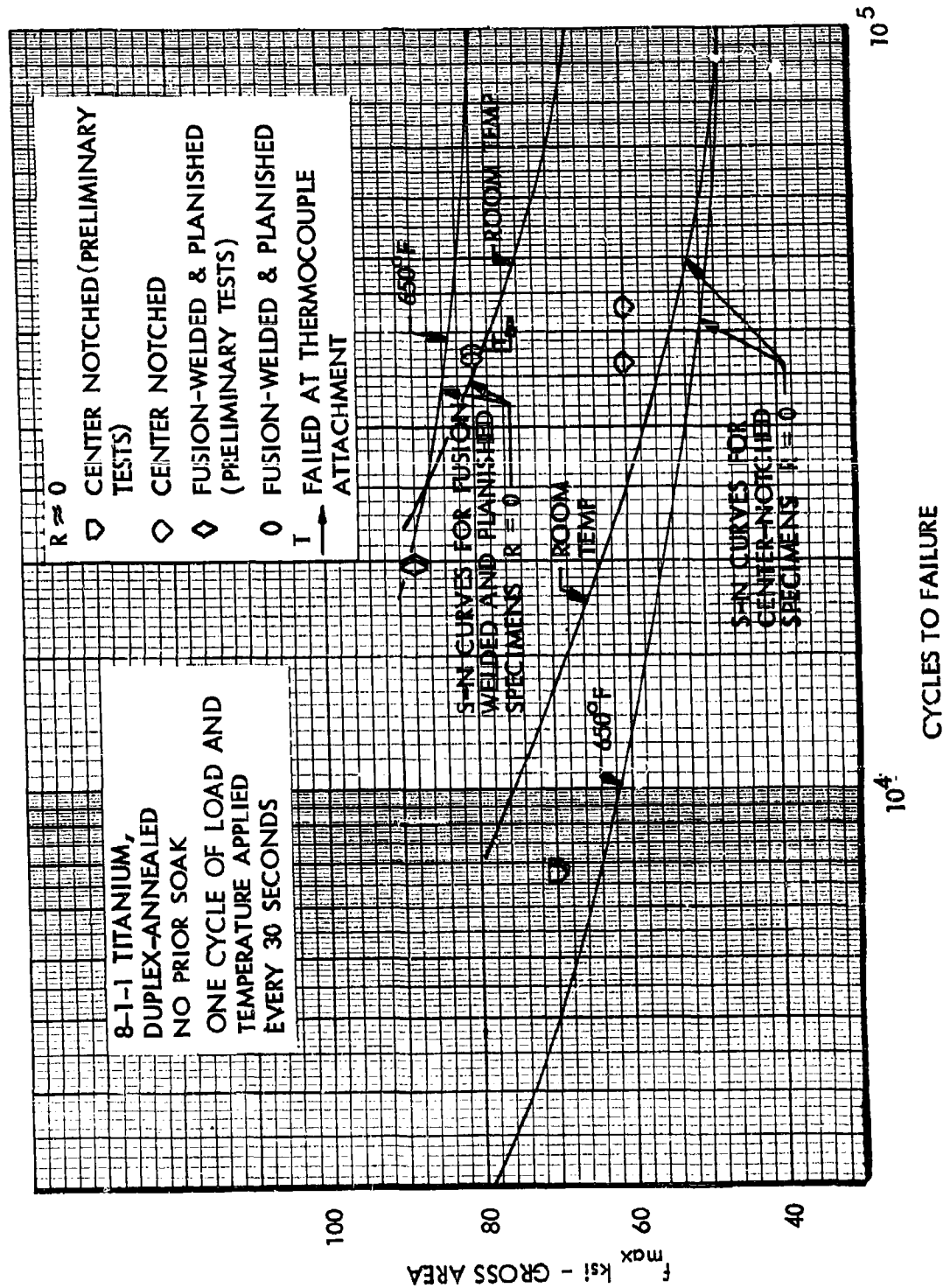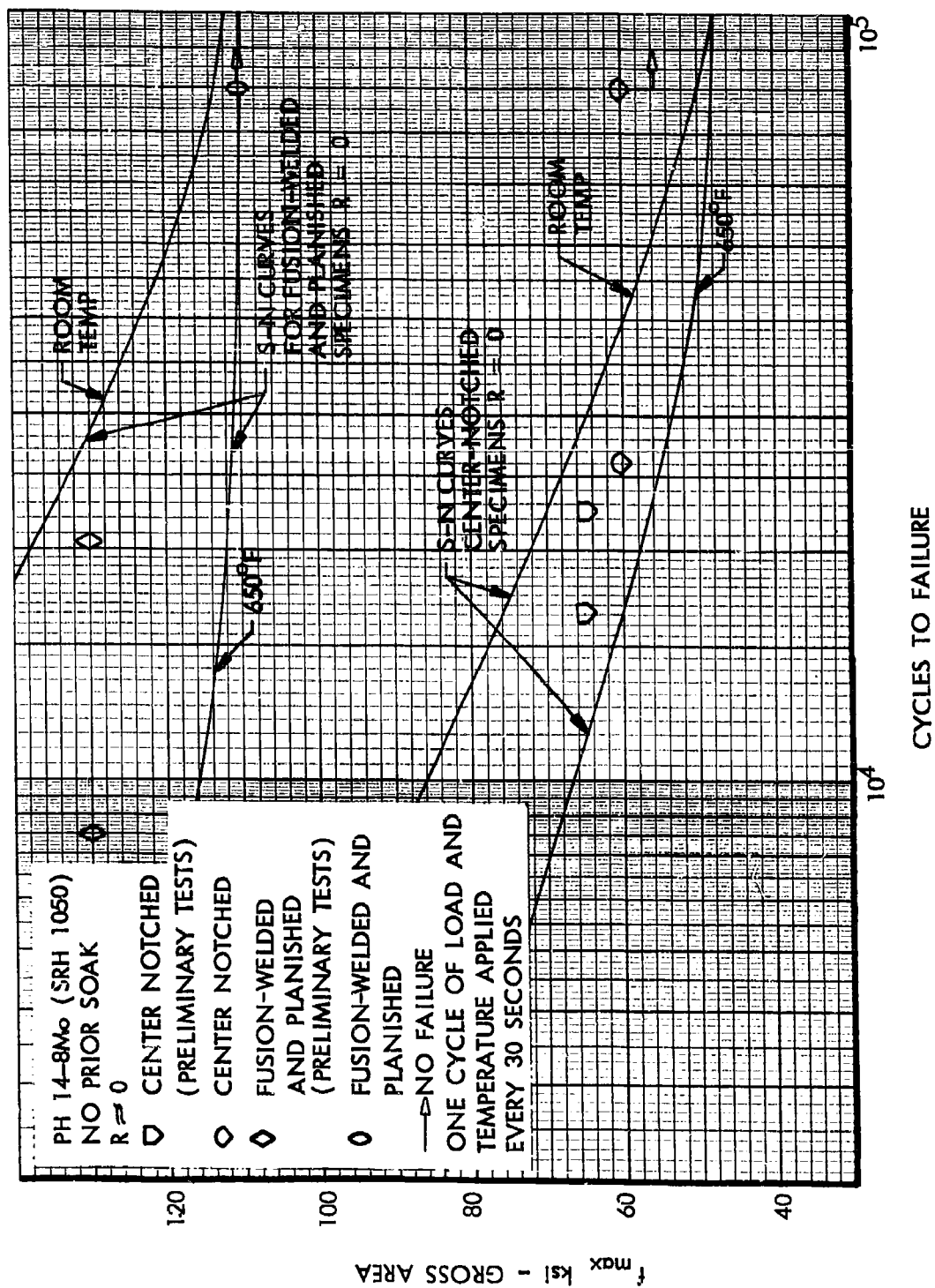
Figure 88. Comparison of Fuselage Loading Test Lives with S-N Curves, Exposed 8-1-1 Titanium

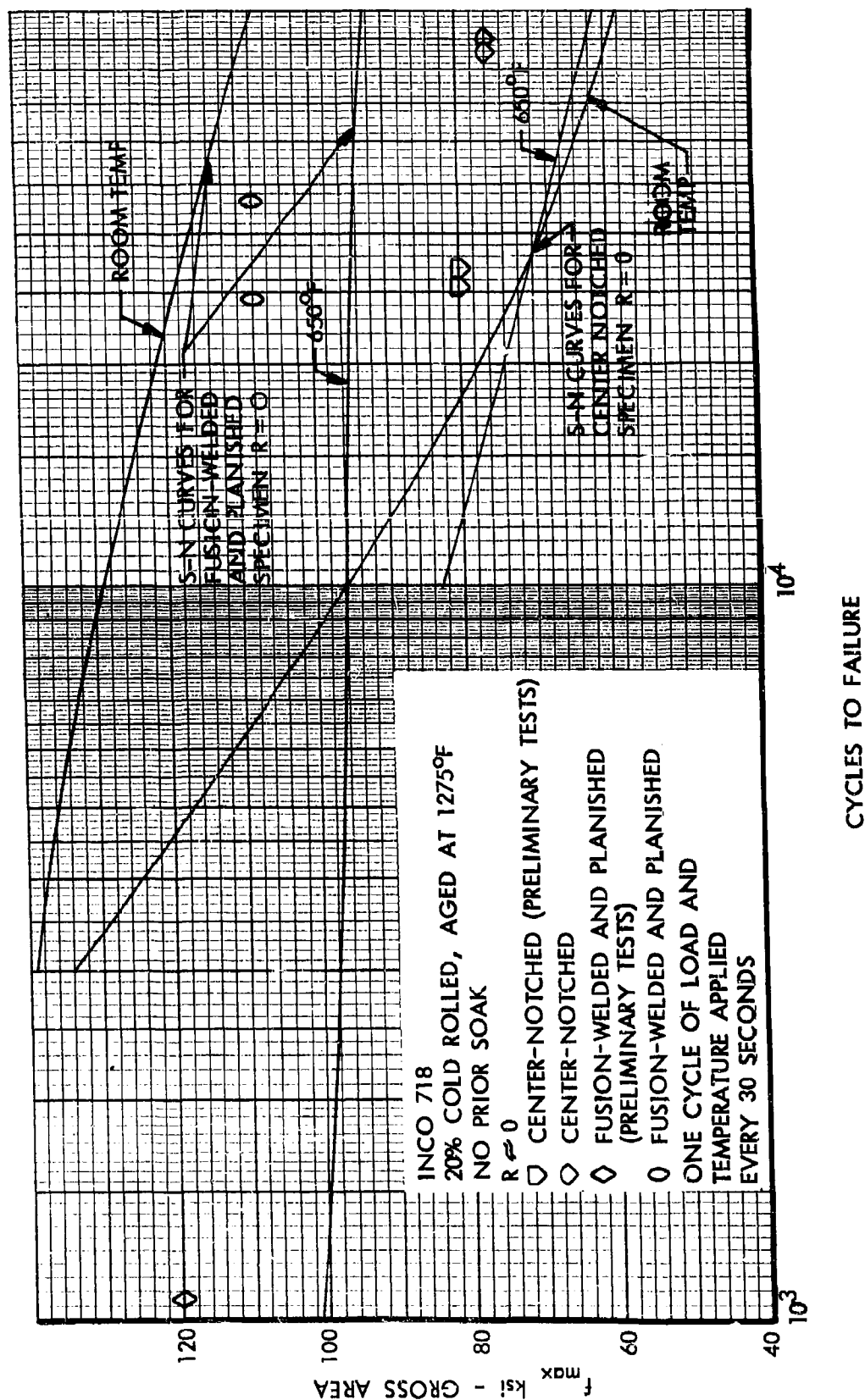Figure 89. Comparison of Fuselage Loading Test Lives with S-N Curves,
Exposed Ph 14-8Mo

137

Figure 90. Comparison of Fuselage Loading Test Lives with S-N Curves, Exposed INCO 718
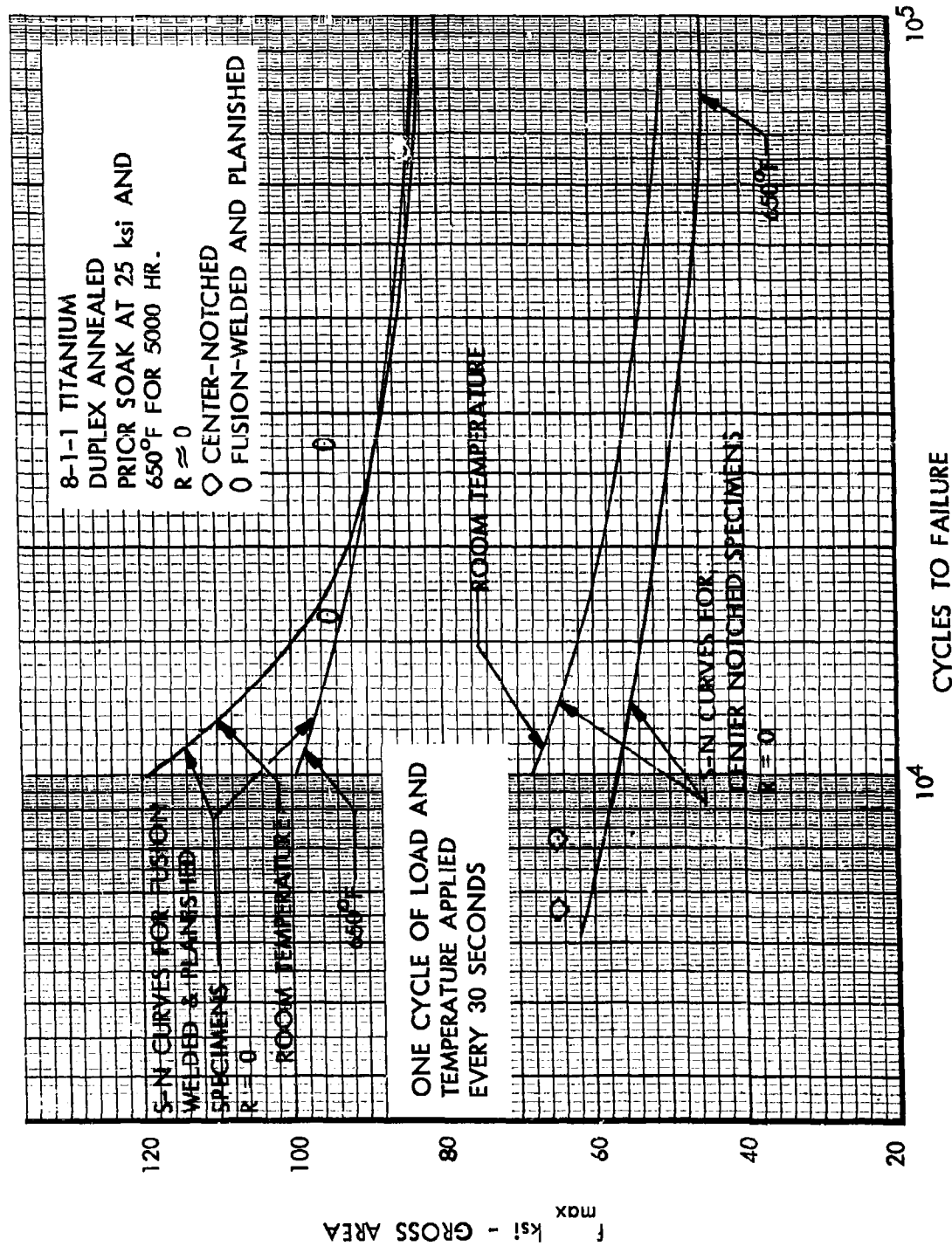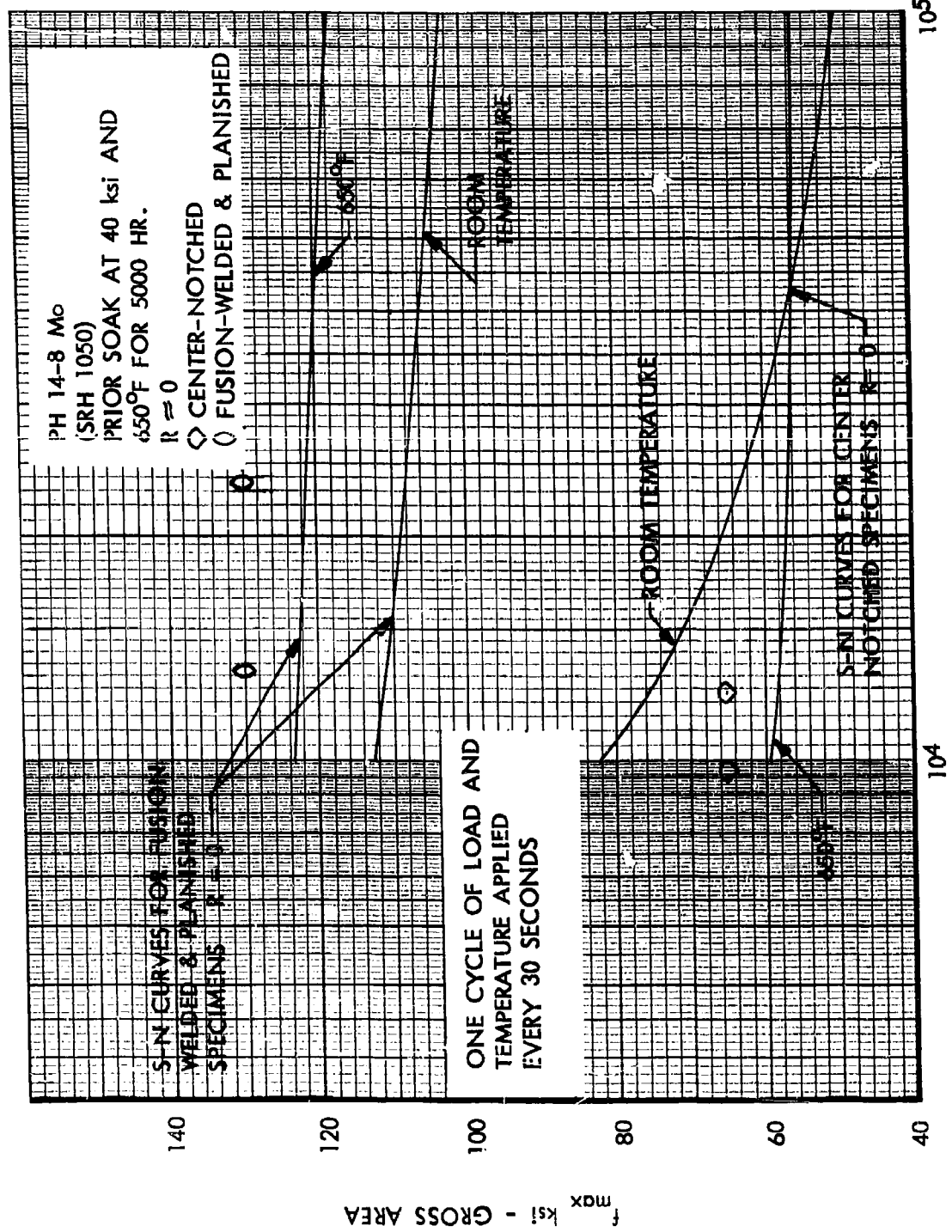
In the test work previously described for this program, no provision was made for evaluating the effect of contaminating or corrosive agents. A series of tests was therefore undertaken to explore the effect of these agents on fatigue test durations and on static tensile properties of the materials at elevated temperature.

Three agents were used in this study. One is a standard ASTM saline solution used for such tests, the second is a super-refined mineral oil produced to MIL-O-7277 which is considered suitable for use as an engine lubricant, and the third is a synthetic material identified as Versilube F-50. This latter material offers promise of satisfactory use in the hydraulic systems on supersonic transports.

In one series of fatigue tests, unnotched, notched and fusion-welded specimens were tested by applying one amplitude of varying load at a stress ratio, R of 0.10, and a temperature of $650°F$. The amplitude for each type of specimen was chosen by referring to the S-N data obtained under Phase I of the program to avoid unduly long test times. Before the start of the test, a potentially contaminating or corrosive material was applied to the specimen test section. At intervals during the test corresponding to approximately one tenth of the anticipated test duration, the oscillatory loading was stopped, the specimens were cooled to approximately room temperature, and the contaminant or corrosive agent was reapplied.

For a subsequent set of tests, three specimens of each of four geometries in each material were loaded by dead weight and heated to $550°F$ intermittently for a total exposure time of approximately 1,000 hours. At intervals of approximately $1\frac{1}{2}$ hours during this exposure, the loading was removed, the temperature was returned to approximately room temperature, a contaminating or corrosive material was painted on both sides of each specimen test section, load was reapplied, and the temperature returned to $550°F$.

For this preconditioning of specimens, the simple enclosed loading rack described in Appendix IV was used.

The effect of this preconditioning on resistance to repeated loading was evaluated by constant load amplitude tests conducted at the same load levels and temperature and with the same sequence of contaminant application as that used in the initial tests described above.

The test lives obtained in these two sets of tests are listed in Tables 25 through 30 and are presented in Figures 91 through 117 where they may be compared with test lives obtained in the absence of contaminants.

An examination of these figures shows that, with the possible exception of short-time salt water exposure on fusion-welded titanium specimens, the exposures to contaminants have had no significant effect on the potential test lives of the specimens. Since exposure of the fusion-welded titanium specimens to salt water in the 1000 hour test led to longer specimen test lives which fall within the range of lives for unexposed specimens, there is

139

probably little practical significance to the relatively short test lives obtained in the short time test.

The effect of the exposure to contaminants for 1000 hours at 550°F on the static tensile properties was obtained using standard tensile strength specimens. The results of these tests are listed in Table 31, Page 174 and are shown graphically on Figures 118, 119 and 120, where they may be compared with results obtained for specimens which were not so exposed.

The data show that Versilube F-50 had the largest effect on each of the materials in the static tests at 650°F. The ultimate strengths, when compared with the average test data obtained after exposure for 1000 hours at 650°F without contaminants, were changed by amounts ranging from plus 3 to minus 11 percent. For the 8-1-1 titanium specimens, the yield strength was increased by 11 percent and, for PH14-Mo and INCO 718 specimens the yield strength was reduced by 11 and 5 percent, respectively. For the titanium specimens, the elongation was reduced by 26 percent and, for the steel and nickel alloy specimens, the elongation was increased by 32 and 10 percent, respectively.

Five of the constant amplitude loading fatigue test specimens were sectioned after test and examined at 20 and 200X magnifications for surface corrosion and subsurface cracks from either the contaminant or from the test loading. The specimens were selected on the basis of the S-N tests to represent either the longest exposure and most severe test loading or the worst combination of material, specimen configuration and contaminant. The metallographic structure of the examined specimens which are shown in Appendix VIII appeared to be the normal ones for each material and showed no evidence of surface corrosion, intergranular attack or subsurface cracks.

In addition to the constant load amplitude fatigue tests, sets of two center-notched specimens of each material were subjected to contaminants during flight-by-flight sequences of loading at a test temperature of 550°F. In these tests the loadings were those defined for Spectra C in Phase II. During each test, the application of loadings was interrupted and the specimens were cooled to approximately room temperature at one hour intervals, a contaminant was reapplied, the specimens were reheated to 550°F and loading was resumed. For these tests, examination of the data previously obtained led to the selection of the Mil-O-7277 oil for application to each material and the selection of salt water for application to two 8-1-1 titanium specimens.

The results obtained in these tests are listed in Table 32, Page 178 and those obtained for exposure to oil are presented graphically on Figure 121 for comparison with data for specimens tested without contaminant. The data listed in the table show that neither the salt water nor the oil had any effect on the test lives of the 8-1-1 titanium specimens. The comparisons shown on this figure indicate that exposure to oil reduced the average test lives of the PH14-8Mo and INCO 718 specimens by approximately 17 and 32 percent respectively.

In view of the small number of test specimens and the severity of the test, the significance of these results is questionable. However, the type of test appears to provide more definite indications of the effects of contaminant than those provided by S-N testing with its larger scatter in test lives.

TABLE 25 CONSTANT AMPLITUDE FATIGUE TEST DATA AT 550 AND 650°F WITH CONTAMINANT
ASTM SYNTHETIC SEA WATER APPLIED DURING TEST
TRANSVERSE GRAIN - NO PRIOR SOAK

Specimen Material	Specimen Type	Max. Stress (ksi) R = 0.1	Test Temp. (°F)	Cycles to Failure
8-1-1 Titanium Duplex Annealed	Center-Notched	50 50 50 40 45 50 50 50	650 650 650 650 650 550 550 550	12,780 16,740 12,600 1,000,000** 375,000* 43,200 26,640 236,340
	Unnotched	92	650	12,420 21,780 14,760
	Fusion-Welded	80	650 650 650 550 550 550	38,340 9,900 25,560 17,100 77,400 17,640
PH14-8Mo (SRH 1050) Stainless Steel	Center-Notched	62	650	10,980 207,360 364,320
	Unnotched	125	650	14,760 56,880 1,000,000**
	Fusion-Welded	115	650	23,400 23,400 1,000,000**
INCO 718 Cold Rolled, Aged at 1275°F	Center-Notched	60	650	108,000 126,540 105,300
	Unnotched	140	650	91,980 130,860 137,880
	Fusion-Welded	90	650	607,860 1,000,000** 656,460

*Failed at the thermocouple attachment
**No failure

141

TABLE 26 CONSTANT AMPLITUDE FATIGUE TEST DATA AT 650°F WITH CONTAMINANT
MIL-O-7277 SUPER-REFINED MINERAL OIL APPLIED DURING TEST
TRANSVERSE GRAIN – NO PRIOR SOAK

Specimen Material	Specimen Type	Max. Stress (ksi) R = 0.1	Test Temp. (°F)	Cycles to Failure
8-1-1 Titanium Duplex Annealed	Center-Notched	50	650	78,660 305,460 148,500
	Unnotched	92	650	589,320* 1,000,000** 470,620
	Fusion-Welded	80	650	1,000,000** 126,540 39,240
PH14-8Mo (SRH 1050) Stainless Steel	Center-Notched	62	650	11,160 10,800 12,960
	Unnotched	125	650	22,860 30,060 108,360
	Fusion-Welded	115	650	419,220 1,000,000** 30,420
INCO 718 Cold Rolled, Aged at 1275°F	Center-Notched	60	650	178,380 98,640 135,180
	Unnotched	140	650	137,340 129,060 134,460
	Fusion-Welded	90	650	81,360 52,740 21,060

* Failed at the thermocouple attachment
** No Failure

TABLE 27 CONSTANT AMPLITUDE FATIGUE TEST DATA AT 650°F WITH CONTAMINANT
VERSILUBE F-50 APPLIED DURING TEST
TRANSVERSE GRAIN - NO PRIOR SOAK

Specimen Material	Specimen Type	Max. Stress (ksi) R = 0.1	Test Temp. (°F)	Cycles to Failure
8-1-1 Titanium Duplex Annealed	Center-Notched	50	650	235,620 179,100 426,780
	Unnotched	92	650	1,000,000** 1,000,000** 95,760
	Fusion-Welded	80	650	1,000,000** 42,660 27,720
PH14-8Mo (SRH 1050) Stainless Steel	Center-Notched	62	650	18,360 1,000,000** 14,220
	Unnotched	125	650	614,880 561,240 510,300
	Fusion-Welded	115	650	203,400 24,120 34,200
INCO 718 Cold Rolled, Aged at 1275°F	Center-Notched	60	650	16,560 148,500 189,540
	Unnotched	140	650	140,940 144,900 77,580
	Fusion-Welded	90	650	677,880 40,140 1,000,000**

**No Failure

143

TABLE 28 CONSTANT AMPLITUDE FATIGUE TEST DATA AT 650°F WITH CONTAMINANT SPECIMENS EXPOSED TO ASTM SYNTHETIC SEA WATER BEFORE AND DURING TEST

Specimen Material	Specimen Type	Prior Soak	Max. Stress (ksi) R=0.1	Cycles to Failure
8-1-1 Titanium Duplex Annealed	Center-Notched	1000 HRS AT 25 ksi and 550°F	50	109,620 356,580 267,480
	Unnotched		92	48,240 27,540 171,900
	Fusion-Welded		80	53,820 773,100 105,920
PH14-8Mo (SRH 1050) Stainless Steel	Center-Notched	1000 HRS AT 40 ksi and 550°F	62	18,180 19,980 10,620
	Unnotched		125	17,730 135,180* 895,680
	Fusion-Welded		115	62,820 51,840 41,580
INCO 718 Cold Rolled, Aged at 1275°F	Center-Notched	1000 HRS AT 40 ksi and 550°F	60	118,260 160,380 150,300
	Unnotched		140	50,220 46,260 44,460
	Fusion-Welded		90	1,000,000** 1,000,000** 698,000

* Failed at clamp
** No failure

TABLE 29 CONSTANT AMPLITUDE FATIGUE TEST DATA AT 650°F WITH CONTAMINANT
SPECIMENS EXPOSED TO MIL-O-7277 SUPER REFINED MINERAL OIL BEFORE AND DURING TEST

Specimen Material	Specimen Type	Prior Soak	Max. Stress (ksi) R=0.1	Cycles to Failure
8-1-1 Titanium Duplex Annealed	Center-Notched	1000 HRS AT 25 ksi and 550°F	50	25,740 24,120 21,060
	Unnotched		92	18,000* 9,720 78,000*
	Fusion-Welded		80	1,000,000** 138,780*** 1,000,000**
PH14-8Mo (SRH 1050) Stainless Steel	Center-Notched	1000 HRS AT 40 ksi and 550°F	62	17,100 18,720 16,020
	Unnotched		125	21,420 10,260 13,680
	Fusion-Welded		115	1,000,000** 1,000,000** 1,000,000**
INCO 718 Cold Rolled, Aged at 1275°F	Center-Notched	1000 HRS AT 40 ksi and 550°F	60	169,380 131,760 107,280
	Unnotched		140	78,480 69,660 70,200
	Fusion-Welded		90	712,800 730,080 1,000,000**

* Failed at thermocouple attachment
** No failure
*** Failed at clamp

TABLE 30 CONSTANT AMPLITUDE FATIGUE TEST DATA AT 650°F WITH CONTAMINANT
SPECIMENS EXPOSED TO VERSILUBE F-50 BEFORE AND DURING TEST

Specimen Material	Specimen Type	Prior Soak	Max. Stress (ksi) R=0.1	Cycles to Failure
8-1-1 Titanium Duplex Annealed	Center-Notched	1000 HRS AT 25 ksi and 550°F	50	-- 748,800 362,700
	Unnotched		92	349,000* 35,280 158,000*
	Fusion-Welded		80	1,000,000** 1,000,000** 1,000,000**
PH14-8Mo (SRH 1050) Stainless Steel	Center-Notched	1000 HRS AT 40 ksi and 550°F	62	1,000,000** 32,040 1,000,000**
	Unnotched		125	10,260 8,820 11,340
	Fusion-Welded		115	25,200 38,880 19,620
INCO 718 Cold Rolled, Aged at 1275°F	Center-Notched	1000 HRS AT 40 ksi and 550°F	60	100,080 128,520 118,980
	Unnotched		140	184,500 63,360 100,440
	Fusion-Welded		90	--- 5,400 54,180

*   Failed at thermocouple attachment
** No failure
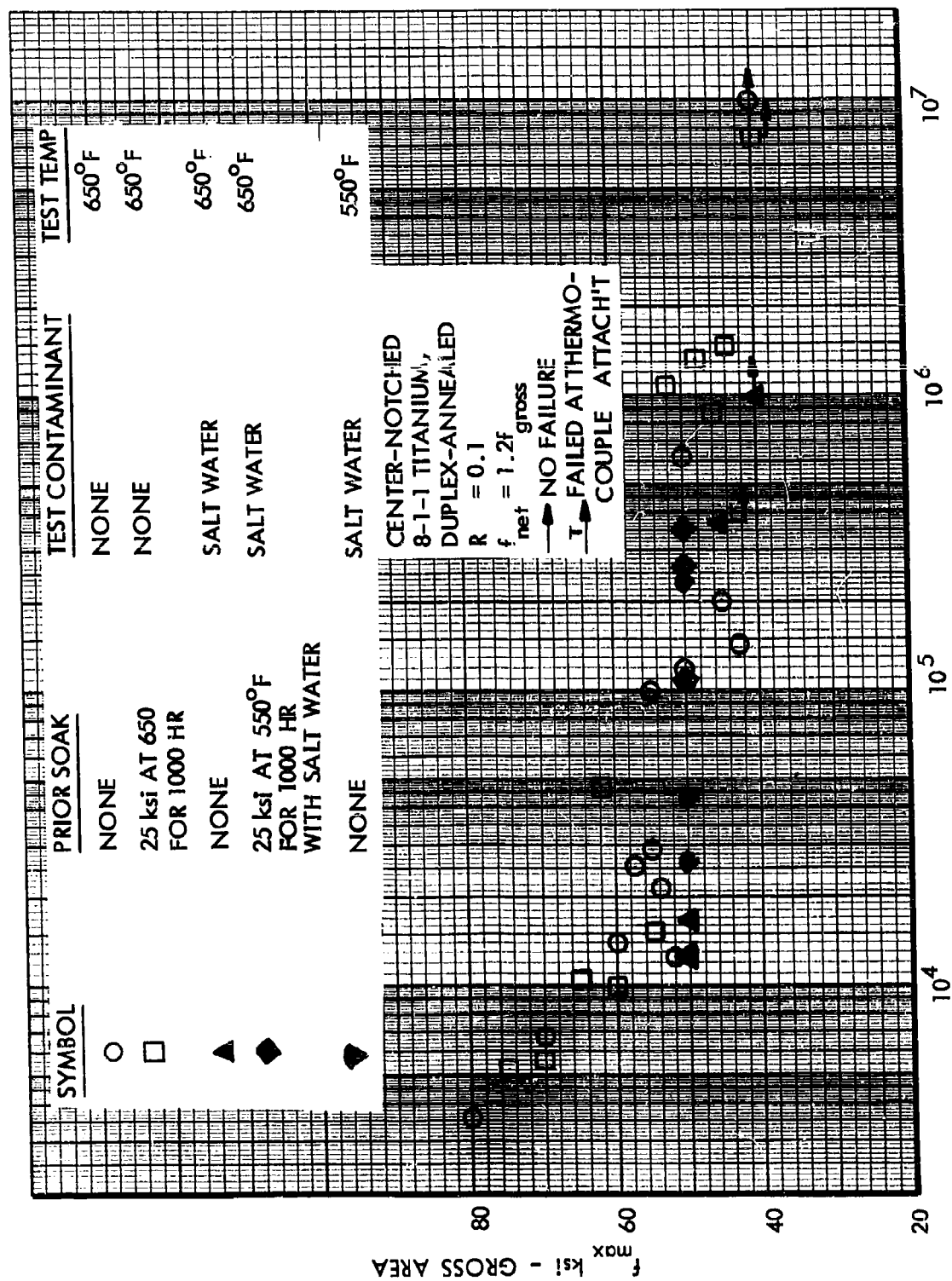
Figure 91. Effects of Salt Water on S–N Data at 550 and 650°F, Center-Notched 8-1-1 Titanium

147
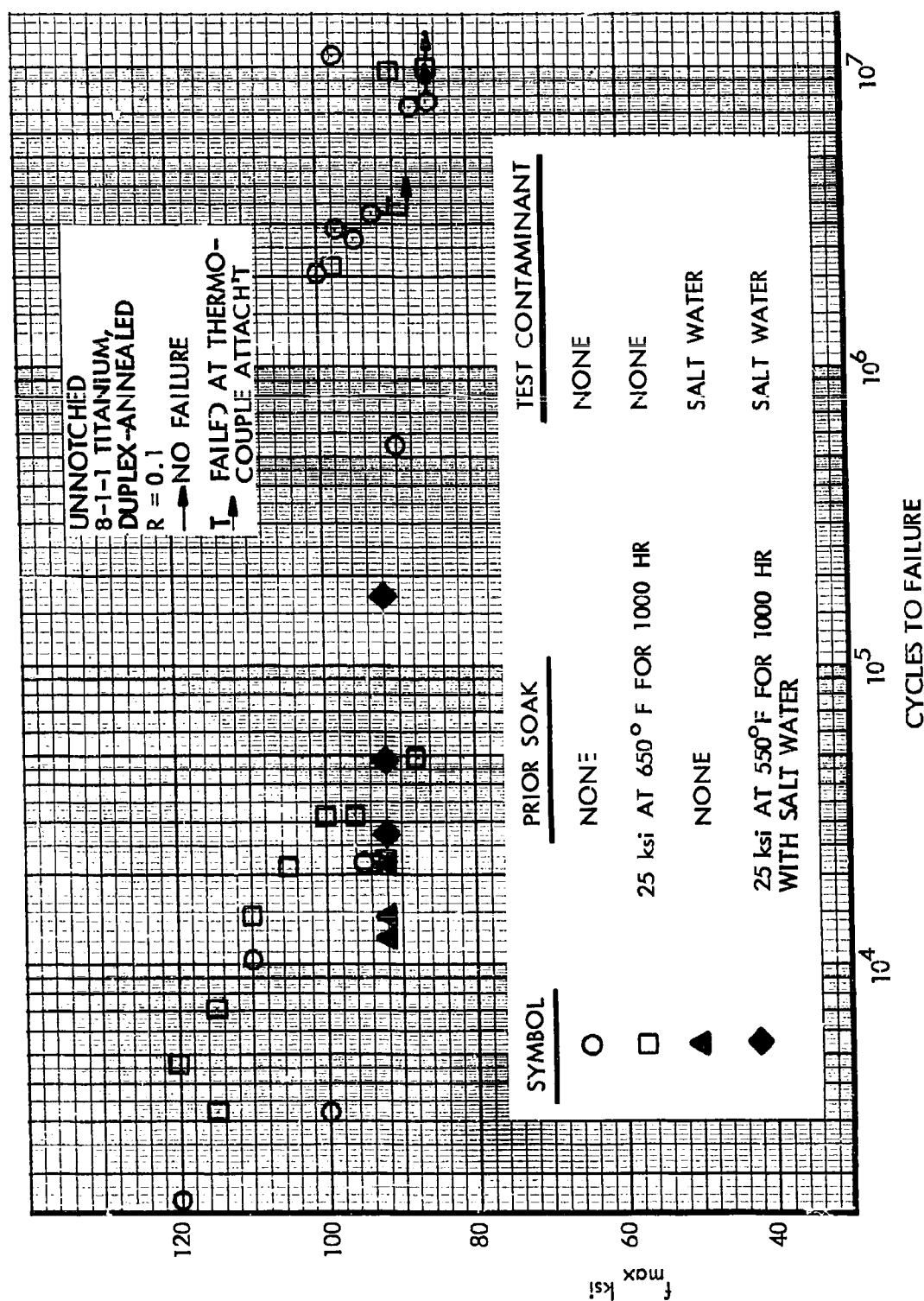
Figure 92. Effects of Salt Water on S-N Data at 650°F, Unnotched 8-1-1 Titanium
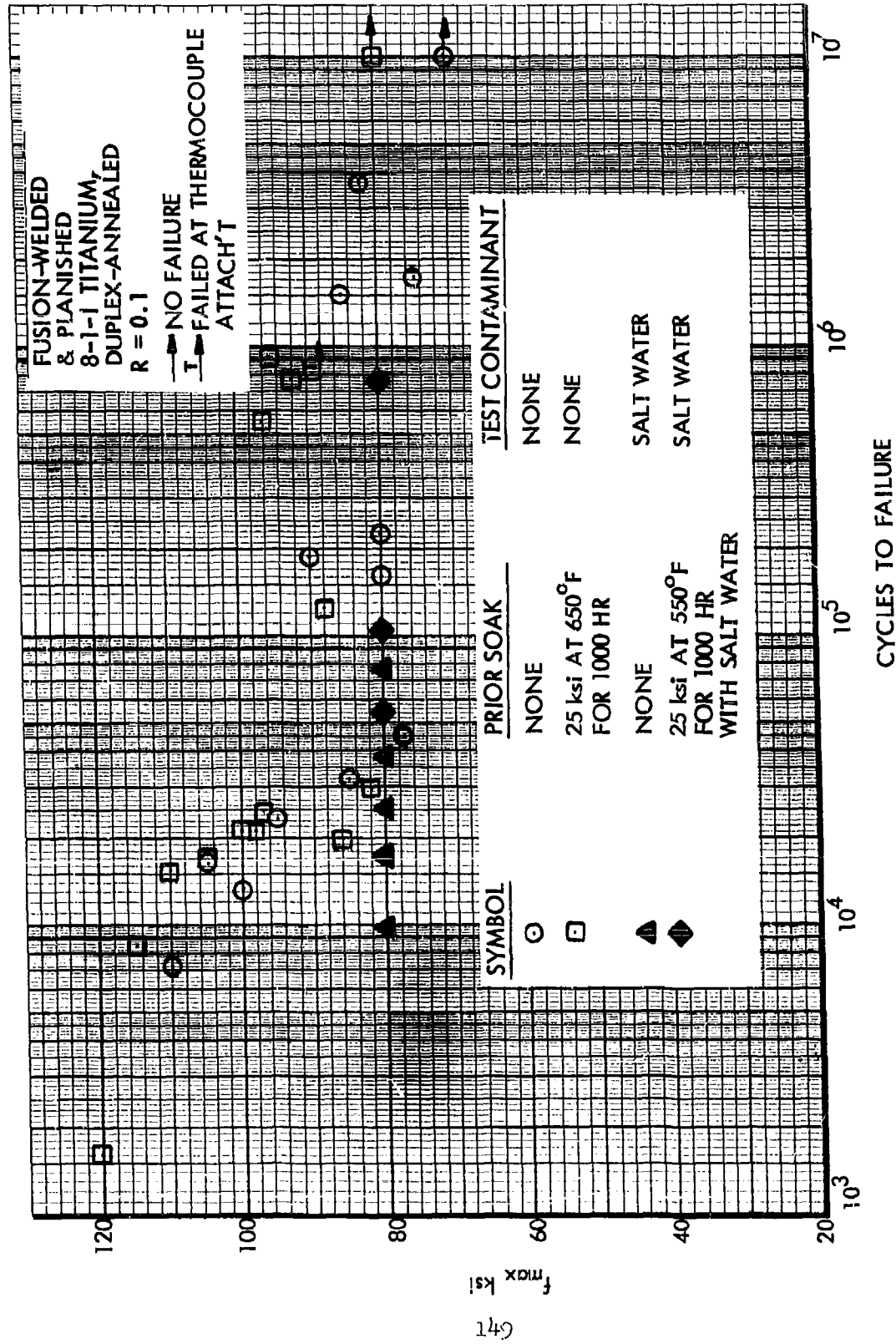
Figure 93. Effects of Salt Water on S-N Data at 650°F, Fusion-Welded 8-1-1 Titanium
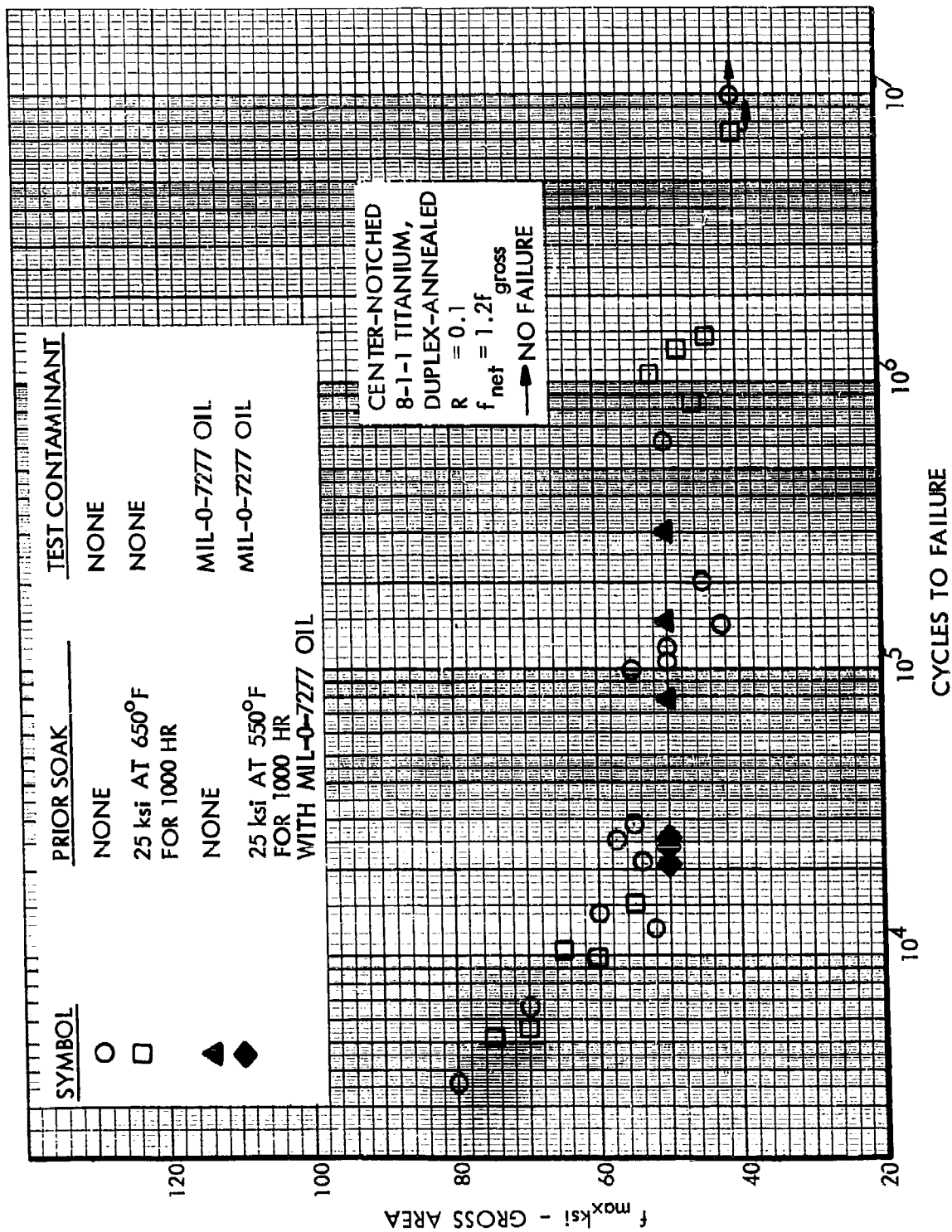
Figure 94. Effects of MIL-O-7277 Oil on S-N Data at 650°F, Center-Notched 8-1-1 Titanium

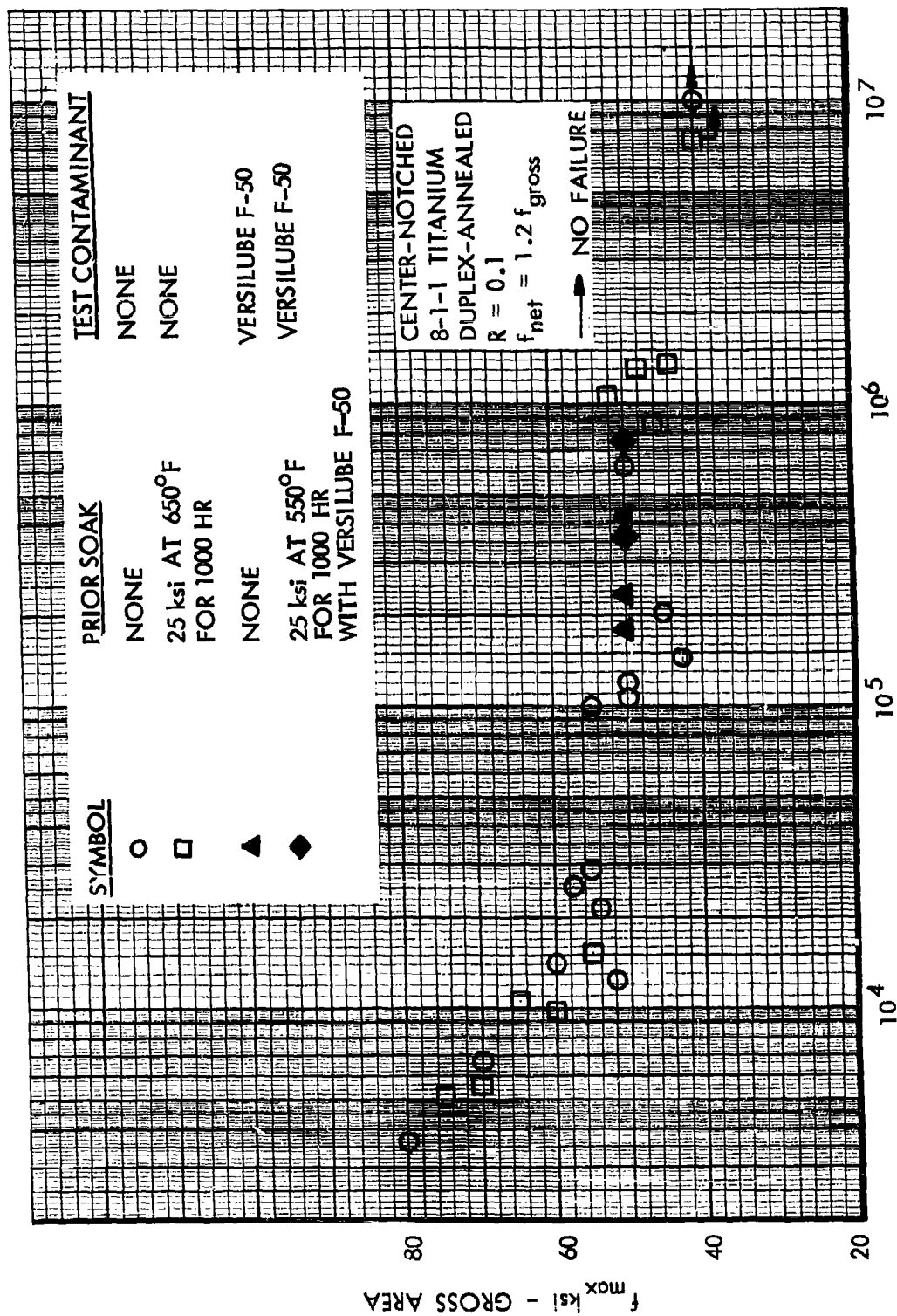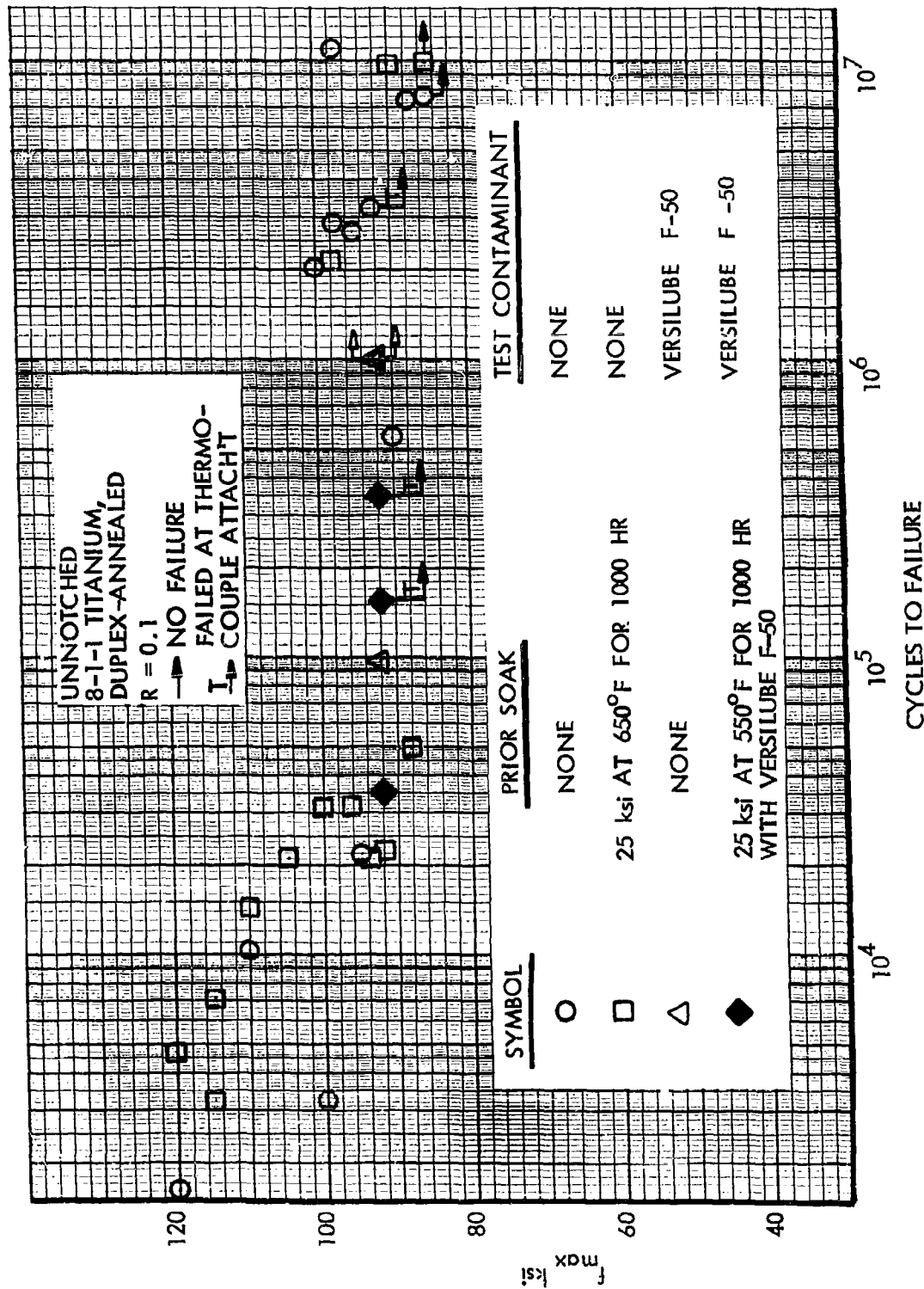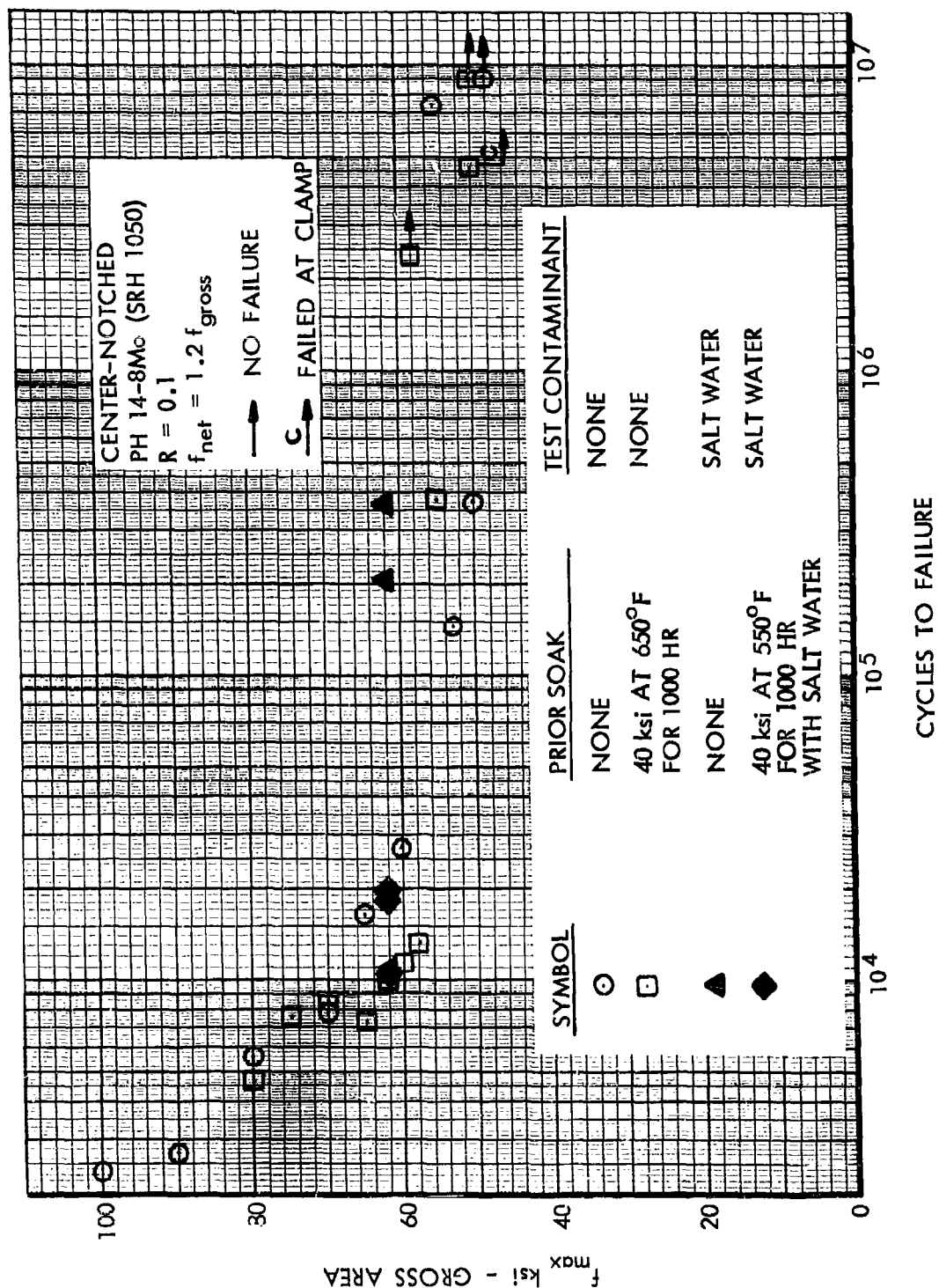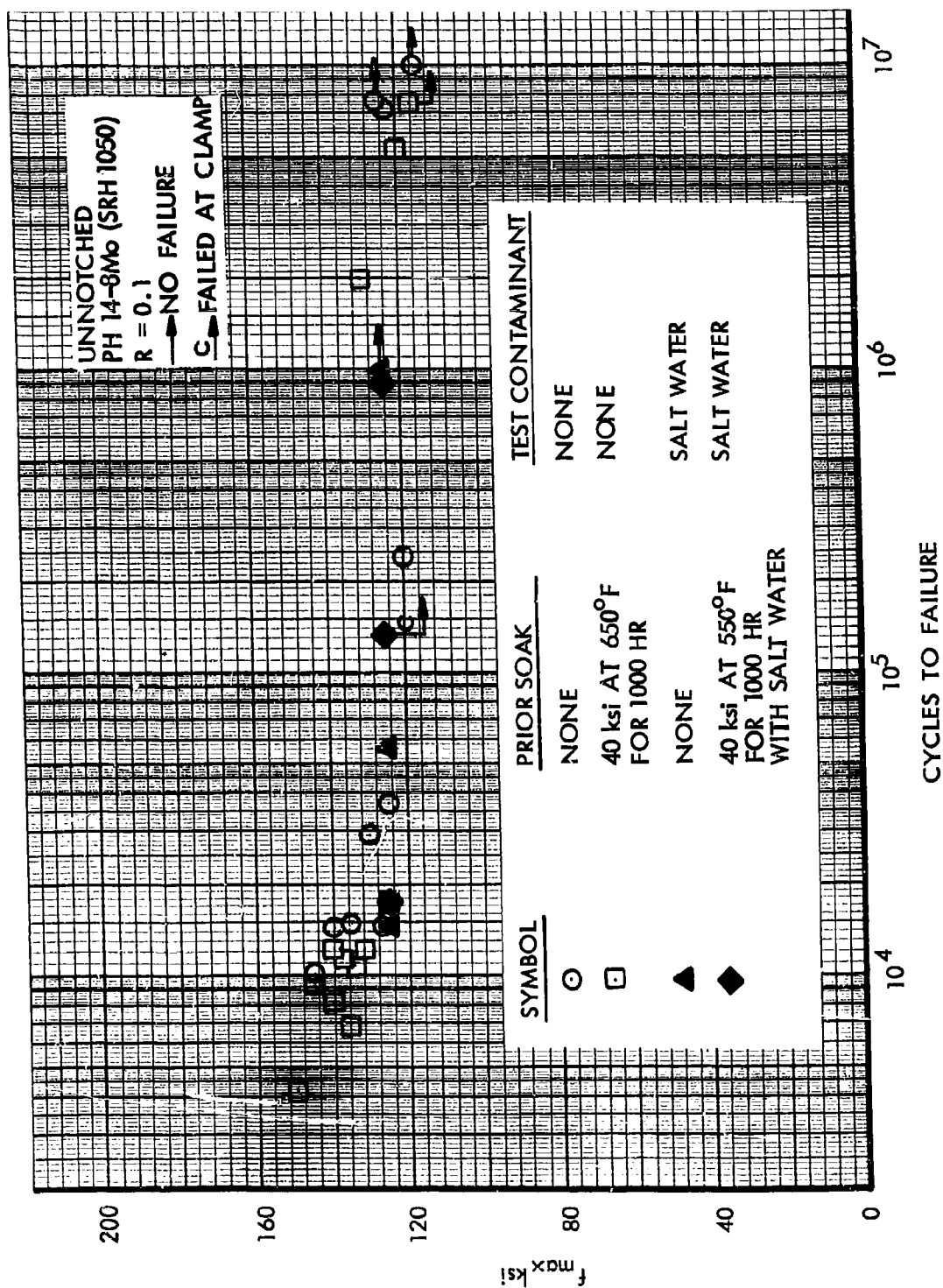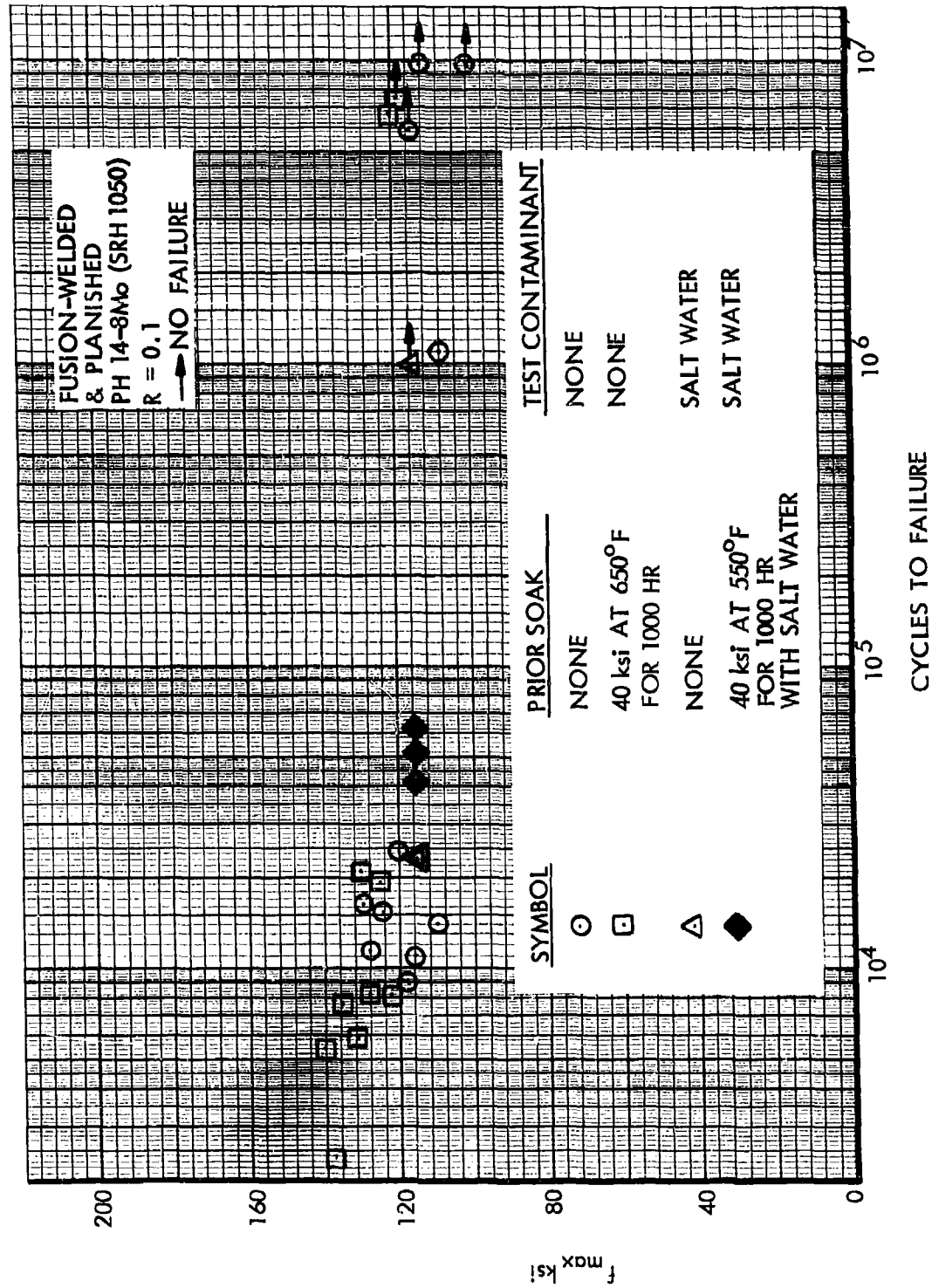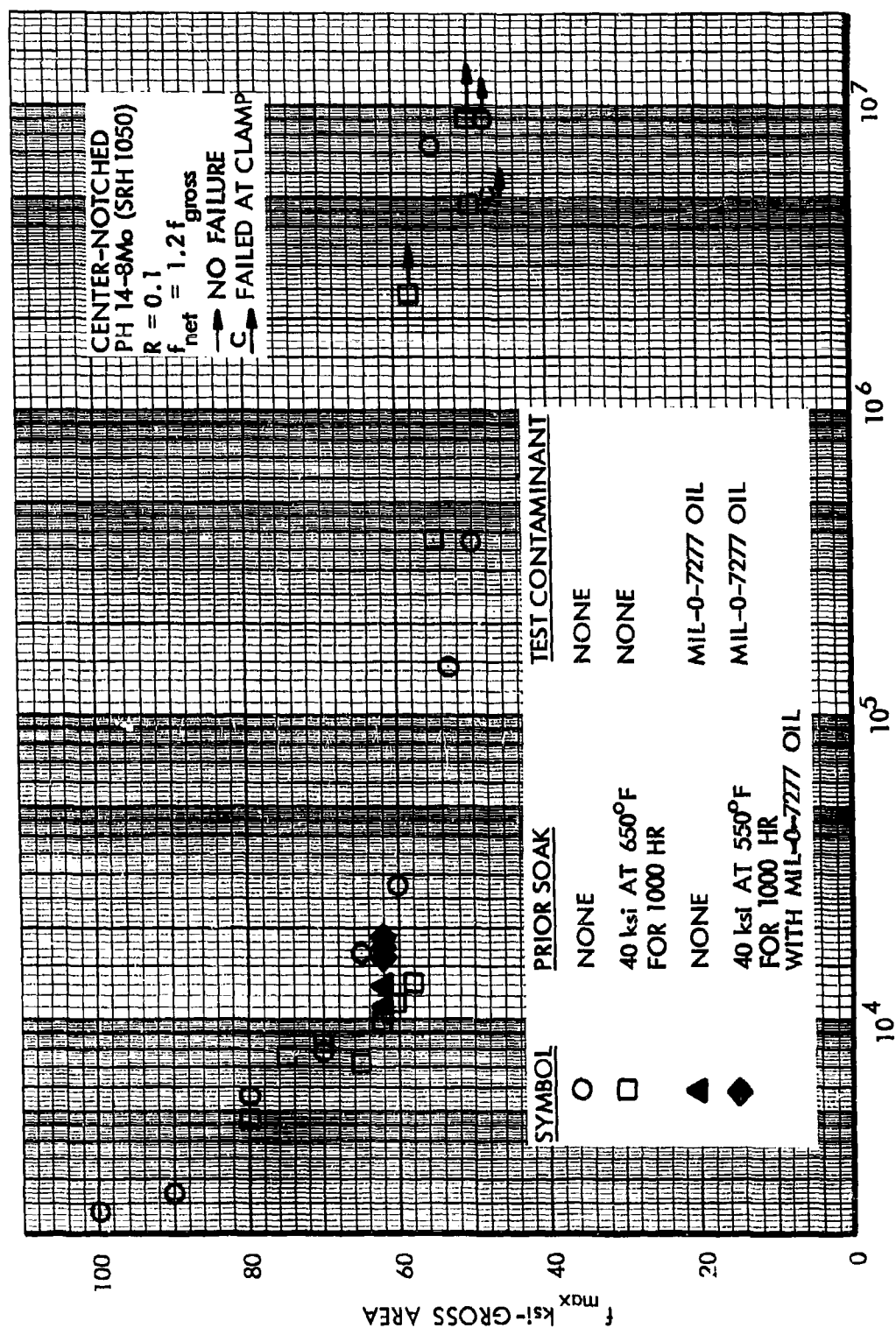Figure 95.   Effects of MIL-0-7277 Oil on S-N Data at 650°F, Unnotched 8-1-1 Titanium

151
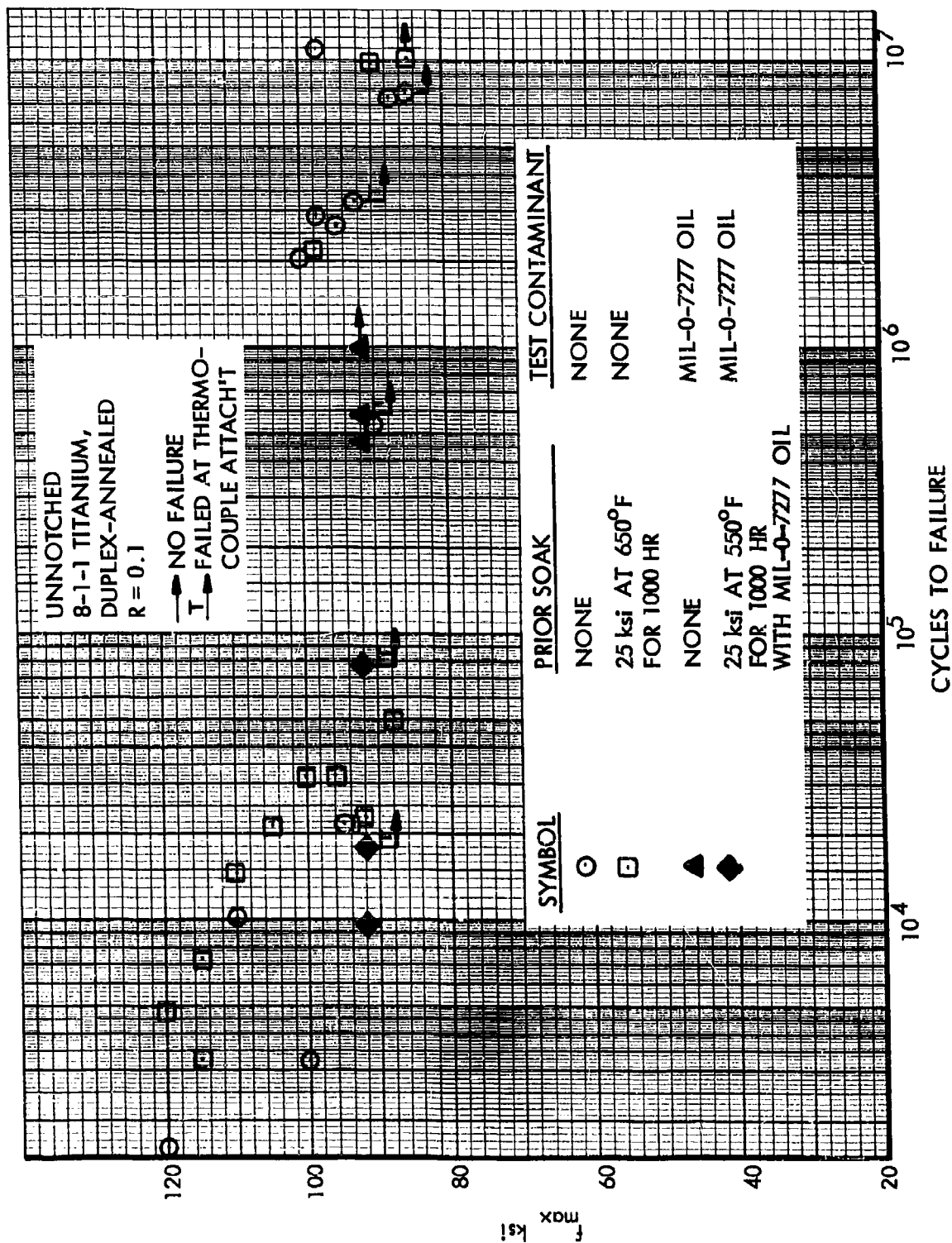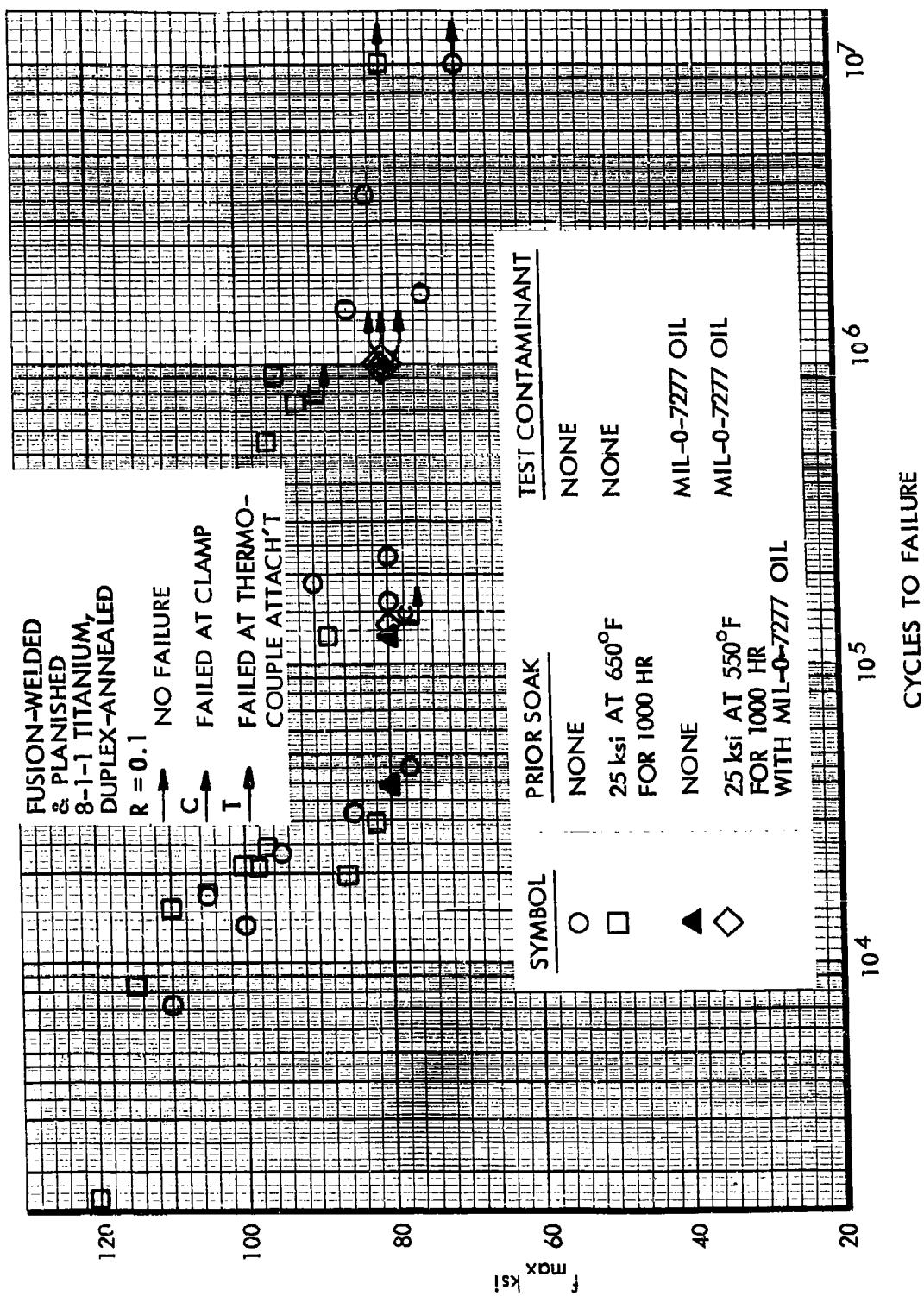
Figure 96. Effects of MIL-0-7277 Oil on S-N Data at 650°F, Fusion-Welded 8-1-1 Titanium

152

Figure 97. Effects of Versilube F-50 on S-N Data at 650°F, Center-Notched 8-1-1 Titanium

Figure 98. Effects of Versilube F-50 on S-N Data at 650°F, Unnotched 8-1-1 Titanium
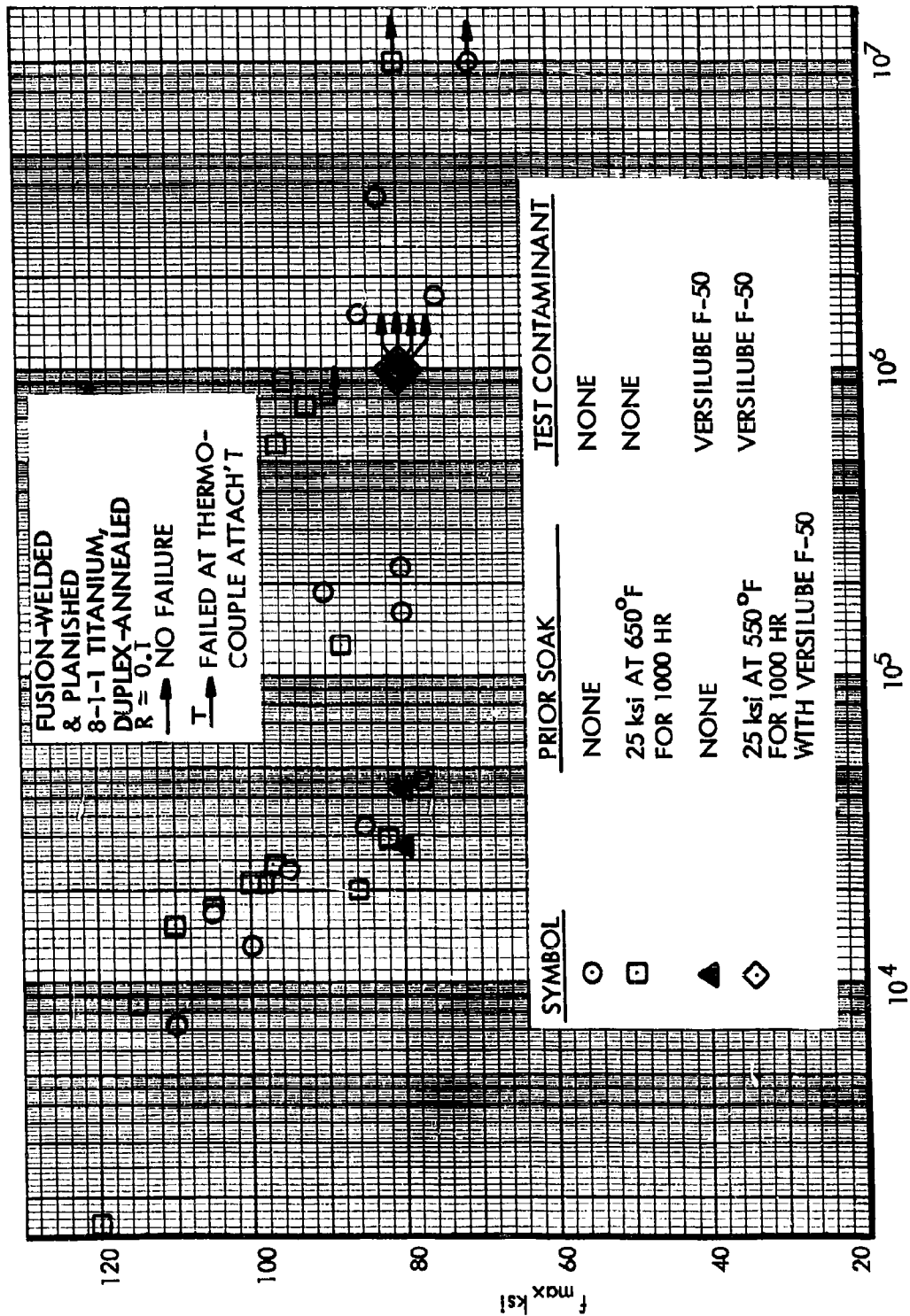
Figure 99. Effects of Versilube F-50 on S-N Data at 650°F, Fusion-Welded 8-1-1 Titanium

155

Figure 100. Effects of Salt Water on S-N Data at 650°F, Center-Notched PH 14-8Mo

156

Figure 101. Effects of Salt Water on S-N Data at 650°F, Unnotched PH 14-8Mo

Figure 102. Effects of Salt Water on S-N Data at 650°F, Fusion-Welded PH 14-8Mo

158

Figure 103. Effects of MIL-0-7277 Oil on S-N Data at 650°F, Center-Notched PH14-8Mo
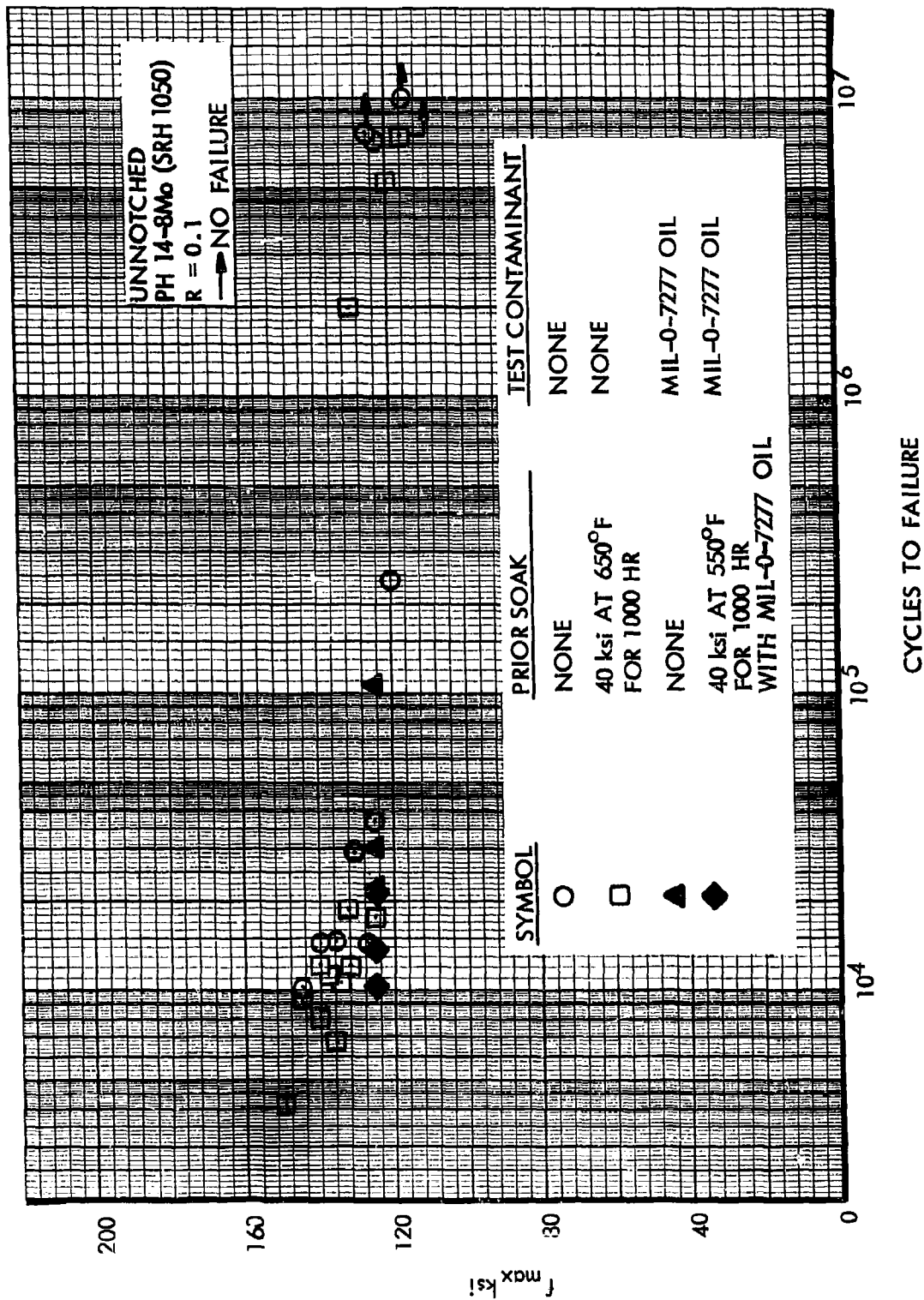
159

Figure 104. Effects of MIL-O-7277 Oil on S-N Data at 650°F, Unnotched PH 14-8Mo
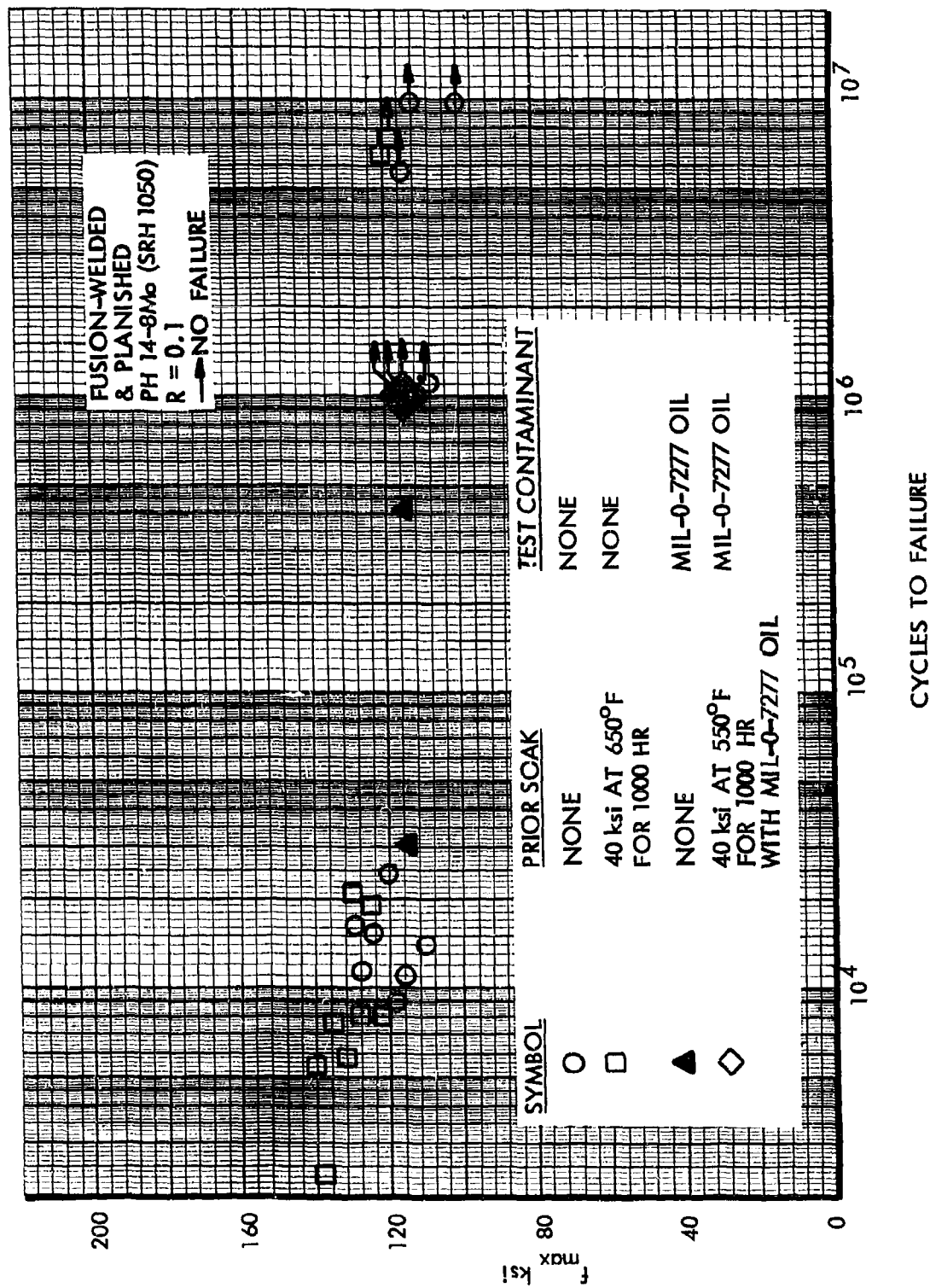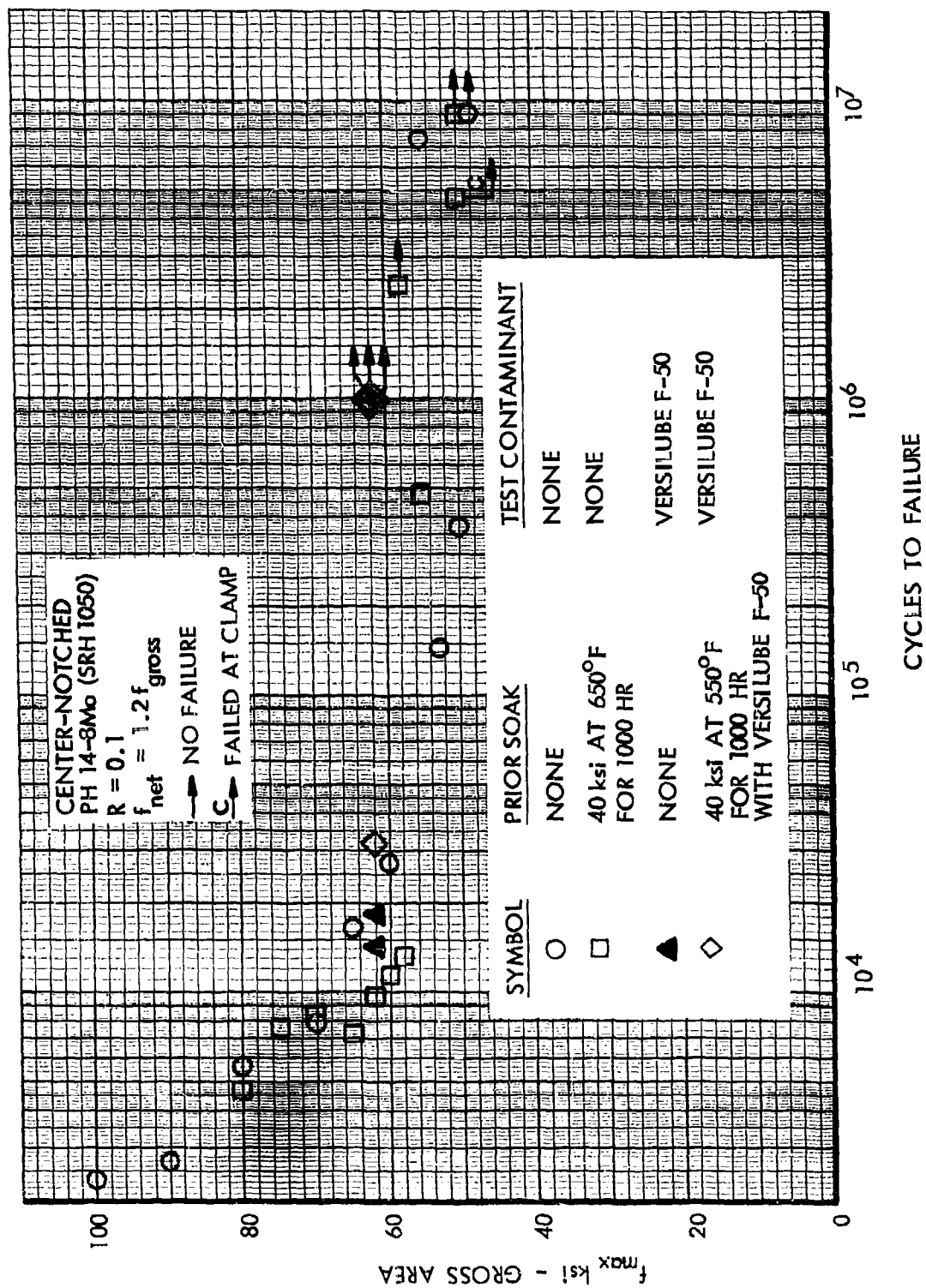
UNNOTCHED
PH 14-8Mo (SRH 1050)
R = 0.1
→ NO FAILURE

SYMBOL	PRIOR SOAK	TEST CONTAMINANT
O	NONE	NONE
□	40 ksi AT 650°F FOR 1000 HR	NONE
▲	NONE	MIL-O-7277 OIL
◆	40 ksi AT 550°F FOR 1000 HR WITH MIL-O-7277 OIL	MIL-O-7277 OIL

CYCLES TO FAILURE

f_{max} ksi

Figure 105. Effects of MIL-0-7277 Oil on S-N Data at 650°F, Fusion-Welded PH 14-8Mo

161

Figure 106. Effects of Versilube F-50 on S-N Data at 650°F, Center-Notched PH 14-8Mo
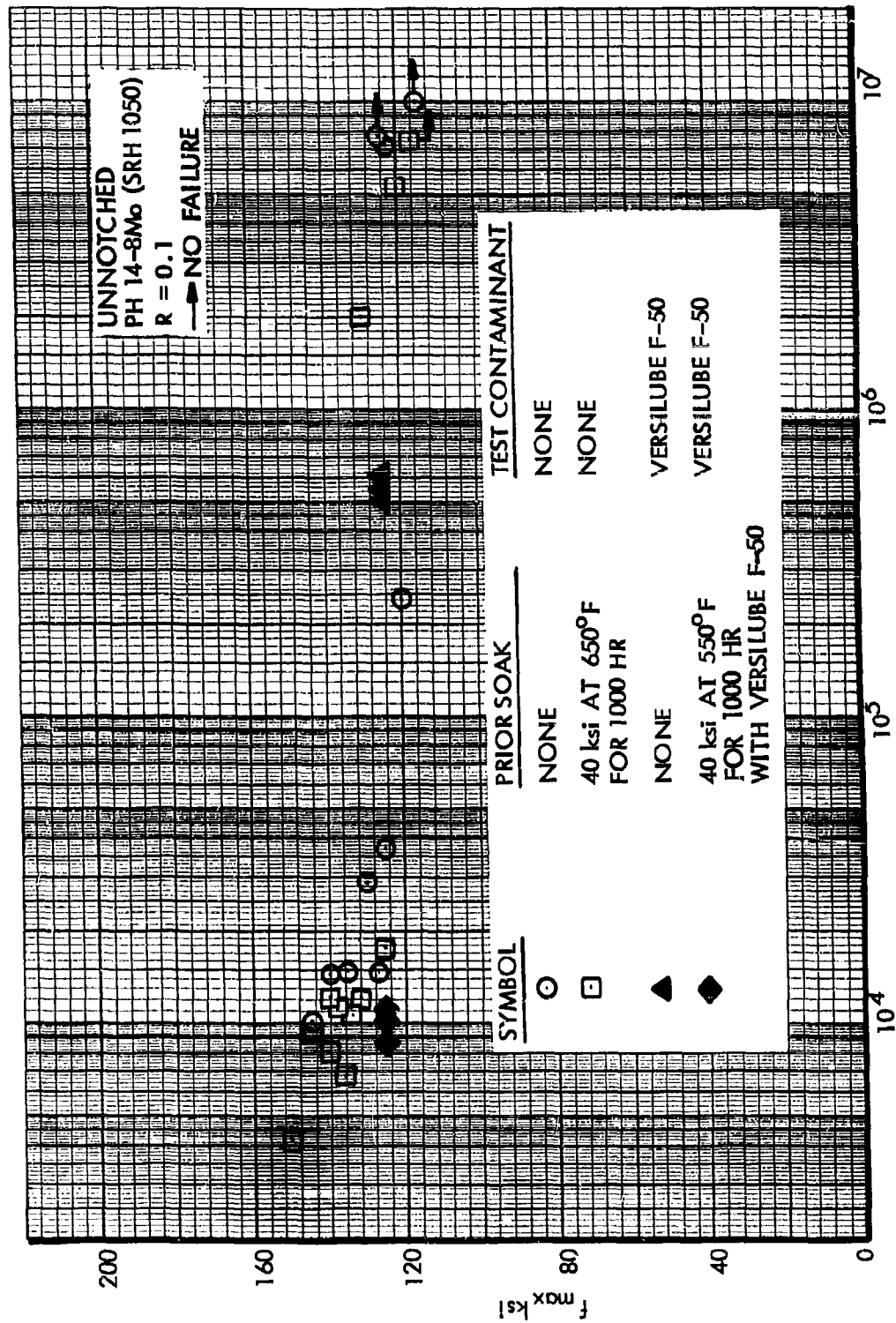
162

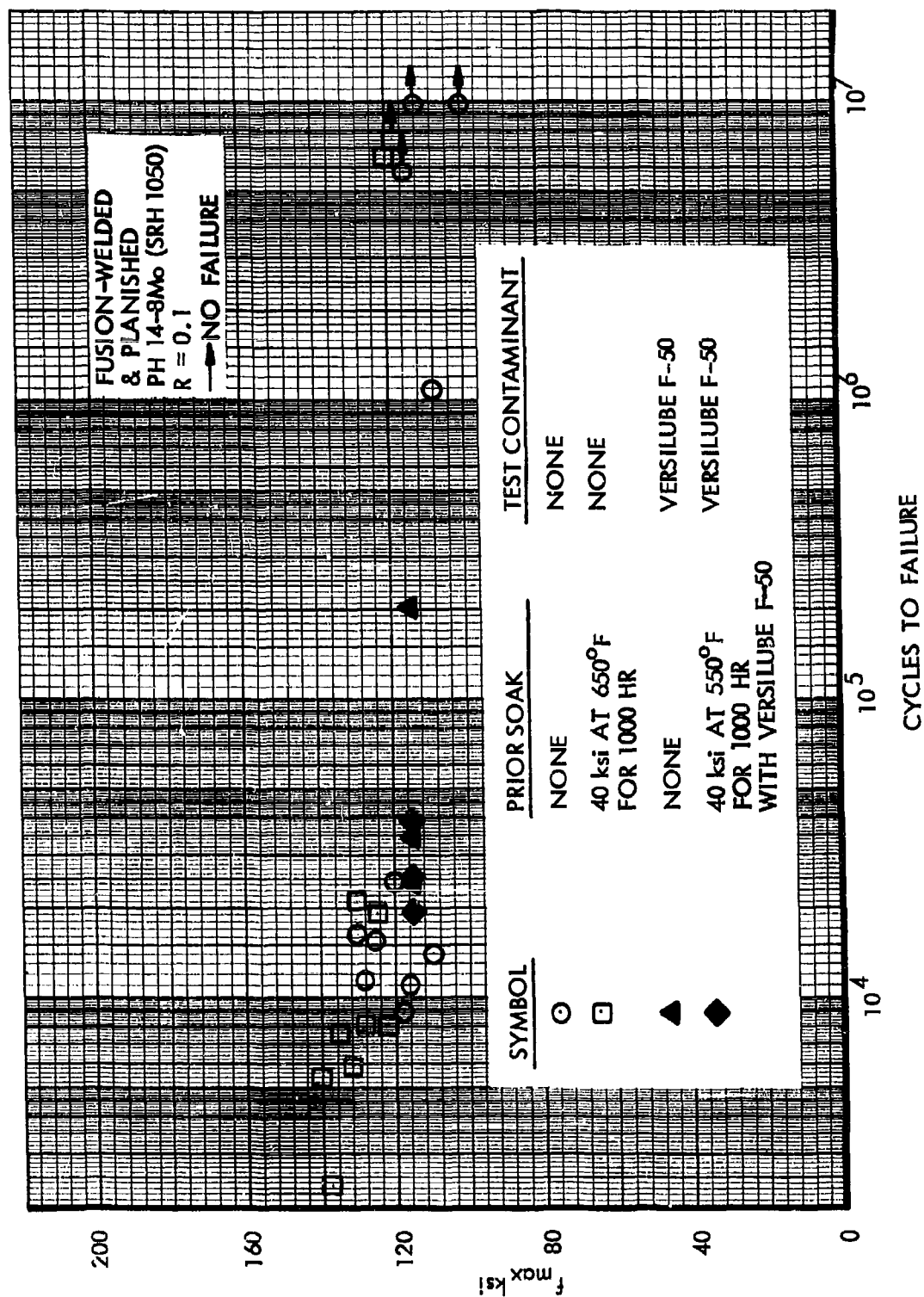Figure 107. Effects of Versilube F-50 on S-N Data at 650°F, Unnotched PH 14-8 Mo

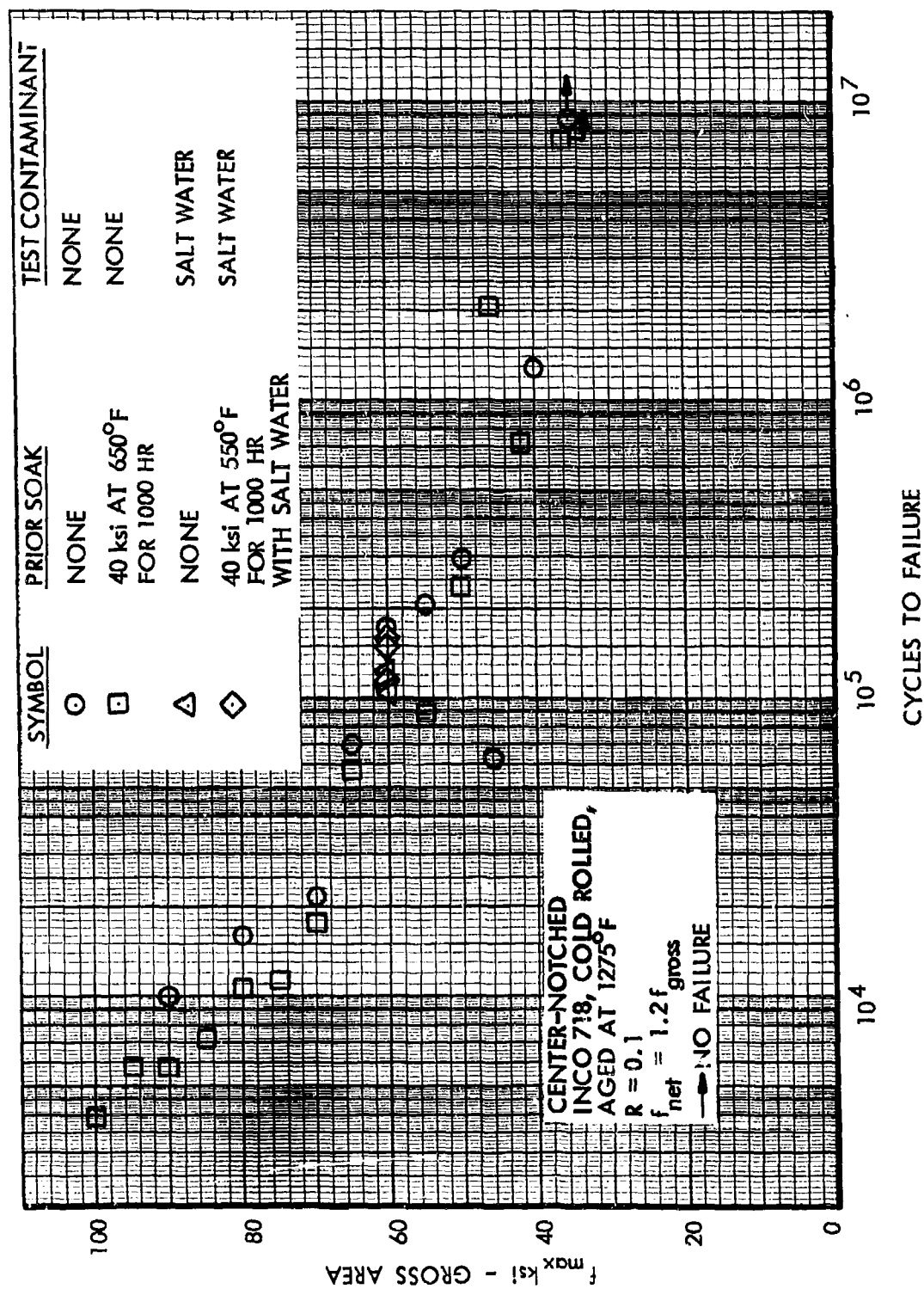Figure 108. Effects of Versilube F-50 on S-N Data at 650°F, Fusion-Welded PH 14-8Mo

164

Figure 109. Effects of Salt Water on S–N Data at 650°F, Center–Notched INCO 718
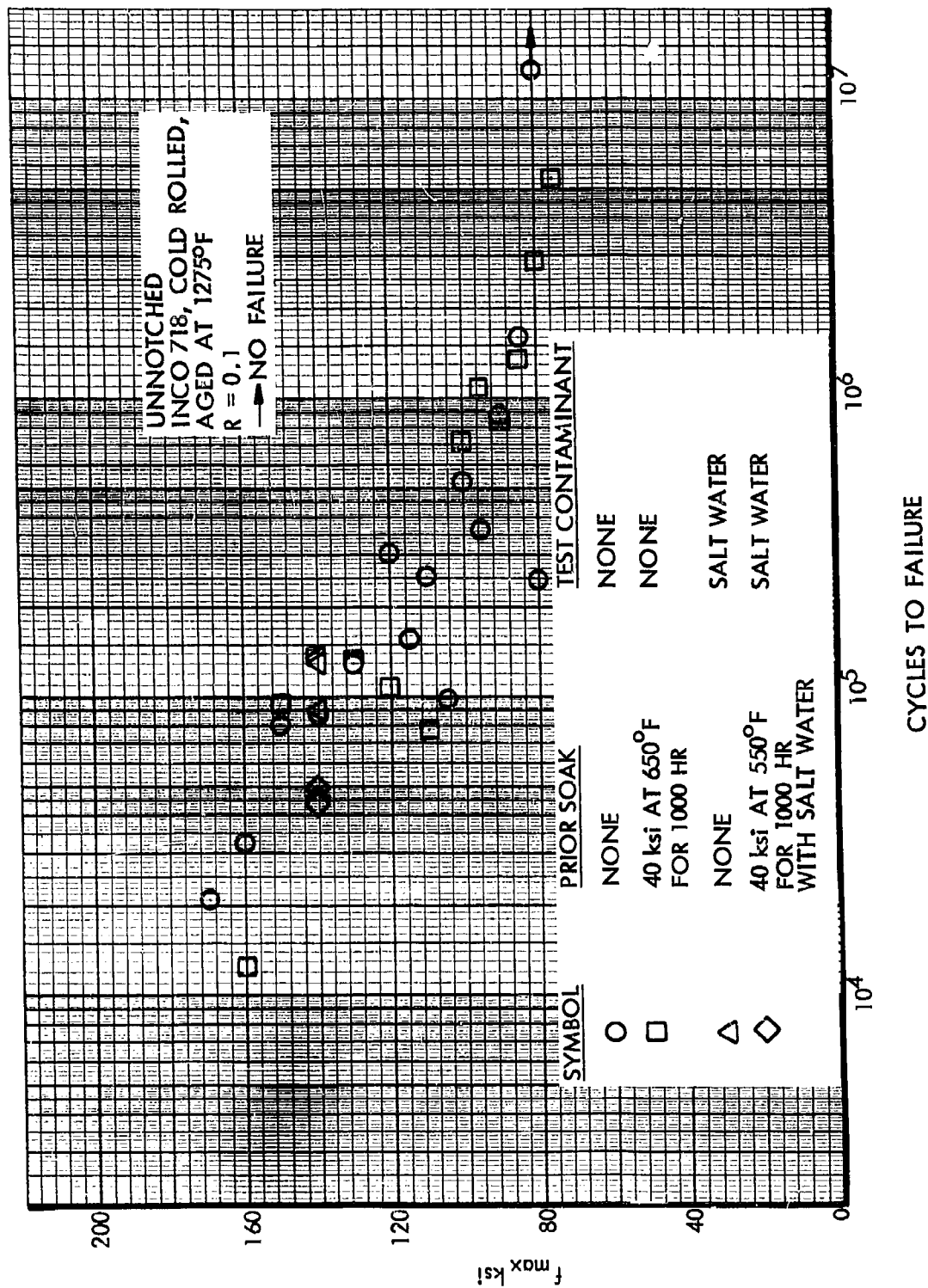
165

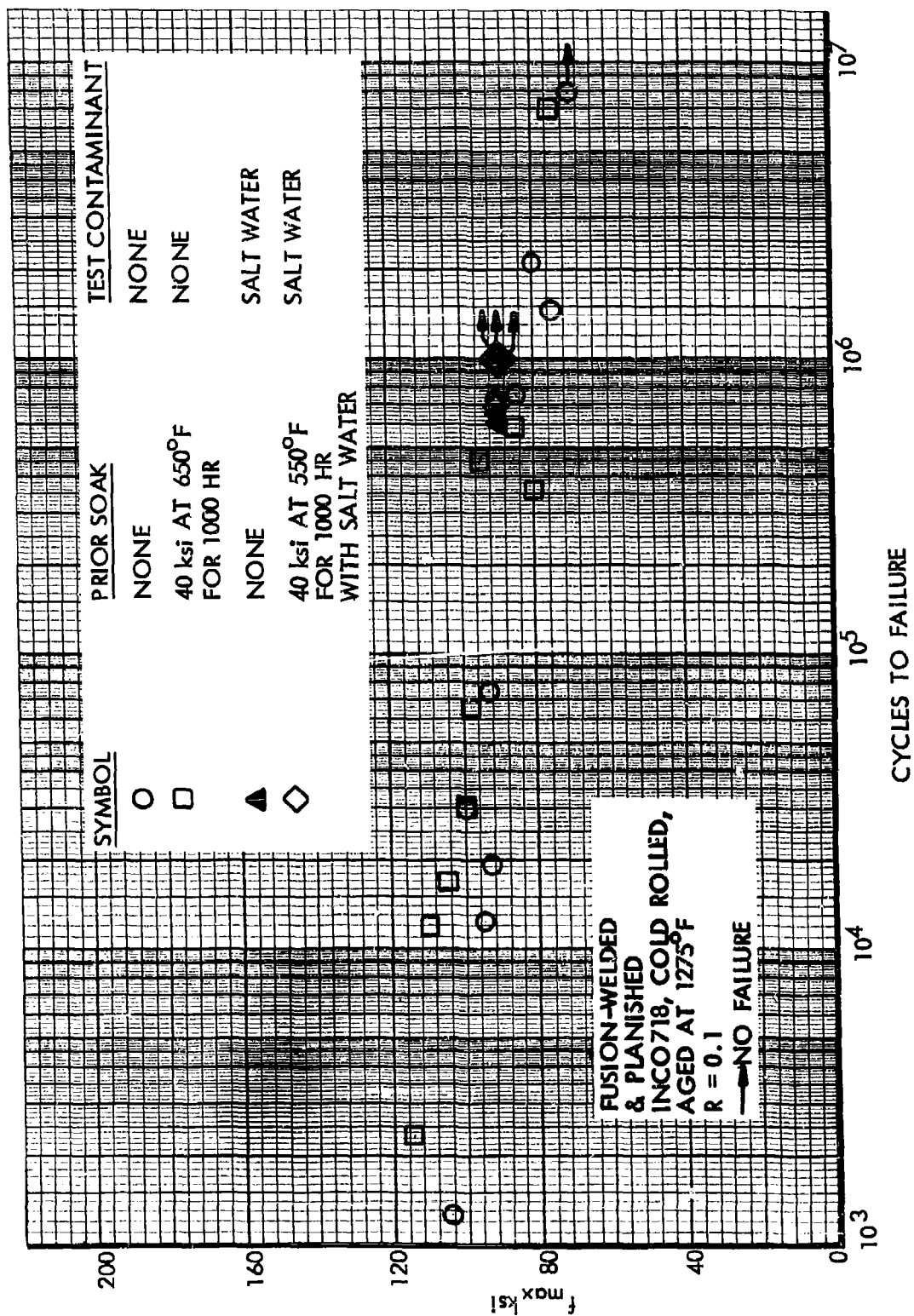Figure 110. Effects of Salt Water on S–N Data at 650°F, Unnotched INCO 718

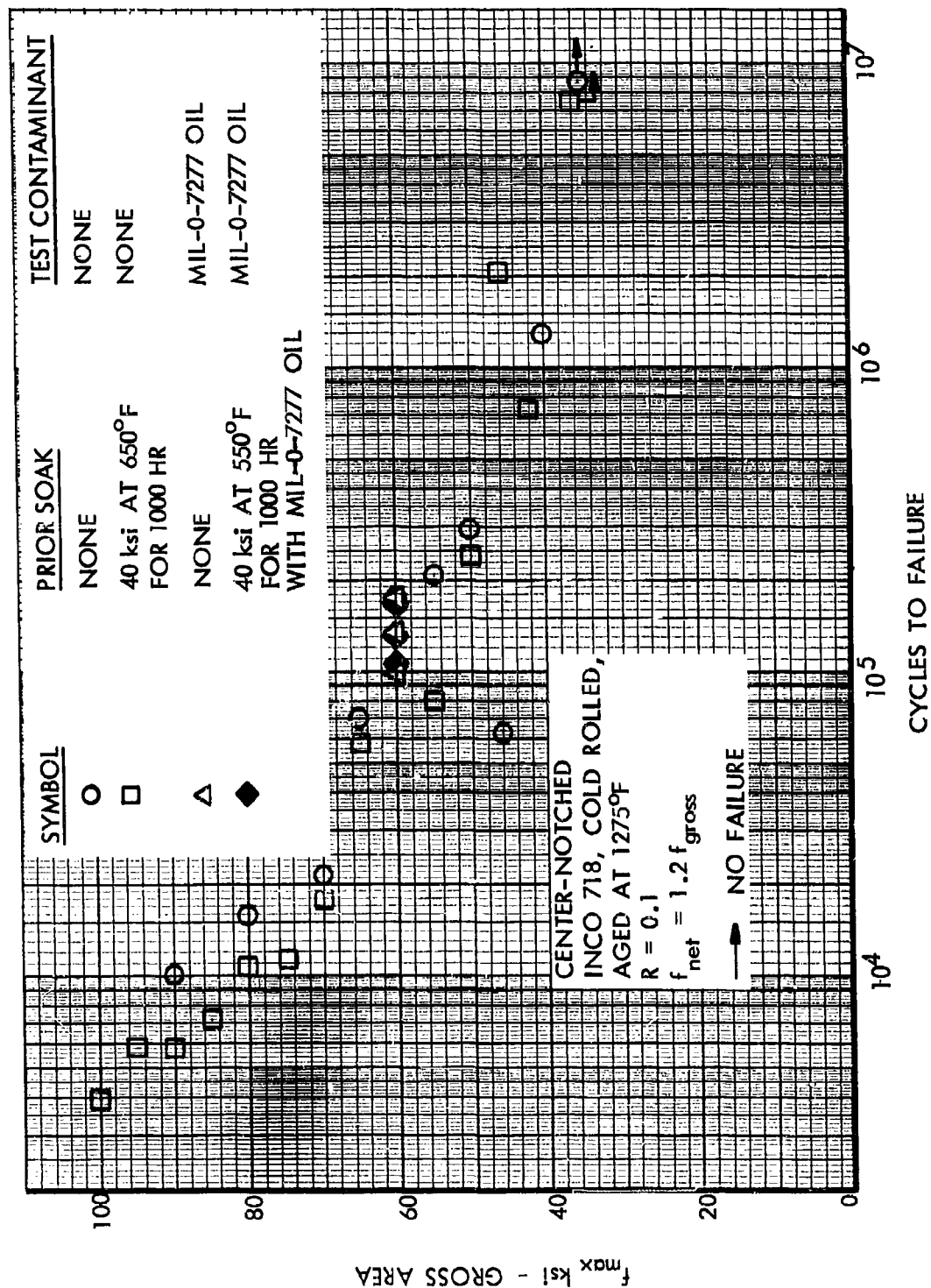Figure 111. Effects of Salt Water on S–N Data at 650°F, Fusion–Welded INCO 718

Figure 112. Effects of MIL-O-7277 Oil on S-N Data at 650°F, Center-Notched INCO 718
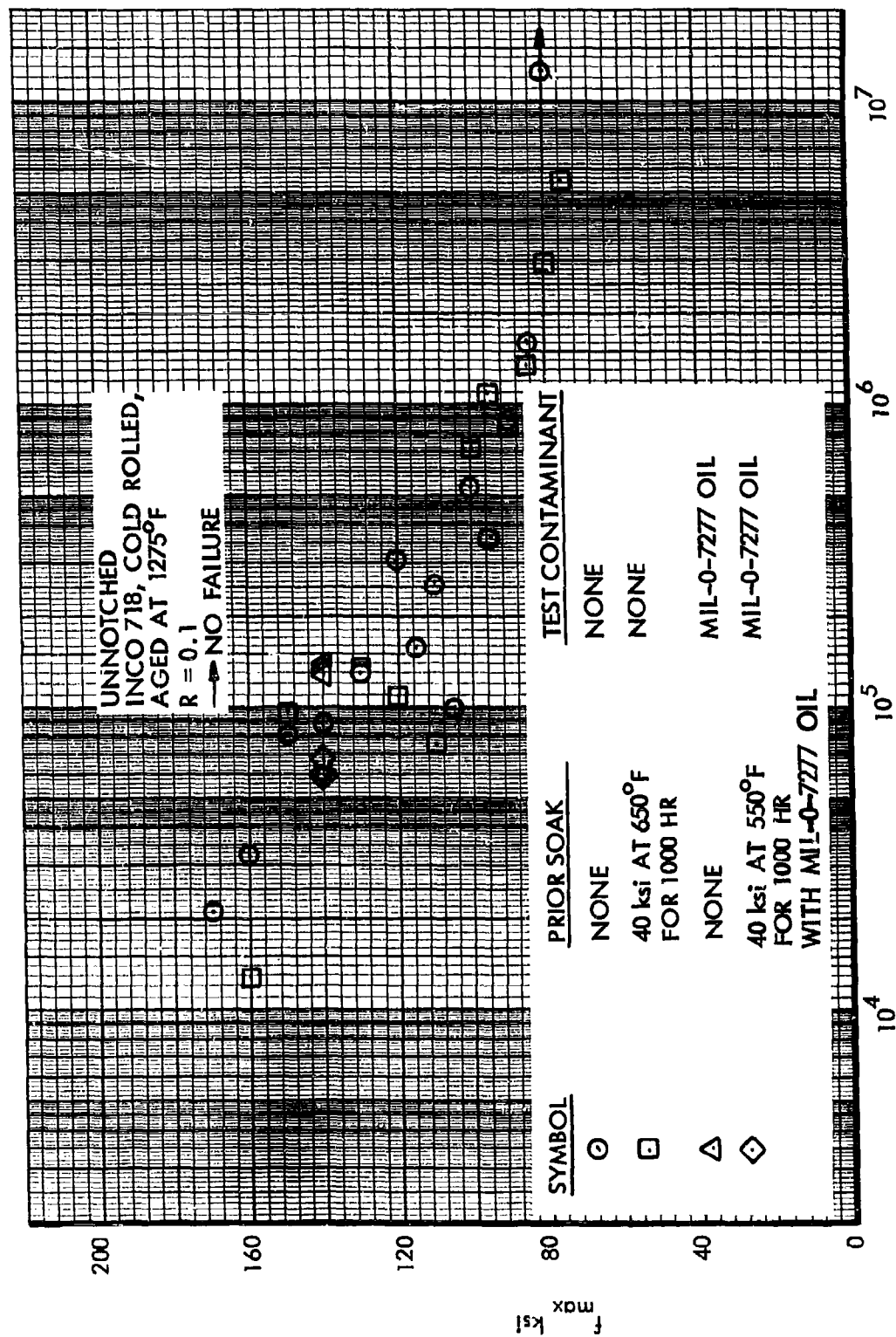
Figure 113. Effects of MIL-0-7277 Oil on S-N Data at 650°F, Unnotched INCO 718
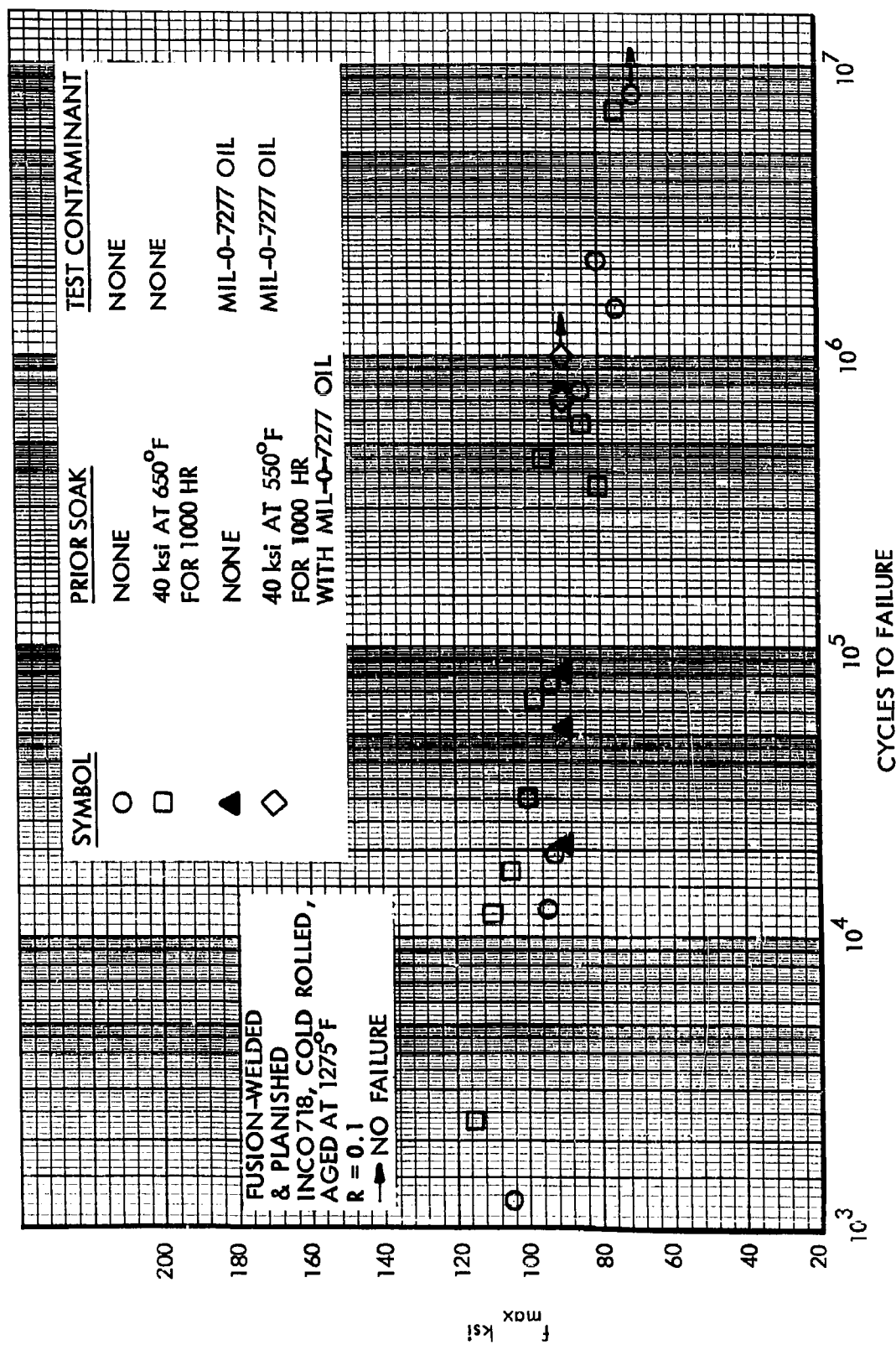
Figure 114. Effects of MIL-0-7277 Oil on S-N Data at 650°F, Fusion-Welded INCO 718

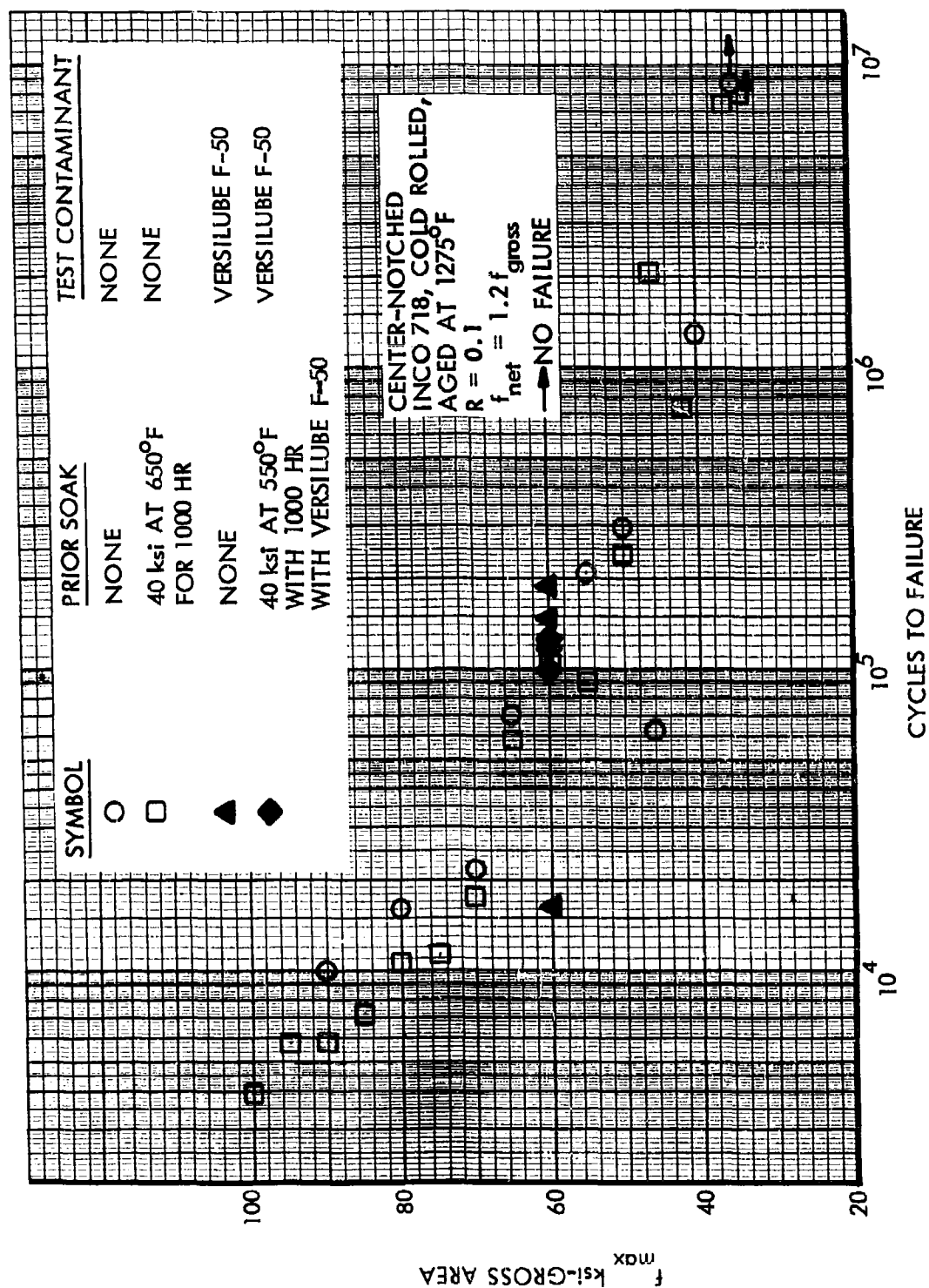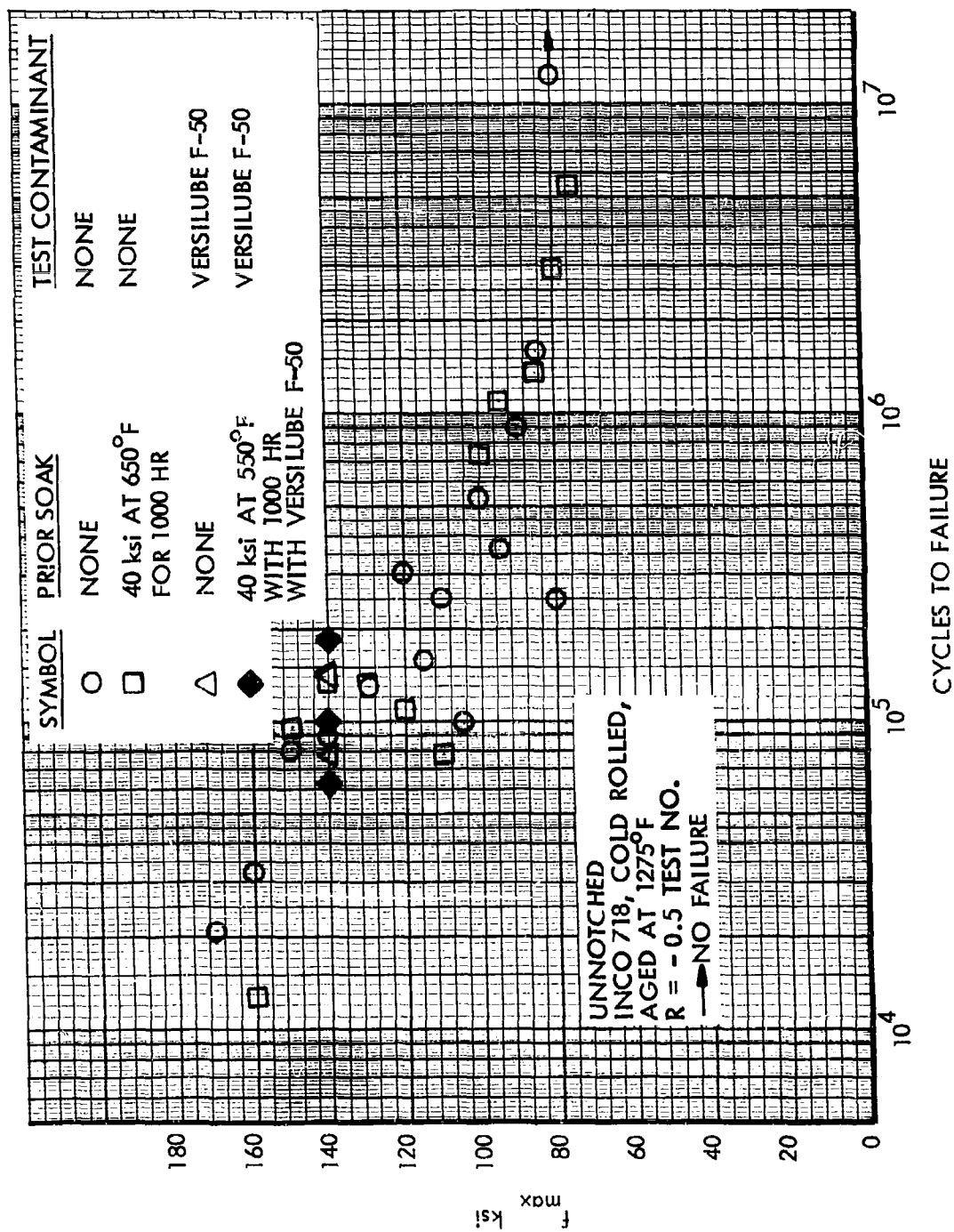Figure 115. Effects of Versilube F-50 on S-N Data at 650°F, Center-Notched INCO 718

171

Figure 116. Effects of Versilube F-50 on S-N Data at 650°F, Unnotched INCO 718

Figure 117. Effects of Versilube F-50 on S-N Data at 650°F, Fusion-Welded INCO 718

TABLE 31 STATIC TEST DATA AT 650° F WITH CONTAMINANT
PLAIN SPECIMENS WITH PRIOR EXPOSURE TO STRESS AND CONTAMINANT AT 550° F

Material	Gage (Nom.)	Prior Soak	Contaminant	F_{tu} (ksi)	F_{ty} (ksi)	e* (%)
8-1-1 Titanium Duplex Annealed	.050	1000 HRS AT 25 ksi AND 550°F	Salt Water	108.3 109.1 111.7	87.6 86.2 90.1	10.0 12.0 10.5
			MIL-O-7277 oil	108.3 111.5 108.5	85.8 90.3 86.2	10.5 9.5 9.5
			Versilube F-50	117.9 116.4 119.2	99.1 97.1 99.4	7.5 8 8
PH14-8Mo (SRH 1050) Stainless Steel	.025	1000 HRS AT 40 ksi AND 550°F	Salt Water	188.5 188.5 184.0	169.3 166.4 163.9	2 2 2.5
			MIL-O-7277 oil	186.1 186.1 184.4	166.8 162.7 170.9	2 2 2
			Versilube F-50	174.8 175.0 177.0	159.3 158.4 164.8	4 4 2
INCO 718 Cold Rolled, Aged at 1275°F	.025	1000 HRS AT 40 ksi AND 550°F	Salt Water	196.8 197.7 196.5	180.9 182.2 181.5	9 7.5 6.5
			MIL-O-7277 oil	196.8 197.7 196.1	182.9 182.9 178.3	6.5 6 7.5
			Versilube F-50	192.3 191.6 188.6	178.3 176.6 173.1	9 8 6

* 2-in. gage length

174

% ELONGATION IN 2 INCH GAGE LENGTH

ONE
SPECIMEN

PLAIN SPECIMENS
8-1-1 TITANIUM
DUPLEX-ANNEALED
.050 GAGE
TRANSVERSE GRAIN

120
110 — F_{tu}
100
90
80 — F_{ty}
70

STRESS ksi

15
10 — % ELONG
5

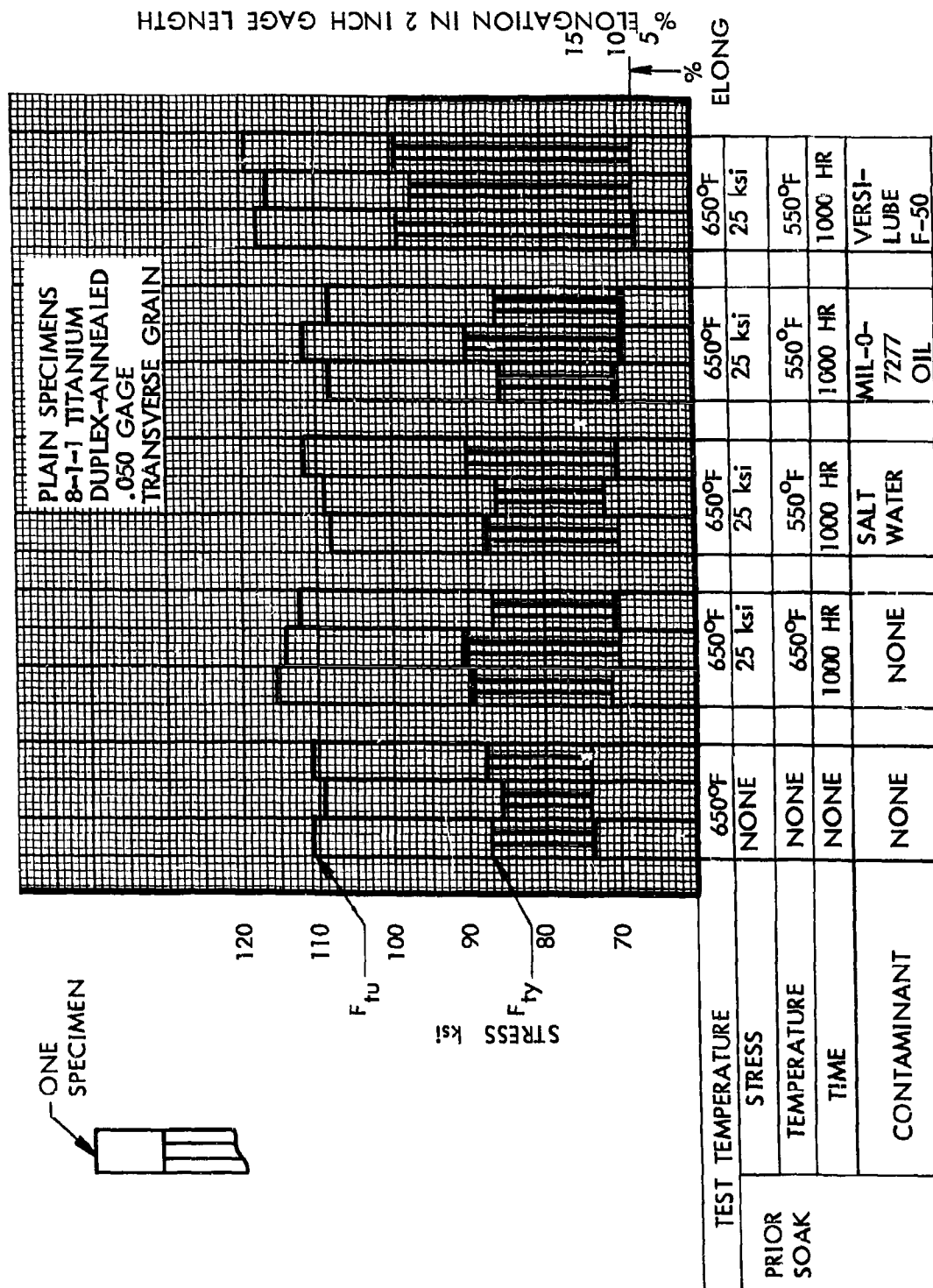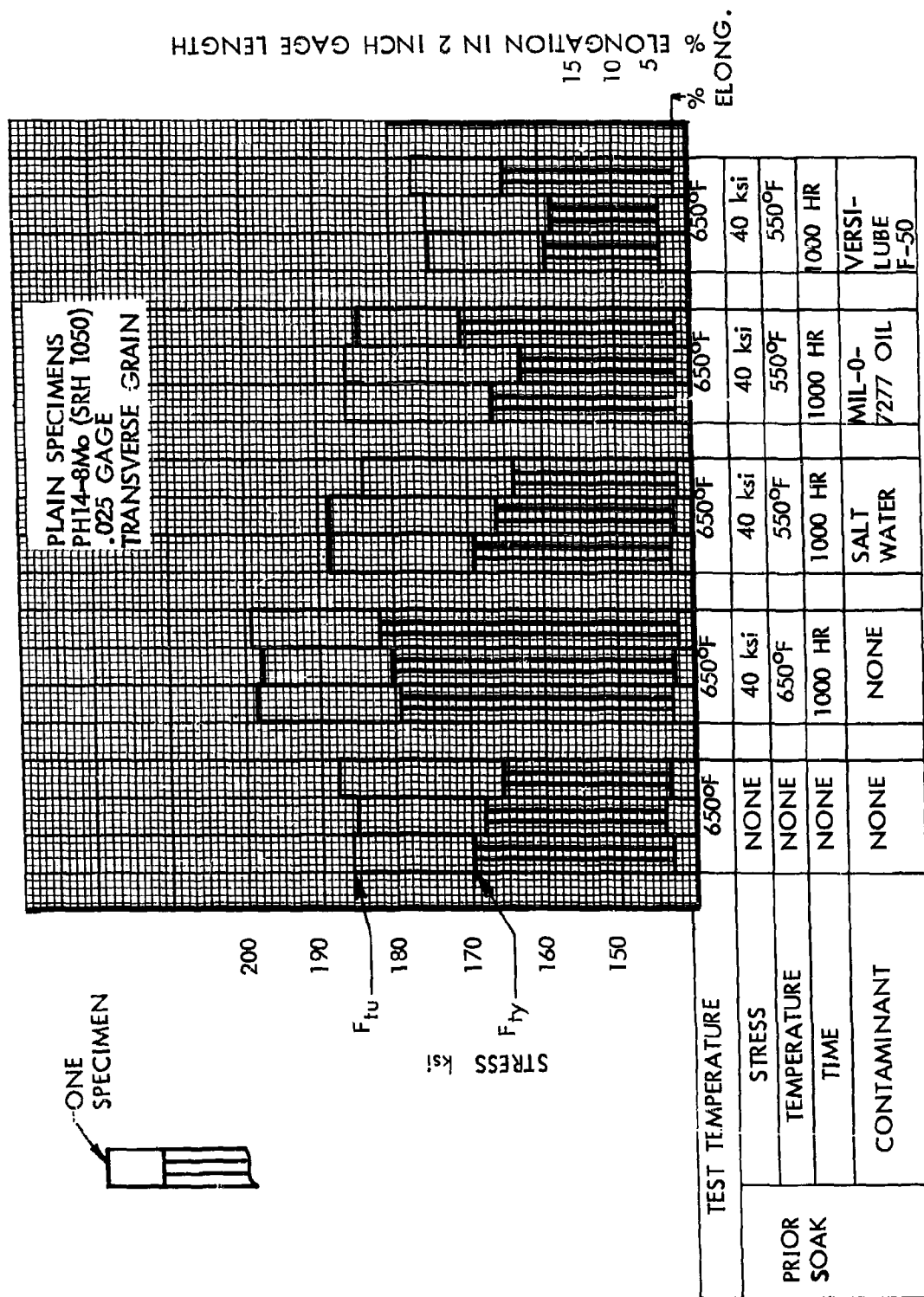| TEST TEMPERATURE		650°F	650°F	650°F	650°F	650°F
PRIOR SOAK	STRESS	NONE	25 ksi	25 ksi	25 ksi	25 ksi
	TEMPERATURE	NONE	650°F	550°F	550°F	550°F
	TIME	NONE	1000 HR	1000 HR	1000 HR	1000 HR
	CONTAMINANT	NONE	NONE	SALT WATER	MIL-O-7277 OIL	VERSI-LUBE F-50

Figure 118.   Effects of Prior Soak with Contaminants on Static Tensile Properties, Plain Specimens,
8-1-1 Titanium

175

Figure 119. Effects of Prior Soak with Contaminants on Static Tensile Properties, Plain Specimens, PH 14-8Mo

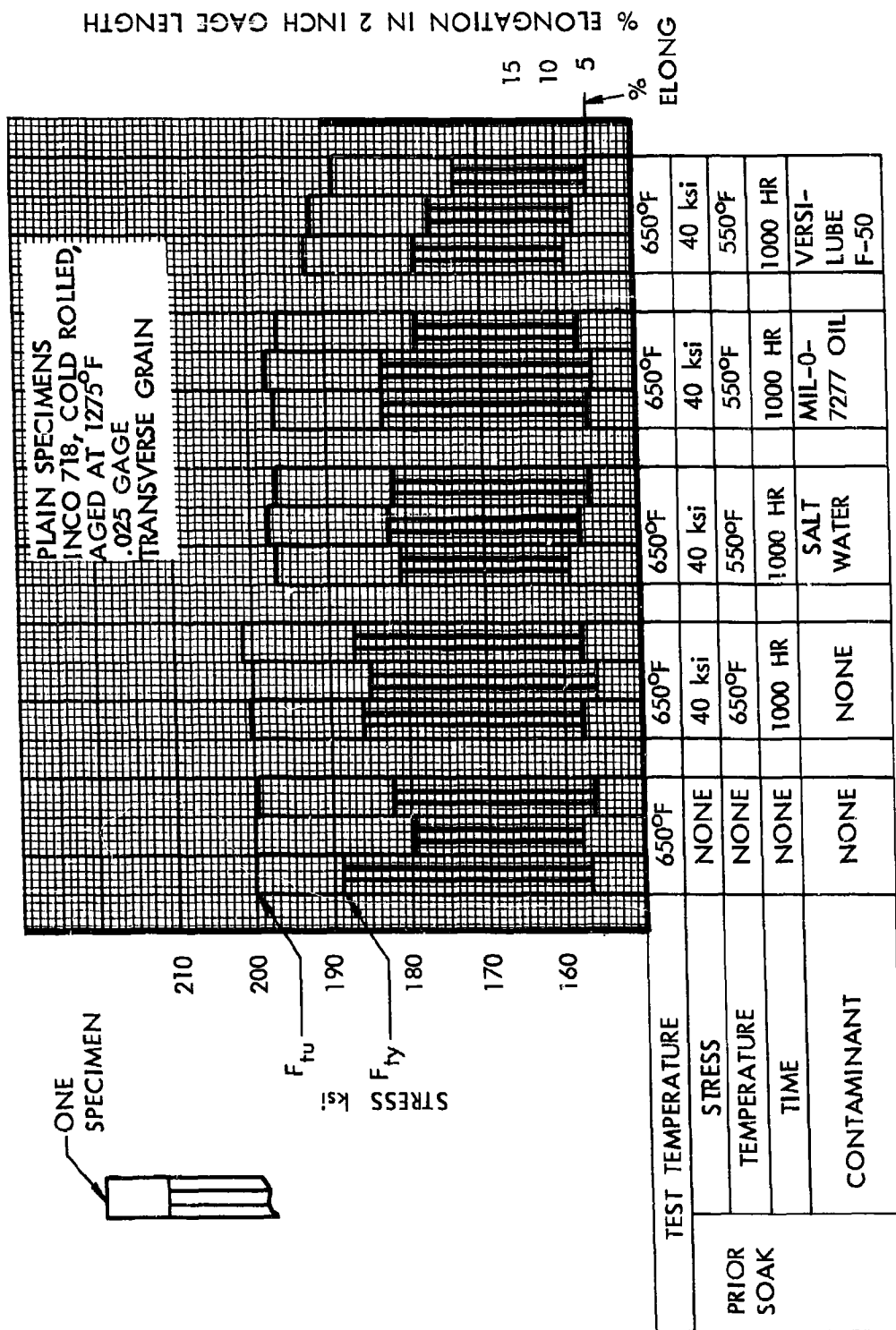| TEST TEMPERATURE		650°F	650°F	650°F	650°F	650°F
PRIOR SOAK	STRESS	NONE	40 ksi	40 ksi	40 ksi	40 ksi
	TEMPERATURE	NONE	650°F	550°F	550°F	550°F
	TIME	NONE	1000 HR	1000 HR	1000 HR	1000 HR
	CONTAMINANT	NONE	NONE	SALT WATER	MIL-0-7277 OIL	VERSI-LUBE F-50

176

Figure 120. Effects of Prior Soak with Contaminants on Static Tensile Properties, Plain Specimens, INCO 718

TABLE 32 ACCELERATED FLIGHT-BY-FLIGHT TEST RESULTS FOR SPECTRA C
WITH CONTAMINATS AT 550°F, NO PRIOR SOAK

SPECIMEN MATERIAL	SPECIMEN TYPE	REF. 1g STRESS (ksi)	CONTAMINANT APPLIED DURING TEST	TIME AT 550°F (hr)	NO. OF FLIGHTS TO DEVELOP. OF VISUAL CRACKING
8-1-1 Titanium Duplex Annealed	Center Notched	25	MIL-O-7277 Oil MIL-O-7277 Oil Salt Water Salt Water	25.8 26.4 25.9 25.9	17,200 17,600 17,250 17,250
PH14-8Mo (SRH 1050) Stainless Steel	Center Notched	40	MIL-O-7277 Oil MIL-O-7277 Oil	3.4 4.4	2,300 2,900
INCO 718 Cold Rolled, Aged at 1275°F	Center Notched	40	MIL-O-7277 Oil MIL-O-7277 Oil	10.8 13.4	7,200 8,900

178

NO PRIOR SOAK

NO. OF SPECIMENS	4	2	4	2	4	2
MATERIAL	8-1-1 TITANIUM		PH 14-8Mo		INCO 718	
CONTAMINANT APPLIED DURING TEST	NONE	MIL-O-7277 OIL	NONE	MIL-O-7277 OIL	NONE	MIL-O-7277 OIL
TEST TEMPERATURE	550°F	550°F	550°F	550°F	550°F	550°F

I   SCATTERBAND
◇   AVERAGE TEST LIFE
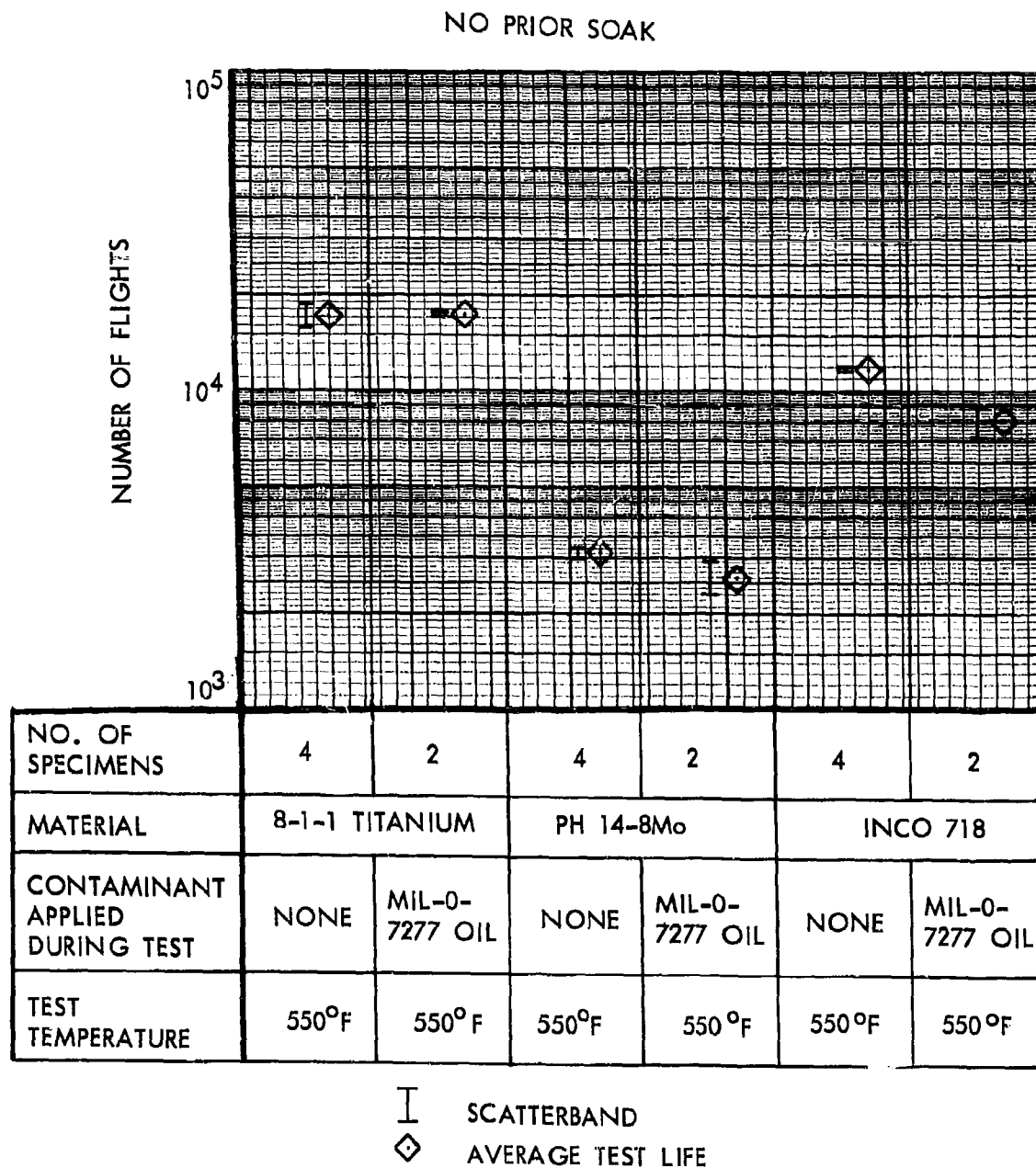
Figure 121. Comparison of Flight-by-Flight Test Results for Spectra C
with and without Contaminants, Center-Notched Specimens

SECTION 6

CONCLUSIONS

1. For the range of specimen exposure and test conditions covered by the fatigue test program, 8-1-1 duplex-annealed titanium sheet specimens showed marked superiority for SST airframe applications over specimens of PH14-8Mo (SRH 1050) steel and Inco 718 cold rolled 20 percent and aged.

2. The test data re-emphasize the variations in comparative evaluations of materials due to the use of differing types of test. For all fatigue tests carried out by the application of constant load amplitudes, an examination of the fatigue strength to density ratios leads to the following ratings.

RATING OF MATERIALS BASED ON S-N DATA

	RATING	TYPE OF SPECIMEN		
		CENTER NOTCHED	UNNOTCHED	FUSION-WELDED & PLANISHED
LOW STRESS	1	8-1-1 TITANIUM	8-1-1 TITANIUM	8-1-1 TITANIUM
HIGH CYCLE	2	INCO 718	INCO 718	PH 14-8Mo
RANGE	3	PH 14-8Mo	PH 14-8Mo	INCO 718
HIGH STRESS	1	8-1-1 TITANIUM	8-1-1 TITANIUM	8-1-1 TITANIUM
LOW CYCLE	2	PH 14-8Mo	PH 14-8Mo	PH 14-8Mo
RANGE	3	INCO 718	INCO 718	INCO 718

For the tests carried out by the application of flight-by-flight sequences of varying load amplitudes, the data for center-notched specimens lead to the simpler, more clearly defined, rating of 8-1-1 titanium, Inco 718 and PH14-8Mo, in that order. For fusion-welded specimens, the data for all materials in this type of test indicate very long potential service lives. For the specimens with single spotwelds which were added in this type of test, the data show test lives for 8-1-1 titanium specimens which were slightly less than those for center-notched specimens while the data for such spotwelded specimens in both of the other materials showed much longer test lives than those for the notched specimens.

The data obtained in the static tensile tests did not correlate with the fatigue test data. For example, exposures of Inco 718 specimens to steady load at elevated temperature had little effect on static tensile properties but they had significant effects on S-N data.

3. For all of the materials, the S-N data obtained after stressed exposure to elevated temperatures for periods up to 5000 hours indicated non-uniform trends in the resistance to repeated loadings. These trends may indicate changes in the stability of the materials. However, the data for each material are based on tests of a relatively small number of specimens taken from sheets of a single thickness produced from a single heat and tested in a type of test which is expected to produce large scatter in test data. A rating of the materials on the basis of their indicated stability in these tests is not justified. An informative rating of material stability will be provided by the results obtained in the tests in which flight-by-flight sequences of loading are being applied with approximately one hour at 500°F during each "flight."

4. Relatively crude measurements of creep elongations on unnotched rectangular specimens after exposure under moderate load for 5000 hours at 400°F or 650°F were made. The measurements showed essentially zero creep for the 8-1-1 titanium and Inco 718 specimens and very small values for the PH14-8Mo specimens.

5. Center notching of specimens after exposure for 5000 hours at 400°F or 650°F under moderate load had no effect on S-N data for PH14-8Mo specimens but produced slightly lower test lives for 8-1-1 titanium and Inco 718 specimens.

6. Comparisons of the data obtained in this program with data reported by Boeing-North American under contract AF33(657)-11461 showed that shorter test lives were obtained for the transverse unnotched specimens used in this program than those for the longitudinal specimens tested by Boeing-North American. The agreement between the two sets of S-N data for fusion welded specimens is considered to be good.

7. In tests using one set of fuselage loading conditions in which a cycle of load representing fuselage pressurization was applied simultaneously with a thermal cycle representing the effect of aerodynamic heating, the results indicate that conventional S-N data obtained at constant temperature can be used to conservatively predict the results in the more complex test.

8. Intermittent application of synthetic sea water, MIL-O-7277 mineral oil or Versilube F-50 during 1000 hours of exposure to moderate load at 550°F had no significant, consistent, effect on the constant load amplitude test lives subsequently obtained for any material-specimen geometry combination. However, in a limited series of tests in which contaminants were intermittently applied during the application of flight-by-flight loading sequences at a constant temperature of 550°F, more clearly defined effects were obtained. In these tests, the mineral oil was applied to center notched specimens of each material and salt water was applied to center notched 8-1-1 titanium specimens. In comparison with the test lives obtained without contaminant, the application of the mineral oil reduced the test lives of center notched specimens of Inco 718 and PH14-8Mo by 32 and 17 percent, respectively. The application of neither synthetic sea water nor the mineral oil had any effect on the test lives for center notched specimens of 8-1-1 titanium.

In static tensile tests of unnotched specimens at 650°F after the 1000-hour exposure to contaminants at 550°F, small effects were produced by the contaminants.

9. Metallographic examination of selected test specimens indicated that none of the test or exposure conditions including those with contaminants had produced evidence of surface corrosion, intergranular attack or subsurface cracking.

SECTION 7

RECOMMENDATIONS

1. Because of the superiority demonstrated in the test program by 8-1-1 duplex-annealed titanium sheet specimens, it is recommended that additional fatigue testing of this material in different sheet gages and of material from different heats be undertaken.

2. Because of superiority demonstrated by the 8-1-1 titanium sheet material, it is recommended that testing of other titanium alloys and other titanium forms, such as extrusions and forgings, be vigorously pursued.

3. Because of the trends demonstrated for all materials and specimen geometries by the fatigue test data after increasing times of exposure to load and elevated temperature, it is recommended that the effects of longer exposures to such conditions be undertaken.

4. Because of the smaller test scatter and the more direct applicability in many design situations of material comparisons based on the results of spectrum loading tests using flight-by-flight loading sequences, more extensive use of such tests is recommended.

5. To obtain the necessary comparison of the number of flights obtained in tests with real time at temperature with those obtained in tests with minimum time at temperature, continuation of the "real time" tests is recommended.

APPENDIX I

TEST SPECIMEN PREPARATION

8-1-1 TITANIUM

Specimen blanks were sheared from sheets of duplex-annealed 8-1-1 titanium, fusion welded as required, and machined. The fusion welding procedure, the equipment and the results of visual inspection and inspections using dye penetrants and X-rays, are shown in Table 33. This Table also contains the results of static tests of weld quality. A typical photomacrograph and photomicrographs of the fusion-welded grain structure are presented in Figure 122, Page 191.

For spotwelded specimens, welding schedules were developed to obtain nugget diameters, nugget penetration and shear strengths similar to those obtained in the Boeing North American Joint Venture under Contract AF 33(657)-11461, "Welding Characteristics of SST Skin Materials". All coupons were wire-brushed locally in the area to be welded and then wiped clean with isopropyl alcohol. For each of the spotweld schedules, three single-spot shear specimens and one metallurgical section were made and evaluated prior to the welding of the fatigue-test specimens. The weld-schedule development data and specimen-fabrication data are given in Table 34.

No additional heat treatment or aging of specimens was performed. Before testing, the unnotched, notched, and fusion-welded specimens were cleaned according to Lockheed Process Bulletin C-362-M which defines the following steps.

1. Soak in hot alkaline solution for fifteen minutes.
2. Rinse in tap water.
3. Pickle in nitric-hydrofluoric acid for one minute.
4. Rinse in tap water.
5. Rinse with de-mineralized water.
6. Dry in hot air (200°F).

This cleaning procedure was also applied to specimen blanks before spotwelding. All subsequent handling of the specimens up to installation in the testing machines was performed while wearing clean white cotton gloves.

PH14-8Mo STEEL

The shearing, welding and machining of PH14-8Mo stainless steel specimens followed the pattern described above. Details of the fusion-welding procedures are given in Table 33. The plain specimens were heat-treated to

187

SRH 1050 condition after machining. The fusion-welded specimens were heat-treated after welding. Their metallographic structures are shown in the as-welded condition in Figure 124 and in the heat-treated condition in Figure 125. Before testing, the plain and fusion-welded specimens were cleaned according to Lockheed Process Bulletin C-364-M.

The heat treating and cleaning procedure was:

1. Heat to 1700 ± 25°F for 40 ± 5 minutes.
2. Air cool.
3. Within 10 hours after austenite conditioning, transform at -100°F for 8 to 9 hours and air-warm to room temperature.
4. Precipitation harden at 1050 ± 10°F for 60 ± 5 minutes and air cool.
5. Clean by vapor honing.

The specimen blanks for the spotwelded specimens were heat-treated and cleaned according to the above schedule before the welding as described in Table 34.

INCO 718 NICKEL ALLOY

All Inco 718 Nickel alloy specimens were aged, with the aging of welded specimens performed before welding. The aging sequence was as follows:

1. Solvent clean.
2. Heat at 1275 ± 25°F for 8 hours.
3. Furnace cool at 20°F/hour to 1150°F.
4. Hold temperature at 1150°F for 10 hours.
5. Air cool.

Details of the fusion welding and spotwelding of specimens are given in Tables 33 and 34. The fusion-welded metallographic structure shown in Figure 123 is typical for materials aged before welding.
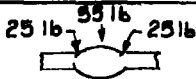
Because initial attempts to spotweld the Inco 718 resulted in constant spitting (metal expulsion at faying surfaces), the Inco coupons were given the following additional cleaning before spotwelding.

1. Hot alkaline clean - 10 minutes.
2. Tap water rinse.
3. Pickled in nitric hydrofluoric acid - three minutes.
4. Rinse in cold tap water.
5. Rinse in hot tap water.
6. Hot air dry - 200°F.

This additional cleaning cycle reduced the metal expulsion tendency but did not eliminate it.

In the preparation of the Inco 718 static test specimens used in the initial evaluation of the materials response to aging, cleaning was not required after aging. However, staining occurred during the aging of the large number of specimens required for the main test program. These stains were removed from the specimen test area by light vapor honing.

188

TABLE 33 FUSION-WELDED SPECIMEN FABRICATION DATA

MATERIAL	.050 8-1-1 Ti	.025 PH14-8Mo	.025 INCO 718
Condition when welded	Duplex-Annealed	Annealed	Aged
Length (in)	88.5	44	70.5
Edge Prep.	Draw Filed	Draw Filed & Sand	Draw Filed & Sand
Cleaning Solvent	Acetone	Acetone	Acetone
Etchant	48HNO$_3$-4HF	None	None
Filler Wire	None	.020 ARMCO 14-8	None
WELDING DATA	TIG Automatic DC	TIG Automatic DC	TIG Automatic DC
Amps	75	87	46
Voltage or Arc Gap	11.5 volts	7.25 volts	3/64 in. gap
Hold Down Pres.(psi)	30	20	20
Weld Vel.(in/min.)	5.5	31	30 1/2
Wire Vel.(in/min.)	None	23	None
Electrode dia. (in)	1/16	1/16	1/16
Electrode type	2% Th	2% Th	2% Th
Shielding Gas	75A/25He	100A	42A/58He
Shielding Gas Flow	40 CFH	15 CFH	12 CFH
Back up Gas	Argon	None	Argon
Weld Equipment:			
Package Weld	Miller SR200	Weldtronic 600	Miller 330A/BF
Torch Type	Linde HW-13	Airco M-50	Linde HW-13
Stake Type	ALW - FAM 11324	AW&E FAL 11313	AW&E FAL 11313
ROLL PLANISH PRESSURE (1 PASS EACH LOCATION)	35 lb — 75 lb — 35 lb	25 lb — 35 lb — 25 lb	35 lb — 35 lb — 35 lb
TESTS OF WELDED SAMPLES FOR WELDING MACHINE SET-UP			
Bend Angle	180° (N.F.)	180° (N.F.)	180° (N.F.)
Bend Radius	7-1/2 to 10T	4T	4T
Avg. of 3 F$_{tu}$ (ksi)	147.88 ± 1%	137.83 ± 1%	144.55 ± 3%
Avg. of 3 F$_{ty}$ (ksi)	146.88 ± 0%	61.97 ± 4%	96.65 ± 1%
Fracture Location	All base metal	All base metal	All in center of weld

NOTE: All welds were subjected to 100% radiographic inspection
per LAC Process Specification 1422

N.F. = No failure

TABLE 34   SPOTWELDED SPECIMEN FABRICATION DATA*

MATERIAL	8-1-1 Titanium (.050-.050)		PH 14-8Mo (.025-.025)	INCO 718 (.025-.025)
	SINGLE SPOT	MULTIPLE SPOT		
Machine Number	7	7	7	22
Transformer Tap	Parallel	Parallel	Parallel	Low Range
Welding Force - lb.	1115	1115	1257	1500
Squeeze - Cycles	30	30	30	30
Heat-Phase	50%	50%	55%	230 Volts
Pulse Cycles	4	4	2	3
Weld Cycles	4	4	2	2
Cool Cycles	1.5	1.5	1.5	1.0
Hold Cycles	30	30	30	50
Electrodes (Top & Lower Electrode the Same)				
Class	RWMA III	RWMA III	RWMA III	RWMA III
Shank Diameter	5/8"	5/8"	5/8"	5/8"
Tip Diameter	3/8"	3/8"	3/8"	3/8"
Tip Radius	3"	3"	3"	8"
Nugget Diameter (Average)	.187	0.220	.108	.125
Penetration % (Average)	75	75	56	60
X-Ray Quality	Not X-Rayed	Clear	Clear	**
Condition When Welded	Duplex Annealed	Duplex Annealed	Heat Treated	Aged
Test Condition	As-Welded	As-Welded	As-Welded	As-Welded
Single Spot Shear Strength (lb.)				
Specimen 1	2400	2950	860	1140
Specimen 2	2500	2950	860	1120
Specimen 3	2500	3000	870	1050
Lbs/Specimen Average	2466	2965	863	1103
Range Lbs.	100	50	10	90
Variation	.04	0.017	.01	.08
Number of Fatigue Specimens Welded	60	12	60	60

*The 8-1-1 titanium and PH 14-8Mo specimens were welded on a Federal three-phase 75 KVA, press welder (CALAC Machine #7) and the INCO 718 specimens were welded on a Sciaky three-phase, 75 KVA, rocker arm welder (CALAC Machine #22).

**Approximately 50% of specimens indicated slight metal expulsion at faying plane.

Cross-Sectional View (Mag. 11X)

| Base Metal (Mag. 280X) | Base Metal (Right) - Heat-Affected Zone Interface - (Mag. 280X) | Weld Metal (Mag. 280X) |

Typical metallographic structure of .050" 8-1-1 titanium welds. Welded in duplex annealed condition. Planished after welding. Shown as planished. Etchant - 4% nitric, 2% hydrofluoric acid.
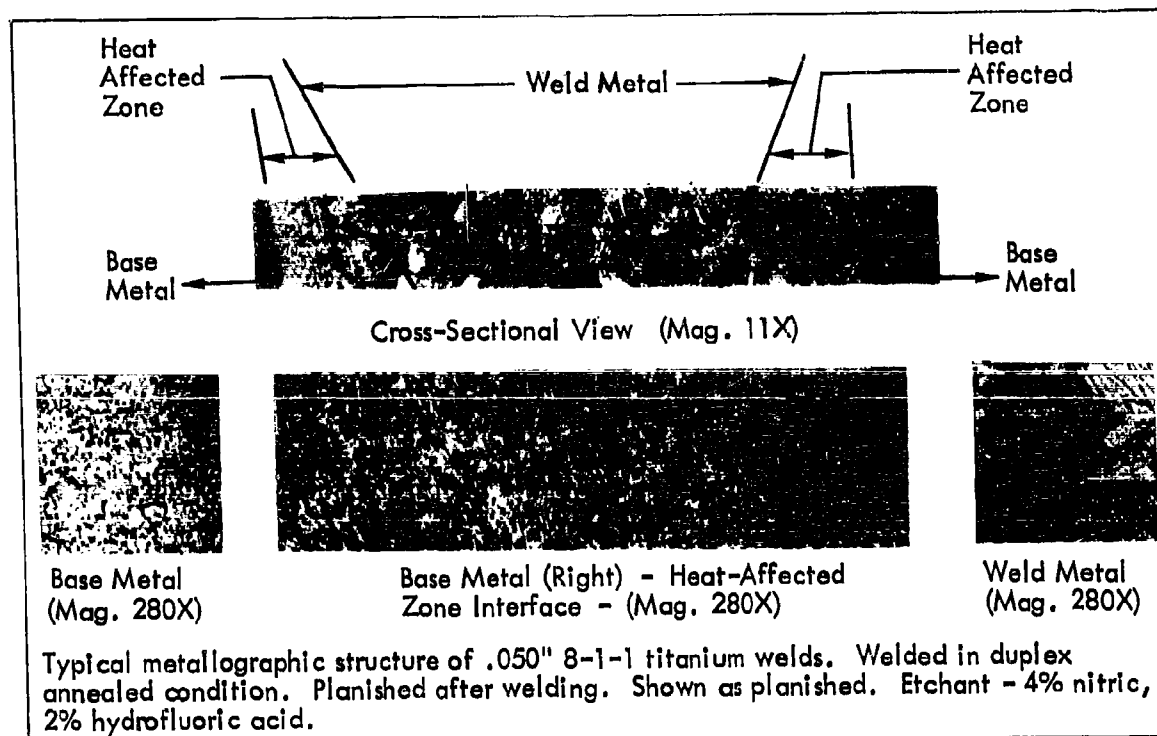
Figure 122. Typical Metallographic Structure of Fusion-Welded 8-1-1 Titanium

Cross-Sectional View (Mag. 35X)

Base Metal (left) Heat-affected zone interface. (Mag. 280X)

Weld Metal (Mag. 280X)

Weld Metal (left) Heat-affected zone interface. (Mag. 280X)

Typical metallographic structure of .025" Inco 718 weld. Welded in 20% cold rolled plus aged condition. Planished after welding. Shown as planished. Etchant - Electrolytic 10% oxalic acid.
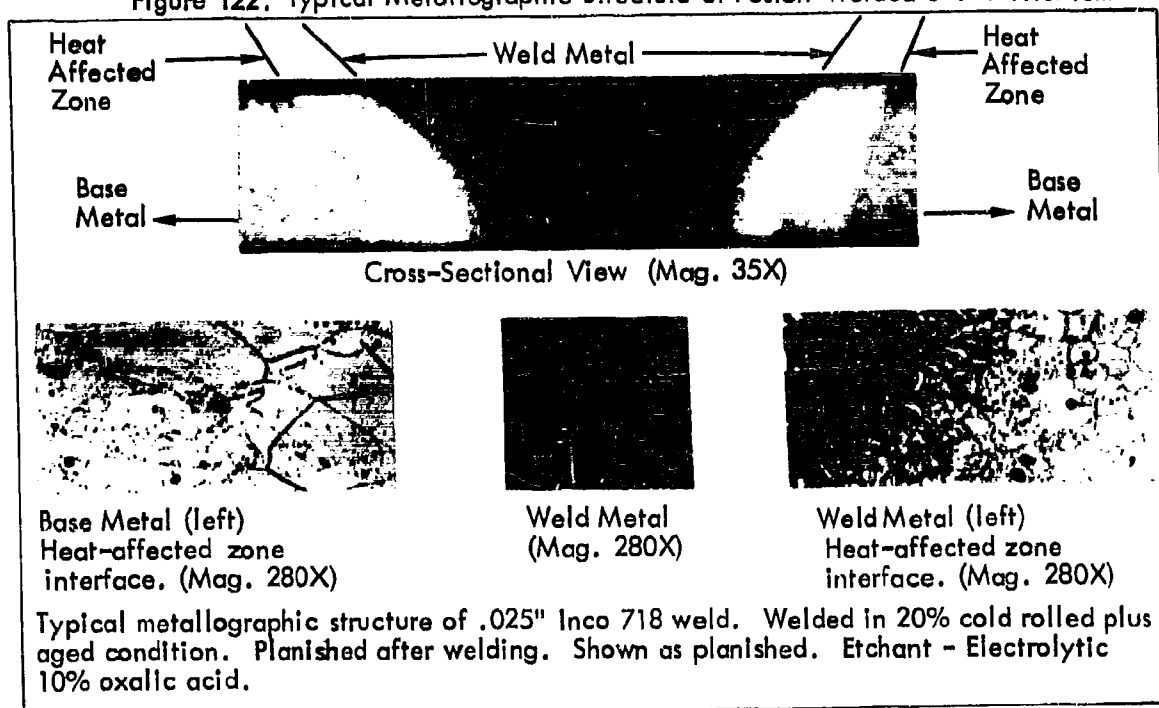
Figure 123. Typical Metallographic Structure of Fusion-Welded INCO 718

Typical metallographic structure of .025" PH 14-8Mo weld. Welded in the solution annealed condition and planished after welding. Shown as planished. Etchant - Electrolytic 10% oxalic acid.
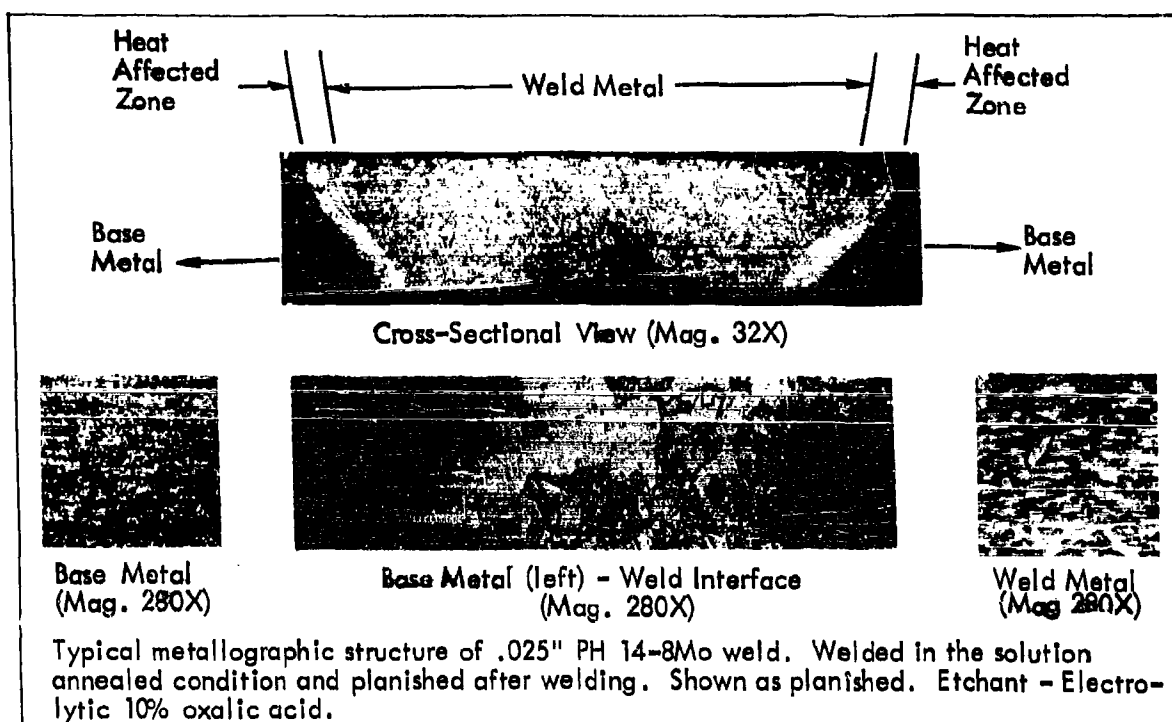
Figure 124. Typical Metallographic Structure of Fusion-Welded PH 14-8Mo as Welded

Typical metallographic structure of .025" PH 14-8Mo weld. Welded in the solution annealed condition and planished and heat treated to the SRH 1050 condition after welding. Shown after heat treatment. Etchant - Electrolytic 10% oxalic acid.
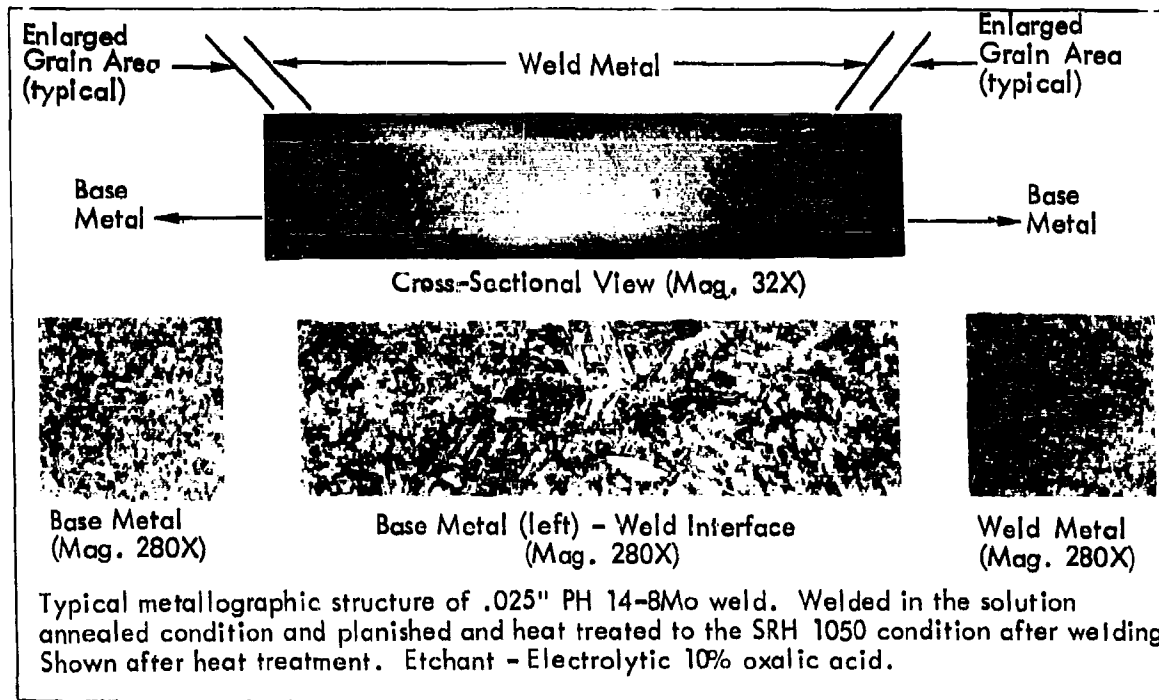
Figure 125. Typical Metallographic Structure of Fusion Welded PH 14-8Mo, Heat Treated after Welding

APPENDIX II

SPECIMEN SUPPORT IN TESTS

Since the application of compressive loads was required in many of the fatigue tests, support of the thin flat test specimens posed a problem. This problem was made more difficult by the requirement of minimum effect of the support on heating and cooling rates and on the distribution of temperature in the specimens. In addition, as is usually the case, the specimens of each material varied slightly in thickness.

To meet the problem, a number of edge support clamp designs were studied over a three month period. The clamps had to be simple to manufacture and easy to install with a sliding contact which would not permit pick up of specimen load. In addition to these basic requirements, the clamps had to be non-corrosive and of such a design that fretting and galling would be held to a minimum, particularly when used on the titanium specimens. The clamps had to have a small mass and be arranged so that the critical test area of each specimen configuration was exposed in order to permit rapid temperature cycling. Finally, the clamp had to be rigid enough to prevent both overall buckling and canning in the central portion of the specimen.

The first practical clamps produced are shown as specimens "B" and "C" in Figure 126. These were simple, machine-slotted, U-sections made from 0.091 gage, stainless steel sheet. They were used exclusively for the constant amplitude (S-N) tests.

The compressive loads produced during the spectrum loading tests were considerably larger than those generated in the S-N tests and required the development of a more rigid clamp. This clamp is shown as Specimen "A", in Figure 126. The specimen is supported by four, 1/4 inch, replaceable, stainless steel rods held in place by four notched steel yokes. The whole assembly is centered on the test specimen by four, 3/16 inch attachment bolts.

Although the heavier clamp acts as a larger heat sink, pre-set temperature cycling rates of three (3) cycles per minute were easily maintained in the accelerated time tests. Both types of clamps caused some temperature variation at the contact surfaces. However, temperatures were continually monitored near the critical test areas where they were maintained within ± 10°F.
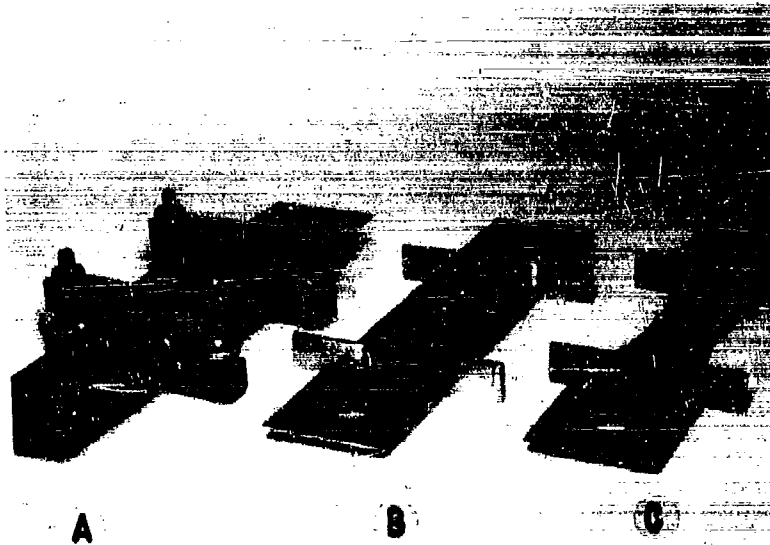
A. Clamp used in all spectrum loading tests
B. Clamp used on center-notched specimen in constant amplitude loading tests
C. Same clamp used on unnotched specimen in constant amplitude loading tests

Figure 126. Test Specimen Support Clamps

APPENDIX III

THERMOCOUPLE INSTALLATION FOR CYCLIC TEMPERATURE TESTS

To measure and control the temperatures of specimens in tests calling for elevated temperatures, it was necessary to attach thermocouple wires at points near the specimen centers.

For the constant elevated temperature tests, this presented no problem. The thermocouple wires were twisted together and simply held tightly against the test specimens by light-weight spring clamps.

For the temperature cycling tests, however, this simple approach did not work. There was too much temperature lag with the use of clamps. For these tests, then, it was necessary to find a more direct means of attachment.

The first few attempts to solve this attachment problem centered around the technique of spotwelding the thermocouples to the test material using a small 80 watt-second capacitor discharge welder. This technique has been used successfully by Lockheed in the past for attaching thermocouples to many steel alloys. However, a preliminary investigation indicated that spotwelding thermocouples to the surface of the 8-1-1 titanium alloy using the conventional Lockheed spotwelding techniques led to premature test cracking at the welds. A study was therefore undertaken in which a number of specimens (center notched with a hole) were used with four successively refined spotwelding techniques.

All of the spotwelding techniques described below involved the welding of 20-gage iron-constantine thermocouple wires at nominally the same point on each test specimen (i.e.: 1/2" from the center of the 1/4" hole on the longitudinal axis of the specimen). This location was far enough from the hole to avoid interference with its normal stress-raising effect, but close enough to be at essentially the same temperature as the material at the center of the specimen. The adequacy of the thermocouple location was checked in special tests in which longitudinal and transverse temperature gradients were defined by use of multiple thermocouples.

The adequacy of each spotwelding technique was evaluated in simple constant load amplitude fatigue tests. The same fatigue loading parameters were used throughout the testing: f_{max} = 37.5 ksi (gross area) at a stress ratio of R = 0.1. All fatigue testing was done at room temperature.

1. In the conventional application, the two thermocouple wires were first twisted together, then welded directly to the 8-1-1 titanium using approximately seven pounds pressure on #2 tweezer electrodes and a meter setting of 80 watt-seconds. The resulting attachment was poor,

195

the titanium was badly pitted, and fatigue tests showed that the spot weld stress concentration effect exceeded that of the hole itself.

2. For a more positive contact, the thermocouple wires were left separated. They were hammered out flat and installed in juxtaposition using the same electrode pressure and meter setting as used above. The test results were the same.

3. To minimize pitting and to produce a more tenacious weld, 2-mil vanadium foil was used as a filler metal between the thermocouple wires and the 8-1-1 titanium. In application, the foil was first welded to the flattened and separated thermocouple wires with a meter setting on the welder of 40 watt-seconds. The excess foil was then removed and the assembly welded to the 8-1-1 titanium as in the previous two cases. Again, all test failures were located in the thermocouple area and not at the hole.

4. A final attempt to reduce the spotwelding effect on the 8-1-1 titanium was made by first welding a 2-mil vanadium foil to the iron wire, then welding both of the flattened wires to a strip of 2-mil stainless steel foil. The stainless steel foil was then welded to the 8-1-1 titanium (with the thermocouple side placed against the specimen) using 18 watt-seconds on the welding meter setting and two pounds pressure on a #3 tweezer electrode.

This fourth method produced welds with twice the fatigue life of those produced by any of the previous methods. However, all failures were again confined to the spotweld areas. It was further discovered that whenever the electrode came in contact with the 8-1-1 titanium, it produced a stress raiser in excess of that caused by the original 1/4" hole used to notch the test specimen. This was true in areas where small hold-down clips had been used, in places where the electrode had accidentally brushed against the material, and at points where the specimen had been grounded.

Spotwelding of thermocouples was, therefore, considered to be unsatisfactory for the specimens to be tested in this program.

A more effective means of thermocouple attachment was developed which involves a "riveting" technique. In this method, a pair of small holes the size of the #20 thermocouple wire (0.032" dia.) were drilled through the test specimen. These holes were located on the longitudinal axis of the specimen 1/2" on either side of the transverse axis (see Figures 127-128). The thermocouple wires were fed through these two holes, gripped in a special holding fixture, then tapped lightly with a hammer. This upsets the thermocouple wires on either side of the specimen and keeps them from rotating in the holes or from pulling out. The advantages of this "riveted" method are as follows:

1. The thermocouple wires did not become detached from the specimen as a result of repeated test loadings and exposure to elevated temperature. Such failures had often occurred with spotwelded thermocouples.

2. This method produced an effective stress concentration smaller than that caused by the 1/4" hole in the center of the specimen. All failures took place at this hole, with test lives being equivalent to those of the original control specimens.

3. Specimen temperatures are defined with greater assurance than with the welded thermocouples. This is due, no doubt, to the fact that the thermocouple wire is in contact with both surfaces of the test specimen. Readings using the "riveted" method were approximately 3-1/2 percent higher than those for spotwelded thermocouples when radiant heat was applied in an open air installation to the side of the specimen away from the thermocouple wires. In this situation a temperature gradient through the specimen thickness is generated which would be minimized in enclosed oven applications.

4. Riveted thermocouples "follow" much more closely in temperature cycling operations.

5. The method of application of "riveted" thermocouples is quick and relatively cheap.

This method of attaching thermocouples was therefore adopted for all specimens subjected to temperature cycling.
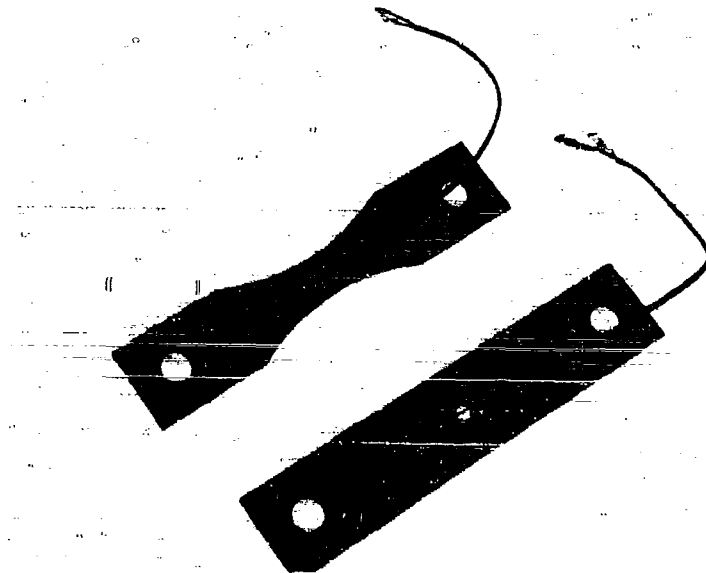
Figure 127.   Thermocouple Installation on Fusion-Welded and
Notched Fatigue Test Specimens
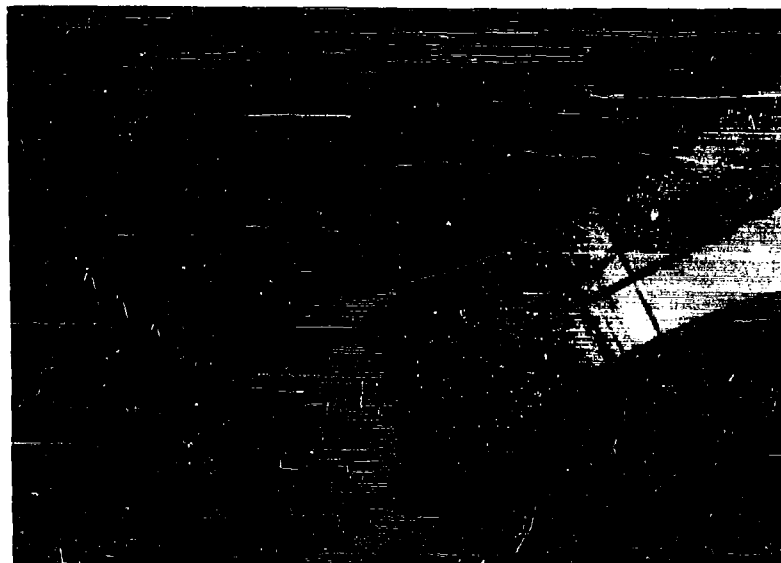
Figure 128.   Enlarged View of Thermocouple Installation on
Fusion-Welded Specimen

APPENDIX IV

DESCRIPTION OF TEST EQUIPMENT

A variety of standard equipment and equipment designed and constructed at Lockheed was used to precondition test specimens and to perform the different types of material evaluation tests required during the test program. This equipment, which is described below, includes the soak ovens, the static test machine, the constant load amplitude fatigue test machines, the accelerated and real time flight-by-flight test machines and the fuselage loading apparatus.

OVENS FOR SOAKING SPECIMENS WITHOUT CONTAMINANTS

Two ovens, each with a capacity of 2500 specimens, were used for exposing specimens to load at temperature without the application of contaminants. The equipment for the exposure of specimens to contaminants is described in the next section.

One of the ovens operated at $400°F$ and the other at $650°F$ with the specimen temperatures being maintained within $\pm 20°F$. Specimen temperatures were monitored within each oven by the use of 10 (ten) thermocouples. Located in each oven was a 16 column rack used to load the specimens through a system of static weights. The specimens were connected by close tolerance pins in a combined series-parallel arrangement, as shown in Figure 129, with specimen heating being provided by calrod elements mounted below heavy plates. Views of one of these soak ovens with the top cover removed are shown in Figures 130-131.

EQUIPMENT FOR SOAKING SPECIMENS WITH CONTAMINANTS

The equipment for soaking specimens under stress at temperature with intermittent application of contaminants consisted of a simple loading rack in an enclosed area. A maximum of 72 specimens were mounted on this rack and loaded by static weights through a system of links and whiffletrees. Banks of heat lamps were used to heat these specimens to $550°F \pm 20°F$. An exhaust system was provided to remove vapors. All controls were manually operated. The equipment and internal views of the specimen arrangement are shown in Figures 132, 133, and 134.

STATIC TENSILE TEST MACHINES

All of the static tensile tests were conducted on a 5,000 pound capacity Baldwin-Lima-Hamilton static test machine. This machine has a calibrated accuracy equal to ± 0.5 percent of the indicated load level and is capable of maintaining a constant strain rate of 0.005 inches/inch/minute. To obtain specimen strain measurements, a conventional O.S. Peters extensometer was used during the room temperature tests and a modified Arcweld extensometer was used in the tests conducted at elevated temperatures. During the elevated temperature tests, a radiant heat oven was used to maintain temperatures within ± 5°F along the two inch gage length of the specimen. This oven is similar to the one shown in Figure 137 for use on the constant load amplitude fatigue test machines.

CONSTANT LOAD AMPLITUDE FATIGUE TEST MACHINES

The constant load amplitude fatigue tests were performed on the machines shown in Figure 135. These machines were designed and constructed at Lockheed. Each machine has a loading column with a single specimen connected in series with a calibrated electrical strain gage transducer. This loading column is held stationary at the upper end and is attached to a hinged beam at the lower end. The free end of this hinged beam carries a motor-driven eccentric disk plus either springs or static weights for maintaining constant loads. Dynamic loads of ± 10,000 pounds can be maintained indefinitely within ± 2% accuracy at a normal operating frequency of 30 cycles per second (1800 cycles per minute).

A close-up of a specimen with stabilizing edge guides installed in one of these machines is shown in Figure 136. The edge guides are described in Appendix II.

Details of the ovens used to heat specimens during the fatigue tests conducted at elevated temperatures are illustrated in Figures 137 and 138.

ACCELERATED FLIGHT-BY-FLIGHT TEST MACHINES

Two test machines of the type shown in Figure 139 and illustrated schematically in Figure 141 were employed to conduct the accelerated flight-by-flight tests in which variable amplitude loadings are applied. These machines were designed and constructed at Lockheed. Each machine consists of a pair of servo jacks mounted in parallel within a simple loading rack. Each jack loads two specimens, as shown in Figure 140. These specimens are connected in series with a calibrated load transducer. The loads applied by these dual jack machines are programmed by two-track magnetic tape units such as those shown in Figure 142. In these machines, loads of ± 10,000 pounds can be controlled within an accuracy of ± 2% at frequencies up to 45 cycles per second.

During operation, the output voltage from the programmer is fed into the servo loop of one of the servo jacks through a summing junction as shown schematically on Figure 141. This signal programs the action of a servo valve

to meter the cyclic flow of oil to the fore and aft ports of the servo jack. Loadings are applied to the specimens and the load transducer by the resulting movement of the jack piston. The servo loop is closed by feeding the signal resulting from the load felt by the transducer back into the summing junction. The instantaneous summing of these opposing signals at the input side of the servo loop results in the specimen experiencing the same loading history as that represented by the signal on the magnetic tape.

The equipment used to obtain a complete thermal cycle in the cyclic temperature tests is indicated schematically in Figure 141 as the heat-cool control. The once-per-flight thermal cycle is triggered by a mean load level detector and is applied once every 20 seconds by the alternate use of a bank of quartz lamps and normal shop air. Traces of the temperature-load relationships produced by this equipment are shown in Figure 143.

As shown in Figure 141, the pressure and return line to each servo jack contains a solenoid-operated safety lock-up valve which stops the oil flow to the jack in the event of a loss in servo control due to an interruption of power. In addition, the use of a safety device in the form of a load limiter is also shown on the schematic diagram. This device was designed to protect the test specimen from spurious signals by simply limiting the maximum amplitude of the signals.

A combination of floating stiffeners and flexure plates were used to keep the specimens from buckling under compressive loads. The stiffeners are described in Appendix II.

FLIGHT-BY-FLIGHT TEST MACHINE FOR TESTS WITH REAL TIME AT TEMPERATURE

The conduct of the real-time at temperature flight-by-flight tests with variable amplitude loadings required the development of specialized equipment. The real-time test machine which is shown in Figure 144 consists of columns of six specimens with the columns installed in parallel within a single reaction frame. Each column is loaded by a double acting hydraulic jack mounted in series with a load-measuring transducer. The test areas of the six series connected specimens in each loading column are enclosed by the heating-cooling ducts shown in Figures 144 and 145. The action of the jacks is controlled so as to apply the loadings in the flight sequence which is shown in Figure 146. The load programmer consists of a rack of eight components, as shown in Figure 147. A block diagram of the control equipment is shown in Figure 148.

The cyclic loads are controlled by a system that uses partial load feedback. In this system, stepping switches program both the loadings and the heating and cooling. The load sensing is obtained by using a Zener trigger device along with one of the load transducers. On this trigger, a pair of preset voltages are used to represent the positive and negative halves of a load cycle. For every change in load on the specimen, the transducer generates a voltage increment. When the net voltage on the transducer is equal to one of the preset voltages on the trigger, the trigger fires to reverse the direction of oil flow in all of the hydraulic jacks. This reversal changes the action of the jacks on all of the specimens, with two such changes required to complete a loading cycle which is then recorded on a counter. When the

required number of each varying load level has been applied, the switches are rotated to a new position to establish the next varying load level felt by the specimen.

To apply the three differing mean load levels required for the climb, cruise and descent phase of flight, sets of weights rather than electrically controlled hydraulic jacks are used. Use of the weights was dictated by the need to minimize the possibility of inadvertent load change during the hour (at constant load) in each flight, which is defined in Figure 146. The load produced by the weights is applied to the pistons of the hydraulic jacks to generate a steady static load on the test specimens. During operation, the mean load produced by the weights is varied by the movement of a weight support platform. This platform movement is provided by the action of electric motor driven Acme screws. The platform is shown in Figure 149 in the 0.2g position for the descent phase of flight with a portion of the total weight supported by the platform. The weight system is diagrammed on Figure 150. The signals to the actuators for moving the platform are supplied by points on the load control stepping switch. The position of the platform is controlled by a system of micro switches.

The specimens are restrained from buckling under compression loadings by using a combination of flexure plates and edge support clamps on the specimens.

To heat the specimens, a number of quartz lamps are used. These lamps are mounted immediately below and at right angles to the specimens. They are located in the Alzac-lined stainless steel tunnels which act as cooling ducts during the last half of the temperature cycle. Power is supplied to these lamps by a 480 volt Research Incorporated Thermac Controller that operates at 100 amperes.

A total of 36 specimens are tested at one time. These consist of 12 specimens for each of the three materials tested. Twelve of the 36 specimens, located throughout the specimen pattern, are equipped with iron-constantine thermocouples which were "riveted" to the specimens as described in Appendix III. Temperatures of these twelve specimens are continuously recorded on the strip chart of a Minneapolis-Honeywell Temperature Recorder. The cyclic temperature changes are monitored by the output from one of these thermocouples.

During operation, a signal to the temperature controller is provided by a trigger action at the completion of loading cycles associated with the "climb" phase of the flight. Full power is applied to the heat lamp at the negative peak of the last load cycle applied during climb. When the load cycle has been completed, the mean load level for the cruise phase of flight is applied. The maximum power is reduced in approximately three minutes to permit the 0.025 gage PH14-8Mo and Inco 718 specimens to reach a stabilized temperature of 500°F without overheating. At this time, the thicker 0.050 gage titanium specimens are at a temperature of 480°F and require an additional three minutes at the reduced power level to reach the stabilized 500°F temperature. At the negative peak of the last cycle of cruise loadings, the power to the lamps is shut off and a 15-horsepower centrifugal blower is turned on to force ambient air across the specimens to reduce their temperature to 90°F for application of the descent load cycles. This cooling takes place in approximately two

minutes for the 0.025 gage specimens and three minutes for the 0.050 gage specimens. The manifold from the blower is shown connected to each of the six stainless steel ducts in Figure 144. Traces of the temperature-loading relationships produced by the equipment are shown in Figures 151 and 152.

Several safeguards were designed into this equipment to minimize the possibility of accidental damage to the specimens through operator error or from malfunction of the equipment. In addition to the previously mentioned use of static weights for maintaining mean load levels, the following design features were incorporated to safeguard the specimens.

1. During the repetitions of the standard flight sequence which are generated by the control apparatus, hydraulic pressures are limited to values a few percent over those required for the maximum loads during each flight.

2. Pre-set pressure regulators protect the specimens against accidental over-loads which might occur during the manually controlled application of the larger loadings which are required to represent the growth of peak loadings with time.

3. Mechanical stops were installed to prevent excessive and damaging system deflections in the event of specimen failures.

4. In the event of a power failure, normally open by-pass valves act to reduce the system oil pressure to zero. As an added safety feature, a 4-way solenoid valve operates to prevent the application of a large compressive load to the specimens in case the by-pass valves do not function.

5. In the event of a drop in operating pressure because of a malfunction of the hydraulic pump or because of a leak in the oil system, a pressure switch shuts off the complete system.

6. To prevent overheating, a device was installed to shut off the complete system if the temperature measured by any of the thermocouples exceeds 530°F.

FUSELAGE LOADING APPARATUS

In the fuselage loading apparatus, a group of four test specimens is loaded through a whiffletree installed in series with a load transducer and a pneumatic loading jack. The maximum jack force is controlled by a regulated pressure source. A peak temperature of 550°F is reached at the center of the test specimen in about 12 seconds through the use of radiant heat lamps. Cooling to 120°F is attained in approximately 18 seconds by the use of a large centrifugal blower moving air through a manifold fitted with a solenoid-operated air diverter. During operation, the load is applied by metering air at a given pressure to the pneumatic jack. The heating cycle is phased with this load increase and controlled through a regulated power supply to peak out at 550°F ± 10°F. When this temperature has been reached, the power to the lamp automatically shuts off, the ambient air from the blower is directed to the four specimens and the load is reduced to a very small positive value by

release of air contained in the pneumatic jack. When the temperature of the test specimen reaches the lower limit, the blower air is directed away from the specimens, the lamps and jack pressure are switched on, and the cycle is repeated.

The safety devices on this apparatus include a regulated pressure source and a load limiter device that works off the load transducer to shut down the system if the desired load is exceeded.

A schematic of the fuselage loading apparatus is presented in Figure 153. The apparatus, its controls and the specimen installation are shown in Figures 154-155. The load and temperature relationship during the fuselage loading tests is shown on Figure 156.
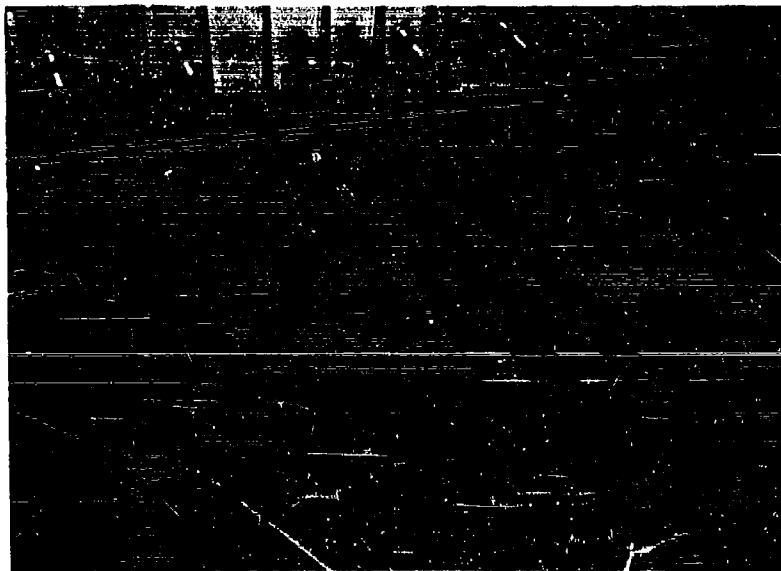
Figure 129. Installation of Test Specimens in Series-Parallel Arrangement in Soak Oven

Figure 130. Oven for Preconditioning Test Specimens, Cover Removed
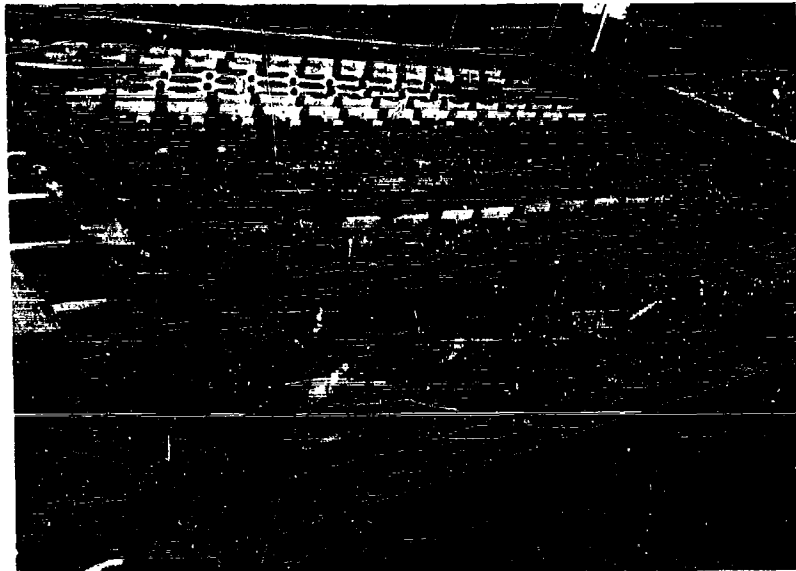
Figure 131. Specimen Installation in Preconditioning Oven
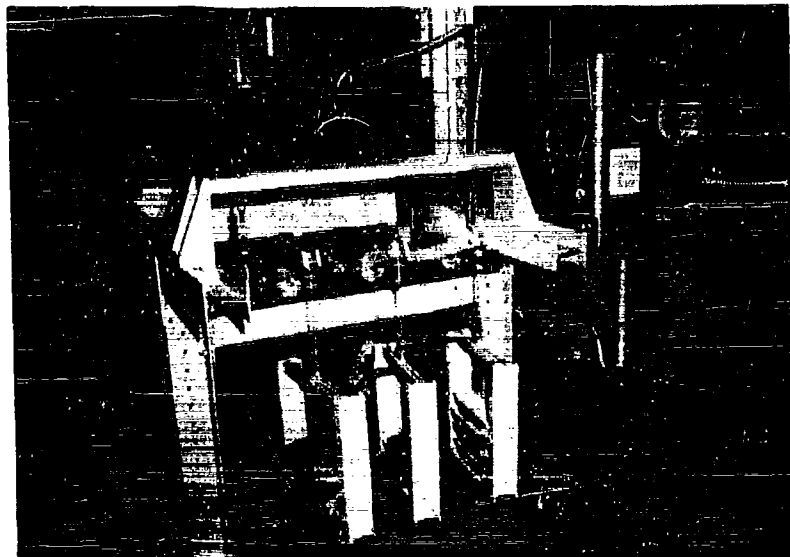
Figure 132. Apparatus for Preconditioning of Specimens with Corrosive or Contaminating Materials
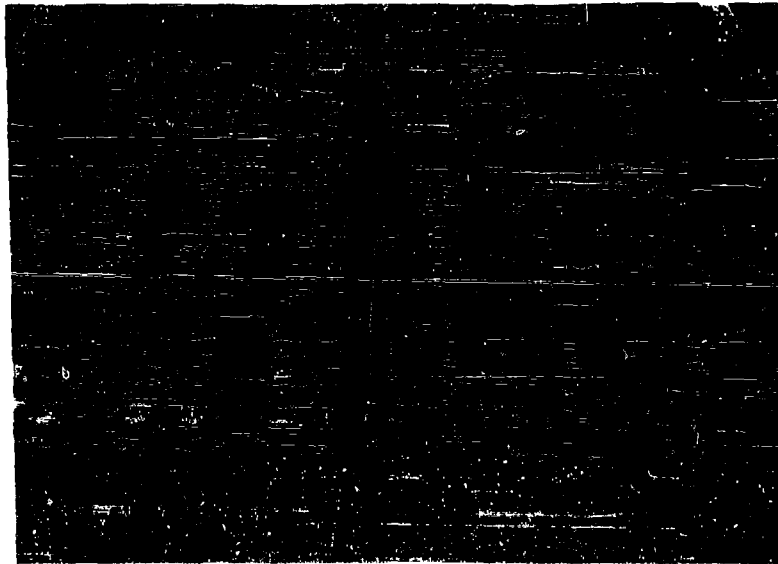
Figure 133.   View of Specimens in Contaminant
Preconditioning Apparatus

Figure 134.   Close-Up of Specimens in Contaminant
Preconditioning Apparatus

Figure 135. Constant Amplitude Fatigue Test Machines

Figure 136. Close-Up of Specimen In Fatigue Test Machine
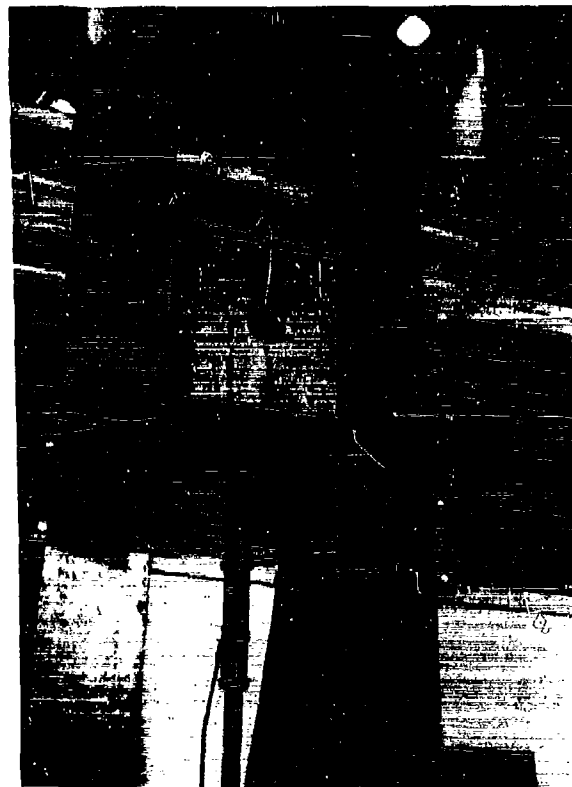
Figure 137. Close-Up of Oven Installation
and Loading Column In Fatigue
Test Machine
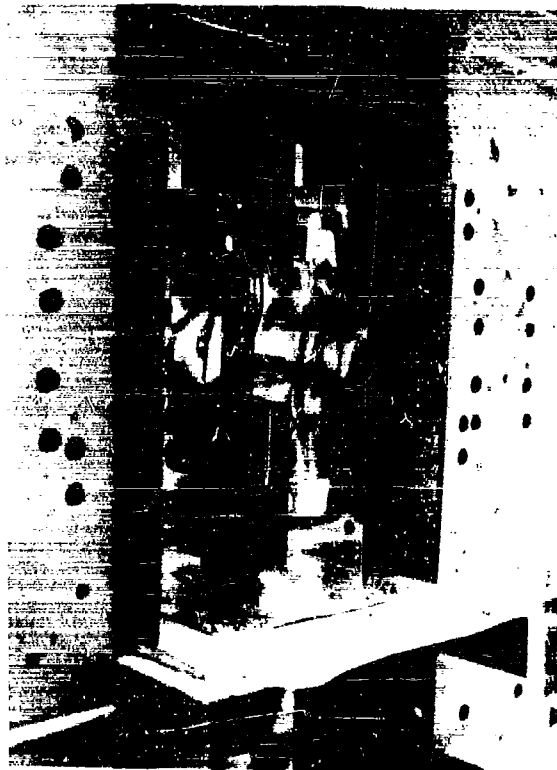
Figure 138. Close-Up of Specimen Installed in
Oven on Fatigue Test Machine
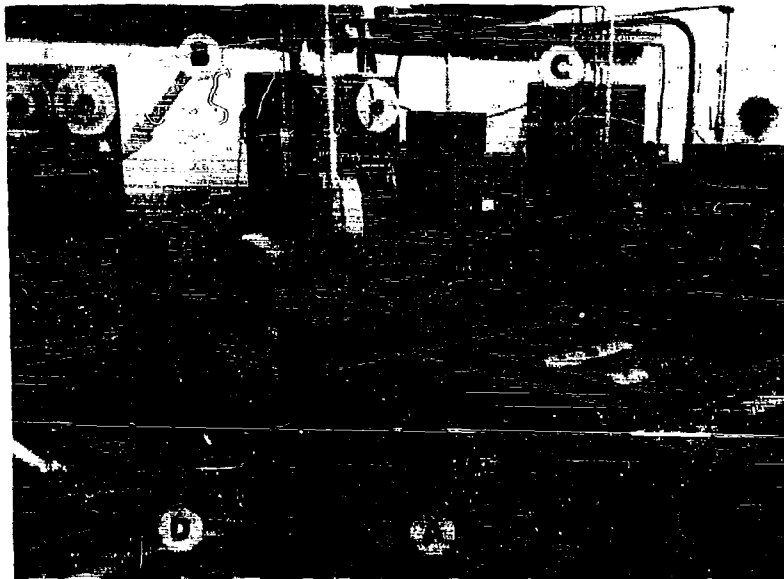
A. Servo-Jack Fatigue Test Machine
B. Magnetic Tape Control Unit for Loads
C. Power Supply and Temperature Controller for Heat Lamps
D. Brown Temperature Recorder

Figure 139. Servo-Controlled "Accelerated Flight-By-Flight" Fatigue Test Machine

A. Test Specimen - 4 Per Machine
B. Compression Edge Support Clamp Assembly
C. Thermocouple Installation
D. Radiant Heat Lamps

Figure 140. Close-Up of Specimen Installation in "Accelerated Flight-by-Flight" Loading Tests
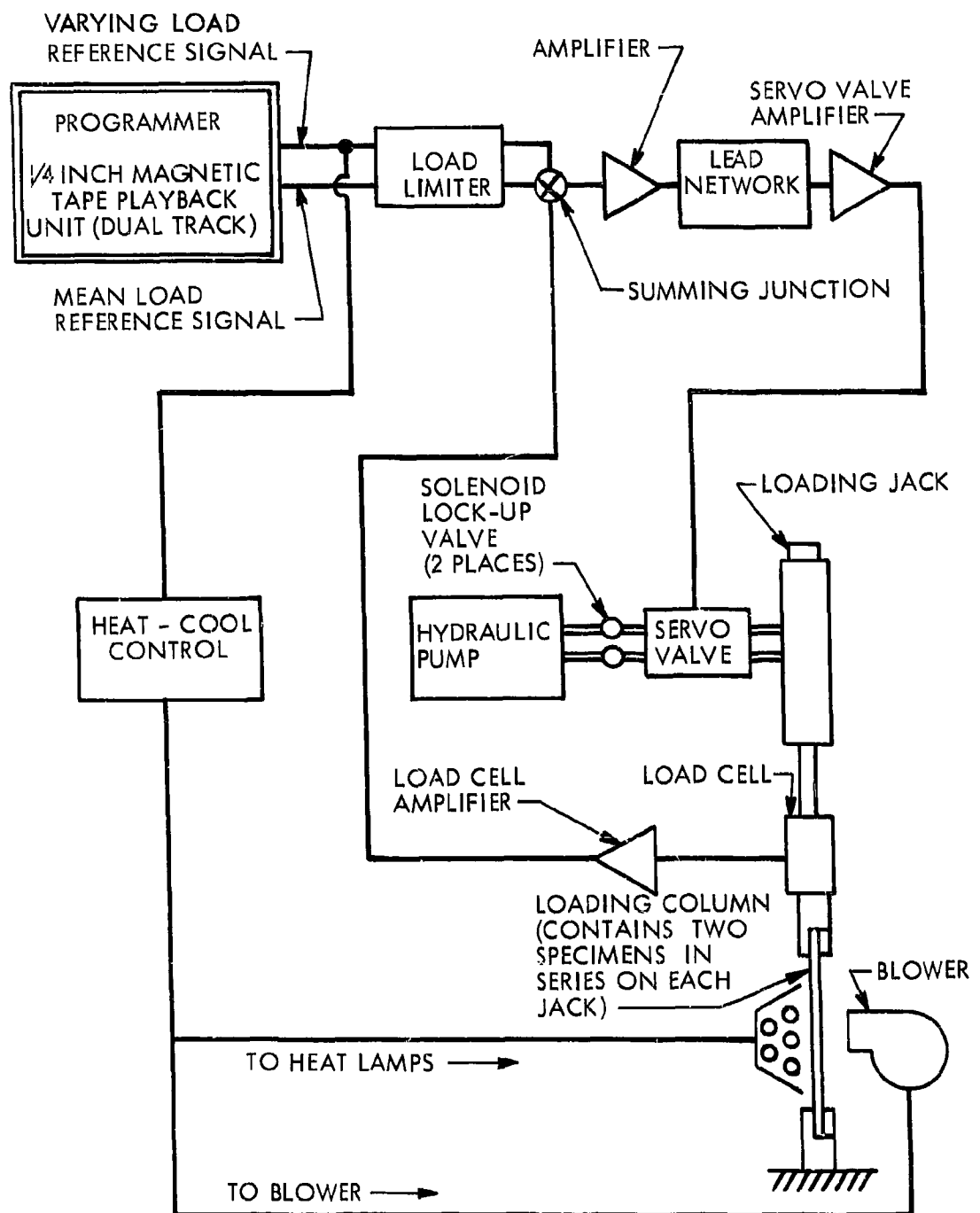
Figure 141. Block Diagram of Test Set-Up for "Accelerated Flight-by-Flight" Loading Tests
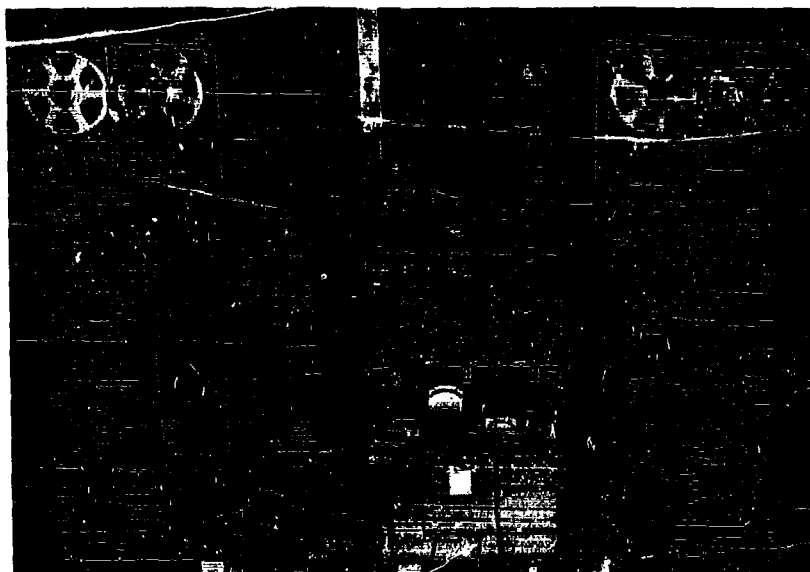
Figure 142. Magnetic Tape Loading Control Units for Servo-Controlled Machines
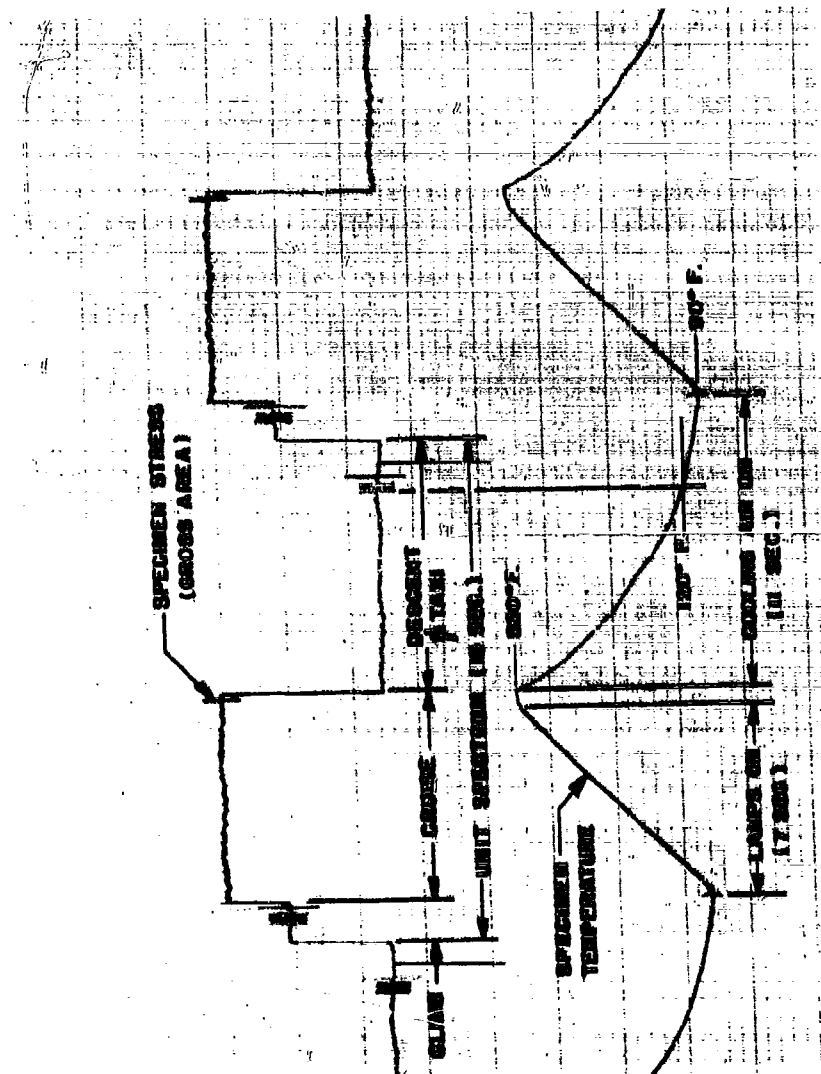
Figure 143. Stress and Temperature Traces for Accelerated Time Tests with Cyclic Temperature
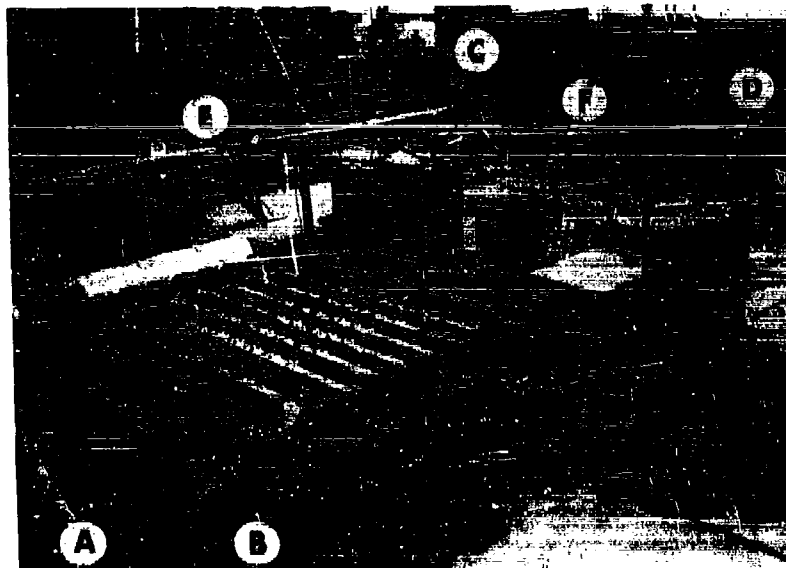
A. Manifold From Centrifugal Blower
B. Heating and Cooling Ducts
C. Load Programmer
D. Hydraulic Control Equipment
E. Power Supply & Temperature Controller for
   Heat Lamps
F. Temperature Recorder

Figure 144.   Test Apparatus for "Real Time" Spectrum
              Loading Tests
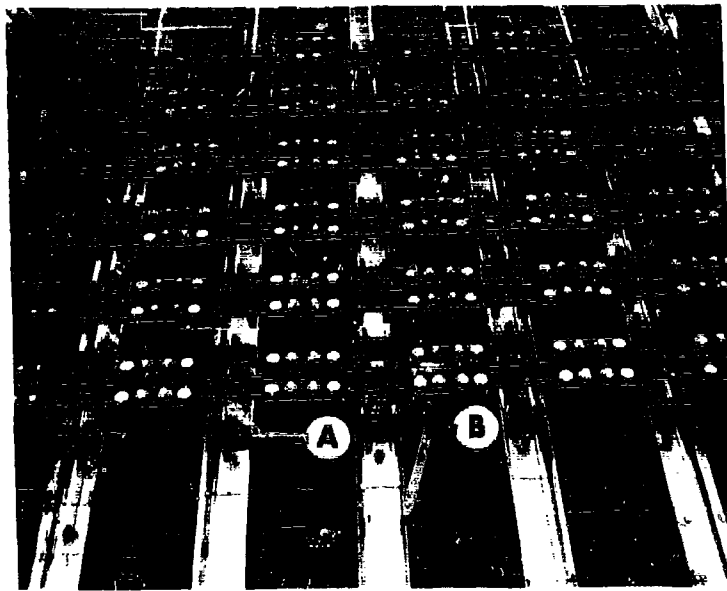
A - Edge Support Clamp
B - Heating-Cooling Tunnel, Lower Half

Figure 145. Close-up of Specimen Installation in Real Time Machine
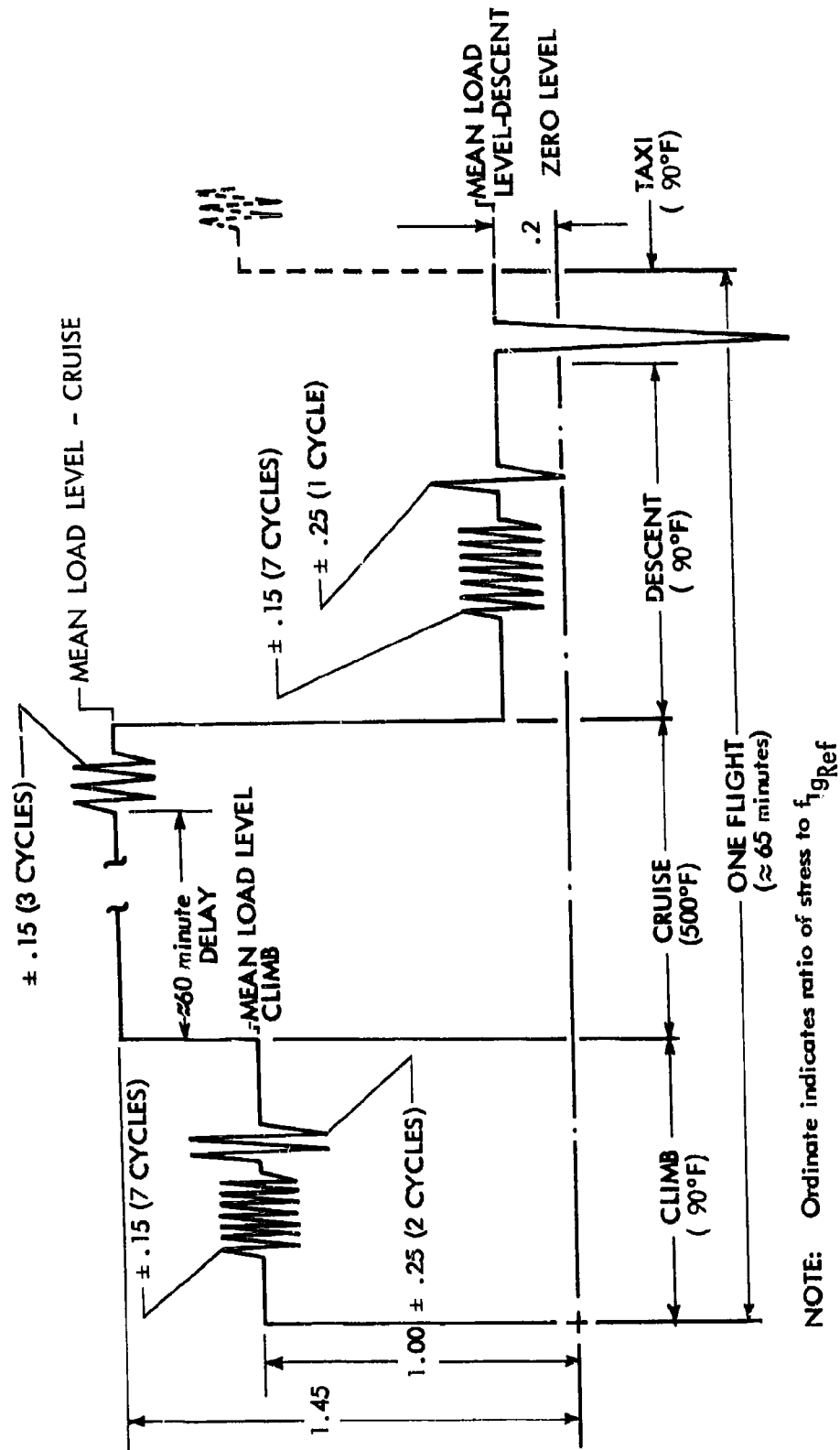
NOTE: Ordinate indicates ratio of stress to $f_{1g_{Ref}}$

where $f_{1g_{Ref}}$ = 25000 psi for 8-1-1 Titanium and

40000 psi for PH 14-8Mo Steel and INCO 718

Growth in magnitude of cyclic loads with time is given in Tables 13-15 and 19.

Figure 146. Unit Flight-by-Flight Loading Sequences and Magnitudes for Real Time Tests — Spectra C

217

A. Load Monitor Chassis
B. "Flight" Recorder
C. Load Sequence Chassis
D. Trigger Chassis
E. 6 - Channel Sanborn Carrier Amplifier,
   Model 956-111
F. Valve Control Chassis
G. Actuator Chassis
H. 28 - Volt Power Supply

Figure 147. Electronic Control Equipment for "Real Time" Spectrum Loading Tests
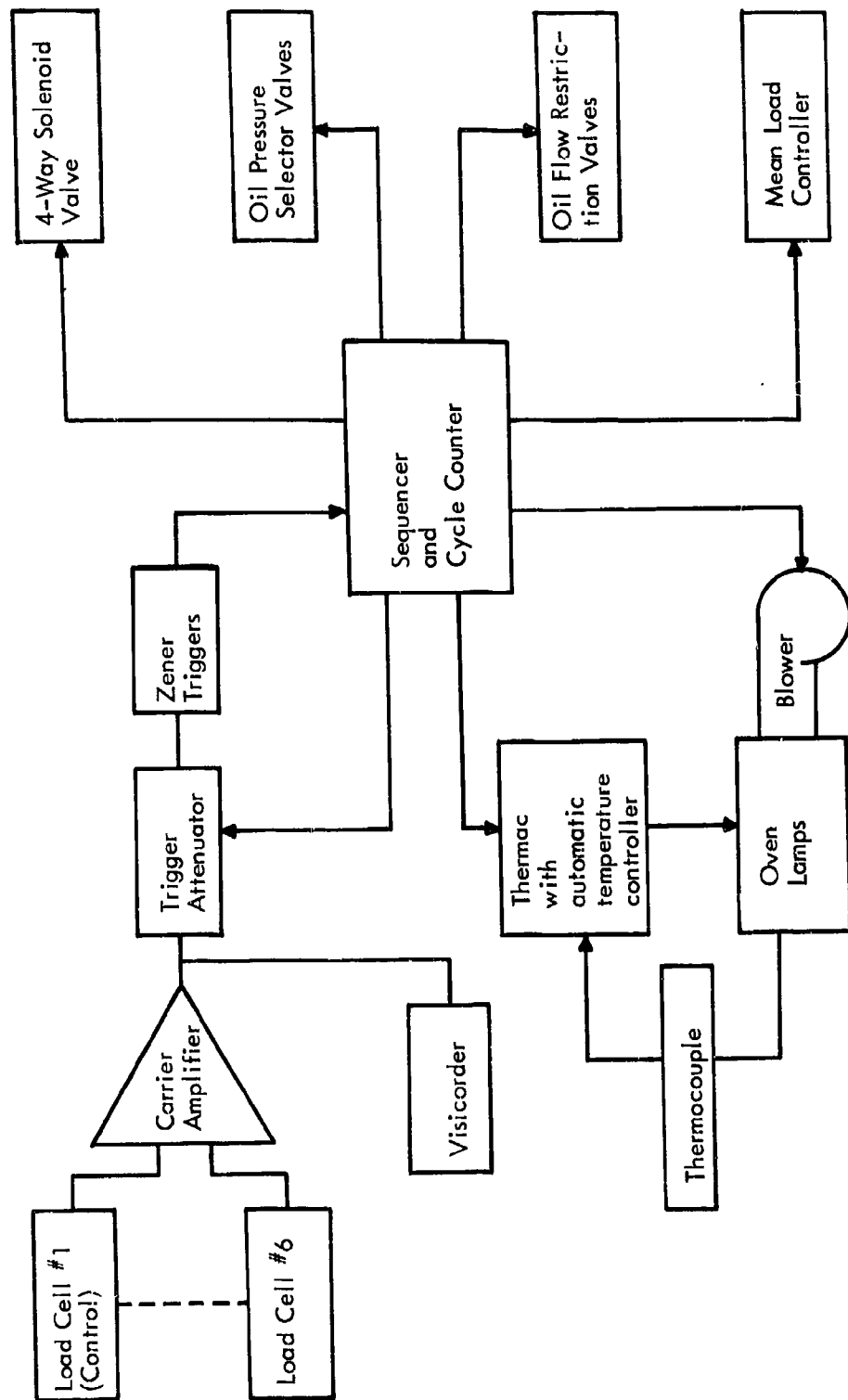
Figure 148. Block Diagram of Control Equipment in Real Time Spectrum Loading Tests
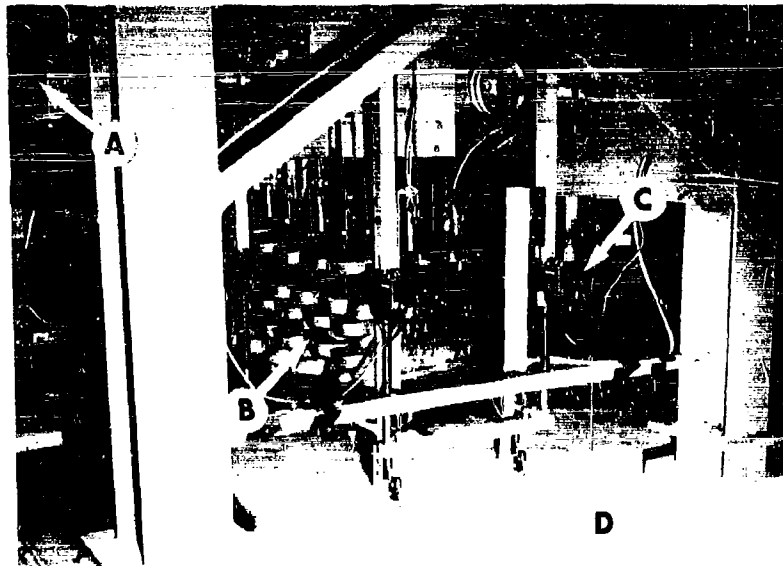
A. Hydraulic Actuator
B. Static Weights
C. Actuator for Lifting Static Weights
D. Micro Switches for Static Weight Positioning

Figure 149. Static Loading System for Controlling Mean Loads on Real Time Spectrum Loading Machine
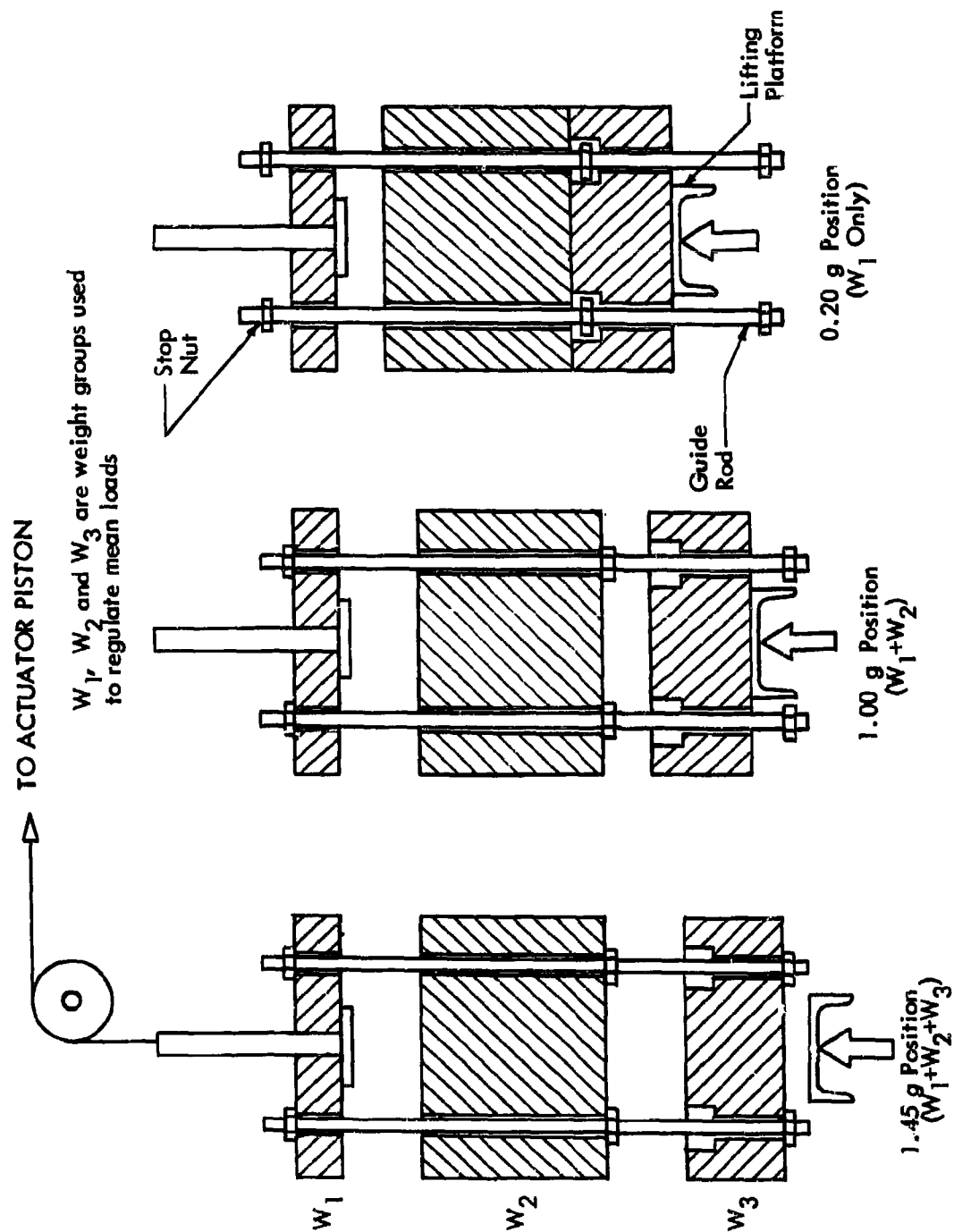
Figure 150. Static Weight Loading System for Maintaining Mean Loads on Real Time Spectrum Loading Machine
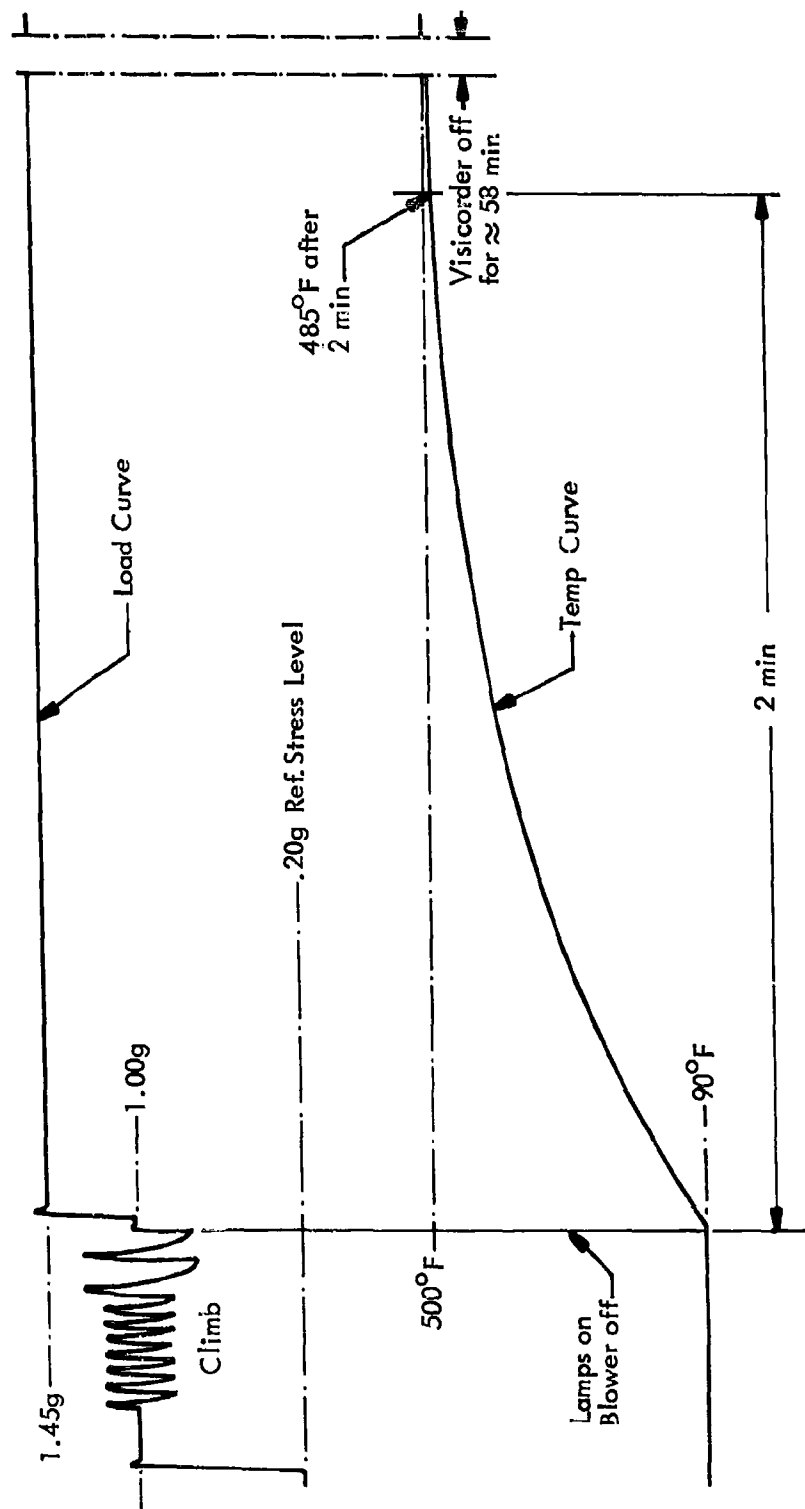
Figure 151. Trace of the Heating Phase of the Real-Time Spectrum Tests of Center-Notched INCO 718
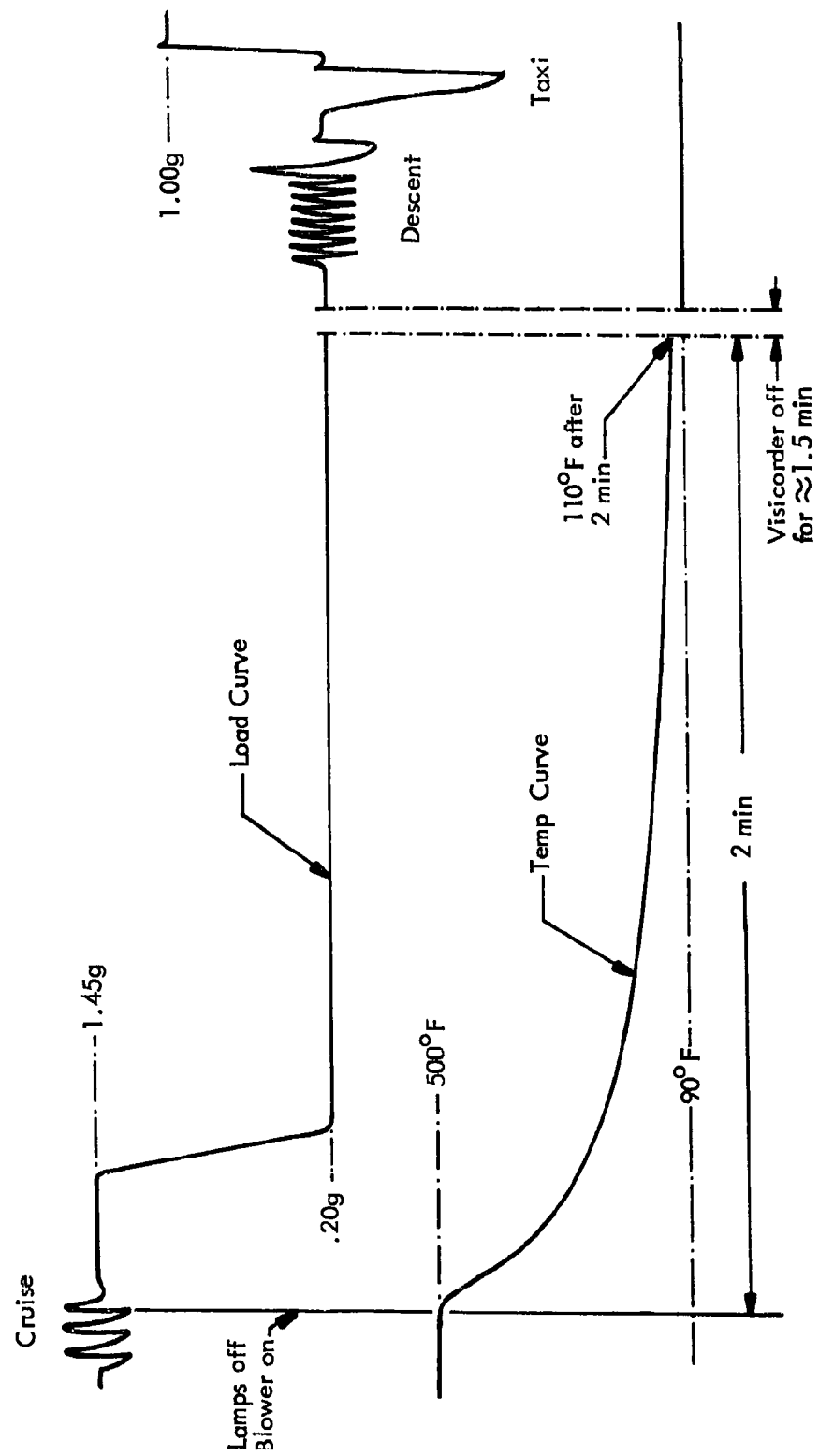
Figure 152. Trace of the Cooling Phase of the Real–Time Spectrum Tests of Center–Notched INCO 718

223
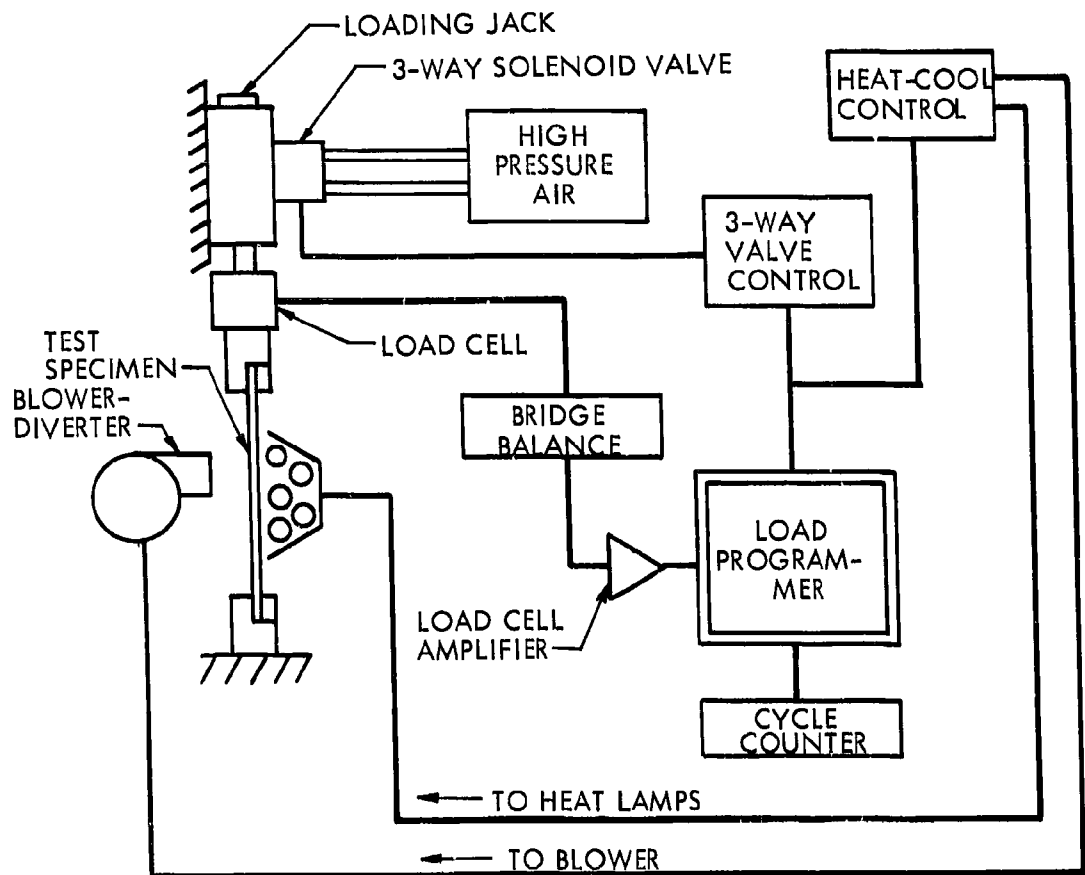
Figure 153. Block Diagram of Test Set-Up for Fuselage Loading Tests
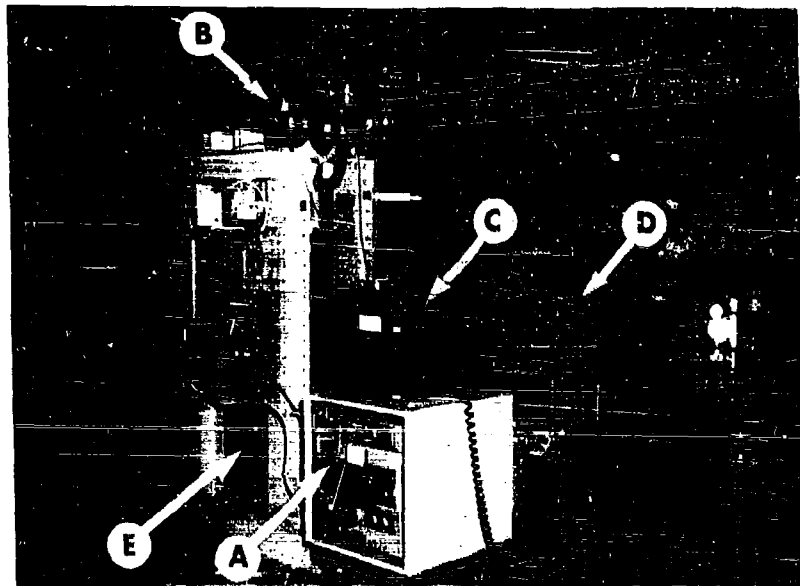
A. Power Supply for Heat Lamps
B. Cooling Air Manifold
C. Temperature Read-Out Equipment
D. Viscorder for Load-Temperature Control
E. Jack

Figure 154. Test Set-Up for Fuselage Loading Evaluation
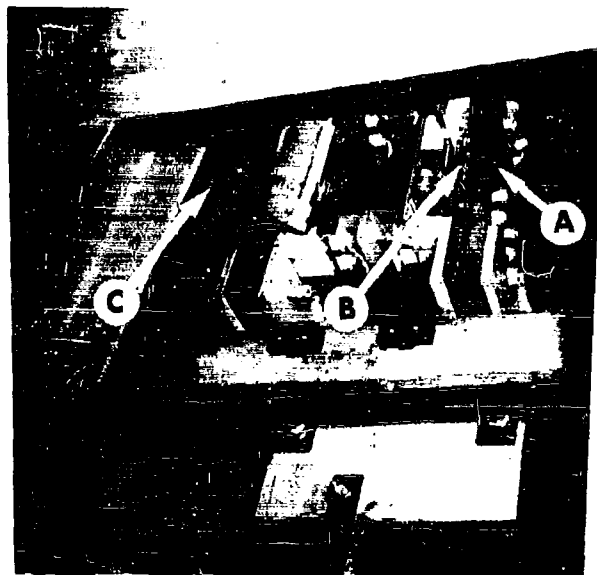
A. Test Specimen
B. Heat Lamps
C. Cooling Air Duct

Figure 155. Close-Up of Specimen Installation (Reflector Removed for Clarity)

225
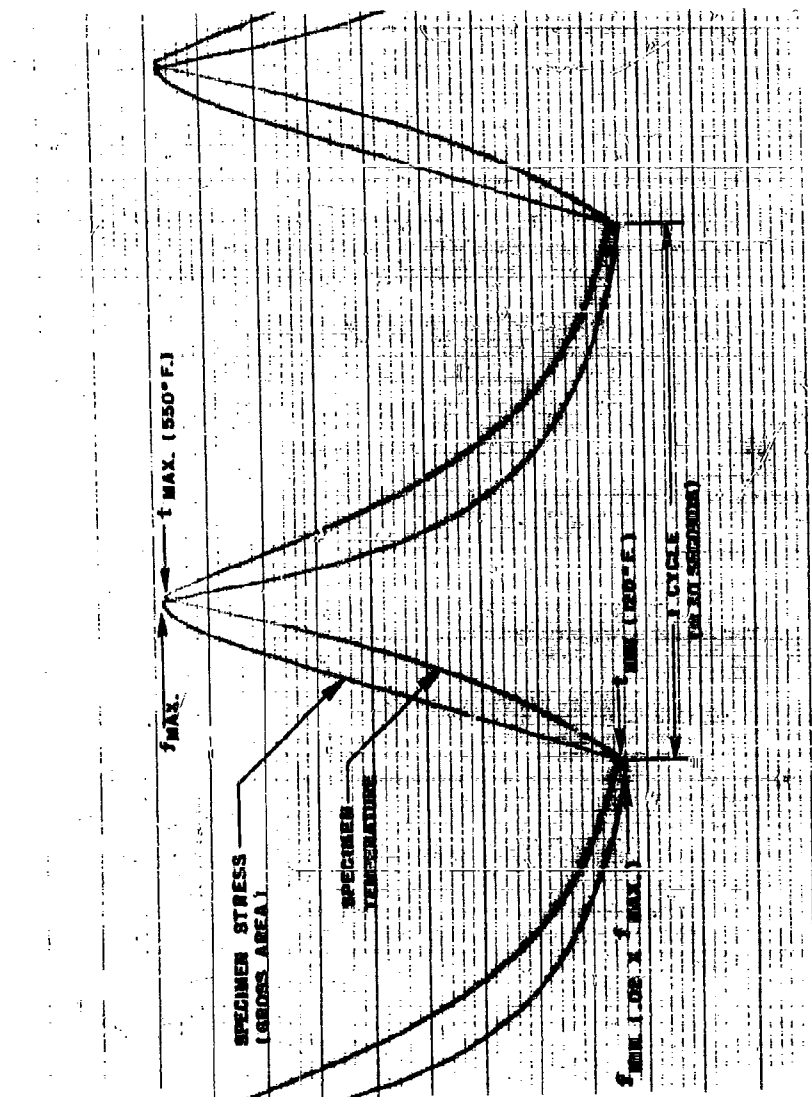
Figure 156. Oscillographic Record of Load and Temperature Phasing in Fuselage Loading Tests

APPENDIX V

DERIVATION OF S-N CURVES

Because of the number of variables - material, specimen geometry, exposure time, exposure temperature, and test temperature - the number of data points obtained for each combination of variables is necessarily rather small. This factor and the relatively large scatter of data always associated with constant load amplitude fatigue testing led to the need for a consistent method of drawing a curve to represent each group of data points. For this purpose, trial use was made of the general method of linear regression as suggested by Weibull[*] for use with small groups of test data. The following derivation of this method of calculation was presented in a recent ASD technical Report.[**]

In Weibull's use of the method of linear regression with small sample sizes, all of the test specimens defining an S-N curve are pooled together. The following equation is then assumed to apply to the pooled S-N data.

$$f_{vary} = f_E + pN^u \tag{V-1}$$

where

f_{vary} = varying stress of constant amplitude

f_E = the constant amplitude varying stress corresponding to endurance limit

N = cycles to failure for f_{vary}

and p and
u = regression coefficients

The endurance limit f_E is a statistical variate in itself and Equation (V-1) must be solved for known or estimated values of f_E. For a given value of f_E, Equation (V-1) can be written in the form

---

[*] Weibull, W., "Statistical Handling of Fatigue Data and Planning of Small Test Series." The Aeronautical Research Institute of Sweden (FAA), Report No. 69, October 1956.

[**] Crichlow, W. J., A. J. McCulloch, L. Young, and M. A. Melcon, "An Engineering Evaluation of Methods for the Prediction of Fatigue Life in Airframe Structures". ASD-TR-61-434, March 1962.

$$\log \left(f_{vary} - f_E\right) = \log p + u \log N \qquad (V-2)$$

Designating $y = \log \left(f_{vary} - f_E\right)$ as the dependent variable and $x = \log N$ as the independent variable, the method of linear regression can be applied to the following equation,

$$y = y_o + ux \qquad (V-3)$$

where the coefficients u and y_o of the linear regression line are determined from

$$u = \frac{\displaystyle\sum_{i=1}^{n} (x_i - \bar{x})(y_i - \bar{y})}{\displaystyle\sum_{i=1}^{n} (x_i - \bar{x})^2} \qquad (V-4)$$

and

$$y_o = \log p + \bar{y} - u\bar{x} \qquad (V-5)$$

where

$$\bar{x} = \frac{\displaystyle\sum_{i=1}^{n} x_i}{n} \qquad (V-6)$$

and

$$\bar{y} = \frac{\displaystyle\sum_{i=1}^{n} y_i}{n} \qquad (V-7)$$

with

$\quad$ n = to the number of pooled test specimens

The above equations are exact only if the variances of y are homogeneous in the population. This is to say, that the standard deviation in y is independent of x. In addition the deviations from the linear regression line should be normally distributed. An unbiased estimate $s_{y \cdot x}^2$ of the variance from the regression of the population is given by

$$s_{y \cdot x}^2 = \frac{\displaystyle\sum_{i=1}^{n} \left[y_i - (y_o + ux_i)\right]^2}{n - 2} \qquad (V-8)$$

228

where

$$S_{y \cdot x} = \text{the standard error of estimate}$$

For any particular value of x, such as x*, confidence limits for the computed mean value y* = $(y_0 + ux*)$ are easily set with the upper confidence limit given by

$$y_u^* = (y_0 + ux*) + t_{\alpha/2, n-2} \, S_{y \cdot x} \left[\frac{1}{n} + \frac{(x* - \bar{x})^2}{\sum\limits_{i=1}^{n} (x_i - \bar{x})^2} \right]^{\frac{1}{2}} \qquad (V-9)$$

and the lower confidence limit given by

$$y_1^* = (y_0 + ux*) - t_{\alpha/2, n-2} \, S_{y \cdot x} \left[\frac{1}{n} + \frac{(x* - \bar{x})^2}{\sum\limits_{i=1}^{n} (x_i - \bar{x})^2} \right]^{\frac{1}{2}} \qquad (V-10)$$

where

$$y* = \text{the estimate of the mean value of y at the value of } x*$$

$$t = \text{value of sampling distribution}$$

and $\quad \alpha = \text{confidence level}$

Values of $t_{\alpha/2, n-2}$ must correspond to the required confidence coefficient $(1-\alpha)$ and the given degree of freedom $(n-2)$. These values can be readily found in any standard text book on statistics.

To apply the above procedure to S-N data, plausible values must be assumed for the endurance limit. The actual value selected for the endurance limit, f_E, will have only a small effect on the analytical matching of the S-N data in the midstress range. Sometimes, a more accurate linear regression fit to the entire stress range of the S-N data is obtained by setting f_E equal to zero in Equation (V-1). An example of the derivation of the parameters for this equation with f_{max} substituted for f_{vary} is given in Table 35 . The use of f_{max} can be justified by adding f_{mean} to both sides of equation (V-1) and letting f_{max} equal the mean plus varying stress on the left hand side of the

229

equation. The term $(f_E + f_{mean})$ on the right hand side of the equation could then be replaced by f_{max_E} or the maximum stress at the endurance limit to obtain

$$f_{max} = f_{max_E} + p N^u \qquad \text{(V-11)}$$

where

p, N and u are defined under Equation (V-1)

In Table 35, the parameters u and p are derived for Equation (V-11) by setting f_{max} equal to zero. Once these parameters have been derived, this equation can be used to plot linear regression lines. Figures 157 to 159 illustrates the correlation between test data and the linear regression lines obtained by using Equation (V-11) in the form presented at the bottom of Column 15 in Table 35. The linear regression lines in these figures were obtained by assuming arbitrary values for N and calculating the applicable value of the maximum stress. The above procedure was followed because of inadequate definition of the endurance limit.

Regression lines need not be limited to the two parameters of a single straight line but may be defined by any number of parameters. Segmented straight regression lines such as those shown on Figures 157 - 159 will provide a significantly better fit to existing data than nonsegmented straight lines. These may be applied in the analysis above, for example, as

$$y = \max(y_1, y_2) = \frac{1}{2}(y_1 + y_2) + |y_1 - y_2| \qquad \text{(V-12)}$$

with

$$y_1 = y_1(x) = y_{1_0} + u_1 x \quad \text{and} \quad y_2 = y_2(x) = y_{2_0} + u_2 x \qquad \text{(V-13)}$$

as in Equation (V-3), y_{1_0}, u_1, y_{2_0}, u_2 are the parameters to be estimated.

Comparisons of the conventional semi-log representations of these segmented and nonsegmented lines are shown in Figures 160-162. The criterion used for determining whether additional segments are justified is that the improvement in fit more than offsets the effect of the loss in number of degrees of freedom due to the additional parameters to be estimated. Because of the small number of pooled data points used to define each S-N curve, no statistically significant gain can be obtained by the use of the type of computations represented by Equation (V-11) to estimate a segmented linear regression line as distinct from a visual best fit. Consequently, after an extensive investigation of numerous plots such as those shown in Figures 157 - 159 and Figures 160 - 162, the definition of S-N curves by a visual best fit of segmented linear regression lines was adopted to generate the constant R curves presented with the test data points in Volume II of this report.

TABLE 35   DERIVATIONS OF PARAMETERS FOR STATISTICAL LINEAR REGRESSION EQUATION CENTER-NOTCHED 8-1-1 TITANIUM AT ROOM TEMPERATURE, NO PRIOR SOAK

①	②	③	④	⑤	⑥	⑦	⑧
R	N CYCLES	f_{max} PSI	$x=\log_{10} N$	$y=\log f_{max}$	$\bar{x}$	$x-\bar{x}=a$	$\bar{y}$
			$\log_{10}$ ②	$\log_{10}$ ③	Σ④ /No. of Specs.	④-⑥	Σ⑤ /No. of Specs.
0.1 ↑	5400	90000	3.73239	4.95424	5.27017 ↑	-1.53778	4.72185 ↑
	7380	80000	3.86806	4.90309		-1.40211	
	18200	70000	4.26007	4.84510		-1.01010	
	21600	65000	4.33445	4.81291		- .93572	
	29700	60000	4.47276	4.77815		- .79741	
	67700	55000	4.83059	4.74036		- .43958	
	53600	50000	4.72916	4.69897		- .54101	
	1342300	47500	6.12775	4.67669		.85758	
	1496160	47500	6.17493	4.67669		.90476	
	1489200	45000	6.17289	4.65321		.90272	
	3776000	42500	6.57703	4.62839		1.30686	
	1579200	40000	6.19838	4.60206		.92821	
	1475300	38000	6.16879	4.57978		.89862	
0.1	1365300	36000	6.13513	4.55630	5.27017 ↓	.86496	4.72185 ↓

⑨	⑩	⑪	⑫	⑬	⑭	⑮
$y-\bar{y}=b$	Σa^2	Σab	u	$\bar{y}-u\bar{x}$	P	$f_{max}=P/N^{-u}$
⑤-⑧	Σ⑦²	Σ⑦ ⑨	⑪÷⑩	⑧-⑥ ⑫	anti log ⑬	⑭ /N⁻ ⑫
.23239	2.36477	- .35736				
.18124	4.36136	- .61148				
.12325	5.38166	- .73598				
.09106	6.25723	- .82118				
.05630	6.86242	- .86608				
.01851	7.05565	- .87422				
-.00288	7.34854	- .86134				
-.04516	8.08464	- .90057				
-.04516	8.90323	- .94142				
-.06864	9.71813	-1.00339				
-.09346	11.42602	-1.12553				
-.11979	12.60759	-1.23670				
-.14207	13.03511	-1.36435				
-.16555	13.24306	-1.50755	-.10890	5.09577	197500	$f_{max}=\dfrac{197500}{N^{.10890}}$

231

Figure 157. Use of Best Fit and Linear Regression for S-N Curves — Room Temperature

232

Figure 158. Use of Best Fit and Linear Regression for S-N Curves – Room Temperature

233
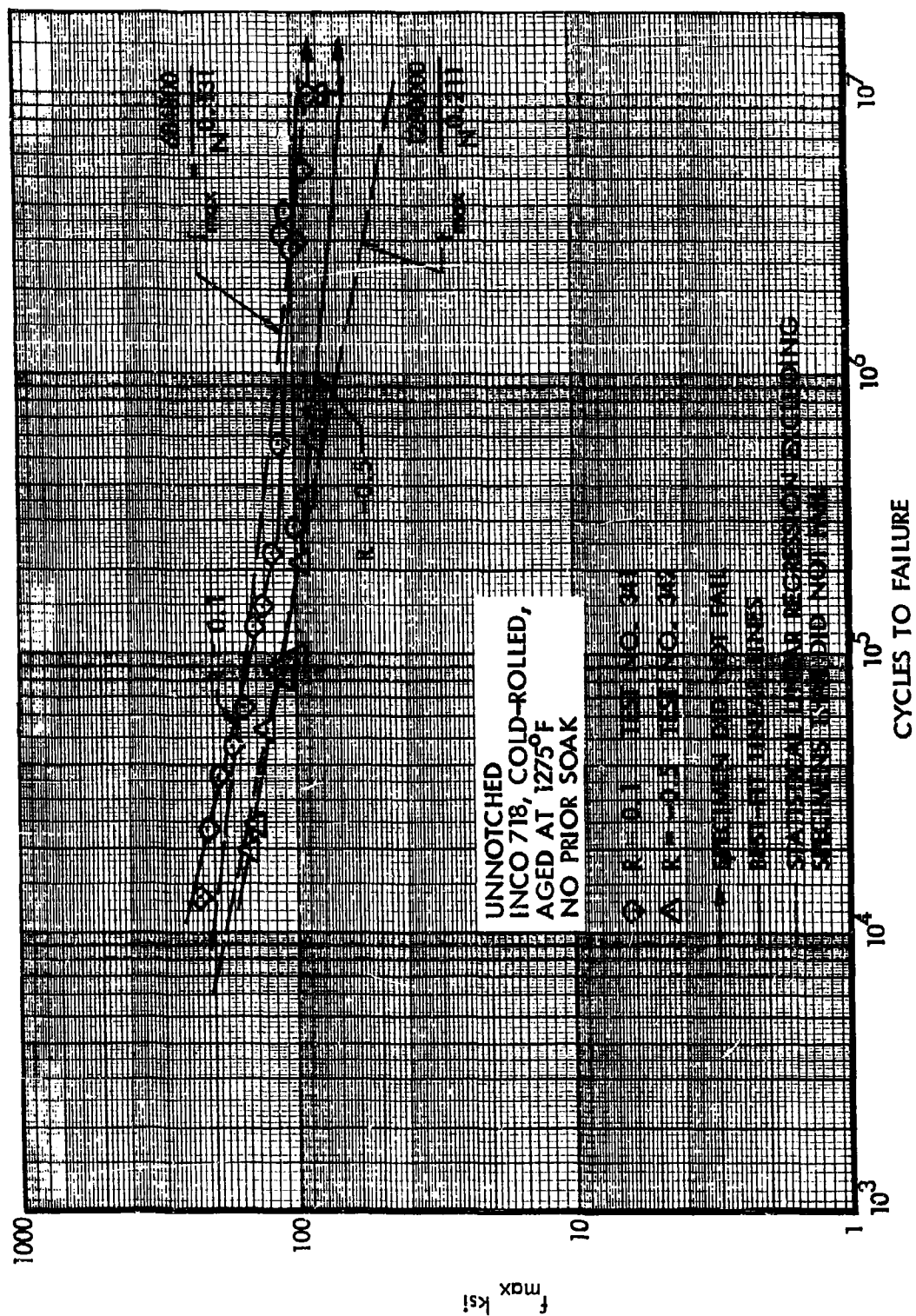
Figure 159. Use of Best Fit and Linear Regression for S-N Curves — Room Temperature

234
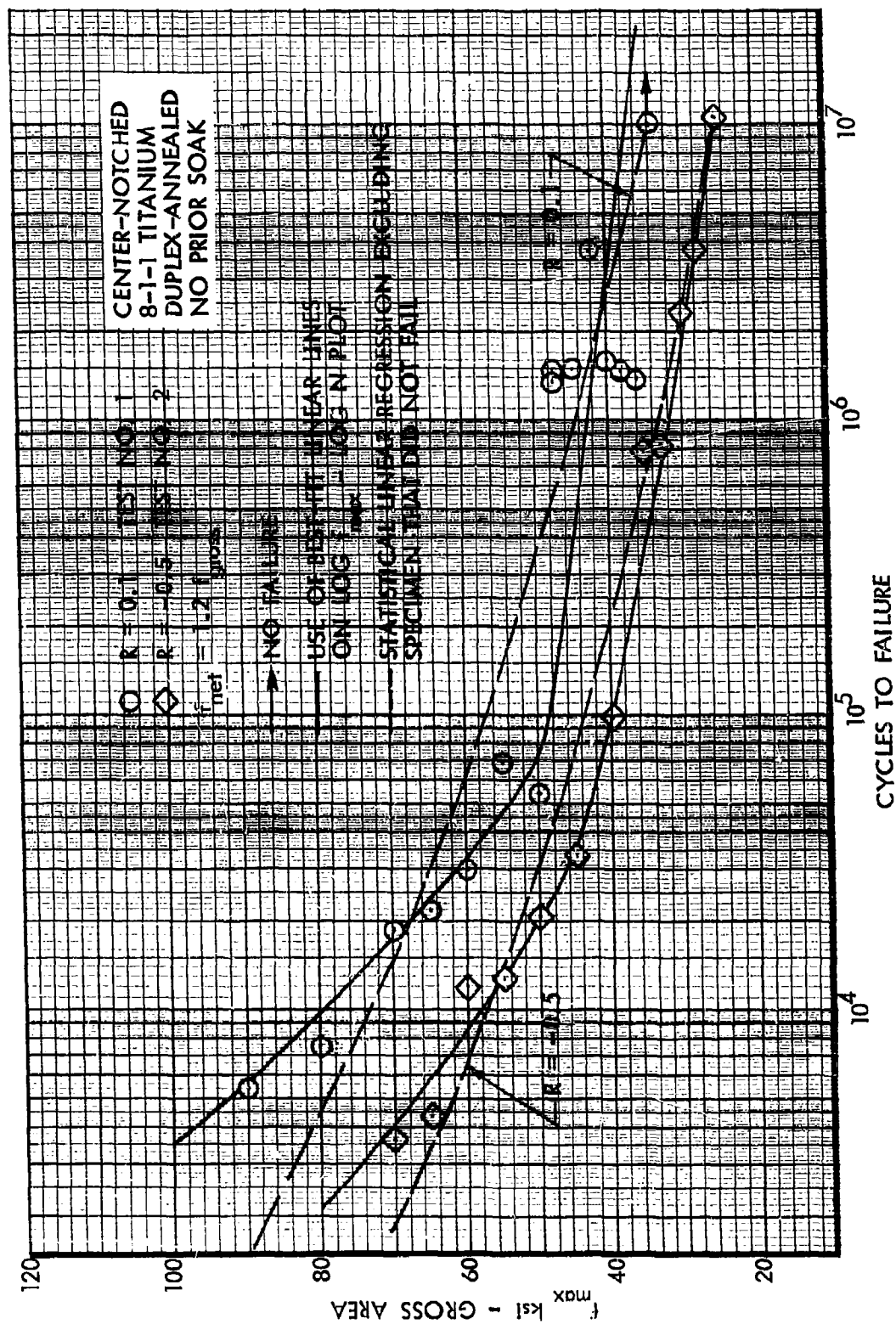
Figure 160. Use of Best Fit and Linear Regression for S-N Curves — Room Temperature

235

Figure 161.   Use of Best Fit and Linear Regression for S-N Curves – Room Temperature

236
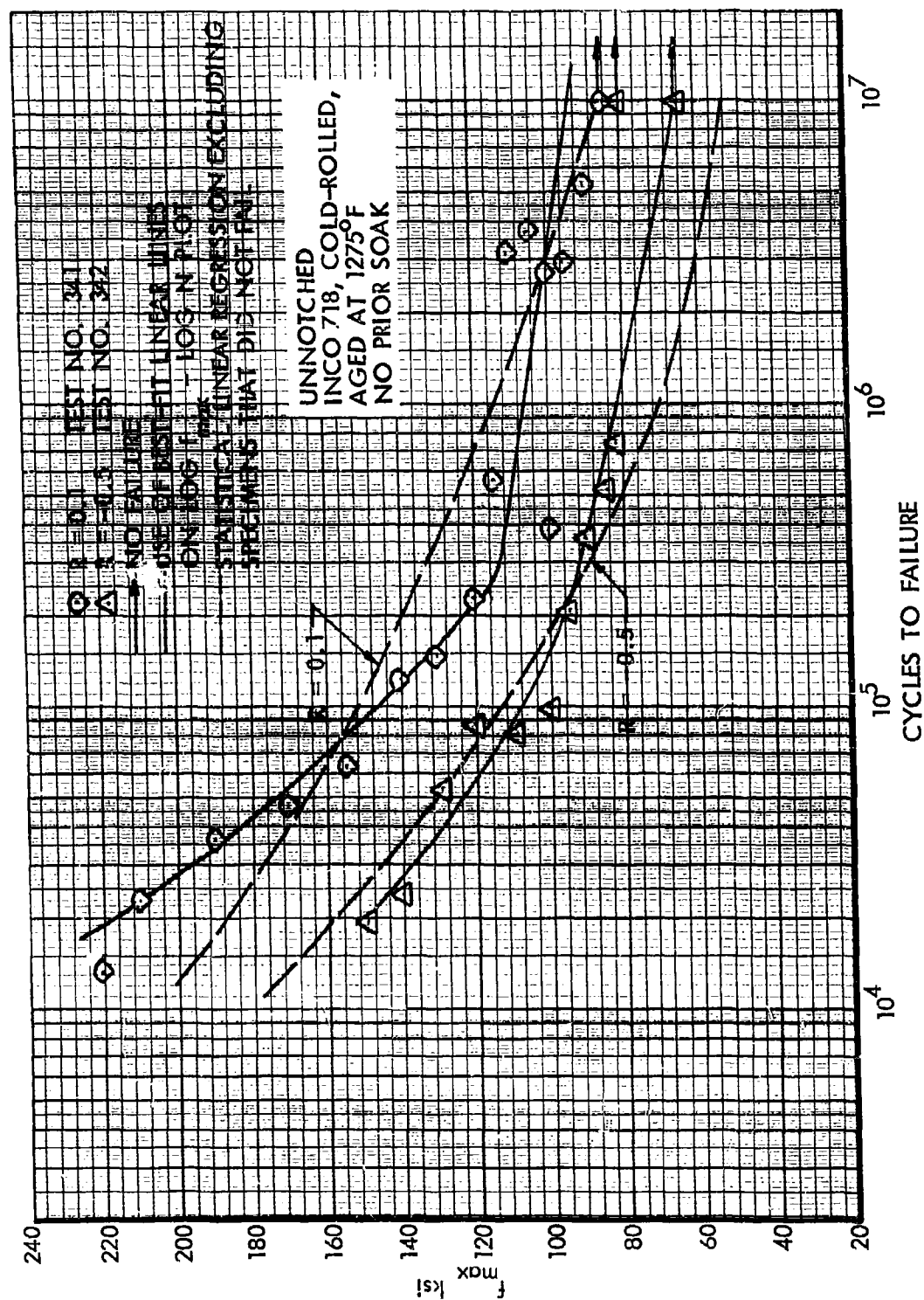
Figure 162. Use of Best Fit and Linear Regression for S-N Curves — Room Temperature

APPENDIX VI

COMPARATIVE S-N CURVES - CONSTANT STRESS RATIO

Volume II of the report presents S-N curves for constant values of stress ratio, R, of 0.1 and -0.5 which were drawn to provide a best fit to the S-N data points obtained in the basic constant load amplitude fatigue test program. To provide a basis for examination of the data in this form in terms of specimen exposure conditions and test temperatures, all of the constant R curves presented in Volume II have been grouped by material, specimen geometry and test temperature. These groupings are presented in this Appendix. The location of these groupings is given in Table 36.

TABLE 36 LOCATION OF COMPARATIVE S-N CURVES - CONSTANT R

R = 0.1 and - 0.5

Material	Specimen Configuration	Test Temp (°F)	Curves Plotted in Figure
8-1-1 Titanium Duplex Annealed	Center-Notched	Room 400 650	163, 164 165, 166 167, 168
	Unnotched	Room 400 650	169, 170 171, 172 173, 174
	Fusion-Welded and Planished	Room 400 650	175, 176 177, 178 179, 180
PH14-8Mo (SRH 1050)	Center-Notched	Room 400 650	181, 182 183, 184 185, 186
	Unnotched	Room 400 650	187, 188 189, 190 191, 192
	Fusion-Welded and Planished	Room 400 650	193, 194 195, 196 197, 198
INCO 718, Cold Rolled, Aged at 1275°F	Center-Notched	Room 400 650	199, 200 201, 202 203, 204
	Unnotched	Room 400 650	205, 206 207, 208 209, 210
	Fusion-Welded and Planished	Room 400 650	211, 212 213, 214 215, 216
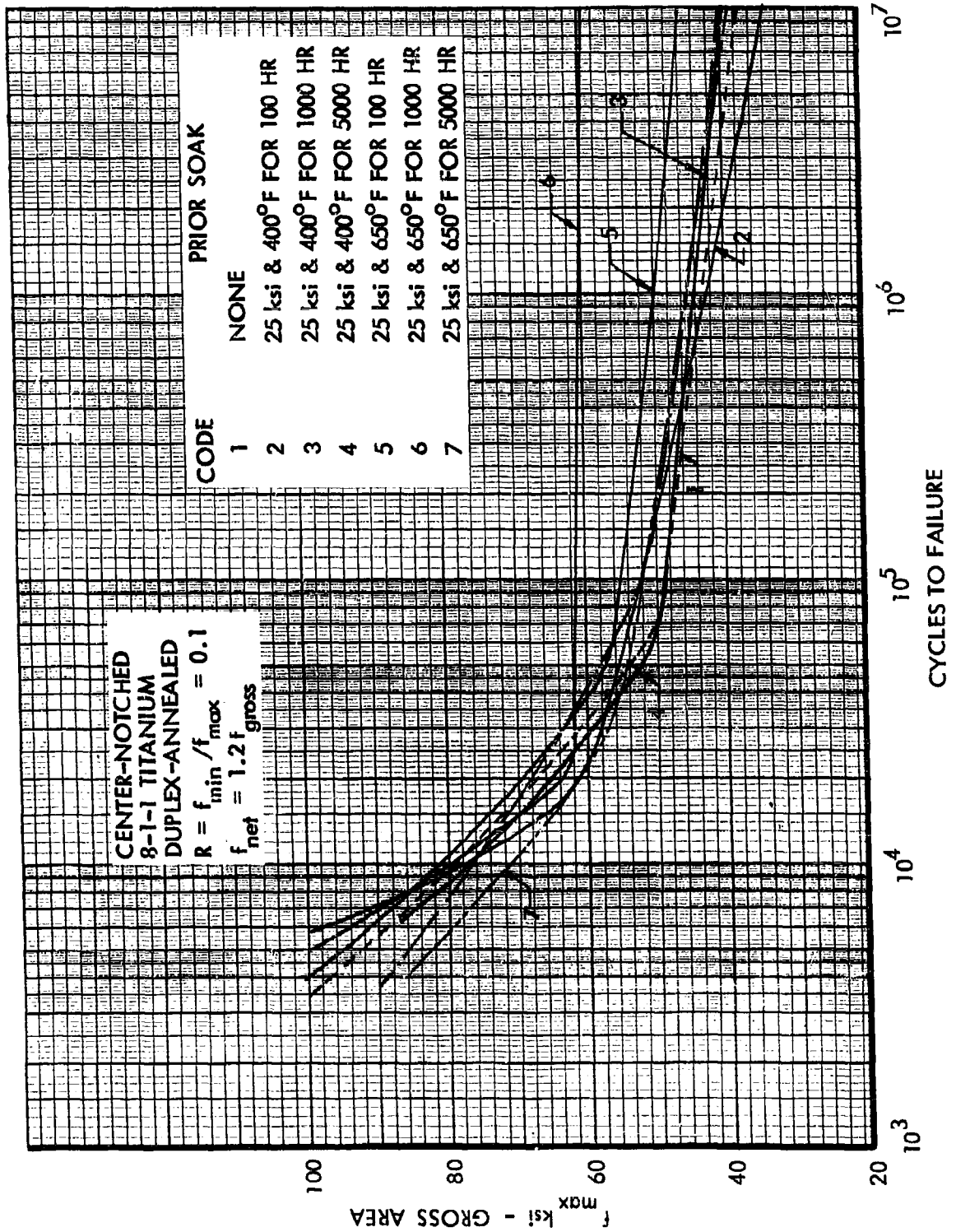
Figure 163. Effects of Prior Soak on S-N Curves at Room Temperature, Center-Notched 8-1-1 Titanium, R = Constant
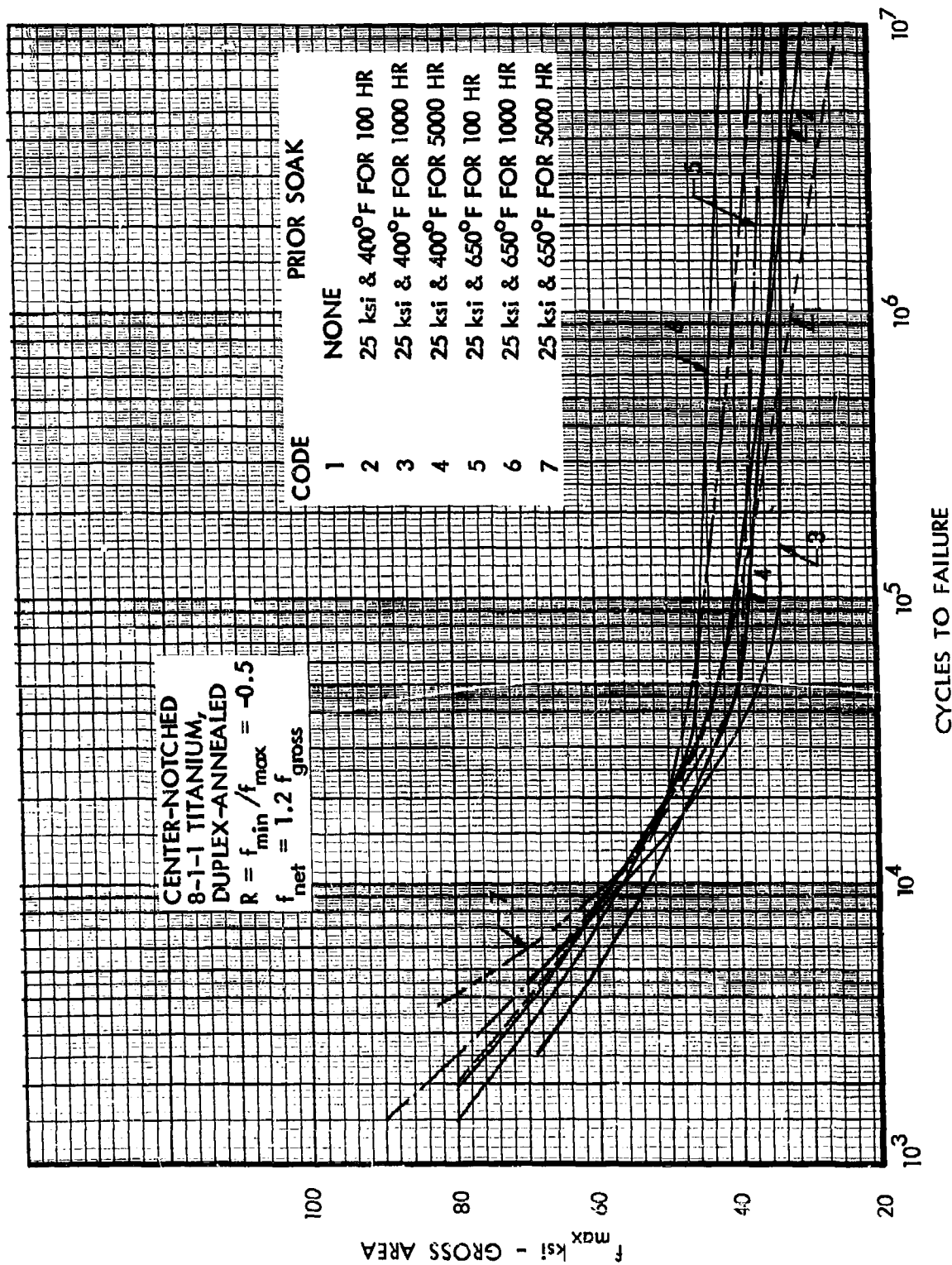
Figure 164. Effects of Prior Soak on S-N Curves at Room Temperature, Center-Notched 8-1-1 Titanium, R = Constant
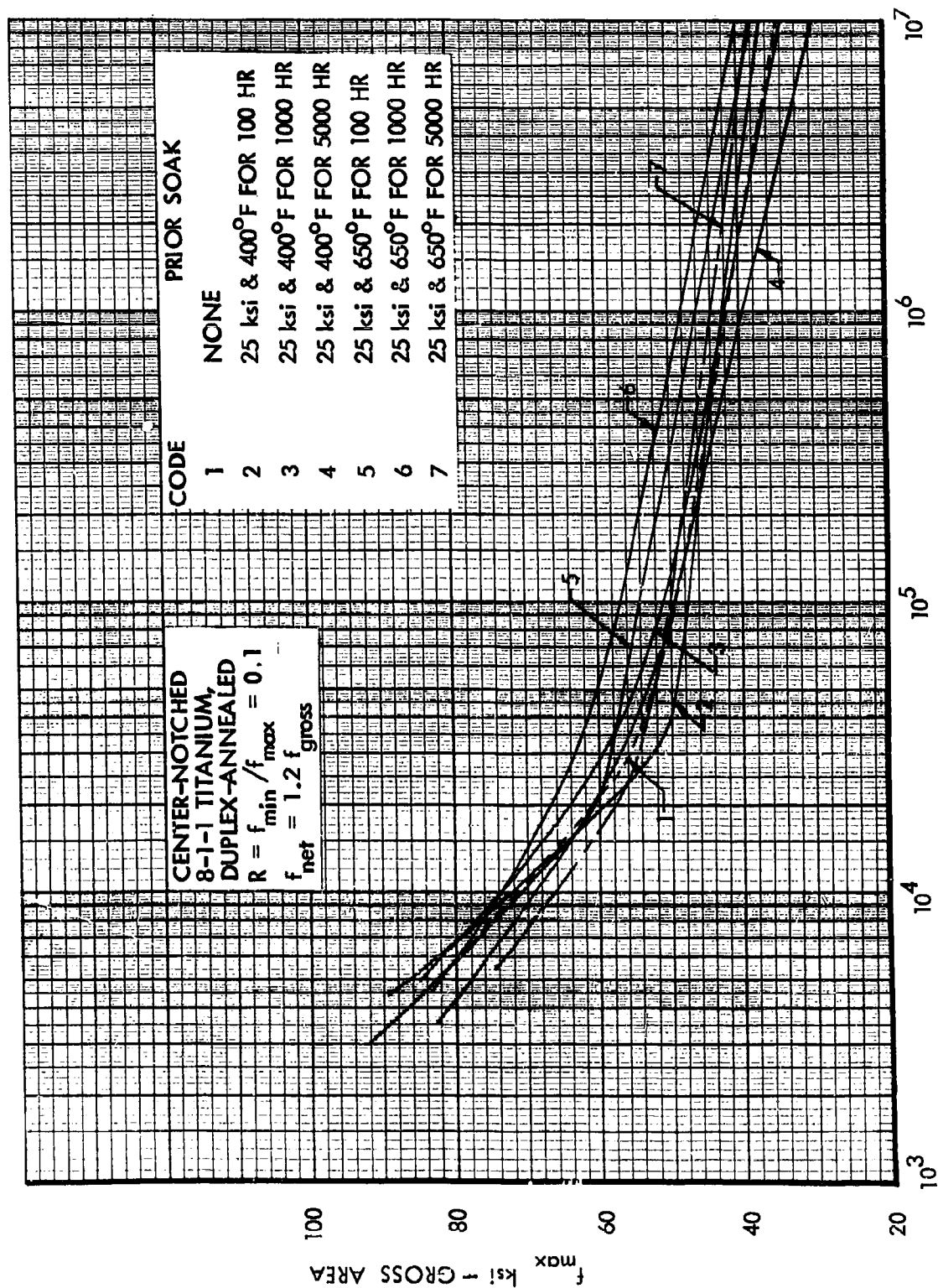
Figure 165. Effects of Prior Soak on S-N Curves at 400°F, Center-Notched 8-1-1 Titanium; R = Constant
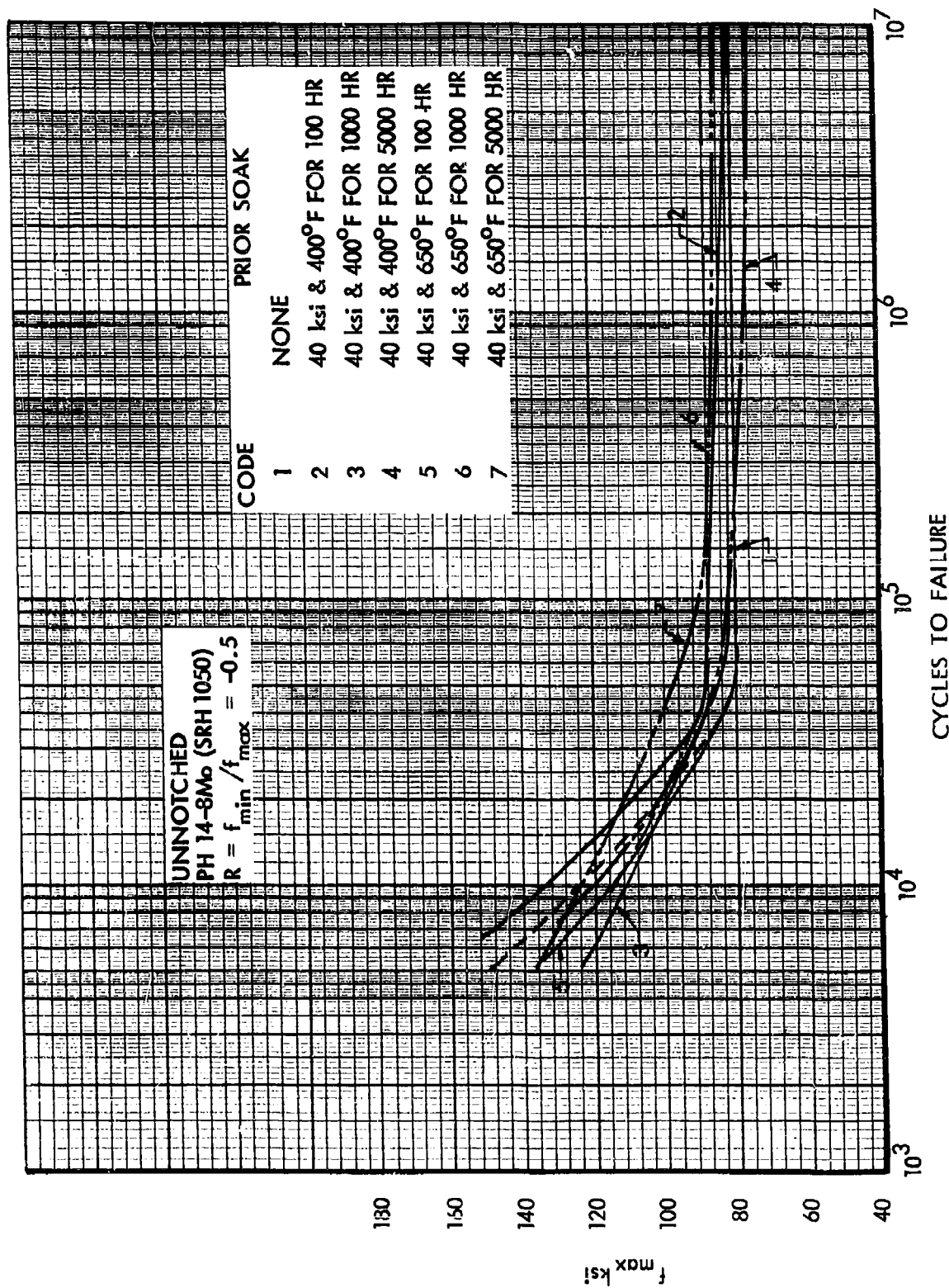
243
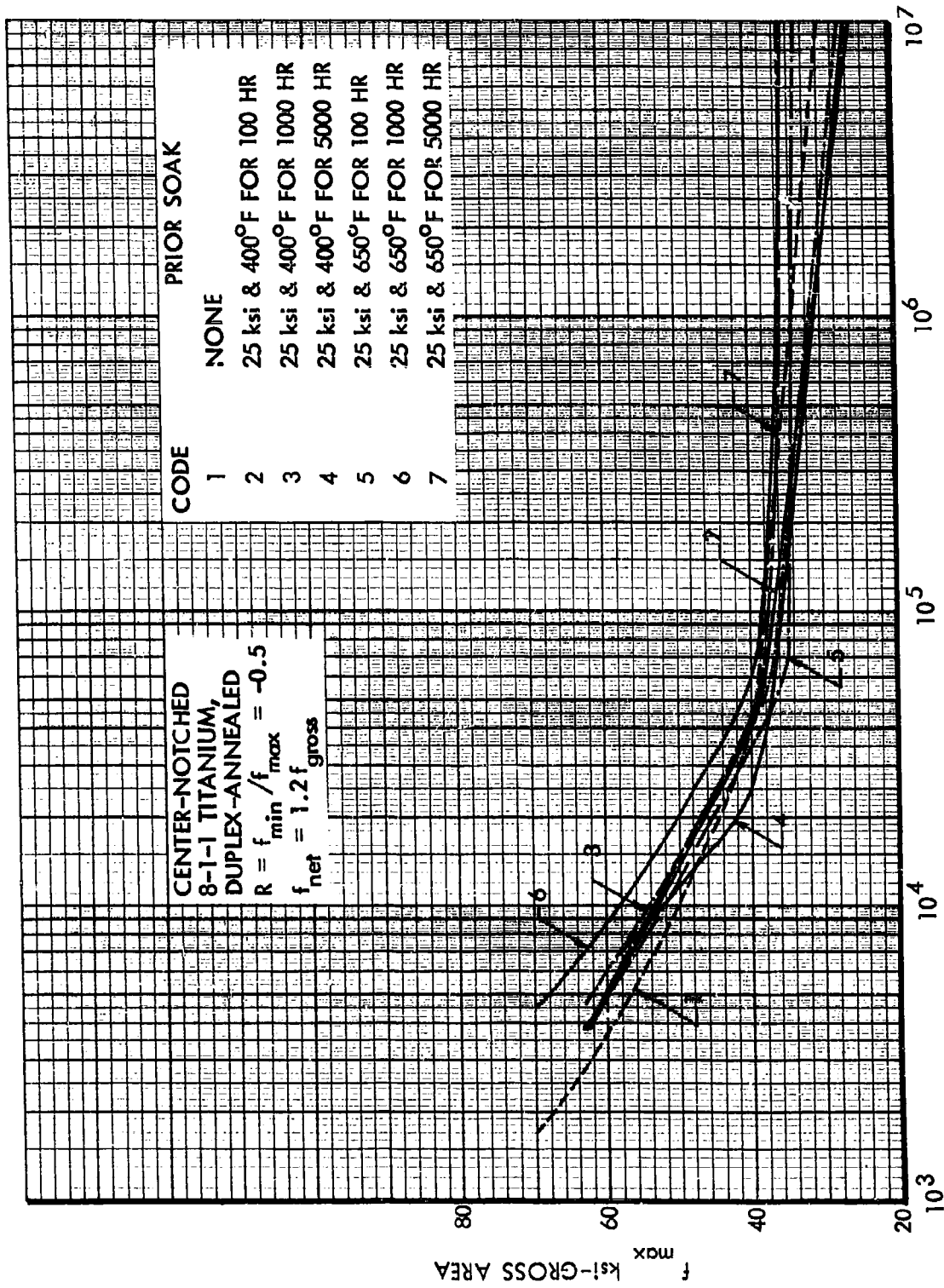
CYCLES TO FAILURE

Figure 166.   Effects of Prior Soak on S-N Curves at 400°F, Center-Notched 8-1-1 Titanium, R = Constant
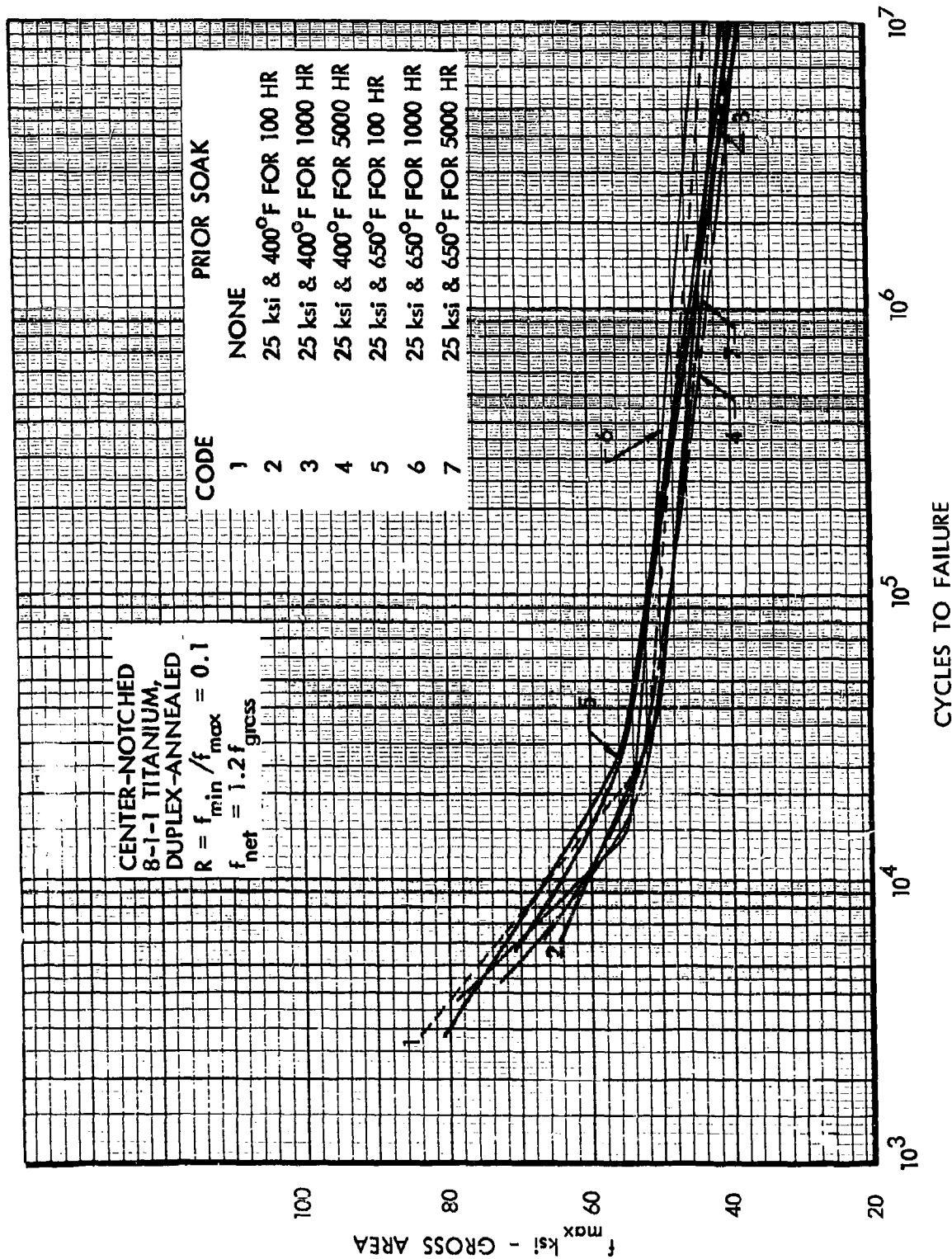
Figure 167. Effects of Prior Soak on S-N Curves at 650°F, Center-Notched 8-1-1 Titanium, R = Constant

245
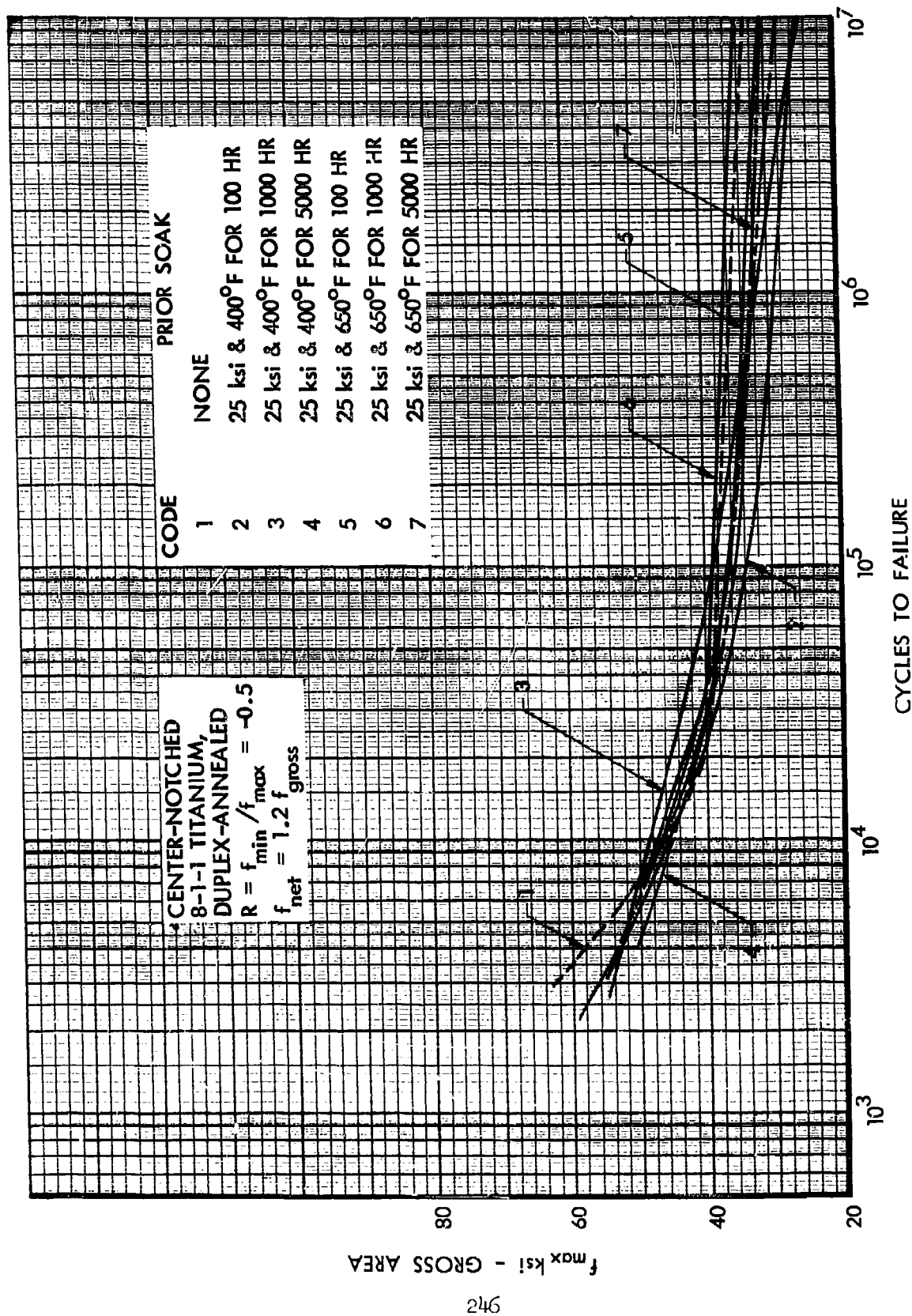
Figure 168.   Effects of Prior Soak on S-N Curves at 650°F, Center-Notched 8-1-1 Titanium, R = Constant

246
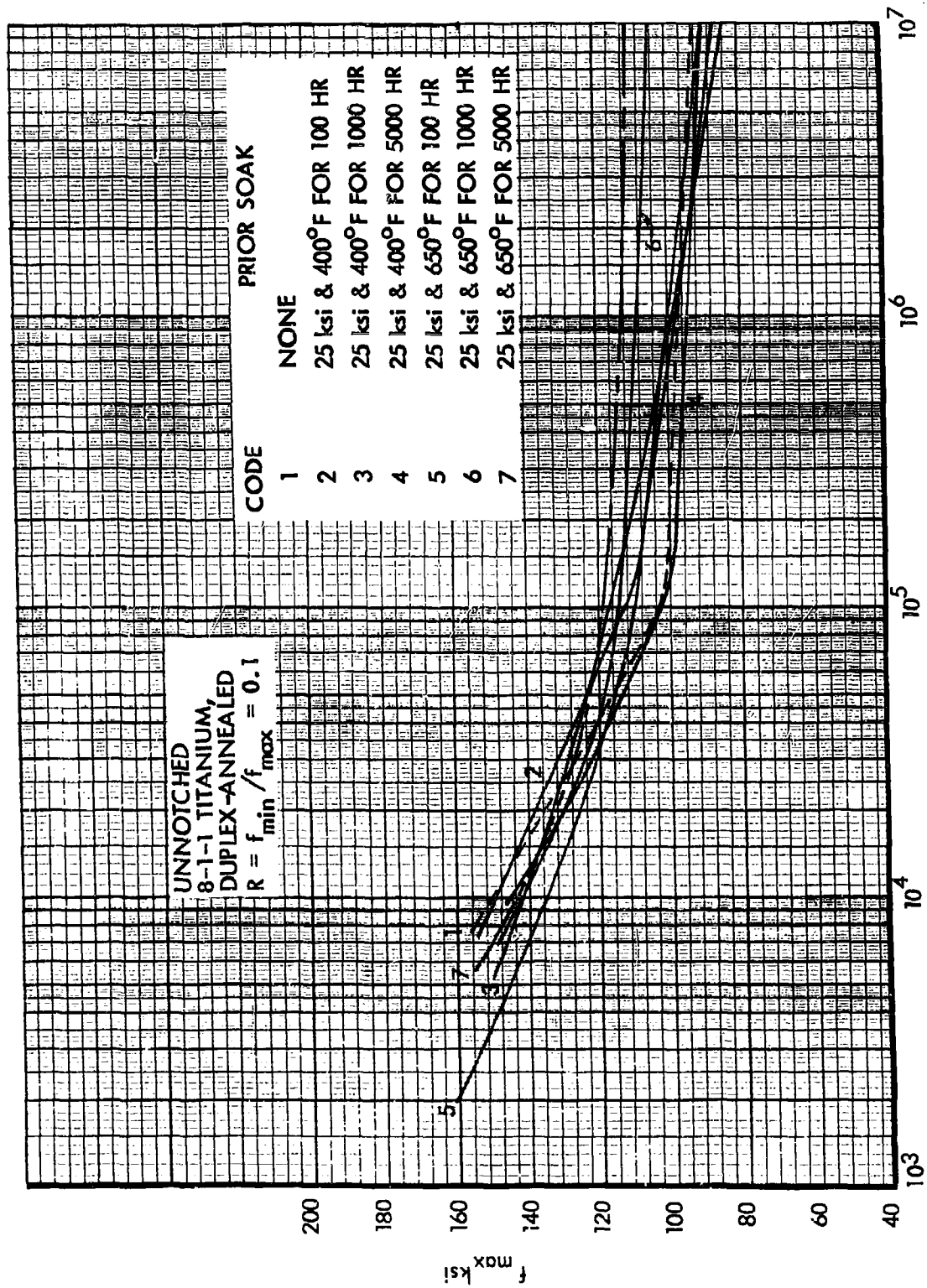
Figure 169. Effects of Prior Soak on S-N Curves at Room Temperature, Unnotched 8-1-1 Titanium. R = Constant

247
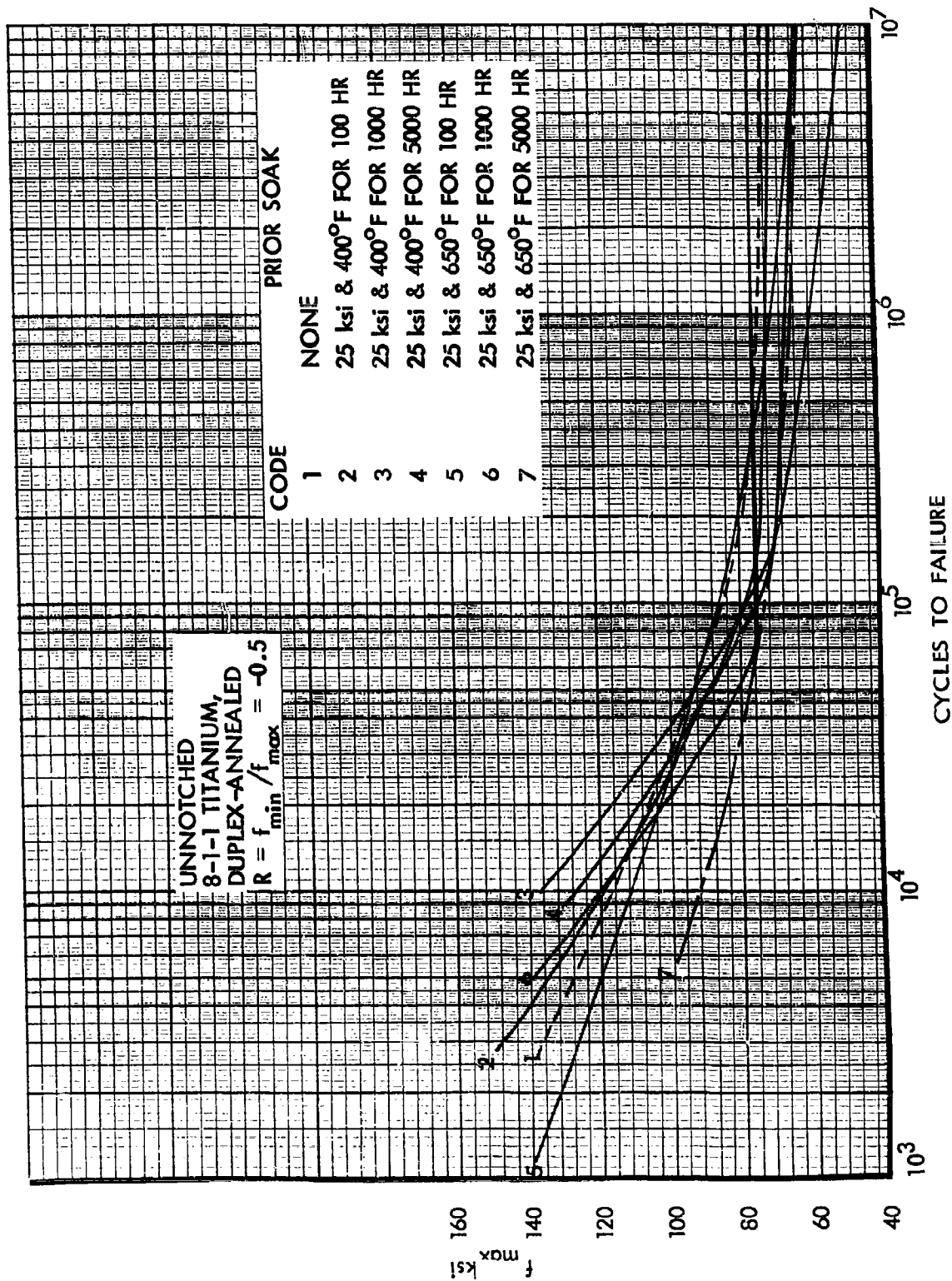
Figure 170. Effects of Prior Soak on S-N Curves at Room Temperature, Unnotched 8-1-1 Titanium, R = Constant
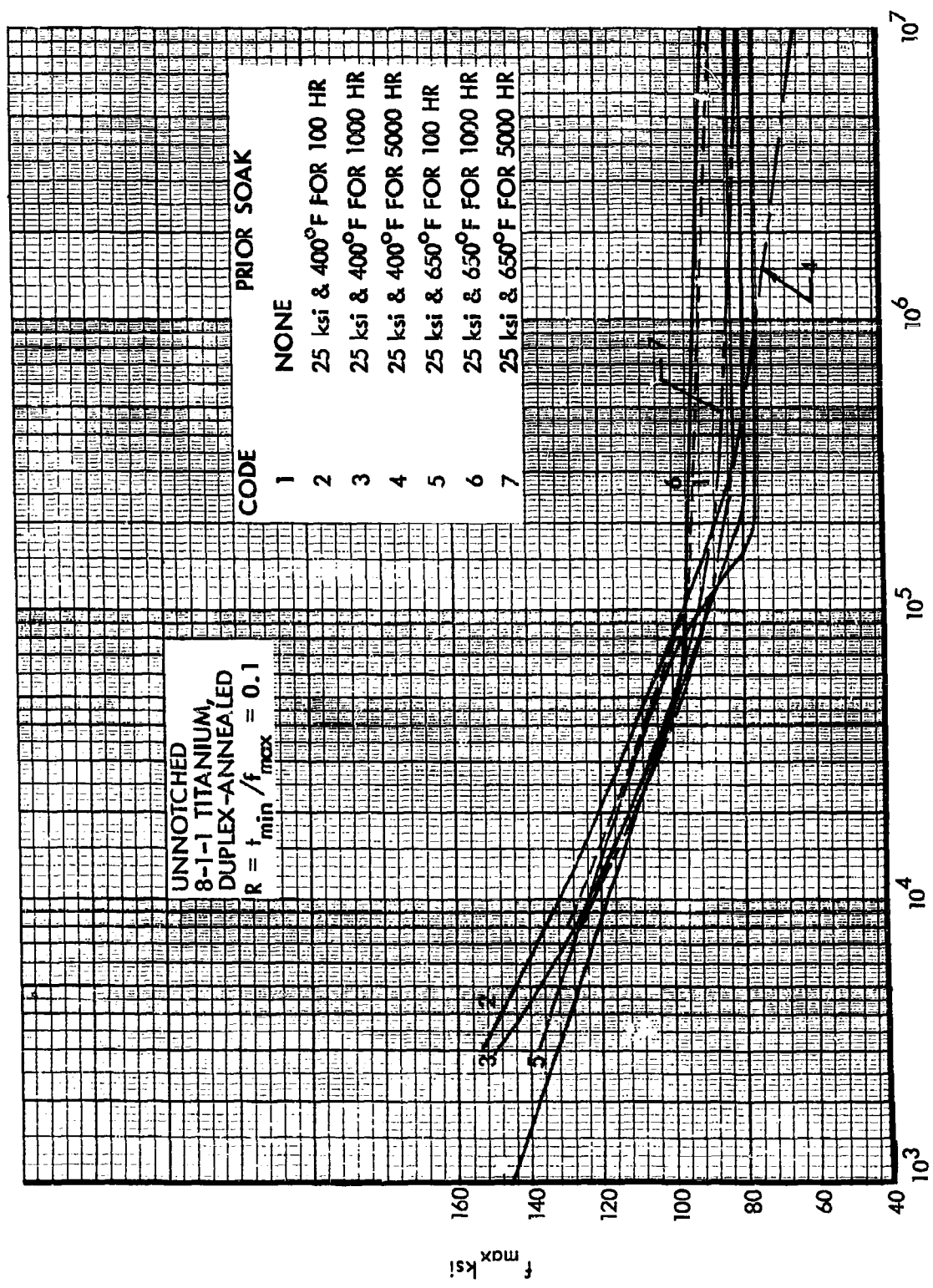
CYCLES TO FAILURE

Figure 171.   Effects of Prior Soak on S-N Curves at 400°F, Unnotched 8-1-1 Titanium, R = Constant

PRIOR SOAK

CODE	
1	NONE
2	25 ksi & 400°F FOR 100 HR
3	25 ksi & 400°F FOR 1000 HR
4	25 ksi & 400°F FOR 5000 HR
5	25 ksi & 650°F FOR 100 HR
6	25 ksi & 650°F FOR 1000 HR
7	25 ksi & 650°F FOR 5000 HR

UNNOTCHED
8-1-1 TITANIUM,
DUPLEX-ANNEALED
$R = f_{min}/f_{max} = 0.1$

f_{max}, ksi

249

CODE	PRIOR SOAK
1	NONE
2	25 ksi & 400°F FOR 100 HR
3	25 ksi & 400°F FOR 1000 HR
4	25 ksi & 400°F FOR 5000 HR
5	25 ksi & 650°F FOR 100 HR
6	25 ksi & 650°F FOR 1000 HR
7	25 ksi & 650°F FOR 5000 HR

UNNOTCHED
8-1-1 TITANIUM,
DUPLEX-ANNEALED
$R = f_{min}/f_{max} = -0.5$

CYCLES TO FAILURE

f_{max} ksi
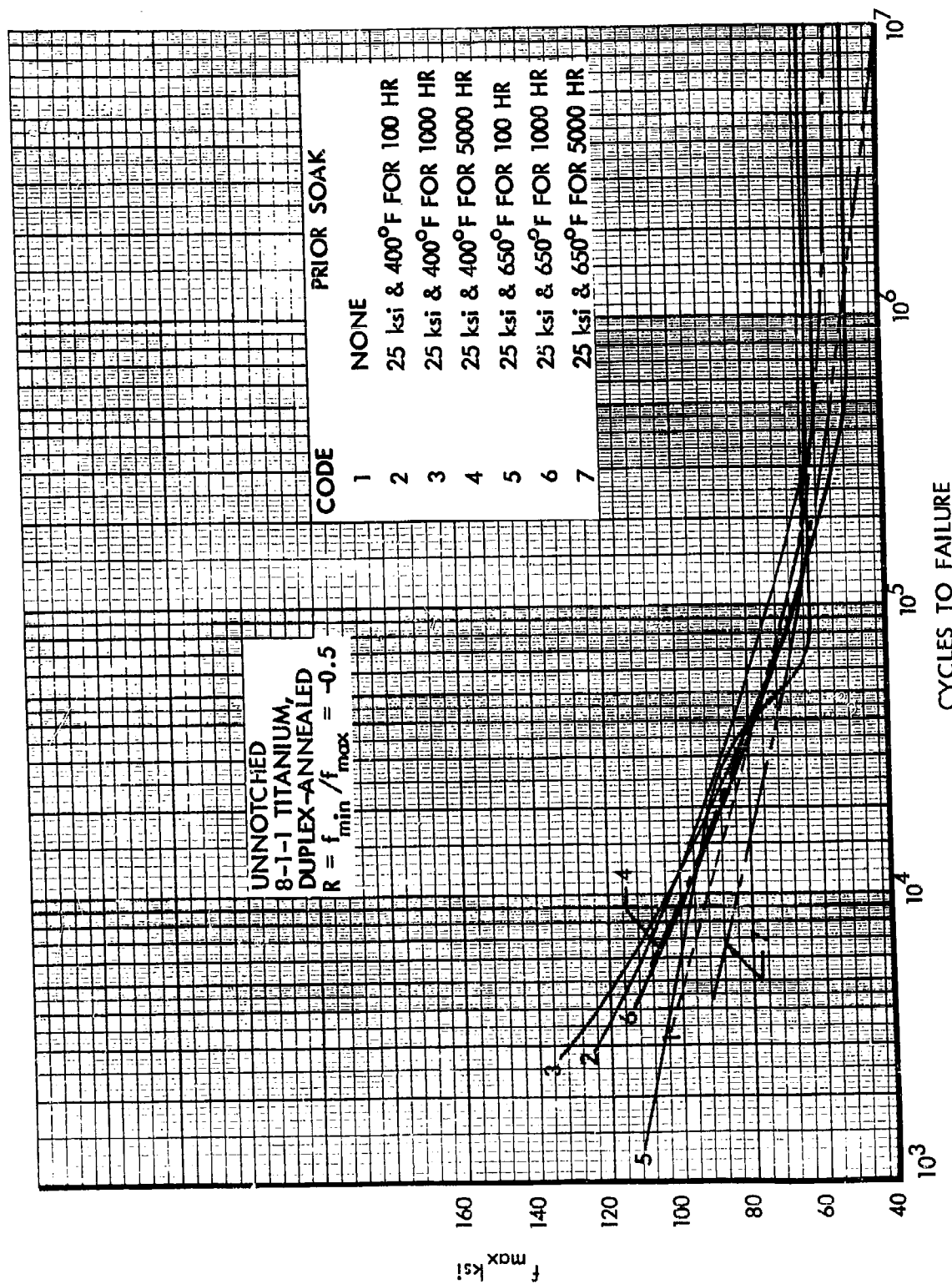
Figure 172.   Effects of Prior Soak on S-N Curves at 400°F, Unnotched 8-1-1 Titanium, R = Constant
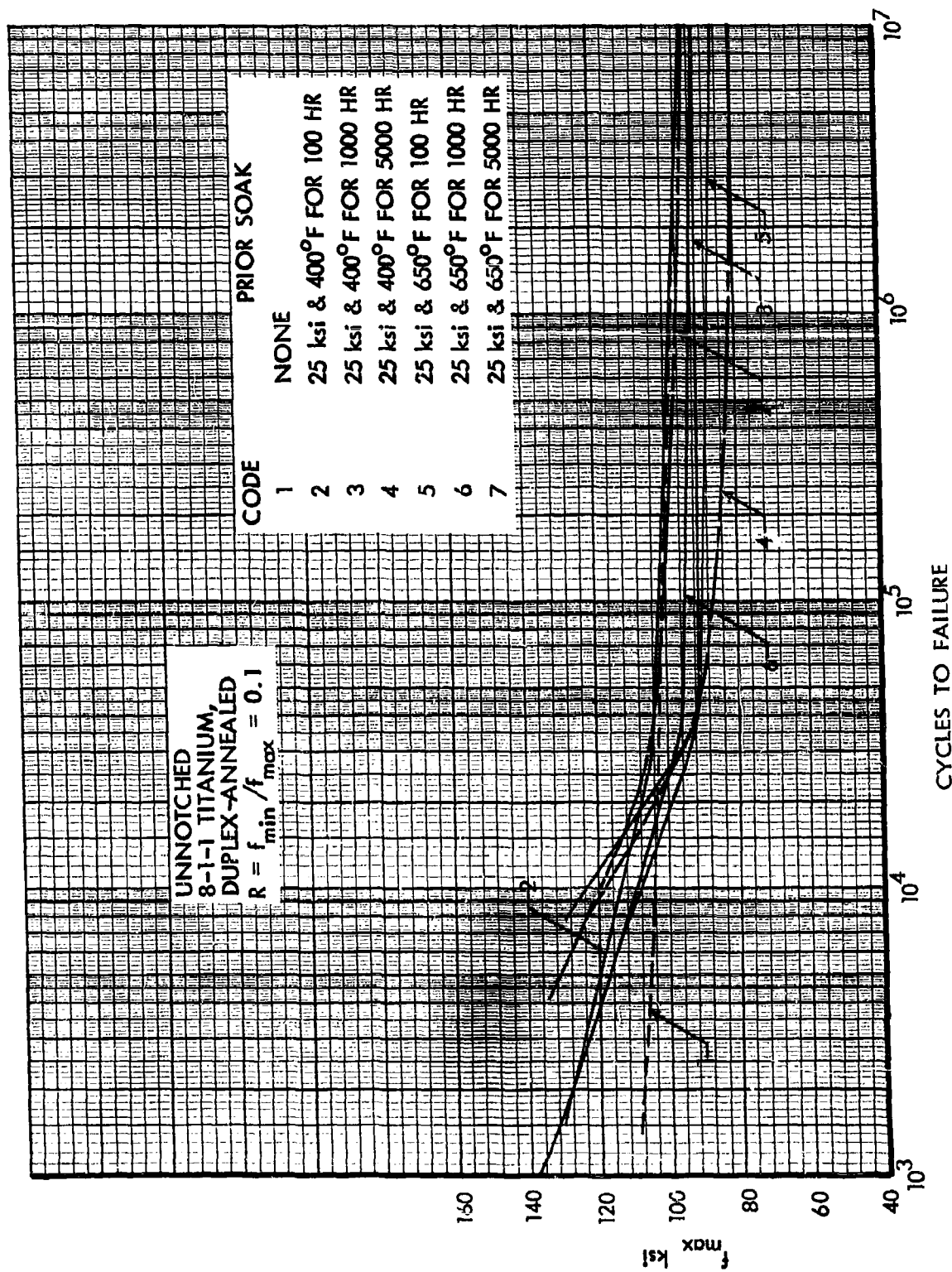
Figure 173. Effects of Prior Soak on S-N Curves at 650°F, Unnotched 8-1-1 Titanium, R = Constant

251
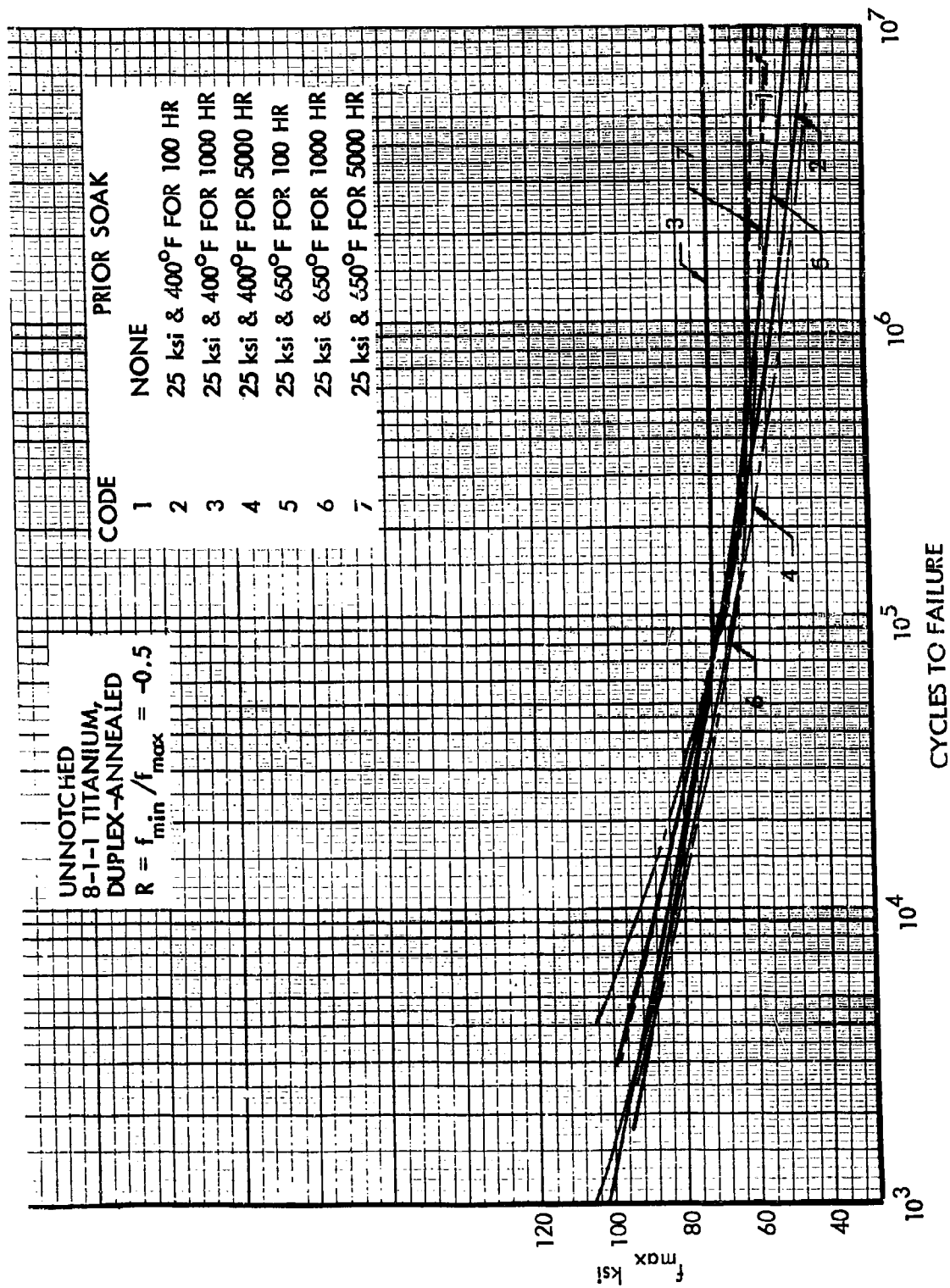
Figure 174. Effects of Prior Soak on S-N Curves at 650°F, Unnotched 8-1-1 Titanium, R = Constant

252
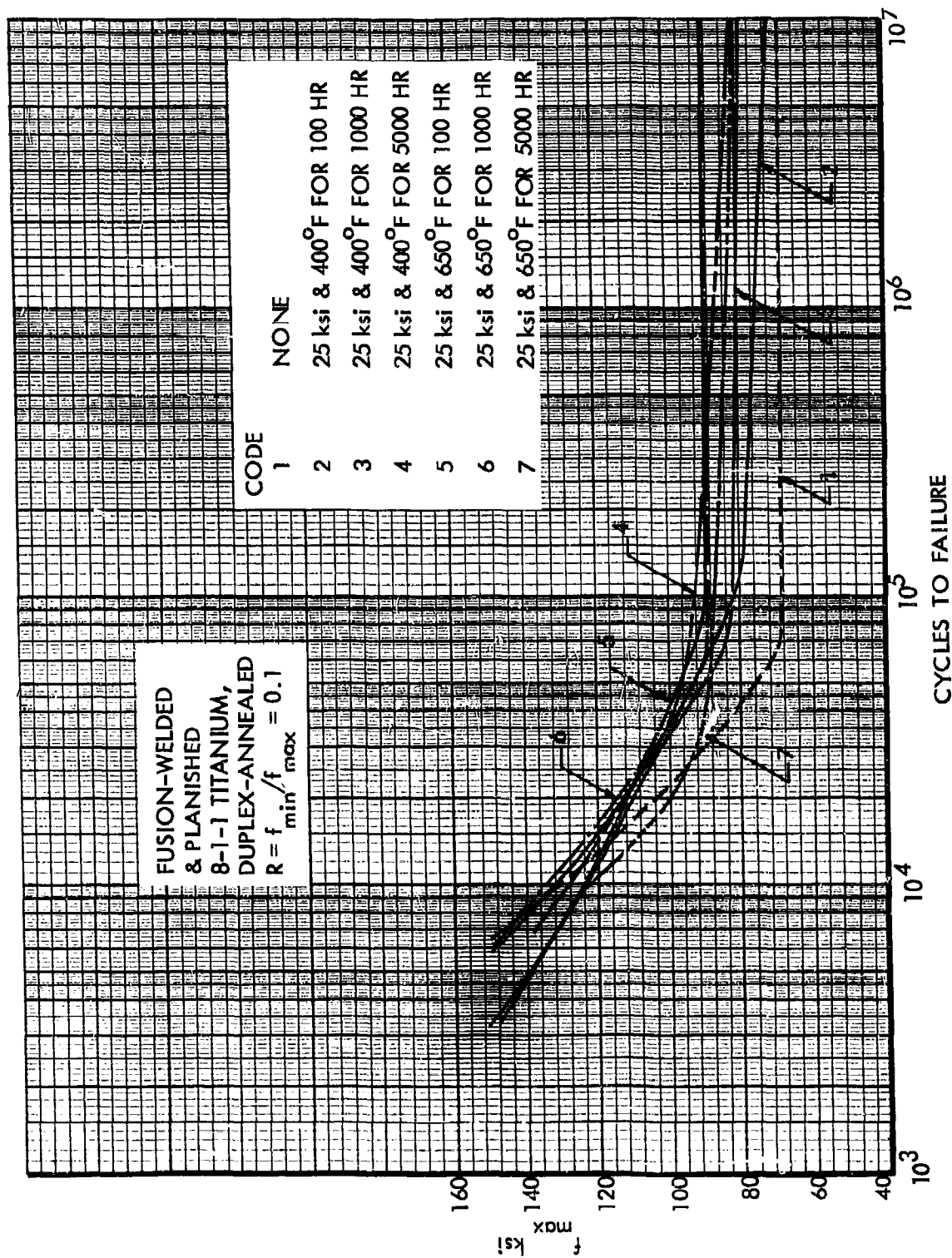
Figure 175.   Effects of Prior Soak on S-N Curves at Room Temperature, Fusion-Welded 8-1-1 Titanium,   R = Constant

253
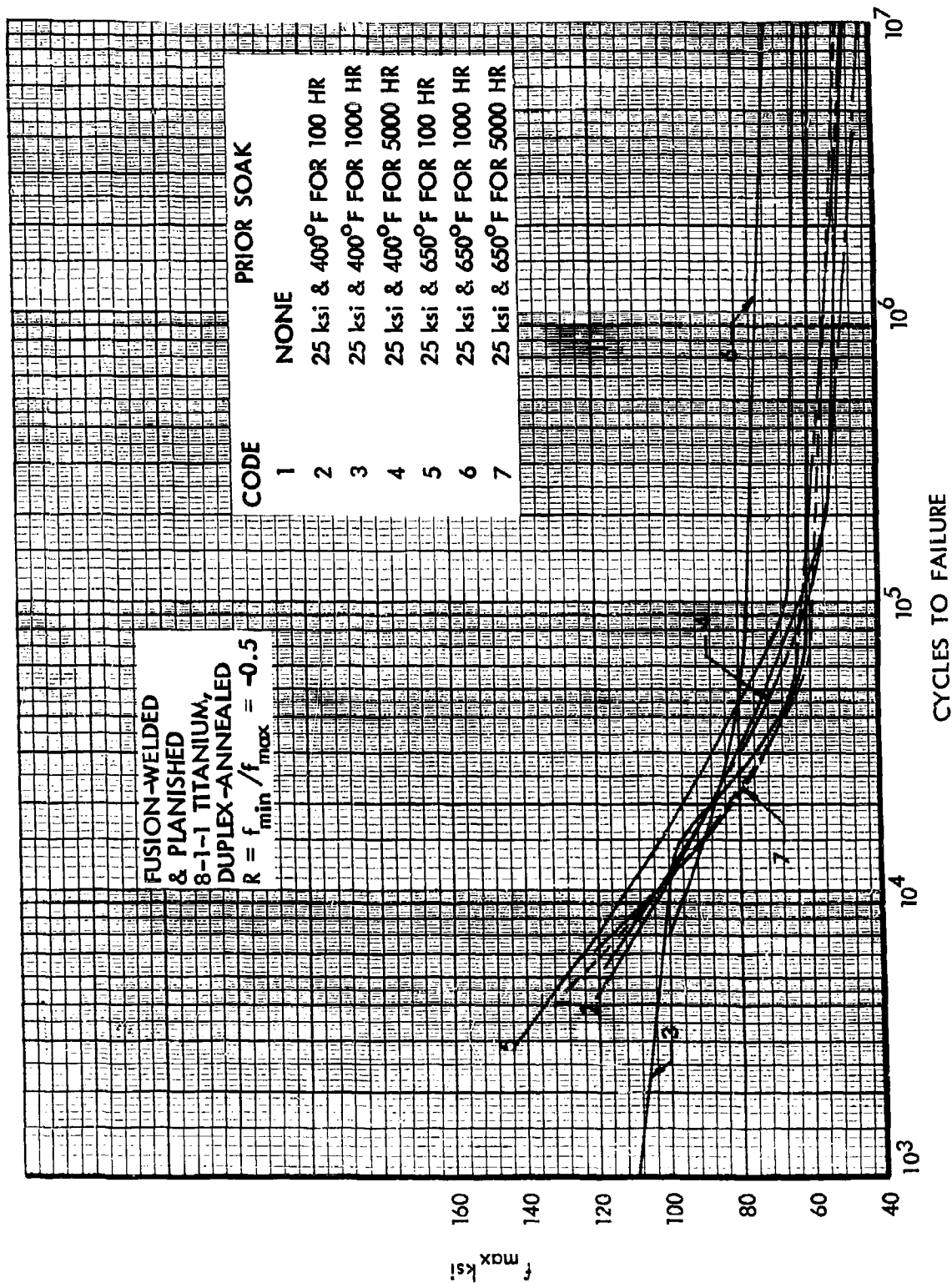
Figure 176. Effects of Prior Soak on S-N Curves at Room Temperature, Fusion-Welded 8-1-1 Titanium, R = Constant
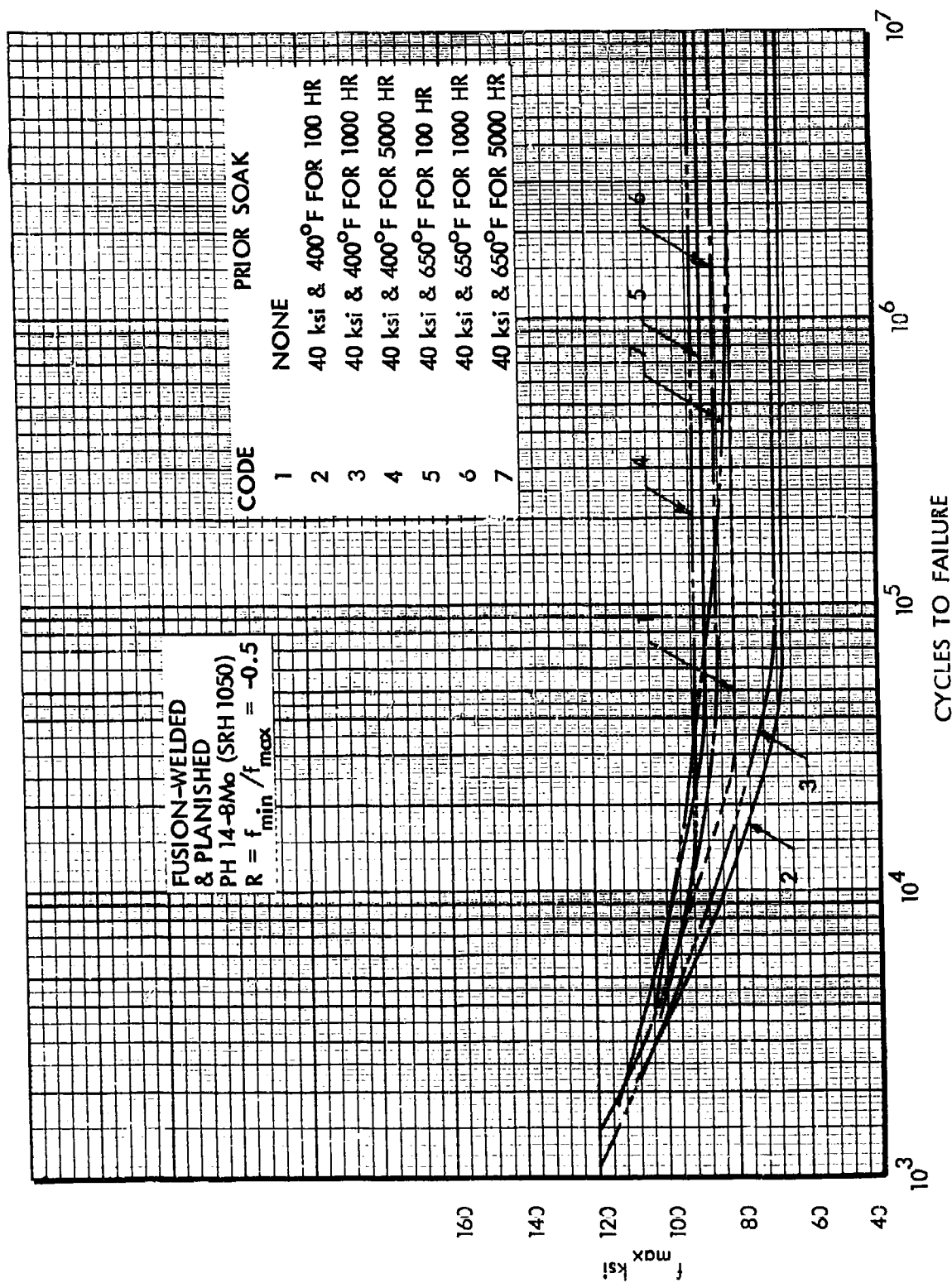
254
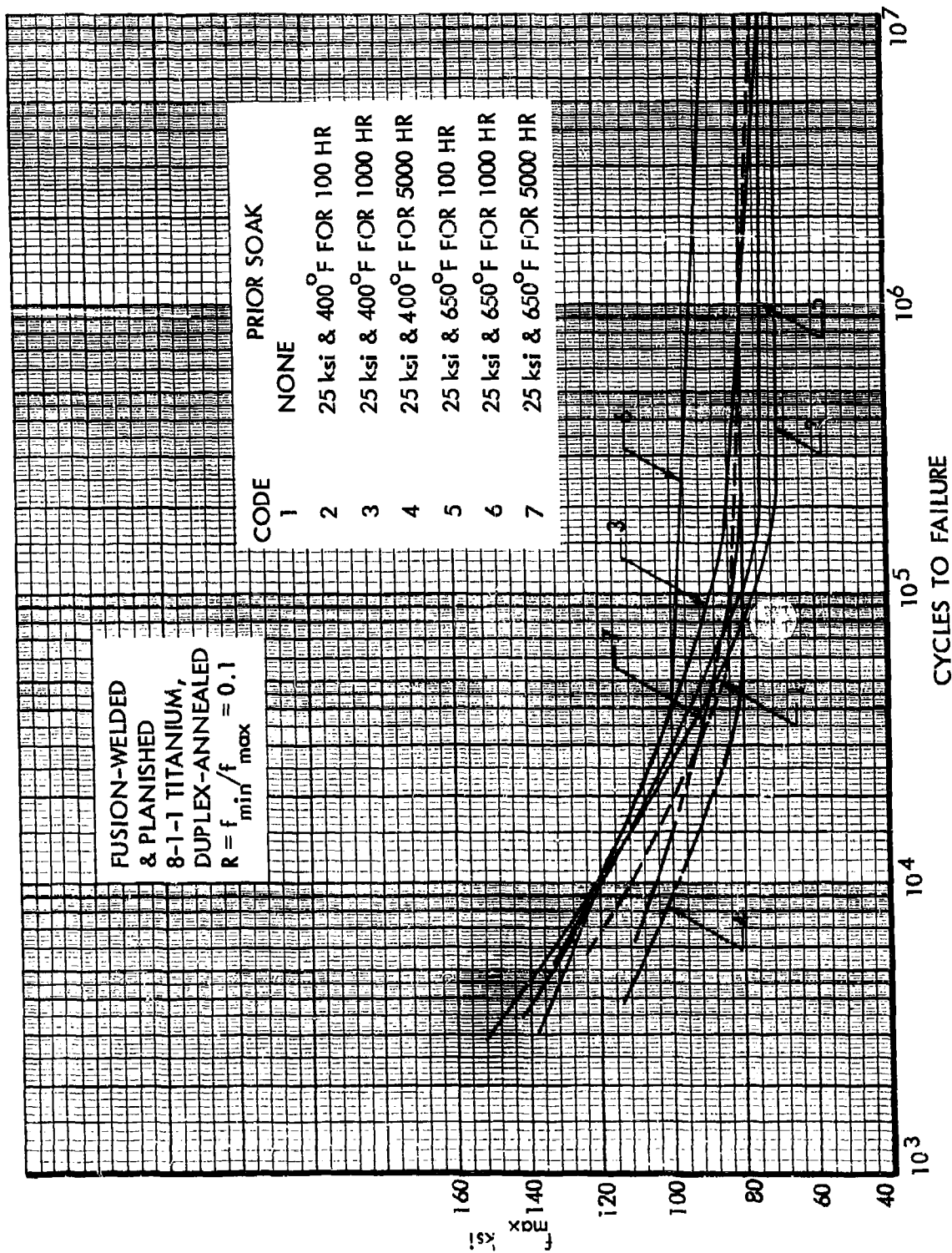
Figure 177. Effects of Prior Soak on S-N Curves at 400°F, Fusion-Welded 8-1-1 Titanium, R = Constant

255
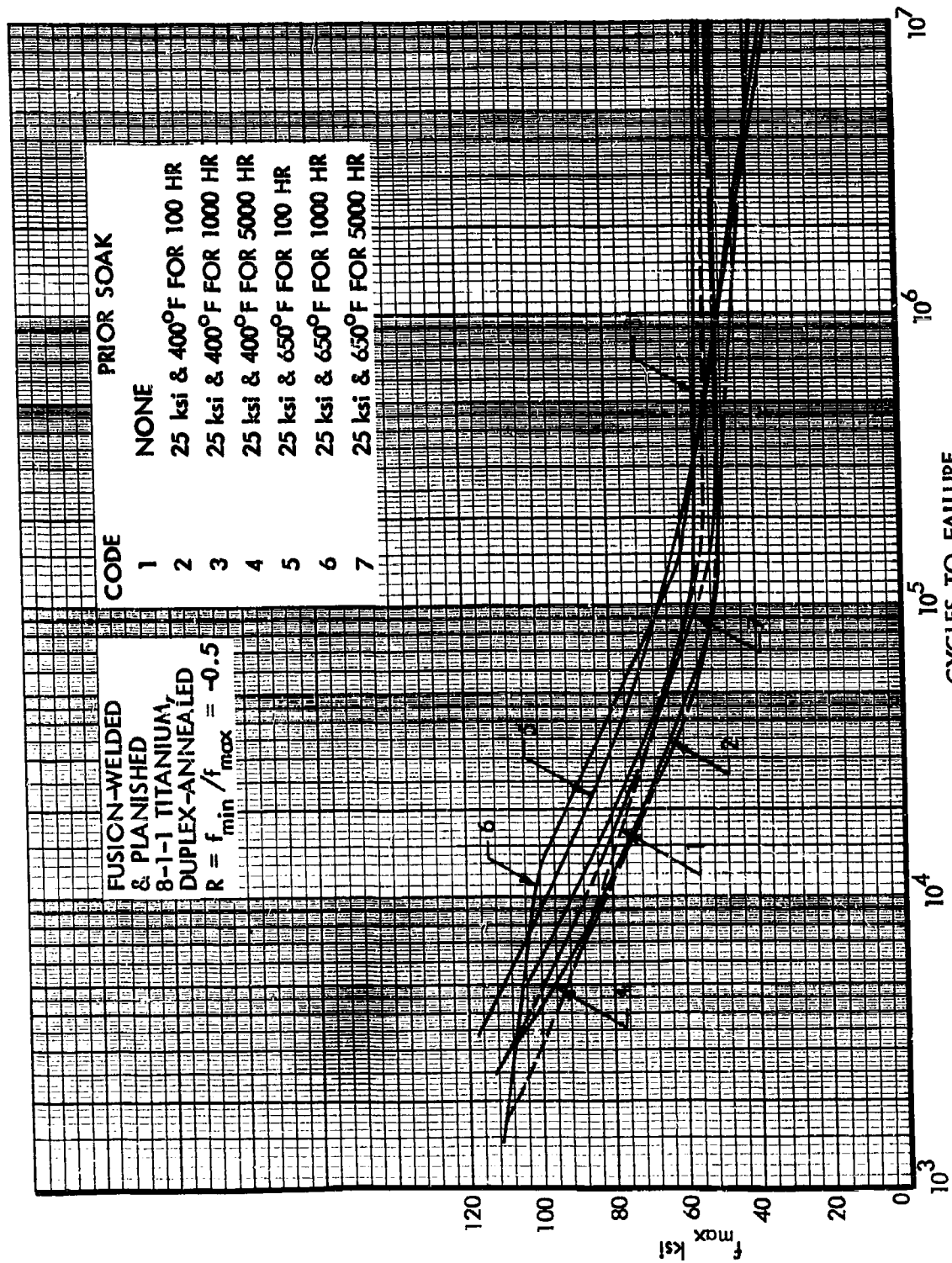
Figure 178. Effects of Prior Soak on S–N Curves at 400°F, Fusion–Welded 8–1–1 Titanium, R = Constant
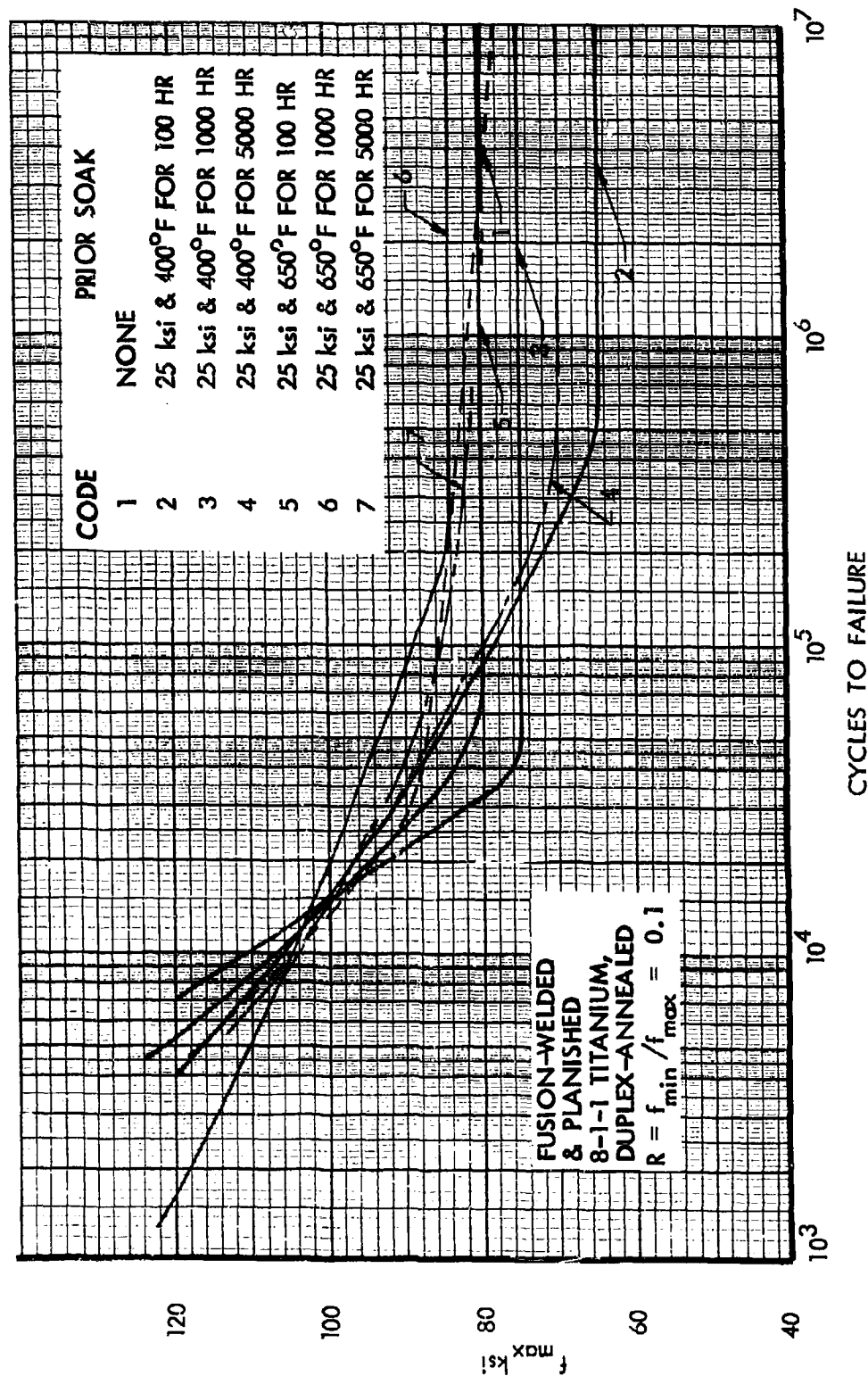
Figure 179. Effects of Prior Soak on S-N Curves at 650°F, Fusion-Welded 8-1-1 Titanium, R = Constant

257
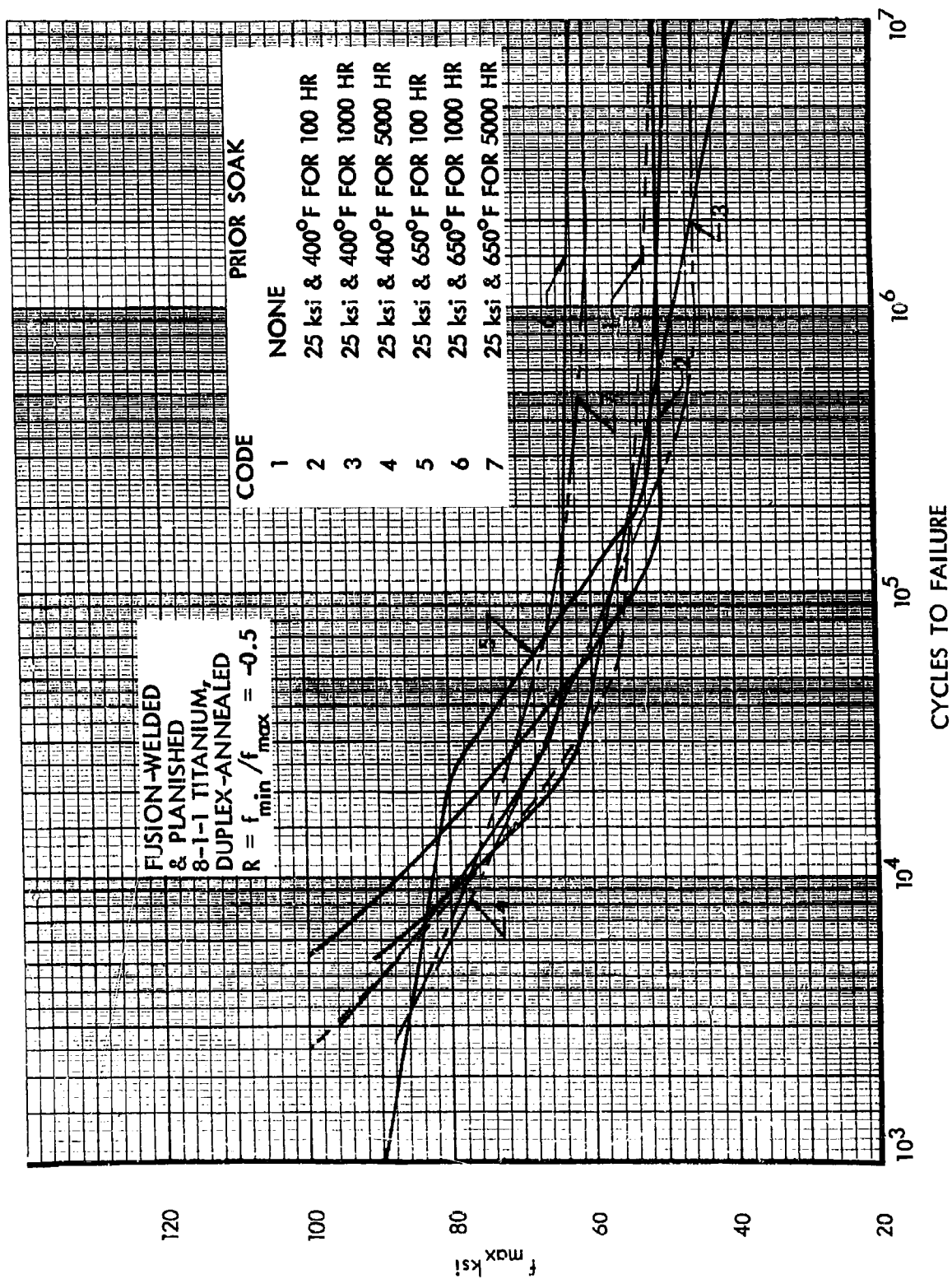
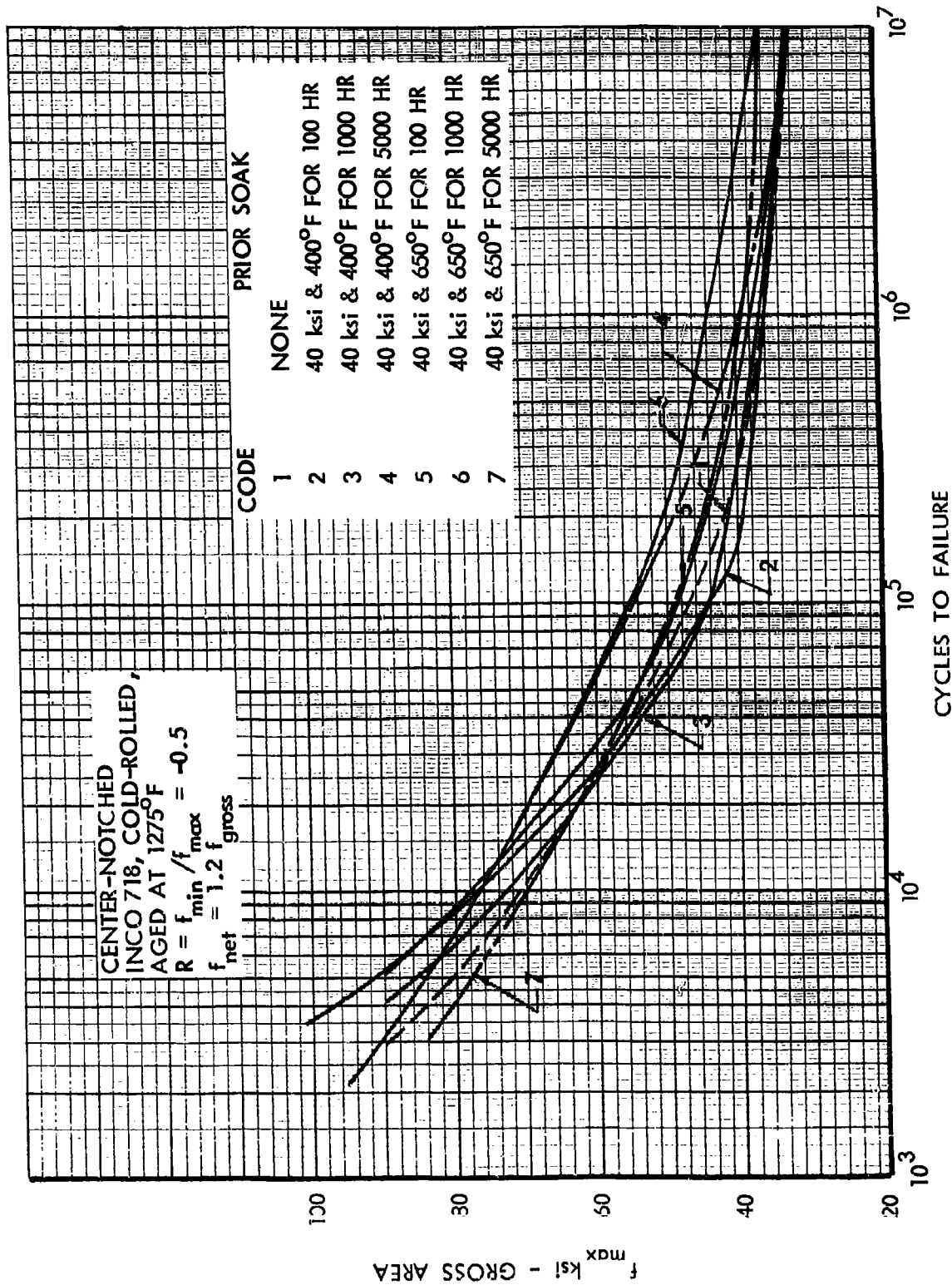Figure 180.   Effects of Prior Soak on S-N Curves at 650°F, Fusion Welded 8-1-1 Titanium, R = Constant
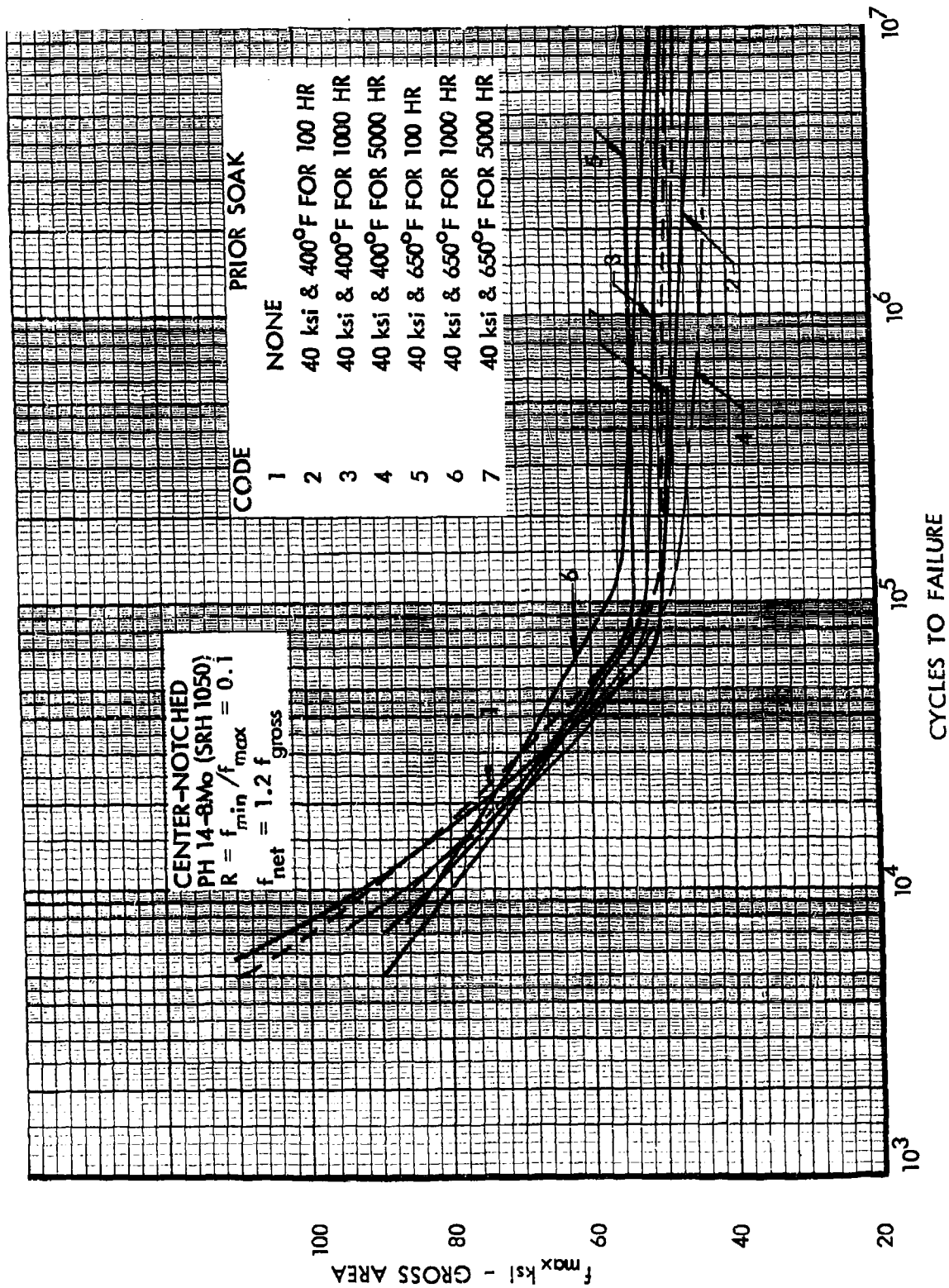
Figure 181. Effects of Prior Soak on S-N Curves at Room Temperature, Center-Notched PH14 – 8Mo, R = Constant

259
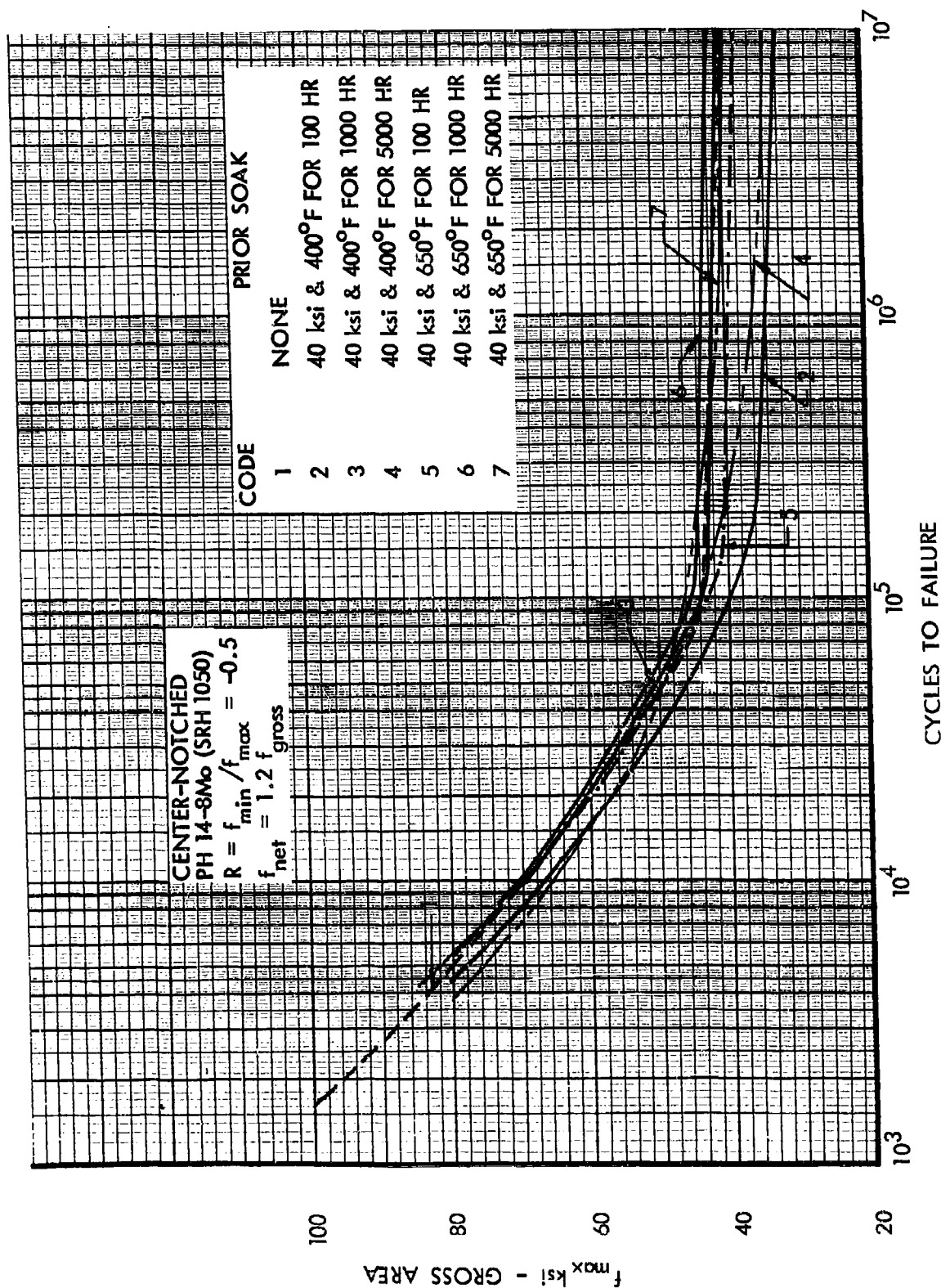
Figure 182. Effects of Prior Soak on S-N Curves at Room Temperature, Center-Notched PH14 - 8Mo, R = Constant

CODE	PRIOR SOAK
1	NONE
2	40 ksi & 400°F FOR 100 HR
3	40 ksi & 400°F FOR 1000 HR
4	40 ksi & 400°F FOR 5000 HR
5	40 ksi & 650°F FOR 100 HR
6	40 ksi & 650°F FOR 1000 HR
7	40 ksi & 650°F FOR 5000 HR

CENTER-NOTCHED
PH 14-8Mo (SRH 1050)
$R = f_{min}/f_{max} = -0.5$
$f_{net} = 1.2 f_{gross}$

CYCLES TO FAILURE

f_{max}, ksi - GROSS AREA

260
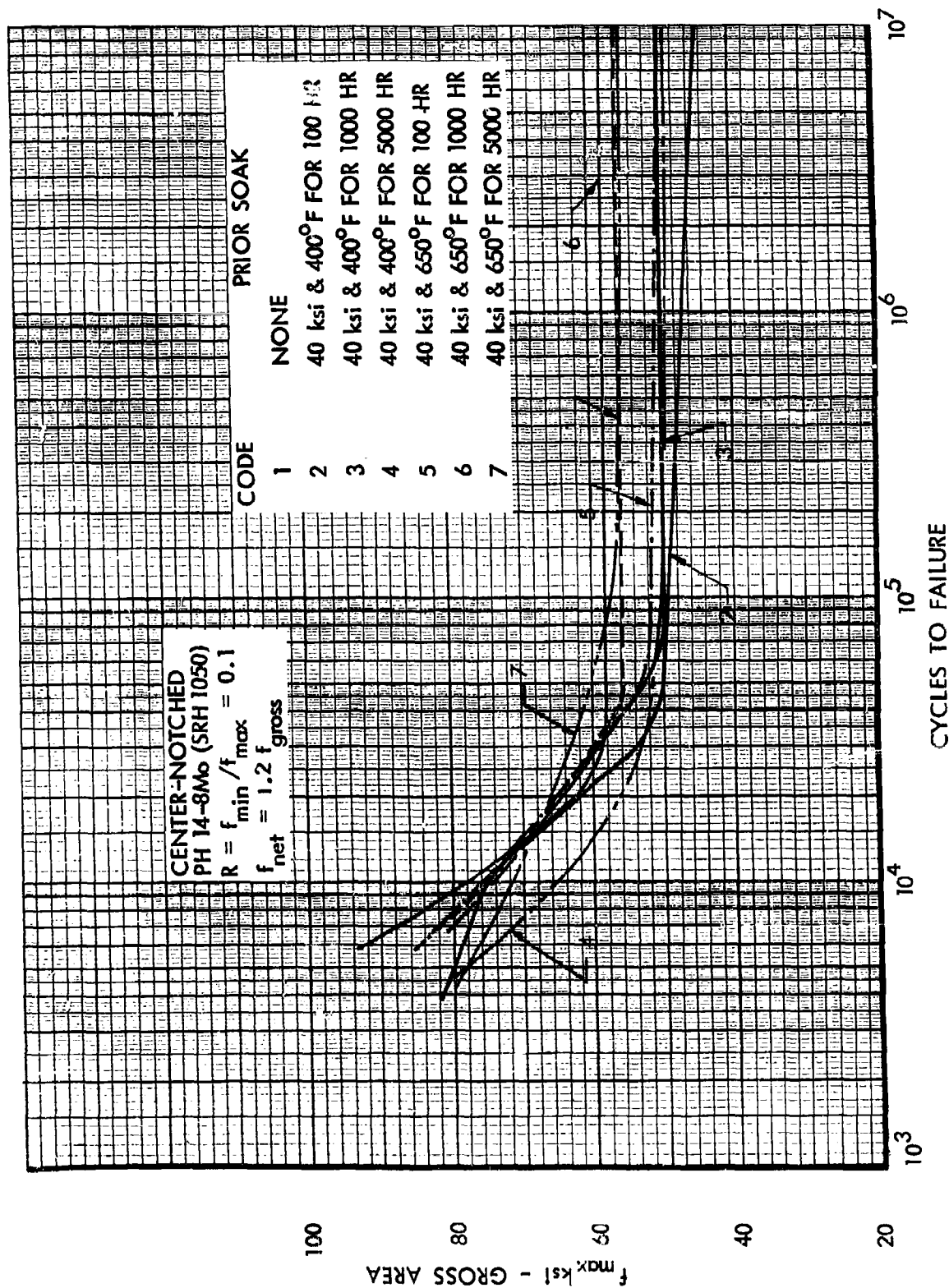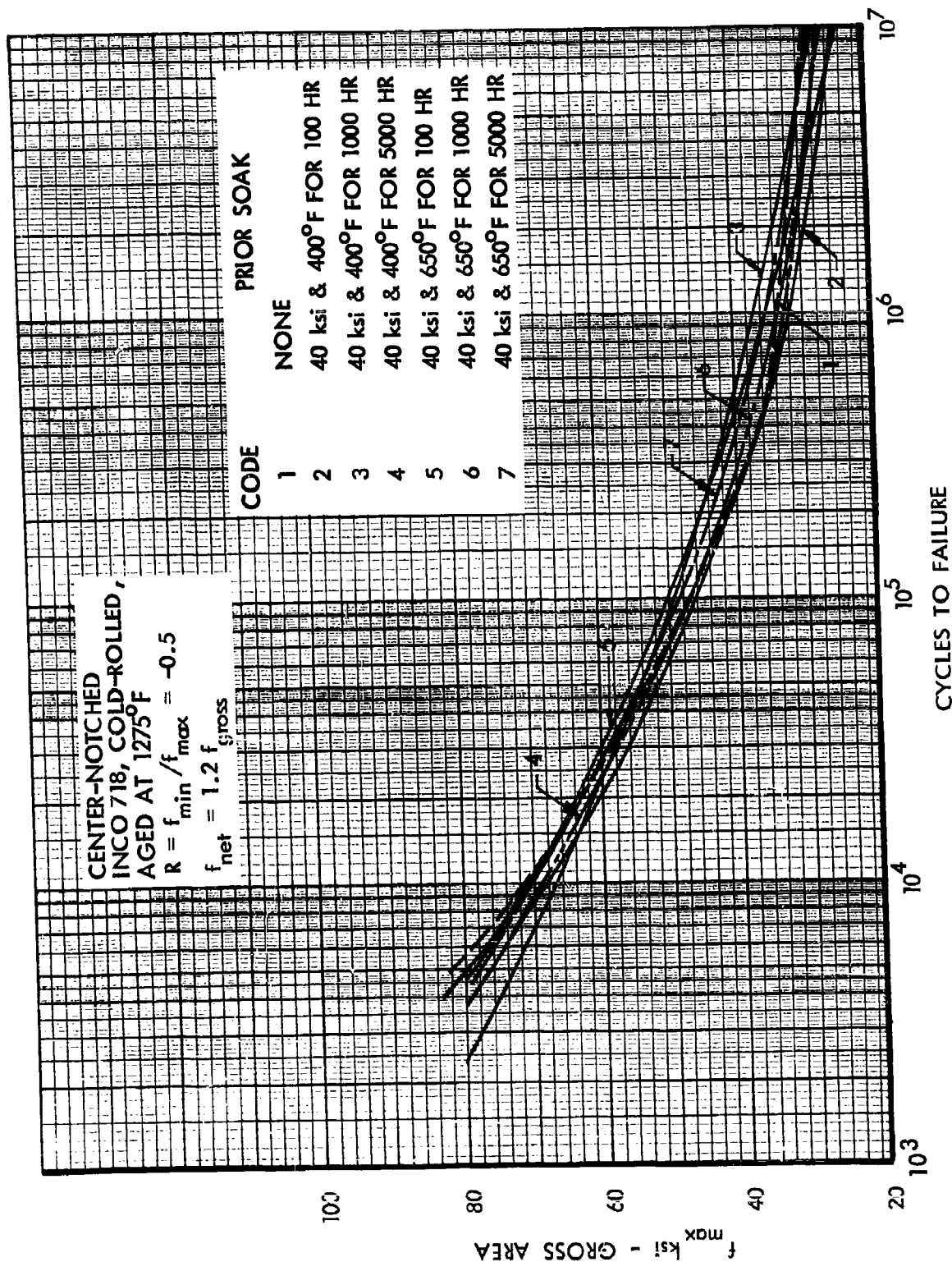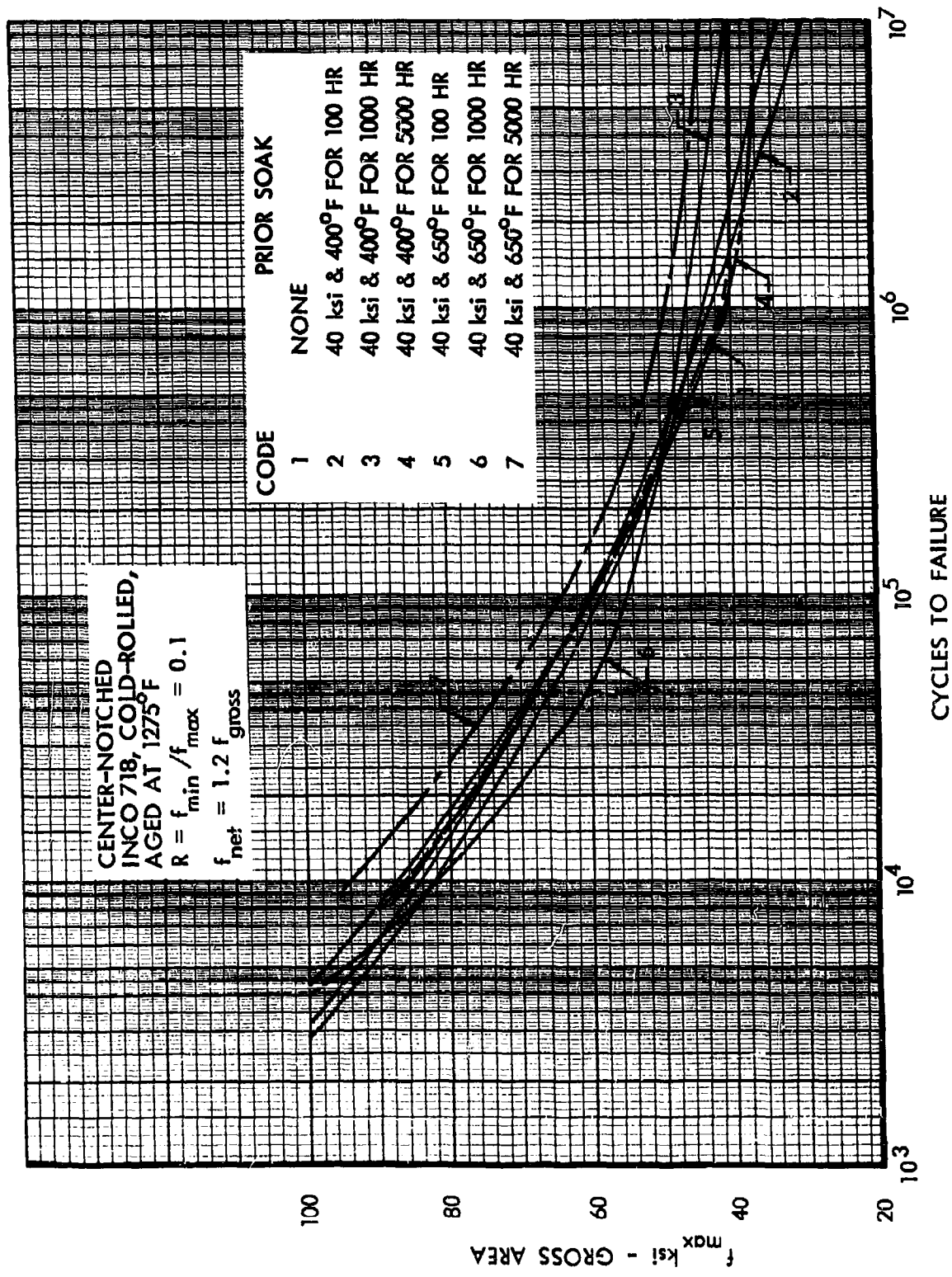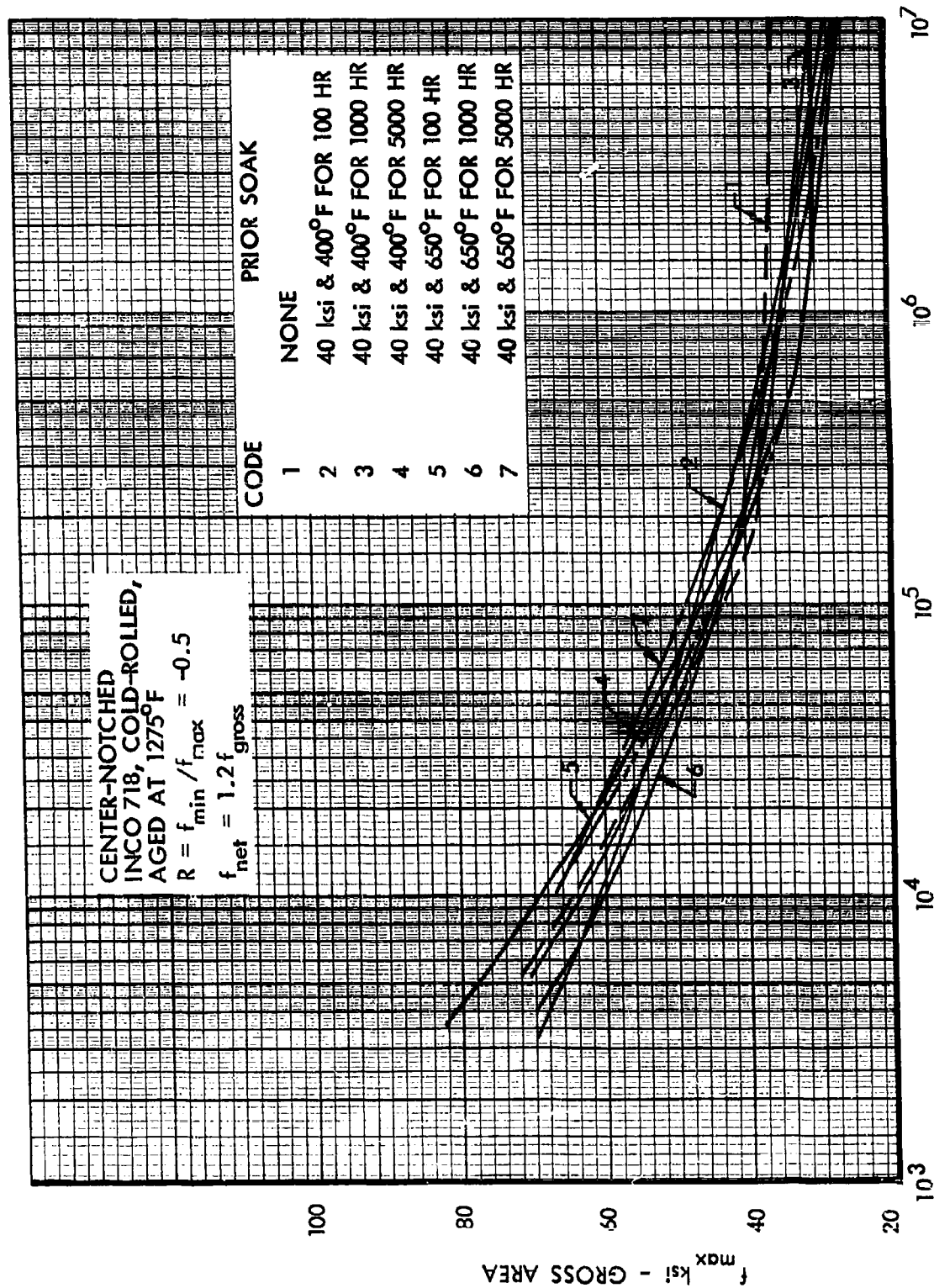
Figure 183.   Effects of Prior Soak on S-N Curves at 400°F, Center-Notched PH14-8Mo, R = Constant
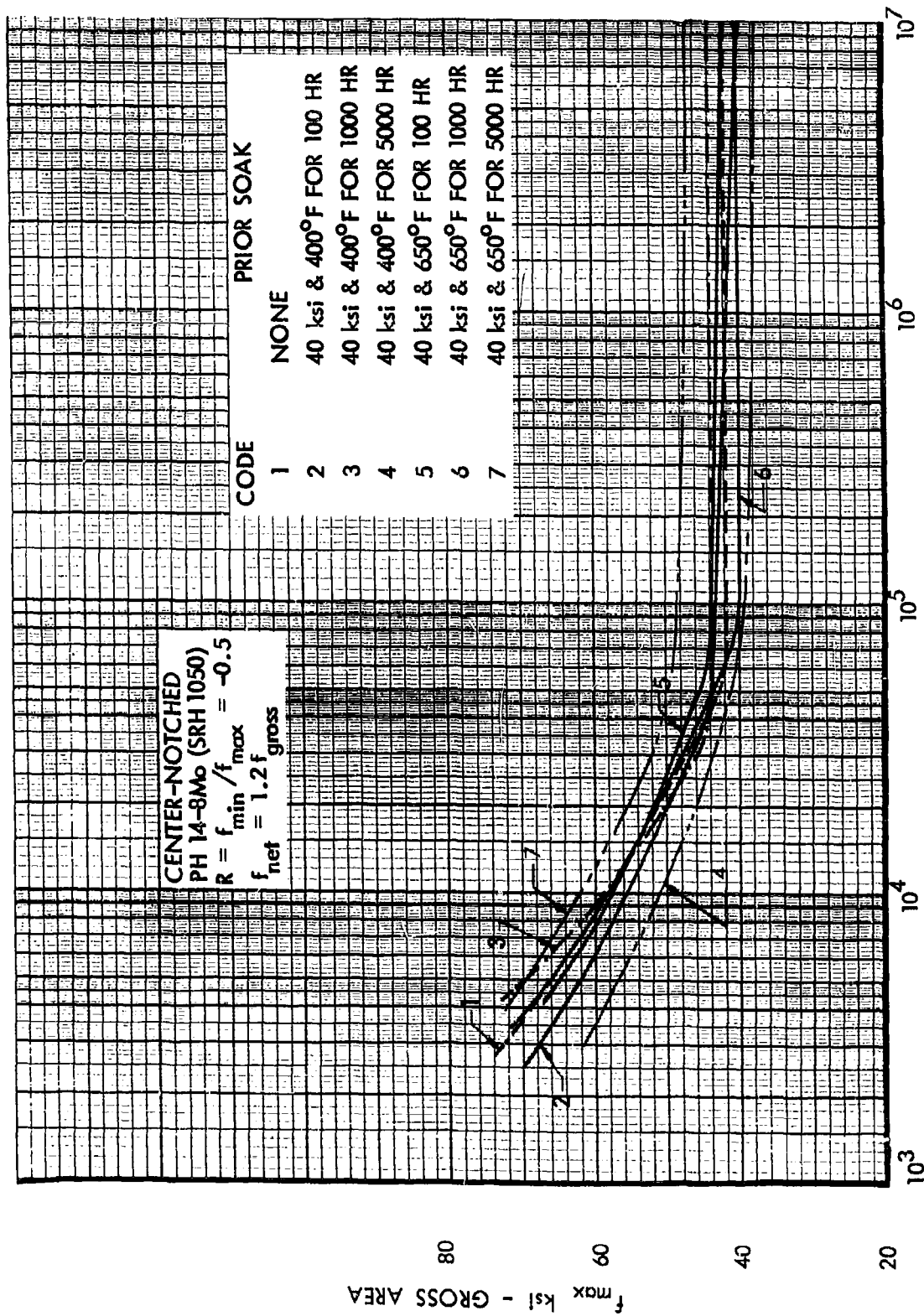
Figure 184. Effects of Prior Soak on S-N Curves at 400°F, Center-Notched PH14-8Mo, R = Constant

CENTER-NOTCHED
PH 14-8Mo (SRH 1050)
$R = f_{min}/f_{max} = 0.1$
$f_{net} = 1.2 f_{gross}$

CODE	PRIOR SOAK
1	NONE
2	40 ksi & 400°F FOR 100 HR
3	40 ksi & 400°F FOR 1000 HR
4	40 ksi & 400°F FOR 5000 HR
5	40 ksi & 650°F FOR 100 HR
6	40 ksi & 650°F FOR 1000 HR
7	40 ksi & 650°F FOR 5000 HR

CYCLES TO FAILURE

f_{max}, ksi – GROSS AREA
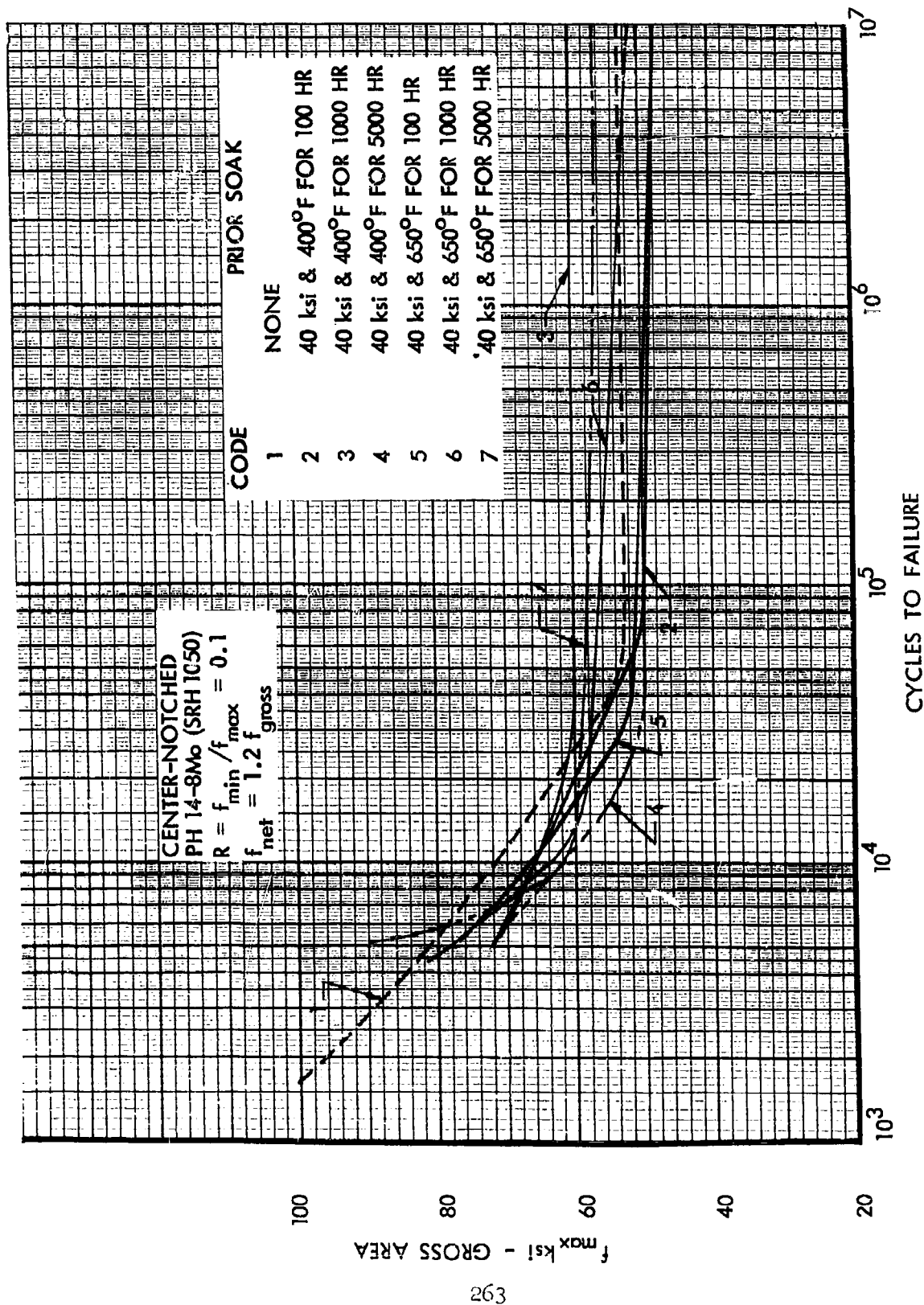
Figure 185.   Effects of Prior Soak on S–N Curves at 650°F, Center-Notched PH14-8Mo, R = Constant

263
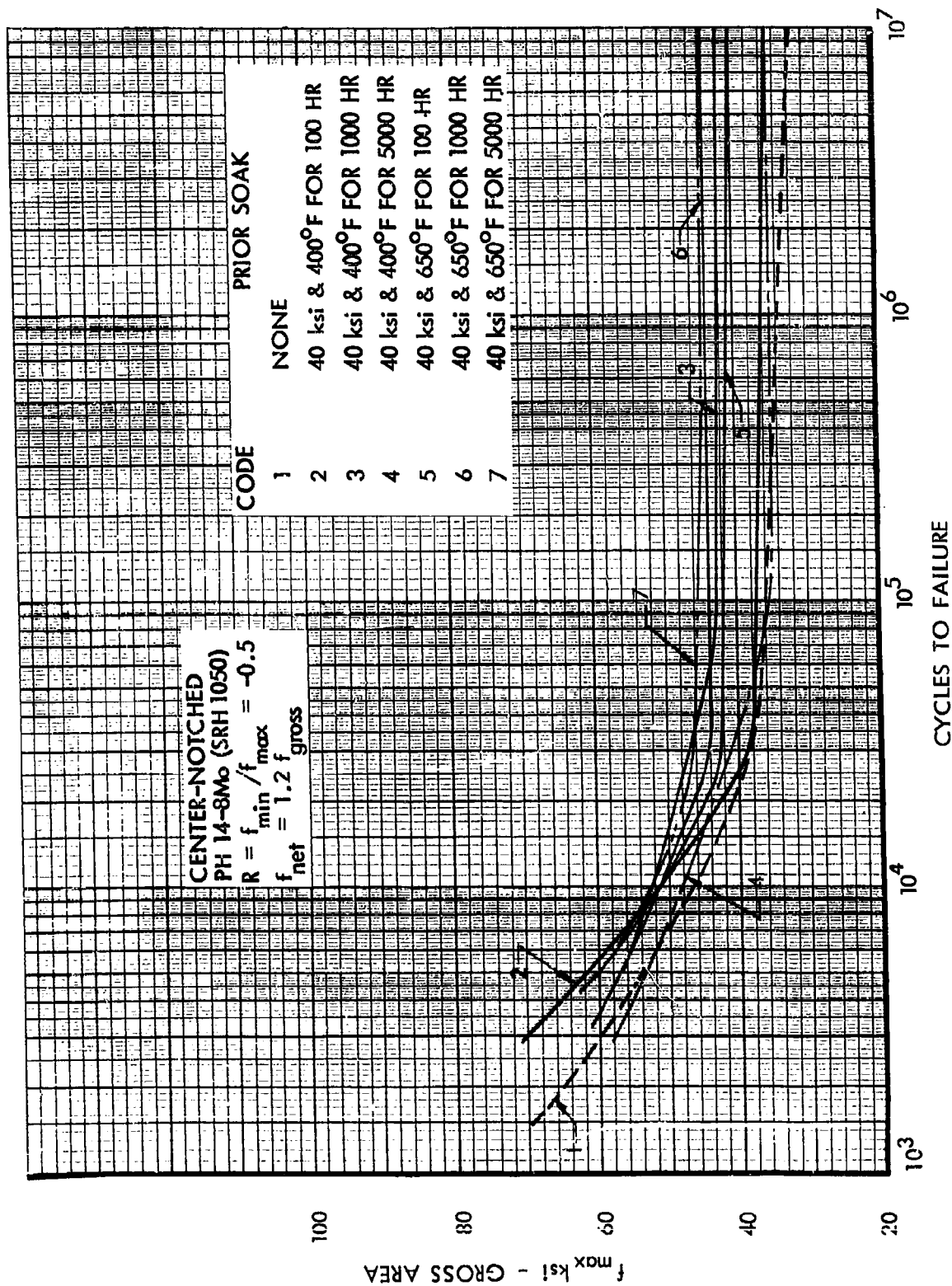
Figure 186.   Effects of Prior Soak on S-N Curves at 650°F, Center-Notched PH14-8Mo, R = Constant
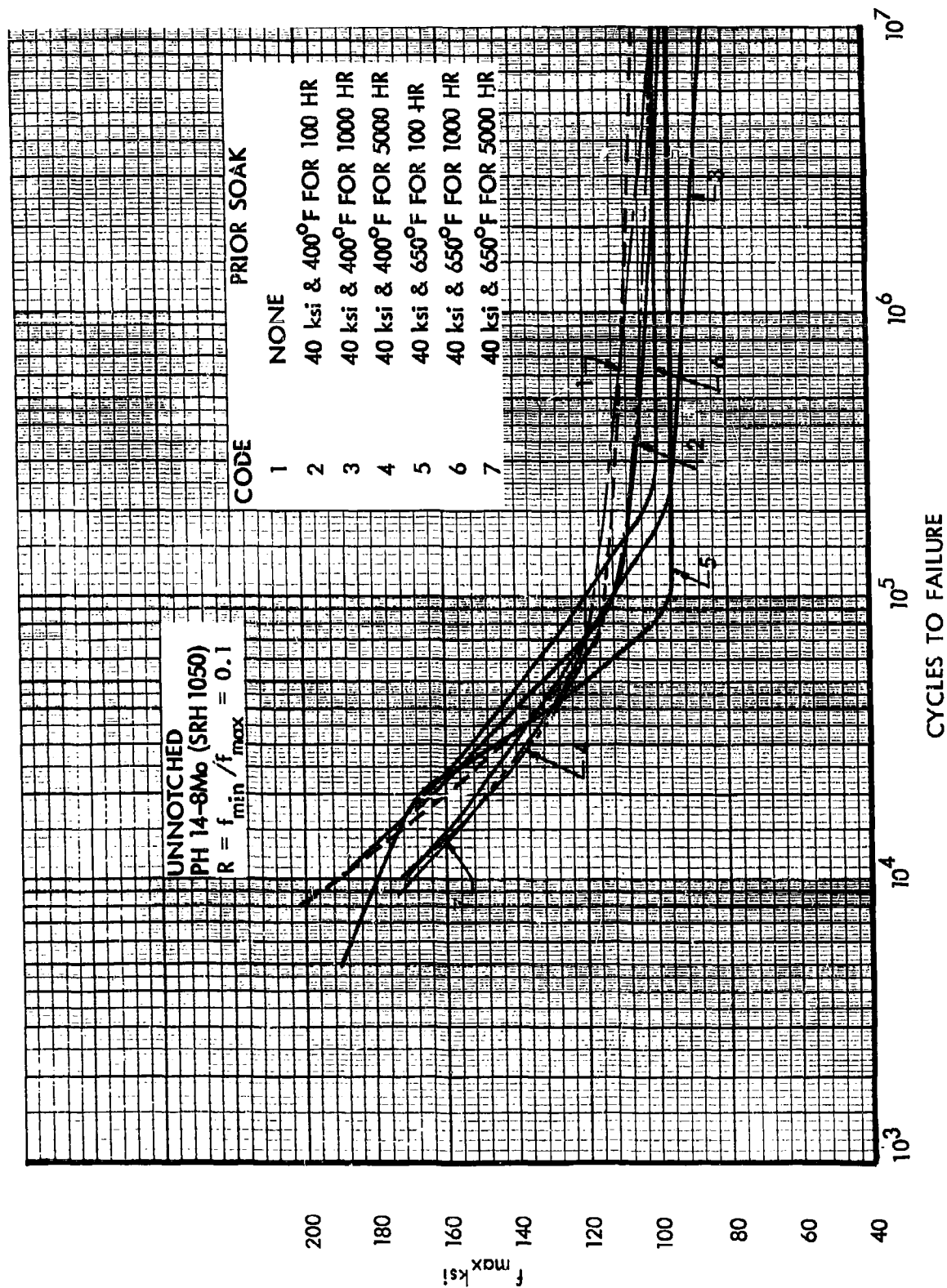
Figure 187. Effects of Prior Soak on S-N Curves at Room Temperature, Unnotched PH14-8Mo, R = Constant

265
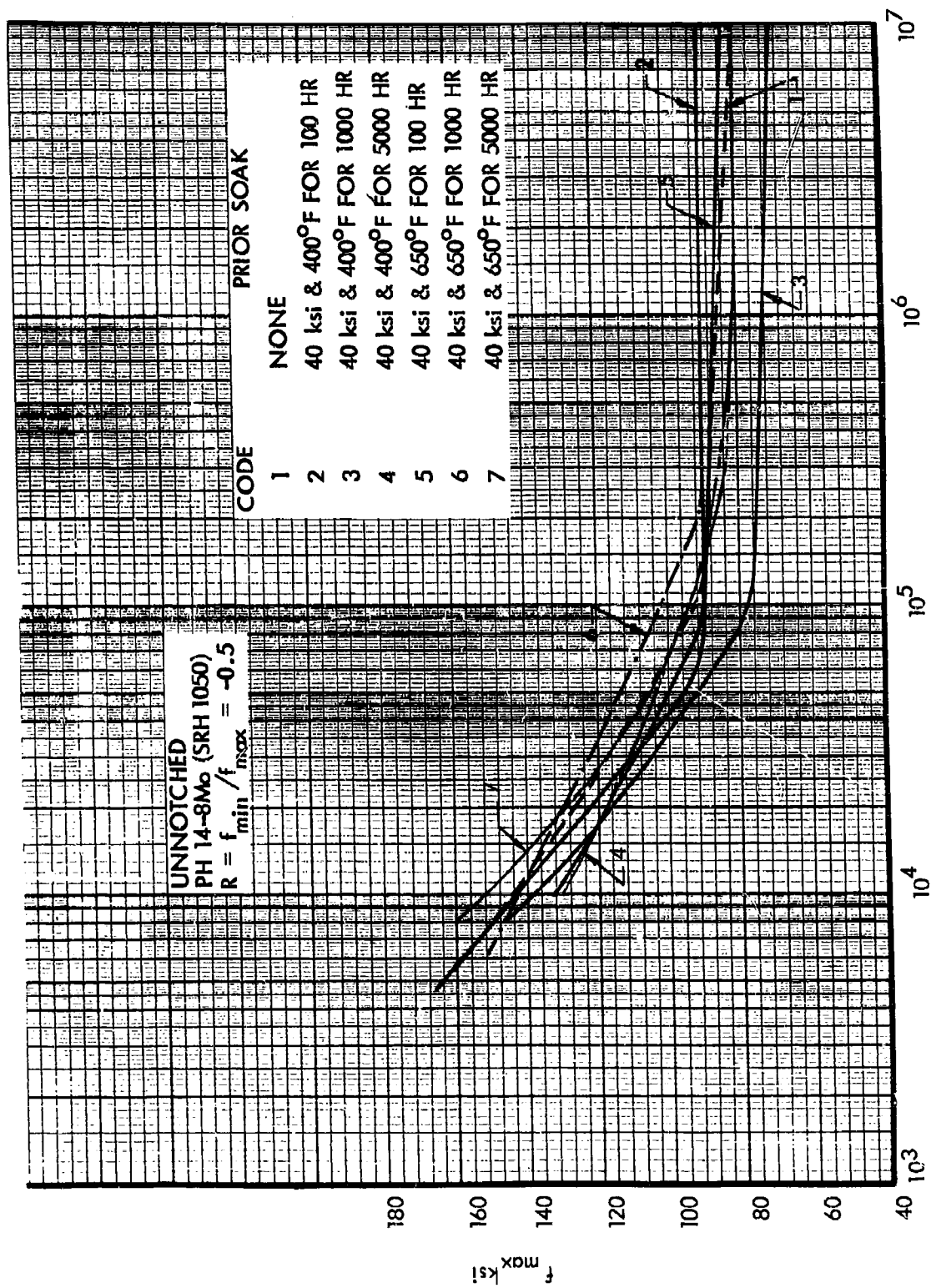
CYCLES TO FAILURE
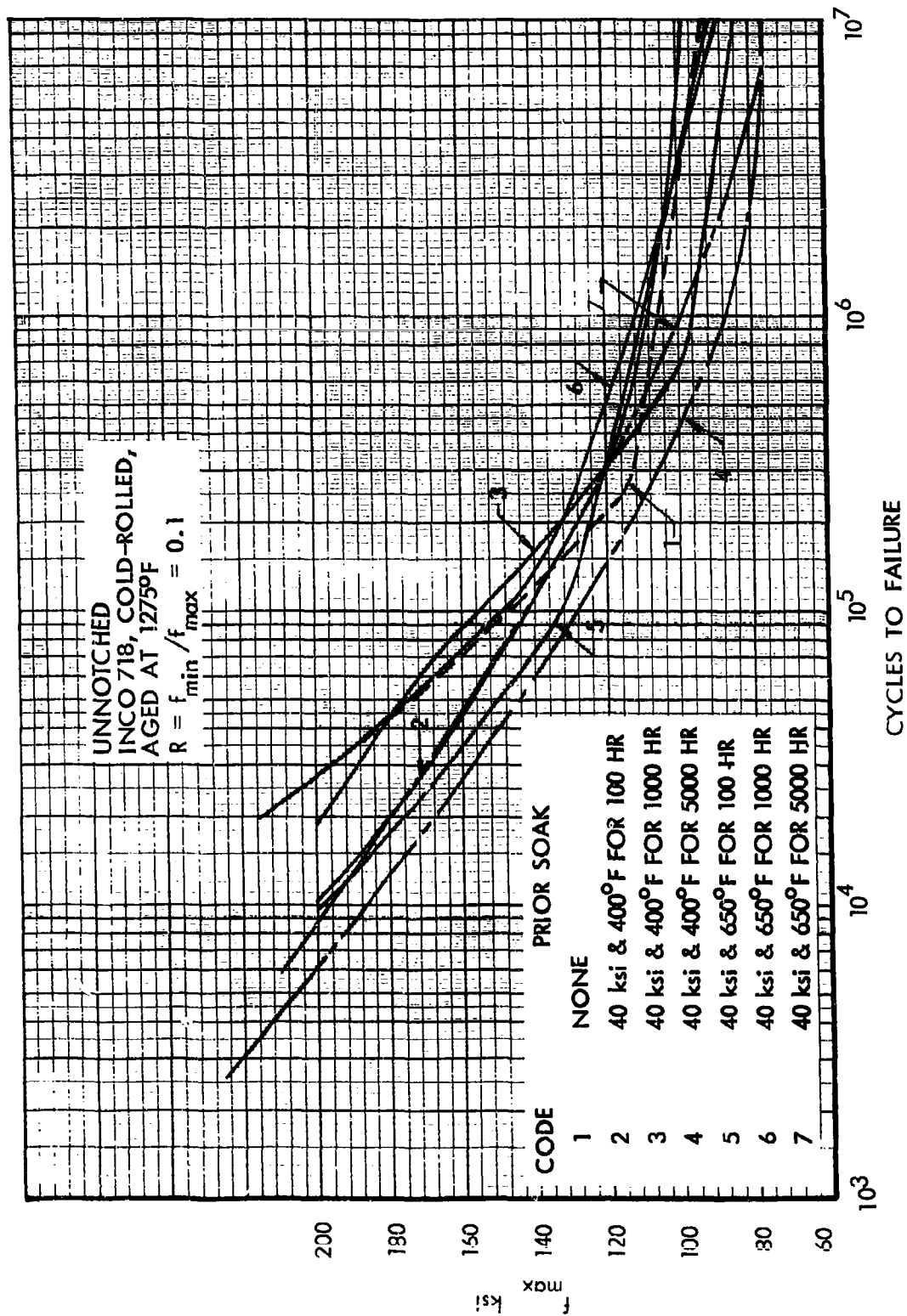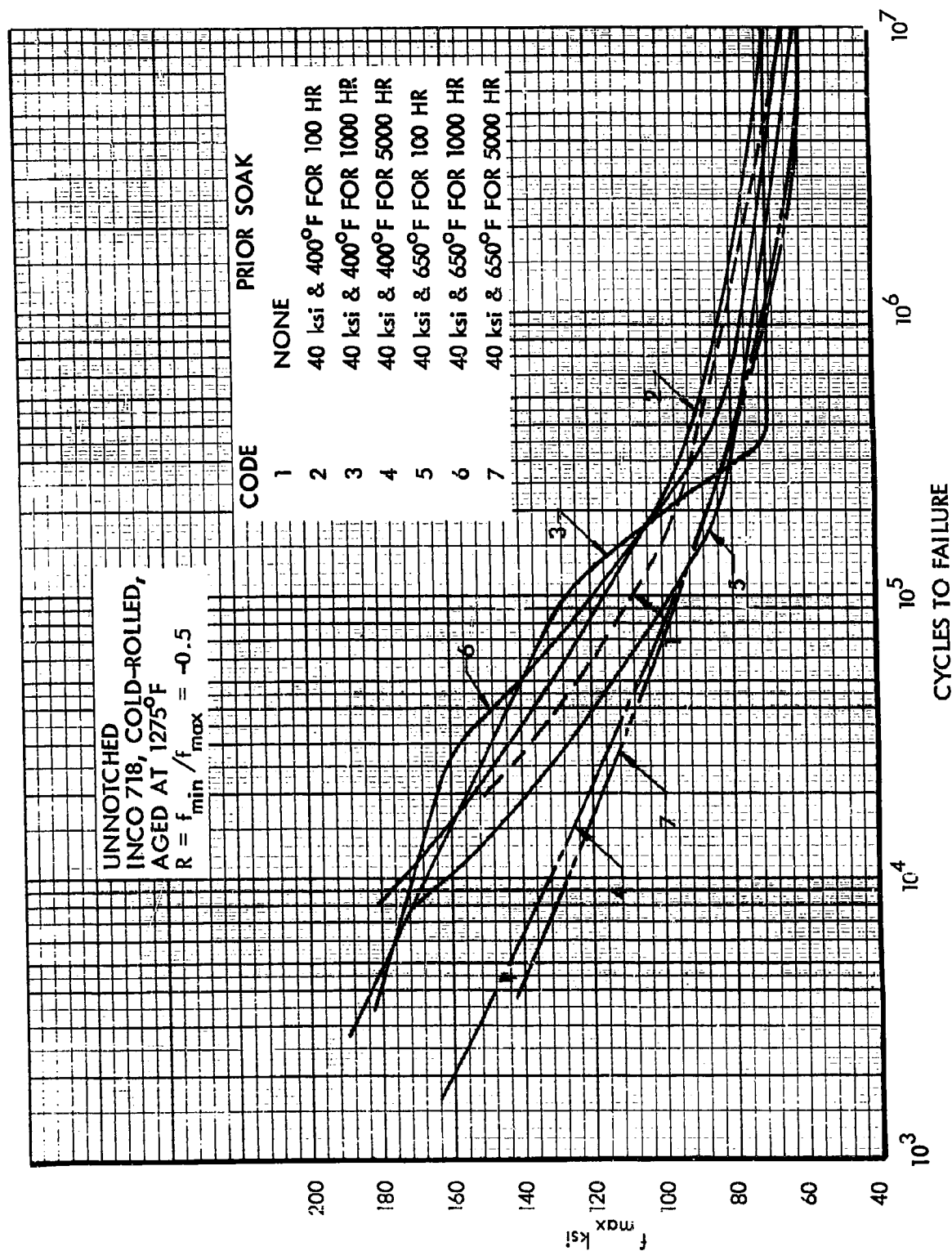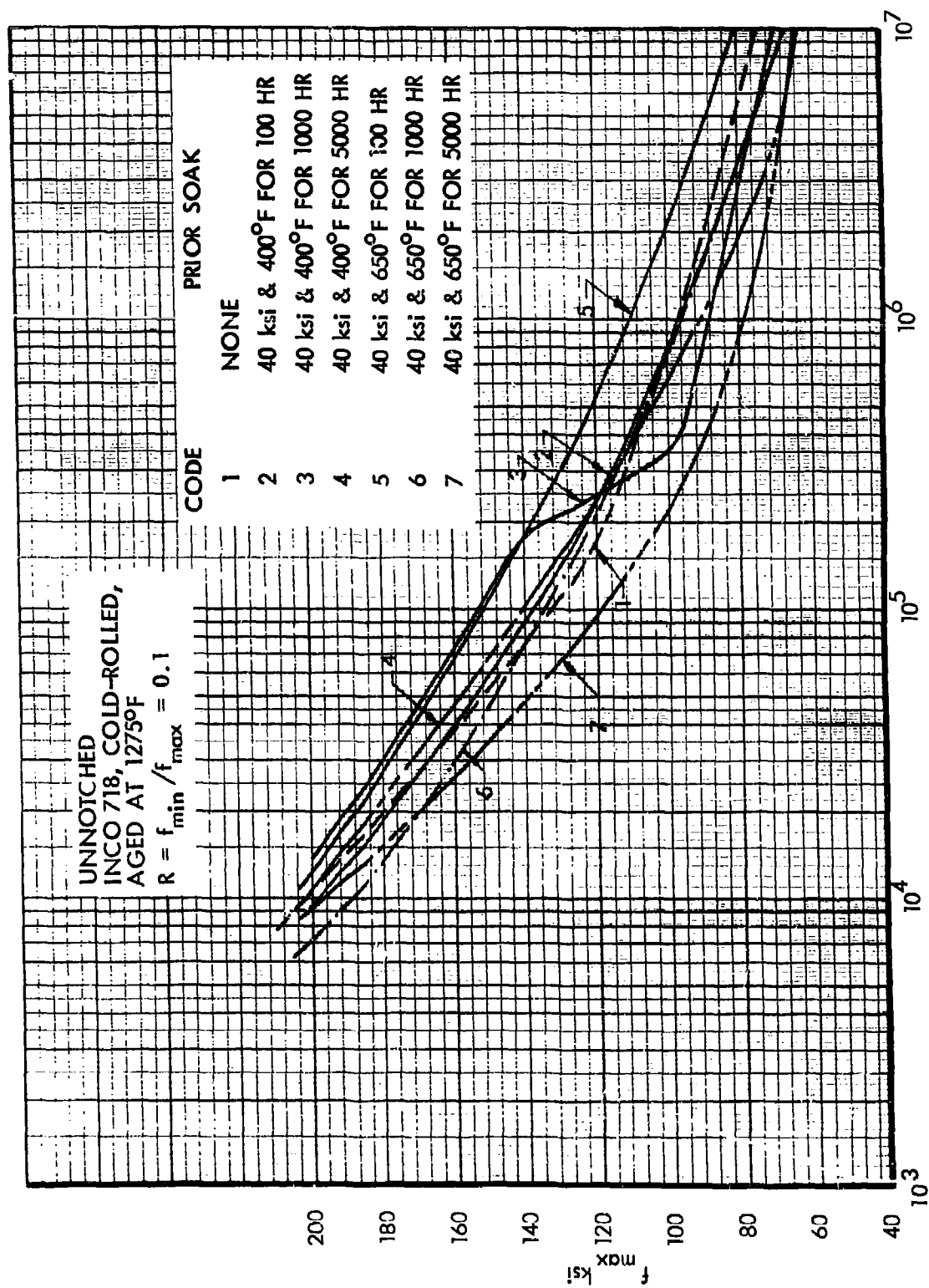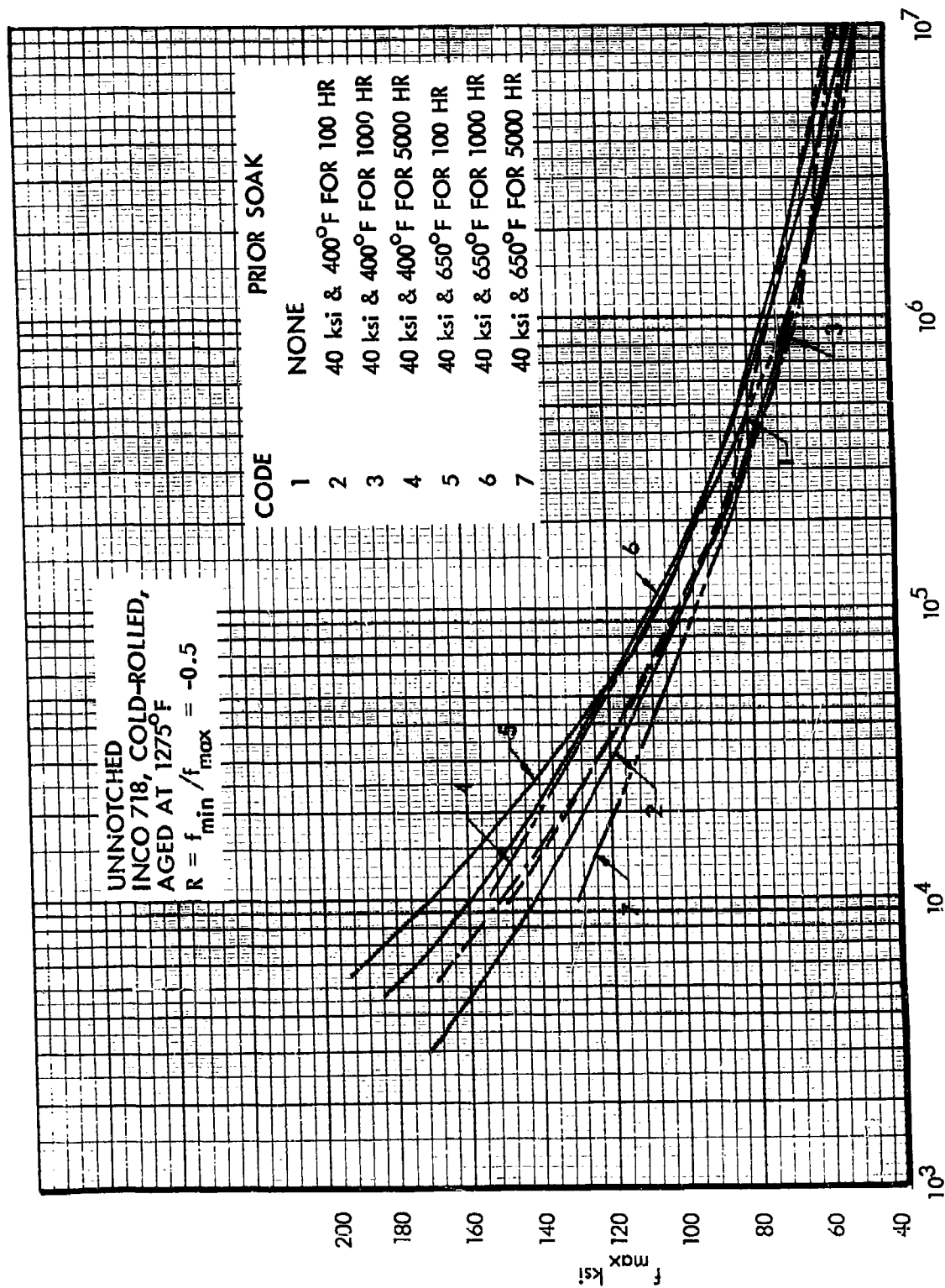
Figure 188. Effects of Prior Soak on S–N Curves at Room Temperature, Unnotched PH14–8Mo, R = Constant

266
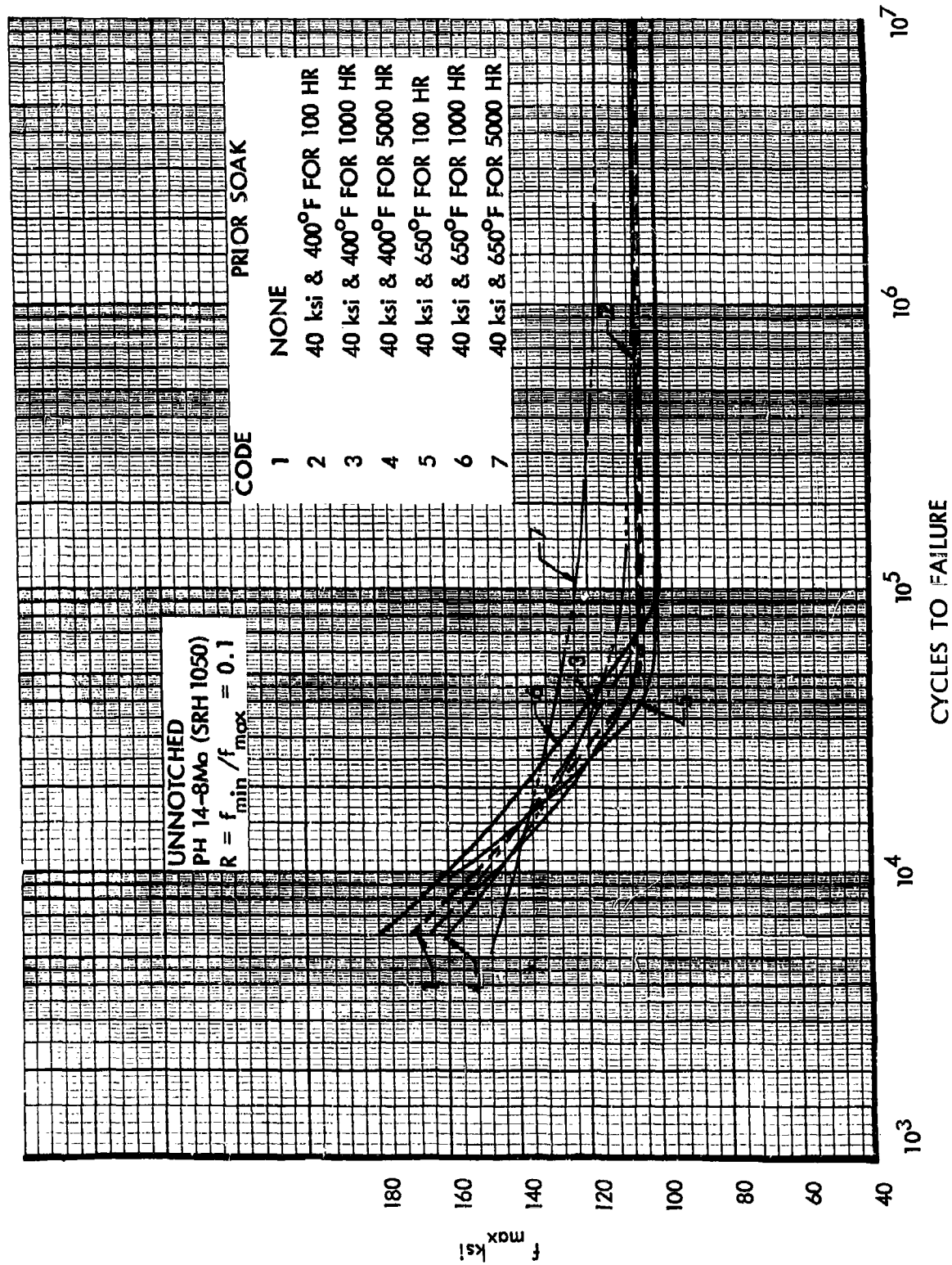
Figure 189. Effects of Prior Soak on S-N Curves at 400°F, Unnotched PH14-8Mo, R = Constant

UNNOTCHED
PH 14-8Mo (SRH 1050)
$R = f_{min}/f_{max} = -0.5$

CODE	PRIOR SOAK
1	NONE
2	40 ksi & 400°F FOR 100 HR
3	40 ksi & 400°F FOR 1000 HR
4	40 ksi & 400°F FOR 5000 HR
5	40 ksi & 650°F FOR 100 HR
6	40 ksi & 650°F FOR 1000 HR
7	40 ksi & 650°F FOR 5000 HR

CYCLES TO FAILURE

f_{max} ksi

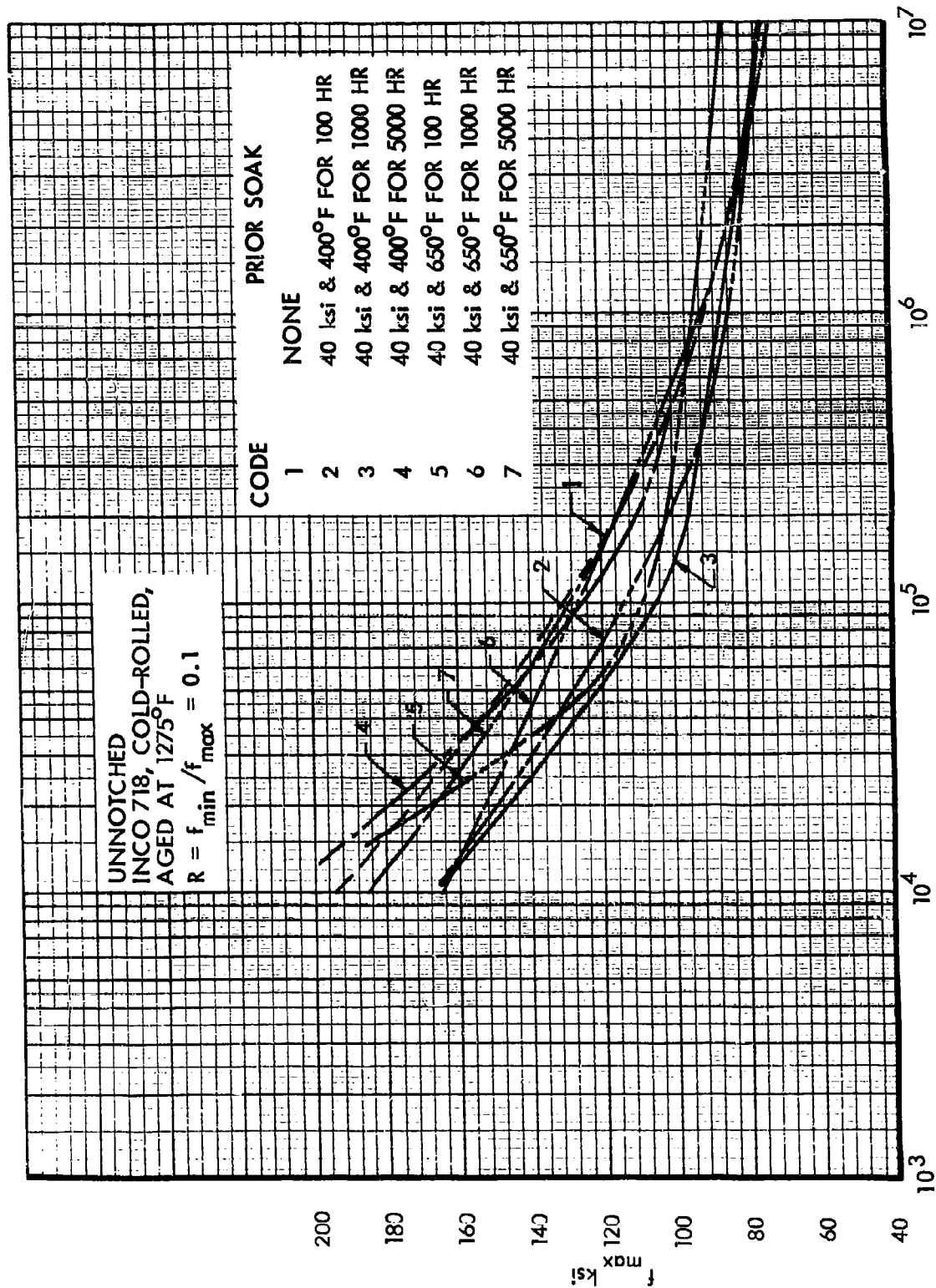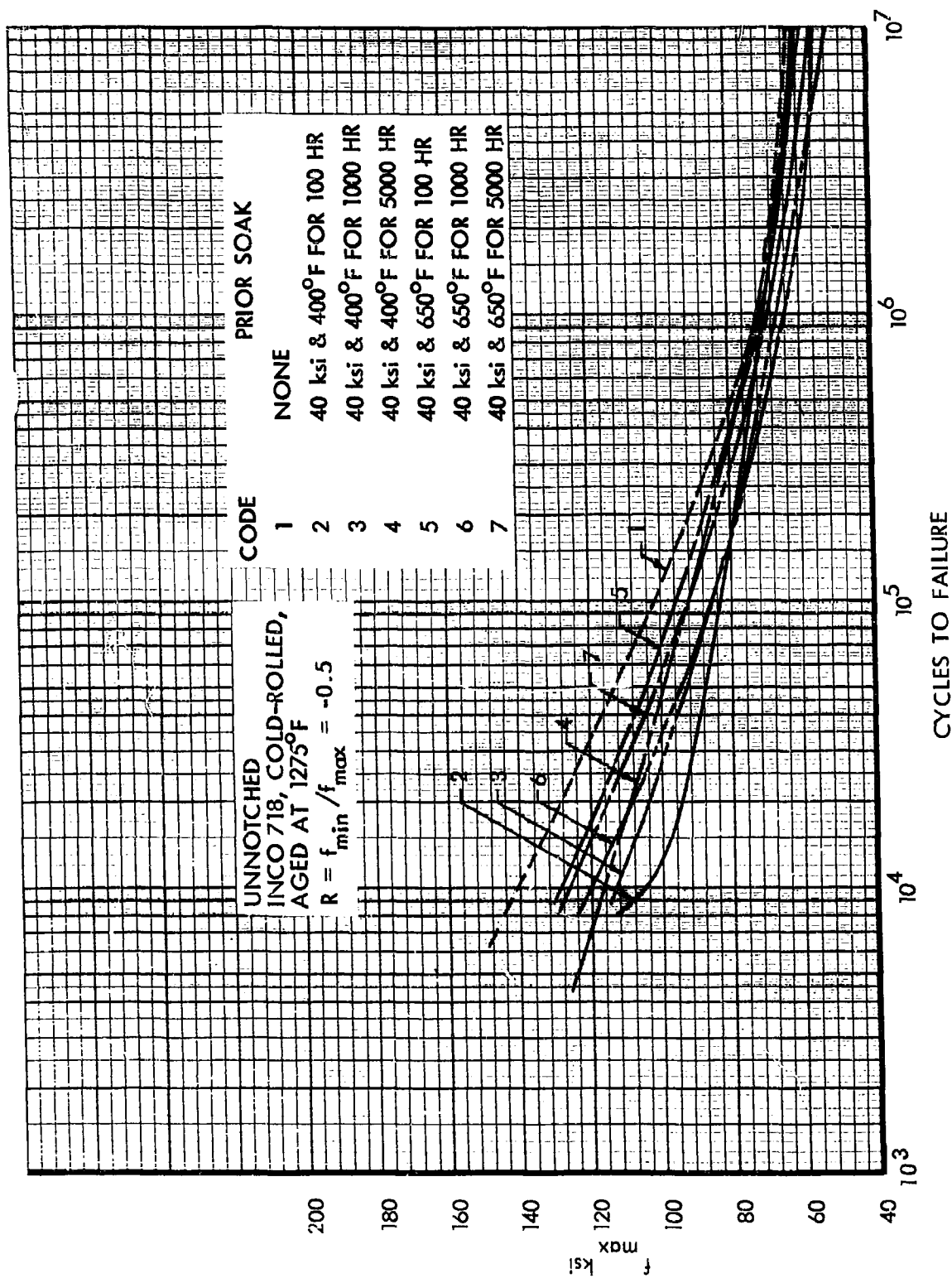Figure 190.   Effects of Prior Soak on S-N Curves at 400°F, Unnotched PH14-8Mo, R = Constant
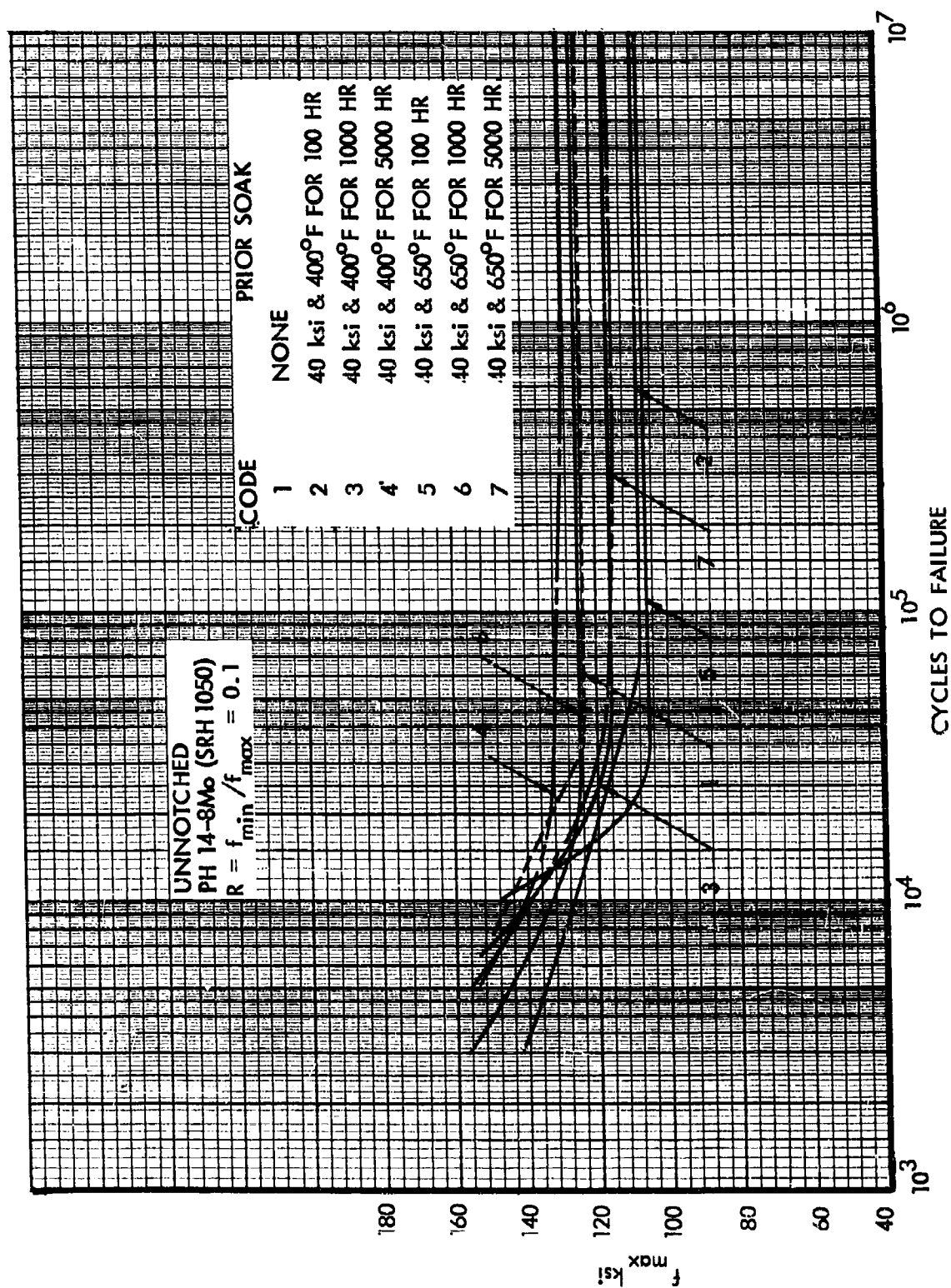
Figure 191. Effects of Prior Soak on S-N Curves at 650°F, Unnotched PH14-8 Mo, R = Constant

269
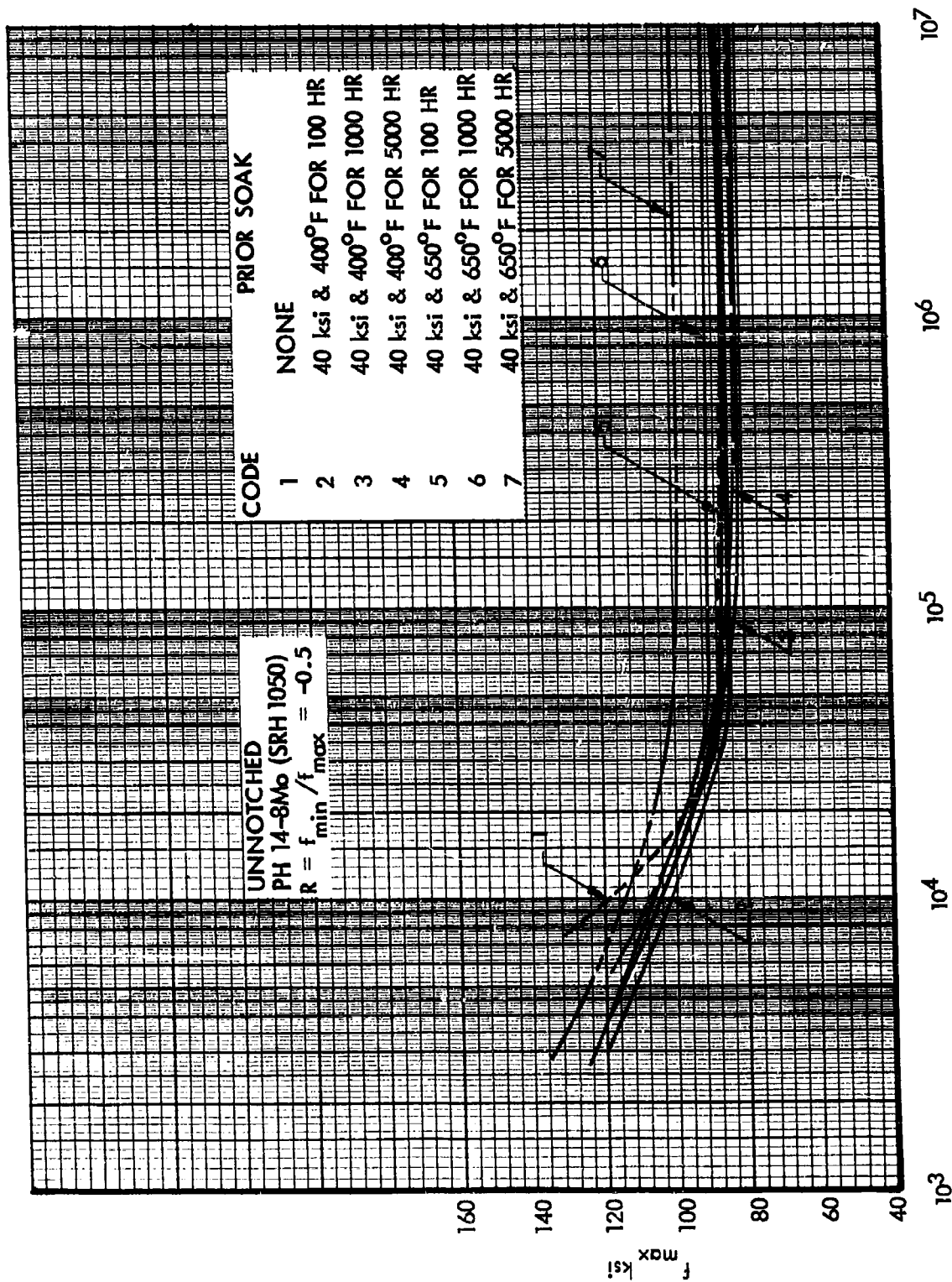
Figure 192. Effects of Prior Soak on S-N Curves at 650°F, Unnotched PH14-8Mo, R = Constant
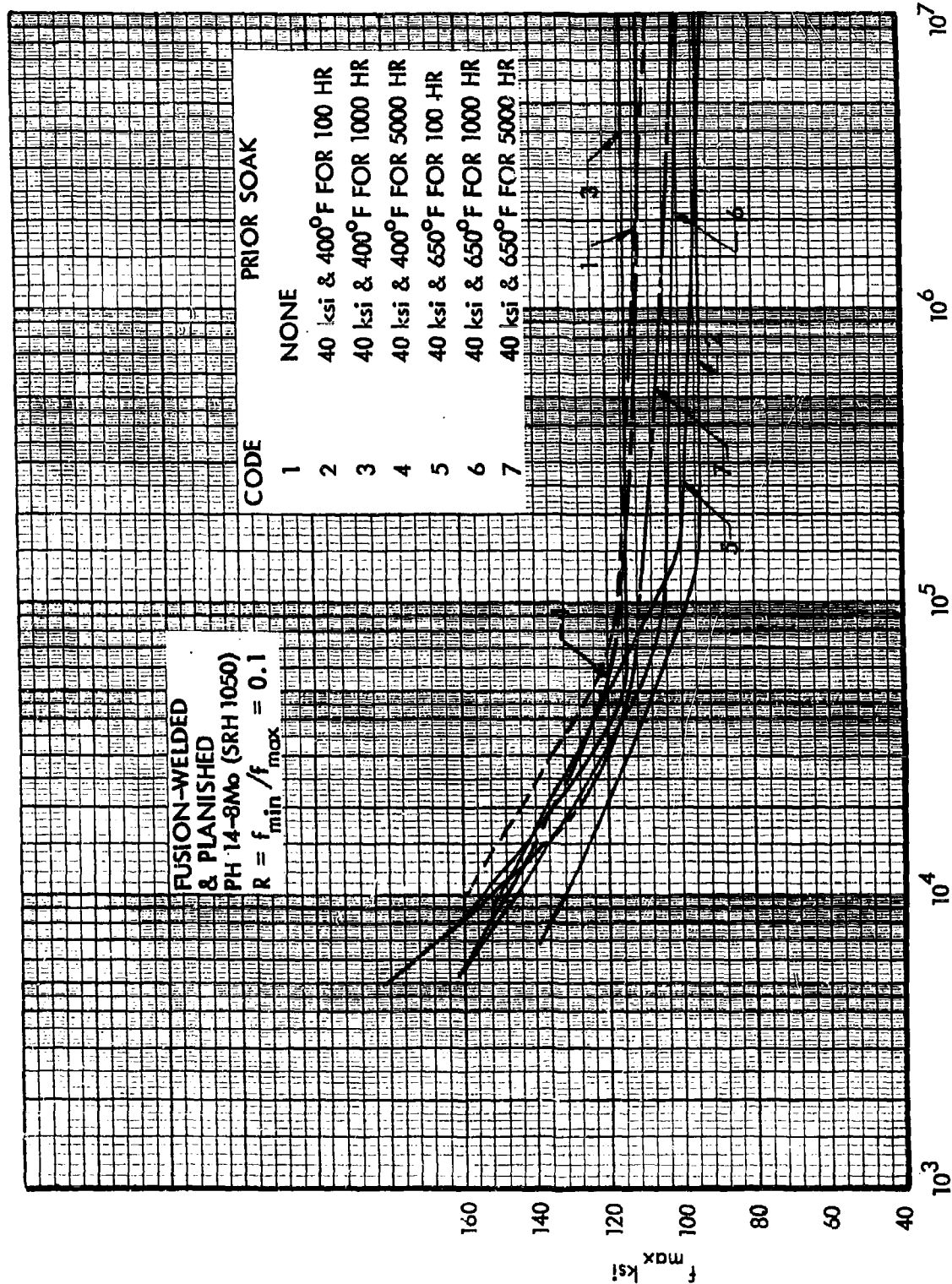
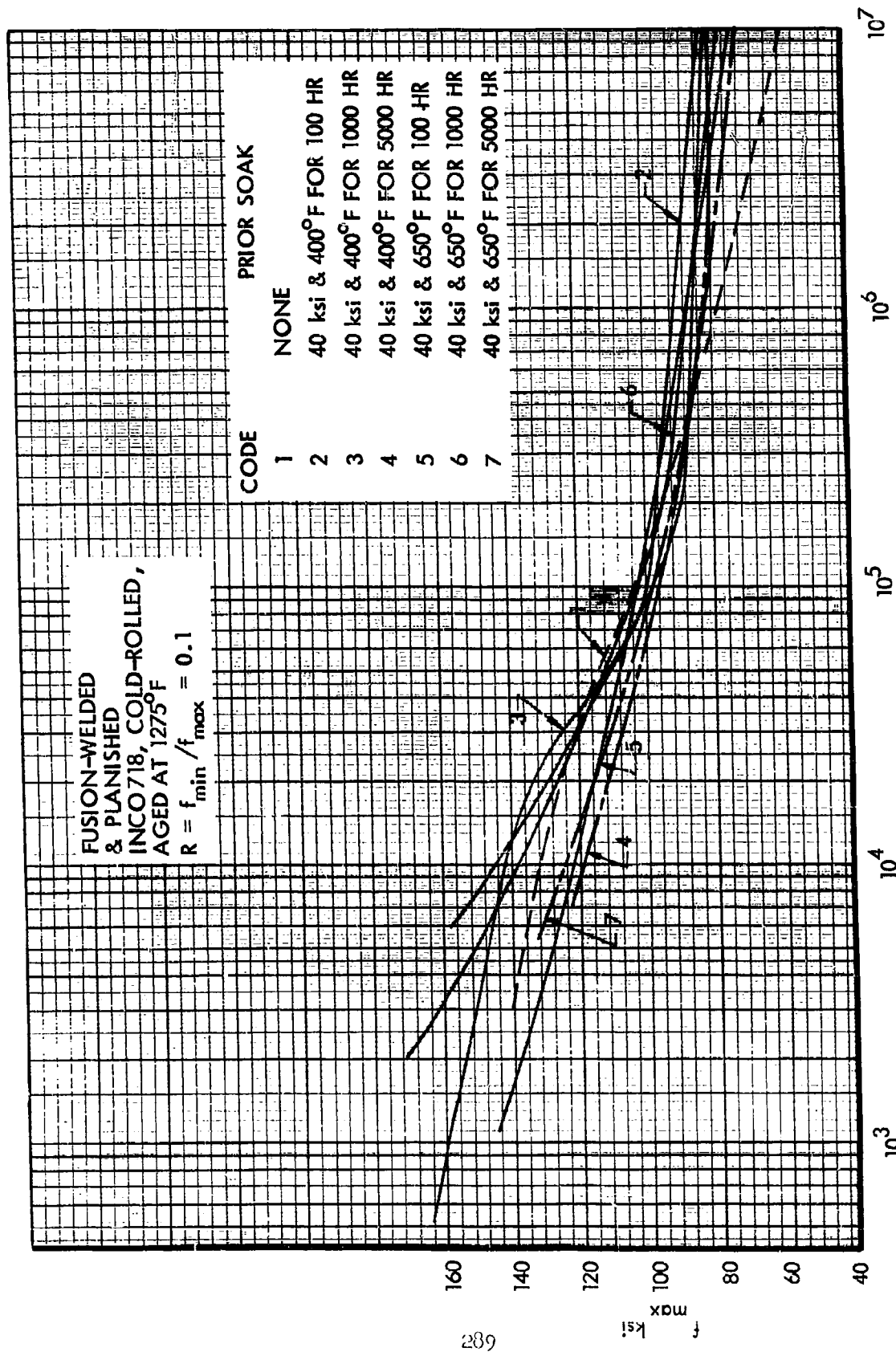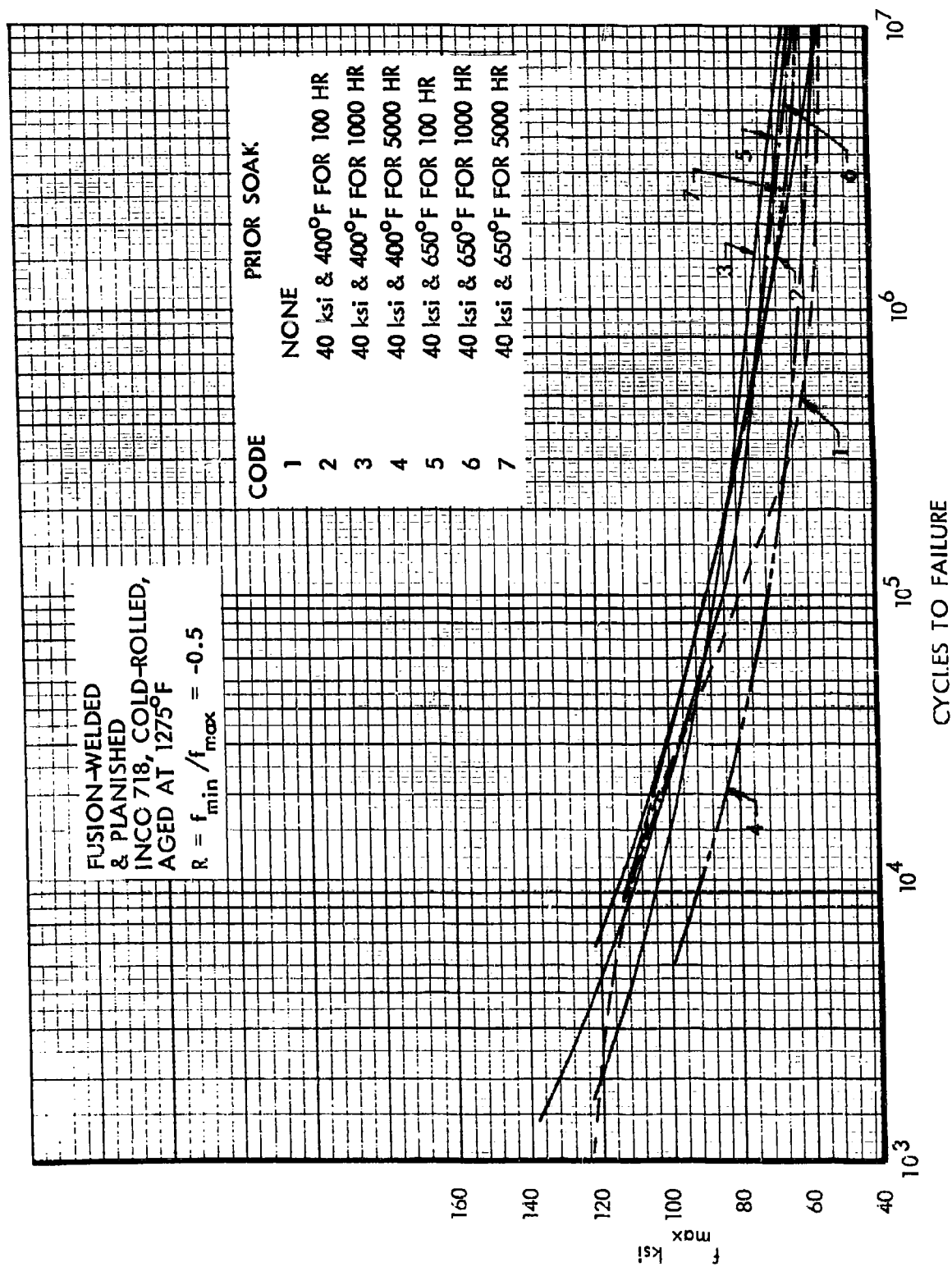Figure 193. Effects of Prior Soak on S-N Curves at Room Temperature, Fusion-Welded PH14-8Mo, R = Constant

271
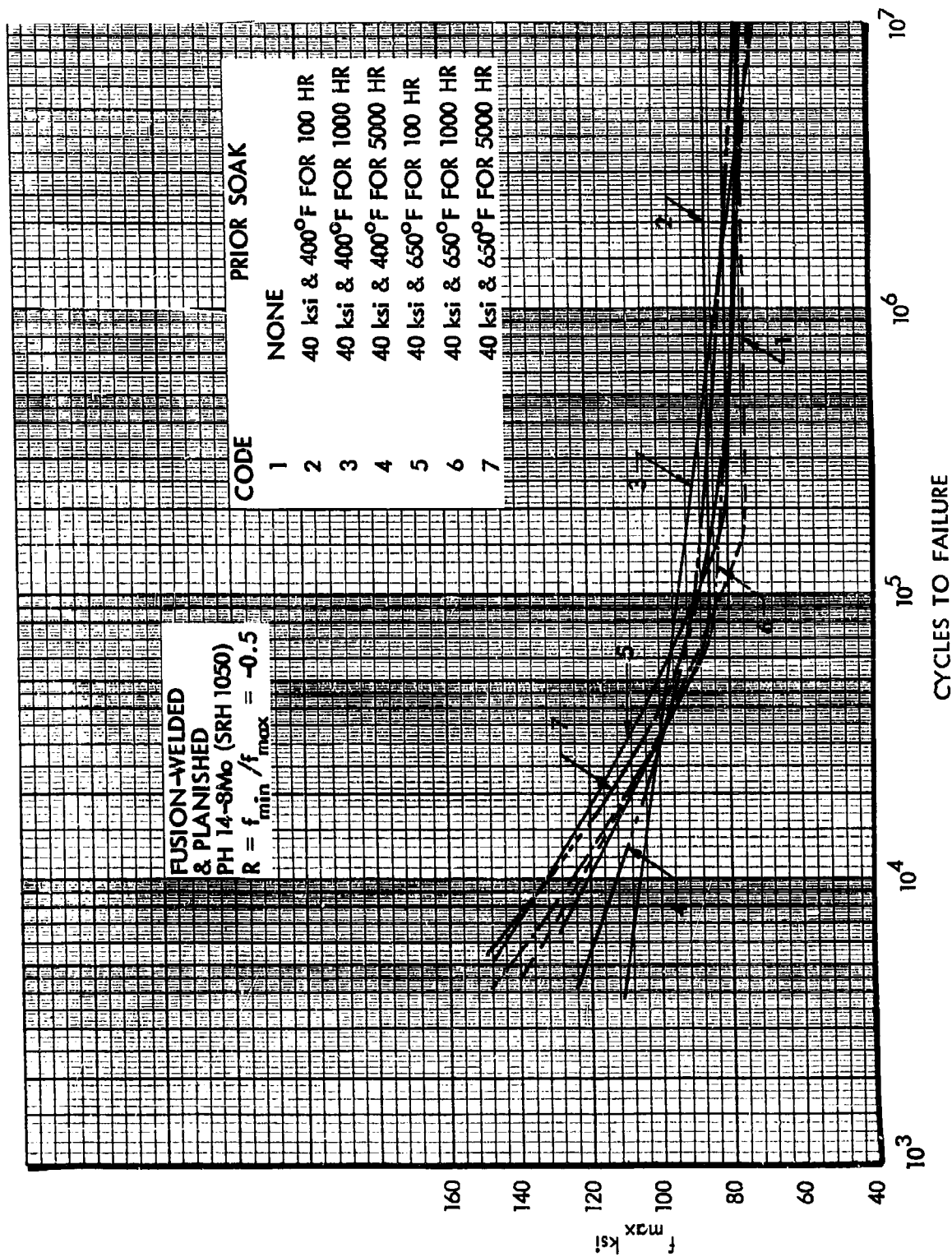
Figure 194. Effects of Prior Soak on S-N Curves at Room Temperature, Fusion-Welded PH14-8Mo, R = Constant

272
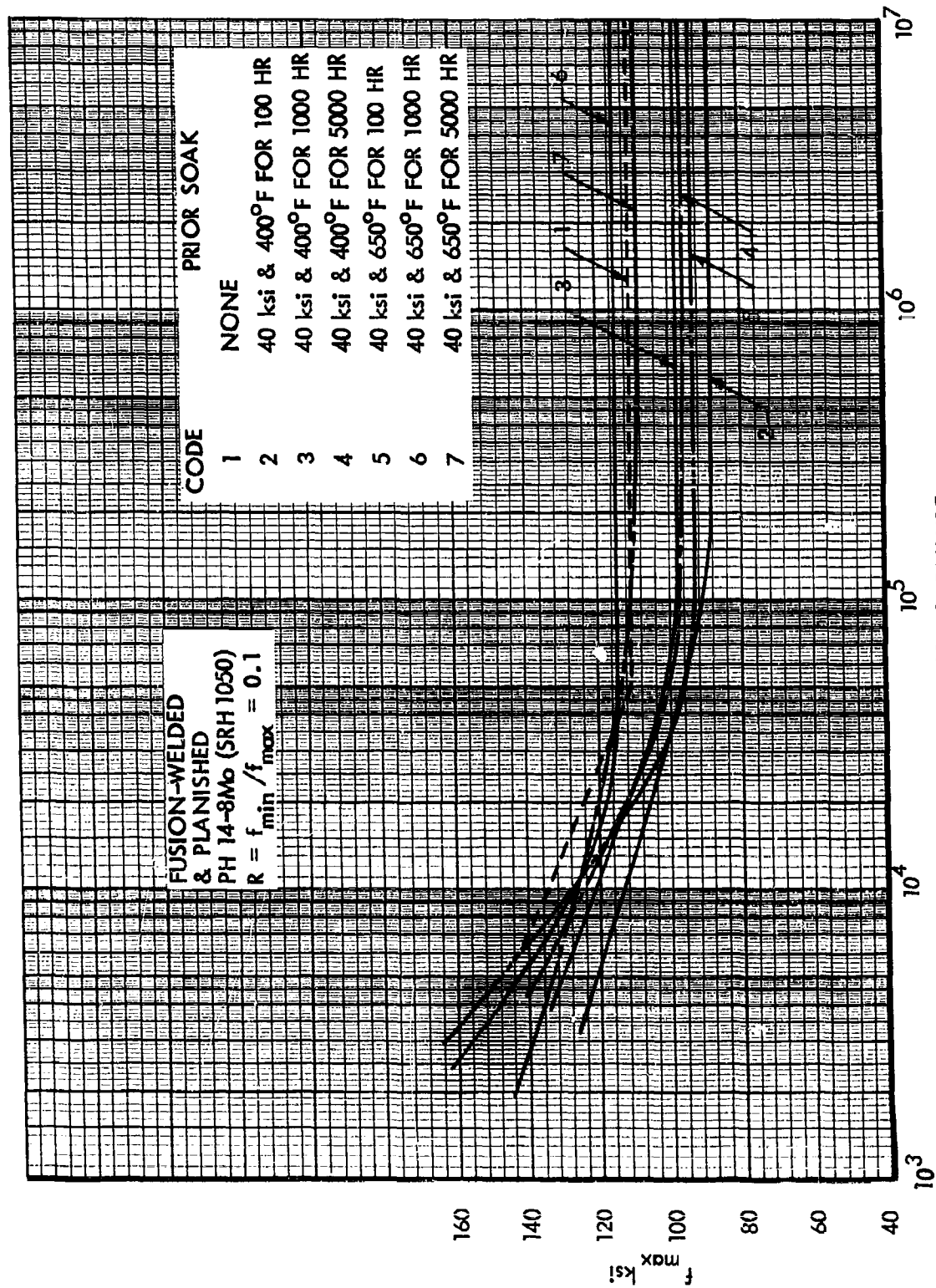
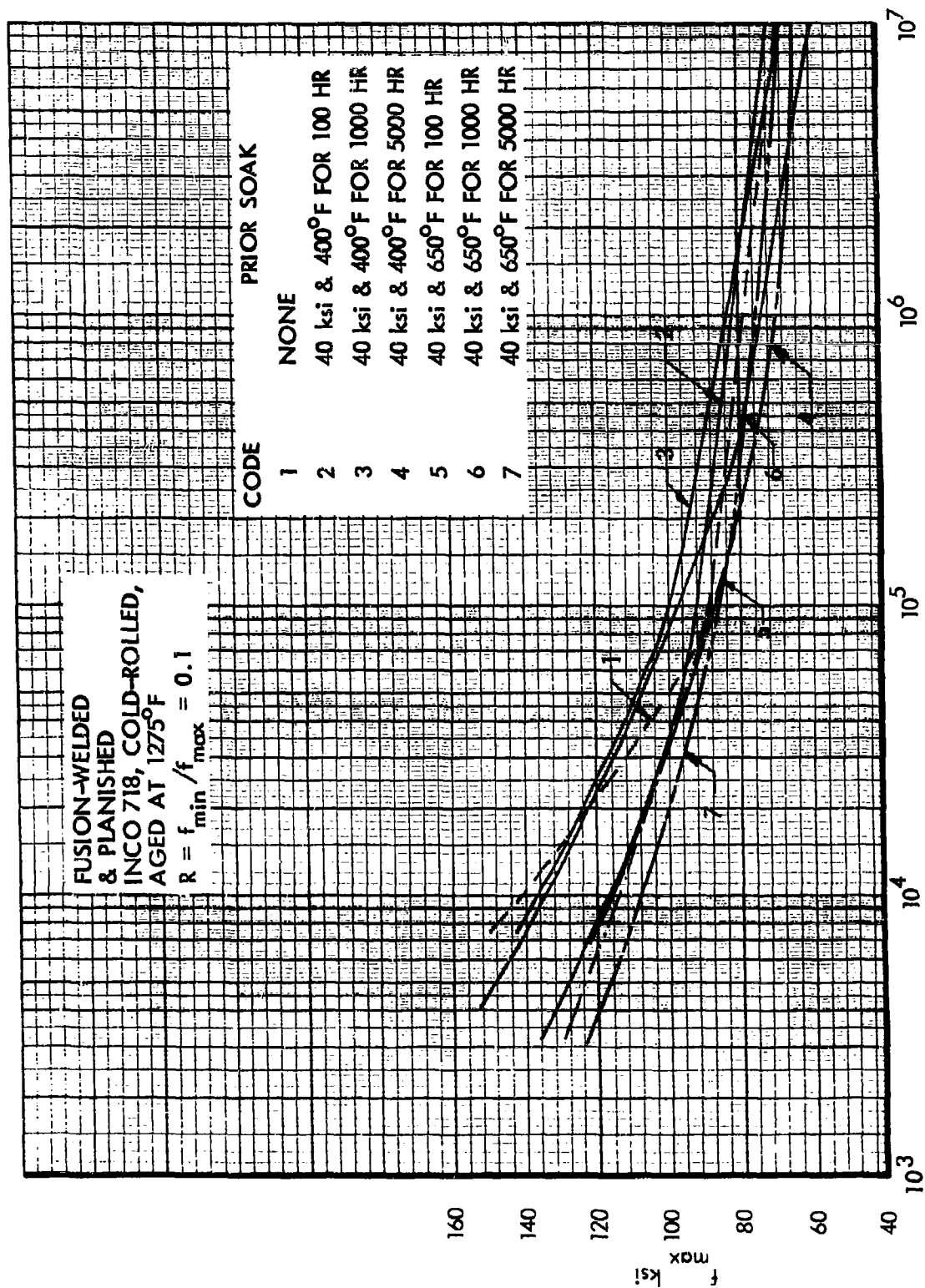Figure 195. Effects of Prior Soak on S-N Curves at 400°F, Fusion-Welded PH14-8Mo, R = Constant

273
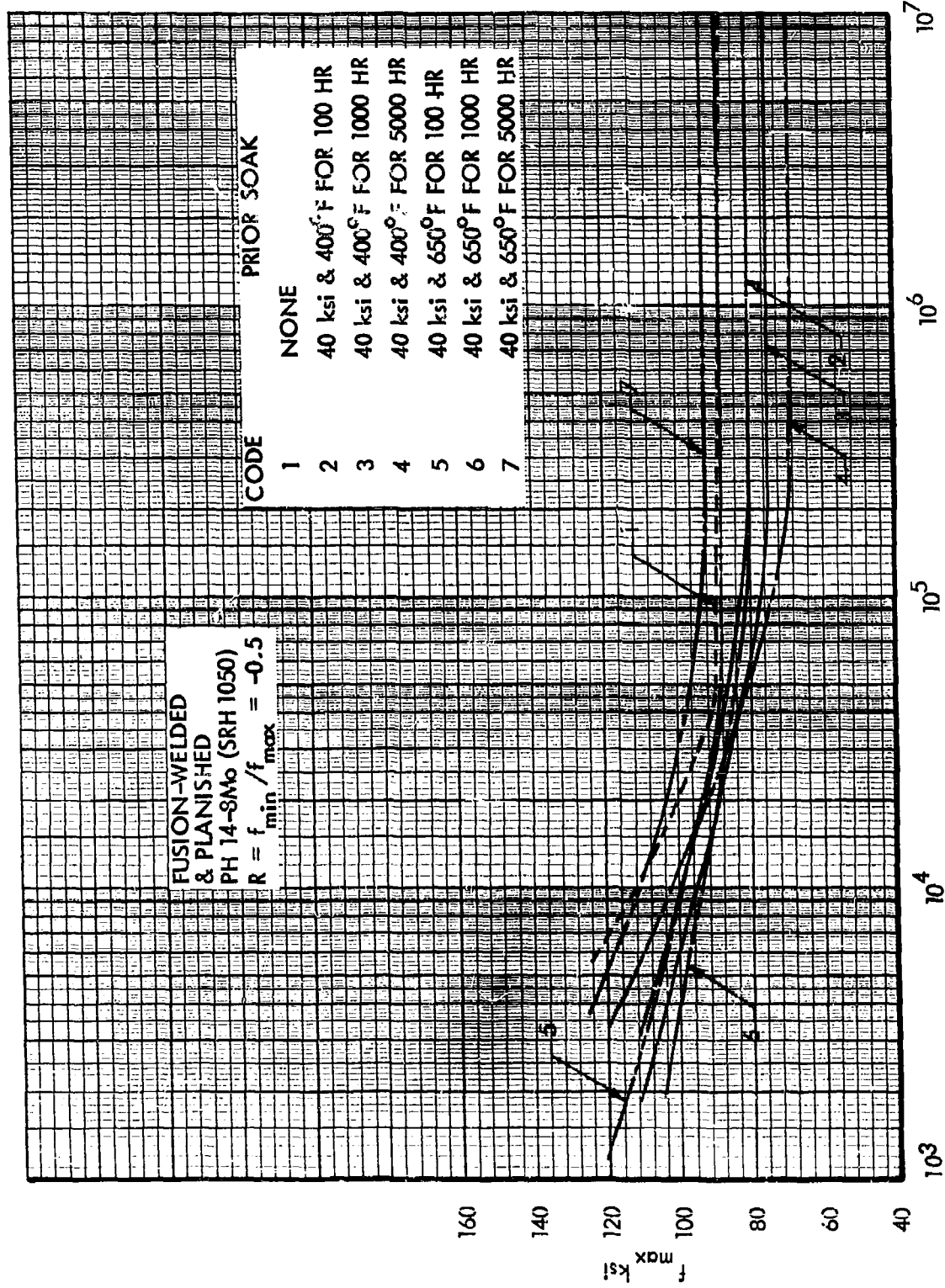
Figure 196. Effects of Prior Soak on S-N Curves at 400°F, Fusion-Welded PH14-8Mo, R = Constant
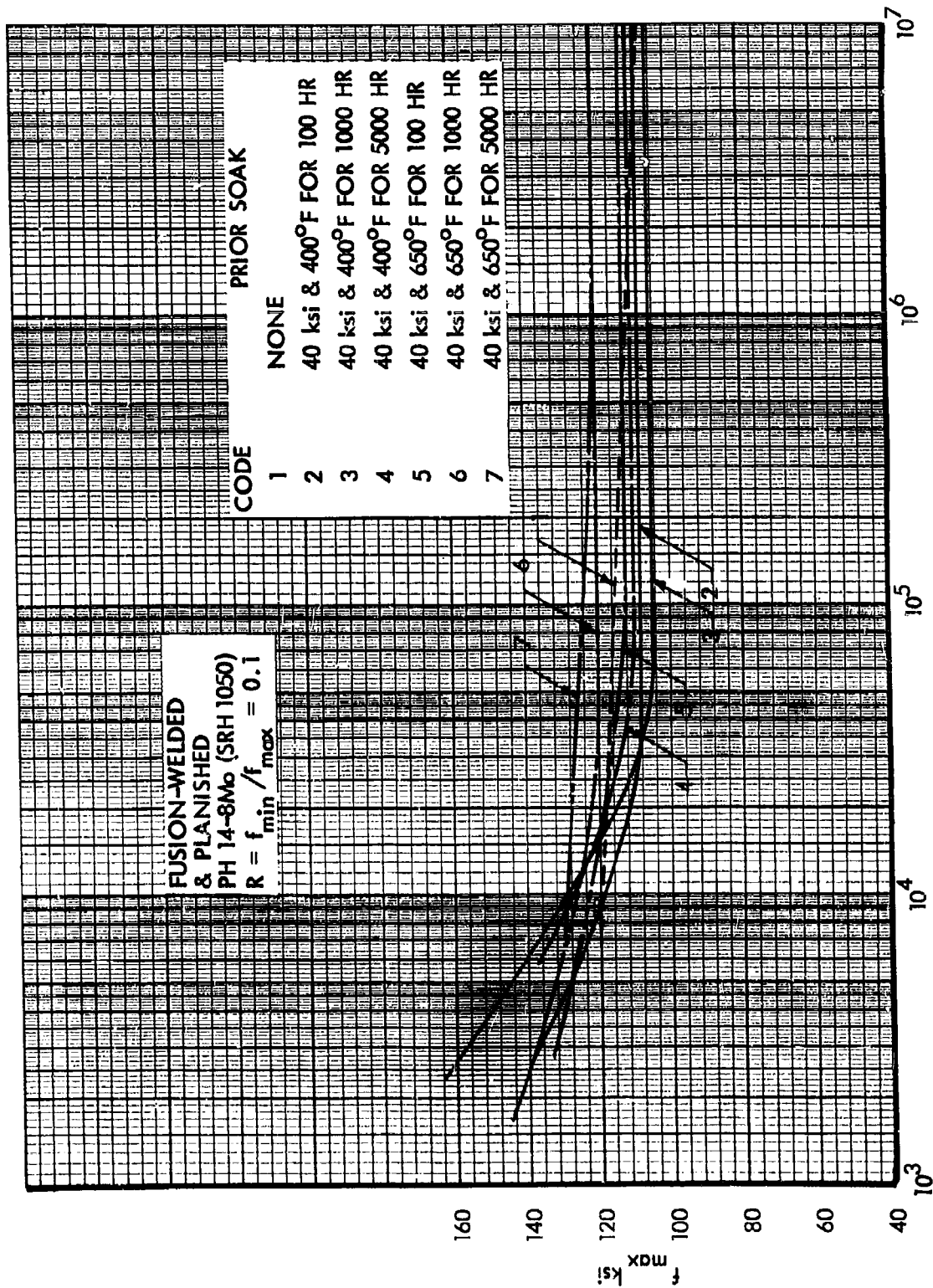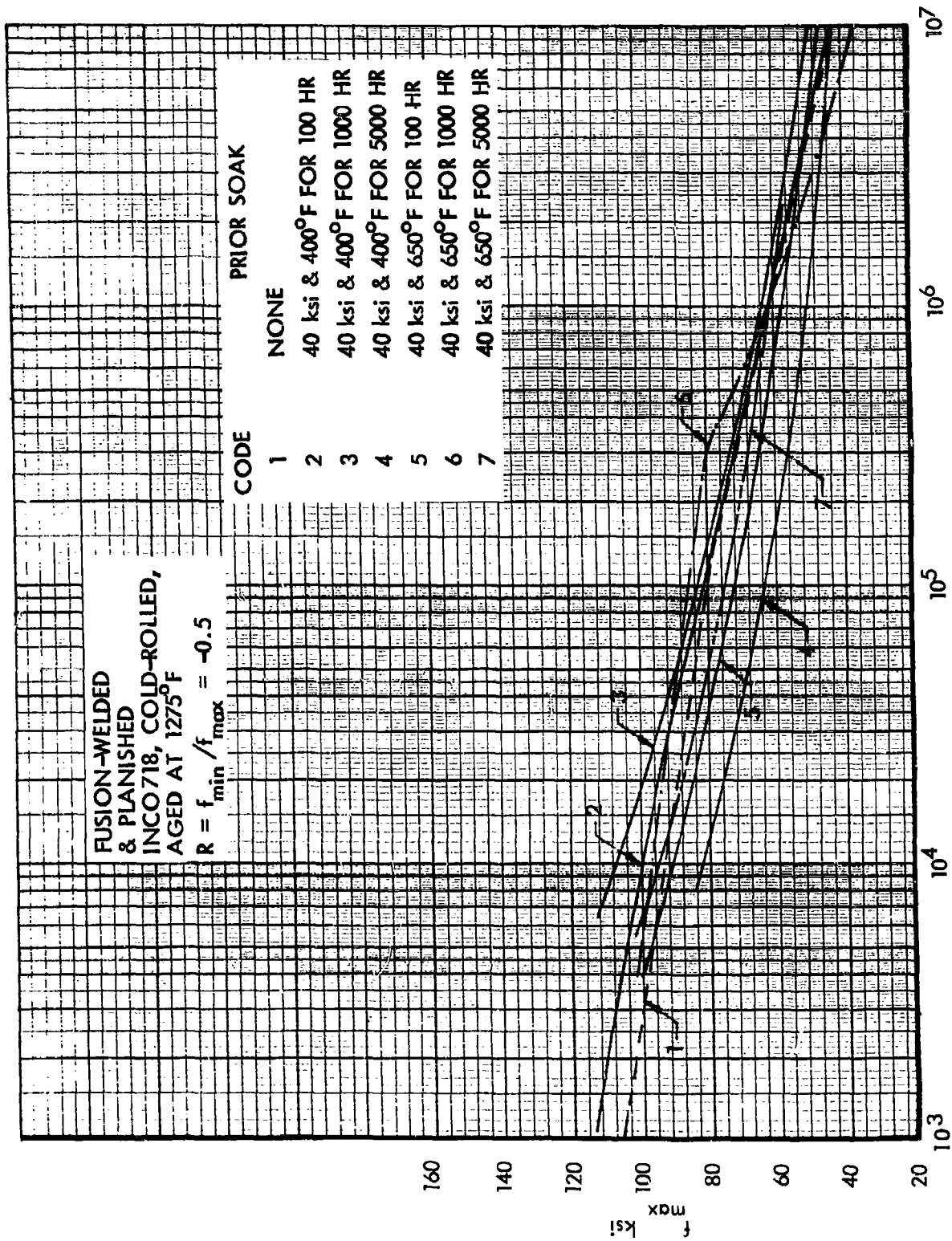
Figure 197. Effects of Prior Soak on S-N Curves at 650°F, Fusion-Welded PH14-8Mo, R = Constant

275

Figure 198. Effects of Prior Soak on S-N Curves at 650°F, Fusion-Welded PH14-8Mo, R = Constant

CENTER-NOTCHED
INCO 718, COLD-ROLLED,
AGED AT 1275°F
$R = f_{min}/f_{max} = 0.1$
$f_{net} = 1.2 f_{gross}$

CODE	PRIOR SOAK
1	NONE
2	40 ksi & 400°F FOR 100 HR
3	40 ksi & 400°F FOR 1000 HR
4	40 ksi & 400°F FOR 5000 HR
5	40 ksi & 650°F FOR 100 HR
6	40 ksi & 650°F FOR 1000 HR
7	40 ksi & 650°F FOR 5000 HR

f_{max}, ksi - GROSS AREA

CYCLES TO FAILURE
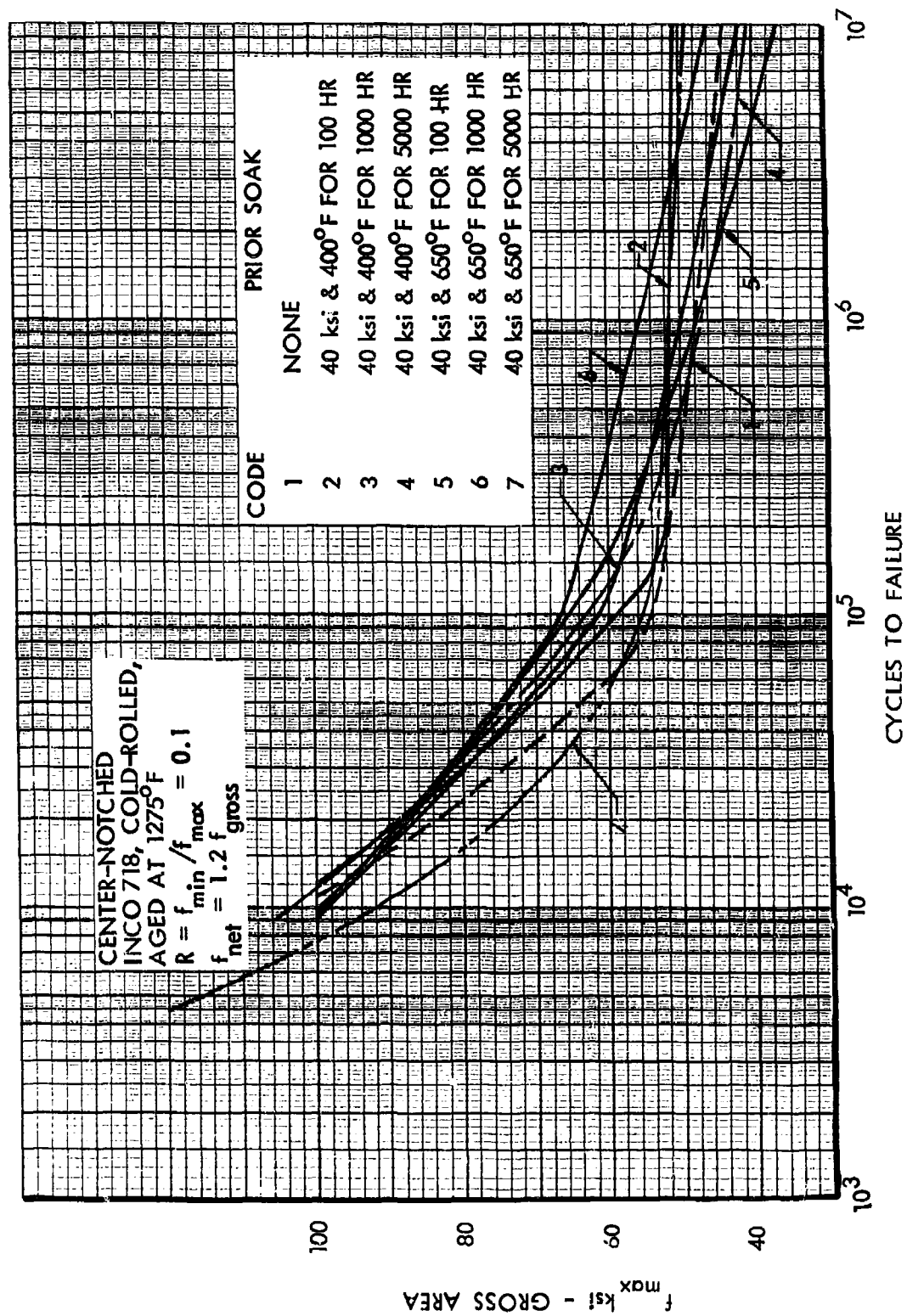
Figure 199. Effects of Prior Soak on S-N Curves at Room Temperature, Center-Notched INCO 718, R = Constant

277

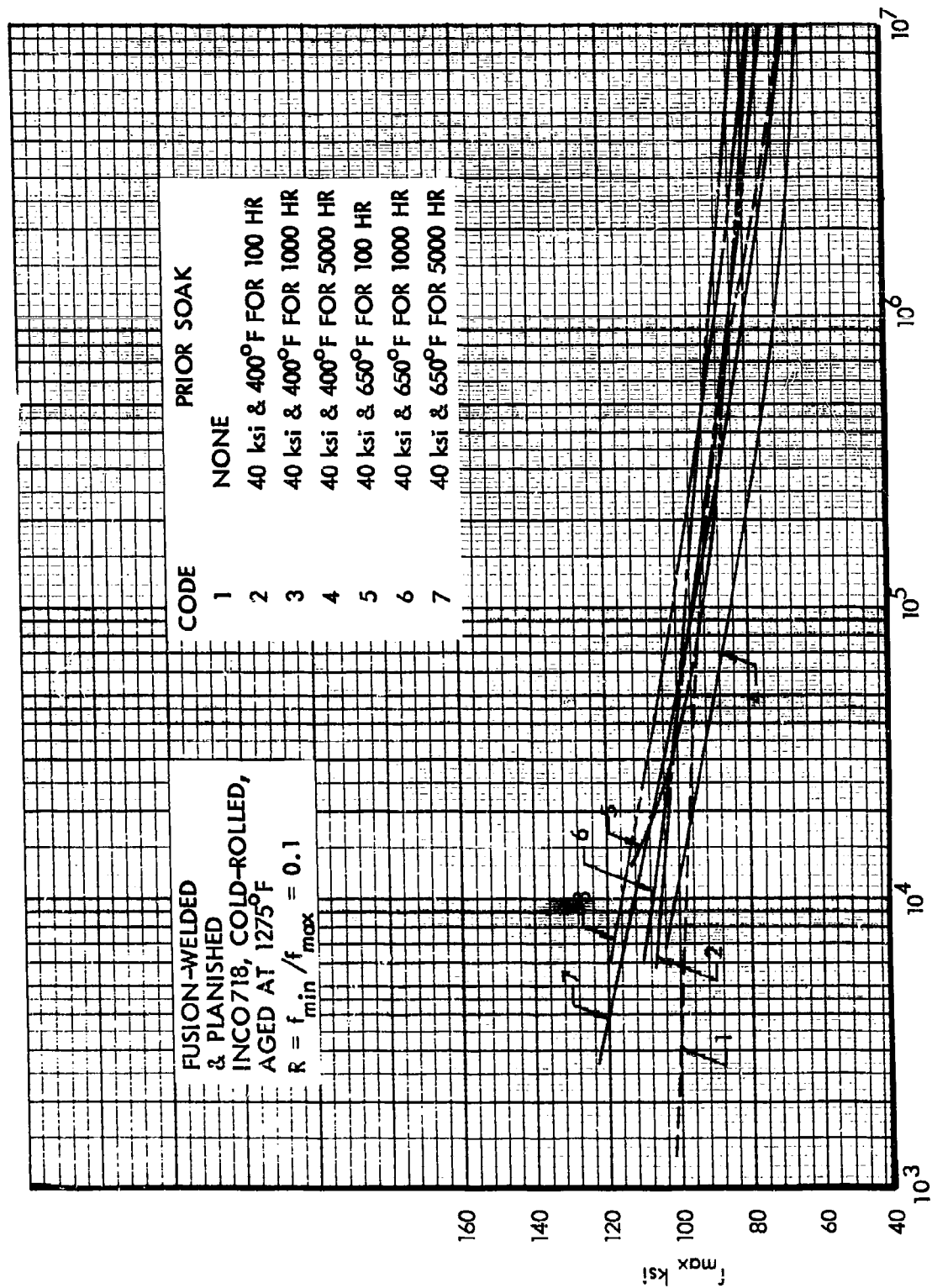Figure 200. Effects of Prior Soak on S-N Curves at Room Temperature, Center-Notched INCO 718, R = Constant
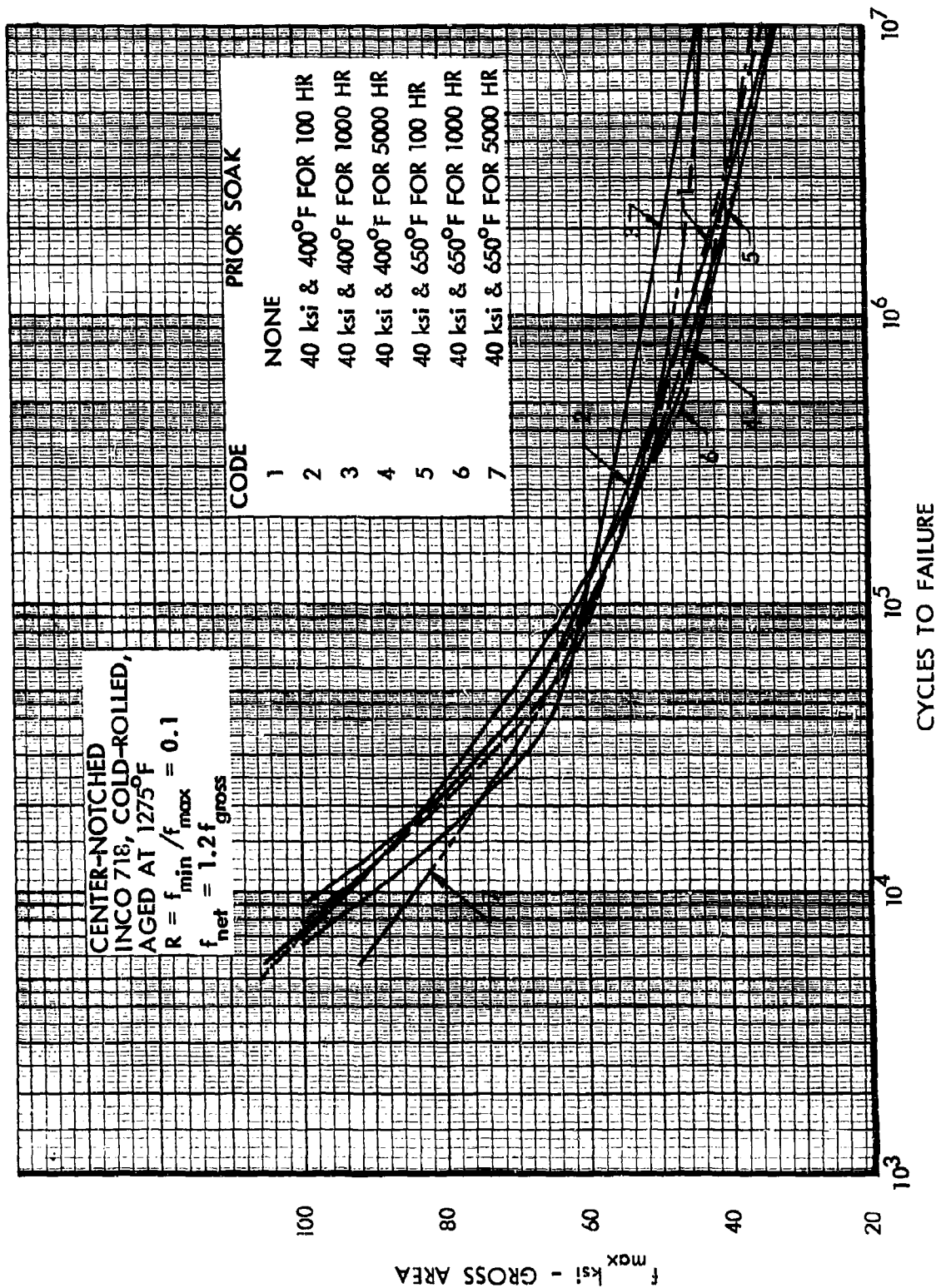
Figure 201. Effects of Prior Soak on S-N Curves at 400°F, Center-Notched INCO 718, R = Constant

Figure 202.   Effects of Prior Soak on S-N Curves at 400°F, Center-Notched INCO 718, R = Constant

The chart contains the following labels:

CENTER-NOTCHED
INCO 718, COLD-ROLLED,
AGED AT 1275°F
$R = f_{min}/f_{max} = -0.5$
$f_{net} = 1.2\ f_{gross}$

CODE	PRIOR SOAK
1	NONE
2	40 ksi & 400°F FOR 100 HR
3	40 ksi & 400°F FOR 1000 HR
4	40 ksi & 400°F FOR 5000 HR
5	40 ksi & 650°F FOR 100 HR
6	40 ksi & 650°F FOR 1000 HR
7	40 ksi & 650°F FOR 5000 HR

CYCLES TO FAILURE

f_{max}, ksi - GROSS AREA

Figure 203. Effects of Prior Soak on S-N Curves at 650°F, Center-Notched INCO 718, R = Constant

281

Figure 204. Effects of Prior Soak on S-N Curves at 650°F, Center-Notched INCO 718, R = Constant

The chart contains the following legend:

CENTER-NOTCHED
INCO 718, COLD-ROLLED,
AGED AT 1275°F

$R = f_{min} / f_{max} = -0.5$

$f_{net} = 1.2 f_{gross}$

CODE	PRIOR SOAK
1	NONE
2	40 ksi & 400°F FOR 100 HR
3	40 ksi & 400°F FOR 1000 HR
4	40 ksi & 400°F FOR 5000 HR
5	40 ksi & 650°F FOR 100 HR
6	40 ksi & 650°F FOR 1000 HR
7	40 ksi & 650°F FOR 5000 HR

Axis labels:
CYCLES TO FAILURE
f_{max}, ksi - GROSS AREA

Figure 205. Effects of Prior Soak on S-N Curves at Room Temperature, Unnotched INCO 718, R = Constant

283

Figure 206. Effects of Prior Soak on S–N Curves at Room Temperature, Unnotched INCO 718, R = Constant

Figure 207. Effects of Prior Soak on S-N Curves at 400°F, Unnotched INCO 718, R = Constant

285

Figure 208. Effects of Prior Soak on S-N Curves at 400°F, Unnotched INCO 718, R = Constant

Figure 209. Effects of Prior Soak on S-N Curves at 650°F, Unnotched INCO 718, R = Constant

Figure 210.   Effects of Prior Soak on S-N Curves at 650°F, Unnotched INCO 718, R = Constant

288

Figure 211. Effects of Prior Soak on S-N Curves at Room Temperature, Fusion-Welded INCO 718, R = Constant

Figure 212.   Effects of Prior Soak on S-N Curves at Room Temperature, Fusion-Welded INCO 718, R = Constant

Figure 213. Effects of Prior Soak on S-N Curves at 400°F, Fusion-Welded INCO 718, R = Constant

291

Figure 214. Effects of Prior Soak on S-N Curves at 400°F, Fusion-Welded INCO 718, R = Constant

Figure 215. Effects of Prior Soak on S-N Curves at 650°F, Fusion-Welded INCO 718, R = Constant

293

CYCLES TO FAILURE
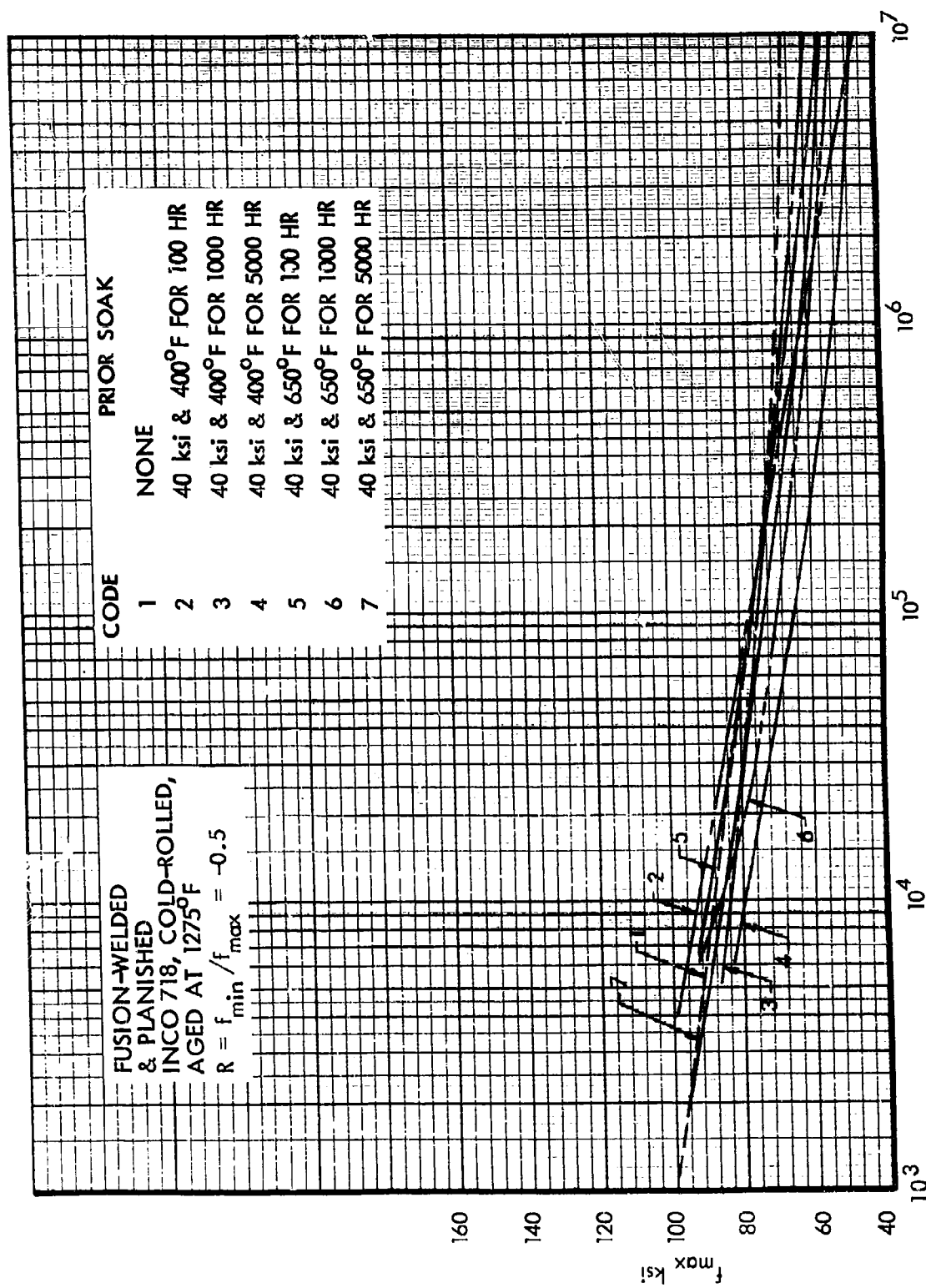
Figure 216.   Effects of Prior Soak on S-N Curves at 650°F, Fusion-Welded INCO 718, R = Constant

APPENDIX VII

COMPARATIVE S-N CURVES - CONSTANT MEAN STRESS

Volume II of the report presents S-N diagrams derived from sets of S-N curves for constant values of R which were drawn to represent the S-N data obtained in the basic constant load amplitude fatigue test program. These S-N diagrams have been used to define S-N curves for a constant mean stress of 25,000 psi for 8-1-1 duplex-annealed titanium specimens and 40,000 psi for specimens of PH14-8Mo (SRH 1050) steel and Inco 718 cold rolled 20 percent and aged. The S-N curves for constant mean stresses are more directly useful in many airframe design situations than the constant R curves.

The constant mean stress curves have been grouped by specimen material, geometry and test temperature and these groupings are presented in this Appendix. These groupings provide the basis for the more condensed representation of the data presented in the body of the report under Phase I. The location of these groupings is given in Table 37.

TABLE 37 LOCATION OF COMPARATIVE S-N CURVES - CONSTANT MEAN STRESS

f_{mean} = 25,000 psi for 8-1-1 titanium and 40,000 psi for PH14-8Mo
and INCO 718

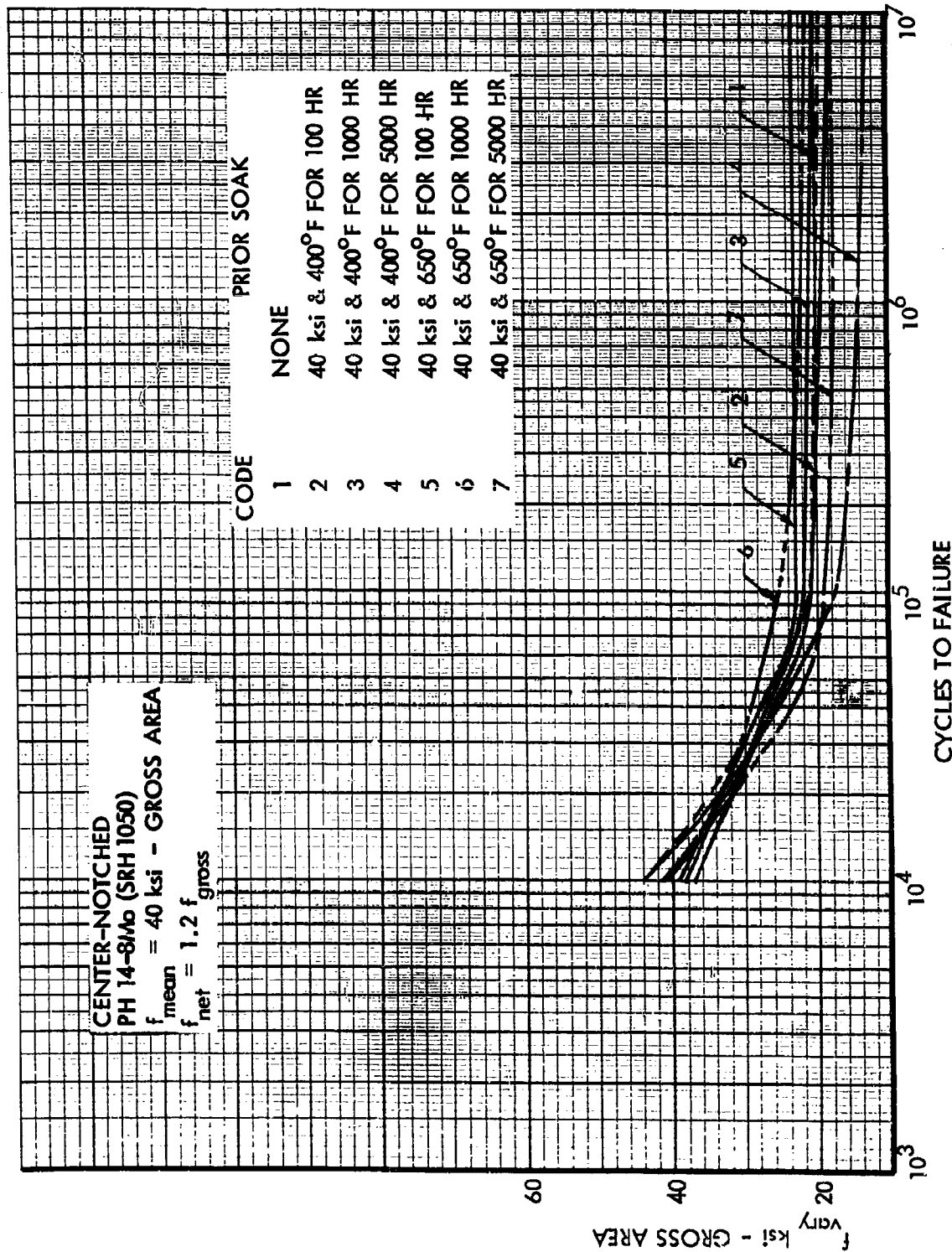| Material	Specimen Configuration	Test Temp (°F)	Curves Plotted in Figure
8-1-1 Titanium Duplex Annealed	Center-Notched	Room 400 650	217 218 219
	Unnotched	Room 400 650	220 221 222
	Fusion-Welded and Planished	Room 400 650	223 224 225
PH14-8Mo (SRH 1050)	Center-Notched	Room 400 650	226 227 228
	Unnotched	Room 400 650	229 230 231
	Fusion-Welded and Planished	Room 400 650	232 233 234
INCO 718, Cold Rolled Aged at 1275°F	Center-Notched	Room 400 650	235 236 237
	Unnotched	Room 400 650	238 239 240
	Fusion-Welded and Planished	Room 400 650	241 242 243

Figure 217.   Effects of Prior Soak on S-N Curves at Room Temperature, Center-Notched 8-1-1 Titanium, f_{mean} = Constant
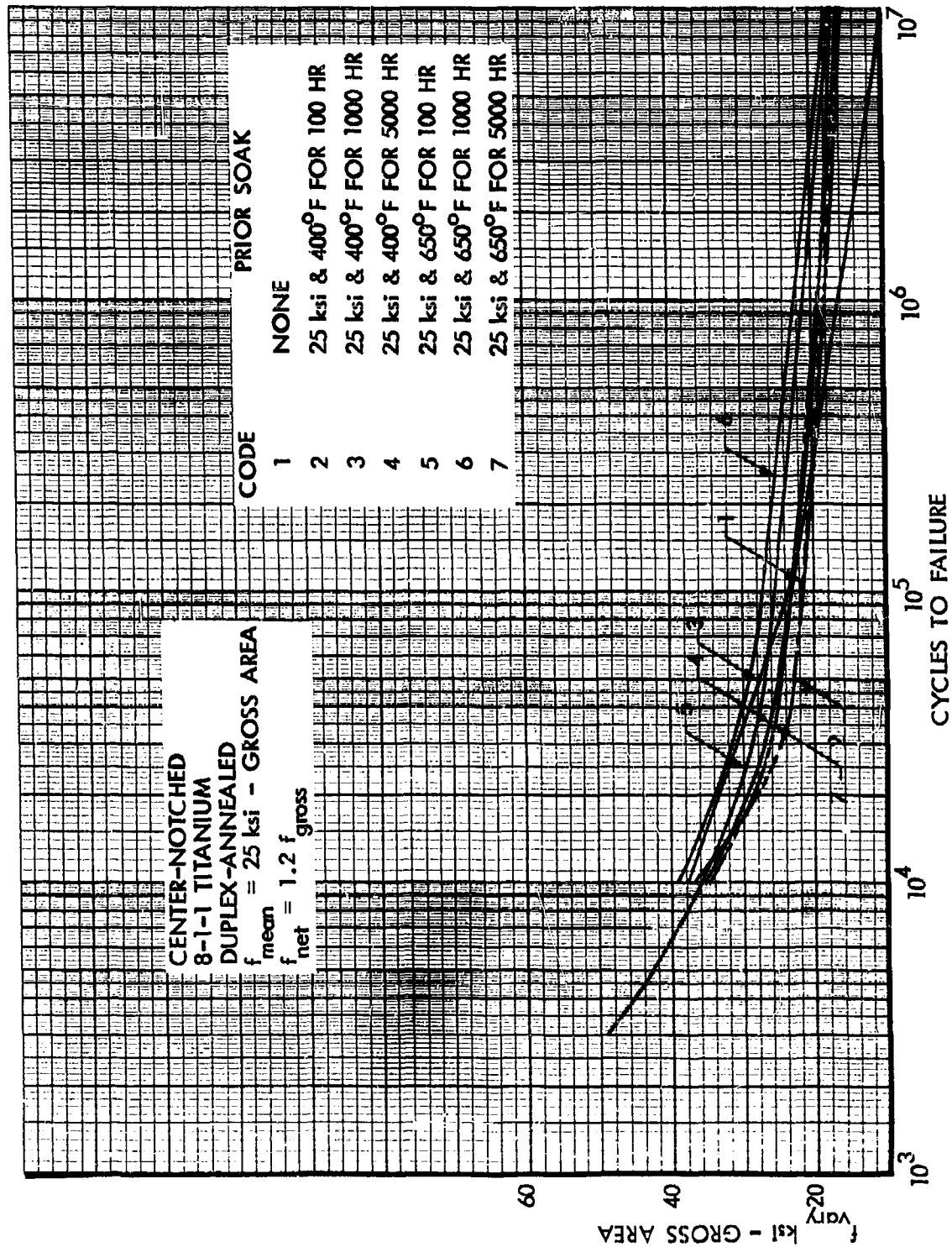
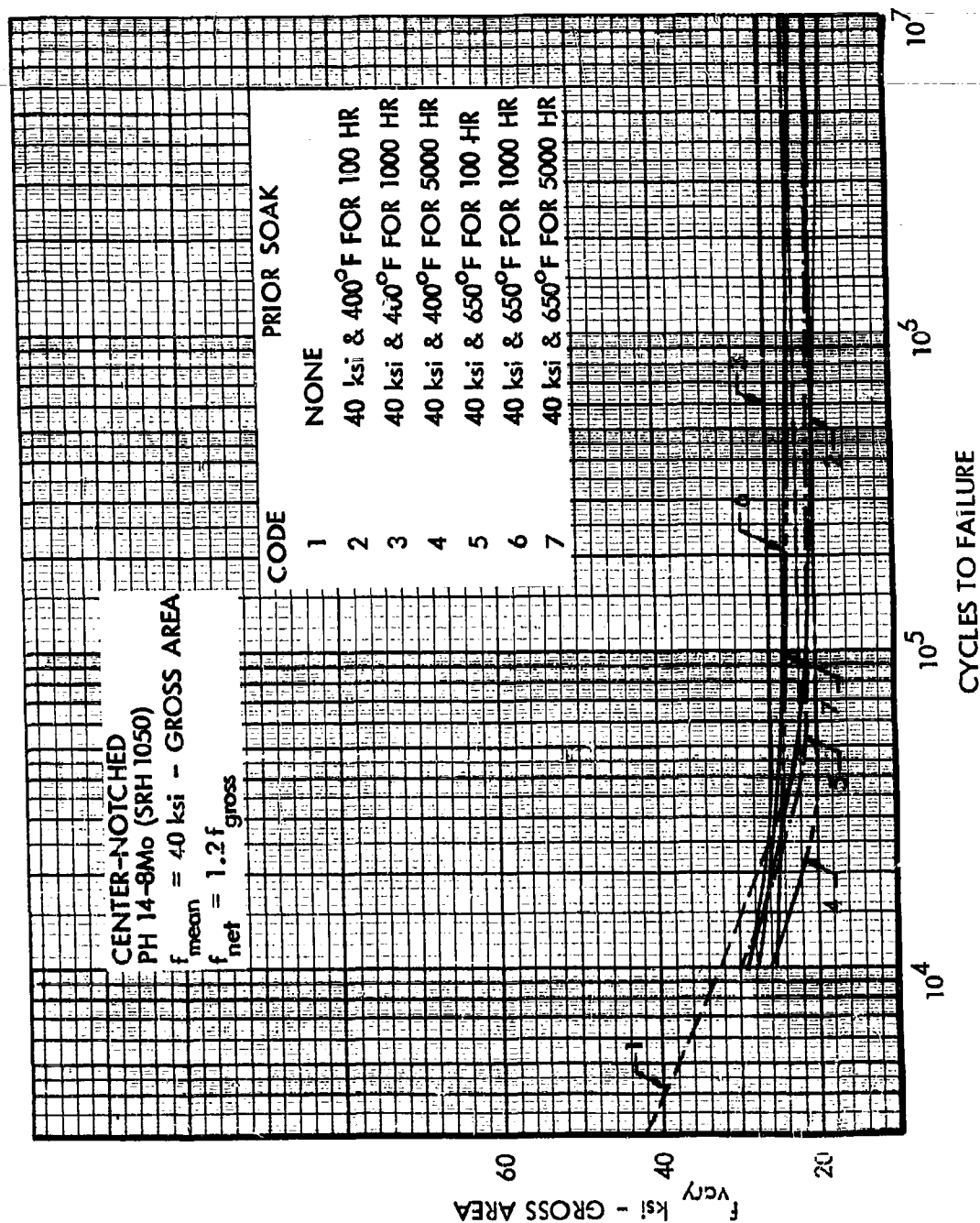Figure 218.   Effects of Prior Soak on S-N Curves at 400°F, Center-Notched 8-1-1 Titanium, f_{mean} = Constant
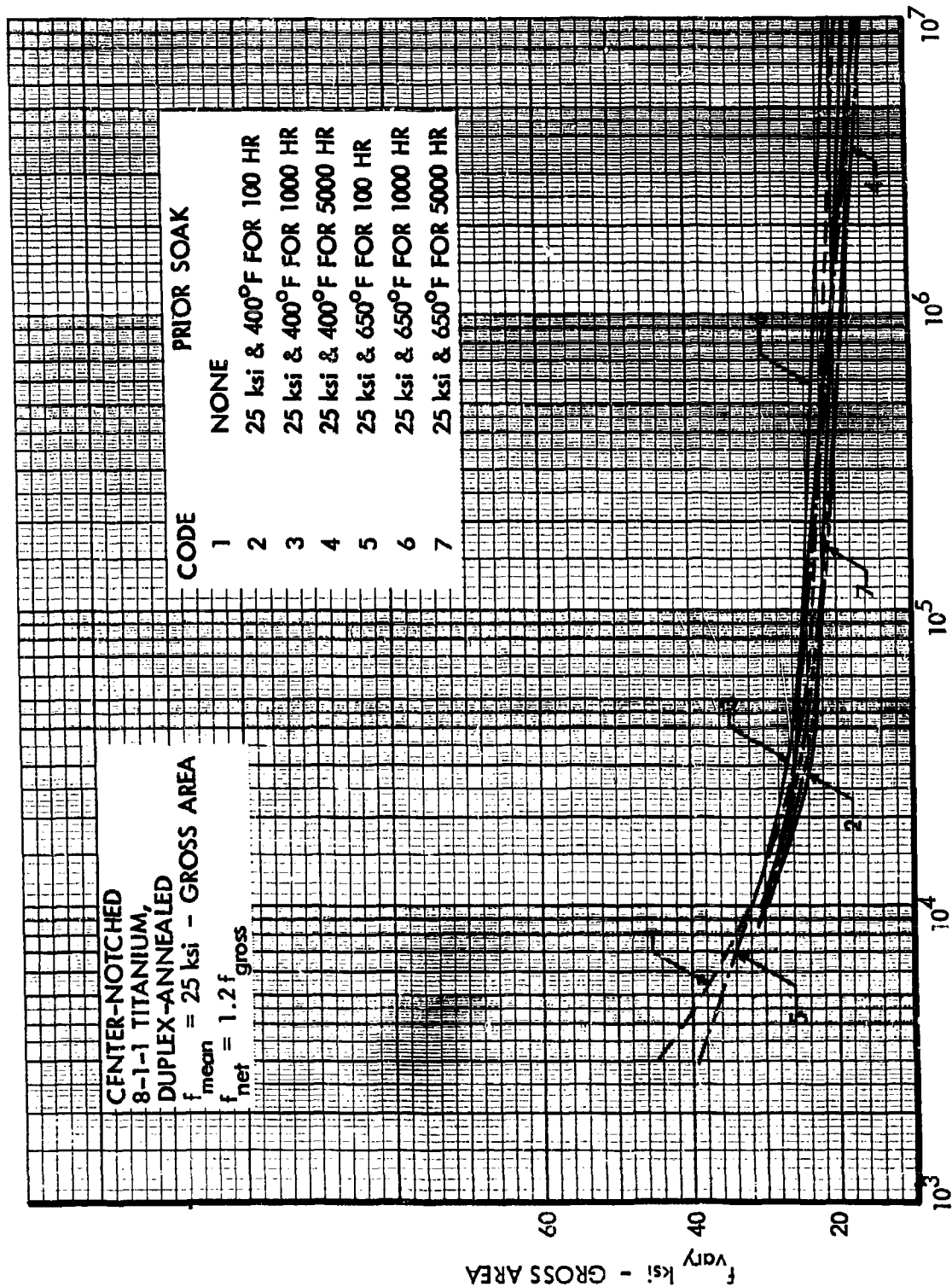
Figure 219. Effects of Prior Soak on S-N Curves at 650°F, Center-Notched 8-1-1 Titanium, f_{mean} = Constant
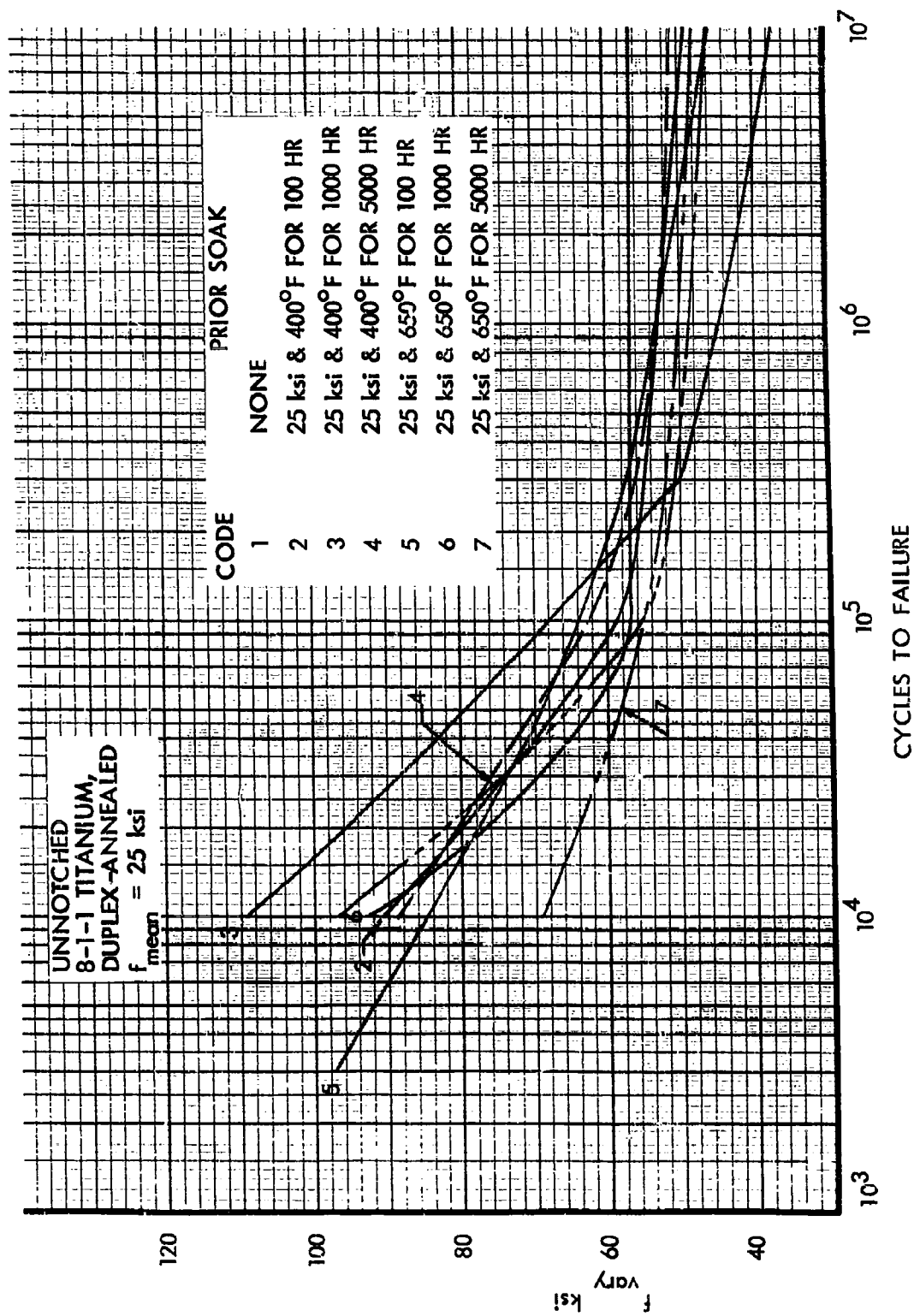
Figure 220. Effects of Prior-Soak on S-N Curves at Room Temperature, Unnotched 8-1-1 Titanium, f_{mean} = Constant
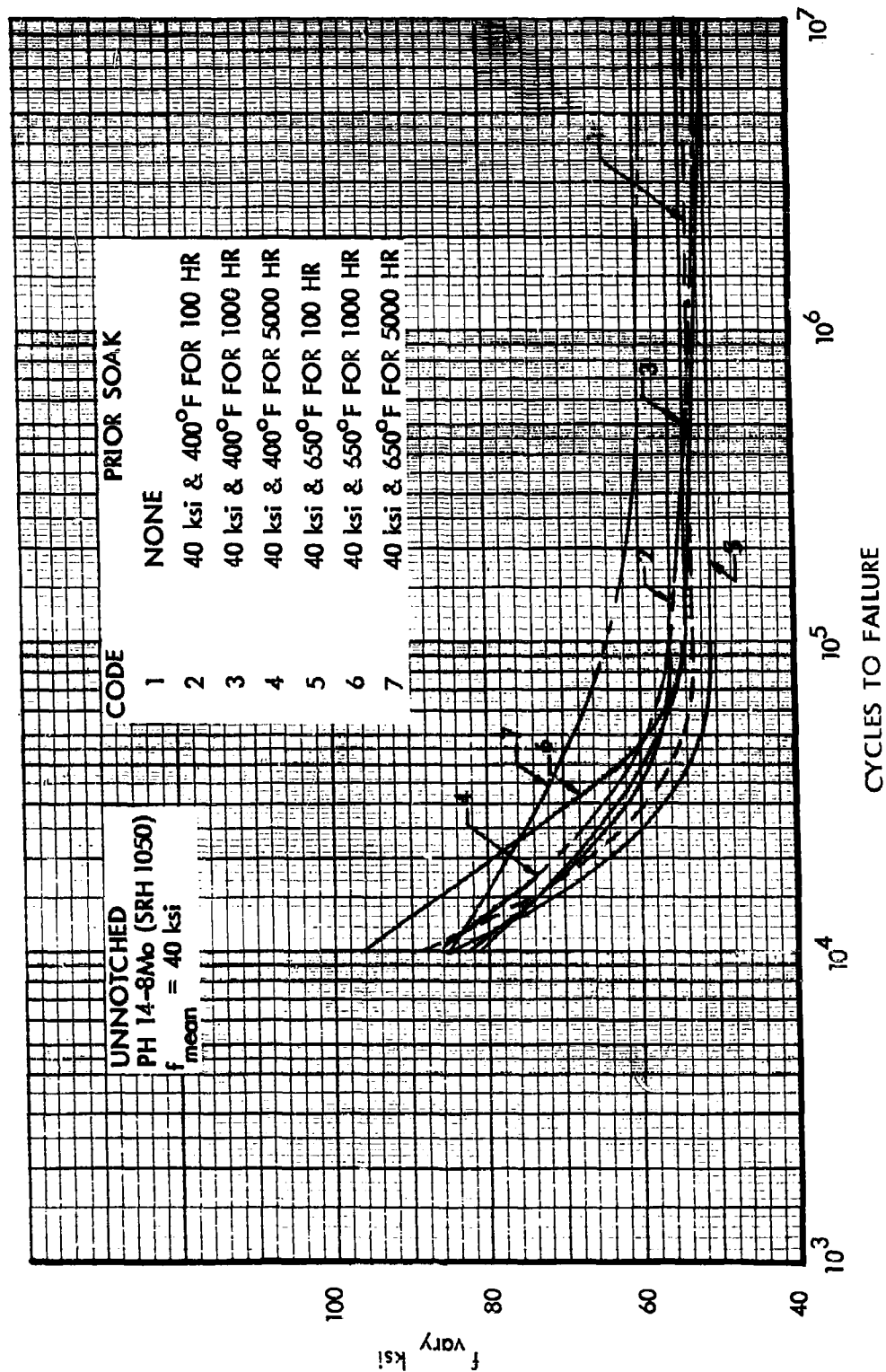
300
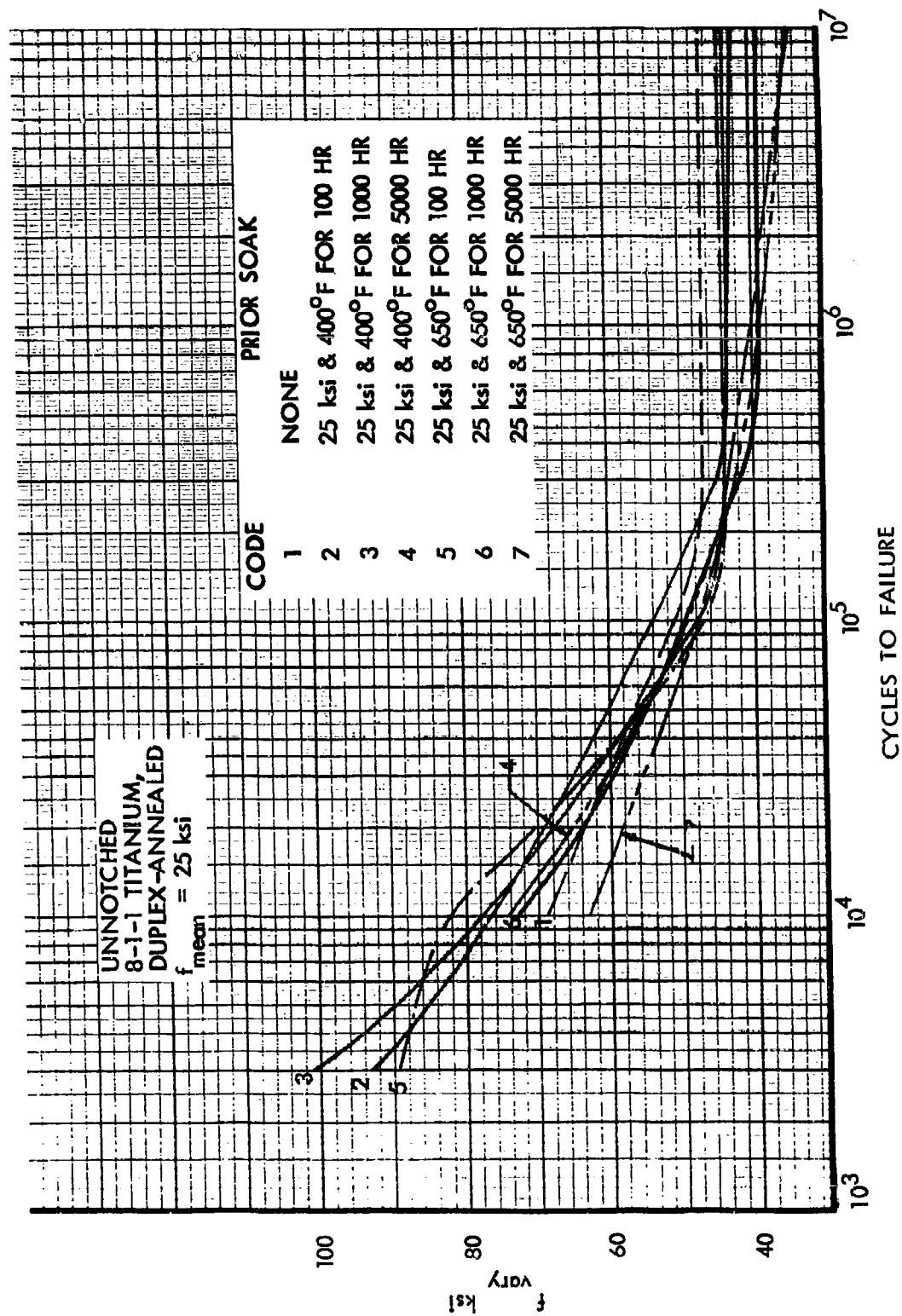
Figure 221. Effects of Prior Soak on S-N Curves at 400°F, Unnotched 8-1-1 Titanium, f_{mean} = Constant

301
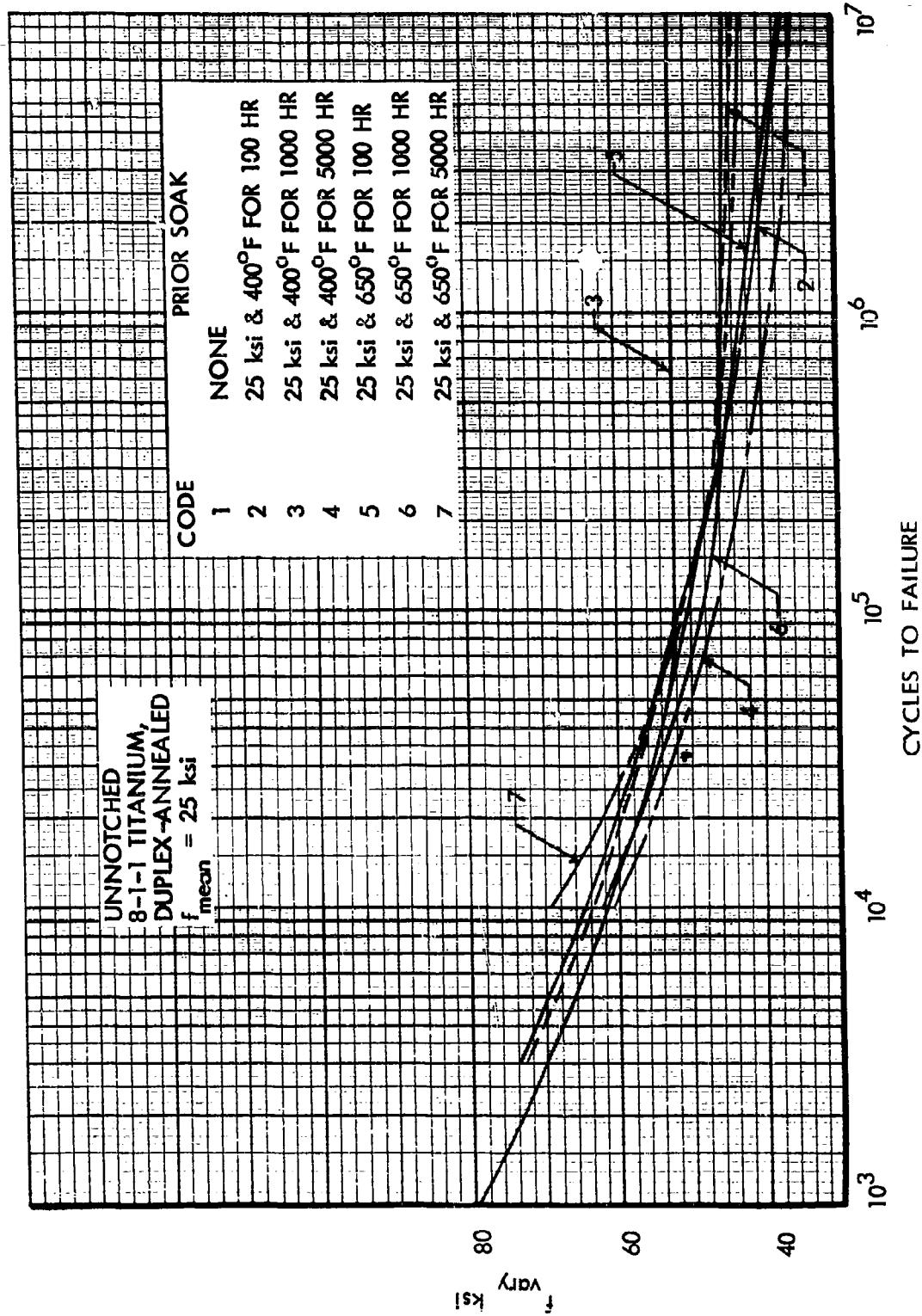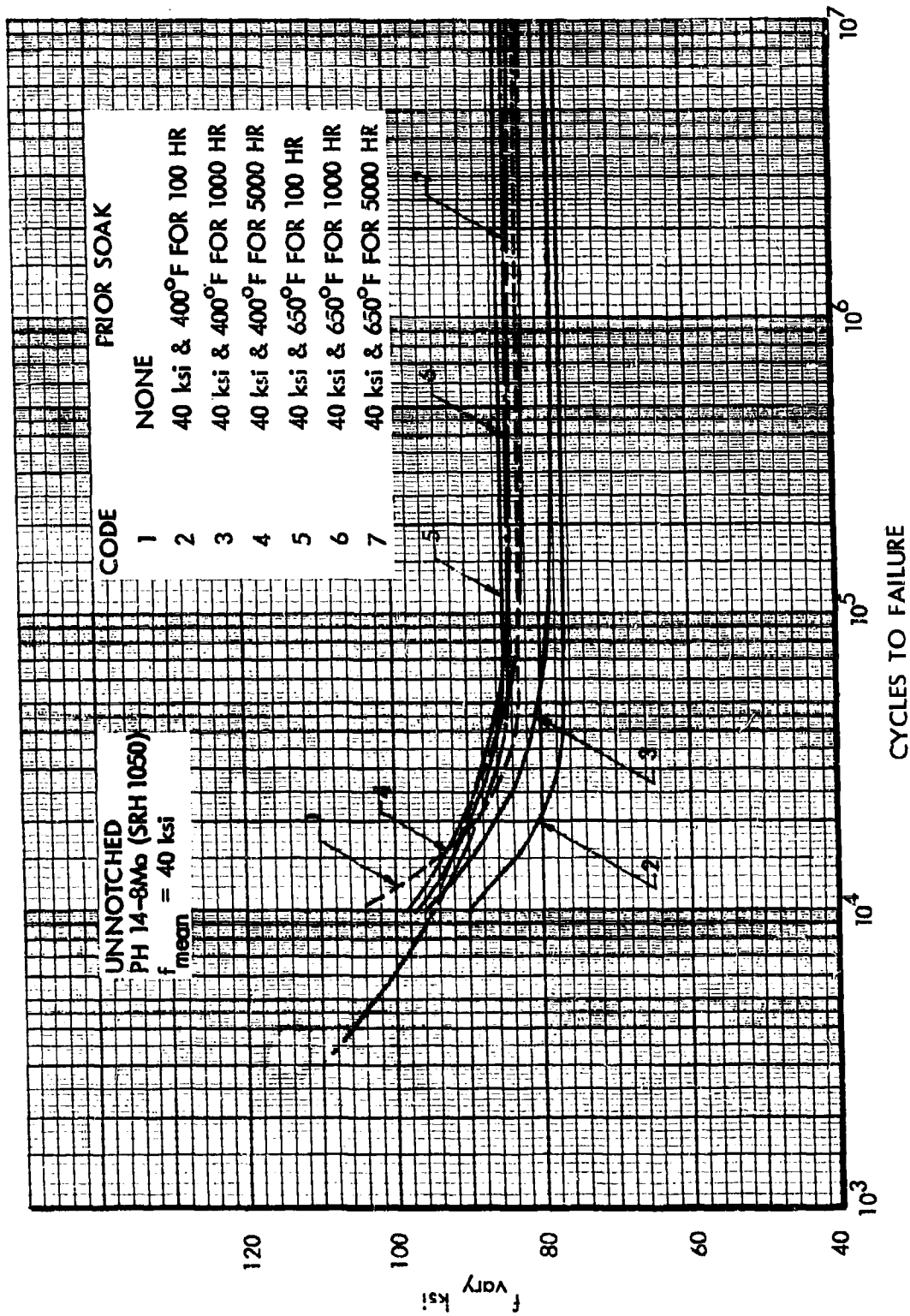
Figure 222. Effects of Prior Soak on S-N Curves at 650°F, Unnotched 8-1-1 Titanium, f_{mean} = Constant
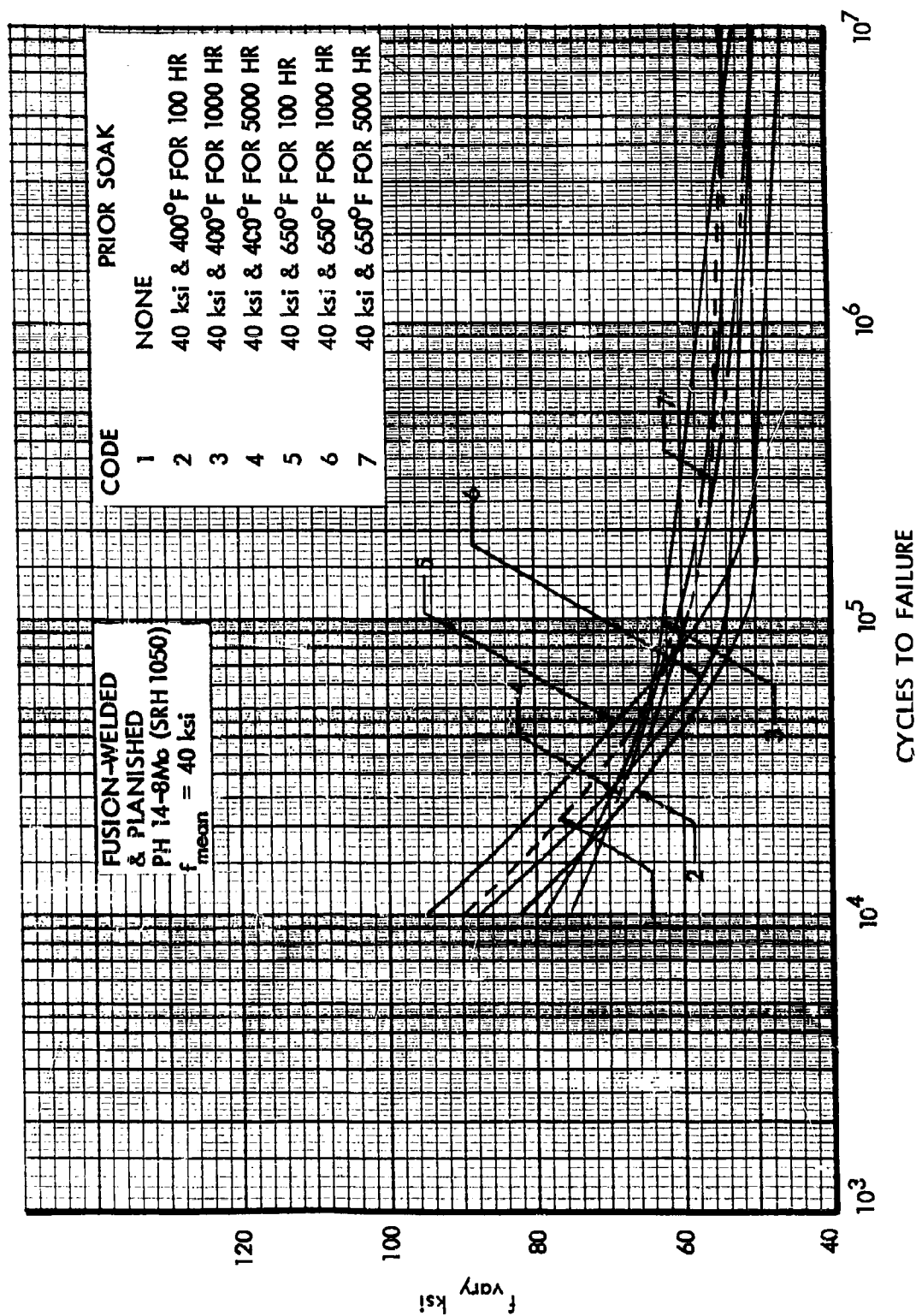
302
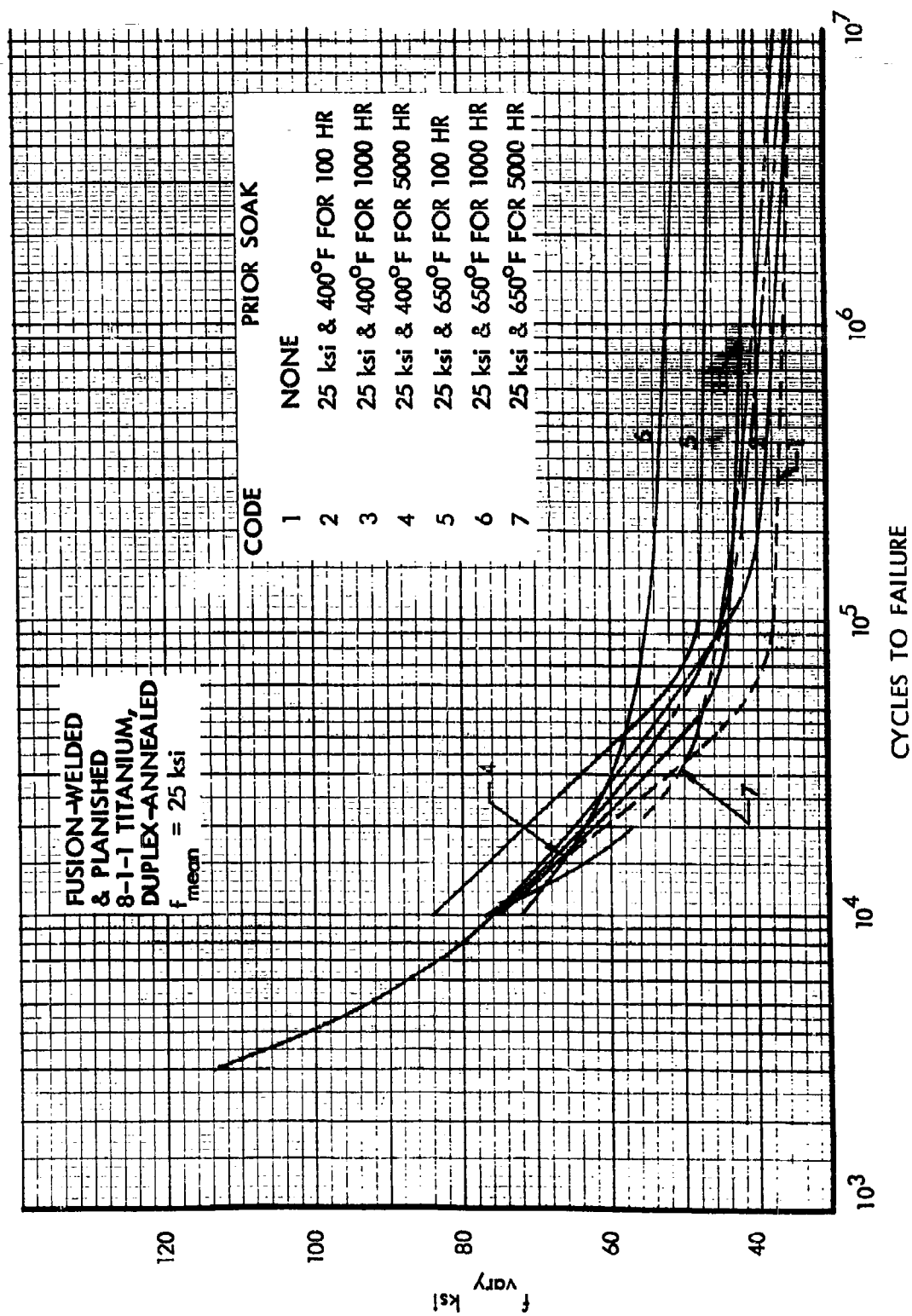
Figure 223.   Effects of Prior Soak on S-N Curves at Room Temperature, Fusion-Welded 8-1-1 Titanium, f_{mean} = Constant
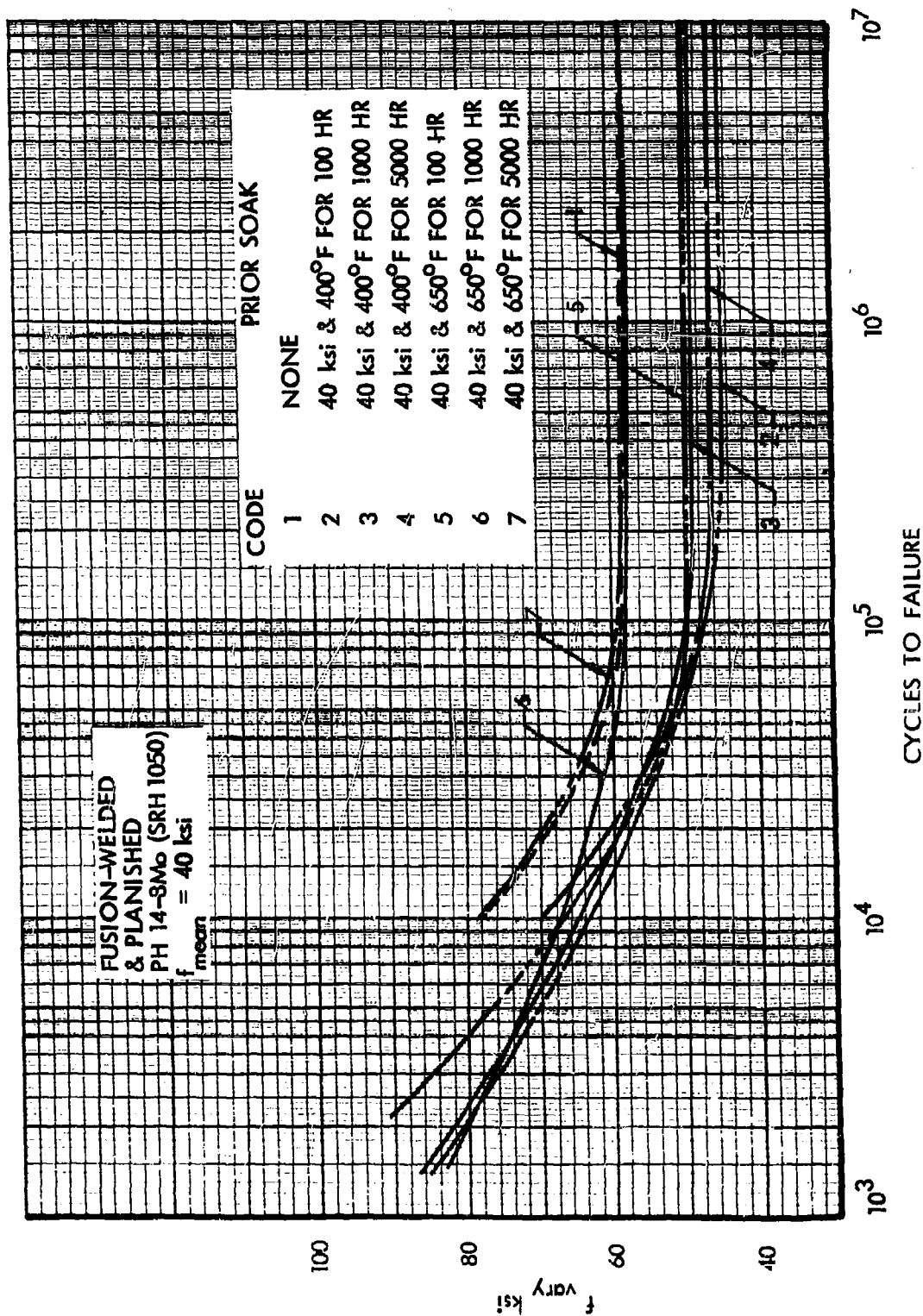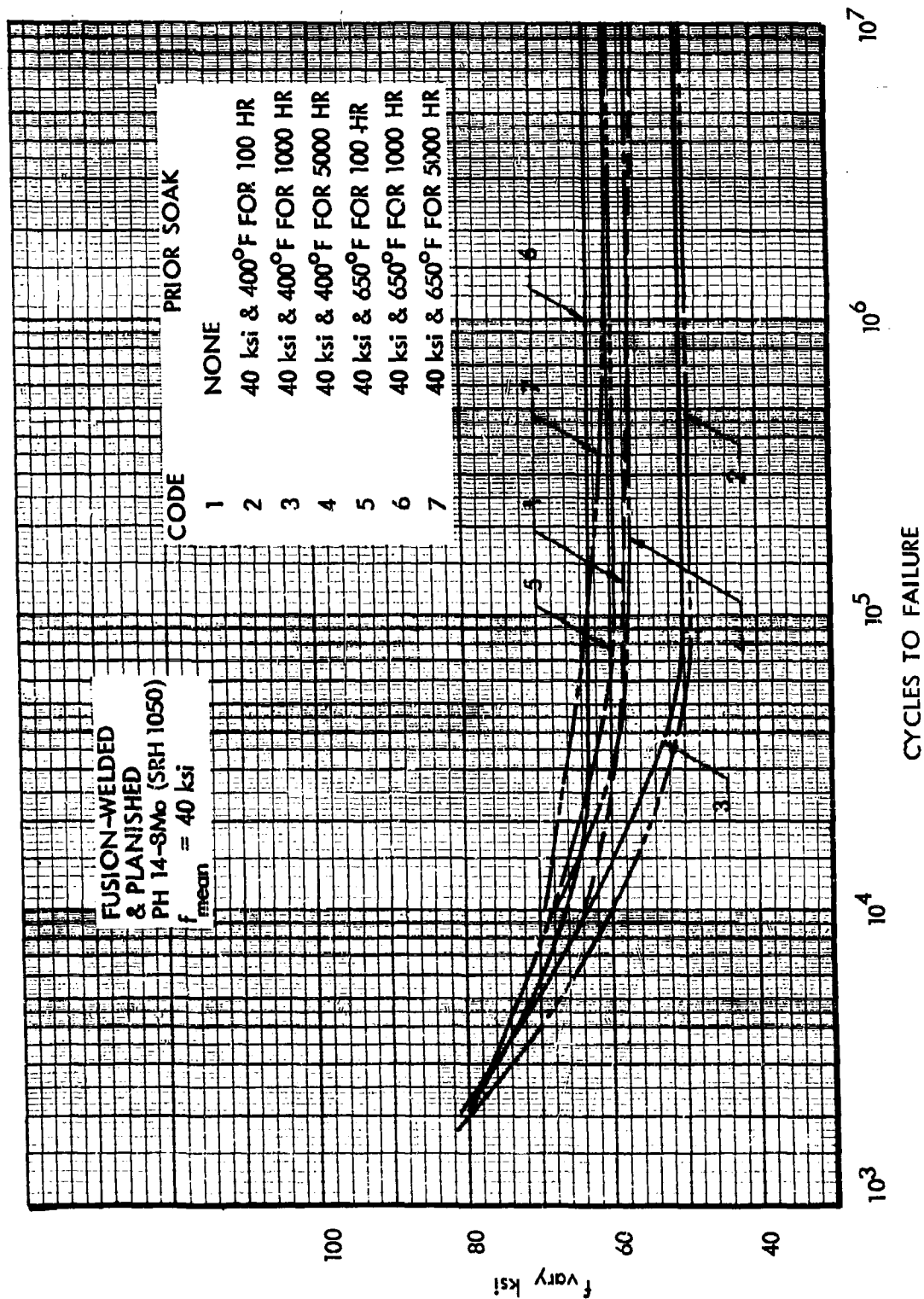
303
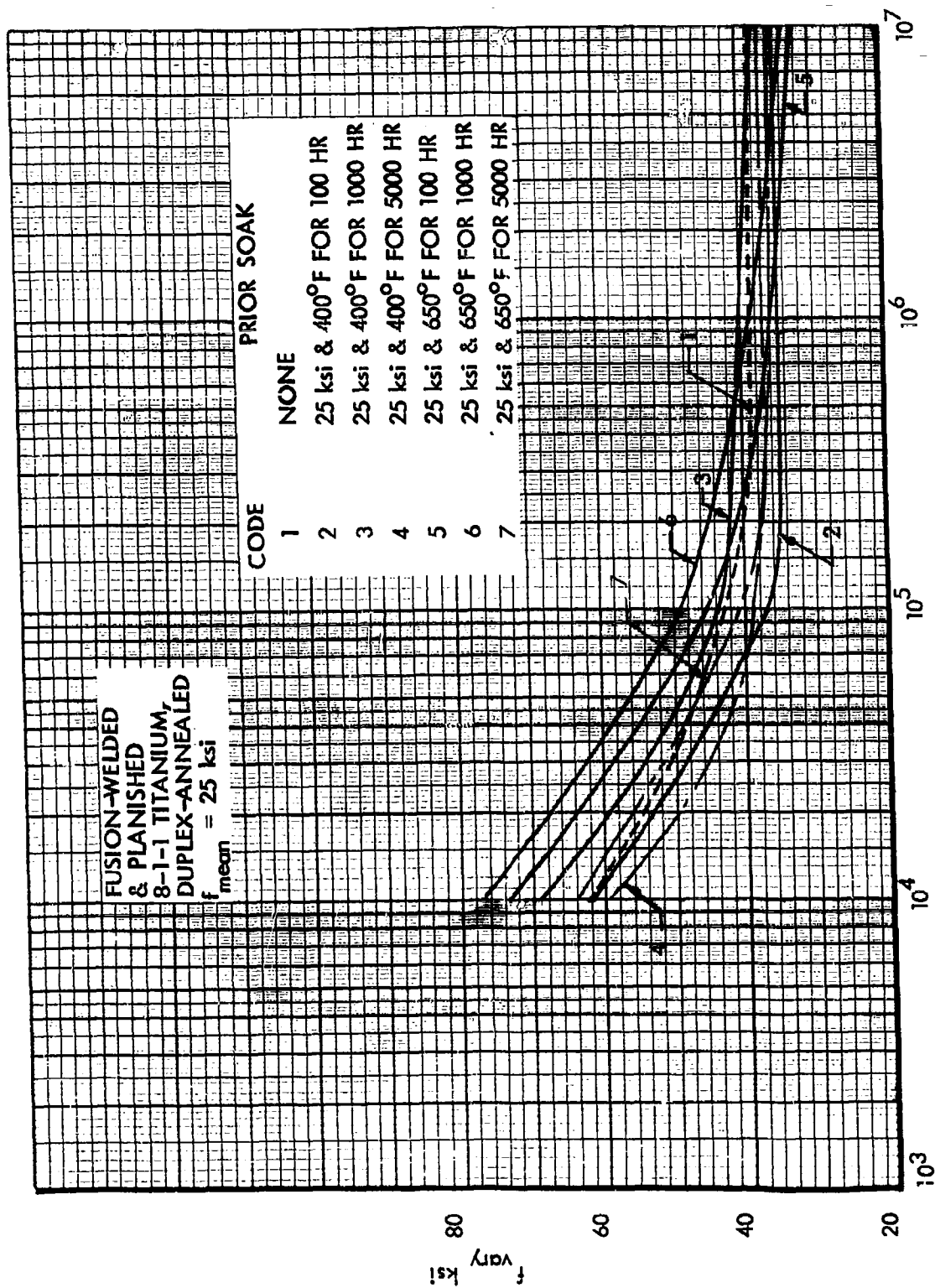
Figure 224. Effects of Prior Soak on S-N Curves at 400°F, Fusion-Welded 8-1-1 Titanium, f_{mean} = Constant
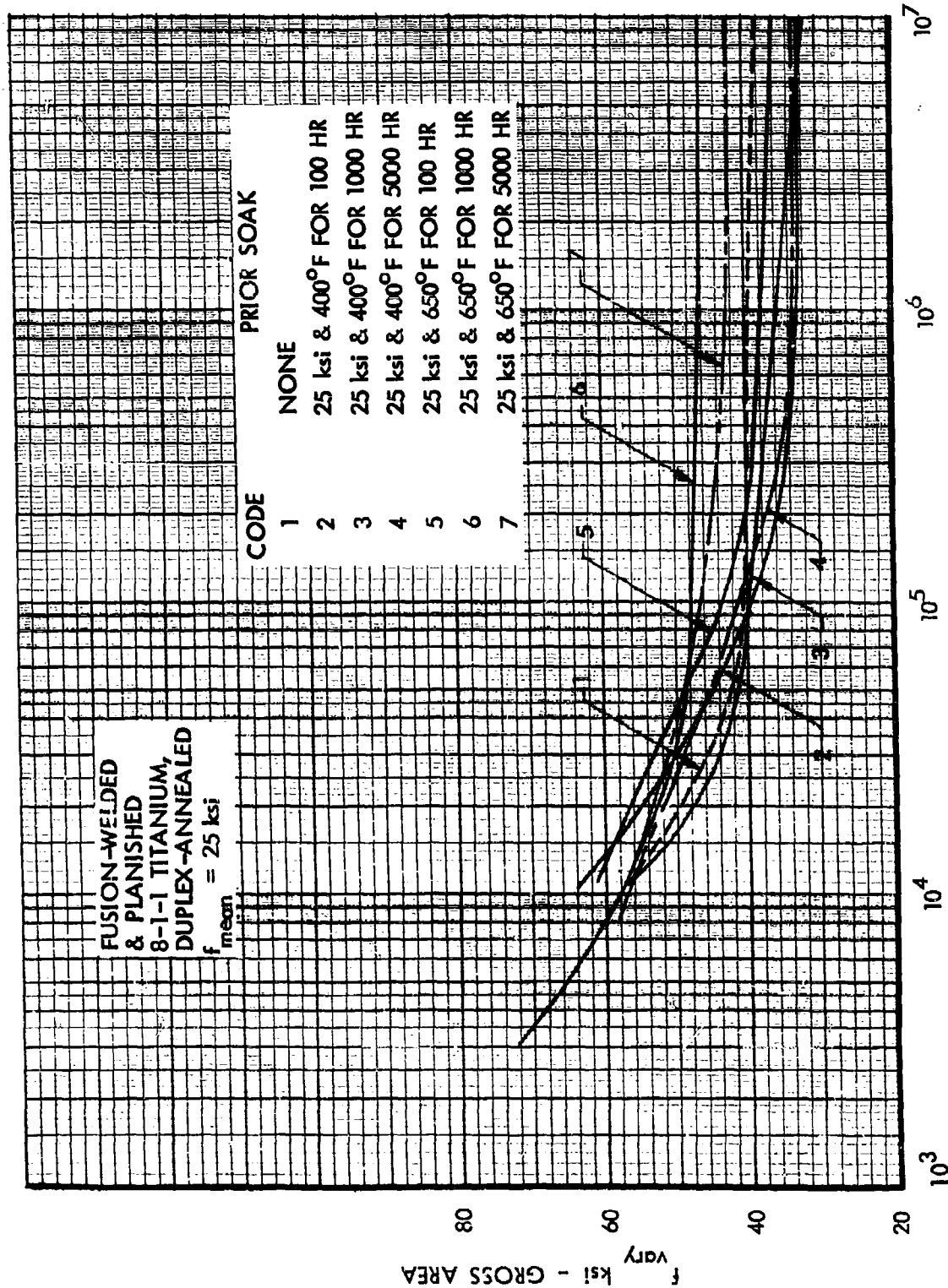
Figure 225.   Effects of Prior Soak on S-N Curves at 550°F, Fusion-Welded 8-1-1 Titanium, f_{mean} = Constant

305

CENTER-NOTCHED
PH 14-8Mo (SRH 1050)
f_{mean} = 40 ksi - GROSS AREA
f_{net} = 1.2 f_{gross}

CODE	PRIOR SOAK
1	NONE
2	40 ksi & 400°F FOR 100 HR
3	40 ksi & 400°F FOR 1000 HR
4	40 ksi & 400°F FOR 5000 HR
5	40 ksi & 650°F FOR 100 HR
6	40 ksi & 650°F FOR 1000 HR
7	40 ksi & 650°F FOR 5000 HR

CYCLES TO FAILURE

f_{vary} ksi - GROSS AREA
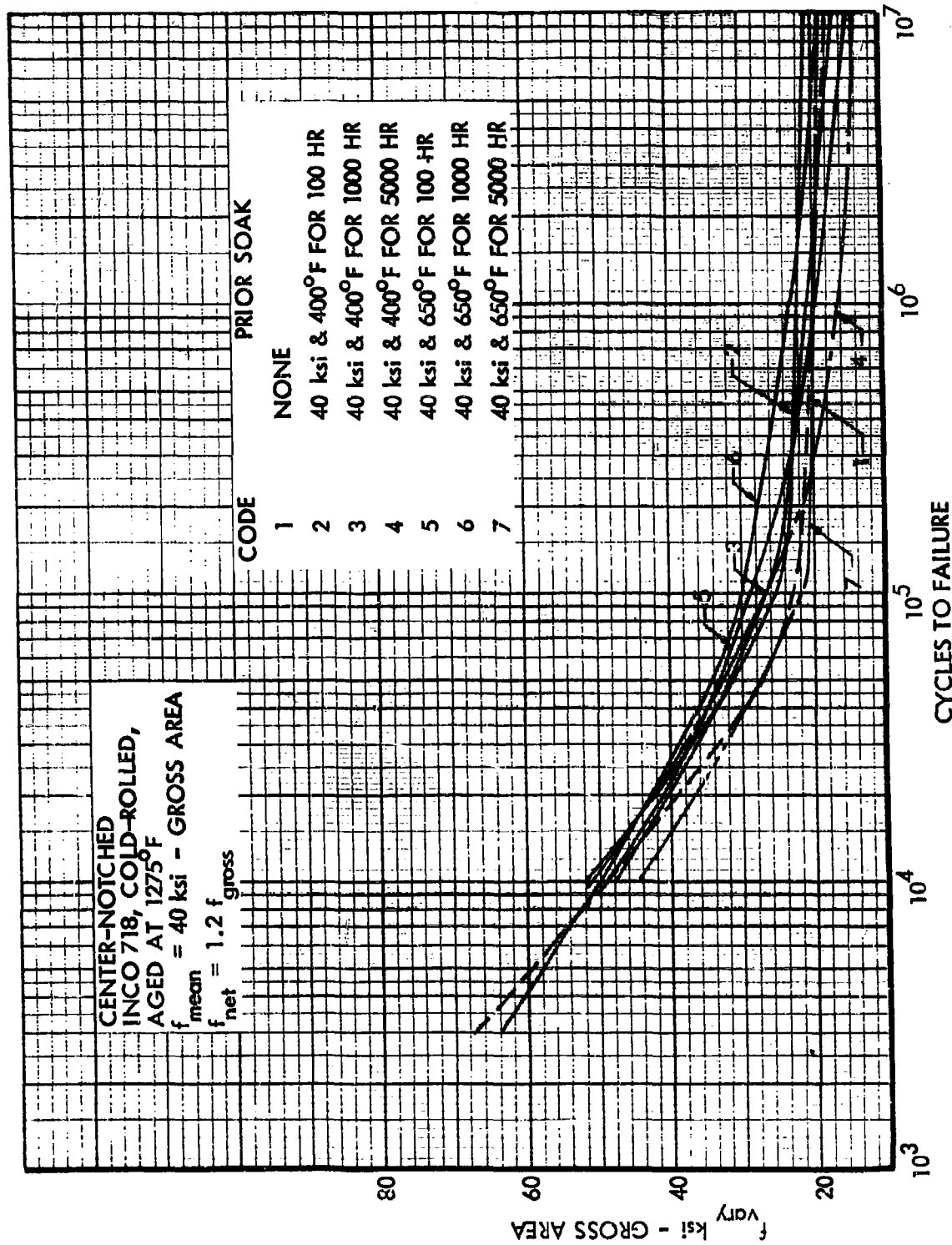
Figure 226. Effects of Prior-Soak on S-N Curves at Room Temperature, Center-Notched PH14-8Mo, f_{mean} = Constant
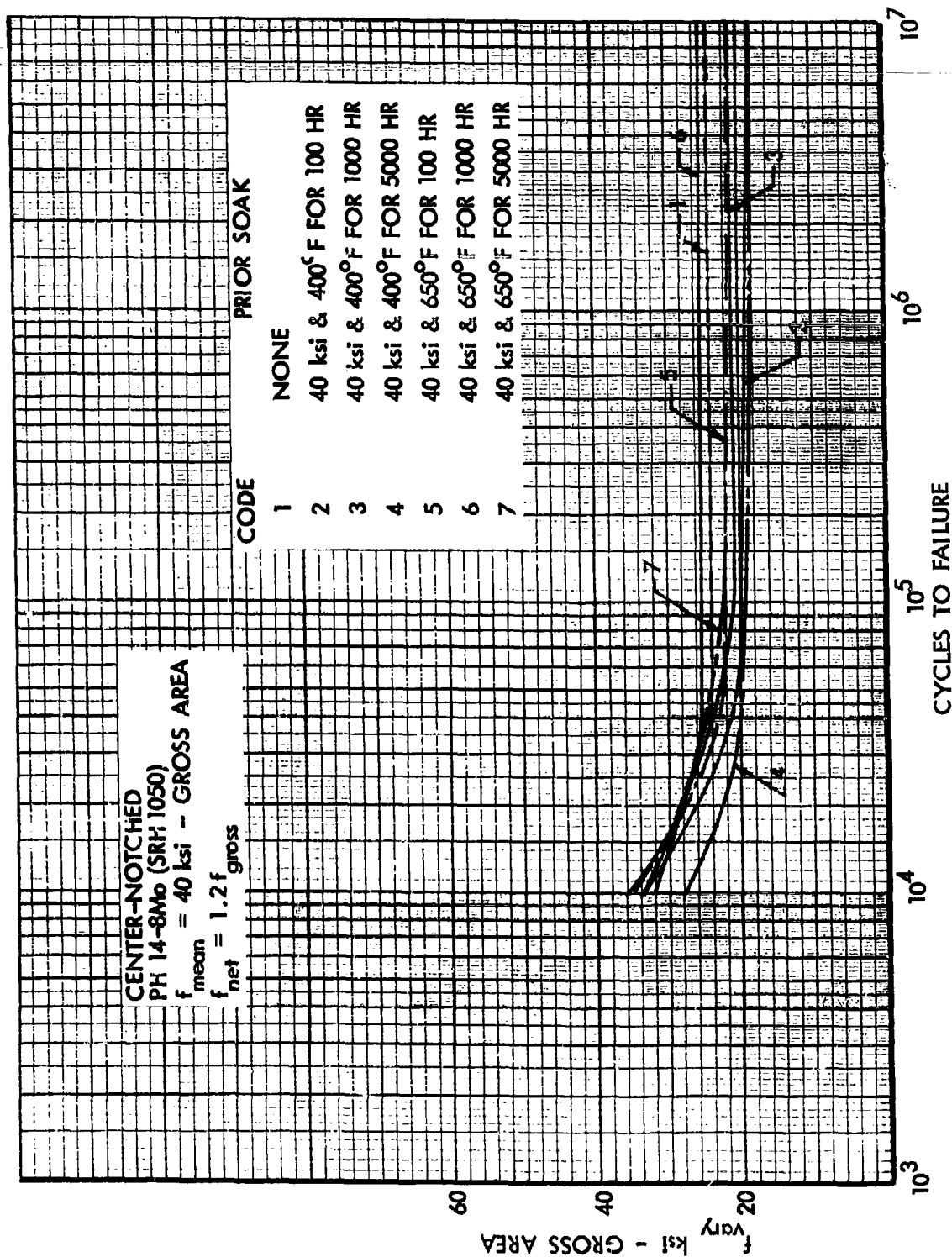
Figure 227. Effects of Prior Soak on S-N Curves at 400°F, Center-Notched PH14-8Mo, f_{mean} = Constant

CENTER-NOTCHED
PH 14-8Mo (SRH 1050)
f_{mean} = 40 ksi - GROSS AREA
f_{net} = 1.2 f_{gross}

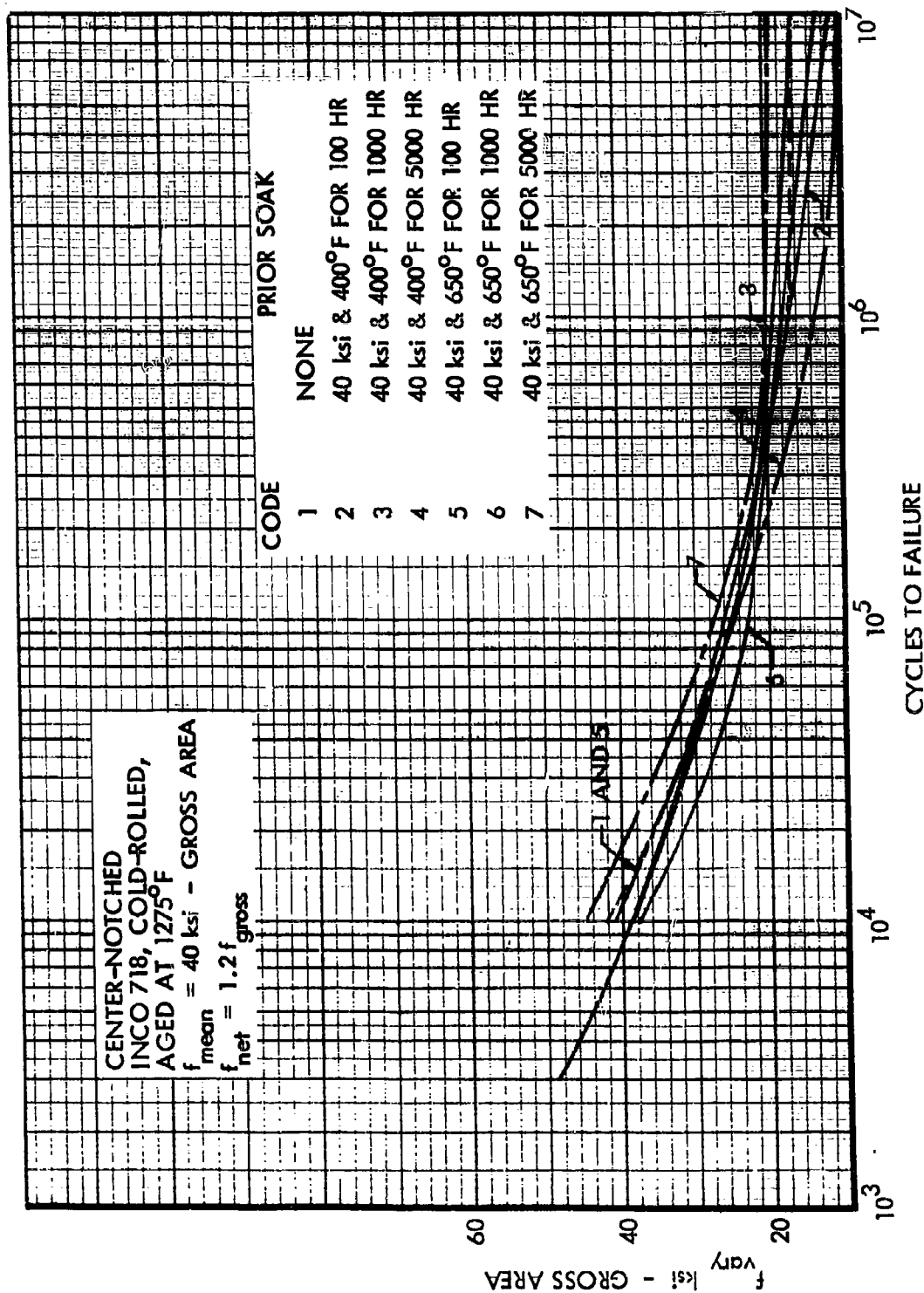| CODE	PRIOR SOAK
1	NONE
2	40 ksi & 400°F FOR 100 HR
3	40 ksi & 400°F FOR 1000 HR
4	40 ksi & 400°F FOR 5000 HR
5	40 ksi & 650°F FOR 100 HR
6	40 ksi & 650°F FOR 1000 HR
7	40 ksi & 650°F FOR 5000 HR

CYCLES TO FAILURE

f_{vary} ksi - GROSS AREA

307

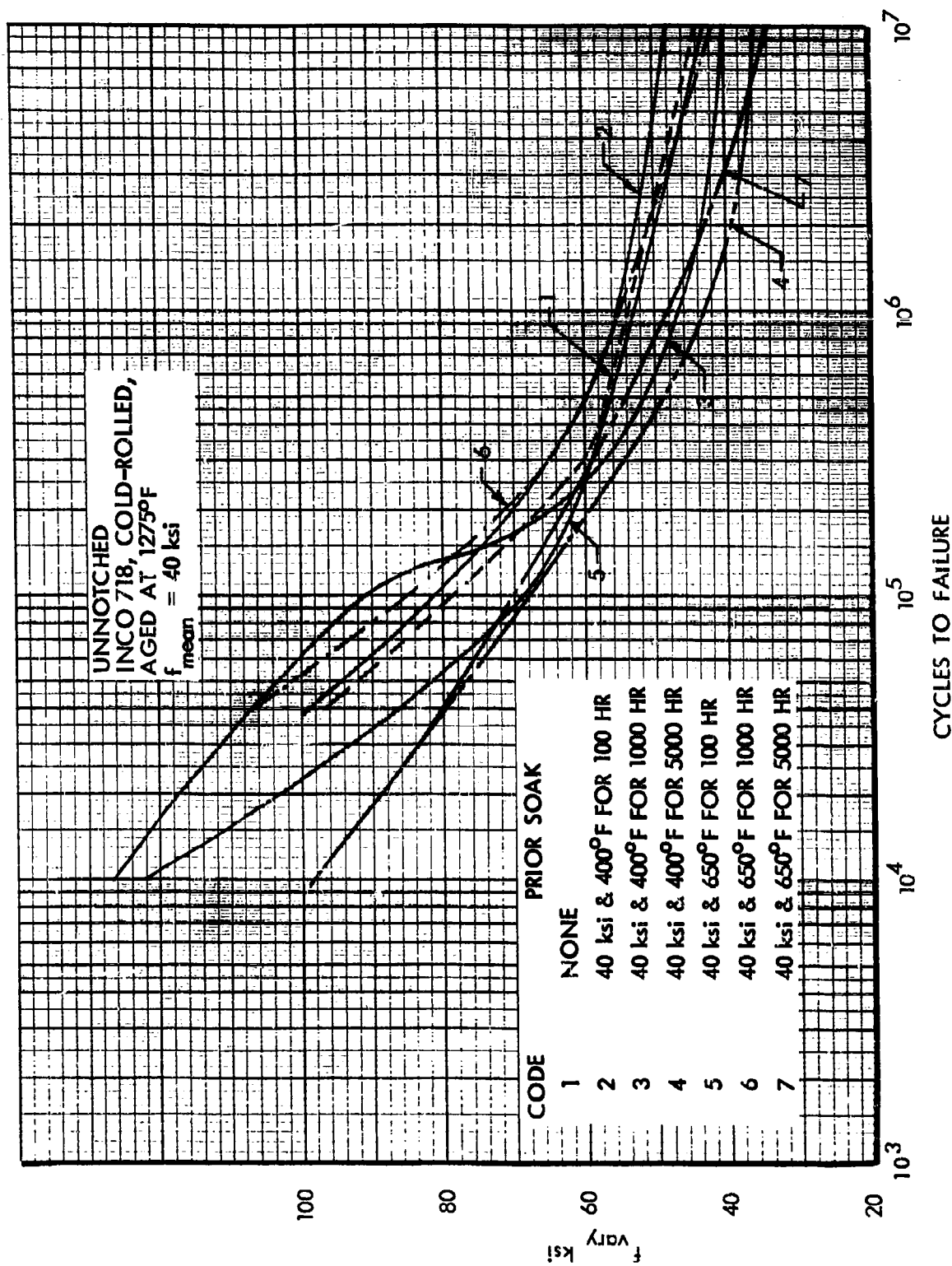Figure 228. Effects of Prior Soak on S-N Curves at 650°F, Center-Notched PH14-8Mo, f_{mean} = Constant

308
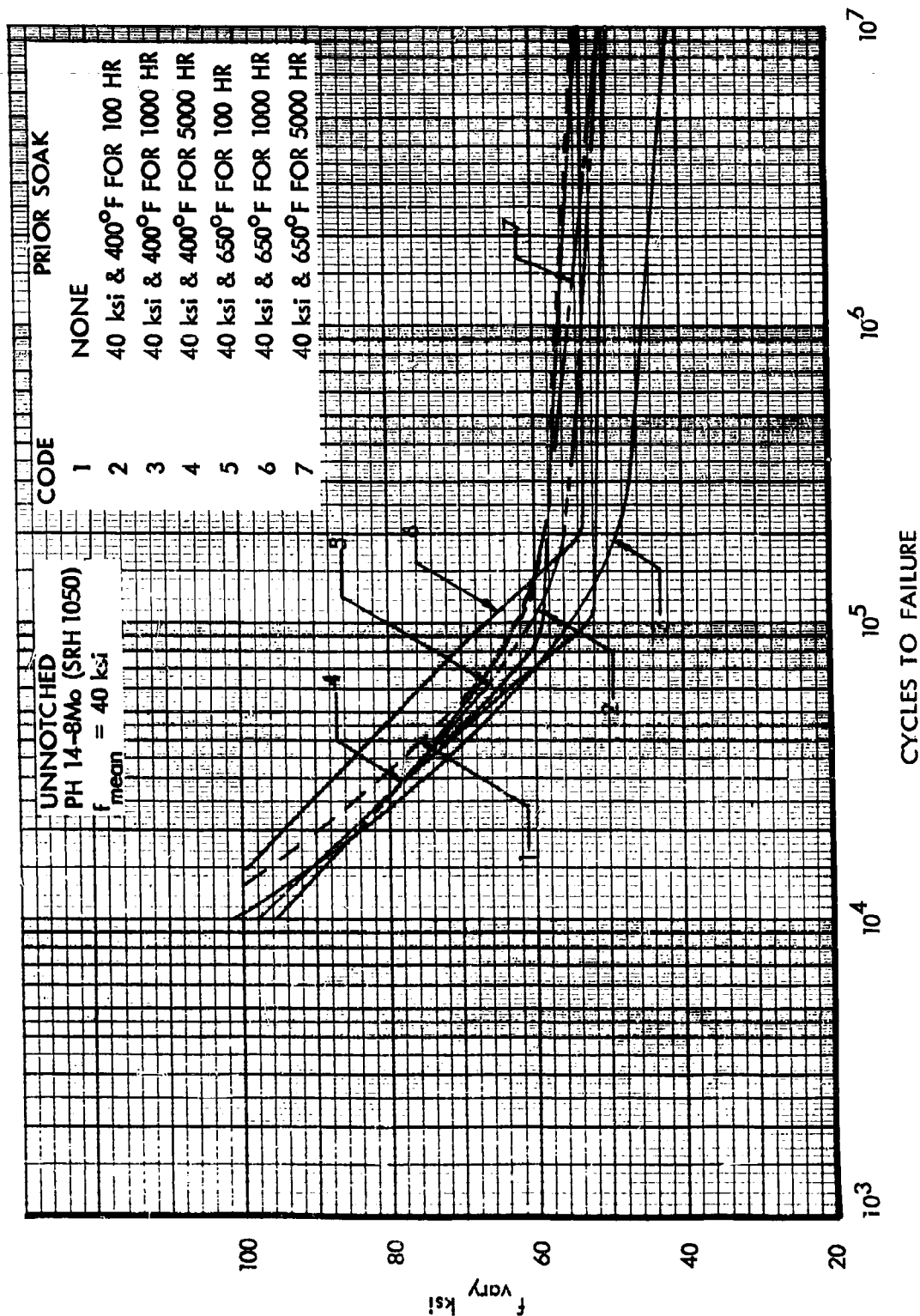
Figure 229. Effects of Prior Soak on S-N Curves at Room Temperature, Unnotched PH14-8Mo, f_{mean} = Constant
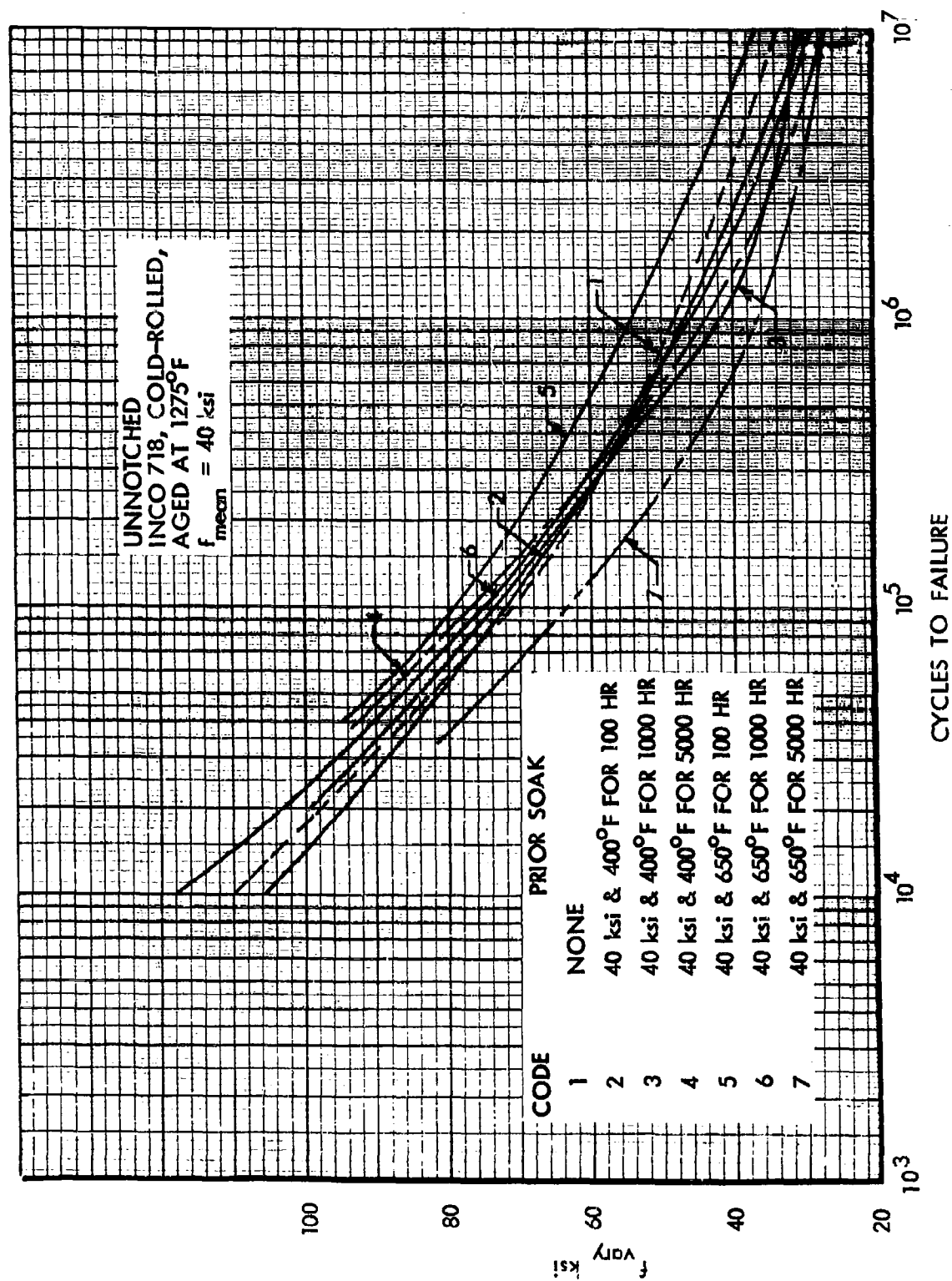
Figure 230. Effects of Prior Soak on S-N Curves at 400°F, Unnotched PH14-8Mo, f_{mean} = Constant

Figure 231. Effects of Prior Soak on S-N Curves at 650°F, Unnotched PH14-8Mo, f_{mean} = Constant

311

Figure 232. Effects of Prior Soak on S-N Curves at Room Temperature, Fusion-Welded PH14-8Mo, f_{mean} = Constant

Figure 233. Effects of Prior Soak on S-N Curves at 400°F, Fusion-Welded PH14-8Mo, f_{mean} = Constant

313

Figure 234. Effects of Prior Soak on S–N Curves at 650°F, Fusion–Welded PH14–8Mo, f_{mean} = Constant

314

Figure 235. Effects of Prior-Soak on S-N Curves at Room Temperature, Center-Notched INCO 718, f_{mean} = Constant
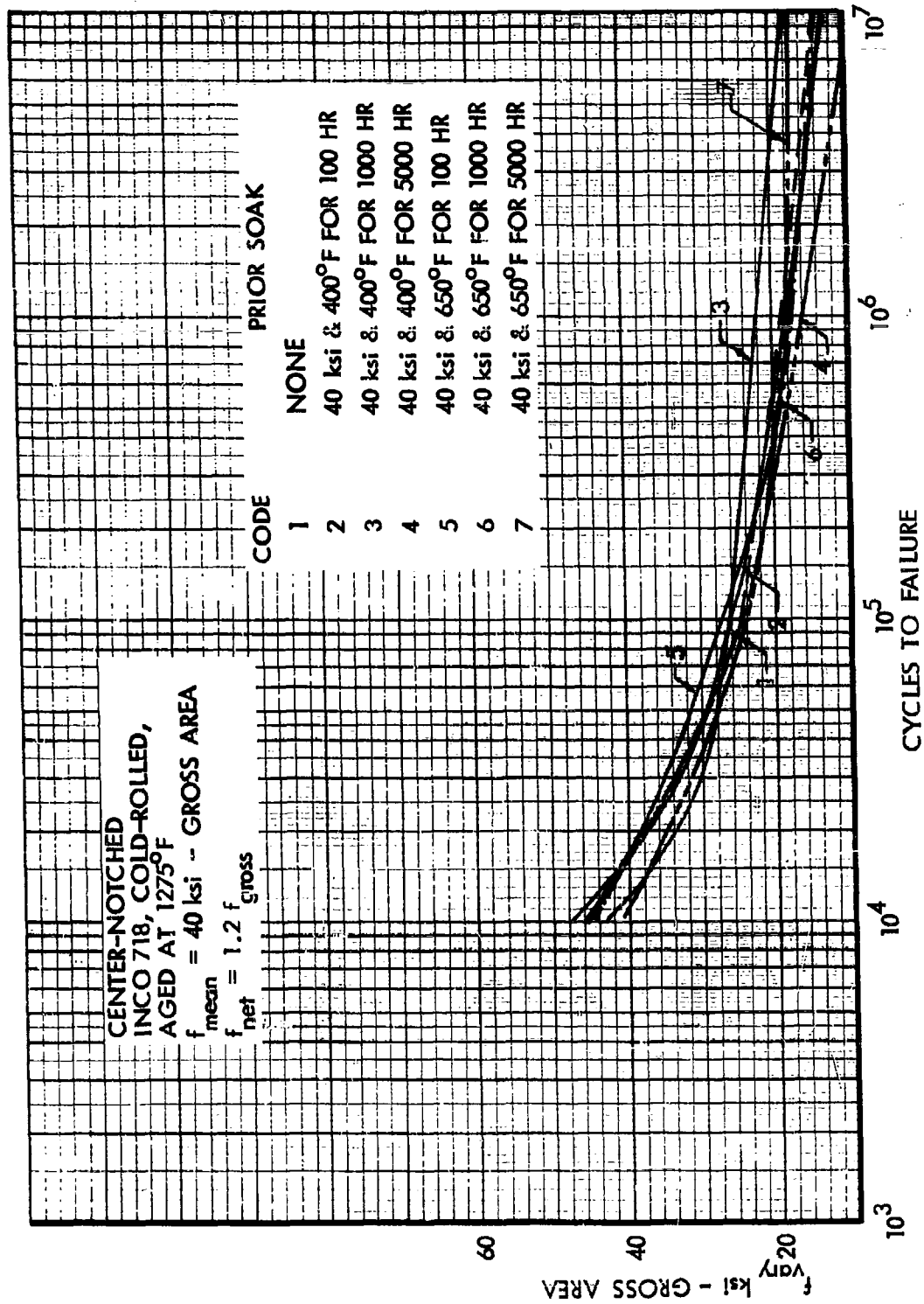
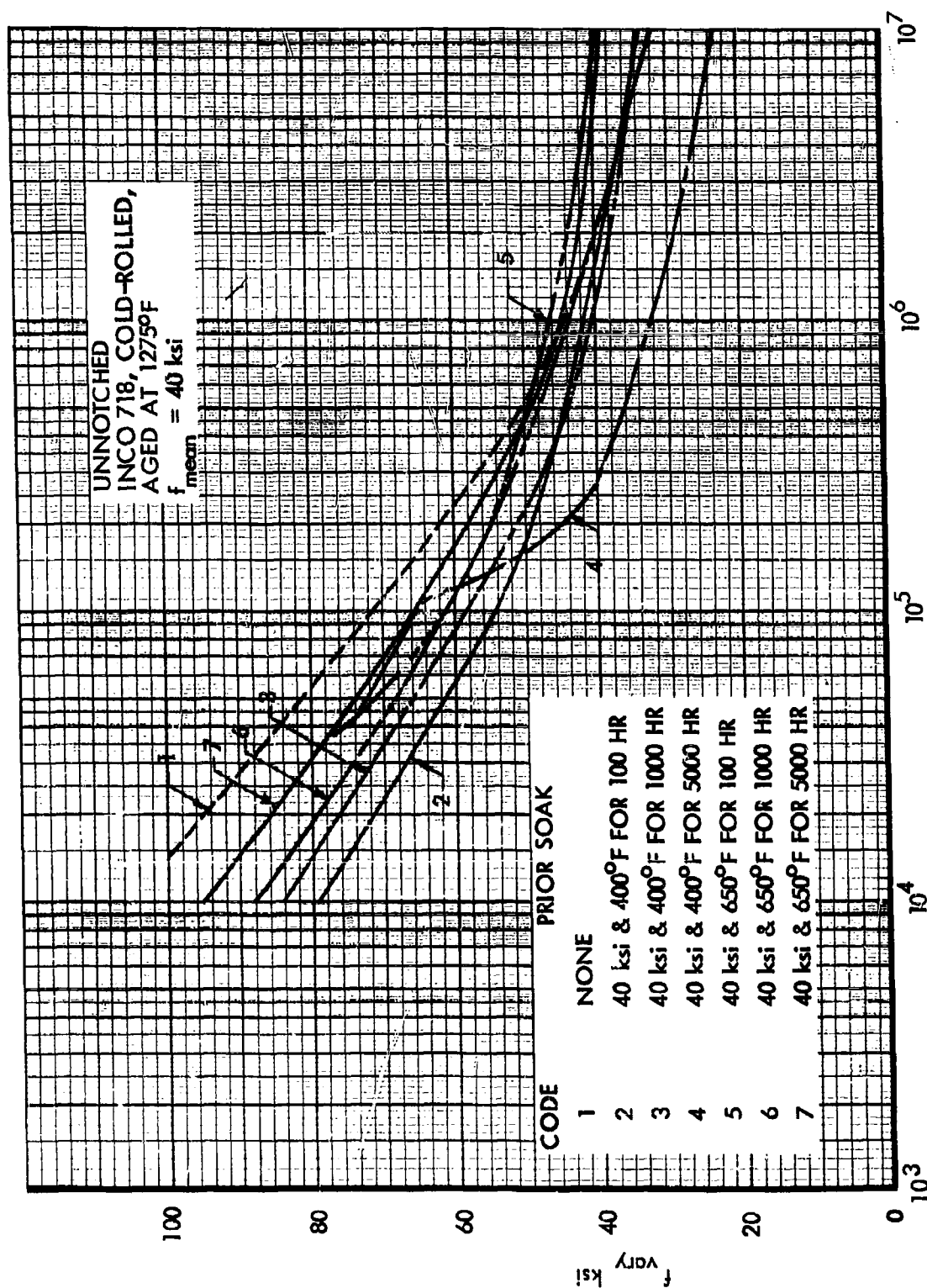Figure 236. Effects of Prior Soak on S-N Curves at 400°F, Center-Notched INCO 718, f_{mean} = Constant

316

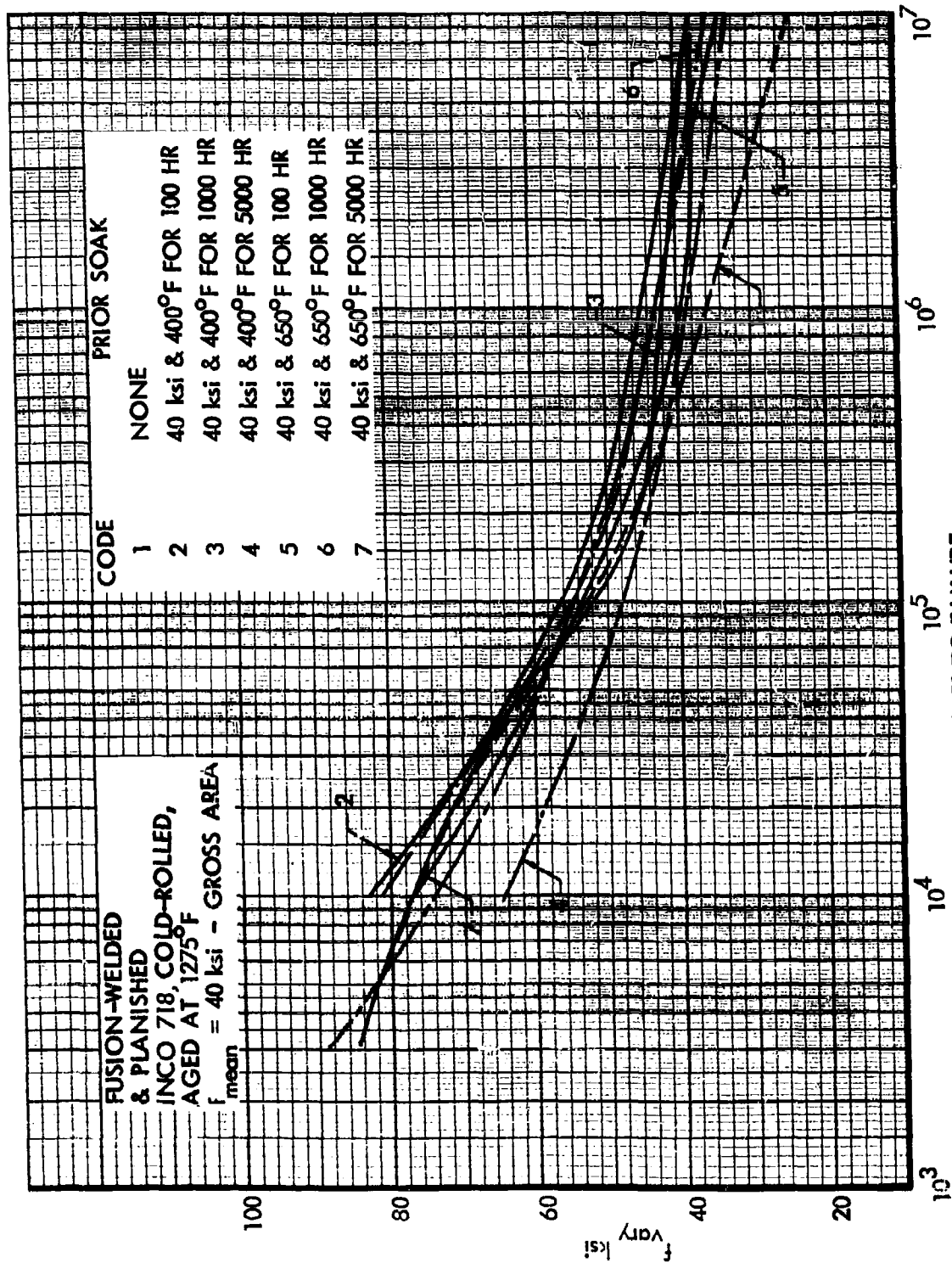Figure 237. Effects of Prior Soak on S-N Curves at 650°F, Center-Notched INCO 718, f_{mean} = Constant

Figure 238. Effects of Prior Soak on S-N Curves at Room Temperature, Unnotched INCO 718, f_{mean} = Constant

Figure 239. Effects of Prior Soak on S-N Curves at 400°F, Unnotched INCO 718, f_{mean} = Constant

UNNOTCHED
INCO 718, COLD-ROLLED,
AGED AT 1275°F
f_{mean} = 40 ksi

CODE	PRIOR SOAK
1	NONE
2	40 ksi & 400°F FOR 100 HR
3	40 ksi & 400°F FOR 1000 HR
4	40 ksi & 400°F FOR 5000 HR
5	40 ksi & 650°F FOR 100 HR
6	40 ksi & 650°F FOR 1000 HR
7	40 ksi & 650°F FOR 5000 HR

CYCLES TO FAILURE

f_{vary} ksi

319

Figure 240. Effects of Prior Soak on S-N Curves at 650°F, Unnotched INCO 718, f_{mean} = Constant

Figure 241. Effects of Prior Soak on S-N Curves at Room Temperature, Fusion-Welded INCO 718, f_{mean} = Constant

321
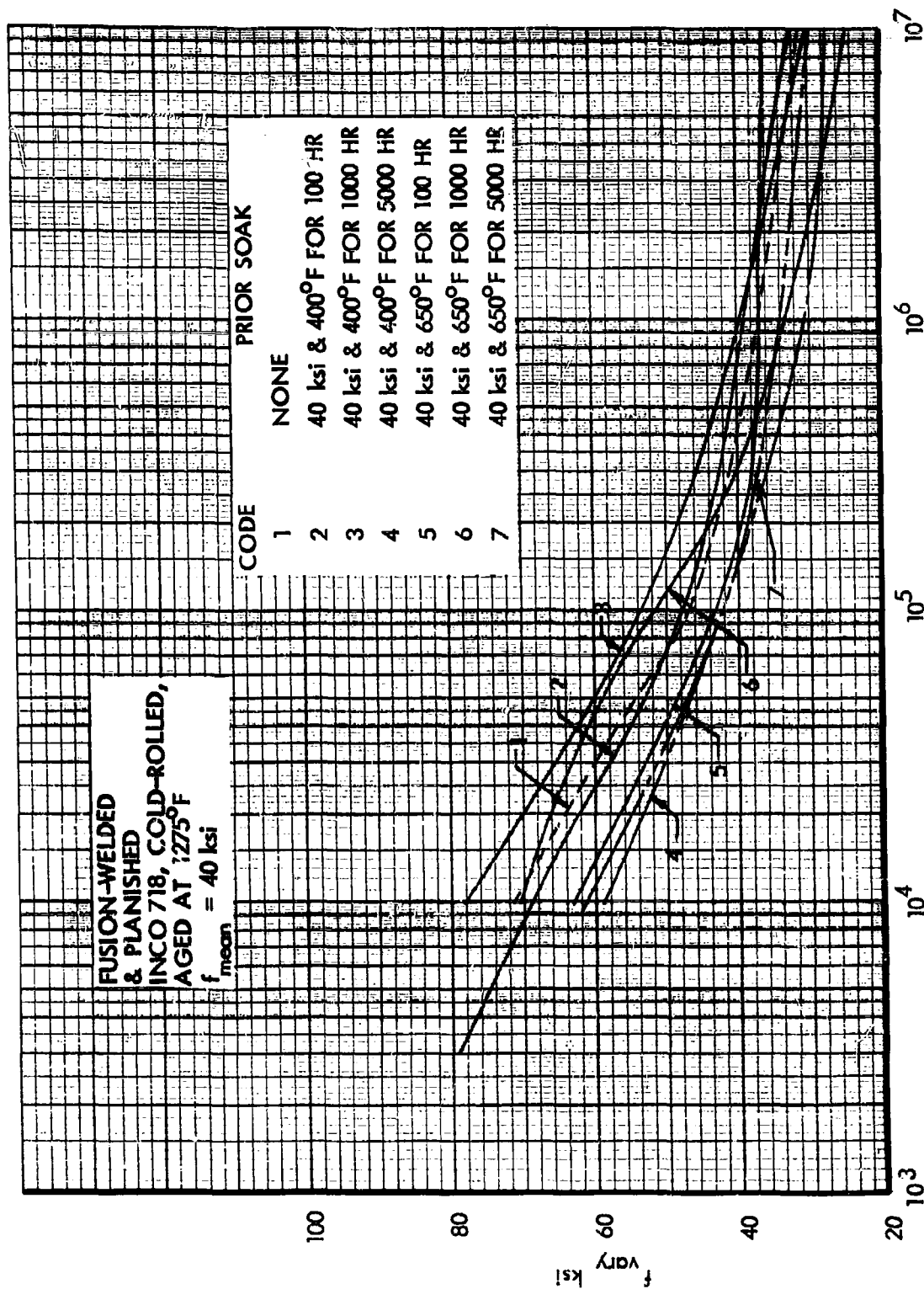
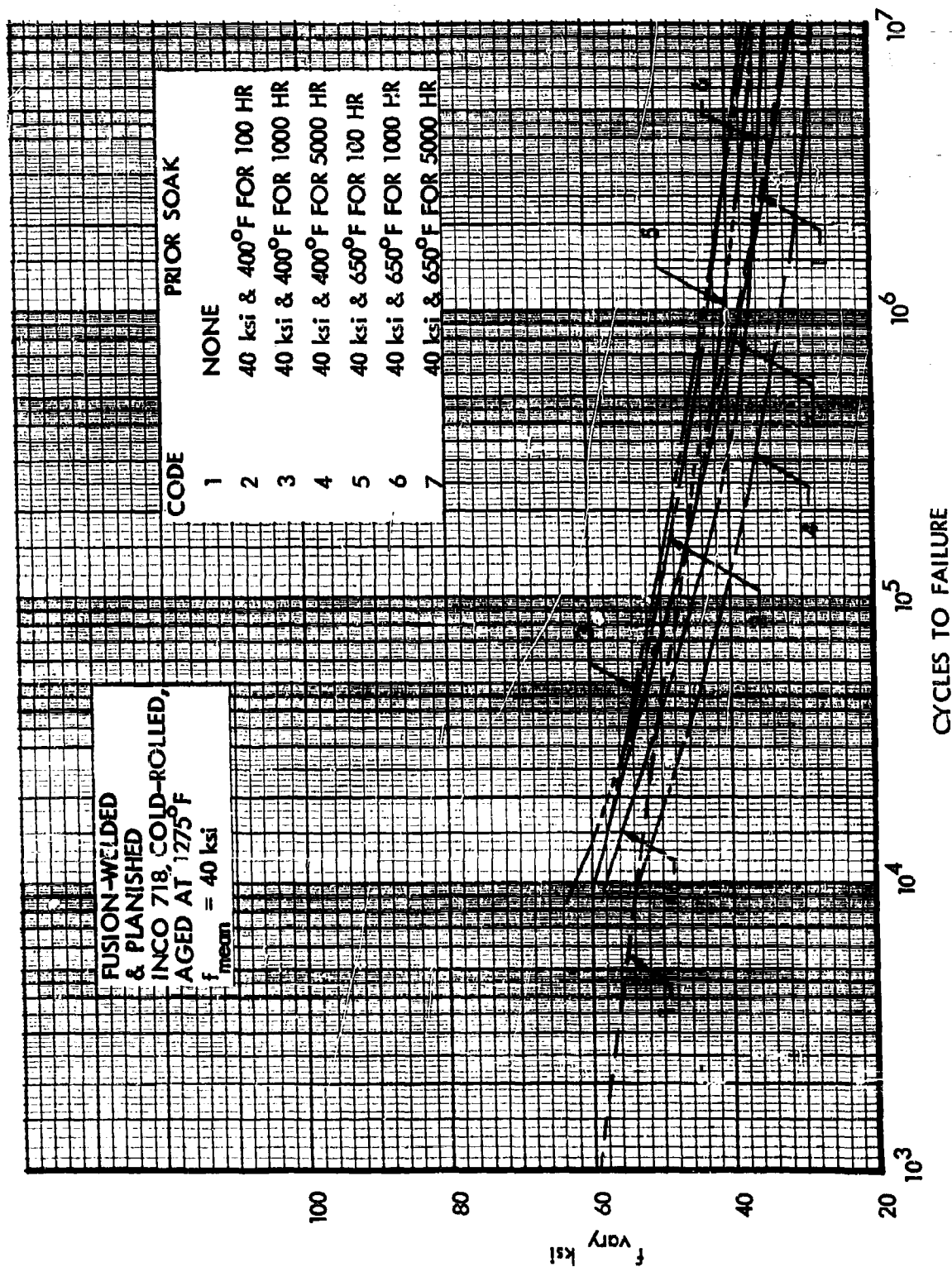Figure 242. Effects of Prior Soak on S-N Curves at 400°F, Fusion-Welded INCO 718, f_{mean} = Constant

322

Figure 243. Effects of Prior Soak on S-N Curves at 650°F, Fusion-Welded INCO 718, f_{mean} = Constant

323

APPENDIX VIII

METALLOGRAPHIC EXAMINATION OF TEST SPECIMENS

After testing, eleven center-notched and fusion-welded specimens were
selected, sectioned and examined metallographically. These specimens were
selected by using the results of S-N tests conducted with and without con-
taminants as a guide. They had been subjected to the longest exposure periods,
the most severe fatigue test conditions, or the most adverse combination of
specimen configuration, exposure and test condition. In addition, one
unexposed and untested fusion-welded specimen of each material was sectioned
and examined. The latter specimens provided a basis for judging the effects
of exposure and test conditions on the metallographic structure of duplex
annealed 8-1-1 titanium, PH14-8Mo (SRH 1050) stainless steel and Inco 718
nickel alloy in the 20 percent cold rolled and aged at 1275°F condition.

The specimens were sectioned and examined at 20X and 200X for evidence of
subsurface attack, cracking and similar defects. These sections were taken
parallel to the axis of the specimen through the weldments, notches and
fracture surfaces. Examination of the metallographic structures shows no
evidence of surface corrosion, intergranular attack or sub-surface cracking.

The results of visual examinations are given along with the specimen
identification and prior history in Table 38. Photomacrographs and photo-
micrographs of sections of the specimens are presented in Figures 244 to 257.
The chemicals used to etch the specimens for microscopic examinations were:

Alloy	Etchant
8-1-1 Titanium	2% HF - 8% HNO_3 - 90% H_2O
PH14-8Mo Steel	10% Ammonium Persulfate, Electrolytic
Inco 718	7% Chromic Acid, Electrolytic

MATERIAL	SPECIMEN *	SPECIMEN NO.	PRIOR SOAK				TEST HISTORY	REMARKS	FIGURE NO.
			STRESS (ksi)	CONTAMINANT	TEMP (°F)	TIME (hr)			
8-1-1 Titanium Duplex Annealed	Center Notched	479	25	Mil-O-7277 Oil	550	1000	Fatigue tested with Mil-O-7277 Oil at 650°F	No corrosion or discoloration	244
	Center Notched	404	25	—	650	5000	Fatigue tested at high stress at 650°F	Discolored and no corrosion	245
	Fusion Welded	655	—	—	—	—	Not tested	No corrosion or discoloration	246
	Fusion Welded	308	25	Salt Water	550	1000	Fatigue tested with salt water at 650°F	No corrosion or discoloration. Failed outside weld zone.	247
	Fusion Welded	527	25	—	650	5000	Fatigue tested at high stress at 650°F	Discolored and no corrosion. Failed outside weld zone.	248
PH14-8Mo (SRH 1050)	Center Notched	577	40	Mil-O-7277 Oil	550	1000	Fatigue tested with Mil-O-7277 Oil at 650°F	Very dark discoloration and no corrosion.	249
	Center Notched	524	40	—	650	5000	Fatigue tested at high stress at 650°F	Very dark discoloration and no corrosion	250

* All fusion-welded specimens were planished.

TABLE 38 VISUAL EXAMINATION OF TEST SPECIMENS AT 20X MAGNIFICATION

(2 of 2)

MATERIAL	SPECIMEN *	SPECIMEN NO.	PRIOR SOAK				TEST HISTORY	REMARKS	FIGURE NO.
			STRESS (ksi)	CONTAM-INANT	TEMP (°F)	TIME (hr)			
PH14-8Mo (SRH 1050)	Fusion Welded	503	—	—	—	—	Not tested	Dark grey color and no corrosion	251
	Fusion Welded	570	40	—	650	5000	Fatigue tested at high stress at 650°F	Very dark discoloration and no corrosion. Failed in weld transition zone (HAZ).	252
	Center Notched	707	40	MIL-O-7277 Oil	550	1000	Fatigue tested with MIL-O-7277 Oil at 650°F	Dark discoloration and no corrosion.	253
INCO 718 Cold Rolled, Aged at 1275°F	Center Notched	498	40	—	650	5000	Fatigue tested at high stress at 650°F	Very dark discoloration and no corrosion.	254
	Fusion Welded	653	—	—	—	—	Not tested	No corrosion	255
	Fusion Welded	614	40	Versi-lube F-50	550	1000	Failure tested with Versilube F-50 at 650°F	Gray color and no corrosion. Failed in weld metal	256
	Fusion Welded	267	40	—	650	5000	Fatigue tested at high stress at 650°F	Very dark discoloration and no corrosion.	257

* Fusion-welded specimens were planished.
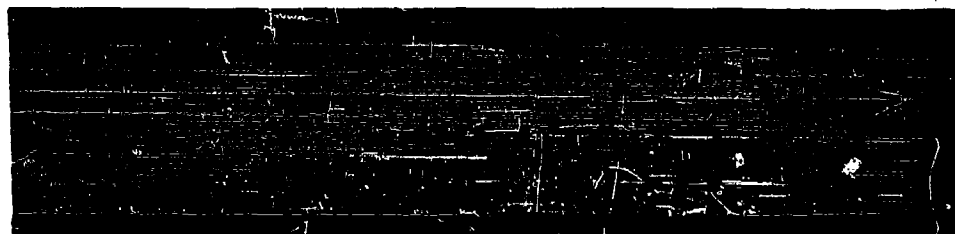
BASE METAL   (20X)
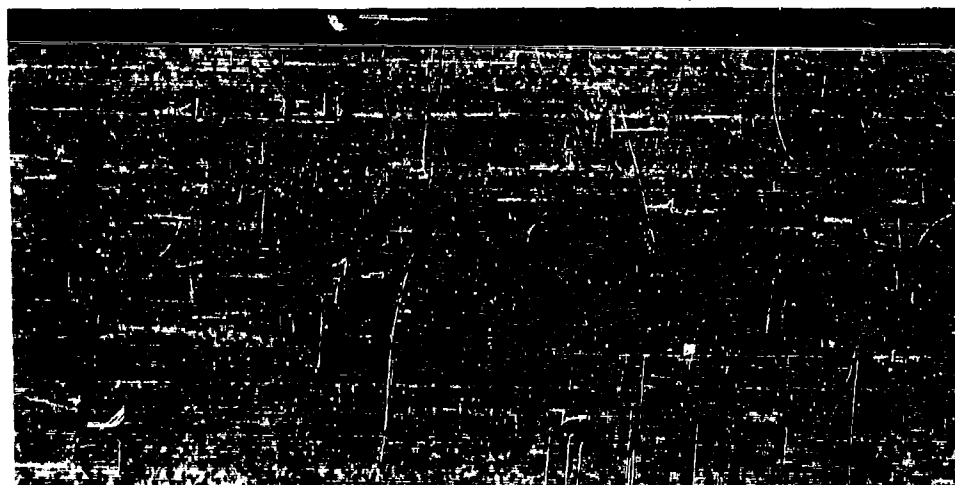
BASE METAL   (200X)

SPECIMEN NO. 479
EXPOSED AT 25 ksi AND 550°F FOR
1000 HR. TO MIL-O-7277 OIL IN
DUPLEX-ANNEALED CONDITION
FATIGUE TESTED WITH MIL-O-7277 OIL AT 650°F

Figure 244. Metallographic Structures of 8-1-1 Titanium,
Exposed to MIL-O-7277 Oil.

328

BASE METAL   (20X)

BASE METAL   (200X)

SPECIMEN NO. 404
EXPOSED AT 25 ksi AND 650°F FOR
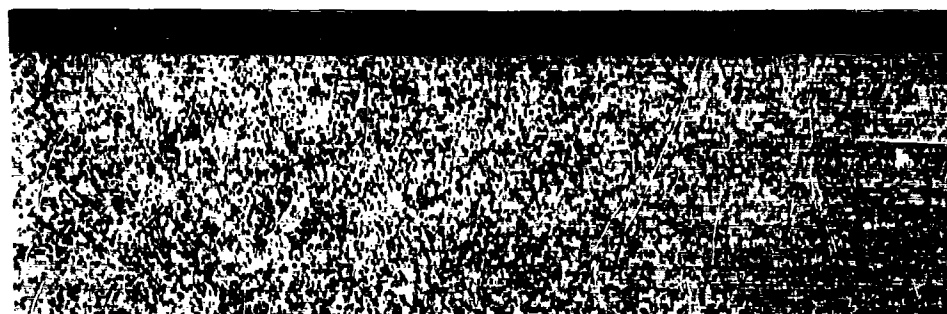5000 HR. IN THE DUPLEX-ANNEALED CONDITION
FATIGUE TESTED AT 650°F

Figure 245. Metallographic Structure of 8-1-1 Titanium, Exposed

WELD METAL, HEAT AFFECTED ZONE AND BASE METAL (20X)

WELD METAL (200X)

HEAT AFFECTED ZONE AND BASE METAL (200X)

SPECIMEN NO. 655
WELDED IN THE DUPLEX-ANNEALED CONDITION
NOT EXPOSED
NOT TESTED

Figure 246. Metallographic Structure of Fusion-Welded 8-1-1 Titanium
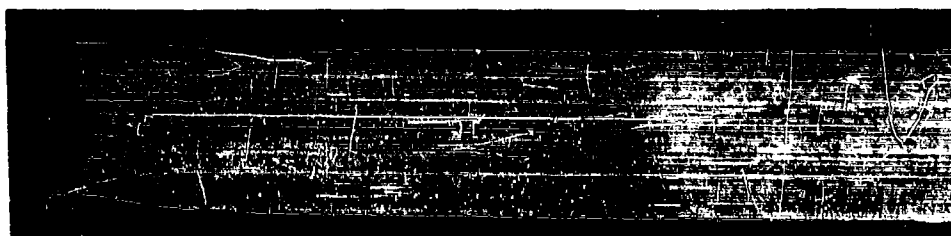
BASE METAL, HEAT AFFECTED ZONE AND WELD METAL (20X)
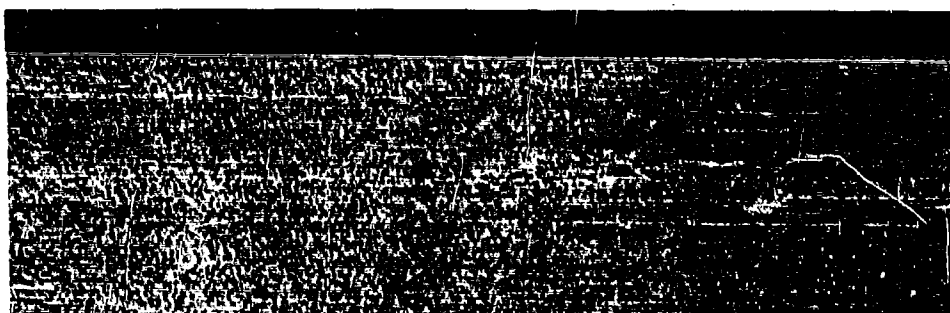
HEAT AFFECTED ZONE AND BASE METAL (200X)

WELD METAL   (200X)

SPECIMEN NO. 308
WELDED IN THE DUPLEX-ANNEALED CONDITION
EXPOSED AT 40 ksi AND 550°F
FOR 1000 HR. TO SALT WATER
FATIGUE TESTED WITH SALT WATER AT 650°F

Figure 247. Metallographic Structure of Fusion-Welded 8-1-1
Titanium, Exposed to Salt Water
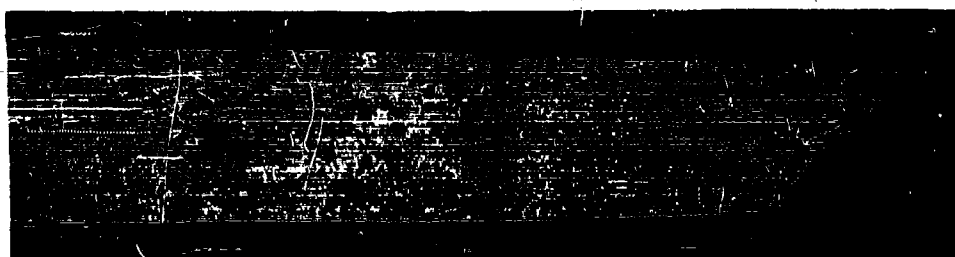
331

WELD METAL, HEAT AFFECTED ZONE AND BASE METAL (20X)

HEAT AFFECTED ZONE AND BASE METAL (200X)

WELD METAL   (200X)

SPECIMEN NO. 527
WELDED IN DUPLEX-ANNEALED CONDITION
EXPOSED AT 25 ksi AND 650°F FOR 5000 HR.
FATIGUE TESTED AT 650°F

Figure 248. Metallographic Structure of Fusion-Welded 8-1-1 Titanium, Exposed

332
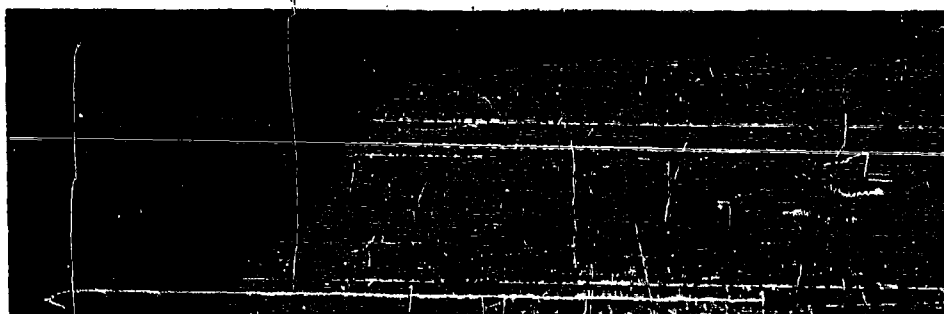
BASE METAL   (20X)

BASE METAL   (200X)

BASE METAL   (200X)

SPECIMEN NO. 577
EXPOSED AT 40 ksi AND 550°F FOR
1000 HR. TO MIL-0-7277 OIL IN SRH 1050
CONDITION
FATIGUE TESTED WITH MIL-0-7277 OIL AT 650°F

Figure 249. Metallographic Structures of PH14-8 Mo
Exposed to MIL-0-7277 Oil

333
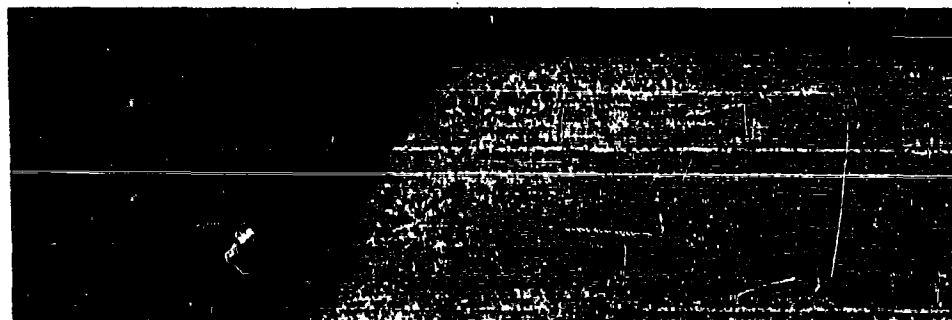
BASE METAL   (20X)

BASE METAL   (200X)

BASE METAL   (200X)

SPECIMEN NO. 524
EXPOSED AT 40 ksi AND 650°F
FOR 5000 HR. IN SRH 1050 CONDITION
FATIGUE TESTED AT 650°F

Figure 250. Metallographic Structure of PH14-8 Mo, Exposed

334
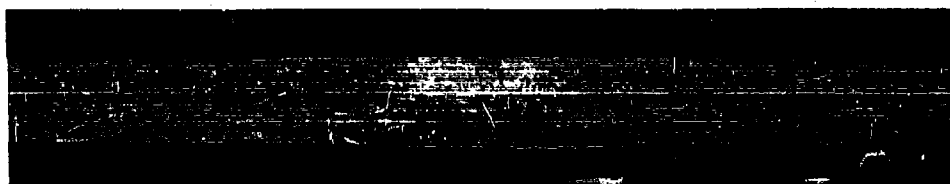
WELD METAL, HEAT AFFECTED ZONE AND BASE METAL (20X)

WELD METAL, HEAT AFFECTED ZONE AND BASE METAL (200X)

BASE METAL   (200X)

SPECIMEN NO. 503
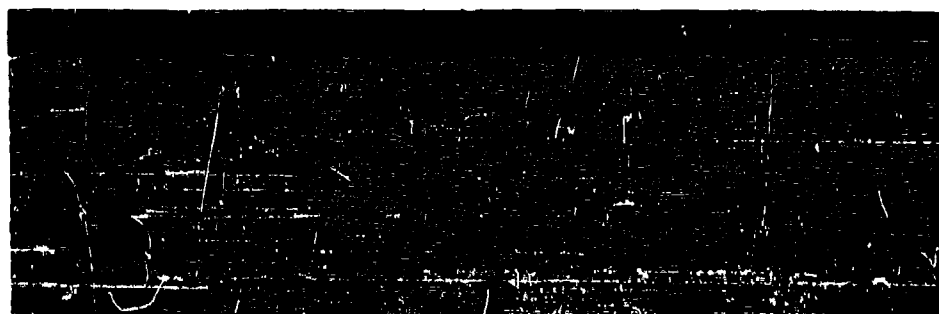WELDED IN ANNEALED CONDITION AND
HEAT TREATED TO THE SRH 1050 CONDITION
NOT EXPOSED
NOT TESTED

Figure 251. Metallographic Structure of Fusion-Welded PH14-8 Mo
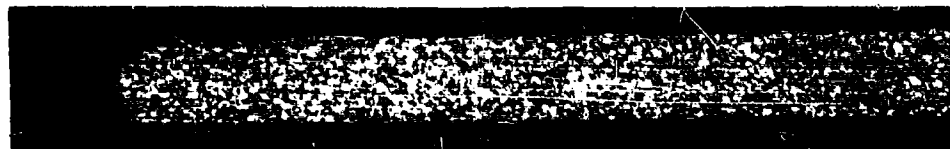
335

WELD METAL, HEAT AFFECTED ZONE AND BASE METAL (20X)
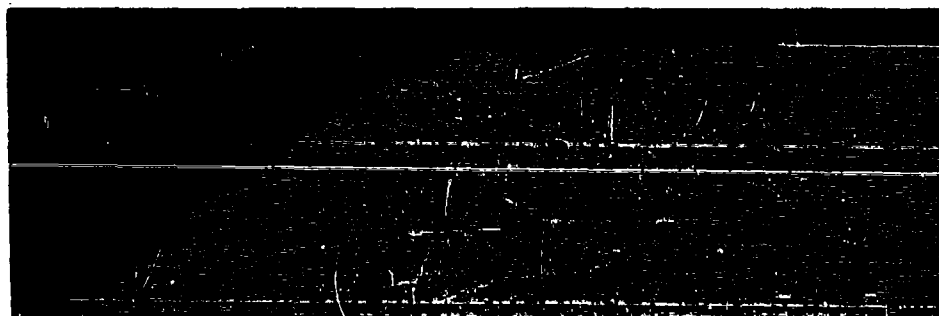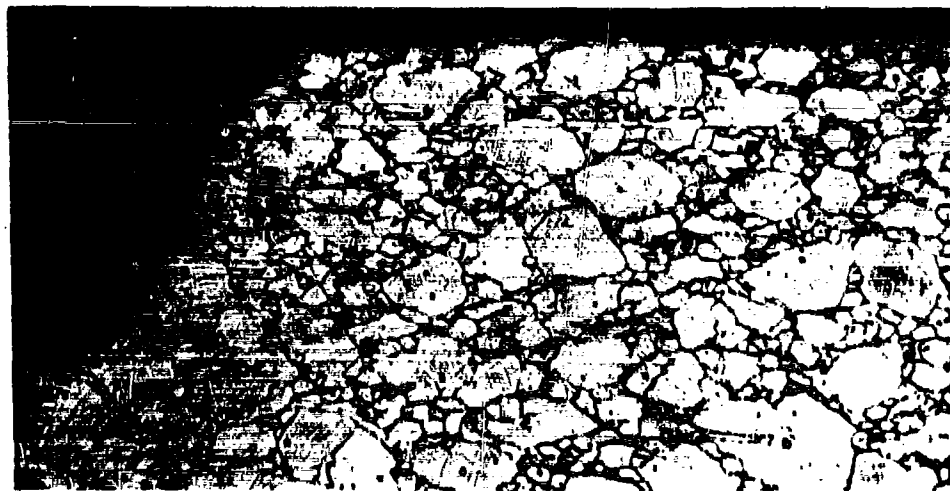

HEAT AFFECTED ZONE (200X)

WELD METAL, HEAT AFFECTED ZONE AND BASE METAL (200X)

SPECIMENT NO. 570
WELDED IN ANNEALED CONDITION
EXPOSED AT 40 ksi AND 650°F FOR
5000 HR. IN SRH 1050 CONDITION
FATIGUE TESTED AT 650°F

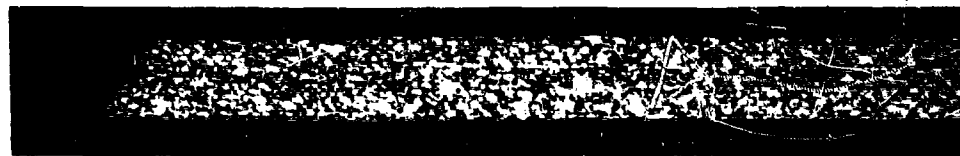Figure 252. Metallographic Structure of Fusion-Welded PH14-8 Mo, Exposed
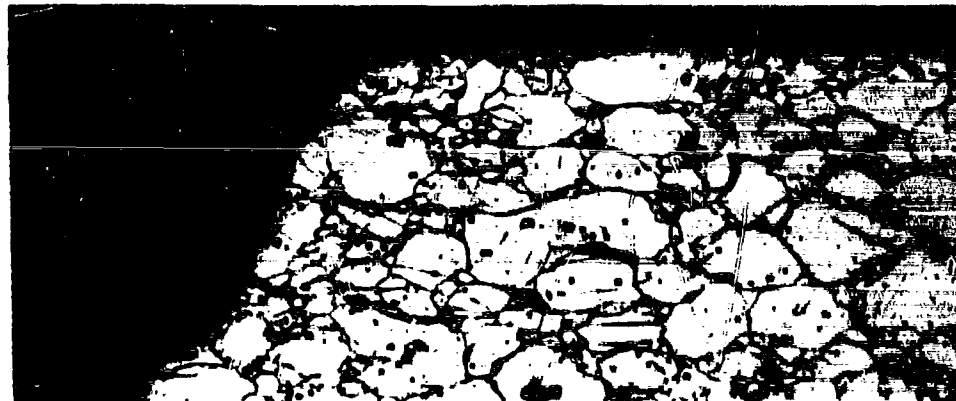
BASE METAL   (20X)

BASE METAL   (200X)

SPECIMEN NO. 707
EXPOSED AT 40 ksi AND 550°F FOR
1000 HR. TO MIL-O-7277 OIL IN THE
20% COLD ROLLED AND AGED AT 1275°F CONDITION.
FATIGUE TESTED WITH MIL-O-7277 OIL AT 650°F

Figure 253. Metallographic Structure of INCO 718,
Exposed to MIL-O-7277 Oil
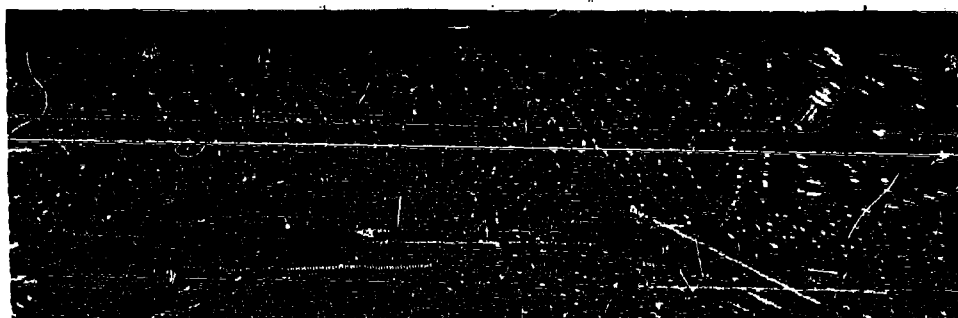
337

BASE METAL   (20X)

BASE METAL   (200X)

SPECIMEN NO. 498
EXPOSED AT 40 ksi AND 650°F FOR
5000 HR. IN THE 20% COLD ROLLED AND
AGED AT 1275°F CONDITION
FATIGUE TESTED AT 650°F

Figure 254. Metallographic Structure of INCO 718, Exposed

338

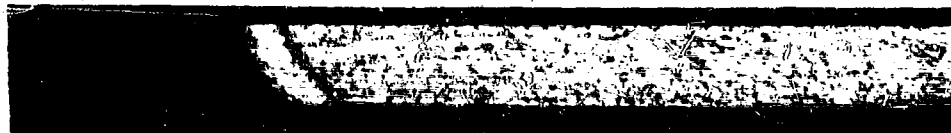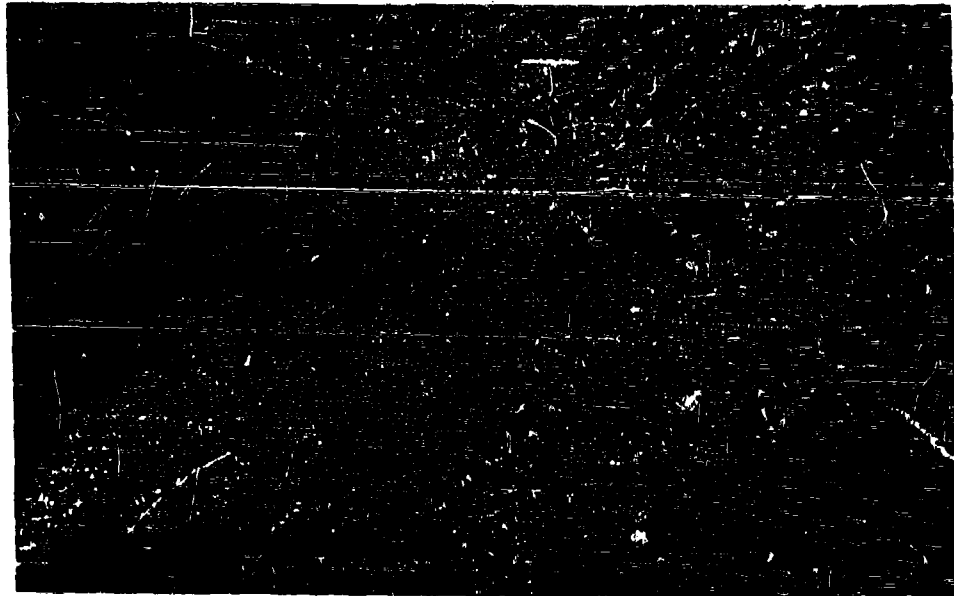WELD METAL, HEAT AFFECTED ZONE AND BASE METAL (20X)

WELD METAL (200X)

WELD METAL, HEAT AFFECTED ZONE AND BASE METAL (200X)

SPECIMEN NO. 653
WELDED IN THE 20% COLD ROLLED AND
AGED AT 1275°F CONDITION
NOT EXPOSED
NOT TESTED

Figure 255. Metallographic Structure of Fusion-Welded INCO 718

339

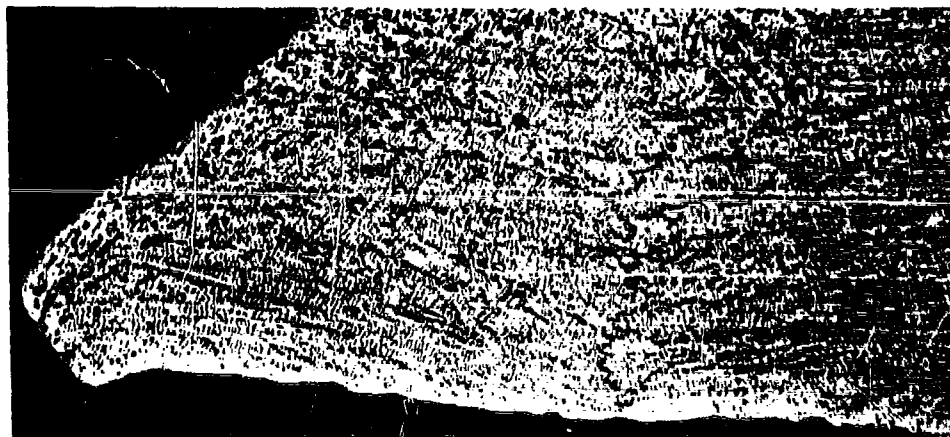WELD METAL, HEAT AFFECTED ZONE AND BASE METAL (20X)

WELD METAL (200X)

WELD METAL, HEAT AFFECTED ZONE AND BASE METAL (200X)

SPECIMEN NO. 614
WELDED IN 20% COLD ROLLED AND AGED
AT 1275°F CONDITION.
EXPOSED AT 40 ksi AND 550°F FOR
1000 HR. TO VERSILUBE F-50
FATIGUE TESTED WITH VERSILUBE F-50 AT 650°F

Figure 256. Metallographic Structure of Fusion-Welded INCO 718,
Exposed to Versilube F-50

WELD METAL, HEAT AFFECTED ZONE AND BASE METAL (20X)

WELD METAL (200X)

WELD METAL, HEAT AFFECTED ZONE, AND BASE METAL (200X)

SPECIMEN NO. 267
WELDED IN THE 20% COLD ROLLED AND
AGED AT 1275°F CONDITION
EXPOSED AT 40 KSI AND 650°F FOR 5000 HR.
FATIGUE TESTED AT 650°F

Figure 257. Metallographic Structure of INCO 718, Exposed

APPENDIX IX

CALCULATED TEST LIVES FOR SPECTRA C LOADINGS

The method of linear cumulative fatigue damage was used to calculate the test life for center-notched coupons under Spectra C Loadings.

For each combination of flight loadings and test temperatures, the appropriate S-N curve was derived from the applicable S-N diagram for no prior exposure. The S-N diagrams for $650°F$ were used for the test loadings applied at $550°F$ since the S-N data for $400°$ and $650°F$ are comparable. Each of the derived S-N curves was based on a constant maximum or mean stress level. For example, the peak (compressive) taxi load levels consisted of the mean taxi stress level and the negative half of the taxi loading cycles. These peak taxi loadings were always applied in terms of stress excursions below the mean stress level for the descent phase of flight. For this reason, the S-N curves derived for the taxi loadings were based on a constant maximum stress level that was equal to the mean stress level for the descent phase of flight. The S-N curves derived for the climb, cruise, descent and the ground-to-air transition cycles between the flight and ground loadings were based on a constant mean stress.

The ground-to-air transition cycle is automatically introduced into the test loadings by the flight-by-flight loading sequence. To indicate fatigue damages, however, required a definition of the transition cycle in terms of a stress range. Three methods were used to define the transition cycle with each method leading to a different value of calculated test life. In the first method, the maximum change in mean load level which occurs between the cruise and taxi phases of flight, as diagramed in Table 39, was employed to define a mean-to-mean transition cycle. This definition led to the least conservative predictions in Table 39.

The next method used the more severe definition of the maximum stress range which occurs during the flights which do not have additional loadings to represent increase of severity with time. This cycle extends, in terms of the actual loads applied during testing, from the maximum tensile stress during cruise to the peak compressive stress for taxi loadings, as illustrated in Table 39. Use of this single flight peak transition cycle led to shorter predicted lives than those obtained by using the mean-to-mean transition cycle.

In the third method, a spectrum of transition cycles was used. The spectrum of transition cycles considers the growth in loading magnitudes felt by the specimens with test time caused by the less than once per flight loading magnitudes. These infrequent loadings were applied at periodic intervals during testing of 100, 500, 1000, 10,000, 20,000, 40,000 and 80,000 flights. The use of larger loadings in the spectrum of transition cycles produced calculated lives that were slightly less than those calculated

for the single flight peak transition cycle as shown in Table 39. The small differences in calculated lives for these two definitions of transition cycles may be applicable only to the loading history employed in this test program and could possibly be much larger for other test loading histories.
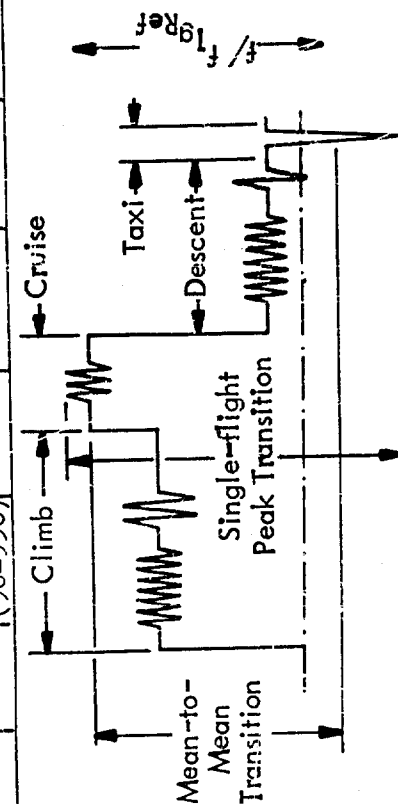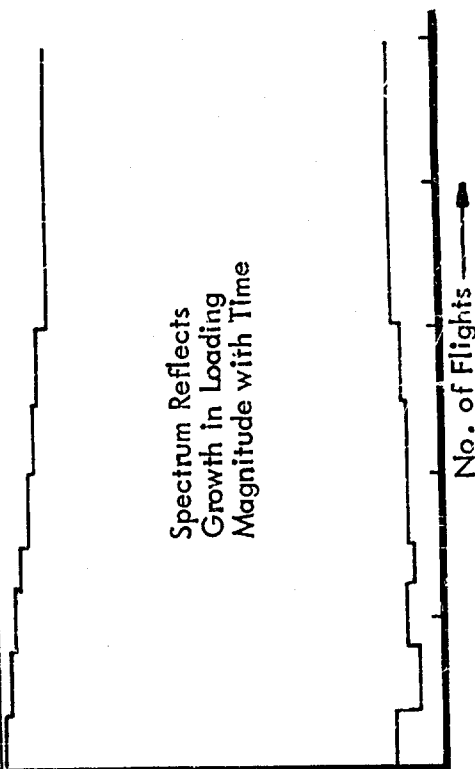
The ratios of average test lives to predicted lives shown in Table 39 indicate that moderately good predictions of test life are provided by the more severe definitions of the transition cycle.

While the use of either the single flight peak or the spectrum of transition cycles led to calculated lives that approximated the test results, extended use of either definition for calculating fatigue damages should be approached with caution. In a recent ASD report[*], the use of the single flight peak transition cycle led to calculated lives that were quite unconservative.

* McCulloch, A. J., Melcon, M. A., Crichlow, W. J., Foster, H. W., and Rebman, J., "Investigation of the Representation of Aircraft Service Loadings in Fatigue Tests." ASD-TR-61-435, January 1962.

TABLE 39 COMPARISON OF CALCULATED LIVES WITH FLIGHT-BY-FLIGHT TEST RESULTS FOR SPECTRA C CENTER-NOTCHED SPECIMENS

Material	No. of Spec.	Test Temp. °F	Test Life			Mean-to-Mean Transition Cycle		Single-Flight Peak Transition Cycle		Spectrum of Transition Cycles	
			Minimum No. of Flights	Average No. of Flights	Maximum No. of Flights	Predicted Life No. of Flights	Avg.Test Life / Pred.Life	Predicted Life No. of Flights	Avg.Test Life / Pred.Life	Predicted Life No. of Flights	Avg.Test Life / Pred.Life
8-1-1 Titanium Duplex Annealed	8	Room	26,500	60,800	105,000	1,360,000	.045	115,000	.524	110,000	.553
	4	550	15,900	17,200	18,600	10,300,000	.0017	26,700	.644	26,000	.662
	3	Cyclic (90-550)	41,900	55,270	64,800	1,360,000	.041	116,000	.476	110,000	.502
PH14-8Mo (SRH 1050)	4	Room	8,100	8,870	10,380	35,500	.250	16,200	.547	15,800	.561
	4	550	3,000	3,125	3,250	9,400	.332	2,400	1.302	2,350	1.330
	4	Cyclic (90-550)	3,900	5,400	6,900	35,500	.152	16,200	.333	15,800	.342
INCO 718 CR, Aged at 1275°F	4	Room	12,750	14,370	16,100	48,200	.298	17,800	.807	17,400	.826
	4	550	11,650	11,825	12,000	42,400	.279	10,000	1.182	9,600	1.232
	4	Cyclic (90-550)	9,500	10,275	11,000	48,200	.213	17,800	.577	17,400	.591

SINGLE FLIGHT

Climb — Cruise — Taxi — Descent

Single-flight Peak Transition

Mean-to-Mean Transition

f/f_{Ref}

SPECTRUM OF TRANSITION CYCLES

Spectrum Reflects Growth in Loading Magnitude with Time

No. of Flights —